

PEG 2011
ARGENTINA

Asociación Geológica Argentina
Serie D: Publicación Especial N° 14
ISSN 0328-2767

CONTRIBUTIONS TO THE 5th INTERNATIONAL SYMPOSIUM ON GRANITIC PEGMATITES



CONICET

MENDOZA

Mendoza, 2011



Diseño editorial: Susana Graciela Farías
Diagramación: Remedios Marín y Silvina Pereyra
Corrección: Silvina Pereyra

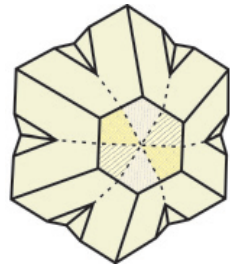
Servicio de Diseño Gráfico. CCT CONICET Mendoza
Mendoza 2010

Front cover: *Photographs of the San Luis I, an albite-spodumene type of granitic pegmatite. The dyke is folded and the core is intruded by a spodumene subtype pegmatite called San Luis II. Outcrops of peripheral pegmatitic lenses of the parental Paso del Rey leucogranite are shown at the upper right part of the landscape.*

Back cover: *Photograph of the texturally heterogeneous Cerro La Torre pegmatitic leucogranite intruding micaschists of the Pringles Metamorphic Complex (SW to NE view). The horizon line is broken by the Los Cerros Largos Tertiary volcanic dome.*

The Organizing Committee of the 5th International Symposium on Granitic Pegmatites disclaims all responsibility for accuracy of the contents of the contributions published in this volume.

**CONTRIBUTIONS TO THE
5TH INTERNATIONAL SYMPOSIUM
ON GRANITIC PEGMATITES**



**PEG 2011
ARGENTINA**

Mendoza, Argentina, February 20-27th 2011

EDITORS

Miguel Ángel Galliski
IANIGLA, CONICET, Argentina

Encarnación Roda Robles,
Universidad del País Vasco, Bilbao, Spain

Frédéric Hatert,
Université de Liège, Belgium

María Florencia Márquez-Zavalía
IANIGLA, CONICET, Argentina

GUEST EDITORIAL BOARD

Hartmut Beurlen
Universidad Federal de Pernambuco, Brazil

Alexander Lima
Universidade do Porto, Portugal

Raúl Lira
Universidad Nacional de Córdoba, Argentina

David London
University of Oklahoma, USA

Robert Martin
McGill University, Canada

Joan Carles Melgarejo
Universidad de Barcelona, Spain

Milan Novák
Masaryk University, Czech Republic

Wm. B. Simmons
University of New Orleans, USA

PREFACE



Petr Černý with a giant crystal of beryl in the La Rosanna pegmatite, San Luis (April 2001).

The 5th biennial edition of the “International Symposium on Granitic Pegmatites” designated “PEG2011 ARGENTINA”, will be held in the city of Mendoza, Argentina from 20 to 27 of February, 2011. This conference follows in the sequence of former meetings held in Brno (2003), Elba (2005), Porto (2007) and Recife (2009).

This meeting has attracted the participation of 125 researchers, from 18 different countries on 5 continents, and will be highlighted by 4 invited lecturers and 55 extended abstracts about mineralogy (28), geochemistry (10), petrology and petrogenesis (21). The three-day conference (February 21-23) will hold the oral and poster presentations. The post-symposium Field Trip (February 24-27) will visit the San Luis ranges, and will permit the observation, discussion and sampling of different kinds of granitic pegmatites outcropping in the southern districts of the Pampean pegmatite province.

The occasion was also considered appropriate to celebrate and honor the life-long academic path of Dr. Petr Černý, for his outstanding dedication to the investigation of the mineralogy, geochemistry and petrogenesis of granitic pegmatites. Dr. Černý has been a Corresponding Member of the Asociación Geológica Argentina since 2001, and has particularly contributed to the knowledge base of Argentinean pegmatites, participating in the description of two new minerals and in studies about the mineralogy of pegmatitic assemblages of oxides, phosphates and silicates.

INVITED LECTURES

CONSTITUTIONAL ZONE REFINING AND THE INTERNAL EVOLUTION OF GRANITIC PEGMATITES David London.....	1
PEARLS OF WISDOM GLEANED FROM MY MENTORS: WAYNE BURNHAM, FRANK TUTLE AND DICK JAHNS Robert F. Martin	5
TOURMALINE IN GRANITIC PEGMATITES Milan Novák	9
GEOCHEMISTRY OF REE-RICH PEGMATITES FROM DIFFERENT TECTONO-MAGMATIC PROVINCES IN SOUTH PLATTE, CO, TROUT CREEK PASS, CO, KINGMAN AND AQUARIUS RANGE, AZ, NORTH AMERICA William Simmons, Karen Webber, Alexander U. Falster, Sarah Hanson & TJ Brown	13

CONTRIBUTIONS

THE DISTRICTS OF THE EASTERN PEGMATITE PROVINCE OF BRAZIL Nelson Angeli.....	17
THE MICROLITE-GROUP MINERALS: NOMENCLATURE Daniel Atencio & Marcelo B. Andrade	21
GEOCHEMICAL EVOLUTION OF PHOSPHATES AND SILICATES IN THE SAPUCAIA PEGMATITE, MINAS GERAIS, BRAZIL: IMPLICATIONS FOR THE GENESIS OF THE PEGMATITE Maxime Bajjot, Frédéric Hatert, André-Mathieu Fransolet & Simon Philippo	25
MORPHOLOGY AND PYROELECTRICITY OF TOURMALINE FROM CENTRAL TRANSBAIKALIA, RUSSIA Vladimir Bermanec, Andrea Čobic, Vladimir Zebec, Snježana Mikulčić Pavlakovic & Victor Zagorsky	29
MINERALOGY OF THE BOA VISTA PEGMATITE, GALILÉIA, MINAS GERAIS, BRAZIL Vladimir Bermanec, Ricardo Scholz, Frane Markovic, Željka Žigovečki Gobac & Mario Luiz De Sá Carneiro Chaves.....	33
BORON-ISOTOPE VARIATIONS IN TOURMALINE FROM GRANITIC PEGMATITES OF THE BORBOREMA PEGMATITE PROVINCE, NE-BRAZIL Hartmut Beurlen, Robert B. Trumbull, Michael Wiedenbeck & Dwight R. Soares	37
CHEMICAL CHARACTERIZATION AND CHROMOPHORE ELEMENTS IN ELBAITES FROM BORBOREMA PROVINCE, BRAZIL Sandra De Brito Barreto, Andrea Čobic, Željka Žigovečki Gobac, Vladimir Bermanec & Goran Kniewald	41
PRELIMINARY FLUID INCLUSION RESULTS FROM THE RUBICON PEGMATITE, KARIBIB, NAMIBIA Luisa Broccardo, Judith A. Kinnaird & Paul A.M. Nex.....	45
A METASTABLE DISEQUILIBRIUM ASSEMBLAGE OF HYDROUS HIGH-SANIDINE ADULARIA + LOW ALBITE FROM LA VIQUITA GRANITIC PEGMATITE, SAN LUIS PROVINCE, ARGENTINA Petr Černý, Miguel A. Galliski, David K. Teertstra, Viviana M. Martínez, Ron Chapman, Luisa Ottolini, Lyndsey MacBride & Karen Ferreira.....	49
CRYSTAL CHEMISTRY OF BLUE GENTHELVITE FROM THE EL CRIOLLO PEGMATITE, CÓRDOBA (ARGENTINA) Fernando Colombo & José González Del Tánago.....	53
THE NYF-TYPE MIAROLITIC-RARE EARTH ELEMENTS PEGMATITES OF THE EL PORTEZUELO GRANITE, PAPACHACRA (CATAMARCA, NW ARGENTINA) Fernando Colombo, Raúl Lira, William Simmons & Alexander U. Falster	57
OCCURRENCE AND CRYSTAL CHEMISTRY OF ZIRCON FROM THE NYF-TYPE MIAROLITIC PEGMATITES OF THE EL PORTEZUELO GRANITE, PAPACHACRA (CATAMARCA, NW ARGENTINA) Fernando Colombo, William Simmons, Alexander U. Falster & Raúl Lira	61

<p>OCCURRENCE, CRYSTAL CHEMISTRY AND ALTERATION OF THORITE FROM THE NYF-TYPE MIAROLITIC PEGMATITES OF THE EL PORTEZUELO GRANITE, PAPACHACRA (CATAMARCA, NW ARGENTINA) Fernando Colombo, William Simmons, Alexander U. Falster & Raúl Lira</p>	65
<p>MINERALOGY OF A HIGHLY FRACTIONATED REPLACEMENT UNIT FROM "ÁNGEL" PEGMATITE, COMECHINGONES PEGMATITIC FIELD, CÓRDOBA, ARGENTINA Manuel Demartis, Joan C. Melgarejo Draper, Pura Alfonso, Jorge E. Coniglio, Lucio P. Pinotti & Fernando J. D'Eramo.....</p>	69
<p>PEGMATITE EMPLACEMENT DURING COMPRESSIONAL DEFORMATION OF THE GUACHA CORRAL SHEAR ZONE, CÓRDOBA, ARGENTINA Manuel Demartis, Lucio P. Pinotti, Fernando J. D'Eramo, Jorge E. Coniglio & Hugo A. Petrelli</p>	71
<p>THE ROLE OF PEGMATITES IN THE "CHESSBOARD CLASSIFICATION SCHEME" (CCS) OF MINERAL DEPOSITS Harald Dill</p>	75
<p>PRELIMINARY RESULTS OF A NEWLY-DISCOVERED LAZULITE-SCORZALITE PEGMATITE-APLITE IN THE HAGENDORF-PLEYSTEN PEGMATITE PROVINCE, SE GERMANY Harald G. Dill, Radek Škoda & Berthold Weber</p>	79
<p>THE WAUSAU SYENITE COMPLEX, MARATHON COUNTY, WISCONSIN Alexander U. Falster, Thomas W. Buchholz & William B. Simmons.....</p>	83
<p>ZONED FOITITE→SCHORL→DRAVITE→MAGNESIOFOITITE CRYSTALS FROM POCKETS IN ANATECTIC PEGMATITES OF THE MOLDANUBIAN ZONE, CZECH REPUBLIC Petr Gadas, Milan Novák, Jan Filip & Josef Staněk.....</p>	87
<p>A MUSCOVITE PEGMATITE FIELD LOCATED IN A LOWER PALEOZOIC OROGENIC ARC: THE VALLE FÉRTIL DISTRICT, SAN JUAN, ARGENTINA Miguel A. Galliski, Brígida Castro de Machuca, Julio C. Oyarzábal, Estela Meissl, Alicia Conte Grand & María Belén Roquet.....</p>	91
<p>ASSOCIATION OF SECONDARY Al-Li-Be-Ca-Sr PHOSPHATES IN THE SAN ELÍAS PEGMATITE, SAN LUIS, ARGENTINA Miguel A. Galliski, Petr Černý, María Florencia Márquez-Zavalía & Ron Chapman</p>	95
<p>THE DUMORTIERITE-BEARING ASSEMBLAGES OF VIRORCO, SAN LUIS, ARGENTINA: ARE THEY PEGMATITIC DYKES OR HYDROTHERMAL VEINS? Miguel A. Galliski, María Florencia Márquez-Zavalía & Raúl Lira</p>	99
<p>THE CRYSTAL CHEMISTRY OF OLIVINE-TYPE PHOSPHATES Frédéric Hatert, Luisa Ottolini, François Fontan, Paul Keller, Encarnación Roda-Robles & André-Mathieu Fransolet.....</p>	103
<p>MAGMATIC LAYERING (UNIDIRECTIONAL SOLIDIFICATION TEXTURES AND Y-ENRICHED GARNET TRAIN TEXTURES) IN APLITE – PEGMATITES OF THE CADOMIAN BRNO BATHOLITH, CZECH REPUBLIC Sven Hönig, Jaromír Leichmann & Milan Novák.....</p>	107
<p>RECENT DEVELOPMENTS IN THE INVESTIGATION OF POLISH PEGMATITES Janusz Janeczek & Eligiusz Szeleg</p>	111
<p>THE OCCURRENCE OF BETAFITE IN PEGMATITIC SHEETED URANIFEROUS GRANITES OF THE CENTRAL ZONE OF THE DAMARA OROGEN Judith Kinnaird, Paul Nex & Guy Freemantle.....</p>	115
<p>GEOCHEMICAL EVOLUTION AND PETROGENESIS OF RARE ELEMENT PEGMATITES IN THE SOLBELDER RIVER BASIN (SOUTH SIBERIA, RUSSIA) Liudmila Kuznetsova</p>	119
<p>UNUSUAL TEXTURAL RELATIONSHIPS BETWEEN SPODUMENE AND PETALITE AT SPODUMENE BEARING APLITE-PEGMATITE OF BARROSO-ALVAO FIELD (NORTHERN PORTUGAL) Alexandre Lima & Tania Martins</p>	123

GRANITIC PEGMATITE CHRYSOBERYL IN A SHEAR ZONE OF THE ACHALA BATHOLITH, CÓRDOBA, ARGENTINA Raúl Lira & Jorge Sfragulla.....	127
COMPETING MODELS FOR THE INTERNAL EVOLUTION OF GRANITIC PEGMATITES David London.....	131
PETALITE RARE-METAL PEGMATITES OF THE EAST SAYAN BELT, EASTERN SIBERIA, RUSSIA: GEOLOGICAL SETTING, MINERALOGY, GEOCHEMISTRY AND GENESIS Vladimir Makagon.....	135
THE REGIONAL DISTRIBUTION OF TRACE ELEMENTS IN QUARTZ OF SOUTH NORWEGIAN PEGMATITES AND ITS TECTONOMAGMATIC IMPLICATIONS Axel Müller.....	139
GEOCHEMISTRY OF GRANITIC APLITE-PEGMATITE VEINS AND SILLS AND THEIR MINERALS FROM CABEÇO DOS POUPOS, SABUGAL, CENTRAL PORTUGAL Ana M. R. Neiva, Paulo B. Silva & João M.F. Ramos.....	141
REGIONAL ZONATION OF PEGMATITES AND SYNCHRONOUS MINERALIZATION IN THE CENTRAL ZONE OF THE DAMARA OROGEN, NAMIBIA Paul Nex, Judith Kinnaird & Luisa Broccardo.....	145
COMPOSITIONAL VARIATIONS IN PRIMARY AND SECONDARY TOURMALINE FROM THE QUINTOS PEGMATITE, BORBO- REMA PEGMATITE PROVINCE, BRAZIL; REDISTRIBUTION OF Cu, Mn, Fe AND Zn IN SECONDARY TOURMALINE Milan Novák, Petr Gadas, Radek Škoda, Hartmut Beurlen & Odúlio J. M. de Moura.....	149
RHEOLOGY OF FLUID-SATURATED GRANITIC AND PEGMATITE-FORMING MELTS Igor S. Peretyazhko.....	153
OCCURRENCE OF COMPLEX PEGMATITES IN THE SOUTH OF TOCANTINS STATE, BRAZIL Hudson Queiroz, Rúbia R. Viana, Gislaïne A. Battilani, Luana Laiame de Oliveira, Gilliard Medeiros Borges & Denis L. Guerra.....	157
CATION PARTITIONING BETWEEN MINERALS OF THE TRIPHYLITE ± GRAFTONITE ± SARCOPSIDE ASSOCIATION IN GRANITIC PEGMATITES Encarnación Roda-Robles, Miguel A. Galliski, James Nizamoff, William Simmons, Paul Keller, Alexander Falster & Frédéric Hatert.....	161
CHEMICAL VARIATION IN TOURMALINE FROM THE BERRY-HAVEY PEGMATITE (MAINE, USA), AND IMPLICATIONS FOR PEGMATITIC EVOLUTION Encarnación Roda-Robles, William Simmons, James Nizamoff, Alfonso Pesquera, Pedro P. Gil-Crespo & José Torres-Ruiz.....	165
THE NYF PEGMATITES OF THE POTRERILLOS GRANITE, SIERRAS DE SAN LUIS, ARGENTINA María Belén Roquet, Federico Bernard, Raúl Lira & Miguel A. Galliski.....	169
TECHNOLOGICAL CHARACTERIZATION OF MUSCOVITE FROM THE PEGMATITES DISTRICTS OF CRISTAIS - RUSSAS (DPCR) AND SOLONÓPOLE - QUIXERAMOBIM (DPSQ) – CEARÁ, NORTHEAST BRAZIL Gabriela Meireles Rosa, Martha Noélia Lima, Débora Macedo do Nascimento, Tereza Falcão de Oliveira Neri, Francisco Diones Oliveira Silva, Andressa de Araujo Carneiro, José de Araújo Nogueira Neto & José Cleyton Vasconcelos.....	173
K-FELDSPAR MINERALS DEFINED FROM THEIR TWIN-STRUCTURE: APPLICATION TO A PRELIMINARY CLASSIFICATION OF PEGMATITES Luis Sánchez-Muñoz, Javier García-Guinea, Victor Zagorsky, Odúlio J. M. de Moura & Peter J. Modresky.....	175
TWIN-STRUCTURES IN K-FELDSPAR FROM OROGENIC AND ANOROGENIC PEGMATITES IN CENTRAL NORTH AMÉRICA Luis Sánchez-Muñoz, Peter J. Modreski & B. Ronald Frost.....	179
Rb-Sr GEOCHRONOLOGY FOR “LA AURORA” ANDALUSITE-BEARING PEGMATITE FROM MAZAN RANGE, NW	

ARGENTINA Fernando Sardi, F. & José Manuel Fuenlabrada Pérez	185
MAGMATIC DIFFERENTIATION IN THE HUACO GRANITE AND ITS ASSOCIATED Be-PEGMATITES FROM THE VELASCO DISTRICT, ARGENTINA Fernando Sardi, Mamoru Murata & Pablo Grosse	189
MINERALOGY OF THE LITHIUM BEARING PEGMATITES FROM THE CONSELHEIRO PENA PEGMATITE DISTRICT (MINAS GERAIS, BRAZIL) Ricardo Scholz, Mário Luiz de Sá Carneiro Chaves & Klaus Krambrock	193
CONCURRENT TREATMENT OF METAMICT AND CRYSTALLINE FERGUSONITE BY U, Th AND Pb-RICH FLUIDS: AN EMPA AND TEM STUDY Radek Škoda, Renata Čopjaková & Mariana Klementová	197
TOWARDS EXPLORATION TOOLS FOR HIGH PURITY QUARTZ AND RARE METALS IN THE SOUTH NORWEGIAN BAMBLE-ØVJE PEGMATITE BELT Benjamin R. Snook, Axel Müller, Ben J. Williamson & Frances Wall	201
MINERAL CHEMISTRY OF ELBAITE FROM THE SERRA BRANCA PEGMATITE, NEAR PEDRA LAVRADA, STATE OF PARAÍBA, NE-BRAZIL Dwight R. Soares, Hartmut Beurlen, Ana Claudia M. Ferreira & Ranjana Yadav	205
SECONDARY Ta-Nb OXIDE MINERALS OF THE ARCHAEOAN WODGINA PEGMATITE DISTRICT, WESTERN AUSTRALIA, AND THEIR SIGNIFICANCE Marcus T. Sweetapple & Gregory R. Lumpkin	209
MINERALS FROM THE CROSS LAKE PEGMATITE, MANITOBA, CANADA Kimberly T. Tait, Frank C. Hawthorne & Petr Černý	213
PARAGENETIC CONTROL AND COMPOSITIONAL EVOLUTION OF THE COLUMBITE-TANTALITE OXIDES FROM THE FREGENEDA- ALMENDRA LITHIUM-RICH PEGMATITES (PORTUGAL & SPAIN) Romeu Vieira, Encarnación Roda-Robles, Alexandre Lima, Alfonso Pesquera, Petr Gadas & Milan Novák	217
U-Pb LA-ICPMS COLUMBITE-TANTALITE AGES FROM THE PAMPEAN PEGMATITE PROVINCE: PRELIMINARY RESULTS Albrecht Von Quadt & Miguel A. Galliski	221
MIAROLITIC PEGMATITES AND GRANITES FROM THE SEARCHLIGHT DISTRICT, COLORADO RIVER EXTENSIONAL CORRIDOR, NEVADA, USA Karen Webber, William Simmons & Alexander Falster	225
THE ZAVITAYA LITHIUM-RICH GRANITE-PEGMATITE SYSTEM, CENTRAL TRANSBAIKALIA, RUSSIA: GEOLOGY, GEOCHEMISTRY, AND PETROGENETIC ASPECTS Victor Zagorsky	229

CONSTITUTIONAL ZONE REFINING AND THE INTERNAL EVOLUTION OF GRANITIC PEGMATITES

David London

ConocoPhillips School of Geology & Geophysics: dlondon@ou.edu.
University of Oklahoma, 100 East Boyd Street, room 710 SEC, Norman, OK USA 73019

Key words: pegmatite, granite, granitic liquid, fluxing components, liquidus undercooling

The most successful models for the origins and internal evolution of granitic pegmatites are those that have been the most holistic in their approach and with the strongest scientific basis. The longstanding success of the Jahns-Burnham model (1969) combines these attributes: the breadth of Jahns' knowledge of pegmatites strengthened by Burnham's innovative and exacting experimental programs. What made the Jahns-Burnham model so successful was its claim to a scientific proof through experimental petrology. Except for a few early abstracts, however, the details of that experimental evidence were not published by Jahns or Burnham. Some experimental programs completed by their students contradicted the underlying precepts of the Jahns-Burnham model (e.g., Kilinc 1969; Fenn 1986).

A holistic model for the origin and internal evolution of granitic pegmatites must focus on those that are most abundant. These "common" pegmatites are represented, for example, by the tens of thousands of dikes exposed along the Appalachian Mountains, and typified by occurrences in the Spruce Pine district, NC. They possess bulk compositions very close to those of the haplogranite (Ab-Or-Qtz) minimum; deviations from the metaluminous minimum occur toward peraluminous, not peralkaline compositions (this does not pertain to or include syenite-associated alkaline pegmatites). With only accessory levels of tourmaline, micas, apatite, or fluorite, they lack evidence for high concentrations of the fluxing components of B, P, or F. Other than the subsolidus formation of microcline perthite, internal hydrothermal alteration is absent. Other than a rare and thin (1-2 mm) border reaction that produces tourmaline or metasomatic biotite, hydrothermal alteration of host rocks is nil. Mirolitic cavities are essentially nonexistent. Most common pegmatites lack foliation, and hence their emplacement postdates tectonism and its associated metamorphism. They possess sharp contacts with their host rocks. These and other pegmatites are completely devoid of entrained phenocrysts, and hence appear to be emplaced in the fully liquid state.

Common granitic pegmatites are not hydrothermal in origin. This is because hydrothermal fluids of metamorphic rocks or of typical granitic plutons are Cl-dominant aqueous fluids in which Al is notably insoluble (e.g., Anderson & Burnham 1983). Such fluids can transport alkalis and silica, but not Al. Porphyry Cu deposits represent a case in point. Although they achieve saturation in a Cl-brine early in their magmatic history (Cline & Bodnar 1991), they are devoid of pegmatitic textures. Their hydrothermal systems transport and deposit massive quartz, but not feldspars and micas. Alkali-H exchange reactions occur in and around the porphyries, but all can be balanced with conservation of Al (i.e., Al is immobile). In contrast, porphyry-Mo deposits and so-called rare-element or "apo-" granites, which contain elevated concentrations of B, P, and/or F, always possess some domains of pegmatitic texture. It appears that H₂O alone in granitic systems does not produce pegmatites, but H₂O in combination with B, P, and/or F does promote the formation of pegmatitic textures in granites.

The fluxes of B, P, and F, together with H, have been implicated with pegmatite formation since the earliest proposed models (see London 2008), for the reason that these components reduce the liquidus and especially solidus temperatures (which extends the interval of magmatic crystallization), they lower the viscosity of melt (which facilitates the mass transfer needed to grow large crystals), and, they enhance the solubility and miscibility between otherwise less soluble or miscible components. The quantities of fluxing components conserved within pegmatite minerals increases from nil in common pegmatites to locally abundant in the rare-element pegmatites. However, the Tanco pegmatite, Manitoba, which is arguably the most fractionated igneous body known, contains ~ 1 wt% total of B, P, and F components (Stilling *et al.* 2006). Morgan and London (1989) calculated the mass transfer associated with the loss of rare alkalis, B, and F from the pegmatite to the mafic host rocks. When added back into the Tanco bulk composition, the fluxes increase only to ~ 2 wt% of the

pegmatite total. *Therefore, a model that addresses the origins of granitic pegmatites, which is as applicable to the common pegmatites as the rare-element-enriched bodies, must explain their origins in terms of the known rheological properties and crystallization behavior of hydrous haplogranitic granitic liquids, with non-negligible but small quantities of the fluxing components of H (up to H₂O-saturation at 6-7 wt% of melt), B, P, and F (from < 1 wt% total up to ~ 1-2 wt % each), and without the fluxing effects of excess alkalis in their bulk compositions (i.e., the liquids are metaluminous to peraluminous).*

Granitic pegmatites of all types mostly occur near the margins and are concentrated in the cupolas of their source granites, from which they emanate hundreds of meters to several km from their source. By virtue of this occurrence, pegmatite-forming melts are juxtaposed against cooler host rocks. The relations of crystal nucleation to cooling (Fenn 1977; Swanson 1977; London 2008) indicate that pegmatite-forming melts are likely to be undercooled by 150-250°C below their liquidus temperatures, regardless of the rate of cooling, before appreciable crystal nucleation and growth commences. For H₂O-saturated haplogranitic liquids at pressures > ~ 200 MPa and liquidus temperature (~ 700°C), the temperatures of crystallization, therefore, should be ~ 550 to 450°C. Numerical cooling models for proximal common pegmatites to distal rare-element bodies predict rapid cooling of melt at the dike margins to 500°-450°C (London 2008). Temperatures calculated from coexisting integrated perthite-plagioclase are 500°-450°C (London 2008), and where present, wallrock alteration assemblages are indicative of zeolite to lower greenschist facies conditions (~ 350°-500°C: e.g., Morgan & London, 1987). Thus, there is good agreement among four distinctly different data sources: experiments on nucleation in the granite system, numerical modeling of heat flow, measured feldspar compositions within pegmatites, and wallrock alteration assemblages where present. This application exemplifies the value of the holistic approach to understanding pegmatites.

If the crystallization of pegmatite from margin to center keeps pace with cooling along the 450°-500°C isotherm, as is suggested by two-feldspar thermometry, then the rates of crystal growth must be ~ 10⁴ faster than those that are recorded from experiments (Swanson 1977; Fenn 1977). The published crystal growth rate experiments do not account for the nucleation delay or the cessation of crystal growth after nucleation; the actual rates of crystal growth in natural systems could be orders of magnitude faster than the experimentally-derived values.

The effects of liquidus undercooling dominate the textures of the outer zones of pegmatites, which are fine-grained and strongly anisotropic. From a kinetic standpoint, even giant crystals of graphic

granite are fine-grained in terms of the short diffusive distance of Al and of Si between nucleation centers for feldspar and for quartz, respectively. These are all attributable to rapid growth from a silicate liquid that is highly supersaturated with respect to feldspar- and quartz-forming components. The high degree of supersaturation results from a long nucleation delay in the granite system. The delay in nucleation derives principally from the viscosity of the liquid, not the rate of cooling. At the magnitude of liquidus undercooling that is indicated for most granitic pegmatites (200°-250°C), the calculated viscosity of an H₂O-saturated granitic liquid will be near 10⁷⁻⁸ Pa-s, which is greater than the viscosity of asphaltic tar at 25°C. High viscosity of the undercooled granitic liquid is the primary cause for the graphic intergrowths (Fenn 1986) and other anisotropic fabrics of granitic pegmatites. The viscous granitic melt can deliver high fluxes of the slow-diffusing components, Al and Si, but only over short distances at the rate of pegmatite cooling; hence, the fine-grained nature of the outer zones.

The coarse-grained textures of pegmatites tend to be located in the central portions of pegmatite bodies, where the rock fabric lacks much of the anisotropy that is evident in the outer zones. In order to grow exceptionally large crystals of feldspars and quartz from melt, one of two conditions must be met: (1) either the time frame of crystallization must be exceedingly long (i.e., the rate of cooling must be exceedingly slow), such that a large flux of Al and Si can migrate even at their exceedingly low rates of diffusion through viscous granitic melt, or else (2) the viscosity of the melt must be lowered substantially by the accumulation of fluxing components and excess alkalis, so that a large flux of Al and Si can diffuse to growing crystal surfaces in the (rapid) time frame of magmatic cooling. Among the two choices, the effects of increased fluxes appear to be the most likely based on the calculated cooling histories of model pegmatite dikes. The problem of low flux content in the bulk compositions of pegmatite-forming magmas can be resolved by the process of constitutional zone refining (CZR), in which fluxes and other quartz-feldspar incompatible elements are enriched in a boundary layer of melt adjacent to growing crystal surfaces (London 2008). Pegmatite crystallization at ~ 450°C provides the ideal environment for CZR to operate. At this condition, the rate of crystal growth is maximal (Swanson 1977; Fenn 1977), and the high viscosity of the bulk granitic melt prevents the back-diffusion of excluded components. Flux-rich boundary layers have been quenched even in the chemically evolved (lower viscosity) liquid composition of the hydrous Macusani obsidian at 450°-500°C and 200 MPa (London *et al.* 1989). The accumulation of fluxing components of B, P, and F in the boundary layer liquid leads to a substantial increase in the solubility of H₂O (London 2009). Suppression of aqueous vapor separation is the

key to pegmatite formation, because increasing H₂O lowers the viscosity of silicate melt, which enhances the diffusion of Al and of Si. The boundary layer liquids that have been documented in experiments are identical in all important respects to crystal-rich fluid inclusions found in minerals from some pegmatite localities (e.g., Tanco, Manitoba: London 1986). The experimentally-produced flux-enriched boundary layer liquids, like the natural inclusions, are alkaline, Na-rich, and contain upwards of 15-20 wt% H₂O (i.e., in excess of 80 mol% H₂O). At 500°C and 200 MPa, a liquid of this approximate composition possessed a viscosity of ~ 10 Pa·s (London 1986, 2008). An experimental analog to this composition at 800°C and 200 MPa transports normally slow-diffusing Si at a flux (mass/volume) that is 10⁷ times greater than an equal volume of H₂O fluid and at a rate (distance/time) that is 10⁷ times greater than H₂O-saturated haplogranite liquid ($D_{Si} \sim 2.5 \cdot 10^{-15} \text{ m}^2\text{s}^{-1}$) without other fluxing components (London 2009). Hence, a flux-rich boundary layer liquid resolves the problems of low bulk concentrations of fluxes, high bulk viscosity of granitic liquid at low temperatures, and commensurately, low rates of diffusion for Al and Si that would prohibit the formation of large monophase crystals of quartz and feldspars.

REFERENCES

- Anderson, G.M. & Burnham, C.W. (1983). Feldspar solubility and the transport of aluminum under metamorphic conditions. *Am. J. Sci.* **283-A**: 283-297.
- Cline, J.S. & Bodnar, R.J. (1991). Can economic porphyry copper mineralization be generated by a typical calc-alkaline melt?. *J. Geophys. Res.* **96** (B5): 8113-8126.
- Fenn, P.M. (1977). The nucleation and growth of alkali feldspars from hydrous melts. *Can. Mineral.* **1**: 135-161.
- Fenn, P.M. (1986). On the origin of graphic granite. *Am. Mineral.* **71**: 325-330.
- Jahns, R.H. & Burnham, C.W. (1969). Experimental studies of pegmatite genesis: I. A model for the derivation and crystallization of granitic pegmatites. *Econ. Geol.* **64**: 843-864.
- Kilinc, I.A. (1969). Experimental metamorphism and anatexis of shales and graywackes. Ph.D. Thesis. Pennsylvania State University, University Park, Pennsylvania, U.S.A. 191 p.
- London, D. (1986). The magmatic-hydrothermal transition in the Tanco rare-element pegmatite: evidence from fluid inclusions and phase equilibrium experiments. *Am. Mineral.* **71**: 376-395.
- London, D. (2008). Pegmatites. *Sp. Pub.* **10**, Can. Mineral. 368 p.
- London, D. (2009). The origin of primary textures in granitic pegmatites. *Can. Mineral.* **47**: 697-724.
- London, D., Morgan, G.B., VI, & Hervig, R.L. (1989). Vapor-undersaturated experiments in the system macusanite-H₂O at 200 MPa, and the internal differentiation of granitic pegmatites. *Contrib. Mineral. Petrol.* **102**: 1-17.
- Morgan, G.B., VI & London, D. (1987). Alteration of amphibolitic wallrocks around the Tanco rare-element pegmatite, Bernic Lake, Manitoba. *Am. Mineral.* **72**: 1097-1121.
- Morgan, G.B., VI & London, D. (1989). Experimental reactions of amphibolite with boron-bearing aqueous fluids at 200 MPa: Implications for tourmaline stability and partial melting in mafic rocks. *Contrib. Mineral. Petrol.* **102**: 281-297.
- Stilling, A., Černý, P., & Vanstone, P.J. (2006). The Tanco pegmatite at Bernic Lake, Manitoba. XVI. Zonal and bulk compositions and their petrogenetic significance. *Can. Mineral.* **44**: 599-623.
- Swanson, S.E. (1977). Relation of nucleation and crystal-growth to the development of granitic textures. *Am. Mineral.* **62**: 966-978.

PEARLS OF WISDOM GLEANED FROM MY MENTORS: WAYNE BURNHAM, FRANK TUTTLE AND DICK JAHNS

Robert F. Martin

Earth and Planetary Sciences, McGill University, Montreal, Canada; robert.martin@mcgill.ca

Key words: granite, pegmatites, rock–fluid interaction, element mobility, metasomatism, ichors.

INTRODUCTION

Early on in my professional career, as an undergraduate student, in fact, I developed a strong interest in the mineralogy and petrology of felsic igneous rocks. So much so, that I applied to do graduate-level work at a university where “big names” had made the place a veritable mecca in the study of granites and granitic pegmatites. It is nothing short of providential, career-wise I mean, that I was accepted to attend The Pennsylvania State University. There, I took courses from Wayne Burnham and Frank Tuttle, both leaders in their respective fields; Dick Jahns was in the picture, but rather remotely for me, as he was the Dean of the College of Mineral Sciences, and not involved in teaching activities, at least not to incoming M.Sc. candidates.

LESSONS LEARNED FROM C. WAYNE BURNHAM

Professor C. Wayne Burnham was a no-nonsense kind of guy in class as well as out. I remember being very nervous in my one-semester seminar course entitled Hydrothermal Mineralogy in which, as the name implies, we focused on the power of hydrothermal fluids to change the mineralogy of solid rocks. In class, students sat around a large oval table with the master; two or three papers had been assigned to all in order to prepare the week’s seminar, and a student among the twelve or so was chosen at random, on the spot, to distill the main message for all present. I survived, and do remember discussing metasomatic overprints in mineralized granites and in kimberlites in the mantle. Prof. Burnham was a very innovative experimentalist, who took great pride in his inventions. He seemed able to address any challenge associated with high-pressure experimentation in silicate systems. I remember discussions on the solubility of minerals, for example albite, the P–V–T properties of H₂O at high pressure, the solubility of H₂O in felsic magmas, and experimentation with mixed H₂O–CO₂ fluids. He clearly had carried out polythermal experiments on

granite – H₂O and granite – H₂O – HCl, mostly with applications to porphyry-copper deposits. In the course, nothing specific was presented on the role of an aqueous fluid phase during the crystallization of granitic pegmatites. There was no hint of what was to come five years later, when the high-impact-factor paper by Jahns and Burnham was published in 1969. Other problems were more fascinating than the origin of granitic pegmatites!

Professor Burnham’s fame rests not only on his experimental prowess, but also on his classic work on the high-temperature skarns at Crestmore, California, probably the source of much of his early inspiration on element mobility in a thermal gradient involving a mixed H₂O–CO₂ fluid phase. Incidentally, wasn’t the title of his course a great one???

LESSONS LEARNED FROM O. FRANK TUTTLE

Whereas C. Wayne Burnham was not discreet about his prowess in the lab, Orville Frank Tuttle, also an experimentalist, was completely the opposite. Perhaps for this reason, they had no use for each other. Professor Tuttle became an important person in my professional life very late in his career. He retired prematurely owing to ill health two years before I defended my Ph.D., and was not even present at my defense. However, Wayne Burnham was brought in to grill me!

Course work with Frank Tuttle focused on systematic presentations of the phase equilibria along the binary joins in the granite system, then building up to the ternary and quaternary systems. Imagine an entire semester of lectures on “Petrogeny’s Residua”, the system NaAlSi₃O₈ – KAlSi₃O₈ – SiO₂ – H₂O, its mineralogical aspects and the petrological applications! We had classes on the α – β transition in quartz, the phase diagram for the system Ab – Or, the ramifications of the hypersolvus and subsolvus textures in granites and nepheline syenites, and discussions on fractionation in the silica-undersaturated and silica-

oversaturated parts of the system. The main textbook used in the course was the bible of granite petrologists, then as now, GSA Memoir 74 by O.F. Tuttle and his mentor in the experimental approach, Norman Levi Bowen, Canada's lasting gift to petrology.

The strong message in the course was that there was no doubt at all, granites are products of the crystallization of felsic magmas. We did read up on the heated and epic debates involving Bowen, an experimentalist, on one side, and field-oriented types like Sederholm and Read, working in Archean terranes of northern Europe, on the other. We thus learned about the mythical "ichors" that Sederholm believed could transform quartzofeldspathic sedimentary units into granitic rocks without going through a melt stage. In class, the case was cut-and-dried... granites truly are igneous. In private discussions, however, Prof. Tuttle stressed upon me the importance of keeping a very open mind about the matter. Basically, he felt that people of the caliber of Sederholm, arguing for "granitization" in the deep crust, were probably not completely naive. He was working at the time with a postdoctoral fellow named William C. Luth, who was finding rather startling results on the solubility of H₂O in granitic magmas at elevated pressure, and on the solubility of the magma in the coexisting H₂O. Could such fluids in the deep crust represent the ichors? I do believe so.

Although Frank Tuttle was very much an experimentalist, he went to the field every summer to interact with students working on granite-related projects. For example, he came to visit me in New Brunswick, and became familiar with my embryonic ideas that there were granites related to orogenic suites, and other granites related to anorogenic suites that had nothing directly to do with an orogeny. If he had not been forced to retire early, I can see that we could have gone on to define O- and A-type granites. Remember that all this was going on just before the plate-tectonic revolution and before the birth of the "genetic alphabet" of the Australian school in the late sixties and the concept of A-type granites in the late seventies.

Frank had exceptional insight into the workings of petrological systems, be they SiO₂-oversaturated or not, and was in the same league as Bowen. He was aware that rocks in Petrogeny's Residua formed from magmas that are not anhydrous. What is the role of H₂O once that magma freezes? He knew that most granites contain microcline, but he also knew that microcline does not crystallize from a magma. He was fascinated by what goes on in the subsolidus chapter of the history of a granite body. He suggested that I work on the alkali feldspars for a Ph.D. thesis, strictly from the point of view of subsolidus phenomena. His main message to all his students? Rocks are like a book, and threads of the story are contained in the rock-forming minerals. Learn to read the minerals and

to interpret their textural attributes, and you will be able to unravel the story.

LESSONS LEARNED FROM RICHARD H. JAHNS

With the move of Frank Tuttle and Dick Jahns to Stanford University, and Peter Wyllie (also my professor) to the University of Chicago, the powerhouse at Penn State lost its superstars. At Stanford, Dr. Tuttle was my main advisor for a year or so, then was forced to retire owing to ill health. I became directly involved with Dick Jahns for the next two years as I worked on my Ph.D., and for two years after that as a postdoctoral fellow making use of the excellent equipment in the so-called "bomb lab", much of it brought in from Penn State.

At Stanford, Dick Jahns did minimal traditional teaching. He was, after all, Dean of the School of Earth Sciences, and as such, responsible for ensuring the well-being of the school. Dick was very affable, and a real go-getter. As Dean, he was active in fund-raising, a vital activity in this high-level private university (*i.e.*, no operating grant from the state or federal government). I am sure that his annual one-semester course offering, run in his large living room at home in the evening, was all that he could handle in the area of teaching. But it was a very popular course, with snacks and beer served at the end of the evening to the appreciative twenty or so attendees. Each week, there was an identified theme, and students were expected to do most of the talking; the atmosphere was MUCH more relaxed than in Wayne Burnham's seminars at Penn State! Then Dick would wade in toward the end of the evening's session to summarize the discussion, and give us his own perspective on things. It was a great experience for me personally, because he used to pick on me rather often to explain to others the finer points having to do with mineralogy and textures. The topic of one seminar was a rectangular table in the center of the living room; it was a slab of the Chelmsford granite showing an aplite dike cross-cutting the granite slab diagonally, and discoloring it rather subtly. At both contacts, it was clear that the melt had begun to crystallize as a pegmatite, with nascent tapering crystals oriented inward, then it abruptly changed to crystallize as an aplite. It was an excellent example to inspire a discussion on nucleation and growth of the nuclei and on the various ways of explaining the aplitic texture.

I can remember trying to pin down Dick Jahns on exactly what he had in mind to explain the strong compositional contrasts between the hanging wall and the footwall of some pegmatites that he had described from Southern California. He kept talking about the solubility of melt constituents in a free aqueous fluid, and the compositional dependence of the solute carried by the supercritical fluid on temperature, but with well-chosen words, without presenting hard

data. He alluded to “little red wagons”, presumably aqueous bubbles, that were circulating in the magma and progressively causing the magma to “disproportionate” into a sodic zone that represented the “compositionally quenched” melt depleted in K, formed at the high-temperature end of a thermal gradient, and a potassic zone, forming in the low-temperature part of that gradient, and more enriched in the incompatible elements. We of course were fully aware of and discussed the interesting paper that Jahns had coauthored with Frank Tuttle on this model.

I stayed on at Stanford for two years after my Ph.D. In those two years, I was building up my portfolio of original publications, on order-disorder relations in the sodic and potassic feldspars, as monitored by X-ray diffraction and infrared absorption spectroscopy, and on boron in K-rich feldspars. I tackled and published on the alkali feldspar solvus at various pressures. I carried out a determination of the melting relations of a sample of graphic granite from Southern California, and one of a high-fluorine topaz-bearing leucogranite from Cornwall, U.K. Dick was particularly interested in my work on polythermal experiments at elevated (crustal) pressures, which I will summarize at this conference. He is the one who inspired me to do this work, and was fascinated to see that I systematically found K and Na to be very mobile in an aqueous fluid ($K > Na$) in a temperature gradient. After I had left Stanford, he provided me with some unpublished data from experiments done years before at Penn State, probably by Wayne Burnham or W.C. Luth. I deemed my results publishable, and I was hoping for a copublication, Martin & Jahns. But it soon became clear that Dick was suppressing my publication of those “vapor-transport” results. Also relevant to this pattern of behavior was his reticence to publish his own work, specifically Parts II, III and IV of the Jahns–Burnham model, *i.e.*, the long-awaited raw data backing up the model. He specifically told me that Parts II and III were already written in 1969, and Part IV was at “an advanced conceptual stage”. When I embarked on a two-year stint as a post-doctoral fellow on a project directly relevant to his model, why did he not provide me with anything???

Dick Jahns was a geopolitician, whose interactions were always interspersed with jokes. One

wondered where he had learned his latest “Did you hear about the poor guy who.....”? He loved to play practical jokes on unsuspecting colleagues. He was fun to be with, in class and in the field. He was a consummate communicator, and was very successful at what he did. He rose to the top, and not only in the area of “pegmatology”; in fact, he is better known in the area of engineering geology. In his communications about granitic pegmatites, in his course, for example, he allowed the audience to believe that he had done a lot of experimental work in his career. In fact, all of that was mirrors and smoke screens, I’m afraid. Dick Jahns was very much a field man who had learned a tremendous amount about crystal growth and phase equilibria in the granite system “by osmosis”, owing to close contacts over many years with top-notch experimental petrologists working in the same institutions, Penn State and Stanford. His model is not without merit, as aqueous fluids are clearly an important part of the story, but not in the way that he conceptualized it in the Jahns–Burnham model, in my opinion.

CONCLUSIONS

Just what is the role of the orthomagmatic fluid phase in the evolution of granitic pegmatites? I do believe that at the magmatic stage, in those pegmatites formed in an epizonal environment, such a fluid can collect in miarolitic pockets. I like the explanations of Dick Jahns about the individuality of such pockets, about pocket rupture due to implosions or explosions, and the formation of gem-quality crystals from this orthomagmatic fluid. I much prefer David London’s explanations of the textural zonation of granite bodies to those of my mentor. In view of my own results on polythermal experiments, I honestly never did believe that they were very relevant to the compositional zonation of individual bodies of granitic pegmatite. Rather, I apply my results to lower crust – mantle interactions, and important metasomatism going on there to fertilize the crust undergoing distension. It seems clear that except for quartz, the minerals that we study in granites and pegmatites are largely pseudomorphs of the minerals that the magma produced.

TOURMALINE IN GRANITIC PEGMATITES

Milan Novák

Department of Geological Sciences, Masaryk University, Kotlářská 2, 611 37 Brno Czech Republic; mnovak@sci.muni.cz

Key words: tourmaline, compositional evolution, geochemical types, crystal-structural constraints, granitic pegmatites

INTRODUCTION

Minerals of the tourmaline group (schorl, dravite > elbaite > foitite, rossmanite, liddicoatite > olenite, uvite, magnesiofoitite, feruvite, buergerite) are typical accessory minerals in many granitic pegmatites. They originated in different stages of pegmatite evolution from primary magmatic to late hydrothermal; moreover, tourmaline also occurs in pegmatite exocontacts. High compositional variability of tourmaline, its refractory properties and abundance of tourmaline in various zones of the individual pegmatites, make tourmaline-group minerals excellent and widely used indicators of geochemical evolution from magmatic to hydrothermal stage and of contamination from host rocks as well. However, crystal-structural constraints, which also control chemical composition of tourmaline, are only poorly known.

TEXTURAL AND MORPHOLOGICAL TYPES OF TOURMALINE

Tourmaline occurs in many textural and morphological types, which manifest their origin in various stages of pegmatite evolution: (i) primary tourmaline crystallized in (ia) various textural-paragenetic units of massive pegmatite and in (ib) pockets; (ii) secondary (subsolidus) tourmaline replacing early minerals (e.g., cordierite, biotite, garnet, Fe,Mn,Mg-phosphates); (iii) hydrothermal tourmaline originated on late fractures within pegmatite or as a very late mineral in pockets; (iv) exomorphic tourmaline on exocontact or in enclaves of host rocks. Size and morphology of crystals and aggregates in the individual textural types are highly variable from large euhedral crystals, up to several m long, to very fine-grained aggregates or graphic intergrowths with quartz. In micro-scale (thin sections, BSE images), tourmaline textures are highly variable from homogeneous (ia), (ib), to simply zoned (ia), (ib),

(iv), oscillatory zoned (ib), (iii), irregularly to patchy zoned (ia), (ii), (iv). Also late microscopic veining in rather homogeneous primary tourmaline is locally common (ia). High variability in macro- and micro-scale is behind the scope of this presentation; hence, only typical cases were given.

CRYSTAL CHEMISTRY OF TOURMALINE

The generalized tourmaline structural formula: $XY_3 Z_6(T_6O_{18})(BO_3)_3V_3W$, where the common ions at each site are: X = Na¹⁺, Ca²⁺ and vacancy; Y = Fe²⁺, Mg²⁺, Al³⁺, Li¹⁺ and Fe³⁺; Z = Al³⁺, Fe³⁺ and Mg²⁺; T = Si⁴⁺, Al³⁺, B³⁺; B = B³⁺; V = OH¹⁻ and O²⁻; and W = F¹⁻, O²⁻ and OH¹⁻. Also other cations are significant in some granitic pegmatites (Bi³⁺, Pb²⁺, Cu²⁺, Zn²⁺, Mn²⁺, Mn³⁺, Ti⁴⁺). Important heterovalent coupled substitutions include: (1) $^X R^{1+} + R^{2+} = ^X \square + R^{3+}$, (2) $^X R^{1+} + R^{3+} = ^X Ca + R^{2+}$, (3) $^Y 2R^{2+} = ^Y Li^{1+} + ^Y Al^{3+}$, (4) $^+ R^{2+} + OH^{1-} = R^{3+} + O^{2-}$ along with several homovalent substitutions e.g., (5) Fe²⁺ = Mg or (6) OH¹⁻ = F¹⁻. Numerous substitutions enable high variability of chemical compositions and thus record compositional evolution of parent medium as well as a change in PTX conditions.

GEOCHEMICAL TYPES OF TOURMALINE-BEARING PEGMATITES

Tourmaline, typically Al_{tot} > 6 apfu, occurs in pegmatites varying from abyssal, muscovite, rare-element to miarolitic class; hence, in a wide range of PT conditions; however, a peraluminous character of parental pegmatite is almost exclusive (London 2008). Also the degree of geochemical fractionation of parental pegmatites is highly variable from very primitive compositions to extremely evolved Li,Cs-rich pegmatites. Compositional evolution in tourmaline was studied in detail in various complex pegmatites and slightly different trends in the lepidolite, elbaite, spodumene and petalite subtypes, respectively, were revealed. In contrast, compositional

trends in tourmaline from primitive Mg-enriched and Li-poor pegmatites, and from Li-poor and extremely Al-rich abyssal pegmatites are less-known as well as the composition of Ca,Mg,(Fe)-enriched and locally relatively Al-poor tourmaline from exocontacts or from evidently contaminated pegmatites.

Only recently, tourmalines with $Al_{tot} \sim 4-6$ apfu were discovered in pegmatites. They include several very distinct geochemical and genetic types such as: intragranitic NYF pegmatites from K,Mg-rich syenogranites of the Třebíč Pluton, Czech Republic (Ca,Ti,Fe³⁺-enriched dravite-schorl; Novák *et al.* accepted; Fig. 1); miarolitic pegmatites with zeolites from the Vitosha Mnts., Bulgaria (schorl-buergerite-foitite); quartz-free, sodalite-

nepheline-cancrinite pegmatite from the Cancrinite Hill, Bancroft, Ontario (Fe³⁺-rich schorl); highly contaminated granitic pegmatites cutting Fe-skarn at Vlastějovice and Mirošov, Moldanubian Zone, Czech Republic (schorl-feruvite, Novák & Kadlec 2010; Fig. 2). Disregarding evident dominance of peraluminous compositions, tourmaline with $Al_{tot} < 6$ apfu also occurs in pegmatites; nevertheless, low Al in tourmaline and parental pegmatite may be controlled by different factors: (i) metaluminous to alkaline composition of the pegmatite melt and (ii) contamination from the host rock. Hence, the elevated contents of Fe³⁺, Ti and Ca may stabilize tourmaline in such specific conditions (Novák *et al.* accepted).

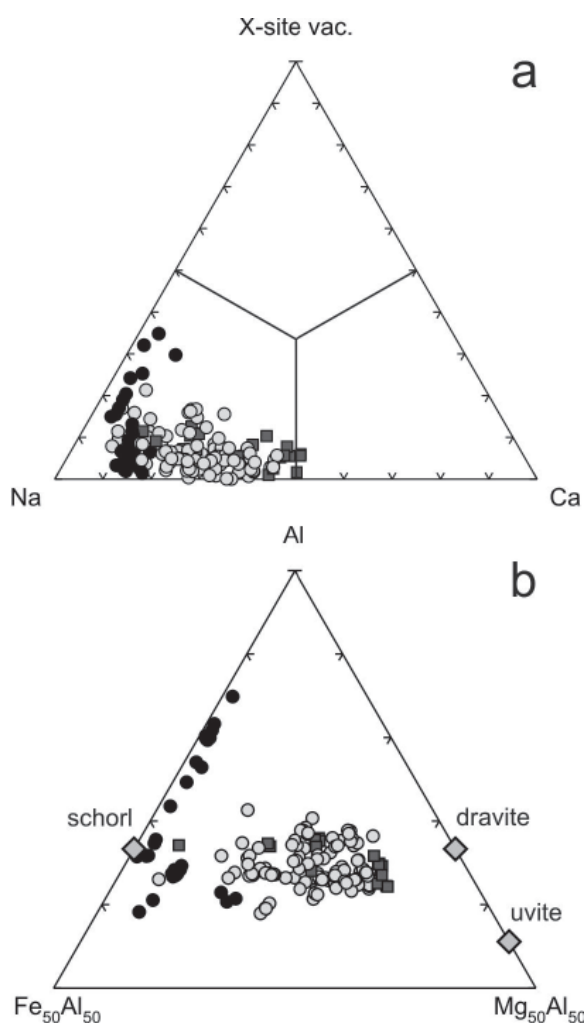


FIGURE 1. Composition of tourmaline from NYF pegmatites of the Třebíč Pluton (slightly modified from Novák *et al.* accepted). a) Na-Ca-X-site vacancy plot, b) Al-Fe-Mg plot. Squares – allanite-type pegmatites, grey circles – euxenite-type pegmatites, solid circles – euxenite-type pegmatite Klučov I.

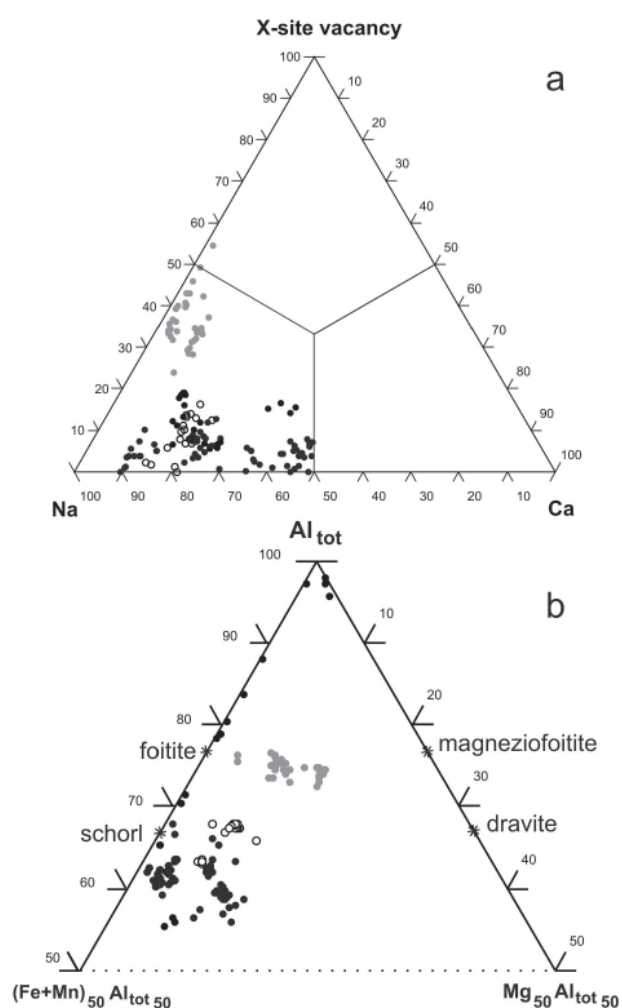


FIGURE 2. Composition of tourmaline from non-contaminated and contaminated pegmatites cutting Fe-skarn in Vlastějovice. (slightly modified from Novák & Kadlec 2010). a) Na-Ca-X-site vacancy plot, b) Al-Fe-Mg plot. Grey circles – pegmatites from gneisses, open circles – pegmatite on the contact of Fe-skarn and orthogneiss, solid circles – pegmatites cutting Fe-skarn including elbaite pegmatite.

ROLE OF CRYSTAL-STRUCTURAL CONSTRAINTS AND THEIR SIGNIFICANCE FOR TOURMALINE COMPOSITION

Role of short-range order and other crystal-structural constraints on tourmaline composition in granitic pegmatites are only exceptionally discussed. The crystal-structural studies (e.g., Hawthorne 1996, 2002, Bosi 2008) revealed that crystal-structural constraints (mainly short-range order) play a significant role in tourmaline compositions (Table 1). For example, tourmaline with high Fe/Mg from pegmatite systems show three distinctive compositions controlled by activities of F and Li in a parental melt and by crystal-structural constraints as well.

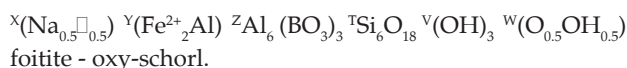
the configuration in the Y site requires $\Sigma Y = 6$ apfu, and it has, owing to incorporation of Li, the most stable configuration ($\text{Li}^+ - \text{Fe}^{2+} - \text{Al}^{3+}$).

The compositional variations in tourmaline from these granitic environments, which are characterized by very similar PT conditions and chemical composition (except for activities of Li and F), suggest significant roles of Li and F. These elements not only enter their appropriate crystallographic sites (Y site and W site, respectively), but significantly control configuration in the Y site and occupancy in the X site. The chemical compositions exhibit combination of both geochemical and crystal-structural constraints.

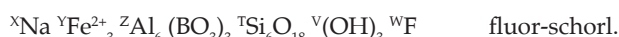
TABLE 1. Stable short-range Y-site cation configurations for anions of different charge at the W site.

General chemical type of tourmaline	W-site anion	Stable short-range configurations
Li-free tourmaline	(OH) ¹⁻ or F ¹⁻	3R ²⁺ or R ³⁺ + 2R ²⁺
Li-free tourmaline	O ²⁻	3R ³⁺ or 2R ³⁺ + R ²⁺
Li-bearing tourmaline	(OH) ¹⁻ or F ¹⁻	2Al ³⁺ + Li ¹⁺ or Al ³⁺ + 2Li ¹⁺
Li-bearing tourmaline	O ²⁻	3Al ³⁺

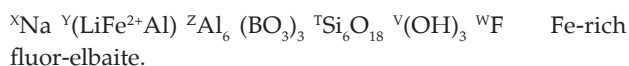
In the rocks with low activities of F and Li (outer zones of complex pegmatites), tourmaline composition commonly tends to the formula (Novák *et al.* 2004):



In the rocks with high activity of F but low activity of Li (F-rich muscovite granites), tourmaline composition tends to the formula:



In the rocks characterized by high activity of F and Li (intermediate zones of some complex pegmatites with Li-muscovite and lepidolite), tourmaline composition tends to the formula:



These well-defined compositions strongly suggest significant role of crystal-structural constraints on the tourmaline composition. In F-,Li-poor rocks, the composition is characterized by high vacancy in the X site, and significant amount of O in the W site; the occupancy of the Y site is controlled by short-range requirements and the configuration R²⁺- R²⁺- Al³⁺ is the most suitable (Table 1). High amount of F at the W site controls the X-site occupancy (high Na and low vacancy) and the configuration at the Y site commonly tends to $\Sigma Y = 6$ apfu ($\text{Fe}^{2+} - \text{Fe}^{2+} - \text{Fe}^{2+}$). In rocks with of high activities of F and Li, the high content of F at W site controls the X site (high Na and low vacancy) and

The first one is marked by concentrations of Li and F; the second one significantly controls occupancies and configurations at the X site, Y site and W site in tourmaline. Consequently, crystal-structural constraints should be considered as a significant factor controlling chemical composition of tourmaline from granitic pegmatites and its stability as well.

ACKNOWLEDGEMENTS

This work was supported by the research project GAČR P210/10/0743.

REFERENCES

- Bosi, F. (2008). Disordering of Fe²⁺ over octahedrally coordinated sites of tourmaline. *Am. Mineral.* **93**: 1647-1653.
- Hawthorne, F.C. (1996). Structural mechanisms for light-element variations in tourmaline. *Can. Mineral.* **34**: 123-132.
- Hawthorne, F.C. (2002). Bond-valence constraints on the chemical composition of tourmaline. *Can. Mineral.* **40**: 789-797.
- London, D. (2008): Pegmatites. Sp. Publ. **10**. Mineral Assoc. Canada. 368 pp.
- Novák, M. & Kadlec, T. (2010). Vlastějovice near Zruc nad Sázavou. Contaminated anatectic pegmatites and tourmaline-bearing granite-pegmatite system cutting Fe-skarn. In: Novák, M. & Cempírek J. eds.; *Acta Mineral. Petrogr., Field Guide Series* **6**: 36-41.

Novák, M., Povondra, P. & Selway, J.B. (2004). Schorl-oxy-schorl to dravite-oxy-dravite tourmaline from granitic pegmatites; examples from the Moldanubicum, Czech Republic. *Eur. J. Mineral.* **16**: 323-333.

Novák, M., Škoda, P., Filip, J., Macek, I. & Vaculovič, T. (2011). Compositional trends in tourmaline from intragranitic NYF pegmatites of the Třebíč Pluton, Czech Republic; electron microprobe, Mössbauer and LA-ICP-MS study. *Can. Mineral.*, in press.

GEOCHEMISTRY OF REE-RICH PEGMATITES FROM DIFFERENT TECTONO-MAGMATIC PROVINCES IN SOUTH PLATTE, CO, TROUT CREEK PASS, CO, KINGMAN AND AQUARIUS RANGE, AZ, NORTH AMERICA

William Simmons¹, Karen Webber¹, Alexander U. Falster¹, Sarah Hanson² & T.J. Brown¹

¹ Department of Earth and Environmental Sciences, University of New Orleans, New Orleans, LA 70148, US. wsimmons@uno.edu,

² Earth Science Department, Adrian College, Adrian, MI 49221, US.

Key Words: REE-rich pegmatite, tectonic-setting, trace-element, South-Platte, Trout-Creek-Pass, Rare-Metals-pegmatite

INTRODUCTION

Pegmatites of the South Platte (SP), Colorado (CO), Trout Creek Pass (TCP), CO, Kingman (K) and Aquarius Range (AQ), Arizona (AZ) have distinctly different tectonic affiliations. Geochemically, pegmatites in these districts are very REE enriched. Each has a distinct mineralogical and geochemical signature.

SOUTH PLATTE

The SP Pegmatite District occurs within the Precambrian core of the Rocky Mountain Front Range in Jefferson County, CO. Located near the northern margin of the Pikes Peak Batholith, it is an extremely REE enriched pegmatite district containing over 75 pegmatites. All of the pegmatites occur as segregations within the parental granite rocks of the 1 Ga Pikes Peak Batholith. More than fifty pegmatites cluster in a relatively small area of only about ten square kilometers. In this area, reddish granite forms the outer zone of the batholith and conforms to the curving contact of the batholith. The pegmatites are large, complex, nearly vertical bodies with a roughly circular to elliptical shape in plan with well-developed concentric zoning. Their diameters or long axes range from less than a meter to almost a hundred meters in length. They have extraordinarily well-developed internal zonal structure and contain abundant rare-earth minerals, zones of massive fluorite, and hematite and albite replacement zones. Strongly enriched yttrian fluorite forms large masses along the core margin of the White Cloud and several other pegmatites. Almost a ton of REE concentrates were recovered from the White Cloud pegmatite alone. Samarskite-(Y) (Fig. 1) is a major sink for the high field strength elements Y, Nb, HREE, Ta and U; and large concentrations were mined from the replacement units of a number of pegmatites. Several hundred tons of samarskite-(Y) were mined from the Quartz Knob pegmatite. Some masses exceeded 60 cm in

maximum dimension. Yb enrichment is exceptionally high in the Little Patsy pegmatite where samarskite-(Yb) was discovered. Columbite group minerals are much less abundant than samarskite-(Y) but are found in a few pegmatites (Fig. 1). Gadolinite-(Ce&Y), thalenite-(Y), synchysite-(Y&Ce), and bastnaesite-(Ce) occur in the fluorite replacement unit of the White Cloud pegmatite, and xenotime-(Y) is abundant in the yttrian fluorite unit of the Big Bertha pegmatite

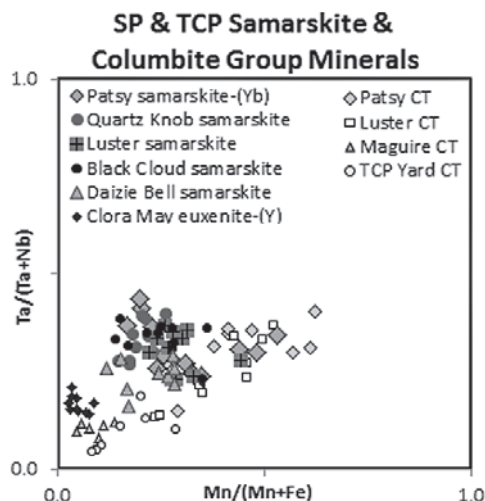


FIGURE 1. Ta/Ta+Nb vs. Mn/Mn+Fe for ferrocolumbite and samarskite-(Y) in SP & TCP.

(Fig. 2). HREE- and Hf-rich zircons in large crystal aggregates up to 15 cm across are abundant in the core margin of the Luster pegmatite and are found in lesser amounts in most other pegmatites. Large anhedral masses of allanite-(Ce) up to 10 cm across occur in the intermediate zones of a number of pegmatites. In terms of Hf, Mn, Ta and Yb enrichment, the Patsy and the Luster are the most evolved pegmatites (Figs. 1, 3). Within the district, a geographical separation exists between pegmatites enriched in LREE vs. HREE. Composite core pegmatites in the southern part of the district contain 'allanite' and are LREE enriched. The

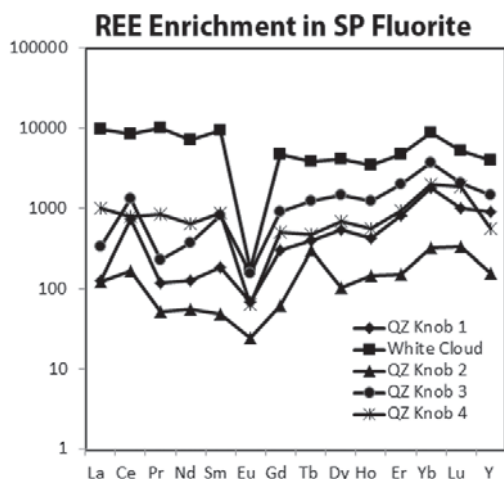


FIGURE 2. Chondrite normalized REE content in various SP fluorite samples.

fluorine-rich quartz-core pegmatites, located in the northern portion of the district, are HREE enriched, containing mainly 'samarskite'. The separation is related to fluorine complexing of HREE over LREE. SP is a classic NYF pegmatite district (Simmons *et al.* 1987).

TROUT CREEK PASS

The TCP pegmatite district is located in the Mosquito Range, Chaffee County, CO. It contains only four pegmatites that were mined for feldspar, but all contain notable concentrations of REE. The district is associated with the catazonal, orogenic, 1.7 Ga Denny Creek pluton of the composite Roubt Plutonic Suite, emplaced during the Boulder Creek Orogeny. Subsequent to this orogenic event, mesozonal granitoids of the Berthoud Plutonic Suite (Silver Plume equivalents) were emplaced as part of the Proterozoic anorogenic 1.4 to 1.45 Ga event. In the Mosquito Range, the Denny Creek pluton consists dominantly of foliated biotite granite, with minor quartz monzonite and a foliated quartz monzodiorite in the southern area. Numerous pegmatites ranging in size from one to several hundred meters are scattered throughout the district. The four largest include the Yard, the Clora May, the Crystal No. 8, and the Tie Gulch. They are structurally well-zoned with a graphic granite wallzone, a composite quartz-microcline core and superimposed albite-rich replacement units. The pegmatites are notably enriched in HREE, Nb, Y and Ti, and depleted in F. Polycrase-(Y) (Fig. 1), found exclusively in the albitic replacement units, is the dominant HREE, Nb and Ti mineral; and monazite-(Ce) and allanite-(Ce), which are found only in the cores, are the dominant LREE minerals in the district. Very minor columbite-(Fe) is found in the core (Fig. 1). The intra-pegmatite separation of the LREE and HREE within these pegmatites cannot be related to fluorine complexing as there is virtually no fluorine in these pegmatites. The presence of 'polycrase' instead

South Platte & Trout Creek Pass Zircons

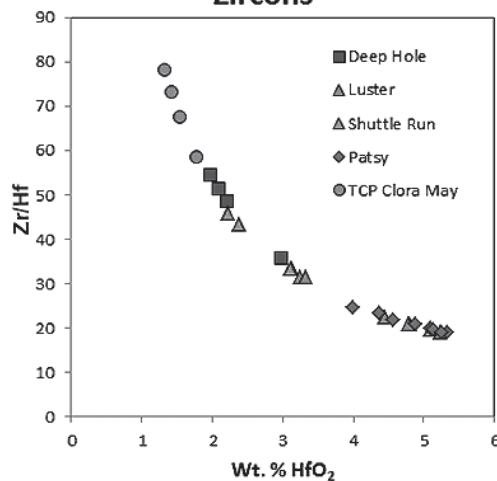


FIGURE 3. Hf enrichment in SP & TCP zircon.

of 'samarskite', as in SP, is related to the stability of 'polycrase' over 'samarskite' in a F-depleted, high Y, Ti, Nb, HREE environment. Here the separation of LREE and HREE appears to be related to late-stage enrichment of HREE caused by early crystallization of the LREE minerals allanite-(Ce) and monazite-(Ce) in the pegmatite cores. Even though the TCP district is associated with an orogenic event, the mineralogy of the pegmatites is distinctly NYF in character (Hanson *et al.* 1992).

KINGMAN AND AQUARIUS RANGE

Five pegmatites from the Basin and Range province near Kingman, AZ have been recently examined. They include the Kingman pegmatite, located in the Cerbat Range (CR) just north of Kingman, AZ, and the Rare Metals, and three Wagon Bow pegmatites located in the Aquarius Range (AQ) about 100 km SW of Kingman. The ranges were formed as a result of block faulting during Miocene extension of SW North America. All pegmatites are hosted in Paleoproterozoic granitic rocks of the Mojave terrane. Ages of the Cerbat plutons are generally contemporaneous with the juxtaposition of the Mojave and Yavapai terranes (1.740–1.720 Ga) (Duebendorfer *et al.* 2001). The AQ Range granites lie within the Boundary Zone between the Mojave and Yavapai terranes and are slightly younger, and associated with the subsequent docking of the sutured Mojave and Yavapai terranes to North America during the Yavapai Orogeny (1.710–1.680 Ga). The Boundary Zone is isotopically mixed and marked by both syn- and post-collisional modification (Duebendorfer *et al.* 2001). All of the pegmatites appear to have been emplaced after docking of the sutured Mojave and Yavapai terranes with North America (Yavapai orogeny, 1.710–1.680 Ga). The cross-cutting nature of the Kingman pegmatite suggests that it is younger and not genetically related to the inferred older ~1.682 Ga host Cerbat granite. However, the Wagon Bow and

Rare Metals pegmatites, which are segregations in the younger AQ Range granitic dikes, appear to be genetically related to their host granites.

The pegmatites are all zoned with border (only Kingman), wall, and intermediate zones and composite quartz-microcline cores. All are REE enriched containing monazite-(Ce), allanite-(Ce), bastnaesite-(Ce), \pm polycrase-(Y) and euxenite-(Y). Like the TCP pegmatites they contain virtually no fluorine. The Kingman pegmatite contains abundant LREE minerals, but Nb- and Ta-phases are notably absent. In the Rare Metals pegmatite, small quantities of Nb and Ta are present in sporadic euxenite-(Y) and polycrase-(Y) in replacement units. Here as in TCP, early 'allanite' and 'monazite' crystallization removed LREE, fractionating HREE into late replacement units which crystallized 'polycrase' or 'euxenite'. The Rare Metals pegmatite contains rare beryl and muscovite. The Wagon Bow pegmatites appear to be less evolved with lower concentrations of Nb, Ta, and REE. The Kingman pegmatite shows strong enrichment of Nd

with the first reported occurrence of "allanite-(Nd)" as crude crystals and anhedral masses up to 20 cm across.

GEOCHEMISTRY

Rare earth element chondrite normalized plots are shown in Figure. 4a-c. SP is distinctly more enriched in total REE than TCP or K-AQ. SP and K-AQ have similar slopes with LREE enrichment but SP is overall more enriched in LREE. The Eu anomalies are prominent in SP and K-AQ, but less pronounced in TCP. The prominent Yb enrichment in some SP pegmatites is also seen in the SP granitic rocks as a positive Yb anomaly. TCP has a prominent positive Gd anomaly, but Gd enrichment in the pegmatites was not noted. The tectonic discriminant Rb vs. Y+Nb plots show the expected within plate (WP) signature for SP (Fig. 5a); TCP falls along the boundary of syn-collisional, volcanic arc (VA) and WP (Fig. 5b). The hybrid character of TCP is further shown in Fig. 5c on the Nb-Y plot. The K-AQ also has a hybrid signature

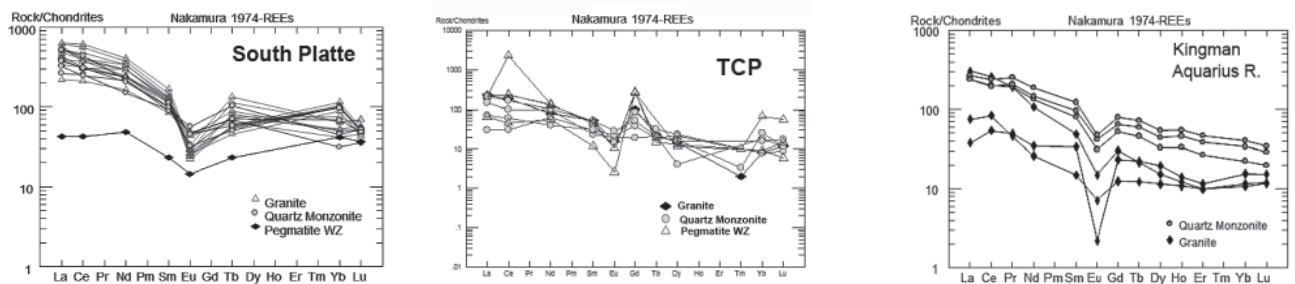


FIGURE 4. Chondrite normalized REE content of: a) SP, b) TCP, c) K-AQ granitic rocks

plotting along VA and WP boundaries (Fig. 5d). Spider diagrams (rock/MORB) are shown in Figure 6. SP shows strong depletion in P, Ba, and Ti and enrichment in Rb, Th, Hf and Yb. TCP shows strong enrichment in Th and Ce and moderate depletion in P and Ti. K-AQ shows depletion in P, Ti, and Ba, and enrichment in Rb, Th, and Ce. These features are consistent with the SP system having formed from partial melting of depleted lower crust or extreme

differentiation of upper mantle melt. TCP granitic rocks show mixed tectonic signatures that appear to be the result of postcollisional melting of mixed sources from the Boulder Creek Orogeny or the Silver Plume anorogenic event. New dates are needed to properly assess the timing. K-AQ granite-pegmatites also show mixed tectonic signatures which reflect the complex Paleoproterozoic tectonic setting. The system shows within plate, subduction and volcanic

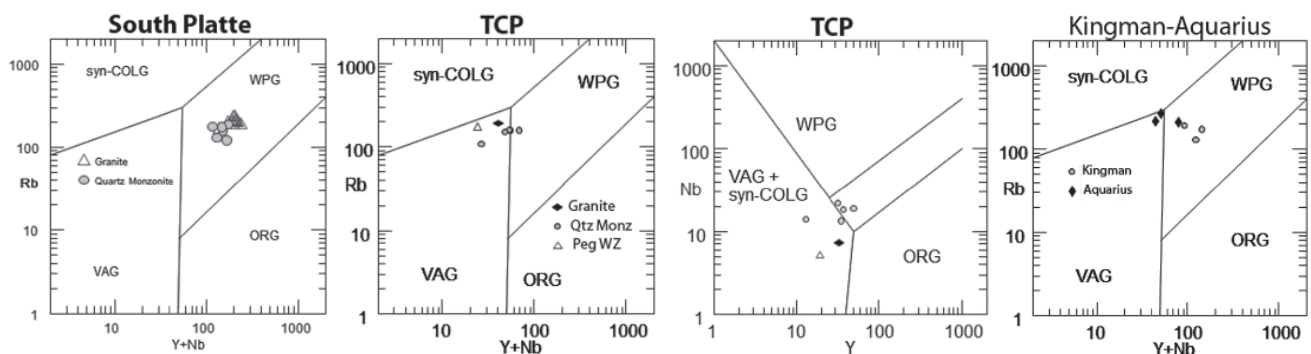


FIGURE 5. Rb vs. Nb+Y tectonic discrimination diagrams for: a) SP, b) TCP, d) K-AQ; c) TCP Nb vs. Y. WPG-within plate, VAG-volcanic arc, syn-COLG-syn-collisional, ORG-ocean ridge, granites.

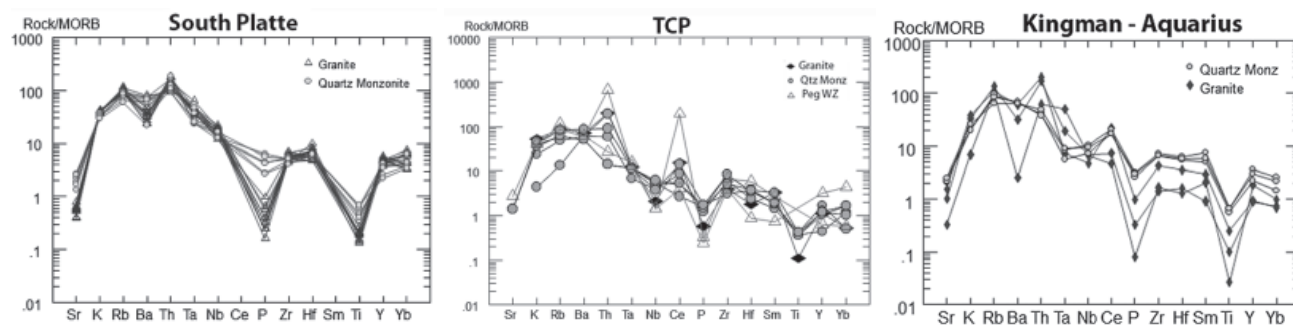


FIGURE 6. Spider diagrams, rock/MORB, for: a) SP, b) TCP, c) K-AQ granitic rocks

arc affinities. This variability is attributed to early Proterozoic rifting which produced crust of both attenuated within plate crust and juvenile volcanic arc composition in the Boundary Zone (Duebendorfer *et al.* 2001). Subsequent remelting of this crust during and after the Yavapai Orogeny produced granites with complex hybrid compositions that are the result of the relative contributions of the diverse rifted crustal material. All REE-rich pegmatites are not created equal.

REFERENCES

- Duebendorfer, E.M., Chamberlain, K.R. & Jones, C.S. (2001). Paleoproterozoic Tectonic History of the Cerbat Mountains, northwestern Arizona: Implications for crustal assembly in the southwestern United States. *GSA Bulletin* **113** (5): 575-590.
- Hanson, S.L., Simmons, W.B., Webber, K. L., and Falster, A.U. (1992) Rare-Earth-Element Mineralogy of Granitic Pegmatites in the Trout Creek Pass Pegmatite District, Chaffee County, Colorado. *Can. Mineral.* **30**: 673-686.
- Simmons, W.B., Lee, M.T., and Brewster, R.H. (1987): Geochemistry and evolution of the South Platte granite-pegmatite system, Jefferson County, Colorado. *Geoch. et Cosmoch. Acta* **51**: 455-471.

THE DISTRICTS OF THE EASTERN PEGMATITE PROVINCE OF BRAZIL

Nelson Angeli

University of State of São Paulo, Rio Claro (SP), Brazil. 24-A Avenue, n°1515, postal code 13506-900: nangeli@rc.unesp.br

Key words: Allanite-monzonite type, REE subclass, Aquamarine, Topaz, NYF family, Magmatic Arc

INTRODUCTION

The Eastern Brazilian Pegmatite Province is known world-wide for its gemstones and occurrences of the minerals of Li, for example spodumene, elbaite, lepidolite, petalite and amblygonite. Its geographic distribution overlaps the huge Late Pre-Cambrian granitic magmatic arc of the Araçuaí Fold Belt, in the states of Minas Gerais and Bahia (Fig. 1). The magmatic arc comprises syn-, late- and post-tectonic intrusive bodies varying from tonalites to syenogranites, associated with metasedimentary and low- to high-grade metamorphic rocks, in the eastern and western portions of the magmatic arc, respectively. The pegmatites of the Salinas–Araçuaí belt [District A] belong to the LCT family (Li subclass), and cut mainly metasedimentary country-rocks and S-type granites. Pegmatites of the NYF family, in the Medina – Pedra Azul area [District B], are hosted by leucocratic equigranular and mesocratic porphyritic granites. The granitic country-rocks have abundant microcline megacrysts. They are considered calc-alkaline, with an overall syenogranitic composition (metaluminous I-type granites). In these rocks, Ba reaches 1000 ppm, Na₂O/K₂O varies between 0.8 and 3.0, and the lineage is 4a according to zircon morphology.

The most outstanding rare-element minerals in pegmatites of District A includes: petalite, lepidolite, amblygonite, beryl, spodumene, variety “kunzite”, triphylite, pollucite, colored tourmaline crystals, cassiterite and columbite-group minerals (Ta > Nb). District A is the best-studied district in the Eastern Brazilian Pegmatite Province.

The pegmatites of District B, which are the focus in this paper (Fig. 1), are located mainly in the poorer metasedimentary portion of the magmatic arc. The pegmatites belong to the REE subclass [beryl – columbite-(Fe) – phosphates – allanite – monazite] of the NYF family, allanite–monazite type. The ⁸⁷Sr/⁸⁶Sr

value of their I-type metaluminous source-granites varies between 0.7062 and 0.7132, which is lower than the values in the A District. Their K₂O content is also higher (7.26–12.91%) than that of the granites in the A District (3.2–4.8%). The mean K₂O (9%) and Rb (1200 ppm) values in muscovite and microcline indicate a lower degree of magmatic differentiation for the B District.

The other districts (C: Governador Valadares – Juiz de Fora, D: Materlândia–Capelinha) consist of unzoned pegmatites that contains microcline, muscovite, biotite and some schorl, and belongs to the muscovite class of pegmatites according to Černý & Ercit (2005).

GEOLOGICAL SETTING AND CHARACTERISTICS OF THE PEGMATITES

The pegmatite bodies of District A were emplaced in the metasedimentary sequences, like Rio Doce, Macaúbas, Jequitinhonha and Salinas groups (Pedrosa Soares *et al.* 2001a). The country rocks display a medium- to high-grade metamorphism (amphibolite facies), and some of them are intruded by granites. Pegmatites in several small mines show precious to semiprecious gemstones, leading to the label Eastern Gemmology Province of Brazil proposed by Pinto & Pedrosa Soares (2001). Also present are phosphates with U–Th, rare metals and an enrichment in REE. To the south, the pegmatites of Governador Valadares – Conselheiro Pena and Juiz de Fora, Minas Gerais are unzoned and show a uniform texture (Muscovite class). The same occurs between Materlândia and Capelinha. These bodies present a simple mineralogy (microcline, muscovite, biotite, minor schorl and beryl). Microcline and muscovite are exploited as industrial minerals in ceramic pegmatites [Districts C and D] (Fig. 1).

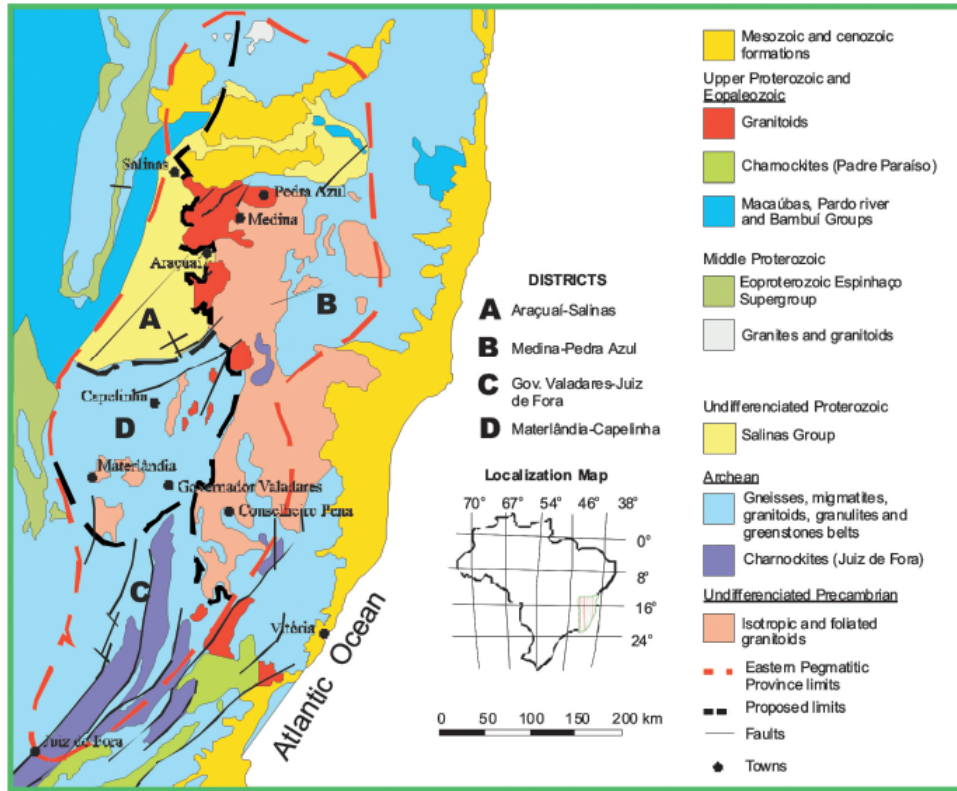


FIGURE 1. Geological sketch of the Eastern Brazilian Pegmatite Province and the proposed Districts (A, B, C and D). Adapted from Biondi (2003).

The pegmatites from District B feature a late development of sodic plagioclase (Fig. 2), coexisting with zircon, magnetite and phosphates. The main accessory minerals comprise: topaz, beryl (in some places as large crystals or as the gemmy variety aquamarine), columbite-(Fe), zircon, apatite, rutile, titanite, fluorite, amethyst, REE-rich allanite, radioactive monazite, samarskite and radioactive

phosphates (goyazite, bobierite and zwieselite), euxenite, autunite, herderite and fergusonite (Figs. 3, 4, 5).

The alteration minerals are kaolinite, epidote, autunite and plumbogummite. The high degree of differentiation of the granites is shown in Figures 6, 7 and 8. The total concentration of the REE and



FIGURE 2. Exposure of NYF granite pegmatite from Medina-Pedra Azul showing the late plagioclase (albite/oligoclase) located near the quartz core, together with microcline and minor muscovite. The albite shows a bladed habit known as «cleavelandite» (District B).



FIGURE 3. Photomicrograph showing a zircon inclusion in biotite, associated with plagioclase and myrmekite; the pleochroic halos are due to inclusions of crystals containing radioactive elements (District B).



FIGURE 4. Photo of beryl, variety aquamarine, close to the quartz core, in a small pocket in the Intermediate Zone exposed in an artisanal mine, Medina (District B)



FIGURE 5. Photo of black crystals of columbite-(Fe) containing a small quantity of Ta, located at the contact of the Wall and Intermediate zones (District B).

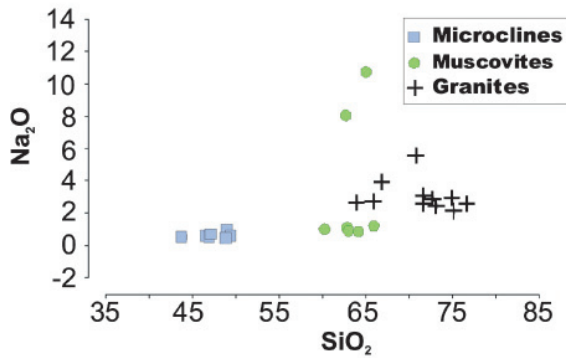


FIGURE 6. Plot of Na_2O versus SiO_2 . Note: two samples showing muscovite and albitized muscovite-bearing granites indicate a late hydrothermal stage in rocks of District B.

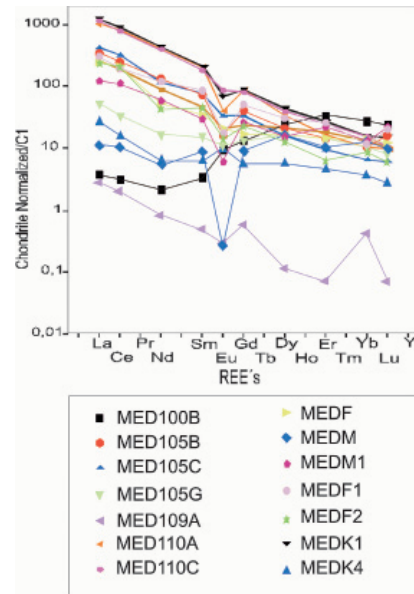


FIGURE 7. Chondrite-normalized REE patterns of rocks and minerals from the Medina – Pedra Azul district (left: samples correspond to granites close to Medina [MED 100B-110C]; right: samples from 10 km to the northeast of Pedra Azul [MEDF-MEDK4]). Normalization: Wakita *et al.* (1971).

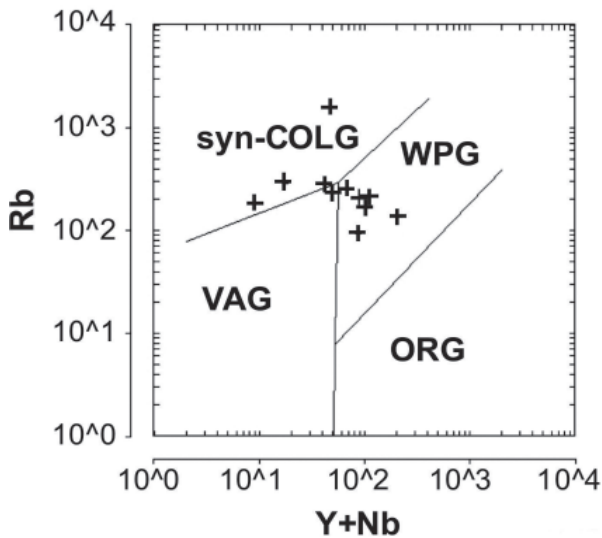


FIGURE 8. Tectonic affiliation of granitic rocks of the Medina – Pedra Azul district, in terms of the diagram of Pearce *et al.* (1984). Fields: Volcanic Arc Granite (VAG), Syn-Collisional Granite (syn-COLG), Intraplate Granite (WPG), and Ocean-Ridge Granite (ORG).

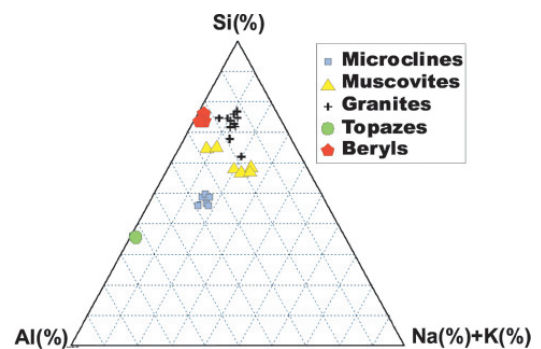


FIGURE 9. Triangular Si – Al – (Na + K) plot summarizing the evolutionary trend defined by the granitic pegmatites in District B, leading to topaz- and beryl-mineralized members.

the ratio $Y/(REE + Y)$, increasing from 0.02 to 0.96, are consistent with a progressive geochemical fractionation of a granitic pegmatite-forming magma of NYF petrogenetic affiliation. The $(La/Lu)_{CN}$ value, 40, and the $(La/Yb)_{CN}$ value, 33, indicate a relatively low degree of fractionation of the LREE in comparison to the HREE. The normalized REE pattern varies in shape from uniformly tilted to flat seagull-wing type, the latter quite similar to the REE pattern of the enclosing granites. A relative depletion in Eu (Fig. 7) is commonly developed. The erratic patterns developed in Figure 7 reflect the presence of various REE-enriched minerals (e.g., zircon, allanite, titanite) in the pegmatites.

A triangular Al – Si – (Na + K) plot shows an evolutionary trend of the pegmatites and their mineralized members, quite similar to the evolution of Caladão Granite (Ferreira *et al.* 2005), except that these only rarely contain garnet (Fig. 9). The granites in this district show a medium to high level of Al_2O_3 , which varies between 11.8 and 17.8%, in comparison to the parental granites in District A, which contain more than 20%. All samples shown in Fig. 9, both of granite pegmatite and the country rocks, are from Medina.

These new data for the Medina – Pedra Azul suite complement the previous information of Pedrosa-Soares (2001a, b) on the tectonic origin and the geochronology of the granitic pegmatites. A program of chemical analyses (mineral chemistry and REE), fluid inclusions, geothermometric and geobarometric studies are planned.

CONCLUSIONS

Granitic pegmatites of District B (Medina – Pedra Azul) suite are enriched in Be–Nb–P–REE–F–U+Th and classified as belonging to the NYF family (Fig. 8), mainly intruded into biotite gneisses, which equilibrated at $P = 3.5$ kbar and $T = 550$ C. The behaviour of the bodies is quite similar from north to the south, between Pedra Azul and Conselheiro Pena. The phosphates of the rare-earth elements in these NYF pegmatites are associated with late-stage replacement in portions of the pegmatites, and have arisen by pneumatolitic or hydrothermal alteration.

In some artisanal mines, crystals of smoky quartz show structural defects owing to the presence of radioactive minerals in the vicinity. The relation of Rb *versus* (Y+Nb) shows a magmatic relationship of this NYF suite to continental arc granitoids (syn- to post-tectonic emplacement) for the parental rocks.

ACKNOWLEDGEMENTS

I acknowledge the anonymous referee for providing extensive help and constructive reviews in this last version.

REFERENCES

- Biondi, J.C. (2003). Processos Metalogenéticos e os Depósitos Minerais Brasileiros. Editora Oficina de Textos, São Paulo: 528 p.
- Černý, P. & Ercit, T.S. (2005). The classification of granitic pegmatites revisited. *Can. Mineral.* **43**(6): 2005-2026.
- Ferreira, M.S.F., Fonseca, M.A. & Pires, F.R.M. (2005). Pegmatitos Mineralizados em Água-Marinha e Topázio do Ponto Marambaia, Minas Gerais: Tipologia e Relações com o Granito Caladão. *Rev. Bras. Geociên.* **35**(4): 463-473.
- Pedrosa-Soares, A.C., Noce, C.M., Wiedemann, C.M. & Pinto, C.P. (2001a). The Araçuaí-West Congo Orogen in Brazil: an overview of a confined orogen formed during Gondwanaland assembly. *Precamb. Res.* **110**: 307-323.
- Pedrosa-Soares, A.C., Pinto, C. P., Netto, C., Araújo, N. C., Castañeda, C., Achtschin, A.B. & Basílio, M.S. (2001 b). A Província Gemológica Oriental do Brasil. In: Gemas de Minas Gerais, Capítulo 1, Castañeda, C.; Addad, J. E. & Liccardo, A. (Organizadores): 16-33.
- Pinto, C. P. & Pedrosa-Soares, A.C. (2001). Brazilian Gem Provinces. *The Australian Gemmologist.* **21**(1): 12-16.
- Wakita, H., Rey, P. & Schmitt, R. A. (1971). Elemental abundances of major, minor, and trace elements in Apollo 11 lunar rocks, soil and core samples. *Proceedings of the Apollo 11 Lunar Science Conference*, 1685-1717.

THE MICROLITE-GROUP MINERALS: NOMENCLATURE

Daniel Atencio¹, Marcelo B. Andrade^{2§}

¹ Instituto de Geociências, Universidade de São Paulo, Rua do Lago, 562, 05508-080, São Paulo, SP, Brazil, § datencio@usp.br

² Instituto de Física de São Carlos, Universidade de São Paulo, 13560-970, São Carlos, SP, Brazil

Key words: nomenclature, pyrochlore supergroup, microlite group.

INTRODUCTION

Microlite-group minerals, which are part of the pyrochlore supergroup, are mainly restricted to moderately to highly fractionated rare-element granitic pegmatites (Lumpkin & Ewing 1995). A new nomenclature scheme for the pyrochlore supergroup, approved by the CNMNC – IMA (Atencio *et al.* 2010), is based on the ions in the *A*-, *B*- and *Y*-sites. What has been referred to until now as the pyrochlore group should be referred to as the pyrochlore supergroup, and the subgroups should be changed to groups. Five groups are recommended, based on the atomic proportions of the *B*-atoms Nb, Ta, Sb, Ti, and W. The recommended groups are pyrochlore, microlite, roméite, betafite, and elsmoreite, respectively.

NAMES

The new names are composed of two prefixes and one root name (identical to the name of the group). The first prefix refers to the dominant anion (or cation) of the dominant valency [or H₂O or □] in the *Y*-site. The second prefix refers to the dominant cation of the dominant valency [or H₂O or □] in the *A*-site. The prefix “keno-” represents “vacancy”. When the first and second prefixes are equal, then only one prefix is applied. Complete descriptions are missing for the majority of the microlite-group species. Only three names refer to valid mineral species on the grounds of their complete descriptions: hydroxykenomicrolite, oxystannomicrolite, and oxystibomicrolite. Fluornatromicrolite is an IMA-approved mineral, but the complete description has not yet been published. The following five names refer to minerals that need to be completely described in order to be approved as valid species: fluorcalciomicrolite, oxycalciomicrolite, kenoplumbomicrolite, hydromicrolite, and hydrokenomicrolite. For these, there are only chemical and/or crystal structure data. Type specimens need

to be defined. Potential candidates for several other species exist but are not characterized well enough to grant them any official status. Ancient chemical data refer to wet chemical analyses and commonly represent a mixture of minerals. These data were not used here. All used data represent microprobe analyses and/or were obtained by crystal structure refinements. We also verified scarcity of crystal-chemical data in the literature. There are crystal structure determinations published for only two microlite-group minerals: hydroxykenomicrolite and kenoplumbomicrolite. The following mineral names were discarded: bariomicrolite, bismutomicrolite, plumbomicrolite, stannomicrolite, stibomicrolite, and uranmicrolite.

The new names are presented below. A table is shown indicating the combinations of dominant species of the dominant-valency group at *A*-site and dominant species of the dominant-valency group at *Y*-site for which there is evidence of a mineral. After the table, references are given for the corresponding species or potential species. The names marked with an asterisk “*” refer to valid mineral species because of their complete descriptions. The other names refer to minerals that need to be completely described in order to be approved as valid species. The names of the species for which there are crystal structure determination studies are marked with a dagger ‘†’. (See table on next page)

FLUORNATROMICROLITE:

The IMA Proposal 98-018 for fluornatromicrolite (Witzke *et al.* 1998) was approved but the complete paper was never published. Some data were published by Atencio (2000). Chemical analyses that correspond to fluornatromicrolite from other occurrences are available in the papers by Ohnenstetter & Piantone (1992), Belkasmí *et al.* (2000), Huang *et al.* (2002) and Baldwin *et al.* (2005).

Dominant species of the dominant-valency group at A-site	Dominant species of the dominant-valency group at Y-site				
	OH	F	O	H ₂ O	□
Na Ca Sn ²⁺ Sr Pb ²⁺ Sb ³⁺ Y U ⁴⁺ H ₂ O □	hydroxykenomicrolite*†	fluornatromicrolite fluorcalciomicrolite	oxycalciomicrolite oxystannomicrolite* oxystibiomicrolite*	hydromicrolite hydrokenomicrolite	kenoplumbomicrolite†

FLUORCALCIOMICROLITE:

There are several analyses of fluorcalciomicrolite in the literature, *e.g.*, Lumpkin *et al.* (1986), Baldwin (1989), Ohnenstetter & Piantone (1992), Tindle & Breaks (1998), Huang *et al.* (2002), Geisler *et al.* (2004), Tindle *et al.* (2005).

OXYCALCIOMICROLITE:

Černý *et al.* (2004) [stibiomicrolite]; Guastoni *et al.* (2008) [microlite].

OXYSTANNOMICROLITE:

Vorma & Siivola (1967) [sukulaite]; Ercit *et al.* (1987) [stannomicrolite]. The type specimen of "sukulaite" described by Vorma & Siivola (1967) should be considered as the type for oxystannomicrolite.

KENOPLUMBOMICROLITE:

Bindi *et al.* (2006): crystal structure study of kenoplumbomicrolite.

OXYSTIBIOMICROLITE:

Groat *et al.* (1987): Type sample for "stibiomicrolite"; Novák & Černý (1998). The type specimen of "stibiomicrolite" described by Groat *et al.* (1987) should be considered as the type for oxystibiomicrolite.

HYDROKENOMICROLITE:

Andrade & Atencio (unpublished data)

HYDROMICROLITE:

Andrade & Atencio (unpublished data)

HYDROXYKENOMICROLITE:

Ercit *et al.* (1993): crystal structure study of "cesstibtantite". The type specimen of "cesstibtantite" described by Voloshin *et al.* (1981) should be considered as the type for hydroxykenomicrolite.

FORMULAE

Formulae are given for the species for which we have analytical evidence. Note that subordinate components on the A-, B-, X- or Y-sites have no nomenclatural significance. We show specific examples here that are typical of the minor components observed, but any of these could be replaced by "#", indicating an unspecified heterovalent species required for charge balance.

oxystannomicrolite*	Sn ₂ Ta ₂ O ₆ O
oxystibiomicrolite*	(Sb ³⁺ ,Ca) ₂ Ta ₂ O ₆ O
hydroxykenomicrolite*†	(□, Na, Sb ³⁺) ₂ Ta ₂ O ₆ (OH)
fluornatromicrolite	(Na, Ca, Bi) ₂ Ta ₂ O ₆ F
fluorcalciomicrolite	(Ca, Na) ₂ Ta ₂ O ₆ F
oxycalciomicrolite	Ca ₂ Ta ₂ O ₆ O
kenoplumbomicrolite	(Pb, □) ₂ Ta ₂ O ₆ (□, O, OH)
hydromicrolite	(H ₂ O, □) ₂ Ta ₂ (O, OH) ₆ (H ₂ O)
hydrokenomicrolite	(□, H ₂ O) ₂ Ta ₂ (O, OH) ₆ (H ₂ O)

ACKNOWLEDGEMENTS

We acknowledge FAPESP (Fundação de Amparo à Pesquisa do Estado de São Paulo) for financial support (processes 2008/04984-7 and 2009/09125-5).

REFERENCES

Atencio, D. (2000). Type Mineralogy of Brazil. 1st. ed. São Paulo: Museu de Geociências - USP. 114p.

- Atencio, D., Andrade, M.B., Christy, A.G., Gieré, R. & Kartashov, P.M. (2010). The pyrochlore supergroup of minerals: nomenclature. *Can. Mineral.* **48**: 673-698.
- Baldwin, J.R. (1989). Replacement phenomena in tantalum minerals from rare-metal pegmatites in South Africa and Namibia. *Mineral. Mag.* **53**: 571-581.
- Baldwin, J.R., Hill, P.G., Finch, A.A., von Knorring, O. & Oliver, G.J.H. (2005). Microlite-manganotantalite exsolution lamellae: evidence from rare-metal pegmatite, Karibib, Namibia. *Mineral. Mag.* **69**: 917-935.
- Belkasmí, M., Cuney, M., Pollard, P.J. & Bastoul, A. (2000). Chemistry of the Ta-Nb-Sn-W oxide minerals from the Yichun rare metal granite (SE China): genetic implications and comparison with Moroccan and French Hercynian examples. *Mineral. Mag.* **64**: 507-523
- Bindi, L., Zoppi, M. & Bonazzi, P. (2006). Plumbomicrolite from the Ploskaya Mountain, Keivy Massif, Kola Peninsula, Russia: composition and crystal structure. *Periodico di Mineralogia* **75**: 51-58.
- Černý, P., Chapman, R., Ferreira, K. & Smeds, S.-A. (2004). Geochemistry of oxide minerals of Nb, Ta, Sn, and Sb in the Varuträsk granitic pegmatite, Sweden: The case of an "anomalous" columbite-tantalite trend. *Am. Mineral.* **89**: 505-518.
- Ercit, T.S., Černý, P. & Siivola, J. (1987) The composition of stannomicrolite. *N. Jb. Miner., Monat.* 249-252.
- Ercit, T.S., Černý, P. & Hawthorne, F.C. (1993) Cesstibtantite—a geologic introduction to the inverse pyrochlores. *Mineralogy and Petrology*, **48**: 235-255.
- Geisler, T., Berndt, J., Meyer, H.-W., Pollok, K. & Putnis, A. (2004) Low-temperature aqueous alteration of crystalline pyrochlore: correspondence between nature and experiment. *Mineral. Mag.* **68**: 905-922.
- Groat, L.A., Černý, P. & Ercit, T.S. (1987) Reinstatement of stibiomicrolite as a valid species. *Geoliska Föreningens i Stockholm Förhandlingar* **109**: 105-109.
- Guastoni, A., Diela, V. & Pezzotta, F. (2008) Vigezzite and associated oxides of Nb-Ta from emerald-bearing pegmatites of the Vigezzo Valley, Western Alps, Italy. *Can. Mineral.* **46**: 619-633.
- Huang, Xiao Long, Wang, Ru Cheng, Chen, Xiao Ming, Hu, Huan & Liu, Chang Shi (2002) Vertical variations in the mineralogy of the Yichun topaz-lepidolite granite, Jiangxi Province, Southern China. *Can. Mineral.* **40**: 1047-1068.
- Lumpkin, G.R. & Ewing, R.C. (1995). Geochemical alteration of pyrochlore group minerals: Pyrochlore subgroup. *Am. Mineral.* **80**: 732-743.
- Lumpkin, G.R., Chakoumakos, B.C. & Ewing, R.C. (1986). Mineralogy and radiation effects of microlite from the Harding pegmatite, Taos County, New Mexico. *Am. Mineral.* **71**: 569-588.
- Novák, M. & Černý, P. (1998). Niobium-tantalum oxide minerals from complex granitic pegmatites in the Moldanubicum, Czech Republic: primary *versus* secondary compositional trends. *Can. Mineral.* **36**: 659-672.
- Ohnenstetter, D. & Piantone, P. (1992). Pyrochlore-group minerals in the Beauvoir peraluminous leucogranite, Massif Central, France. *Can. Mineral.* **30**: 771-784.
- Tindle, A.G. & Breaks, F.W. (1998). Oxide minerals of the Separation Rapids rare-element granitic pegmatite group, Northwestern Ontario. *Can. Mineral.* **36**: 609-635.
- Tindle, A.G., Selway, J.B. & Breaks, F.W. (2005) Liddicoatite and associated species from the McCombe spodumene-subtype rare-element granitic pegmatite, Northwestern Ontario, Canada. *Can. Mineral.* **43**: 769-793.
- Voloshin, A.V., Men'shikov, Yu.P., Pakhomovskiy, Ya.A. & Polezhaeva, L.I. (1981) Cesstibtantite, (Cs,Na)SbTa₄O₁₂ □ a new mineral from granitic pegmatites. *Zapiski Vsesoyuznoye Mineralogicheskogo Obshchestvo* **116**: 345-351 (in Russian).
- Vorma, A. & Siivola, J. (1967) Sukulaite □ Ta₂Sn₂O₇ □ and wodginite as inclusions in cassiterite in the granite pegmatite in Sukula, Tammela, in SW Finland. *Bulletin de la Commission géologique de Finlande*, **229**, 173-187.
- Witzke, T., Steins, M., Doring, T., Schuckmann, W., Wegner, R. & Pollmann, H. (1998) Fluornatromicrolite. IMA CNMMN Submission 98-018.

GEOCHEMICAL EVOLUTION OF PHOSPHATES AND SILICATES IN THE SAPUCAIA PEGMATITE, MINAS GERAIS, BRAZIL: IMPLICATIONS FOR THE GENESIS OF THE PEGMATITE

Maxime Baijot^{1§}, Frédéric Hatert¹,
André-Mathieu Fransolet¹ & Simon Philippo²

¹ Laboratory of Mineralogy, University of Liège, B18, B-4000 Liège, Belgium §mbaijot@doct.ulg.ac.be

² National Museum of Natural History of Luxembourg, Section of Mineralogy, rue Münster, 24, L-2160, Luxembourg, Luxembourg

Key words: phosphate minerals, silicates, evolution, pegmatite, Brazil.

INTRODUCTION

One of the most important pegmatite provinces in the world, the Eastern Brazilian Pegmatite Province (EBPP), occurs in Brazil. This province is located at the East side of the São Francisco craton, mainly in the state of Minas Gerais. Among these pegmatites, the Sapucaia pegmatite was selected for detailed sampling. This pegmatite was probably discovered around 1920-1930 and was initially exploited for beryl and muscovite (Pecora *et al.* 1950, Cassedanne & Baptista 1999). Sapucaia pegmatite is especially famous for its complex phosphate mineral associations, among which six new phosphate mineral species were first described: frondelite, faheyite, moraesite, barbosalite, tavorite, and lipscombite (Atencio 2000). The discovery of these new mineral species leads to a good knowledge of the Sapucaia mineralogy; however, only a brief description of the pegmatite body exists.

The aims of this work are (i) to describe the variations of the mineral assemblages corresponding to the different zones of the pegmatites, (ii) to investigate in detail the petrographic relations among phosphates as well as their chemical compositions in order to better understand the transformation sequences which affected these minerals, and (iii) to shed some light on the genesis of the Sapucaia pegmatite throughout the geochemical evolution of the phosphate minerals and their associated silicates.

GEOLOGICAL SETTING AND DESCRIPTION OF THE PEGMATITE BODY

GEOLOGICAL SETTING

The Eastern Brazilian Pegmatite Province (EBPP) is divided into several districts, among which the Conselheiro Pena district (Pedrosa-Soares *et al.* 2009) in which the Sapucaia pegmatite occurs. During the Brazilian orogeny (700-450 Ma), several pre-, syn-, and post-tectonic granitoids took place in the EBPP (Bilal

et al. 2000), originating most of the pegmatites (Bilal *et al.* 2000; Morteani *et al.* 2000). Two of these intrusions crosscut the cover and the basement rocks of the Conselheiro Pena district: the Galiléia and Urucum magmatic suites which belong to the G1 and G2 supersuites, respectively (Pedrosa-Soares *et al.* 2001). The Galiléia granitoid (595 Ma) is a metaluminous suite characterized by a polydiapiric batholith consisting mainly of granodiorites and tonalites with minor granites. These rocks are associated with the precollisional magmatism of the Brazilian orogeny and have calcalkaline affinities (Nalini *et al.* 2000; Pedrosa-Soares *et al.* 2001). The Urucum suite (582 Ma) is composed by four different types of rocks: a feldspar megacrystal-bearing granite (Urucum facies), a medium to coarse grained granite (Palmital facies), a tourmaline-bearing granite and a pegmatitic granite (Nalini *et al.* 2000). These rocks mainly have a peraluminous composition (S-type granite) due to the syn-collisional character of the orogeny (Nalini *et al.* 2000; Pedrosa-Soares *et al.* 2001).

DESCRIPTION OF THE PEGMATITE BODY

The Sapucaia pegmatite is located 14 km NE of the Galiléia town (18°54'038''S ; 41°29'061''W). The pegmatite occurs in the São Tome formation consisting in subvertical sillimanite-staurolite-garnet-micas-bearing schists and has an elliptic shape of 80 m length, 40 m width and 50 m height. Different zones are observed in the pegmatite (Fig. 1). A border zone of 5 cm width, in direct contact with the host schists, has a granular texture and consists of an interbedding of dark bands of schorl + quartz, and light bands of quartz + albite ± greenish apatite. Muscovite is an accessory mineral in the two types of layers. The wall zone is characterized by K-feldspars showing occasionally coarse graphic texture, associated with biotite and muscovite (M2). Muscovite is coarser than biotite, and shows a fishbone-like habit, in which the crystals can reach 20 cm in length. Accessory schorl, reaching 1 to 2 cm in length, occurs in the matrix as well as in the muscovite flakes. In this wall zone,

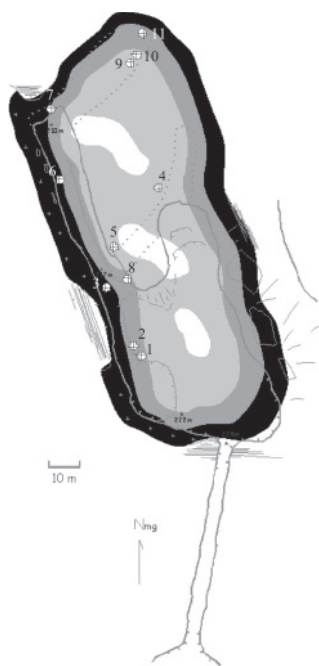


FIGURE 1. Schematic map of the Sapucaia pegmatite showing the zonation and the location of the phosphate nodules (numbers). Black zone = M2 zone: quartz + feldspars + two micas ± small schorl; Dark grey zone = M1 zone: graphic feldspars + muscovite + schorl ± Beryl; Light grey zone = S zone: Spodumene + quartz + yellow mica ± beryl; White zone: Q zone: quartz cores

biotite disappears one or two meters before entering into the intermediate zone, and the paragenesis is then characterized by K-feldspar (sometimes showing graphic textures), large schorl crystals reaching 10 cm long, accessory muscovite and beryl (M1). In the intermediate zone, many large spodumene crystals reaching 2 meters in length are surrounded by yellow mica in a quartz matrix. Beryl and small schorl crystals (2 cm maximum) can be present; larger tourmaline crystals sometimes appear perpendicular to the spodumene crystals. Finally, the quartz core (Q) appears, which can locally contain a few smaller spodumene crystals. The M1, S, and Q zones can be partially albitized.

Phosphate minerals were observed in the M1 and S zones, in which they form nodular masses reaching 2 meters in diameter (Fig. 1). Nine nodules were sampled directly in place in the pegmatite (samples 3 and 6 are not in place), and three different types of phosphate associations occur:

I) Masses showing dendritic or/and skeletal textures involving feldspar and several secondary phosphate minerals.

II) Fresh massive triphylite altered by vivianite, which give its bluish colour to the phosphate.

III) Rim of phosphate minerals and oxides

surrounding a white core of albite; the external feldspar directly in contact with the rim takes a greenish colour

Petrographic observations, X-ray diffraction measurements, and electron-microprobe analyses were performed on the phosphates, to confirm their identification, to calculate their unit-cell parameters, and to characterize their chemistry.

PHOSPHATE MINERALOGY AND CHEMICAL VARIATION

The only primary phosphate mineral is triphylite, $\text{Li}(\text{Fe}^{2+}, \text{Mn}^{2+})\text{PO}_4$. In association I, this mineral progressively oxidizes to ferrisicklerite, $\text{Li}_{<1}(\text{Fe}^{3+}, \text{Mn}^{2+})\text{PO}_4$, and to heterosite, $(\text{Fe}^{3+}, \text{Mn}^{3+})\text{PO}_4$, following the so-called "Quensel-Mason" sequence (Quensel 1937; Mason 1941). Ferrisicklerite is frequently replaced by several secondary phosphates like leucophosphite, phosphosiderite, minerals of the jahnsite group, and minerals of the rockbridgeite-frondelite series. In association II, triphylite is directly replaced by vivianite along cleavage planes under reducing conditions. The association III needs more investigations.

As it was already observed in the literature (Mason 1941; Fontan *et al.* 1976; Fransolet *et al.* 1986), the contents in Fe, Mn and Mg do not show significant variation during the "Quensel-Mason" sequence. For example, ferrisicklerite and heterosite of sample Sap-1 are located close to each other in the $\text{Fe}_{\text{tot}}\text{-Mn-Mg}$ ternary diagram (Fig. 2). So we can also use the $\text{Fe}_{\text{tot}}/(\text{Fe}_{\text{tot}} + \text{Mn})$ and $\text{Mg}/(\text{Fe}_{\text{tot}} + \text{Mn} + \text{Mg})$ ratios in ferrisicklerite and heterosite to estimate the differentiation degree of the pegmatites (Keller *et al.* 1994a, 1994b). The electron-microprobe analyses of samples from Sapucaia show variations of the $\text{Fe}_{\text{tot}}/(\text{Fe}_{\text{tot}} + \text{Mn})$ ratio in these phosphates of the "Quensel-Mason" sequence, with a decrease from sample Sap-1 (around 0.74) to sample Sap-4 (0.71). The $\text{Mg}/(\text{Fe}_{\text{tot}} + \text{Mn} + \text{Mg})$ ratio also decreases, from 0.18 for Sap-1 to 0.13 for Sap-4.

These chemical modifications are due to variations of the differentiation degree, from the border to the centre of the pegmatite: the phosphates from the inner zone, in which Sap-4 is located, show a decrease in Fe and Mg, when compared with the less differentiated phosphates from the outer zone, where Sap-1 and Sap-7b are located. These observations are in agreement with the geochemical evolution of pegmatites described by Ginsburg (1960). Sap-6b was not in place but its Mg-Fe-Mn ratio suggests that this sample has a similar differentiation degree than Sap-1 (Fig. 2). Moreover, the Mn-rich triphylite sample Prb-1b, which was not located on the map, probably corresponds to a second generation of triphylite that crystallized at lower temperature (Fig. 2).

This geochemical trend must be further

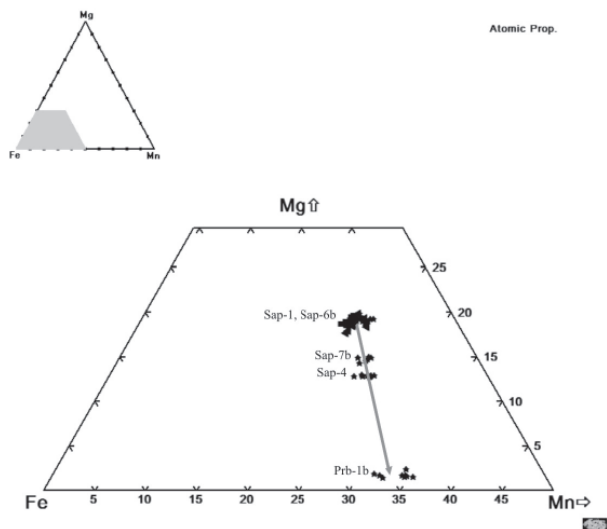


FIGURE 2. Chemical composition of triphylite (star), ferrisicklerite (square) and heterosite (triangle) from different phosphates nodules in a ternary plot Mg-Fe_{tot}-Mn.

confirmed by the investigation of the phosphate samples collected during the last fieldtrip in July 2010, as well as by analyses of the associated silicates.

REFERENCES

- Atencio, D. (2000). Type Mineralogy of Brazil. Universidade de São Paulo, Brazil, 114 p.
- Bilal, E., Horn A.H., Nalini, H.A. Jr., Mello, F.M., Correia-Neves, J.M., Giret, A.R., Moutte, J., Fuzikawa, K. & Fernandes, M.L.S. (2000). Neoproterozoic granitoid suites in southeastern Brazil. *Rev. Brasil.Geociências* **30**: 51-54.
- Cassedanne, J. & Baptista, A. (1999). The Sapucaia Pegmatite, Minas Gerais, Brazil. *Mineral. Record* **30**: 361-366.
- Fontan, F., Huvelin, P., Orliac, M. & Permingeat, F. (1976). La ferrisicklerite des pegmatites de Sidibou-Othmane (Jelibet, Maroc) et le groupe des minéraux à structure de triphylite. *Bull. Soc. Fr. Minéral. Cristallog.* **99**: 274-286.
- Fransolet, A-M, Keller, P. & Fontan, F. (1986). The phosphate mineral associations of the Tsaobismund pegmatite, Namibia. *Contrib. Mineral. Petrol* **92**: 502-517.
- Ginsburg, A.I. (1960). Specific geochemical features of the pegmatitic process. 21st Intern. Geol. Congress Session Norden Rept Part **17**: 111-121.
- Keller, P., Fontan, F. & Fransolet, A-M. (1994a). Intercrystalline cation partitioning between minerals of the triplite-zwieselite-magniotriplite and the triphylite-lithiophilite series in granitic pegmatites. *Contrib. Mineral. Petrol.* **118**: 239-248.
- Keller, P., Fransolet, A-M. & Fontan, F. (1994b). Triphylite-lithiophilite and triplite-zwieselite in granitic pegmatites : Their textures and genetic relationships. *N.Jb.Mineral.Abh.* **168**(2): 127-145.
- Mason, B. (1941). Minerals of the Varuträsk pegmatite. XXIII. Some iron-manganese phosphate minerals and their alteration products, with special reference to material from Varuträsk. *Geol. Fören. Förhandl.* **63**(2): 117-175.
- Morteani, G., Preinfalk, C. & Horn, A.H. (2000). Classification and mineralization potential of the pegmatites of the Eastern Brazilian Pegmatite Province. *Mineral. Deposita* **35**: 638-655.
- Nalini, H.A., Bilal, E., Paquette, J.-L., Pin, C. & Rômulo, M. (2000). Géochronologie U-Pb et géochimie isotopique Sr-Nd des granitoïdes néoproterozoïques des suites Galiléia et Urucum, vallée du Rio Doce, Sud-Est du Brésil. *Comptes Rendus Acad. Sc., Sc. de la Terre et des Planètes* **331**: 459-466.
- Pecora, W.T., Klepper, M.R., Larrabee, D.M., Barbosa, A.L. & Frayha, R. (1950). Mica deposits in Minas Gerais, Brazil. *U.S. Geol. Survey Bull.* **964-C** : 205-305.
- Pedrosa-Soares, A.C., Noce, C.M., Wiedemann, C.M. & Pinto, C.P. (2001). The Araçuaí-West-Congo Orogen in Brazil: an overview of confined orogen formed during Gondwanaland assembly. *Precamb. Res.* **110**: 307-323.
- Pedrosa-Soares, A.C., Chaves, M. & Scholz, R. (2009). Eastern Brazilian pegmatite province. 4th International Symposium on Granitic Pegmatites, Field trip guide: 1-28.
- Quensel, P. (1937). Minerals of the Varuträsk Pegmatite. I. The lithium-manganese phosphates. *Geol. Fören. Förhandl.* **59**(1): 77-96.

MORPHOLOGY AND PYROELECTRICITY OF TOURMALINE FROM CENTRAL TRANSBAIKALIA, RUSSIA

Vladimir Bermanec^{1§}, Andrea Čobić¹, Vladimir Zebec²,
Snježana Mikulčić Pavlaković² & Victor Zagorsky³

¹ Institute of Mineralogy and Petrology, Dept. of Geology, Faculty of Science, Horvatovac 95, Zagreb, Croatia §vberman@public.carnet.hr

² Croatian Natural History Museum, Demetrova 1, Zagreb, Croatia

³ Vinogradov Institute of Geochemistry, Siberian branch, Russian Academy of Science, Russia

Key words: elbaite, morphology, pyroelectric effect, Transbaikalia

INTRODUCTION

Tourmaline crystallizes in a non-centrosymmetric 3m class, and pyroelectric and piezoelectric effects are expected. Measuring the effect of pyroelectricity on crystals of tourmaline could help in determination of true crystallographic and morphological orientation of crystals.

EXPERIMENTAL

Fifteen transparent prismatic tourmaline crystals of elbaite composition, with terminal pyramidal faces and basal pedion were measured on a two-circle goniometer. All samples studied are collected from two localities of gem-bearing miarolitic pegmatites in Central Transbaikalia, Russia – the Vodorazdel'naya mine and the Malkhan deposit. Their geology and mineralogy are described in detail early (Zagorsky & Peretyazhko 1992; 2008). It was not clear from these morphological measurements whether positive or negative end of crystallographic axis *c* is morphologically terminated.

In order of determining true crystallographic and morphological orientation of tourmaline crystals, pyroelectric effect of tourmaline was measured. Crystals were cooled to a temperature below 0°C (approximately -10 °C) and afterwards heated to the room temperature. Relative electrical charge was measured with digital milivoltmeter.

RESULTS AND DISCUSSION

Tourmaline crystals from different localities show considerably different morphology.

Crystals from the Vodorazdel'naya mine are tricolored (from greenish-yellow at the terminated end, through yellow to violetish-pink at the broken end), (Fig. 1).

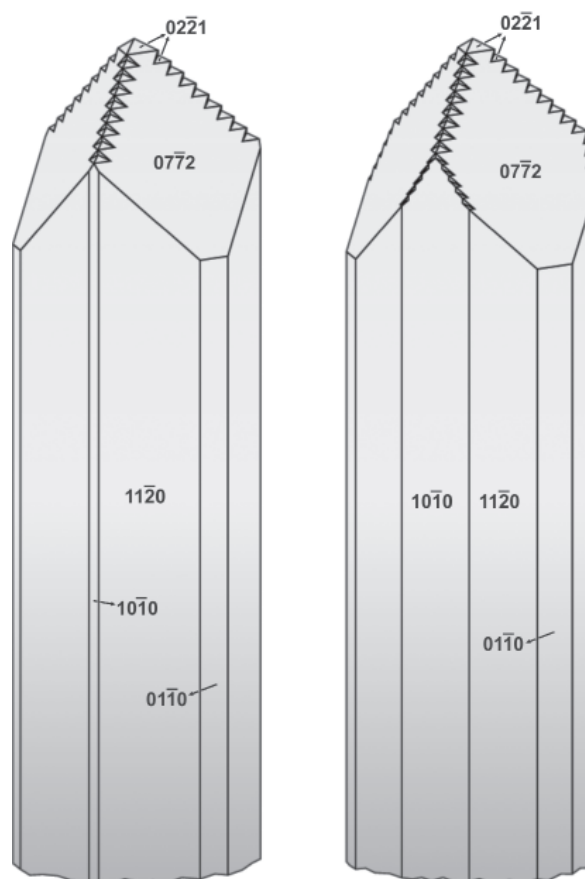


FIGURE 1. Morphology of tourmaline crystals from the Vodorazdel'naya mine, Transbaikalia.

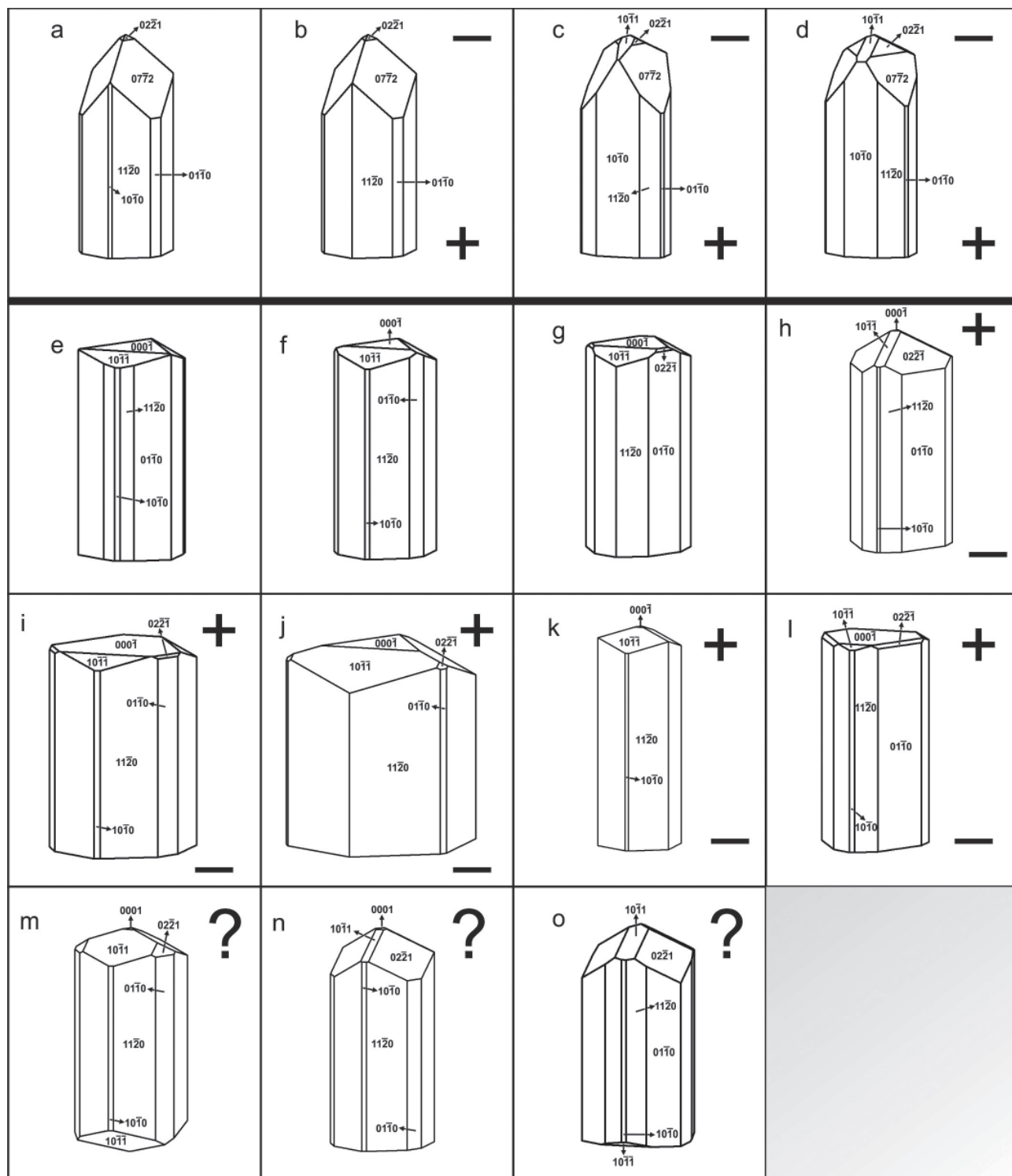


FIGURE 2. Simplified drawings of tourmaline crystal morphology (a-d are crystals from Vodorazdel'naya mine; e-o are crystals from the Malkhan deposit) and indicated pyroelectric effect of measured tourmalines (+ positive; - negative; ? electrical charge was not determined; drawings without any markings were not measured for pyroelectricity).

Crystals are usually terminated only on one side and the other side is broken. Following forms were measured on these crystals: $\{10\bar{1}0\}$, $\{11\bar{2}0\}$, $\{01\bar{1}0\}$, $\{10\bar{1}1\}$, $\{02\bar{2}1\}$ and $\{07\bar{7}2\}$ (Figs. 2a-2d). $\{07\bar{7}2\}$ form gives these crystals extremely sharp termination (Figs. 1, 2a-2d). Terminal form $\{07\bar{7}2\}$ is modified by small faces of $\{02\bar{2}1\}$ form (Fig. 1). Pyroelectric measurements show negative electrical charge at the terminated end of crystals (Figs. 2b-2d).

Terminating faces on the light-purple to brownish-purple crystals from the Malkhan deposit are not as steep as the faces on crystals from the Vodorazdel'naya mine because form $\{07\bar{7}2\}$ is missing. Following forms were determined: $\{10\bar{1}0\}$, $\{11\bar{2}0\}$, $\{01\bar{1}0\}$, $\{21\bar{3}0\}$, $\{10\bar{1}1\}$, $\{02\bar{2}1\}$ and $\{0001\}$. Basal pedion is present on every measured crystal from the Malkhan deposit, but it is more or less dominant. Similar habit was previously described (Goldschmidt 1923). On these crystals, terminated side shows positive electrical charge (fig. 2h-2l).

Three crystals do not show any pyroelectric effect (1m – 1o). Such behavior of tourmaline crystals could be explained with the fact that these crystals are twinned. Twin laws for tourmaline are extremely rare

and tentative (Dietrich 1985), but obtuse angles on crystals which do not show pyroelectric effect suggest that crystallographic axes *c* of twinned crystals are antiparallel.

In order of determining true crystallographic and morphological orientation of tourmaline crystals, detailed investigation is necessary.

REFERENCES

- Dietrich, R.V. (1985). The tourmaline group. New York. Van Nostrand Reinhold Company Inc. 300p.
- Goldschmidt, V. (1923). Atlas der Krystallformen, Tafeln, band IX. Carl Winters Universitätsbuchhandlung, Heidelberg.
- Zagorsky, V.A. & Peretyazhko, I.S. (1992). Gem-bearing pegmatites of Central Transbaikalia. Novosibirsk. Nauka Press. 224 p. (in Rus.).
- Zagorsky, V.Ye. & Peretyazhko, I.S. (2008). The Malkhan Gem Tourmaline Deposit in Transbaikalia, Russia // Mineral Observer: Mineral News from Russia and Beyond. Mineral. Almanac. 13b. M. P. 4-39.

MINERALOGY OF THE BOA VISTA PEGMATITE, GALILÉIA, MINAS GERAIS, BRAZIL

Vladimir Bermanec¹, Ricardo Scholz², Frane Marković¹
Željka Žigovečki Gobac^{1§} & Mario Luiz de Sá Carneiro Chaves³

¹ Institute of Mineralogy and Petrology, Faculty of Science, University of Zagreb, Croatia, §zeljkaz@geol.pmf.hr

² Geology Department, Mining School, Federal University of Ouro Preto, Brazil

³ Geology Department, Geosciences Institute, Federal University of Minas Gerais, Brazil

Key words: pegmatite, lithium bearing pegmatite, spodumene, phosphate.

INTRODUCTION

The Boa Vista pegmatite is located in the Conselheiro Pena pegmatite district, one of the metalogenetic subdivisions of the Eastern Brazilian pegmatite province (EBP) that encompasses an area of about 150,000 km², extending from Bahia to Rio de Janeiro states. Around 90% of the province is located in the eastern part of the State of Minas Gerais. This pegmatite district covers an area of about 500 km² in the municipalities of Conselheiro Pena and Galiléia, in the middle Doce River basin, about 360 km northeasterward from the city of Belo Horizonte.

The Conselheiro Pena pegmatite district is inserted in the central domain of the Araçuaí mobile belt (Almeida 1977), formed during the Brasiliano orogeny (630-490 Ma) by accretion to the eastern margin of the São Francisco craton. In the studied area several suites of granitoid rocks are distinguished (Urucum and Palmital of Eocambrian to Paleozoic age, and Galiléia of Neoproterozoic age), intruding the schists of the Neoproterozoic São Tomé formation.

The São Tomé formation and the granites are found in a north-south extending synclinorium megastructure with metasediments dominating synclines of this structure, granitoid rocks in the adjacent anticlines. Ages of the pegmatite bodies are about 580 Ma (Nalini 1997), and are related to granite G2 supersuite (Pedrosa-Soares *et al.* 2001, 2009) intrusive in the metasediment units. They consist mostly of S-type peraluminous granites and minor metaluminous granites, generated during the syn-collisional stage of the Araçuaí orogen.

The very first description of mineral assemblage of the Boa Vista and others pegmatites in the vicinity were described by Chaves *et al.* (2005).

METHODS

Samples of accessory minerals were collected at the Boa Vista pegmatite for mineralogical studies

and investigated using optical polarizing microscopy followed by mineral phase determination of 34 selected samples using a Philips X'pert powder diffractometer, with CuK α radiation filtered with a graphite monochromator running at 40 kV and 40 mA. X-ray diffraction data sets were collected from 4 to 65°2 θ .

For additional characterization of separated samples Tescan TS 5136 scanning electron microscope (SEM) operating in back scattered (BSE) mode at an accelerating voltage of 20 kV and current of 10 mA was used. The same SEM microscope equipped with the Oxford energy dispersive spectrometer (EDS), coupled with INCA 250 system, was used for elemental distribution analysis in the samples. EDS qualitative analysis and elemental mapping were performed on the carbon coated samples at an accelerating voltage of 20 kV. Quantitative studies by electron probe microanalysis are in progress.

RESULTS

It was possible to distinguish 21 mineral species using optical polarizing microscopy (Fig. 1), X-ray powder diffraction and scanning electron microscopy (Fig. 2). Besides main pegmatitic minerals quartz, microcline, mica and albite, a number of rare minerals were identified (Table 1).

DISCUSSION

Total amount of 21 different mineral species were determined in the Boa Vista pegmatite, half of which belongs to the phosphate mineral group. Common pegmatite minerals found in this pegmatite are albite, microcline, quartz, beryl, spodumene and mica. The other identified minerals are mainly phosphates. The other accessory minerals are cryptomelane, löllingite, fourmarierite, bütschliite, and bismuth. Tantalum and niobium minerals were not found, however, were described by Cassedanne and Cassedane (1979) and Chaves *et al.* (2005).

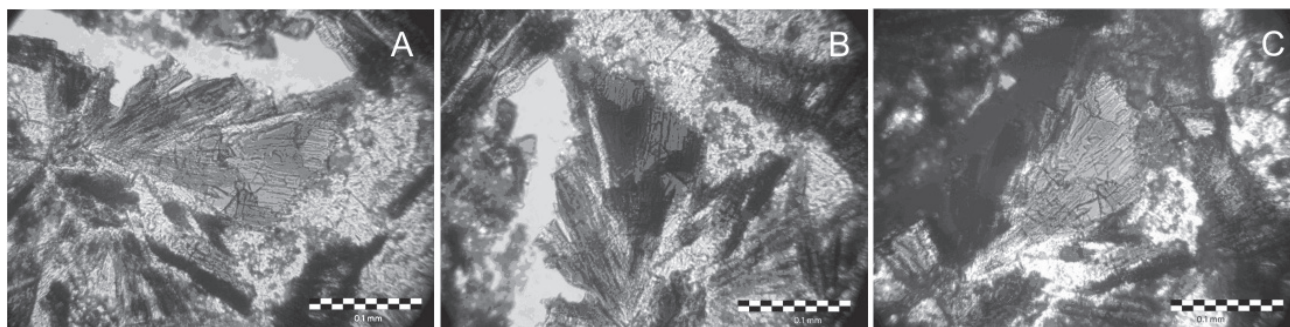


FIGURE 1. Thin sections of rockbridgeite, showing intensive pleochroism. (A) Rockbridgeite spray; mineral is yellowish-brown parallel to X axis of indicatrix. (B) Rockbridgeite spray; mineral is bluish green parallel to Z axis of indicatrix. (C) Rockbridgeite spray (+).

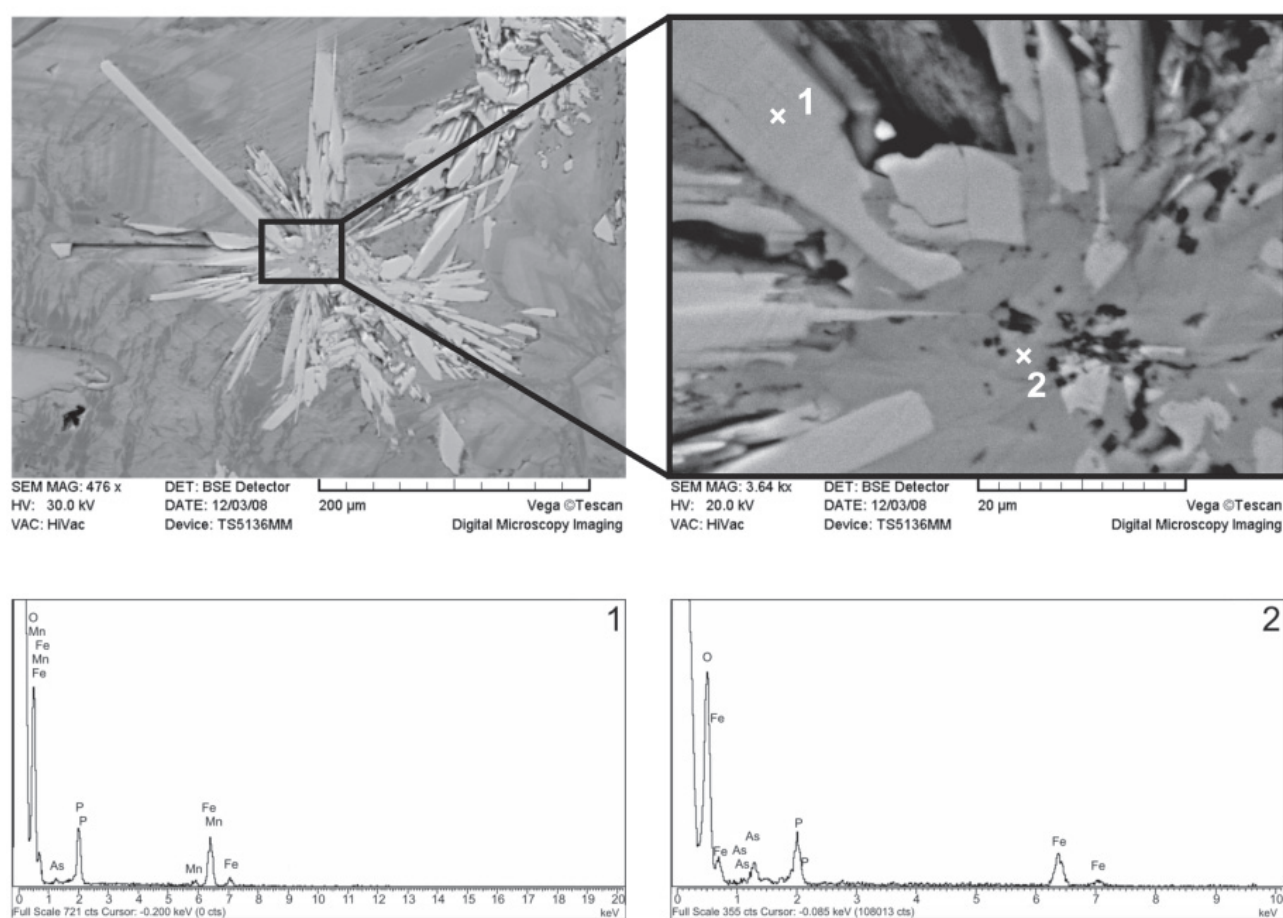


FIGURE 2. BSE photographs and EDS spectrum of rockbridgeite (1) and phosphosiderite (2). Spray of rockbridgeite needles (1 to 20 µm thick and up to 300 µm long) growing from the core of phosphosiderite.

This is the first systematic investigation of mineral samples from Boa Vista pegmatite. Six minerals were described for the first time in that pegmatite (fourmarierite, bütschliite, huréaulite, metatorbenite, strengite and scorodite).

According to minerals determined, Boa Vista pegmatite can be considered as a phosphate-rich pegmatite. Phosphates identified with used methods in the Boa Vista pegmatite are: huréaulite,

cyrilovite, phosphosiderite, variscite, heterosite, strengite, rockbridgeite, metatorbenite, frondelite and scorodite (arsenate).

The phosphate assemblage occurs in miarolitic cavities up to 15 cm or in substitution to triphylite-lithiophilite.

Almost all phosphates identified in the Boa Vista pegmatite are secondary by origin and they belong to the low-temperature hydrothermal mineral

assemblage, and just some of them could be formed by weathering. Only heterosite does not belong to this paragenesis because it is assumed as a metasomatic phosphate (Moore 1973, Hawthorne 1998, Chaves *et al.* 2005, Chaves & Scholz 2008).

TABLE 1. List of identified minerals.

Minerals	
Elements	
Bismuth	Bi
Sulphides (including arsenides)	
Löllingite	FeAs ₂
Oxides	
Cryptomelane	K(Mn ⁴⁺ ,Mn ²⁺) ₈ O ₁₆
Quartz	SiO ₂
*Fourmarierite	PbU ₄ O ₁₃ · 4H ₂ O
Carbonates	
*Bütschliite	K ₂ Ca(CO ₃) ₂
Phosphates (including arsenates)	
Cyrlivite	NaFe ³⁺ ₃ (PO ₄) ₂ (OH) ₄ · 2H ₂ O
Frondelite	(Mn ²⁺ ,Fe ²⁺)Fe ³⁺ ₄ (PO ₄) ₃ (OH) ₅
Heterosite	FePO ₄
*Huréaulite	H ₂ (Mn,Fe) ₅ (PO ₄) ₄ · 4H ₂ O
*Metatorbernite	Cu(UO ₂) ₂ (PO ₄) ₂ · 8H ₂ O
Phosphosiderite	FePO ₄ · 2H ₂ O
Rockbridgeite	(Fe ²⁺ ,Mn)Fe ³⁺ ₄ (PO ₄) ₃ (OH) ₅
*Strengite	FePO ₄ · 2H ₂ O
Variscite	AlPO ₄ · 2H ₂ O
*Scorodite	FeAsO ₄ · 2H ₂ O
Silicates	
Albite	NaAlSi ₃ O ₈
Beryl	Be ₃ Al ₂ Si ₆ O ₁₈
Microcline	KAlSi ₃ O ₈
Mica	-
Spodumene	LiAlSi ₂ O ₆

* Minerals described for the first time in the Boa Vista pegmatite

REFERENCES

- Almeida, F.F.M. (1977). O Craton do São Francisco. *Rev. Bras. Geociências* 7: 349-364.
- Cassedanne J. & Cassedanne J. (1979). Lês minéraux opaques de la pegmatite de Boa Vista (MG) et leur gangue. *Anais da Academia Brasileira de Ciências* 51(2): 311-326.
- Chaves M.L.S.C., Scholz R. & Atencio D. (2005). Assembléias e paragéneses minerais singulares nos pegmatitos da região de Galiléia (Minas Gerais). *Geociência* 24: 143-161.
- Chaves, M.L.S.C. & Scholz, R. (2008). Pegmatito Gentil (Mendes Pimentel, MG) e suas paragéneses mineralógicas de fosfatos raros. *Rev. Escola de Minas* 61: 125-134.
- Hawthorne F.C. (1998). Structure and Chemistry of Phosphate Minerals. *Mineralogical Magazine* 62(2): 141-164.
- Moore, P.B. (1973). Pegmatite phosphates: Descriptive mineralogy and crystal chemistry. *Mineral. Rec.* 4(3): 103-130.
- Nalini Jr. H.A. (1997). Caractérisation des suites magmatiques néoprotérozoïques de la region de Conselheiro Pena et Galiléia (Minas Gerais, Brésil). These de Docteur, Graduate School of engineering, Ecole Nationale Superieure des Mines de Saint Etienne, 237 pp. (in French).
- Pedrosa-Soares, A.C., Noce, C.M., Wiedemann, C.M. & Pinto, C.P. (2001). The Araçuaí-West Congo orogen in Brazil: an overview of a confined orogen formed during Gondwanaland assembly. *Precambrian Res.* 110: 307-323.
- Pedrosa-Soares, A.C., Chaves, M.L.S.C. & Scholz, R. (2009). Eastern Brazilian pegmatite province. In: 4th Internat. Symp. on Granitic Pegmatites (PEG 2009), Recife, Field Trip Guide. 28 pp.

BORON-ISOTOPE VARIATIONS IN TOURMALINE FROM GRANITIC PEGMATITES OF THE BORBOREMA PEGMATITE PROVINCE, NE-BRAZIL

Hartmut Beurlen^{1§}, Robert B. Trumbull²,
Michael Wiedenbeck² & Dwight R. Soares³

¹ Departamento de Geologia, Universidade Federal de Pernambuco(UFPE), Rua Acadêmico Hélio Ramos s.n., 50740-530, Recife, Pernambuco, Brazil § beurlen@ufpe.br

² GeoForschungsZentrum Potsdam, Telegrafenberg B 120 D 14473Potsdam, Germany

³ Instituto Federal de Educação, Ciência e Tecnologia da Paraíba (IFPB), R. Tranquillino Coelho Lemos 671, 58100-000, Campina Grande- Paraíba, Brazil

Key words: B-isotopes, elbaite-schorl-dravite, RE-pegmatites, NE-Brazil.

INTRODUCTION

Soares *et al.* (2008) first analysed the variation of chemical composition of tourmalines from different types of granitic pegmatites and their internal zones in the Borborema Pegmatite Province (BPP), in northeastern Brazil. The results revealed systematic, slightly discontinuous trends from dravitic, to schorlitic and finally to near end-member elbaitic compositions, clearly related to the degree of magma evolution, as observed from the border zones to the cores and replacement bodies in single pegmatite dikes. In this study, selected samples amongst those used by Soares *et al.* (2008) are complemented by ^{11/10}B isotope analyses using SIMS (secondary ion mass spectrometry), aiming to approach the still controversial questions about the igneous or anatectic origin and of the degree of evolution of different pegmatite types in the BPP.

THE STUDIED PEGMATITES

The mineralized pegmatites in the BPP according to the classification proposed by Černý & Ercit (2005) are of the RE class, LCT family, including several types and subtypes established by Soares *et al.* (2008) using mineral chemistry data and ore mineral parageneses. Nearly 80% of the mineralized pegmatites occur intruded into the Neoproterozoic garnet-cordierite-sillimanite bearing biotite-schists of the Seridó Formation, 10% into quartzites and metaconglomerates of the Equador Formation, and less than 10% are hosted by granites or gneissic-granitic rocks of the Paleoproterozoic basement.

The samples used for this study are from five pegmatites, selected to cover a large range of subtypes and with tourmaline found as primary mineral in different pegmatite zones. The Boqueirão pegmatite may be classified tentatively as of the complex spodumene type, Quintos and Capoeira 2 are intermediate between the spodumene and the lepidolite subtype and are known producers of the

Paraíba tourmaline. Carrascão is of the lepidolite subtype (with no spodumene). All of the above are hosted by the quartzites or conglomerates of the Equador formation, while the Fazenda Turmalina is an almost barren homogeneous pegmatite hosted in biotite-schists. Tourmaline crystals were sampled along cross sections from the border zone to the core of the pegmatites. One sample of a probable source granite was also analysed. Detailed geological information of the Boqueirão, Capoeira 2, and Quintos pegmatites may be found in Soares *et al.* (2008) and Beurlen *et al.* (2008).

METHODOLOGICAL AND ANALYTICAL PROCEDURES

All grains and points selected for analysis are interpreted as primary tourmaline (crystallized from the melt) based on the textural relations with other primary pegmatite minerals. The only exception is sample BO-07, with multicolored, zoned elbaite crystals formed on the wall of a vug and therefore likely formed from a late pegmatitic fluid. The samples and sites targeted for SIMS analysis were selected after chemical analyses by EPMA and re-polishing, then ultrasonic cleaning with ethanol and coating with a ~35 nm thick, high purity gold coat. Boron isotope compositions were measured using the CAMECA ims6f SIMS instrument at the GFZ Potsdam. The detailed description of the analytical procedures is given by Trumbull *et al.* (2008).

B-ISOTOPE COMPOSITIONS IN PEGMATITIC TOURMALINE ELSEWHERE

B-isotope compositions of tourmaline from granitic pegmatites reported in the literature are highly variable with values between -27 and +9 ‰ $\delta^{11}\text{B}$. Most values, however, are within a narrow range of $-11.3 \pm 5.4\%$, similar to that of the mostly S-type source granites and metasedimentary sequences from which the granites were derived by crustal anatexis

(Marshall & Ludwig 2006 and references therein). The exceptions are pegmatites intruded into or derived from marine evaporitic sequences, which are enriched in the heavier B-isotope (up to +9‰), or from continental evaporitic sequences with lighter B-isotope compositions, down to -27‰. There have been few systematic studies of B-isotope variations in individual pegmatites. One study of strongly-zoned Elba tourmalines showed unexpectedly small variations with fractionation and decreasing crystallization temperature (Tonarini *et al.* 1998). Trumbull & Chaussidon (1999) found a range in pegmatite-aplite dikes (-12.7 to 21.6‰), and a shift to lower values (-18.0 to -23.0‰) in associated hydrothermal tourmalines due to fluid-related fractionation. Experimental data of $\delta^{11}\text{B}$ fractionation between granitic melt and tourmaline are still unavailable. Experimental results of melt/fluid fractionation by Hervig *et al.* (2002) suggest values of about -5‰ at 650°C to -14‰ at 350°C. This strong temperature dependence of fractionation is much larger than experimental estimates between fluid and tourmaline obtained by Marshall *et al.* (2009) and in disagreement with the smaller variations observed between early magmatic and late magmatic or hydrothermal tourmalines (e.g., Tonarini *et al.* 1998, Trumbull *et al.* 2008 amongst others *apud* Marshall & Ludwig 2006).

BORON ISOTOPE COMPOSITIONS IN TOURMALINE OF THE BPP

The B-isotope composition of tourmaline from the BPP has a total range between -21‰ and +2‰ $\delta^{11}\text{B}$. Most (53 of 66) data are in the range between -17‰ and -9‰, with a strong maximum between -13‰ to -15‰ (Fig. 1). This major part of the dataset will be referred to as the "main population". Its average composition (-13.2 ± 2.0 ‰) is closely similar to the $\delta^{11}\text{B}$ values of tourmaline from a S type pegmatitic granite in the same district (-13.3 to -15.1‰). This granite type is therefore proposed to be the source of the pegmatites. Figures 1A and 1B show that the main population includes all tourmaline varieties from schorl-dravite to varicolored elbaite, suggesting a common magmatic source for the elbaites (including blue "Paraíba Tourmaline") and dravite-schorl. There is no systematic difference in B-isotope composition between different pegmatites, but it is possible to note a slight shift towards lighter isotope compositions for elbaite from inner pegmatite zones (average $\delta^{11}\text{B}$ -14.1 ± 1.3) compared with dravite-schorl from the border and wall-zones (average -12.1 ± 2.0). A lighter isotope composition of the inner zone tourmaline is consistent with crystallization from evolved magma after preferential loss of ^{11}B by volatile exsolution as suggested by Jiang & Palmer (1998) and Trumbull & Chaussidon (1999), but the compositional range of these two groups overlap and with present data it is not possible to confirm that this difference is statistically significant. Figure 2

shows the variation of $\delta^{11}\text{B}$ versus ^{27}Al in tourmaline (^{27}Al as an index of magma fractionation). There is no correlation of isotopic and chemical variations in either of the two groups (elbaite and schorl-dravite), nor were any correlations observed between $\delta^{11}\text{B}$ and other chemical parameters in tourmalines like Li, F or the Fe/(Fe+Mg) ratio.

Some strongly zoned crystals were studied to check for isotopic variations during growth and shifting composition. There are examples of colour-zoned tourmaline lacking any isotopic zonation, as noted in Elba by Tonarini *et al.* (1998). The results in the present case are erratic (Fig. 2). For example a crystal from Carrascão shows a strong zonation (6 ‰ variation) with lighter rims than cores, consistent with Rayleigh fractionation and loss of ^{11}B to exsolved fluid. Another zoned tourmaline from Boqueirão displays the opposite trend, with rims much heavier than cores (10 ‰ difference), and this is possibly due to late influx of an external, isotopically heavy B-source. In addition, crystals without apparent textural differences in the same sample (e.g. CA2-08) may have very different $\delta^{11}\text{B}$ values (-15 and near 0.0) and core – rim trends. This erratic behavior may be due to sporadic contribution of different B-sources, as wall-rock assimilation, external fluids and, as suggested by Thomas *et al.* (2006), coexistence of immiscible melts and volatiles during the pegmatite crystallization process.

ACKNOWLEDGEMENTS

This research was supported by CNPq grants APQ 471064/2006-8 & 301204/2004-7. Review and very constructive comments by David London were greatly appreciated.

REFERENCES

- Beurlen, H., Da Silva, M.R.R., Thomas, R., Soares, D.R. & Olivier, P. (2008). Nb-Ta-(Ti-Sn)-Oxide mineral chemistry as tracers of rare-element granitic pegmatite fractionation in the Borborema Province, Northeastern Brazil. *Mineral. Deposita* 43: 207-228.
- Černý, P. & Ercit, T.S. (2005). The classification of granitic pegmatites revisited. *Can. Mineral.* 43: 2005-2026.
- Hervig, R L., Moore, G. M. , Williams, L.B. Peacock, S.M, Holloway, J.R & Roggensack, K. 2002 Isotopic and elemental partitioning of boron between hydrous fluid and silicate melt. *Am. Mineral.* 87: 769-774.
- Jiang, S-Y. & Palmer, M.R. (1998). Boron isotope systematics of tourmaline from granites and pegmatites: a synthesis. *Eur. J. Mineral.* 10: 1253-1265.
- Marschall, H. R. & Ludwig, T. (2006). Re-examination of the boron isotopic composition of tourmaline from the Lavicky granite, Czech Republic, by secondary ion mass spectrometry: back to normal. *Geochemical Journal* 40: 631- 638.

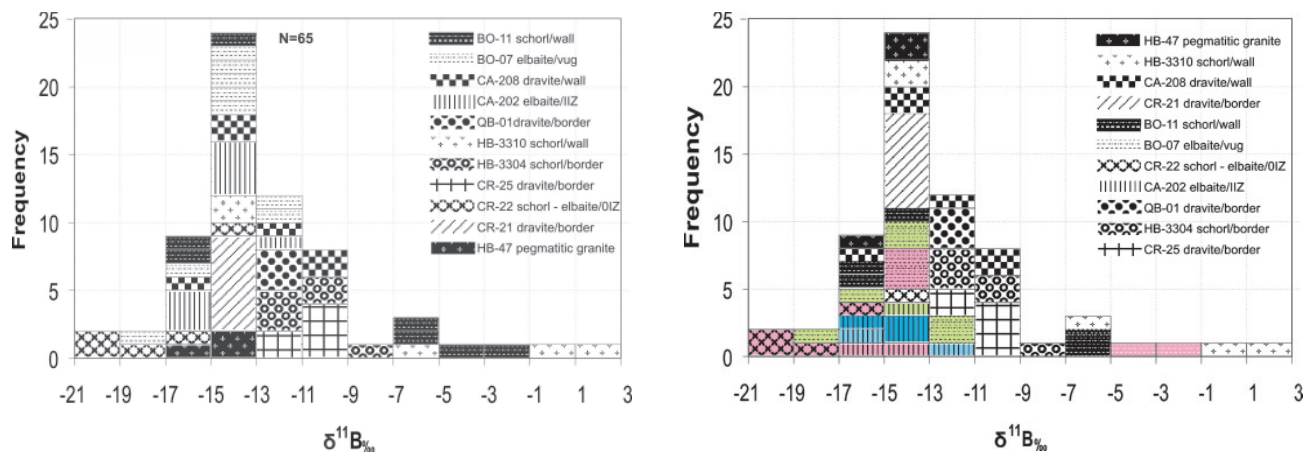


FIGURE 1. **A.** Frequency histogram of B-isotope data arranged according to the hosting pegmatite: BO=Boqueirão; CA=Capoeira2, QB=Quintos, HB33=Fz. Turmalina, CR=Carrascão, HB47=pegmatitic granite. **B.** Frequency histogram of B-isotope data arranged according to the tourmaline species: black and white symbols refer to dravite-schorl and colored symbols to color zoned elbaite crystals. The colors represent the Paraíba Tourmaline (darker blue), the lighter blue portions (light blue), green rims (green) and light pink or colorless cores (pink). The graphic symbols represent the hosting pegmatites and are the same of the upper diagram: elbaite of different colors are not significantly different than the frequency distribution of the whole data set and of dravite-schorl.

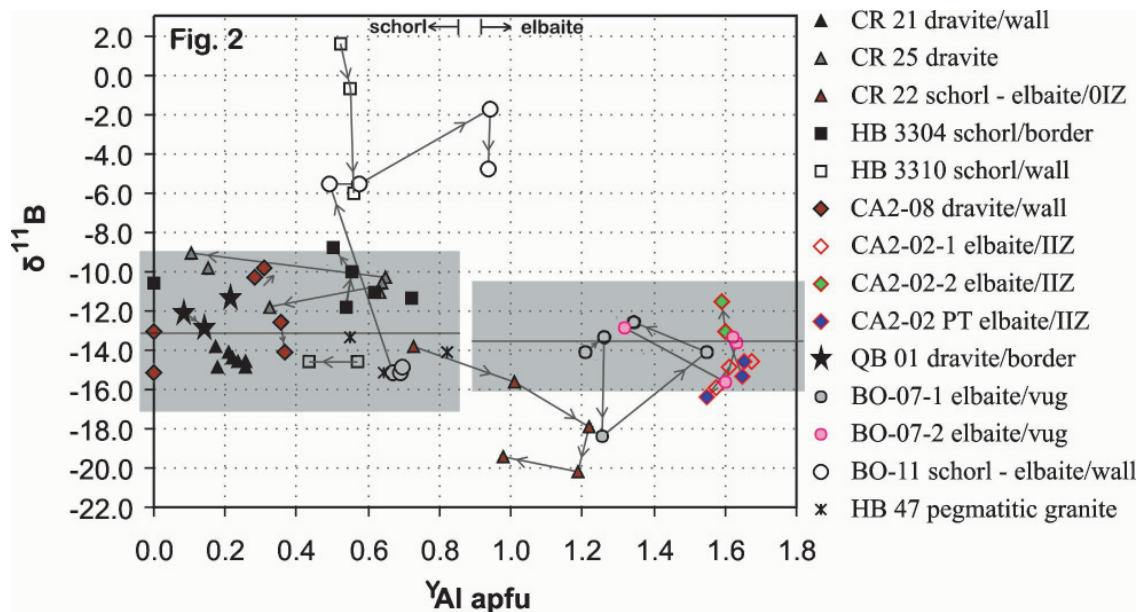


FIGURE 2. Plot of B-isotope compositions *versus* chemical composition in atoms per formula unit (apfu) of Al in the Y-site. Data of zoned tourmaline crystals are linked by arrows indicating the growth direction from core to rim. The B-isotope variations in the zoned crystals are erratic. The heavy lines and gray boxes represent averages ± 1 sd.

Marschall, H.R., Meyer, C., Wunder, Ludwig, T. & Heinrich, W. (2009). Experimental boron isotope fractionation between tourmaline and fluid: confirmation from in situ analyses by secondary ion mass spectrometry and from Rayleigh fractionation modeling. *Contrib. Mineral. Petrol.* **158**: 675-681.

Soares, D.R., Beurlen, H., Barreto, S.B., Da Silva, M.R.R. & Ferreira, A.C.M. (2008). Compositional variation of tourmaline-group minerals in the Borborema Pegmatite Province, northeastern Brazil. *Can. Mineral.* **46**: 1097-1116.

Thomas, R., Webster, J.D. & Davidson, P. (2006). Understanding pegmatite formation: the melt and fluid inclusion approach. *MAC Short Course* **36**: 189-209.

Tonarini, S., Dini, A., Pezzotta, F. & Leeman, W. P. (1998). Boron isotopic composition of zoned (schorl-elbaite) tourmalines, Mt. Capanne Li-Cs pegmatites, Elba (Italy). *Eur. J. Mineral.* **11**: 941-952.

Trumbull, R.B. & Chaussidon, M. (1999). Chemical and boron isotopic composition of magmatic and hydrothermal tourmalines from the Sinceni granite-pegmatite system in Swaziland. *Chem. Geol.*, **153**: 125-137.

Trumbull, R.B., Krienitz, M.S., Gottesmann, B. & Wiedenbeck, M. (2008). Chemical and B-isotope variations in tourmalines from an S-type granite and its source rocks: the Erongo granite and tourmalinites in the Damara Belt, Namibia. *Contrib. Mineral. Petrol.* **155**: 1-18.

CHEMICAL CHARACTERIZATION AND CHROMOPHORE ELEMENTS IN ELBAITES FROM BORBOREMA PROVINCE, BRAZIL

Sandra de Brito Barreto^{1§}, Andrea Čobić², Željka Žigovečki Gobac²,
Vladimir Bermanec² & Goran Kniewald³

¹ Department of Geology, Federal University of Pernambuco, Av. Academico Hélio Ramos. S/N. 5 andar.,
Cidade Universitária. Recife. PE. Brasil, §sandrabrito@smart.net.br

² Institute of Mineralogy and Petrology, Faculty of Science, Horvatovac 95, Zagreb, Croatia

³ Department of Marine and Environmental Research, Rudjer Bošković Institute, Bijenička 54,
10000 Zagreb, Croatia

Key words: elbaite, Borborema pegmatite province, chromophore elements, EMPA, ICP-MS

INTRODUCTION

Tourmalines from the north-east Brazil (Borborema Pegmatite Province - BPP) have attracted attention of mineralogists and gemologists for their extraordinary characteristics, especially their color. The most appreciated are blue-colored, also known as "Paraíba" tourmalines. They have been widely used as gemstones of high quality and value, but nevertheless, there is not much published data on crystal-chemical properties of these tourmalines. The knowledge about the color of these tourmalines is not complete and the cause is always a controversial subject. Most of them are related to transition elements substitutions, such as Fe, Mn and Ti, occurring in different valence states incorporated in the Y site of the tourmaline structure. On the other side, the models for color centers are based on optical absorption data and crystal theory, and generally are assigned to electron-hole traps (Nassau 2001). In this paper we focus on correlation of different colors of these tourmalines and possible chromophore elements.

EXPERIMENTAL CONDITIONS

Samples of blue, green, pink and turquoise tourmaline from BPP were chosen for this study.

Chemical composition of tourmalines with different colored zones was determined by EMPA, model CAMECA SX50 using internal standards of tourmaline enabled to analyze minor and trace elements with good reliability. The current and voltage used for these analyses and the correspondents elements analysed, were respectively, 15nA/6kV (F and B) and 30nA/25kV (Mn, Fe, Cu, Zn, Ca, Bi, Ti, Na, Si, Al, Mg). These internal tourmaline standards were created using samples of tourmaline previously analyzed by ICP-MS, model Perkin Elmer Elan 6000.

RESULTS AND DISCUSSION

All analyzed samples belong to elbaite (Table 1). Figure 1 shows the diagram of Al, Al₅₀Fe_(tot)₅₀ and Al₅₀Mg₅₀ tourmaline (Henry & Guidotti 1985) with plotted data from these analysis. Formulae are calculated on the basis of 6 Si apfu (M. Novák, pers.comm.). Excess of B is probably connected with fluctuation in analysis, although the analysis were

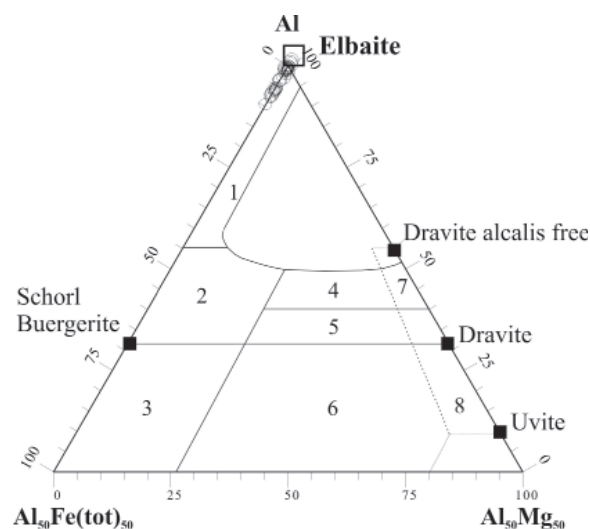


FIGURE 1. Diagram Al-Fe (total)-Mg (molecular proportions) for tourmalines from different rock types with data from the analysis plotted. The fields are: (1) granites and granitic pegmatites rich in Li and aplite, (2) granitoids poor in Li and his pegmatite and aplite associates, (3) rocks quartz-tourmaline-rich Fe³⁺ (hydrothermally altered granites), (4) metapelites and metapsammitic coexisting with minerals saturated in Al, (5) metapelites and metapsammitic without minerals saturated in Al, (6) rock quartz-tourmaline-rich Fe³⁺, calcosilicáticas and metapelites, (7) metaultramafic poor in Ca and metasediments rich in Cr- V (8) and metacarbonates metapiroxenitos. Henry & Guidotti (1985)

TABLE 1. Formula calculations of tourmalines based on microprobe data.

sample color wt. %	PAD-16 blue	C7A blue	C9A greenish blue	S6VA greenish blue	PAD-17 green	PAD-14 turquoise	PAD-08 pink/red	B-11R pink/red
SiO ₂	37.84	37.25	37.44	37.09	37.14	37.43	37.67	39.15
TiO ₂	0.01	0.02	0.00	0.00	0.31	0.01	0.01	0.00
B ₂ O ₃	12.56	14.64	9.54	12.13	14.04	14.19	14.95	15.51
Al ₂ O ₃	37.00	35.62	38.6	40.62	39.43	38.79	42.98	40.71
Bi ₂ O ₃	0.01	0.00	0.00	0.01	0.05	0.00	0.00	0.00
MgO	0.00	0.00	0.03	0.00	0.09	0.00	0.00	0.00
CaO	0.18	0.14	0.28	0.08	0.50	0.13	0.44	0.13
MnO	1.53	1.19	1.09	0.75	0.52	1.95	0.28	0.11
FeO	2.35	3.10	4.94	3.16	2.21	0.36	0.01	0.01
CuO	0.01	0.00	0.00	0.00	0.80	1.54	0.01	0.00
ZnO	2.47	2.71	0.07	0.11	0.09	0.07	0.00	0.00
Na ₂ O	2.45	2.38	2.29	2.00	1.51	1.68	1.17	1.22
H ₂ O	3.00	2.97	2.95	3.33	3.30	3.32	3.58	3.44
F	1.59	1.75	1.43	0.82	1.16	1.07	0.22	0.64
O=F	0.67	0.74	0.60	0.34	0.49	0.45	0.09	0.47
Total	101.00	101.77	98.66	100.10	101.15	100.54	101.32	100.92
apuf								
Si	6.000	6.000	6.000	6.000	6.000	6.000	6.000	6.000
Ti	0.001	0.000	0.000	0.000	0.038	0.001	0.001	0.000
B	3.438	4.071	2.394	3.387	3.915	3.927	4.111	4.103
Al	6.915	6.763	7.291	7.745	7.508	7.329	8.069	7.354
Bi	0.000	0.000	0.000	0.000	0.002	0.000	0.000	0.000
Mg	0.000	0.000	0.007	0.000	0.022	0.000	0.000	0.000
Ca	0.031	0.024	0.048	0.014	0.087	0.022	0.075	0.021
Mn	0.205	0.162	0.148	0.103	0.071	0.265	0.038	0.014
Fe _{total}	0.312	0.418	0.662	0.428	0.299	0.048	0.001	0.001
Cu	0.001	0.000	0.000	0.000	0.098	0.199	0.001	0.000
Zn	0.289	0.322	0.008	0.013	0.011	0.008	0.000	0.000
Na	0.753	0.743	0.712	0.627	0.473	0.522	0.361	0.363
F	0.797	0.891	0.725	0.420	0.593	0.542	0.111	0.310
H ₂ O	1.589	1.598	1.579	1.799	1.781	1.778	1.905	1.761

^{*}B₂O₃- value obtained by calculating stoichiometric. ^{**}H₂O – obtained value based on thermogravimetric and thermodiferencial analysis ATD-TG.

done in analytical conditions suitable for analyzing light elements by microprobe (6 KeV, 15 nA, crystal monochromator multilayer Mo/B4C spacing of 2d = 20.5 nm, with an efficiency 40 times greater (c/s peak) than the classical crystals of lead stearates).

ICP - MS data show small, but significant variations in chemical composition. Different colors can be correlated with several elements or even combinations of these elements, such as common chromophores Fe, Mn, Cu and Ti (Table 2). Although Zn is found in an unusually high concentration for

tourmaline, it is rather characteristic for geochemical environment.

The most probable reason for blue coloration of tourmalines from BPP could be the intervalence charge transfer.

Green tourmalines contain important concentration of Fe, Mn, Ti and Cu. Low concentrations of Cu could be a reason for blue color, but it could also be a result of a rather high iron content which is present in blue and green elbaite samples (Tables 1

TABLE 2. Trace elements of tourmalines of different colors based on ICP-MS data.

ppm	blue	green	turquoise	pink
	PAD-16	PAD-17	PAD-14	PAD-08
Na	19234 ± 457	15833 ± 1355	16184 ± 136	14089 ± 1496
Li	6305 ± 72	7094 ± 198	7218 ± 38	8028 ± 618
Ca	1305 ± 112	<660	<1381	2726 ± 1153
Mg	<125	599 ± 89	<287	<251
Mn	12824 ± 101	4000 ± 86	15324 ± 1617	1925 ± 139
Fe	18265 ± 323	16671 ± 153	3094 ± 356	<45
Ti	<62	1454 ± 15	<138	<120
Zn	20018 ± 161	575 ± 42	543 ± 37	<194
Ga	128 ± 0,4	163 ± 1	169 ± 0,01	121 ± 8
Sr	<5	<5	<5	6 ± 0,4
Bi	42 ± 0,4	318 ± 72	18 ± 1	<828
Sc	<5	<5	<5	7 ± 2
Ce	<1	<2	<2	2 ± 0,4
Nb	<1	6 ± 0,2	<1	4 ± 0,4
K	235 ± 21	1412 ± 118	249 ± 53	<169
Pb	<70	<70	<70	271 ± 14
Sn	31 ± 1	<30	<30	308 ± 27
U	<0,2	2 ± 0,03	<0,2	<0,2
Be	12 ± 0,1	19 ± 0,43	5 ± 0,15	14 ±
Cs	4 ± 0,01	0,7 ± 0,16	<5	1 ± 0,1
Rb	<2	8 ± 2	<2	<2
Ge	20 ± 0,5	3 ± 0,2	2 ±	13 ± 0,4
Cu	25 ± 7	3914 ± 44	11310 ± 67	<44

and 2). According to present analysis (Table 2) it is not clear whether it is heteronuclear or homonuclear intervalence charge transfer.

Many authors (Henn & Bank 1990, Fritsch *et al.* 1990, Hawthorne & Henry 1999, Soares *et al.* 2008, Rossman *et al.* 1991) assumed that light blue coloration of these tourmalines is connected with high copper content. However, this study shows in the investigated tourmaline the presence of lower copper content for the blue (PAD-16, Table 1) and much higher copper content in green and turquoise (Table 1, PAD-17 and PAD-14 respectively). It seems that this element is not the only responsible for the blue color.

Low concentration and almost absence of Fe and high concentrations of Mn in pink elbaite (Table 2) suggest that this color is connected with Mn content.

It is more likely that the blue coloration is a result of intervalence charge transfer connected to iron content. Heteronuclear intervalence charge transfer could involve some other transitional metal, for example Ti⁴⁺ like in blue corundum (Nassau 2001) or to Mn²⁺-Ti⁴⁺ (which give yellow color according to Rossman & Mattson 1986). Unfortunately, there is no clear correlation between iron and titanium content in

differently colored tourmalines from this region (Table 2). Then Ti content does not seem to have important role in coloration of this tourmaline. Due to this, it is more likely that combination of homonuclear intervalence charge transfer (Fe²⁺- Fe³⁺) in combination with low copper concentrations produce blue coloration of "Paraíba" tourmaline. Higher concentrations of copper cover this blue and give green or turquoise color, what is in agreement with earlier observations for other blue and green tourmalines (Warner 1935) and with recent conclusions of Fritsch *et al.* (1990) for blue tourmaline samples from São José de Batalha, Paraíba, Brazil.

Additional spectroscopic studies are necessary to make definite conclusions.

REFERENCES

- Hawthorne, E.C. & Henry, D.J. (1999). Classification of the minerals of tourmaline. *Eur. J. Mineral.* **11**: 201-215.
- Fritsch, E., Shigley, J. E. & Rossman, G. R. (1990). Gem-quality cuprian-elbaite tourmalines from São José de Batalha, Paraíba, Brazil. *Gems & Gemol.* **26**: 189-205.

- Henn, U. & Bank, H. (1990). On the colour and pleochroism of Cu-bearing green and blue tourmalines from Paraíba, Brasil. *N.Jb.Mineral. Mh. H.* **6**: 280-288.
- Henry, D. J. & Guidotti, C. V. (1985). Tourmaline as a petrogenetic indicator mineral: an example from the staurolite-grade metapelites of NW Maine. *Am. Mineral.* **70**: 1-15.
- Nassau, K. (2001). *The physics and chemistry of colors. The fifteen causes of color.* John Wiley and Sons, Inc. New York, 481 p.
- Rossmann, G.R., Fritsch, E. & Shigley, J.E. (1991). Origin of color in cuprian elbaite from Sao José da Batalha, Paraíba, Brasil. *Am. Mineral.* **76**: 1479-1484.
- Rossmann, G. R. & Mattson, S. M. (1986). Yellow, Mn-rich elbaite with Mn-Ti intervalence charge transfer. *Am. Mineral.* **71**: 599-602.
- Soares, D. R., Beurlen, H., de Brito Barreto, S., da Silva, M. R. & Ferreira, A. C. M. (2008). Compositional variation of tourmaline-group minerals in the Borborema pegmatite province, northeastern Brazil. *The Can. Mineral.* **46**: 1097-1116.
- Warner, T. W. Jr (1935). Spectrographic analysis of tourmalines with correlation of color and composition. *Am. Mineral.* **20**: 531-536.

PRELIMINARY FLUID INCLUSION RESULTS FROM THE RUBICON PEGMATITE, KARIBIB, NAMIBIA

Luisa Broccardo^{1§}, Judith A. Kinnaird² & Paul A.M. Nex³

¹ School of Geosciences, University of the Witwatersrand, Johannesburg; §luisa.broccardo@students.wits.ac.za

² Economic Geology Research Unit, School of Geosciences, University of the Witwatersrand.

³ Umbono Group of Companies, Johannesburg.

Key words: LCT pegmatite, fluid inclusion, water, CO₂, daughter minerals, Namibia.

INTRODUCTION

Namibia is well-known for its LCT pegmatites (Rubicon and Helicon) which were mined for lithium in the past, and also pegmatitic granites mined for uranium (Rössing deposit; Basson & Greenway 2004) and tin (Uis deposit; Richards 1986; Fig. 1). We present here the first results, as far as we know, of fluid inclusion studies from the Rubicon LCT pegmatite.

GEOLOGICAL SETTING

A large proportion of Namibia's Li, Be, Nb, Ta and semi-precious gems are hosted within large, internally – zoned LCT pegmatites in the central parts of the Damara Belt, a 560 – 542 Ma orogenic belt extending southwest – northeast through the central parts of Namibia (Roering & Gevers 1964; Diehl 1992a, b; Prave 1996). The Damara Belt has been divided into seven main zones, which are, from north to south, the Northern Platform (NP), Northern Margin Zone (NMZ), Northern Zone (NZ), Central Zone (CZ), Southern Zone (SZ), Southern Margin Zone (SMZ), and the Southern Foreland (SF) (Miller 1983). The CZ is further divided into northern (nCZ) and southern (sCZ) sections (Miller 1983). Lithologies of the SZ and SMZ are dominated by a high pressure, low temperature (~ 600° C at ~ 10 kbar; Kasch 1983) kyanite facies mineral assemblages (Fig. 2), while those of the CZ contain low pressure, high temperature (~ 750° C at ~ 5.0-6.0 kbar; Kasch 1983) cordierite-sillimanite facies minerals (Fig. 2), and are associated with syn- to post-tectonic intrusive bodies, predominantly of granitic composition (Fig. 2; Goscombe *et al.* 2004).

RUBICON PEGMATITE

The Rubicon pegmatite is located on the farm Okangava Ost 72, 30 km southeast of Karibib (Roering & Gevers 1964, Diehl 1992a, b). It is a large, internally-zoned LCT pegmatite which comprises two ellipsoidal orebodies surrounded by quartzo-feldspathic

pegmatite that intruded into quartz monzodiorite and coarse-grained, pegmatitic two-mica granite of Pan African age (Roering 1963, Diehl & Schneider 1990).

Rubicon I is the larger of the two pegmatite bodies, and represents the main orebody (Roering & Gevers 1964). It forms a prominent ridge striking northeast and dipping 18 – 25° northeast (dip increases to 46° at the footwall contact), which measures 320 m in length and 25 – 35 m in width (Diehl 1992b).

Roering & Gevers (1964) identified a number of zones (Figs. 3-4) in the Rubicon pegmatite, based on dominant mineralogy:

- ◆ Border Zone: Fine-grained perthitic feldspar, quartz and garnet.
- ◆ Wall Zone: Albite, quartz, muscovite, tourmaline and garnet (spessartine).
- ◆ Intermediate Zone: Quartz, Li-muscovite, lepidolite, microcline-perthitic feldspar, cleavelandite, with accessory beryl, apatite, and Li-phosphates.
- ◆ Perthite Zone: Pure, coarse-grained perthitic feldspar.
- ◆ Outer Core Beryl Zone: Dominant cleavelandite and muscovite with quartz, beryl and accessory frondelite; frondelite weathers to form black Mn-oxide dendrites, which act as a useful identification tool for the zone.

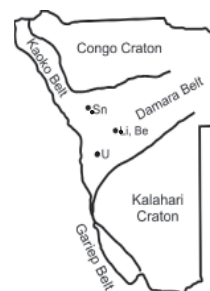


FIGURE 1. Simplified map of Namibia showing the localities of pegmatite-hosted Sn, Li, Be & U.

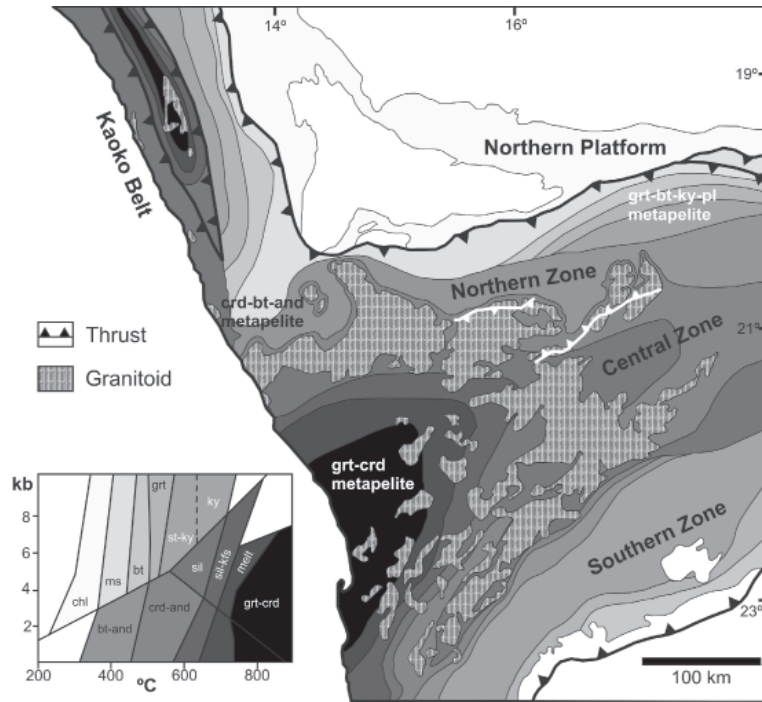


FIGURE 2. Simplified representation of peak metamorphic conditions in the Damara Orogen, as determined from metamorphic studies on metapelites in the Damara and Kaoko Belts (Jung & Mezger 2003; modified after Goscombe *et al.* 2004).

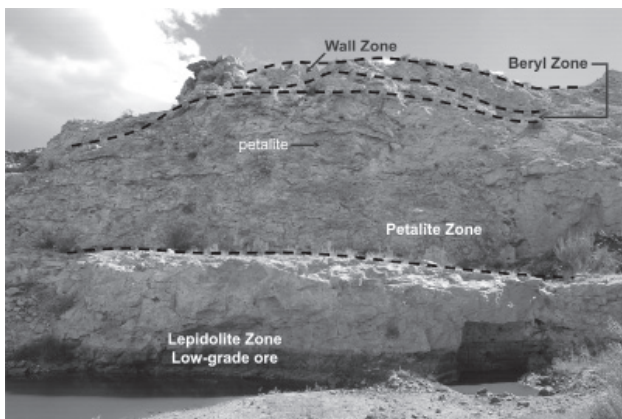


FIGURE 3A. Zonation of Rubicon Pegmatite observed in the footwall.

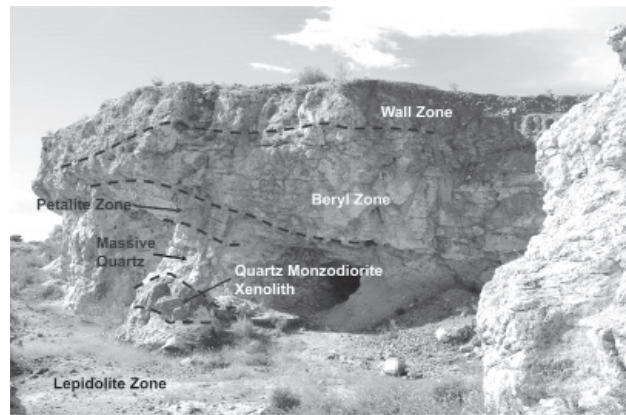


FIGURE 3B. Zonation of Rubicon Pegmatite observed in the hangingwall.

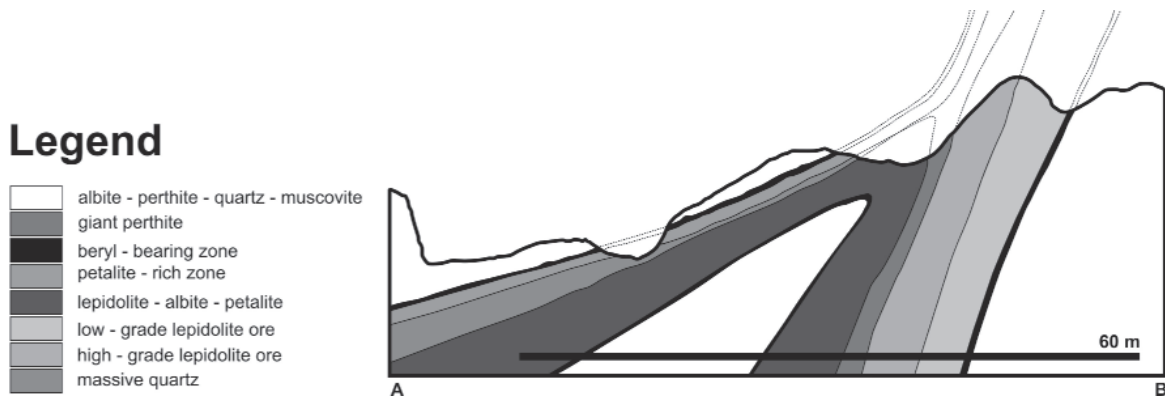


FIGURE 4. Idealised cross-section of the Rubicon Pegmatite (after Roering & Gevers 1964).

- ◆ Outer Core Petalite Zone: Variable mineralogy ranging from pure petalite to an assemblage of petalite, albite, lepidolite, amblygonite, and subordinate quartz, with accessory columbite, apatite, fluorite, and Li-phosphates.
- ◆ Outer Core Lepidolite Zone: Comprising two units; the outer unit contains low grade lepidolite ore, admixed with other minerals, e.g. albite, quartz, amblygonite and petalite, and the inner unit, adjacent to the quartz-rich core, comprising high grade lepidolite ore. The change from low grade ore inwards to high grade ore is transitional, from mainly aplitic albite containing speckles of lepidolite, to almost pure lepidolite.
- ◆ Quartzose Core Zone: Dominant quartz, but also other mineral constituents such as lepidolite, albite, petalite, and amblygonite, as well as small amounts of white beryl. Zonation in this Zone replicates the large-scale zonation of the pegmatite, and the most central part is composed of massive quartz.

FLUID INCLUSIONS IN RUBICON PEGMATITE

Quartz sampled from each zone of the Rubicon Pegmatite contains abundant fluid inclusions. Two populations of fluid inclusions have been identified during preliminary petrographic and microthermometric studies. In both populations, the fluid inclusions are variable in size, ranging from as small as ~ 5 μm to as large as 50 μm .

The first population of fluid inclusions is considered primary. They are polyphase aqueous-carbonic inclusions; the *degree of fill* (F) = 0.95, and they contain as many as four salts and an opaque phase ($S_1 - S_5$, Fig. 5). The composition of all the salts and the opaque phase has not yet been determined. Final melting of ice (T_{mi}) occurs at -0.6 $^{\circ}\text{C}$, indicating



FIGURE 5. Primary inclusion containing H_2O , CO_2 and four salts.

a salinity of ~ 2 wt% NaCl. Homogenization ($L + V \rightarrow L$) temperatures vary from 290 – 335 $^{\circ}\text{C}$.

The second population of fluid inclusions cross cuts the first and comprises three-phase aqueous-carbonic inclusions ($F = 0.7$). At room temperature no daughter minerals are observed (Fig. 6). Clathrate dissociation (T_{mc}) occurs at 8 $^{\circ}\text{C}$, indicating a slightly higher salinity (~ 4 wt% NaCl) than in the primary inclusions.

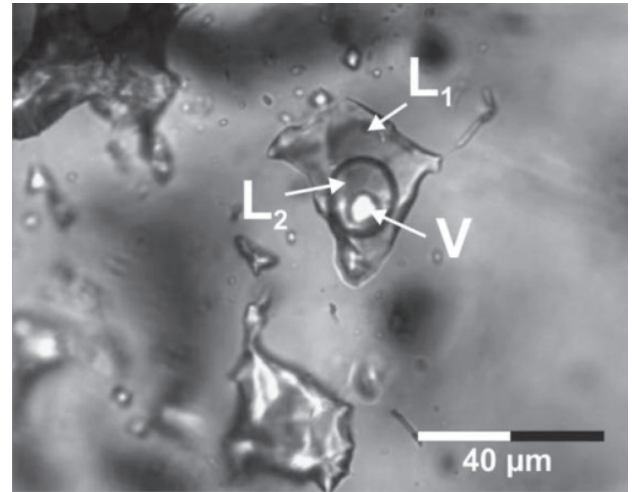


FIGURE 6. Secondary CO_2 – rich fluid inclusion.

REFERENCES

- Basson, I.J. & Greenway, G. (2004). The Rössing uranium deposit: a product of late-kinematic localization of uraniumiferous granites in the Central Zone of the Damara Orogen, Namibia. *J. Afr. Earth Sci.* **38**: 413-435.
- Diehl, B.T.M. (1992a). Lithium, beryllium and cesium. In Miller, R. McG. *Mineral Resources of Namibia*, Ministry of Mines and Energy, Geological Survey of Namibia, Windhoek **6.15**: 1-18.
- Diehl, B.T.M. (1992b). Niobium and tantalum. In Miller, R. McG. *Mineral Resources of Namibia*, Ministry of Mines and Energy, Geological Survey of Namibia, Windhoek **3.5**: 1-20.
- Diehl, B.J.M. & Schneider, G.I.C. (1990). *Geology and mineralisation of the Rubicon Pegmatite, Namibia*. Geological Survey of Namibia Open File Report, 20 pp.
- Goscombe, B., Gray, D. & Hand, M. (2004). Variation in metamorphic style along the northern margin of the Damara Orogen. *J. Petrol.* **45**(6): 1261-1295.
- Jung, S. & Mezger, K. (2003). Petrology of basement-dominated terranes: I. Regional metamorphic $T-t$ path from U-Pb monazite and Sm-Nd

- garnet geochronology (Central Damara Orogen, Namibia). *Chem. Geol.* **198**: 223 – 247.
- Kasch, K.W. (1983). Regional P-T variations in the Damara Orogen with particular reference to early high-pressure metamorphism along the southern margin. *In* Miller, R.McG. (Ed.). *Evolution of the Damara Orogen of South West Africa/ Namibia*. Geological Society of South Africa Special Publication **11**: 243-253.
- Miller, R.McG. (1983). The Pan-African Damara Orogen of South West Africa/Namibia. *In*: Miller, R. McG. (Ed.). *Evolution of the Damara Orogen of South West Africa/ Namibia*. Geological Society of South Africa Special Publication **11**: 431-515.
- Prave, A.R. (1996). Tale of three cratons: tectonostratigraphic anatomy of the Damara Orogen in northwestern Namibia and the assembly of Gondwana. *Geology* **24**: 1115-1118.
- Richards, T.E. (1986). Geological characteristics of rare-metal pegmatites of the Uis type in the Damara orogen, South West Africa/Namibia. *In* Anhaeusser, C.R. and Maske, S. (Eds). *Mineral Deposits of Southern Africa 2*, Geological Society of South Africa, Johannesburg, 1845-1862.
- Roering, C. & Gevers, T.W. (1964). Lithium- and beryllium-bearing pegmatites in the Karibib District, South West Africa. *In* Haughton, S.H. (Ed.). *The Geology of Some Ore Deposits in Southern Africa*, Geological Society of South Africa **2**: 462- 495.

A METASTABLE DISEQUILIBRIUM ASSEMBLAGE OF HYDROUS HIGH-SANIDINE ADULARIA + LOW ALBITE FROM LA VIQUITA GRANITIC PEGMATITE, SAN LUIS PROVINCE, ARGENTINA

Petr Černý^{1§}, Miguel A. Galliski², David K. Teertstra¹, Viviana M. Martínez²,
 Ron Chapman¹, Luisa Ottolini³, Lyndsey MacBride¹ and Karen Ferreira¹

¹ Department of Geological Sciences, University of Manitoba, Winnipeg, MB, Canada R3T 2N2; § p_cerny@umanitoba.ca

² Departamento de Mineralogía y Geoquímica, IANIGLA – CCT Mendoza - CONICET, 5500 Mendoza, Argentina

³ CNR – Istituto di Geoscienze e Georisorse, Sezione di Pavia, Via Ferrata, 1, I-27100 Pavia, Italy

Key-words: high sanidine, adularia, low albite, order-disorder, granitic pegmatite.

INTRODUCTION

Studies of feldspars in granitic pegmatites are mainly devoted to the primary rock-forming phases. Examination of these early feldspar generations substantially contributes to the understanding of pegmatite geochemistry, regional and internal fractionation, solidification and cooling conditions. The geochemical signature of feldspars also aids in pegmatite classification and in evaluation of economic potential.

However, late-crystallizing low-temperature feldspars also attracted attention in pegmatite studies. A broad spectrum of mineral assemblages hosting diverse low-temperature K-feldspars, and the variability in the chemistry and structural state of the feldspars themselves, can illustrate the variety of conditions encountered in late subsolidus stages of pegmatite consolidation and reconstitution. Despite the so far limited number of well examined cases, the occurrences of the late feldspars are undoubtedly much more abundant. However, they easily escape attention because of their commonly inconspicuous appearance in outcrops and hand specimens. Consequently, any new discovery of these feldspars warrants investigation, as it may not only contribute to deciphering late processes at the parent locality, but also to the understanding of the overall spectrum of conditions affecting granitic pegmatites in the waning stages of their evolution.

We describe an occurrence of highly disordered adularia in La Viquita pegmatite, the influence of late fluids on its structural state, and its coexistence with a virtually completely ordered albite. This is, to the best of our knowledge, the first case of a high-sanidine adularia recognized in Argentina, the first documented hydrous adularia, and the second documented case of metastable coexistence of high sanidine with low albite.

THE PARENT PEGMATITE

La Viquita is a rare-element, complex, spodumene-subtype pegmatite in La Estanzuela pegmatite field, located in the San Luis province on the western slope of La Estanzuela range, Eastern Pampean Ranges at approximately 65°06'30" W and 31°51'00" S, close to the southern exposed termination of the Pampean pegmatite province. The peraluminous rare-alkali-enriched LCT pegmatites of this province range from beryl-columbite to spodumene and lepidolite subtypes. La Viquita is representative of the more fractionated members of the overall pegmatite population. A map and a detailed description of the pegmatite, including a preliminary geochemistry of K-feldspar, were published by Martínez & Galliski (2000).

La Viquita is a 190 m long, up to 40 m wide pegmatite of a roughly lenticular shape, emplaced at a moderate but variable dip, discordant with the schistosity of a medium-grade mica schist. A minor border zone (Qtz + Ms) and a volumetrically modest wall (Kfs + Qtz + Ms) envelope a coarse-grained outer intermediate (Kfs + Qtz + Spd + Ms + Ab + Mtb), middle intermediate (Kfs + Qtz + Spd + Ab + Mtb + Ms) and inner intermediate zones (Qtz + Kfs + Spd + Ab + Ms). The core consists of Qtz + Spd + Kfs, whereas fracture-filling units contain Ms + Qtz and replacement units carry Spd + Ab + Qtz. Accessory minerals include beryl, apatite, schorl, eosphorite, ernstite, purpurite, heterosite and an assemblage of (Nb, Ta, Sn, Ti)-oxide phases (Galliski & Černý 2006, Galliski *et al.* 2008).

The perthitic rock-forming K-feldspar shows a moderate degree of fractionation. Across the pegmatite zones, the K₂O content ranges from 10.69 to 14.62 wt.%, Na₂O inversely from 3.05 to 1.75 wt.%, and Rb₂O from 0.15 to 0.74 wt.%, with K/Rb (wt.) from 70 to 18. Structurally, the K-feldspar component is considerably disordered, dominantly monoclinic with subordinate randomly disordered triclinic phases.

THE ADULARIA-BEARING ASSEMBLAGE

The adularia examined occurs closely associated with albite, which is locally earlier but usually coprecipitated. Quartz is present in variable but generally subordinate to minor amounts. Rare apatite is associated with quartz, filling interstices among the euhedral feldspars. Thin veneers of very fine-flaked muscovite coat slightly etched adularia crystals in some cavities but are absent from others. The adularia + albite assemblage follows in part fractures and grain boundaries in the milky quartz and blocky perthitic K-feldspar in the core margin of the pegmatite body, and spreads from them into both the quartz and K-feldspar as replacement aggregates.

ADULARIA

Adularia forms massive aggregates averaging ~1mm in grain size, and euhedral crystals lining small cavities. Sheaf-like radial aggregation of slightly bent crystals is common. The crystals show the typical double-axe habit and the {110}, {10-1} forms, with or without minor {001}. The adularia is highly translucent to opaque milky, white to very pale beige; turbid crystals in cavities are coated with muscovite but clear crystals lack this overgrowth.

Composition of adularia generally corresponds to end-member K-feldspar, with negligible Na and Rb, and mere traces of other components (Table 1, EMPA and SIMS). The compositions of turbid and clear crystals proved to be statistically identical in all their parts (Fig. 1). All compositions, however, display a noticeable shift from the ideal composition, when normalized on the anhydrous basis, in a direction indicative of combined $\square\text{SiO}_4$ and light-element substitutions. Incorporation of H_2O as cationic H^+ overcompensates the discrepancy (Fig. 1), suggesting that some of the hydrogen may be present in a different form bonded to a non-framework oxygen [$\text{H}_2\text{O}^?$, (H_3O^+)?].

TABLE 1. Electron microprobe analyses of representative La Viquita adularia and albite based on eight oxygen anions per unit formula.

	Adularia	Albite
P_2O_5	0.02	0.04
SiO_2	65.46	68.32
B_2O_3	0.0006	0.0002
Al_2O_3	18.00	19.57
Fe_2O_3	0.01	0.01
Li_2O	0.0053	0.0006
Na_2O	0.12	11.77
K_2O	15.73	0.09
Rb_2O	0.24	0.01
Cs_2O	0.01	0.00
CaO	0.00	0.04
SrO	0.03	0.03
BaO	0.09	0.01
PbO	0.01	0.00
H_2O	0.203	0.019
Total	99.93	99.91
P^{5+}	0.001	0.001
Si^{4+}	3.014	2.988
B^{3+}	0.000	0.000
Al^{3+}	0.977	1.009
Fe^{3+}	0.000	0.000
Li^+	0.001	0.000
Na^+	0.011	0.998
K^+	0.924	0.005
Rb^+	0.007	0.000
Cs^+	0.000	0.000
Ca^{2+}	0.000	0.002
Sr^{2+}	0.001	0.001
Ba^{2+}	0.002	0.000
Pb^{2+}	0.000	0.000
H^+	0.062	0.006
$\Sigma\text{Cations}$	4.937	5.004
M^{1+}	1.005	1.009
M^{2+}	0.003	0.003
ΣM	1.008	1.012
$\text{M} +$	1.011	1.015
TO^{2-}	0.976	1.008
$\text{Si} + 2\text{P}$	3.016	2.990
ΣT	3.992	3.998

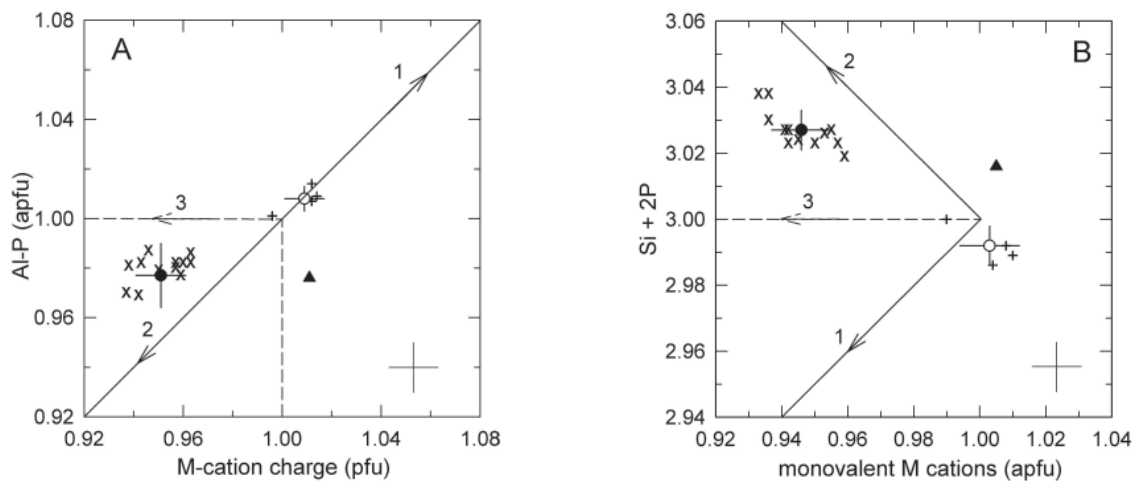


FIGURE 1. Cation variations in La Viquita adularia (x's) and albite (crosses) calculated on anhydrous basis of 8 oxygens: A - (Al-P) vs. M-cation charge with a 1:1 trend line; B - (Si+2P) vs. sum of monovalent cations. Solid and open circles with 1σ standard-deviation bars mark averages for the two feldspars. Crosses indicate the precision (4σ) of measurement for the Eifel sanidine standard. Vectors indicate (1) plagioclase-type substitution M^{2+}Al (M^{1+}Si)₁, (2) the $\square\text{SiO}_4$ substitution, and (3) apparent M-cation deficiency. The triangle marks average adularia adjusted for H^+ from a single analysis.

X-ray powder diffraction shows slight broadening of some peaks at their bases for the turbid material, but the clear crystals generate perfectly shaped monoclinic patterns. Unit-cell dimensions of the clear crystals correspond to virtually disordered high sanidine (Al in $t_1 = 0.260$), whereas those of the turbid crystals are shifted toward low sanidine (Al in t_1 up to 0.308). The b - c data for the most disordered, clear La Viquita crystals plot close to those of gemmy adularia from other localities, and outside the structural end-members (Fig. 2). These data fall outside the quadrangle of end-members as currently defined, possibly affected by the "water" content.

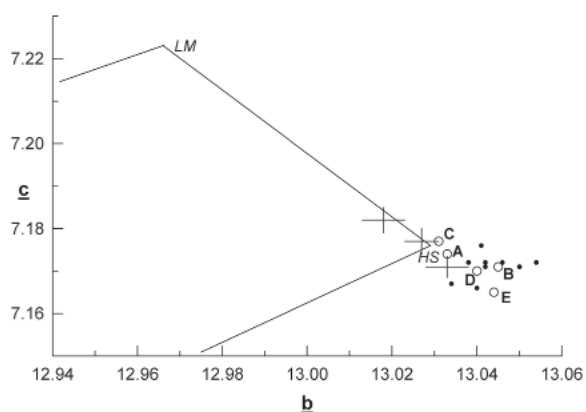


FIGURE 2. The potassic part of the b - c diagram for K-Na feldspars with plots of La Viquita adularia (crosses mark 1σ standard deviation of unit-cell refinements). End-member HS and LM data of the partial quadrilateral from Smith & Brown (1988, Table 7.1). Calculated high-sanidine end-member data (open circles) show data refined for high-sanidine adularia (unlabelled dots) from literature.

CONCLUSIONS

The assemblage of adularia and albite, accompanied by minor quartz and accessory apatite, occurs in La Viquita pegmatite, located in the inner intermediate or core-margin zone. The assemblage was produced by a subsolidus, in part metasomatic, process. Near-end-member chemical compositions of both feldspars and considerable $\square\text{SiO}_4$ and light-element substitutions in hydrous adularia suggest very low temperature of crystallization, probably as low as 200 to 150°C at low pressures of ~2 to ~1 kbar $P(\text{H}_2\text{O})$, well within the stability fields of microcline and low albite. Both feldspars crystallized in a metastable, highly disordered structural state. Whereas (Al,Si) rearrangement in albite proceeded at high rate to virtually complete order (Martin 1969, 1974), adularia is preserved in the original high-sanidine structure (Černý & Chapman 1984, 1986). In general, this adularia was not exposed to late agents that would promote substantial ordering of the tetrahedral

ALBITE

Granular albite and its cavity-lining crystals are thick tabular parallel to {010}, undeformed, with well-developed {001}, {110}, {1-10} and {20-1}. Relatively coarse Albite twinning is common. The chemical composition of albite is very close to $\text{NaAlSi}_3\text{O}_8$, with negligible Ca and K contents. Both the M-cation and tetrahedral populations are statistically identical with those of the ideal composition. Unit-cell dimensions refined from X-ray powder diffraction data and calculated tetrahedral distribution of Al indicate a virtually perfectly ordered low albite (Fig. 3).

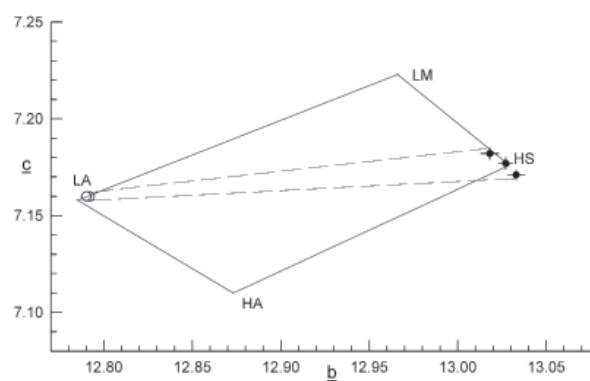


FIGURE 3. The b - c diagram for K-Na feldspars with plots of La Viquita adularia and coexisting albite. Crosses mark standard deviation (1σ) of unit-cell refinements for adularia; for albite, 1σ is within the circle symbols. End-member HS, LM, HA and LA data from Smith & Brown (1988, Table 7.1).

framework. However, some clusters of adularia crystals were subject to mild hydrolytic action of low-pH fluids that etched the crystal faces and precipitated thin films of muscovite. These crystals show variable but generally very modest degrees of incipient (Al,Si) ordering which approaches, but does not attain, the level of low sanidine.

ACKNOWLEDGEMENTS

The field work and postgraduate thesis of VAM were supported by grants Res. 889/94 and PIP 319/98 of CONICET to MAG. The field work also was supported, in part, by the NSERC of Canada Research Grant to PČ. The latter funding financed the laboratory work at the University of Manitoba, together with an NSERC of Canada Major Installation Grant to PČ and Major Equipment plus Infrastructure Grants to Frank Hawthorne. The careful review by E. Roda-Robles is much appreciated.

REFERENCES

- Černý P. & Chapman R. (1984). Paragenesis, chemistry and structural state of adularia from granitic pegmatites. *Bull. Minéral.* **107**: 369-384.
- Černý P. & Chapman R. (1986). Adularia from hydrothermal vein deposits: extremes in structural state. *Can. Mineral.* **24**: 717-728.
- Galliski, M. A., & Černý, P. (2006). Geochemistry and structural state columbite-group minerals in granitic pegmatites of the Pampean Ranges, Argentina. *Can. Mineral.* **44**: 645-666.
- Galliski, M. A., Márquez-Zavalía, M. F., Černý, P., Martínez, V. & Chapman R. (2008). The Ta-Nb-Sn-Ti oxide-mineral paragenesis at La Viquita, a spodumene-bearing rare-element granitic pegmatite from San Luis, Argentina. *Can. Mineral.* **47** (2): 379-393.
- Martin, R.F. (1969). The hydrothermal synthesis of low albite. *Contrib. Mineral. Petrol.* **23**: 323-339.
- Martin, R.F. (1974). Controls of ordering and subsolidus phase relations in the alkali feldspars. In *The Feldspars*, Mackenzie, W.S. and Zussman, J., ed's, Proc. NATO Adv. Studies Institute, Manchester Univ. Press: 313-336.
- Martínez, V.M. & Galliski, M.A. (2000). La Viquita, Sierra de la Estanzuela, San Luis: Geología de una pegmatita de subtipo espodumeno enriquecida en óxidos de Nb-Ta-Ti-Sn. In *Mineralogía y Metalogenia 2000*, Schalamuk, I., Brodtkorb, M. & Etcheverry, R., Eds., INREMI Publ. **6**: 295-303.
- Smith, J.V. & Brown, W.L. (1988). *Feldspar Minerals I. Crystal structures, physical, chemical and microtextural properties*, 2nd ed., Springer-Verlag, Berlin.

CRYSTAL CHEMISTRY OF BLUE GENTHELVITE FROM THE EL CRIOLLO PEGMATITE, CÓRDOBA, ARGENTINA

Fernando Colombo^{1§} & José González del Tánago²

- ¹ CONICET - Cátedra de Geología General, Facultad de Ciencias Exactas, Físicas y Naturales. Pabellón Geología, Universidad Nacional de Córdoba, Vélez Sarsfield 1611, (X5016GCA) Córdoba, Argentina. § fosfatos@yahoo.com.ar
- ² Departamento de Petrología y Geoquímica, Facultad de Ciencias Geológicas, Universidad Complutense, 28040 Madrid, Spain

Key words: helvine group minerals, beryllium, cobalt, copper.

INTRODUCTION

Genthelvite, ideally $Zn_4Be_3(SiO_4)_3S$, is the Zn-dominant member of the helvine group, the other two being danalite and helvine (Fe- and Mn-dominant, respectively). Although helvine-group minerals are not common in granitic pegmatites, a few occurrences are known (see Černý 2002); of the three members, genthelvite is the least common, and almost all of the occurrences are restricted to alkaline rocks.

While chemically pure genthelvite is colorless, the Fe and Mn contents usually impart a yellow, pink, red or brown color; green genthelvite was reported from Niger (Perez *et al.* 1990), but the cause of the coloration was not explored. The first report of blue genthelvite was made by Gay & Gordillo (1976) from Cerro Blanco, Argentina; the same occurrence was later studied by Mas & Peral (1998), who added microthermometric data. To the best of our knowledge, the only other find of blue genthelvite was made in the Vize Pass, San Giacomo, Bolzano Province, Trentino-Alto Adige, Italy, where beautiful zoned green and blue crystals were found in clefts in a meta-quartz porphyry (Gartner & Weiss 2005).

According to Gay & Gordillo (1976), cobalt and nickel (about 300 ppm each) were presumably the chromophores of genthelvite at Cerro Blanco. Copper was found in negligible amounts (approximately between 30 and 100 ppm).

More recent finds revealed a couple of other occurrences at the same quarry, and a range of hues (from pale green to deep greenish blue); color zoning was evident in some samples, but the fine chemical variations had been averaged by the wet chemical methods used by Gay & Gordillo (1976). This prompted us to re-study the genthelvite using electron microprobe analyses, to characterize its chemical composition and explore further the cause of the blue color.

GENTHELVITE OCCURRENCE

Genthelvite occurs as grains and tetrahedral crystals up to about 1 cm long (though usually much smaller) included in masses up to 80 cm, composed of quartz and lamellar to granular hematite, in the second intermediate zone of a small pegmatite located at Cerro Blanco, near Tanti (Córdoba province, Argentina). Its coordinates are $31^{\circ} 21' 22.9'' S - 64^{\circ} 39' 6.1'' W$. Other primary minerals that occur with genthelvite are anatase and, very rarely, tiny inclusions of sphalerite within genthelvite. Rarely, genthelvite crystals are also found scattered in clay minerals (one of them being interstratified illite/smectite) adjacent to the hematite masses. Malachite is a common secondary mineral lining fractures and voids, as well as forming stains in clay minerals.

These hematite masses are only found inside the pegmatite, and are probably related to a hydrothermal stage.

METHODS

Seventy-four electron microprobe analyses were made on eight genthelvite samples in two analytical sessions, using a JEOL JXA 8900M microprobe (WDS mode). The first dataset was measured with a 5 μm beam at 15 kV and 20 nA, with a count time of 10 s at the peak and 5 s at each background position. A second dataset was measured with a 5 μm beam using 10 kV and 150 nA; in addition to those elements which had been detected in the previous analytical session (see below), the following elements were sought: Be, Co, Cu, V, Ni and Cr. The same count times were used, except for Be (20 s at the peak and 10 s at each side of it). $K\alpha$ lines were selected for all elements. Elements measured, and their standards and crystals, include: Si (albite, TAP), Al (sillimanite, TAPH), Zn (gahnite, LIF), Cu (chalcopyrite, LIFH), Fe and Mn (almandine, LIF), Mg (kaersutite, TAP), S (chalcopyrite, PETH), Co

and Ni (Ni-Cr-Co alloy, LIFH), Be (beryl, LDE3H), Ca (kaersutite, PET), V (vanadinite, PET), and Cr (Ni-Cr-Co alloy, PET). Also sought but not detected, and their respective detection limits (2σ , in ppm), were P (fluorapatite, PETH, 440), Ti (kaersutite, PET, 740), Cl (fluorapatite, PETH, 210), and K (microcline, PETH, 250).

RESULTS

Back-scattered electron images reveal that genthelvite grains are slightly to strongly zoned; three patterns can be recognized: A) oscillatory concentric triangular zones, formed during growth of the tetrahedral crystals (Figs. 1A, B & F); B) a patchy zoning with sharp but irregular limits (Figs. 1C & D) late veinlets and patches cross-cutting the crystals, showing strong zoning roughly parallel to the contacts (Figs. 1E & F).

The chemical composition is always dominated by Zn, with a range between 52.77 (Gen₇₇ Dan₂ Hev₁) and 31.77 wt.% (Gen₆₀ Dan₈ Hev₃₂, which at the same time is the Mn-richest analysis). In spite of the fact that Fe was readily available in the environment, genthelvite has Mn slightly dominant over Fe in almost all cases. The Fe-richest composition is Gen₇₅

Dan₁₁ Hev₁₄. There is a poorly defined tendency towards Zn depletion in the rims of the crystals and in the cross-cutting veinlets.

As regards the trace element content, CuO reaches 0.71 wt%, CoO 0.21 wt%, NiO 0.15 wt%, V₂O₃ 0.10 wt%, and Cr₂O₃ 0.13 wt%. There is no relationship between the content of major (Zn, Fe and Mn) and trace elements, nor among trace elements. The chromophores most commonly detected were Cu and Co. The analyses suggest that Cu causes a green color, whereas Co is necessary to produce the bright blue color.

SUBSTITUTIONS IN BLUE GENTHELVITE

In the helvine-group minerals, the most important substitution is among the dominant M^{2+} cations (Zn, Fe and Mn); Ca, Co and Cu are also presumably located in this site.

Trivalent cations (Al, Cr³⁺ and V³⁺) have a charge intermediate between that of Si and the M^{2+} , and therefore it is not straightforward to assign them to either site. In most analyses Al is present in very small amounts, such that the substitution scheme cannot be unambiguously determined. An exception

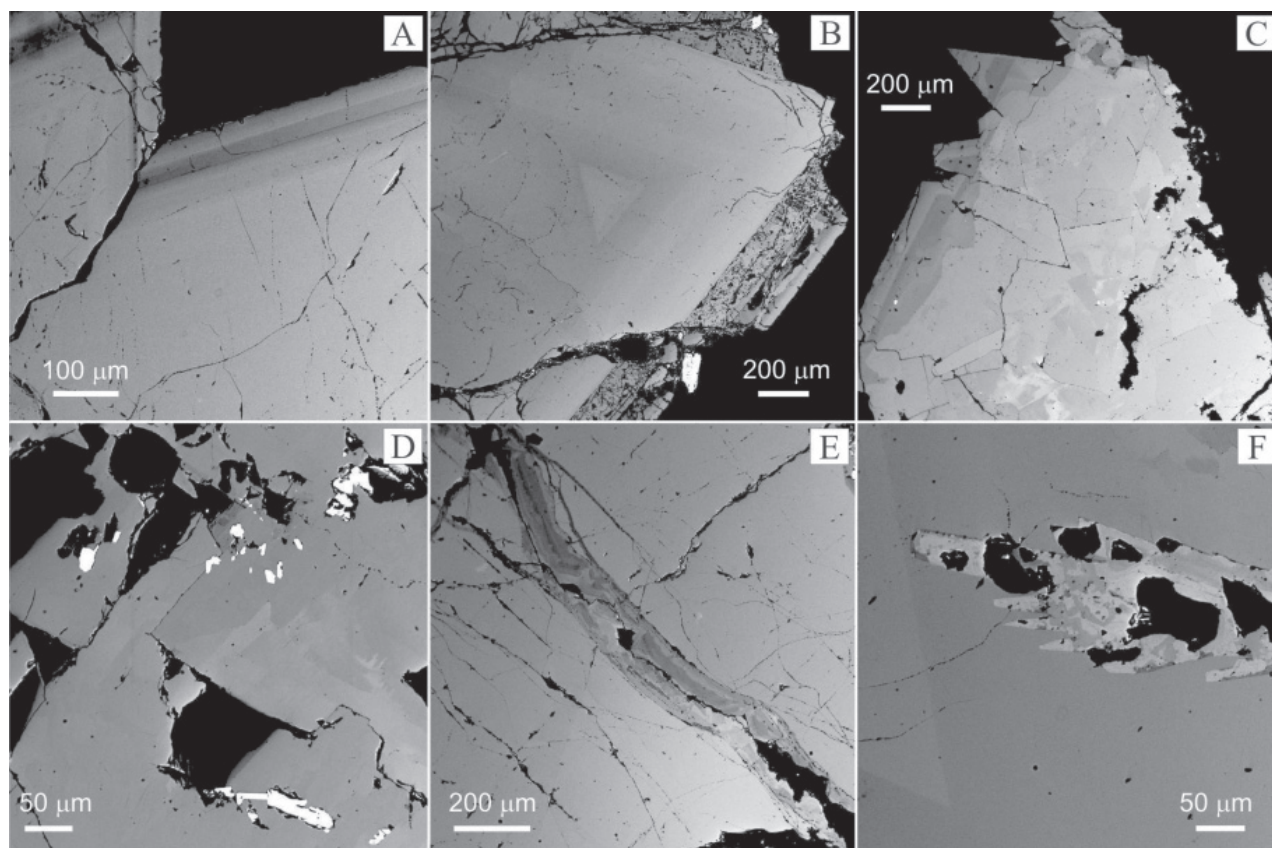


FIGURE 1. BSE images of genthelvite crystals. A and B show concentric zoning, whereas C and D show patchy zoning. E and F are images of cracks and voids filled with a second generation of genthelvite. Bright grains in images B and D are hematite.

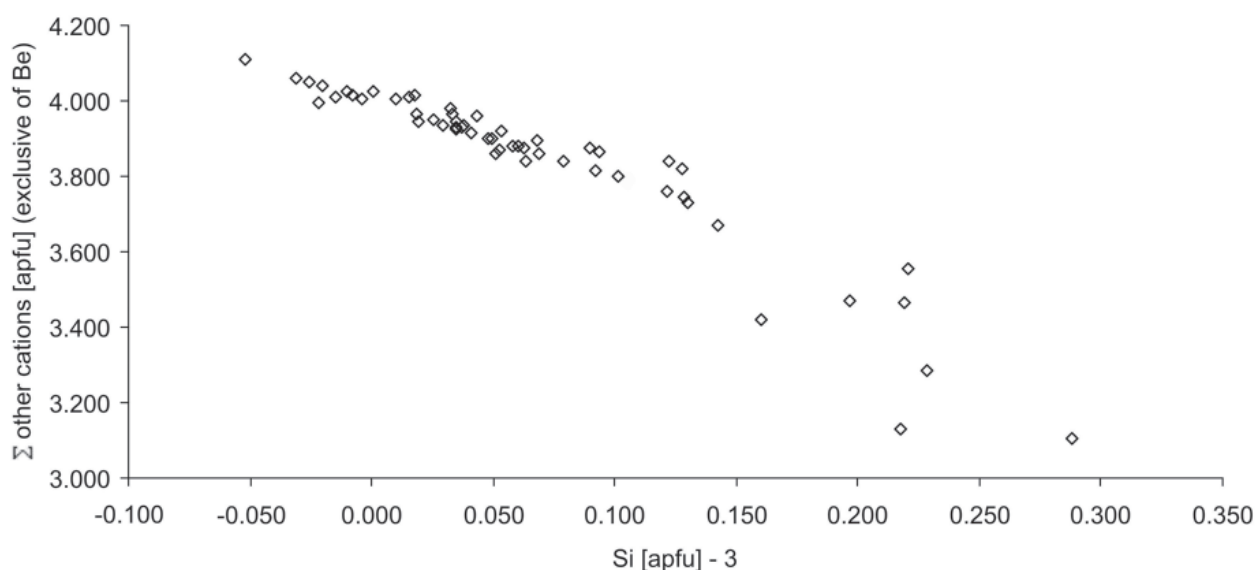


FIGURE 2. Covariation of Si in excess of 3 apfu and the sum of other cations (exclusive of Be), normalized on a 10 (O+S) basis. The ideal formula would be a point located at (0.00;4.00). Data sources: this work plus Mankov (1986), Kwak & Jackson (1986), Finch (1990), Holtstam & Wingren (1991), Raimbault & Bilal (1993), Bilal (1994), Ragu (1994), Nimis *et al.* (1996), Zaw *et al.* (1997), Larsen (1998), Langhoff *et al.* (2000) and Falster (pers. com.)

is the genthelvite analyzed by Finch (1990), with an anomalous Al content (up to 9.68 wt% Al_2O_3) that was negatively correlated with M^{2+} .

An interesting feature of the minerals belonging to the helvine group is the fact that the Si content often exceeds the ideal 3.00 apfu and ΣM^{2+} usually below 4.00 apfu (normalized on a 10 O+S basis, excluding BeO), with a strong negative correlation between the two parameters (Fig. 2).

Despite the difference in X-ray scattering between Si and Be, the SiBe_1 exchange is difficult to prove by structural analysis because of the small amount of Si (≈ 0.1 apfu) typically involved, and also because of the very similar Si-O and Be-O distances in the genthelvite structure. A single-crystal structural refinement (Nimis *et al.* 1996) and the few Be analyses available obtained using electron or ion microprobe (Nimis *et al.* 1996 and this work) suggest that Si and Be are negatively correlated.

Silicon must replace Be (both of which are tetrahedrally coordinated), with charge balance achieved by the introduction of vacancies () at the C site. The scheme (assuming that M^{3+} and M^{2+} share the same site) would be: $\text{Si}^{4+} + \leftrightarrow \text{Be}^{2+} + M^{2+}$ (where $M^{2+} = \text{Zn, Fe, Mn, Co}^{2+}, \text{Cu}^{2+}$, and $1.5 \text{ Al}^{3+}, \text{V}^{3+}, \text{Cr}^{3+}$). This scheme has already been proposed by Finch (1990), who also cautioned about the potential errors that can be introduced by assuming that $\text{Be} = 3.00$ apfu.

ACKNOWLEDGEMENTS

A. Falster kindly provided some unpublished helvite analyses, and D. Holtstam sent copies of his works. We gratefully acknowledge the suggestions made by M. F. Márquez-Zavalía.

REFERENCES

- Bilal, E. (1994). Geochimie et conditions de cristallisation des minéraux du groupe de l'helvite. *Geonomos* **2**: 1-13.
- Černý, P. (2002). Mineralogy of Berillium in Granitic Pegmatites. In: Grew, E.S. (Ed.) *Beryllium-Mineralogy, Petrology and Geochemistry*. *Rev. in Min. & Geochem.* **50**: 405-444.
- Finch, A. (1990). Genthelvite and willemite, zinc minerals associated with alkaline magmatism from the Motzfeld centre, South Greenland. *Mineral. Mag.* **54**: 407-412.
- Gartner, A. & Weiss, S. (2005). Blauer Genthelvin aus Südtirol – ein sensationeller Fund. *Lapis* **30**: 20-23.
- Gay, H.D. & Gordillo, C.E. (1976). Hallazgo de genthelvita $\text{Zn}_8[\text{S}_2/(\text{BeSiO}_4)_6]$ en el Cerro Blanco, Tanti, Córdoba. *Rev. de la Asoc. Arg. de Miner., Petr. y Sedim.* **VII** (3-4): 41-45.

- Holtstam, D. & Wingren, N. (1991). Zincian helvite, a pegmatite mineral from Stora Vika, Nynäshamn, Sweden. *GFF* **113**: 18:3-184.
- Kwak, T.A. & Jackson, P.G. (1986). The compositional variation and genesis of danalite in Sn-F-W skarns, NW Tasmania, Australia. *Neues Jahrbuch Min. Monat.* 452-462.
- Langhof, J., Holtstam, D. & Gustafsson, L. (2000). Chiavennite and zoned genthelvite-helvite as late-stage minerals of the Proterozoic LCT pegmatites at Üto, Stockholm, Sweden. *GFF* **122**: 207-212.
- Larsen A.O. (1998). Helvite group minerals from syenite pegmatites in the Olso region, Norway. *Contributions to the mineralogy of Norway*, No. 68. *Norsk Geol. Tidsskr.* **68**: 119-124.
- Mankov, S. (1986). A new genetic type of helvite mineralization in Bulgaria (in Bulgarian). *Ann. Higher Inst. Mining & Geology, Sofia, Part II: Geol.* **32**: 95-104.
- Mas, G.R. & Peral, H.R. (1998). Genthelvita de la cantera El Criollo, Cerro Blanco; Córdoba. 4° Reunión de Mineralogía y Metalogenia. Universidad Nacional del Sur. Bahía Blanca. *Proceedings*, 185-190.
- Nimis, P., Molin, G. & Visonà, D. (1996). Crystal chemistry of danalite from Daba Shabeli Complex (N Somalia). *Mineral. Mag.* **60**: 375-379.
- Perez, J.-B., Dusauroy, Y., Babkine, J. & Pagel, M. (1990). Mn zonation and fluid inclusions in genthelvite from the Taghouaji complex (Air Mountains, Niger). *Am. Miner.* **75**: 909-914.
- Ragu, A. (1994). Helvite from the French Pyrénées as evidence for granite-related hydrothermal activity. *Can. Mineral.* **32**: 111-120.
- Raimbault, L. & Bilal, E. (1993). Trace-element contents of helvite-group minerals from metasomatic albitites and hydrothermal veins at Sucuri, Brazil and Dajishan, China, *Can. Mineral.* **31**: 119-127.
- Zaw, K., Large, R.R. & Huston, D.L. (1997). Petrological and geochemical significance of a Devonian replacement zone in the Cambrian Rosebery massive sulfide deposit, Western Tasmania. *Can. Mineral.* **35**: 1325-1349.

THE NYF-TYPE MIAROLITIC-RARE EARTH ELEMENTS PEGMATITES OF THE EL PORTEZUELO GRANITE, PAPACHACRA (CATAMARCA, NW ARGENTINA)

Fernando Colombo^{1§}, Raúl Lira², William Simmons³ & Alexander U. Falster³

¹ CONICET - Cátedra de Geología General, Facultad de Ciencias Exactas, Físicas y Naturales. Pabellón Geología, Universidad Nacional de Córdoba, Vélez Sarsfield 1611, (X5016GCA) Córdoba, Argentina.

§ fosfatos@yahoo.com.ar

² CONICET - Museo de Mineralogía, Facultad de Ciencias Exactas, Físicas y Naturales, Vélez Sarsfield 299, (5000) Córdoba, Argentina.

³ Department of Earth and Environmental Sciences, University of New Orleans, New Orleans, LA 70148, United States of America

Key words: Carboniferous, fluorine, beryllium, niobium, aplite, A-type granite

INTRODUCTION

A number of plutons with the chemical attributes of A-type granites (as defined by Collins *et al.* 1982 and Whalen *et al.* 1987) were intruded in NW Argentina during the Carboniferous (Dahlquist *et al.* 2010). Most research has been focused on the petrography, whole-rock chemistry and, to a lesser degree, in radiogenic isotopes (U-Pb, Nd-Sm and Rb-Sr), both for dating and to gain insight about the potential melt sources. Pegmatites derived from them, if any, are bound to have a distinctive mineralogy, reflecting the chemical signature of these granites. Some of them have miaroles, whose formation was favored by the usually shallow emplacement levels of these granites. However, most of these pegmatitic districts have remained largely unexplored. We present here a summary of the aplite-pegmatite system related to the El Portezuelo granite, one of such A-type bodies. This adds even more diversity to the Pampean Pegmatitic Province (Galliski 1994 a,b), where NYF-type pegmatites are represented by just a few examples. We would like to note that the little available information about other plutons suggests that (at least in some of them) their pegmatites have different characteristics, and we do not contend that the features reported here are shared by all the A-type Carboniferous granites of NW Argentina.

THE PARENTAL GRANITE

The El Portezuelo granite is located slightly east of the intersection of coordinates 67° W and 27° S, in Belén Department, Catamarca Province, NW Argentina. The biotite syeno- to monzogranite is composed of quartz + K-feldspar + plagioclase + biotite (annite-siderophyllite series) and fluorite, topaz, zircon, thorite, monazite-(Ce), xenotime-(Y), apatite, magnetite, ilmenite, rutile, uraninite, cerianite-(Ce) and ferrocolumbite as accessories. The granite has a restricted compositional variation; it has high SiO₂

(>75% wt.) and relatively low Al₂O₃, Fe₂O₃^{TOTAL}, CaO and TiO₂. It is very poor in P₂O₅ (<0.03% wt.) and MgO (<0.06% wt.). Alkalis are not particularly enriched [(Na₂O + K₂O) ~ 8.5%]. Rb is high (545-730 ppm), and Sr (5-27 ppm), Ba (4-105 ppm), and Eu (0.37-<0.05 ppm) are low. It has a remarkably elevated content of Nb (69-109 ppm), Th (51-80 ppm), and U (9-31 ppm). The chondrite-normalized REE pattern shows a negative Eu anomaly (0.18-0.01) and a slight fractionation of light and heavy REE, with shallow negative slope in chondrite-normalized diagrams. All samples display the lanthanide tetrad effect. Along with the behavior of other element pairs like Zr/Hf, Y/Ho, and Nb/Ta, this suggests interactions with fluids in the late stages of the magmatic evolution (Irber 1999, Monecke *et al.* 2002, Badanina *et al.* 2006).

The granite plots in the within-plate field of discriminant diagrams and displays the features of A-type granites, and particularly of the A₁ subgroup (as defined by Eby 1992). In this respect the El Portezuelo pluton is different from most other A-type granites in NW Argentina, which show A₂ characteristics.

In the normative Qtz-Ab-Or diagram (Tuttle & Bowen 1958), aplite and granite samples define a cluster around the point corresponding to a haplogranitic melt at 100 MPa; such a melt has a solidus temperature of ~750°C, which was probably depressed by volatiles (mainly H₂O and F) in the case of El Portezuelo aplite-pegmatites.

PEGMATITES: DESCRIPTION AND MINERALOGY

Structurally, pegmatites derived from the biotite granite can be grouped into four types (in this context the term is unrelated to the classification of Černý (1991)):

1) miarolitic cavities enclosed within a volume with pegmatitic texture. The zoning closely follows that described by Černý (2000). Size is very variable,

from a few mm to *ca.* 1.5 m, but most are smaller than ~20 cm;

- 2) rounded segregations in granite with heterogeneous textures, with some aplitic and some pegmatitic sectors;
- 3) aplitic dikes with pegmatitic differentiations parallel to the dike elongation, enclosing aligned cavities;
- 4) pegmatitic pods with zonal structure, very scarce.

Pegmatite size is variable but most bodies tend to be small, less than ~6 m long (except for dikes, that can reach several tens of m).

Miaroles indicate fluid saturation during cooling; fluid inclusions trapped in quartz contain Al, Ca, Na, K, Cl, Fe and Mg, rarely S and Mn, as revealed by EDS analyses of daughter crystals and precipitates left by evaporation of solutions of opened inclusions. No CO₂ was detected in fluid inclusions during optical examination at 25°C of doubly polished quartz chips coming from miaroles.

The most abundant minerals are quartz (usually smoky, rarely amethyst), albite and K-feldspar (microcline >> orthoclase). Members of the tourmaline (schorl, fluor-schorl and foitite) and mica group (siderophyllite-polyolithionite series and muscovite), fluorite, topaz and hematite may be locally common and can occur as relatively large (cm-sized) crystals. Most other phases are found as small crystals (usually mm-sized) and never in significant amounts; some of them are columbite-group minerals (in most cases Nb- and Fe-rich), fergusonite-beta-(Y), tapiolite-(Fe), ilmenite, members of the pyrochlore supergroup (with both Ta- and Nb-dominant species), rutile, bastnäsit-(Ce), parisit-(Ce), siderite, florencit-(Ce), monazit-(Ce), xenotime-(Y) (in some cases very rich in Yb), bertrandite, chamosite, phenakite, illite, thorite, and zircon. Some minerals are very rare in Papachacra, and are known from just a few specimens or a single sample. Examples are pyrite (replaced by goethite), anatase, brookite, cassiterite, possibly ixiolite, magnetite, opal, todorokite, thorianite, uraninite, calcite, scheelite, goyazite, monazit-(Nd) (?), beryl, danalite, hingganite-(Y), and Nb-bearing titanite. Secondary minerals are represented by cerianite-(Ce), members of the pyrochlore supergroup, goethite, bismuthite, and chlorite.

Ferberite, apatite, and synchisite-(Ce), along with abundant beryl, occur in a greisen-like assemblage overprinting part of a pegmatite intruded in the country rock (slate), very close to the contact with the granite.

Mica compositions in the granite-pegmatite system vary towards Al enrichment and Fe, Mg, and Ti depletion, progressing from trioctahedral types to dioctahedral types (Colombo *et al.* 2010).

Chemical compositions of the K-feldspars from biotite granite, pegmatites and miaroles are similar, with Or % between 96 and 99. All crystals are perthitic, with albite being close to An₀. Rubidium content in K-feldspar is low, increasing from an average value of 0.10 wt.% (range 0.03-0.17) Rb₂O in samples from the granite to an average value of 0.15 wt.% (range 0.03-0.39) Rb₂O in samples from miaroles. Cesium is below the detection limit.

Regardless of their origin, most samples are microcline with high but never near-complete Al-Si ordering (*t*₁₀ between 0.85-0.90, *t*_{1m} between 0.04-0.10, 2*t*₂ 0.03-0.06). A few samples show dominant monoclinic symmetry.

It is likely that the structural state of K-feldspar has been homogenized in the presence of fluids at a moderately high subsolidus temperature; compositions were later adjusted by a lower temperature (<300°C) hydrothermal event.

GEOCHEMICAL FEATURES AND CLASSIFICATION OF THE DISTRICT

In general, minerals from the aplite-pegmatites of El Portezuelo pluton show Fe>Mn and (Y+HREE)>LREE. Fluorine is very abundant; fluorite is common as an accessory phase in miaroles, and many minerals that can show F(OH)₁ exchange are very F-rich. The maximum measured F content (expressed as wt.%) is 8.30 (in micas), 20.12 (in topaz), 1.56 (in fluor-schorl) and 2.79 (in microlite). Beryllium is present as bertrandite and phenakite. Beryl, danalite and hingganite-(Y) are exceedingly scarce. Zircon (with thorite exsolutions) is very common, while discrete thorite crystals are rare. Phosphorus is bound in (Y+REE) phosphates [xenotime-(Y) >> monazit-(Ce) and florencit-(Ce)], whereas apatite (probably fluorapatite) is only present in a greisenized portion of a pegmatite. Phases where U is an essential structural constituent are virtually absent (save for a few micrometric uraninite inclusions); most U is present in thorite (up to 26.75 wt.% UO₂), zircon (up to 2.34 wt.% UO₂) and members of the pyrochlore supergroup (up to 4.10 wt.% UO₂) minerals. Primary and secondary pyrochlore-supergroup minerals, complex unidentified Y-Nb-Ti (with subordinate Ta) oxides and scarce columbite-group minerals are the main Nb and Ta carriers, with Nb>Ta. Lithium is inferred to be present in micas of the siderophyllite-protolithionite series (reaching the composition formerly attributed to zinnwaldite, now a discredited species); stoichiometric calculations suggest that tourmalines contain negligible amounts of Li.

The aplite-pegmatites from El Portezuelo belong to the NYF petrogenetic family and are a representative of the miarolitic class, miarolitic-REE subclass, with features more similar to those reported

for the gadolinite-fergusonite type, following the scheme of Černý & Ercit (2005).

ACKNOWLEDGEMENTS

This research was partially funded by CONICET. This is a contribution to the project BID 1728/OC AR PICT N° 1009. We gratefully acknowledge the comments made by an anonymous reviewer, which greatly improved the manuscript.

REFERENCES

- Badanina, E. V., Trumbull, R. B., Dulski, P., Wiedenbeck, M., Veksler, I. V. & Syritso, L. F. (2006). The behavior of rare-earth and lithophile trace elements in rare-metal granites: a study of fluorite, melt inclusions and host rocks from the Khangilay Complex, Transbaikalia, Russia. *Can. Mineral.* **44**: 667-692.
- Černý, P. (1991). Rare-element granitic pegmatites. II. Regional to global environments and petrogenesis. *Geoscience Canada* **18**: 68-81.
- Černý, P. (2000). Constitution, petrology, affiliations and categories of miarolitic pegmatites. In: Pezzotta, F. (Ed.) *Mineralogy and petrology of shallow-depth pegmatites*. First International Workshop. *Memorie della Società Italiana de Scienze Naturali. Museo Civico di Storia Naturale di Milano* **30**: 5-12.
- Černý, P. & Ercit, T.S. (2005). The classification of granitic pegmatites revisited. *Can. Mineral.* **43**: 2005-2026.
- Collins, W. J., Beams, S. D., White, A. J. R. & Chappell, B. W. (1982). Nature and origin of A-type granites with particular reference to Southeastern Australia. *Contrib. Miner. Petrol.* **80**: 189-200.
- Colombo, F., Lira, R. & Dorais, M.J. (2010). Mineralogy and crystal chemistry of micas from the A-type El Portezuelo Granite and related pegmatites, Catamarca (NW Argentina). *J. of Geosciences* **55**: 46-56.
- Dahlquist, J.A., Alasino, P.H., Eby, G.N., Galindo, C. & Casquet, C. (2010). Fault controlled Carboniferous A-type magmatism in the proto-Andean foreland (Sierras Pampeanas, Argentina): Geochemical constraints and petrogenesis. *Lithos* **115**: 65-81.
- Eby, G. N. (1992). Chemical subdivision of the A-type granitoids: Petrogenetic and tectonic implications. *Geology* **20**: 641-644.
- Galliski, M. A. (1994a). La Provincia Pegmatítica Pampeana. I: Tipología y distribución de sus distritos económicos. *Rev. Asoc. Geol. Arg.* **49**: 99-112.
- Galliski, M. A. (1994b). La Provincia Pegmatítica Pampeana. II: Metalogénesis de sus distritos económicos. *Rev. Asoc. Geol. Arg.*, **49**, 113-122.
- Irber, W. (1999). The lanthanide tetrad effect and its correlation with K/Rb, Eu/Eu*, Sr/Eu, Y/Ho, and Zr/Hf of evolving peraluminous granite suites. *Geochim. Cosmo. Acta* **63**: 489-508.
- Monecke, T., Kempe, U., Monecke, J., Sala, M. & Wolf, D. (2002). Tetrad effect in rare earth element distribution patterns: A method of quantification with applications to rock and mineral samples from granite-related rare metal deposits. *Geochim. Cosmo. Acta* **66**: 1185-1196.
- Tuttle, O. F. & Bowen, N. L. (1958). Origin of granite in the light of experimental studies in the system NaAlSi₃O₈ - KAlSi₃O₈ - SiO₂ - H₂O. *Geol. Soc. Am., Memoir* **74**.
- Whalen, J. B., Currie, K. L. & Chappell, B. W. (1987). A-type granites: geochemical characteristics, discrimination and petrogenesis. *Contrib. Miner. Petr.* **95**: 407-419.

OCCURRENCE AND CRYSTAL CHEMISTRY OF ZIRCON FROM THE NYF-TYPE MIAROLITIC PEGMATITES OF THE EL PORTEZUELO GRANITE, PAPACHACRA (CATAMARCA, NW ARGENTINA)

Fernando Colombo^{1§}, William Simmons², Alexander U. Falster² & Raúl Lira³

¹ CONICET. Cátedra de Geología General, Facultad de Ciencias Exactas, Físicas y Naturales. Pabellón Geología, Universidad Nacional de Córdoba, Vélez Sarsfield 1611, (X5016GCA) Córdoba, Argentina.

[§] fosfatos@yahoo.com.ar

² Department of Earth and Environmental Sciences, University of New Orleans, New Orleans, LA 70148, United States of America

³ CONICET. Museo de Mineralogía, Facultad de Ciencias Exactas, Físicas y Naturales. Vélez Sarsfield 299, (5000) Córdoba, Argentina.

Key words: hydrothermal, miarole, aplite-pegmatite, zirconium

INTRODUCTION

Zircon is a widespread accessory mineral in felsic rocks, including granitic pegmatites. The chemical composition of igneous zircon has been well characterized (see Hoskin & Schaltegger 2003, for a review); however, zircon can also precipitate from fluids, even of rather low temperature (Rubin *et al.* 1989, Dempster *et al.* 2004, Rasmussen 2005). Information on such hydrothermal zircon is much more scarce.

The El Portezuelo A-type granite (located slightly East of the intersection of coordinates 67° W and 27° S, in Belén Department, Catamarca Province, NW Argentina) offers an interesting opportunity of studying the compositional variability of zircon, which occurs both in the granite and in different zones of intragranitic aplite-pegmatites, including crystals growing on miarole walls which most probably crystallized from a very fluid-rich medium.

OCCURRENCE

Whole-rock analyses of the El Portezuelo granite show up to 220 ppm Zr, most of which is hosted in zircon microcrystals included in siderophyllite. Zircon is also frequently found in aplite-pegmatites, both in the outer zones and in the miarole walls, and as loose crystals mixed with clay minerals filling the cavity interior. The characteristics of the granite and the related aplite-pegmatites and miarolitic segregations have been summarized by Colombo *et al.* (2010). Following the scheme of Černý & Ercit (2005), the pegmatites belong to the miarolitic class, miarolitic-REE subclass, gadolinite-fergusonite type.

This nesosilicate occurs as crystals up to a few mm long, showing short prismatic habit, with dominant {100} terminated by {101} or {111}; another {hkk} form (possibly {311}) is less common. The surface

may be crisscrossed by fissures. Crystals are opaque to translucent and display different shades of brown, sometimes with a reddish, pink or yellowish cast.

The inner parts of crystals taken from miaroles have myriads of vacuoles (Figs. 1A, B), considered by Hoskin & Schaltegger (2003) as a characteristic feature of hydrothermal zircon. Crystal rims are vacuole-free.

Thorite inclusions are very common, either grouped in certain zones or distributed in patches inside the crystals (Figs. 1B, C). Xenotime-(Y) is another commonly associated species, as anhedral inclusions (sometimes arranged concentrically) or forming chemically zoned epitactic overgrowths in corroded zircon (Fig. 1C). Cerianite-(Ce) and Fe oxide inclusions are less frequent, whereas thorianite and uraninite are exceptional. It is likely that the environment during the crystallization of zircon was oxidizing, according to the abundance of hematite in the miaroles.

CHEMICAL COMPOSITION

Electron microprobe analyses (WDS mode) were obtained from zircon from the host biotite granite, from the outer zone of a pegmatitic segregation (referred to henceforth as *pegmatite*), and from miarole walls. Detected elements include P, Si, Zr, Hf, Ti, U, Th, Y, Al, Fe, Mn, Ca and Pb; Mg and Sn were sought but found to be below the detection limits. The composition of every crystal was checked using EDS, and no elements (other than those analyzed) were detected, save for trace quantities of heavy rare earth elements in some points. BSE images show that most crystals are unzoned, except for a thin rim with fine-scale zoning.

The composition of zircon can be represented as ABO_4 , where $A = Zr$ and $B = Si$ in zircon with ideal composition. In the El Portezuelo granite-pegmatite system, the main homovalent substitution is $HfZr_{-1}$,

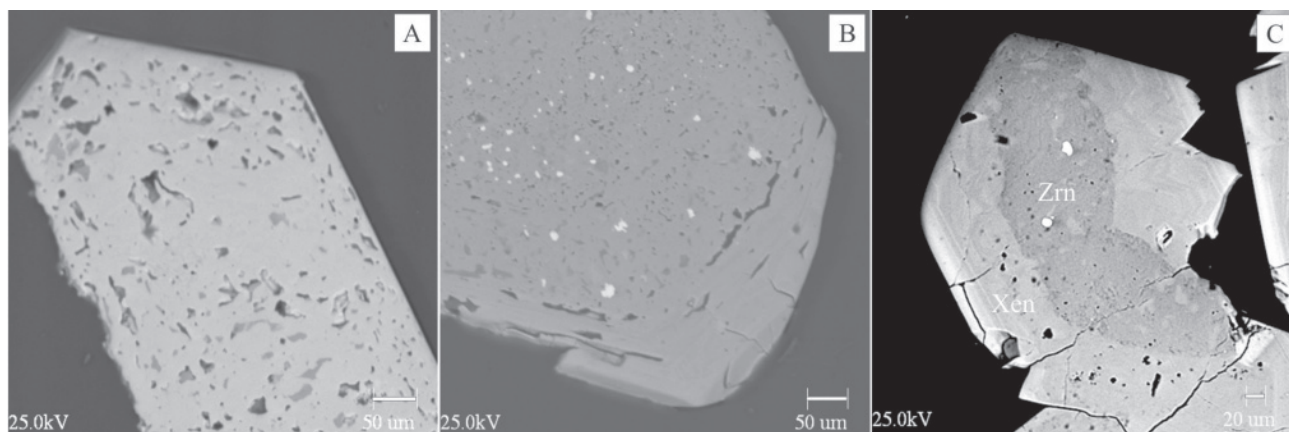


FIGURE 1. SEM-BSE images of polished sections of zircon crystals from miarolitic cavities. A) Crystal showing vacuoles. B) Thorite inclusions (white) and vacuoles inside a crystal. The rim is free of inclusions and vacuoles. C) Zoned xenotime-(Y) overgrowth on a corroded zircon crystal, with thorite inclusions (white).

with different values among different crystals but little intracrystalline variation. There is a partial overlap between the Hf content (2.45-3.92 wt.% HfO_2) of zircon from the granite and pegmatite. With a single exception, crystals from miarolitic cavities are richer in Hf (4.30-7.21 wt.% HfO_2 , with an average value of 5 ± 1 wt.%). The average Zr/Hf ratio of zircon from the granite and pegmatite is rather variable (24-40 and 29-42, respectively), whereas zircon from miaroles has a ratio between 12 and 46 (average = 21 ± 9 , $n = 26$), much lower than the chondritic value of *ca.* 38 (Anders & Grevesse 1989).

Among the trivalent cations, the most abundant is Fe^{3+} (oxidation state inferred from the dominance of hematite over magnetite), followed by Y and then Al. Yttrium decreases in the sequence granite-pegmatite-miarole, whereas Al and Fe show a positive covariation. Calcium is rather variable, with contents ranging from below the detection limit up to 0.23 wt.% CaO.

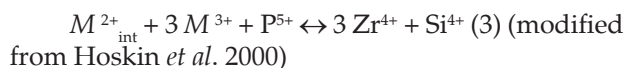
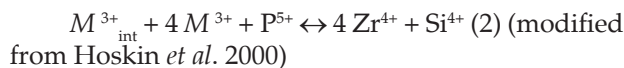
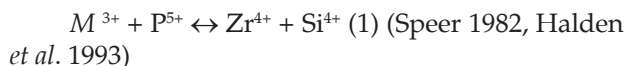
Thorium and U are very depleted in the zircon from the pegmatite; these elements are widely variable in crystals from miaroles, reaching up to 2.34 wt.% UO_2 and 0.99 wt.% ThO_2 . Most crystals from the granite and the pegmatite have molar Th/U ≥ 0.5 , typical of igneous zircon (Hoskin & Schaltegger 2003). Many miarolitic crystals show a ratio lower than 0.5 (and as low as 0.08), suggesting crystallization in a fluid-rich environment. The covariation of $\Sigma(\text{U}+\text{Th})$ and Pb is very poor, suggesting removal of radiogenic Pb.

Most analytical totals in crystals from the pegmatite and miaroles are between 98 and 101 wt.%, but they drop drastically in analyses from the granite (80-89 wt.%). Although these analyses are incomplete (they include only Si, P, Zr, Hf, Th, U, Y and Pb), it is very unlikely that the deficit could be compensated for by the other elements mentioned above. Instead,

the low values reflect a strong alteration, as also suggested by the low birefringence color displayed in thin section.

Regardless of the zircon origin, most analyses show a systematic departure from the ABO_4 stoichiometry; formulae calculated on a 4 O basis have B contents above 1.00 atom per formula unit (apfu), whereas the occupation of the A site is usually below 1.00 apfu. Since alteration can cause mobilization of both A and B cations (Geisler *et al.* 2003, Rayner *et al.* 2005), the choice of an appropriate normalization scheme is very difficult. The lower occupancy of the A site suggests that Si and P are more easily leached; if analyses are normalized on a basis of 1 ($\text{Zr}+\text{Hf}+\text{Ti}+\text{U}+\text{Th}+\text{Y}+\text{Al}+\text{Fe}+\text{Ca}+\text{Pb}+\text{Mn}$) apfu, the (Si+P) deficiency becomes more evident, and increases with decreasing analytical totals.

Several schemes have been proposed for heterovalent substitutions, to explain the incorporation of P^{5+} , M^{2+} ($M = \text{Mg}, \text{Mn}^{2+}, \text{Fe}^{2+}$) and M^{3+} ($M = \text{Y}, \text{Fe}, \text{Al}, \text{REE}$):



Substitution 1 involves two crystallographic sites, whereas 2 and 3 also include an interstitial site (marked *int*).

Figure 2 shows that there is an excess of ($\text{Fe}^{3+}+\text{Al}+\text{Y}$) compared with the P content, indicating that other substitution schemes must be operative. This coincides with the finds of Hanchar *et al.* (2001), who detected a deficit of P compared with the HREE content in doped synthetic zircon. Since the

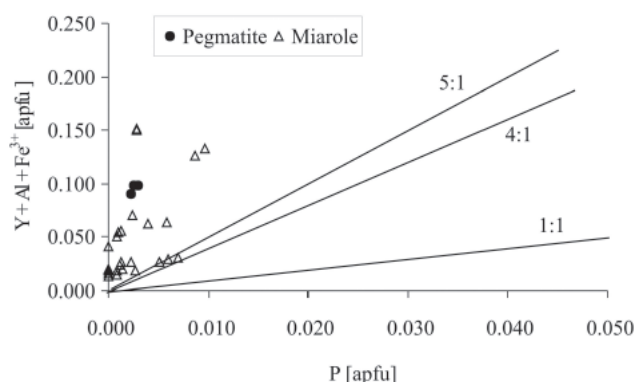


FIGURE 2. Covariation of P and ΣM^{3+} . The straight lines represent the substitution schemes 1 (1:1), 2 (5:1) and 3 (4:1).

substitution of Zr^{4+} for divalent or trivalent cations would produce a charge imbalance, we suggest that the incorporation also involves a coupled substitution of O^{2-} by F^- or $(OH)^-$, as proposed by Pointer *et al.* (1988).

ACKNOWLEDGEMENTS

This research was partially funded by CONICET. Eduardo L. Jawerbaum kindly loaned samples for study.

REFERENCES

- Anders, E. & Grevesse, N. (1989). Abundances of the elements: Meteoritic and solar. *Geochim. Cosmochim. Acta* **53**: 197-214.
- Černý, P. & Ercit, T.S. (2005). The classification of granitic pegmatites revisited. *Can. Miner.* **43**: 2005-2026.
- Colombo, F., Lira, R. & Dorais, M.J. (2010). Mineralogy and crystal chemistry of micas from the A-type El Portezuelo Granite and related pegmatites, Catamarca (NW Argentina). *J. of Geosciences* **55**: 46-56.
- Dempster, T.J., Hay, D.C. & Bluck, B.J. (2004) Zircon growth in slate. *Geology* **32**: 221-224.
- Geisler, T., Rashwan, A.A., Rahn, M.K.W., Poller, U., Zwingmann, H., Pidgeon, R.T., Schleicher, H. & Tomaschek, F. (2003). Low-temperature hydrothermal alteration of natural metamict zircon from the Eastern Desert, Egypt. *Miner. Mag.* **67**: 485-508.
- Halden, N.M., Hawthorne, F.C., Campbell, J.L., Teesdale, W.J., Maxwell, J.A. & Higuchi, D. (1993). Chemical characterization of oscillatory zoning and overgrowths in zircon using 3 MeV μ -PIXE. *Can. Mineral.* **31**: 637-647.
- Hanchar, J.M., Finch, R.J., Hoskin, P.W.O., Watson, E.B., Cherniak, D.J. & Mariano, A.N. (2001). Rare earth elements in synthetic zircon: Part 1. Synthesis, and rare earth element and phosphorus doping. *Am. Mineral.* **86**: 667-680.
- Hoskin, P.W.O. & Schaltegger, U. (2003). The Composition of Zircon and Igneous and Metamorphic Petrogenesis. In: Hanchar, J. M. & Hoskin, P.W.O. (Eds.) *Zircon. Rev. in Miner. and Geochem.* **53**: 27-62. Mineralogical Society of America & Geochemical Society.
- Hoskin, P.W.O., Kinny, P.D., Wyborn, D. & Chappell, B. W. (2000). Identifying Accessory Mineral Saturation during Differentiation in Granitoid Magmas: an Integrated Approach. *J. of Petrol.* **41**: 1365-1396.
- Pointer, C.M., Ashworth, J.R. & Ixer, R.A. (1988). The Zircon-Thorite Mineral Group in Metasomatized Granite, Ririwai, Nigeria. 2. Zoning, Alteration and Exsolution in Zircon. *Min. and Pet.* **39**: 21-37.
- Rasmussen, B. (2005). Zircon growth in very low grade metasedimentary rocks: evidence for zirconium mobility at $\sim 250^\circ\text{C}$. *Contrib. Mineral. Petrol.* **150**: 146-155.
- Rayner, N., Stern, R.A. & Carr, S.D. (2005). Grain-scale variations in trace element composition of fluid-altered zircon, Acasta Gneiss Complex, northwestern Canada. *Cont. Mineral. Pet.* **148**: 721-734.
- Rubin, J.N., Henry, C.D., Price, J.G. (1989). Hydrothermal zircon and zircon overgrowths, Sierra Blanca Peaks, Texas. *Am. Mineral.* **74**: 865-869.
- Speer, J.A. (1982). Zircon. In: Ribbe, P.H. (Ed.) *Orthosilicates. Rev. in Miner.* **5**: 67-112. Mineralogical Society of America.

OCCURRENCE, CRYSTAL CHEMISTRY AND ALTERATION OF THORITE FROM THE NYF-TYPE MIAROLITIC PEGMATITES OF THE EL PORTEZUELO GRANITE, PAPACHACRA (CATAMARCA, NW ARGENTINA)

Fernando Colombo^{1§}, William Simmons², Alexander U. Falster² & Raúl Lira³

¹ CONICET - Cátedra de Geología General, Facultad de Ciencias Exactas, Físicas y Naturales. Pabellón Geología, Universidad Nacional de Córdoba, Vélez Sarsfield 1611, (X5016GCA) Córdoba, Argentina. § fosfatos@yahoo.com.ar

² Department of Earth and Environmental Sciences, University of New Orleans, New Orleans, LA 70148, United States of America

³ CONICET - Museo de Mineralogía, Facultad de Ciencias Exactas, Físicas y Naturales, Vélez Sarsfield 299, (5000) Córdoba, Argentina.

Key words: hydrothermal, thorongumite, aplite-pegmatite, thorium, uranium, vanadium

INTRODUCTION

The A-type granites of NW Argentina are quite rich in Th (Dahlquist *et al.* 2010), although no economic concentrations are known. Monazite-(Ce), frequent in these granites, is usually assumed to be one of the main Th hosts. However, a detailed examination of the rich variety of accessory phases reveals that thorite can be quite abundant. The El Portezuelo granite, one of the northernmost representatives of this Carboniferous magmatic event, is an epizonal pluton parental to a suite of intragranitic aplite-pegmatite bodies and small miarolitic segregations. Thorite precipitated during the whole crystallization sequence, from biotite granite to the miarole walls, affording an interesting study case to examine chemical and textural variations along the sequence, as well as the effects of hydrothermal alteration.

OCCURRENCE

The El Portezuelo granite is located slightly east of the intersection of coordinates 67° W and 27° S, in Belén Department, Catamarca Province, NW Argentina. The characteristics of the granite and the

related aplite-pegmatites and miarolitic segregations have been summarized by Colombo *et al.* (2010). Following the scheme of Černý & Ercit (2005), the pegmatites belong to the miarolitic class, miarolitic-REE subclass, gadolinite-fergusonite type.

Single crystals of thorite, up to *ca.* 2 mm long, are scarce and show the {100} prism terminated by the {101} bipyramid (Fig. 1A). Color varies from dark red to bright yellow, they are translucent to almost opaque, and have greasy luster in the fracture surfaces and almost dull in the crystal faces. Crystals usually show a network of fractures (Fig. 1A). Unlike zircon, no voids (possibly fluid inclusions) are found inside thorite crystals.

Thorite also occurs as myriads of micrometric amoeboid inclusions in zircon (Fig. 1B, C); this is so common that thorite-free zircon is almost nonexistent. The inverse correlation between size and abundance suggests that the inclusions are exsolutions. No epitactic overgrowths on zircon were found. More rarely, thorite forms inclusions in bastnäsite-(Ce) associated with hingganite-(Y), and in monazite-(Ce).

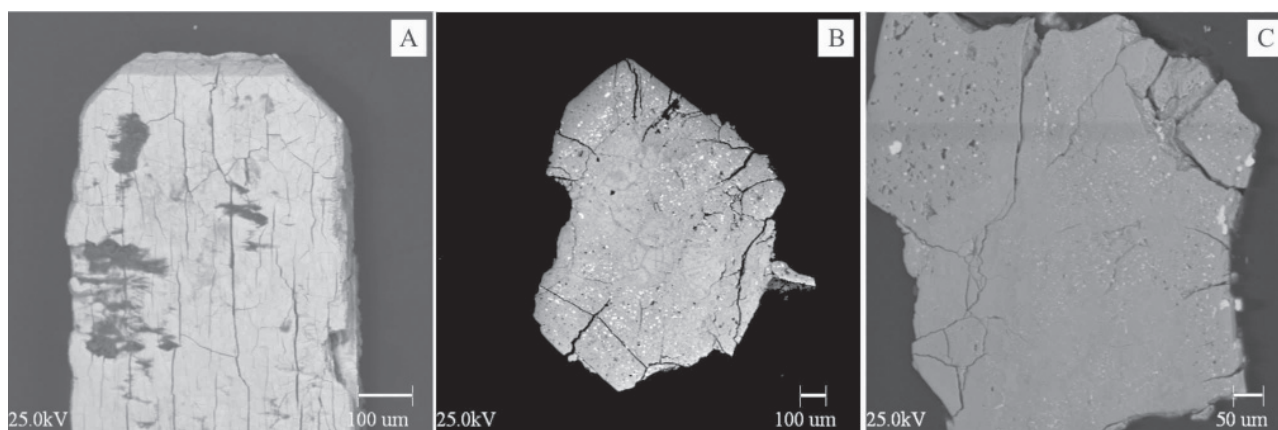


FIGURE 1. SEM-BSE images. A) Thorite crystal with a fracture network. B and C) Thorite inclusions (white) in zircon. In C note the inverse relationship between size and number of the inclusions.

CHEMICAL COMPOSITION

Electron microprobe analyses were obtained from thorite from the host biotite granite, from the outer zone of a pegmatitic segregation (referred to henceforth as *pegmatite*), and from miarole walls (both single crystals and exsolutions within zircon). Detected elements include P, V, Si, Zr, Hf, Ti, U, Th, Y, Al, Fe, Mn, Ca and Pb; Mg and Sn were sought but found to be below the detection limits. The composition of every crystal was checked using EDS, and no elements (other than those analyzed) were detected, save for trace quantities of heavy rare earth elements (Gd, Dy) in some points. Unaltered crystals look homogeneous in BSE images.

The composition of thorite can be represented as ABO_4 , where $A = Th$ and $B = Si$ in thorite with ideal composition. Thorium is mainly substituted by U, with up to 27.12 wt.% UO_2 (0.375 atoms per formula unit, *apfu*, on a basis of 4 O) in crystals from miaroles. In general, thorite exsolutions are richer in U than individual crystals. Thorite from the granite and the pegmatite is much poorer in U (up to 6.76 and 1.59 wt.%, respectively). The Th/(Th+U) molar ratio is between 1.00 and 0.91 in granite and pegmatite, decreasing to 0.74-0.65 in miaroles. Other tetravalent cations (Zr, Hf and Ti) rarely exceed 0.03 wt.%, although Ti may reach up to 0.15 wt.%.

Other elements detected (listed in decreasing abundance) include Fe, Y, Ca and Al. Manganese is rarely present above the detection limit.

Lead, mostly of radiogenic origin, is below the detection limit in thorite from the granite and the pegmatite, whereas it varies between 0.67 and 2.03 wt.% PbO in the miaroles. It is noteworthy that, in spite of being a mineral so rich in parent isotopes, some grains have such low Pb content. This shows Pb loss, a very common feature of thorite (Speer 1982).

Silicon is partially replaced by P and V. Vanadium is present above the detection limit in all of the analyzed points, and in most cases it exceeds P (in molar amounts). The highest V content is 3.12 wt.% V_2O_5 .

Like in zircon (see Colombo *et al.* this volume), thorite analyses normalized on a 4 O basis usually show $A > 1.00$ apfu and $B < 1.00$ apfu.

By analogy with zircon, which is isostructural with thorite (though there is very limited Zr-for-Th substitution), the following coupled substitution schemes could be postulated:

$M^{3+} + (P,V)^{5+} \leftrightarrow Th^{4+} + Si^{4+}$ (1) (Speer 1982, Halden *et al.* 1993)

$M^{3+}_{int} + 4 M^{3+} + (P,V)^{5+} \leftrightarrow 4 Th^{4+} + Si^{4+}$ (2)
(modified from Hoskin *et al.* 2000)

$M^{2+}_{int} + 3 M^{3+} + (P,V)^{5+} \leftrightarrow 3 Th^{4+} + Si^{4+}$ (3)
(modified from Hoskin *et al.* 2000)

Where M stands for *metal* ($M^{3+} = Y, HREE, Fe^{3+}, Al$, and $M^{2+} = Fe^{2+}, Mn, Ca$) and *int* means that it is located in an interstitial site.

In Figure 2 it can be seen that points plot on and between the lines representing the schemes 1 (line 1:1) and 2 and 3 (line 4:1 and the very similar 5:1, not drawn), indicating that in most cases a combination of substitutions is necessary to accommodate the 3+ and 5+ cations. Altered thorite (see below) contains much more P and V than can be expected by any or the substitutions mentioned above, or their combinations. No other phases that could host these elements were detected using BSE imagery at moderate ($\leq 5,000\times$) magnification.

ALTERATION

Low analytical totals, fractures (Fig. 3A), a mottled aspect in BSE images (Figs. 3B, C), varying Th/Si ratios and the presence of higher quantities of Ca, P and V are characteristic of thorite showing signs of alteration. No covariation is evident between any element (including U+Th) and the analytical deficit below 100 wt.%. It is very likely that alteration is associated with the entry of F^- and H^+ (see Pointer *et al.* 1988) and the creation of submicrometric voids. Two powder X-ray diffraction patterns show that the crystal structure is partially conserved, with broadened peaks. It is possible that some of the analyzed grains correspond to thorogummite, $Th(SiO_4)_{1-x}(OH)_{4x}$. The dimensions of the a unit cell parameter of the samples from El Portezuelo [7.140(3)-7.141(1) Å] are very similar to thorite, but the c parameters [6.242(1)-6.259(4) Å] are smaller and more akin to thorogummite.

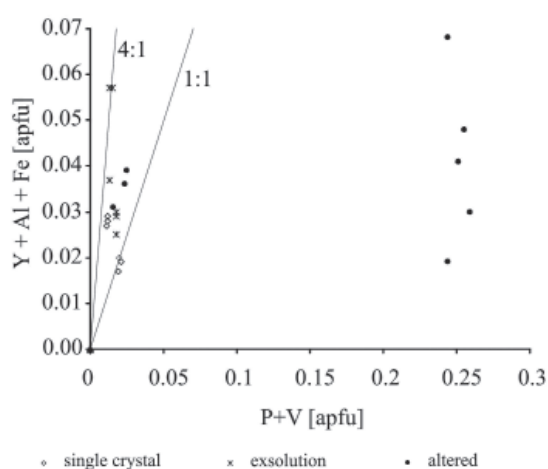


FIGURE 2. Covariation of (P+V) and SM^{3+} . The straight lines represent the substitution schemes 1 (1:1) and 3 (4:1).

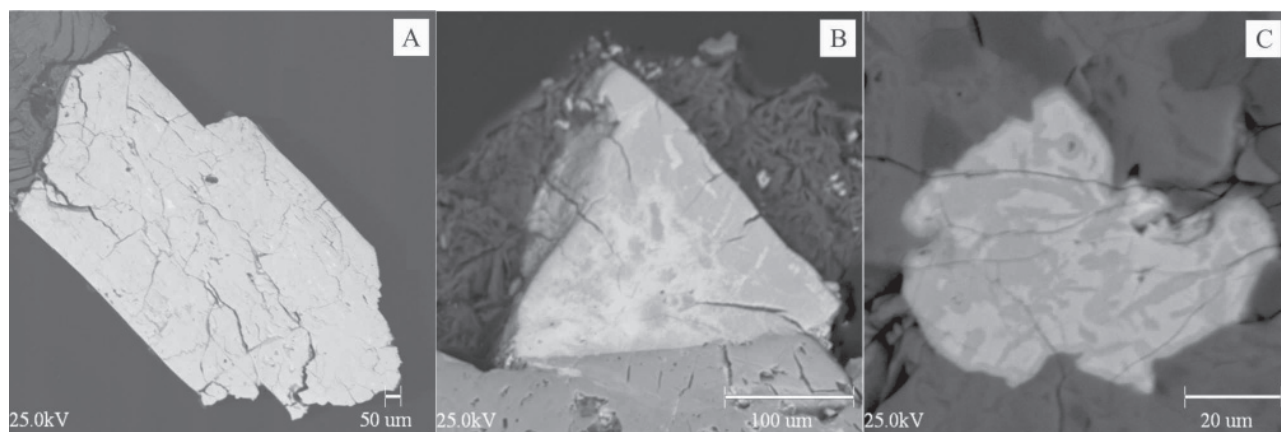


FIGURE 3. SEM-BSE images of polished thorite crystals showing signs of alteration. Note the fractures and the mottled aspect of B and C. These last two grains are hosted in zircon.

ACKNOWLEDGEMENTS

This research was partially funded by CONICET. Eduardo L. Jawerbaum kindly loaned samples for study. This abstract was improved by the suggestions of an anonymous reviewer.

REFERENCES

- Černý, P. & Ercit, T.S. (2005). The classification of granitic pegmatites revisited. *Can. Mineral.* **43**: 2005-2026.
- Colombo, F., Lira, R. & Dorais, M.J. (2010). Mineralogy and crystal chemistry of micas from the A-type El Portezuelo Granite and related pegmatites, Catamarca (NW Argentina). *J. of Geosciences* **55**: 46-56.
- Dahlquist, J.A., Alasino, P.H., Eby, G.N., Galindo, C. & Casquet, C. (2010). Fault controlled Carboniferous A-type magmatism in the proto-Andean foreland (Sierras Pampeanas, Argentina): Geochemical constraints and petrogenesis. *Lithos* **115**: 65-81.
- Halden, N.M., Hawthorne, F.C., Campbell, J.L., Teesdale, W.J., Maxwell, J.A. & Higuchi, D. (1993). Chemical characterization of oscillatory zoning and overgrowths in zircon using 3 MeV μ -PIXE. *Can. Mineral.* **31**: 637-647.
- Hoskin, P.W.O., Kinny, P.D., Wyborn, D. & Chappell, B. W. (2000). Identifying Accessory Mineral Saturation during Differentiation in Granitoid Magmas: an Integrated Approach. *J. of Pet.* **41**: 1365-1396.
- Pointer, C.M., Ashworth, J.R. & Ixer, R.A. (1988). The Zircon-Thorite Mineral Group in Metasomatized Granite, Ririwai, Nigeria. 2. Zoning, Alteration and Exsolution in Zircon. *Miner. and Pet.* **39**: 21-37.
- Speer, J. A. (1982). The actinide orthosilicates. In: Ribbe, P. H. (Ed.) *Orthosilicates*. *Rev. in Miner.* **5**: 113-135. Mineralogical Society of America.

MINERALOGY OF A HIGHLY FRACTIONATED REPLACEMENT UNIT FROM “ÁNGEL” PEGMATITE, COMECHINGONES PEGMATITIC FIELD, CÓRDOBA, ARGENTINA

Manuel Demartis^{1§}, Joan C. Melgarejo Draper², Pura Alfonso³, Jorge E.
Coniglio⁴, Lucio P. Pinotti¹ & Fernando J. D'Eramo¹

- ¹ CONICET – Departamento de Geología, Universidad Nacional de Río Cuarto. Ruta Nac. N° 36, km 601, Río Cuarto, provincia de Córdoba (Argentina). § mdemartis@exa.unrc.edu.ar
- ² Departament de Cristallografia, Mineralogia i Dipòsits Minerals. Universitat de Barcelona. C/ Martí i Franquès s/n. 08028 Barcelona (Catalonia, Spain).
- ³ Departament d'Enginyeria Minera i Recursos Naturals. Campus Manresa. Universitat Politècnica de Catalunya. Av/ Bases de Manresa 61-73. 08242 Manresa (Catalonia, Spain).
- ⁴ Departamento de Geología, Universidad Nacional de Río Cuarto. Ruta Nac. N° 36, km 601, Río Cuarto, provincia de Córdoba (Argentina).

Key words: LCT pegmatite; replacement unit; Comechingones Pegmatitic Field; BSE-SEM.

INTRODUCTION

The Comechingones Pegmatitic field (CPF), southeastern Pampean Pegmatitic Province (Galliski 1994a and b; Hub 1994 and 1995; Galliski 1999), locates in the northwestern Sierra de Comechingones, Córdoba province, Argentina. It is composed of a great number of Be–Nb–Ta–P–U-rich pegmatites of the rare-element class (some of them grading to the muscovite class), beryl–columbite–phosphate subtype (Galliski 1994a). These pegmatites were emplaced synkinematically during the compressive deformation of the crustal scale Guacha Corral shear zone (Demartis 2010).

The pegmatites are generally well zoned. Border and wall zones are composed of fine- to medium-grained quartz + muscovite ± microcline ± albite. Coarse- to very coarse-grained intermediate zones are composed of graphic microcline + quartz + muscovite ± albite ± garnet; phosphates and uranium minerals occur in these zones. Core is composed of milky quartz with subordinated microcline and muscovite, with accessory crystals of beryl and minerals of the columbite series.

Replacement units are rare and have been found only in a few cases, as in the “Ángel” pegmatite, and they generally affect graphic microcline + quartz intermediate zones. “Ángel” pegmatite, cropping out in the southern part of the CPF (~ 32° 18' S and 64° 54' W), is particularly known because of its varied primary and secondary uranium mineralogy (Angelelli 1950).

The aim of this contribution is to describe the extremely fractionated minerals from the replacement units.

THE REPLACEMENT UNIT FROM “ÁNGEL” PEGMATITE

This unit consists of an extremely foliated and ductily deformed rock mostly composed of fine- to medium-grained albite + micas + quartz. It was generated by an almost complete metasomatic replacement of the graphic microcline. Radial platy variety of albite (cleavelandite) is commonly present in crystals of a few centimetres long, but tabular euhedral polysynthetic albite grains predominate. Accessory minerals such as zircon, Ta-rich oxides, and phosphates were also recognized.

SILICATES

Li-rich micas (lepidolite or polyolithionite-trilithionite series; Tischendorf *et al.* 2004) generally show a pink to pale pink color in hand samples. A zoned pattern can be usually recognized using both optical and BSE-scanning electron microscopy, reflecting changes in the Rb content of the micas.

Zircon usually crystallizes in ~100 µm euhedral to subhedral grains. They are zoned and strongly corroded, either in the crystal centers and the grain borders. The rims tend to be euhedral and are strongly enriched in Hf. Černý *et al.* (1985) and Corbella & Melgarejo (1993) also found extreme enrichment in Hf in crystals produced during late events in evolved pegmatites, and emphasized in the progressive enrichment in Hf from core to rim in individual zircon grains.

Albite uses to be present in tabular crystals, some hundreds of microns in dimension.

OXIDES

Tantalite-(Mn) and members of the microlite subgroup are found as anhedral crystals scattered among the albite grains. These minerals are very common, although fine-grained (less than 100 microns in size). Tantalite-(Mn) is not zoned and is partially replaced by metamictic microlite. On its turn, several generations of microlite are distinguished, owing to changes in the contents of Na, Bi and U in the A position.

NATIVE ELEMENTS

Native bismuth is widespread in these units, and it is found only as fine-grained crystals of less than 5 microns in diameter. These grains are found filling small veinlets in microlite and in the cleavages of the surrounding micas. Hence, bismuth may correspond to a product of alteration of bismutomicrolite.

PHOSPHATES

Primary phosphates in the albite units comprise F-rich members of the amblygonite-montebrazite series, and they are widespread as anhedral grains of ~1 mm in diameter. These phosphates are intergrown with albite and lithium micas.

In addition, secondary phosphates are found as vein and porosity infillings, and also as some pseudomorphs of the primary phosphates. Crandallite occurs in fine-grained crystals, and it can be associated with an undefined interstitial Hf- and Zr- bearing phosphate which may correspond to a new mineral species. This phosphate is found as fine-grained interstitial intergrowns between albite and mica crystals.

DISCUSSION AND CONCLUSIONS

According to primary K-feldspar (Demartis 2010) and columbite-group mineral (Galliski & Černý 2006) geochemistry, pegmatites from the southern CPF could represent poorly evolved melts with at least intermediate fractionation degree. However, the mineral assemblage found in this replacement unit suggests a metasomatic event produced by highly fractionated fluids during the late stages of pegmatite crystallization. Extreme fractionation is indicated by relatively high Ta and Mn contents in members of the columbite group and pyrochlore supergroup, and by relatively high Hf content in zircon, as was determined by EDS spectra. Positive correlation between Hf and Ta has been also described in some cuppolas of extremely evolved granites (Ru Cheng Wang *et al.* 1996). The occurrence of Hf-bearing phosphates need more study.

REFERENCIAS

- Angelelli, V. (1950). Recursos minerales de la República Argentina – I – Yacimientos Metalíferos. Revista del Instituto Nacional de Investigaciones de las Ciencias Naturales 'Bernardino Rivadavia', Ciencias Geológicas, Tomo II, Bs. As.
- Černý, P., Meintzer, R.E. & Anderson, A. J. (1985). Extreme fractionation in rare-element granitic pegmatites: selected examples of data and mechanisms. *Can. Mineral.* **23**: 381-421.
- Corbella, M. & Melgarejo, J.C. (1993). Rare-element pegmatites of the Cap de Creus Peninsula, NE Spain: a new field of the Beryl-Phosphate subtype. In Proc. 8th. Quadriennial IAGOD meeting (Y.T. Maurice, ed.). E. Schweizerbart'sche Verlagsbuchhandlung (295-302).
- Demartis, M. (2010). Emplazamiento y petrogénesis de las pegmatitas y granitoides asociados. Sector central de la Sierra de Comechingones, Córdoba, Argentina. Unpublished PhD Thesis, Depto de Geología, Universidad Nacional de Río Cuarto, Argentina, p. 265.
- Galliski, M.A. (1994a). La Provincia Pegmatítica Pampeana. I: Tipología y distribución de sus distritos económicos. *Revista de la Asociación Geológica Argentina* **49**(1-2): 99-112.
- Galliski, M.A. (1994b). La Provincia Pegmatítica Pampeana. II: Metalogénesis de sus distritos económicos. *Revista de la Asociación Geológica Argentina* **49**(1-2): 113-122.
- Galliski, M.A. (1999). Distrito pegmatítico Comechingones, Córdoba. In: Recursos Minerales de la República Argentina (Ed. E. O. Zappettini), Instituto de Geología y Recursos Minerales SEGEMAR, *Anales* **35**: 361-364, Buenos Aires.
- Galliski, M.A. & Černý, P. (2006). Geochemistry and structural state of columbite-group minerals in granitic pegmatites of the Pampean ranges, Argentina. *Can. Mineral.* **44**: 645-666.
- Hub, C.C. (1994). Estudio geológico-económico de pegmatitas del Distrito Comechingones. Informe Beca CONICOR. 156p.
- Hub, C.C. (1995). Estudio geológico-económico de pegmatitas del Distrito Comechingones. Informe Beca CONICOR. 172p.
- Ru Cheng Wang, Fontan, F., Shi Jin Xu, Xiao Ming Chen & Monchoux, P. (1996). Hafnian zircon from the apical part of the Suzhou granite, China. *Can. Mineral.* **34**: 1001-1010.
- Tischendorf, G., Rieder, M., Förster, H.J., Gottesmann, B. & Guidotti, C.V. (2004). A new graphical presentation and subdivision of potassium micas. *Mineral. Mag.* **68**(4): 649-667.

PEGMATITE EMPLACEMENT DURING COMPRESSIONAL DEFORMATION OF THE GUACHA CORRAL SHEAR ZONE, CÓRDOBA, ARGENTINA

Manuel Demartis^{1§}, Lucio P. Pinotti¹, Fernando J. D'Eramo¹,
 Jorge E. Coniglio² & Hugo A. Petrelli²

¹ CONICET – Departamento de Geología, Universidad Nacional de Río Cuarto. Ruta Nac. N° 36, km 601.

[§] mdemartis@exa.unrc.edu.ar

² Departamento de Geología, Universidad Nacional de Río Cuarto. Ruta Nac. N° 36 – km 601.

Key words: pegmatite emplacement; LCT pegmatite; Comechingones Pegmatitic Field; Guacha Corral shear zone.

INTRODUCTION

In the Sierra de Comechingones, Córdoba province, Argentina, a great number of Be–Nb–Ta–U–P-rich pegmatites were grouped by Galliski (1994, 1999) in the Comechingones Pegmatitic Field (CPF), southeastern Pampean Pegmatitic Province (Fig. 1a). These pegmatites have a LCT signature and belong principally to the rare-element class, beryl–columbite–phosphate subtype, and some of them grade to the muscovite class (Galliski 1994).

These pegmatites were emplaced at pressures of approximately 500 MPa, synkinematically with the crustal scale Guacha Corral shear zone (GCSZ) development (Demartis 2010). At first sight, the transfer of magma through such a ductile, middle pressure continental crust seems to require a huge amount of energy. However, the GCSZ deformation provided open spaces for the migration and ascent of pegmatite magmas, and the high volatile content of the pegmatites enhanced significantly the buoyant force of these pegmatite magmas. These two points suggest a mechanism of easy-intrusion for the pegmatite magmas through the ductile continental crust. In this contribution, we present field and microstructural data from the southern part of the CPF (Fig. 1b) that evidences syntectonic pegmatite emplacement during the compressional deformation of the GCSZ. We also propose two main deformation related mechanisms for space generation that triggered magma ascent and emplacement.

GEOLOGICAL SETTING

The GCSZ deformation took place during the Ordovician to Devonian Famatinian orogeny, (Rapela *et al.* 1998, Otamendi *et al.* 2004) and it reworked previous gneissic and migmatitic fabrics developed during Neoproterozoic to Cambrian Pampean orogeny. This reworking generated a pervasive submeridional striking moderately dipping mylonitic foliation.

According to deformation evidences, two domains with contrasting finite deformation intensity were defined in the studied area of the GCSZ: “high strain domain” (HSD; Fig. 1c), dominated by mylonites and ultramylonites; and “low strain domain” (LSD; Fig. 1d), where gneisses and migmatites predominate. A transition zone between these two end-member domains also occurs. Thus, a westward increasing of deformation intensity can be established.

Granitic pegmatites of the CPF occur as countless bodies with lens or sheet geometry of relatively small size (<50 m thick and 200 m long), that often come into contact, forming larger composite dykes with more than 1 km long. Internal zonation can be usually recognized individually in each lenticular pegmatitic body. Border and wall zones are composed of fine- to medium-grained quartz + muscovite ± microcline ± albite. Coarse- to very coarse-grained intermediate zones are composed of graphic microcline + quartz + muscovite ± albite ± garnet; phosphates and uranium minerals occur in these zones. Core is composed of milky quartz with subordinated microcline and muscovite, with accessory crystals of beryl and columbite. Highly fractionated replacement units occur only locally in some pegmatites (Demartis *et al.* 2011, this volume). P–T crystallization conditions of the pegmatites from southern CPF are 500 MPa and 600–700 °C (Demartis 2010).

STRUCTURAL ANALYSIS

Field and microstructural analysis was carried out both in country rocks and pegmatites from HSD and LSD. Mylonitic, gneissic and migmatitic foliations, as well as mineral stretching lineation and kinematic indicators, were measured in country rocks. Orientation, internal foliations, stretching lineations and kinematic indicators were also measured in pegmatites.

In HSD, mean mylonitic foliation plane strikes submeridionally and dips moderately toward E, but

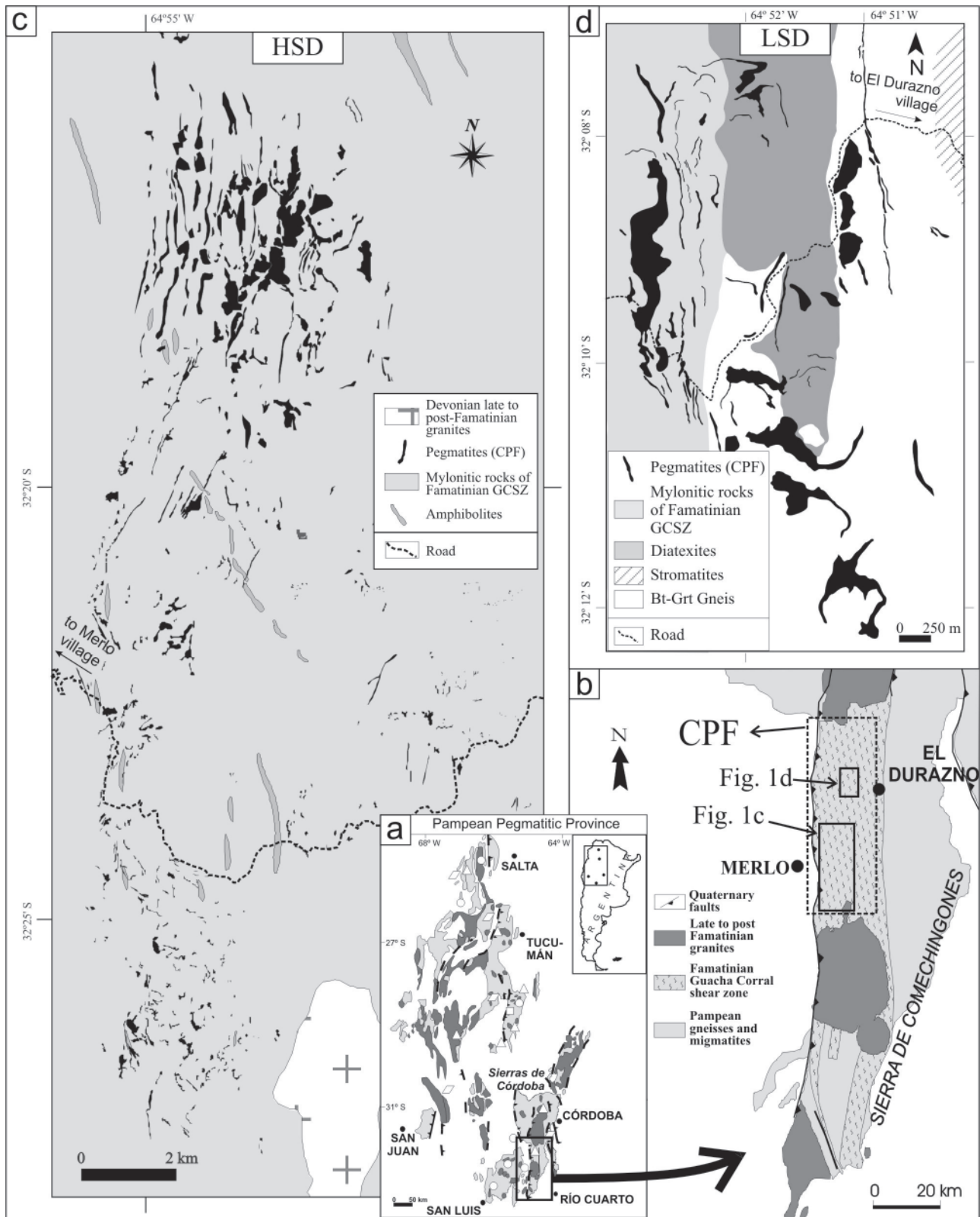


FIGURE 1. a) Pampean Pegmatitic Province, simplified from Galliski (1994). b) Sierra de Comechingones with the insets of Comechingones Pegmatitic Field (CPF), High Strain domain (HSD; figure 1c) and Low Strain domain (LSD; figure 1d). c) Lithological map of the HSD. d) Lithological map of the LSD.

orientation variations throughout this domain are very common and an anastomosed mylonitic foliation pattern is therefore defined. Kinematic analysis using mylonitic foliation and mineral stretching lineation indicates an almost reverse shear sense with an east-to-west tectonic transport, in a simple shear deformation context, where rotational elements are represented by sigma and delta-type porphyroclasts and S/C structures. Pegmatites in this domain generally crop out conformably with mylonitic foliation, even though where its orientation changes significantly, harmonically with anastomosing mylonitic foliation pattern. An internal foliation defined by stretched and reoriented microcline, quartz and muscovite of the intermediate zone also develops in the pegmatites, and a stretching mineral lineation can be locally observed, yielding an analogous sense of shear to that measured in mylonitic country rocks. Contrary to the higher strain domains, pegmatites of the LSD are usually discordant with NNW-striking, moderately E-dipping gneissic and migmatitic foliations. Pegmatite orientations also strike submeridionally and dip eastwards, but two different mean dipping angles were measured: low dipping angles (<30-40°) and high dipping angles (>70°).

Both pegmatites from the LSD and the HSD display deformation textures and microstructures developed from submagmatic to low temperature subsolidus state.

PEGMATITIC MAGMA ASCENT AND EMPLACEMENT MECHANISMS

Field and microscopic structural data from the country rocks and pegmatites indicate synkinematical emplacement and crystallization for pegmatitic magmas during compressive deformational event of the GCSZ.

Two different magma ascent and emplacement mechanisms are proposed for space generation in both different strain domains.

Discordant pegmatites cropping out in the LSD are thought to represent magmas emplaced in Riedel fractures that were developed in response to simple shear deformation, unrelated to any previous anisotropy, hereafter called "fracture-controlled" mechanisms (Clemens & Mawer 1992; Weinberg & Regenauer-Lieb 2010). Therefore, low dipping pegmatites are regarded as magmas intruding T extensional fractures, normal to the minimum compressive stress (σ_3), while high dipping pegmatites represent magmas ascended through synthetic P fractures that acted as feeding channels, transferring magmas from lower structural levels.

Many pegmatites from the HSD outcrop concordantly, even where anastomosed mylonitic foliation changes its orientation. They are regarded to represent pegmatitic magmas emplaced in local

spaces generated by "magma pumping" mechanism. This mechanism takes place when spaces begin to open due to anastomosing mylonitic foliation laminae sliding during deformation, originating a local pressure gradient due to the vacuum generated between two adjacent laminae. This pressure gradient, together with enhanced magma buoyancy force, induces the ascent and migration of pegmatitic magmas towards these sites, separating mylonitic foliation laminae and pumping the magma into these spaces. Similar mechanism has been described for granitic magmas by D'Lemos *et al.* (1992) and Weinberg *et al.* (2009). Relatively high volatile contents (pegmatite mineralogy and geochemical signature indicate relatively high proportions of P, B and H₂O in these melts) reduce magma viscosity (Dingwell *et al.* 1996), thus increasing buoyancy force. Moreover, during transport these volatile-rich magmas also favour mylonitic foliation laminae sliding, enhancing further deformation, generating a feed-back relationship between magma migration and progressive deformation.

Fracture-controlled mechanism seems to have dominated magma ascent and emplacement during the initial stages of deformation, allowing magma transfer previously to anastomosed mylonitic foliation development. Once emplaced, with further deformation pegmatites were rotated and sheared by mylonitic flow, parallelising them with mean mylonitic foliation plane and losing their original orientation. Moreover, magma pumping mechanism began to take place when deformation originated anastomosed mylonitic foliation pattern. However, pegmatites emplaced in the LSD, which experienced almost none further rotation, represent the former stages of pegmatite emplacement and allowed reconstructing a general model for magma ascent and emplacement throughout this crustal scale shear zone. This model for mass transfer within ductile crust contributes to resolve energetic and rheological problems for magma ascent from lower to middle crustal zones.

REFERENCES

- Clemens, J.D. & Mawer, C.K. (1992). Granitic magma transport by fracture propagation. *Tectonophysics* **204**(3-4): 39-360.
- D'Lemos, R.S., Brown, M. & Strachan, R.A. (1992). Granite magma generation, ascent and emplacement within a transpressional orogen. *Journal of the Geological Society, London* **149**(4): 487-490.
- Demartis, M. (2010). Emplazamiento y petrogénesis de las pegmatitas y granitoides asociados. Sector central de la Sierra de Comechingones, Córdoba, Argentina. Unpublished PhD Thesis, Depto de Geología, Universidad Nacional de Río Cuarto, Argentina, p. 265.

- Demartis, M., Melgarejo Draper, J.C., Alfonso, P., Coniglio, J.E., Pinotti, L.P. & D'Eramo, F.J. (2011). Mineralogy of a highly fractionated replacement unit from "Ángel" Pegmatite, Comechingones Pegmatitic Field, Córdoba, Argentina. 5th Internacional Symposium on granitic pegmatites, Mendoza, Argentina (this volume).
- Dingwell, D.B., Hess, K.-U. & Knoche, R. (1996). Granite and granitic pegmatite melts: volumes and viscosities. *Transactions of the Royal Society of Edinburgh: Earth Sciences* **87**: 65-72.
- Galliski, M. (1994). La Provincia Pegmatítica Pampeana. I: Tipología y distribución de sus distritos económicos. *Revista de la Asociación Geológica Argentina* **49**(1-2): 99-112.
- Galliski, M. (1999). Distrito pegmatítico Comechingones, Córdoba. En: *Recursos Minerales de la República Argentina* (Ed. E. O. Zappettini), Instituto de Geología y Recursos Minerales SEGEMAR, *Anales* **35**: 361-364, Buenos Aires.
- Otamendi, J.E., Castelarini, P.A., Fagiano, M., Demichelis, A. & Tibaldi, A. (2004). Cambrian to Devonian geologic evolution of the Sierra de Comechingones, eastern Sierras Pampeanas: evidence for the development and exhumation of continental crust on the proto-pacific margin of Gondwana. *Gondwana Research* **7**(4):1143-1155.
- Rapela, C.W., Pankhurst R.J., Casquet, C., Baldo, E., Saavedra, J., Galindo, C. & Fanning, C.M. (1998). The Pampean orogeny of the southern proto-Andes: Cambrian continental collision in the Sierras de Córdoba. In: Pankhurst, R.J. & Rapela, C.W. (eds) *The Proto-Andean Margin of Gondwana*. Geol. Soc., London, Special Publication **142**: 181-217.
- Weinberg, R.F., Mark, G. & Reichardt, H. (2009). Magma ponding in the Karakoram shear zone, Ladakh, NW India. *Geological Society of America Bulletin* **121**: 278-285.
- Weinberg, R.F. & Regenauer-Lieb, K. (2010). Ductile fractures and magma migration from source. *Geology* **38**(4): 363-366.

THE ROLE OF PEGMATITES IN THE CHESSBOARD CLASSIFICATION SCHEME (CCS) OF MINERAL DEPOSITS

Harald G. Dill[§]

Federal Institute for Geosciences and Natural Resources, P.O. Box 510163, D-30631 Hannover, Germany, [§]dill@bgr.de

Key words: Pegmatite, chessboard classification scheme, mineralogy, economic geology

INTRODUCTION - PRINCIPLES OF THE CLASSIFICATION SCHEME

The "CHESSBOARD CLASSIFICATION SCHEME" (CCS) (Dill 2010) is designed as an interactive classification scheme open for amendments in an electronic spreadsheet version and adjustable to the needs and wants of application, research and training in geosciences.

Mineralogy and geology act as x- and y-coordinates of a classification chart of mineral resources. Magmatic and sedimentary lithologies together with tectonic structures (1-D / pipes, 2-D / veins) are plotted along the x-axis in the header of the spreadsheet diagram representing the columns in this chart diagram. 63 commodity groups, encompassing minerals and elements are plotted along the y-axis, forming the rows of the spreadsheet. These commodities are subjected to a tripartite subdivision into ore minerals, industrial minerals/rocks and gemstones/ ornamental stones.

The code of each type of deposit can be created by combining the commodity (rows) shown by numbers plus lower caps with the host rocks or structure (columns) given by capital letters.

Further information on the various types of mineral deposits, as to the major ore and gangue minerals, the current models and the mode of formation or when and in which geodynamic setting these deposits mainly formed throughout the geological past may be obtained from an explanatory text by simply using the code of each deposit in the chart.

Each commodity has a small preface on the mineralogy and chemistry and ends up with an outlook into its final use and the supply situation of the raw material on a global basis, which may be updated by the user through a direct link to the commodity database of the US Geological Survey. The internal subdivision of each commodity section corresponds to the common host rock lithologies (magmatic, sedimentary, metamorphic) and structures.

PEGMATITES IN THE CLASSIFICATION SCHEME

THE COMMODITY TYPES

Metallic resources bound to pegmatites are important for the succeeding element associations: Mo-Re, Sn-W, Nb-Ta-Sc, Be, Li-Cs-Rb, REE-Y, U-Ra, Th, F, Si. Pegmatites are used in the field of industrial minerals and rocks in search of the following minerals and rocks: borate-bearing dimension stones, fluorite, quartz (mineral, aggregate, dimension stones), feldspar (mineral, aggregate, dimension stones), nepheline (mineral, dimension stones), zeolite, garnet (dimension stones), corundum /emery, muscovite, graphite. Pegmatites are among the most looked-for target areas when it comes to the exploitation of gemstones and ornamental stones.

THE COLUMNS

Pegmatitic mineral deposits are almost exclusively bound to the felsic igneous rocks (column D) and the alkaline igneous rocks (column E). Only beryllium deposits and gemstone deposits containing varieties of precious corundum also occur in or related to ultrabasic (column A) and intermediate igneous rocks (column C). Pegmatite deposits of columns E and A evolved in a geodynamic setting characterized by divergent plate boundaries, those of column C and D mainly along convergent plate boundaries. As far as the economic geology of pegmatite-related deposits is concerned one has to take into consideration also the duricrusts, regolith and vein-like deposits (column H) developing on top of these pegmatite stocks, plugs and sheets and the clastic aureole draped around them (column I). This apron is host of economic alluvial-fluvial placer deposits, while the residual and eluvial types bridge the gap into the afore-mentioned chemical sediments (column H).

THE ROWS

The rows describe in detail the various types of pegmatite deposits for each commodity group.

Mo-Re pegmatites are associated with granitic complexes which developed during the waning stages

of the orogenic plutonism. In these mineralized sites, molybdenite is accompanied by scheelite, cassiterite, and wolframite.

Sn-Ta-Nb pegmatites are known from Brazil, Russia, DR Congo, Great Britain, Burundi, Rwanda and Uganda. Metalliferous pegmatites carry cassiterite and stokesite. Stockscheider which is a pegmatitic part of the tin granite also falls into this category.

Locally, calc-alkaline and alkaline pegmatites are also host of Sn-Ta-Nb mineralization. The zoned petalite-subtype Tanco granitic pegmatite at Bernic Lake, Canada, is one of the main producers of Ta in the world. Rare-element pegmatites may host several economic commodities, such as tantalum (Ta-oxide minerals), tin (cassiterite), lithium (ceramic-grade spodumene and petalite), and cesium (pollucite). Other renowned examples of rare-metal pegmatite is the Sn-Ta-Nb deposits of Manono-Kitotolo, DR Congo and the Be-Li-Ta-Nb-REE-U pegmatites of the Alto Ligonha province, Mozambique. The Sc silicates are normally found in granite pegmatites.

Beryllium minerals are found in four different groups of pegmatites. Be-F-B-Sn-(Cs) mineralization with beryl, aquamarine, chrysoberyl, emerald, euclase, hambergite, phenakite and rhodizite is related to LCT granitic pegmatites. Chrysoberyl coexists with REE in pegmatites of alkaline igneous rocks. Beryl also shows up in pegmatitic mobilizates in metamorphic rocks. A very complex process led to the Be-(Li)- (emerald, spodumene) pegmatites in suture zone- and/ or pegmatite-related schist-hosted deposits. This is also true for the contact deposits with chrysoberyl. Li-Cs-(Rb-Nb-Ta-P) mineralization developing among other minerals spodumene and amblygonite in their deposits also occur in LCT pegmatites.

Pegmatites are important sources of Li and Cs (Bessemer City, USA, Greenbushes, Australia, and Bikita, Zimbabwe). Normally these pegmatitic deposits are exploited for Nb and Ta and the light metals Li and Cs won as byproducts (Bernic Lake, Canada, Manono-Kitotolo, DR Congo). Spodumene, Li mica and pollucite are extracted from these deposits to produce Cs and Li concentrates. The Li-Cs-(Rb) pegmatite, Bikita, Zimbabwe, is besides Bernic Lake (Lac-du-Bonnet), Canada, the only site where another alkaline element rubidium was found at such a high level so as to make its recovery from the ore feasible. The Hagedorf-Pleystein pegmatite province was also mined for some years for Li which is accommodated in a wide range of Li phosphates. This chain of Variscan Li-bearing pegmatites may be extended through the Czech Republic into Poland with lepidolite pegmatite near Rožná and Dobrá Voda. Gem quality kunzite, the rose colored spodumene variety formed together with cleavelandite, black tourmaline, morganite and aquamarine in many Brazilian pegmatites

REE-U-Nb-bearing pegmatites which in places are transitional into intragranitic deposits with Mo-W-U-Be are known from Kyrgyzstan (Kuperlisay/ Kalesay REE-Th-Be deposit). The Radium Hill REE-U deposit is located in eastern South Australia where segregations bearing Fe, Ti, U and REE led to the development of davidite. Granite-type Nb-REE deposits are also found in southern Hunan and eastern Guangxi, China.

Uraniferous pegmatites were discovered among others at Bancroft, and Campbell Island, Canada, but only a few pegmatites may be called U deposits. Many pegmatites and aplites contain U in form of uraninite or uraniferous Ta-Nb oxides but mostly at a subeconomic level. Often U yellow ores indicate remobilized black ore mineralization that are no longer present or at relatively low level, as is the case with Hagedorf, Germany.

Tin and boron are continuously enriched during the evolution of granitic magmas and finally concentrated in pegmatites and greisen zones where it may reach contents of more than 12% B₂O₃ at temperatures from the pegmatitic stages down to temperatures of hydrothermal fluids. Tourmalines are taken from pegmatites that are intrusive into schistose or granitoid rocks. Where the pegmatites are deeply weathered, tourmalines can be extracted from the kaolinitic saprolite with perfect crystal faces preserved (Nepal (Hyakule, Phakuwa), Russia (Mursinska Mts. in the Ural), Kenya (Voi-Taveta) and Zambia (Chipata). Danburite and dumortierite in gem quality are observed in granites and pegmatites. Jeremejevite is a rare constituent of the late stage hydrothermal alteration of pegmatites.

Fluorine is also concentrated within pegmatites. The pegmatite at Crystal Mountain in Montana, USA is one of the few fluorite-bearing pegmatites. Topaz crystals of gem-quality are bound to granites and pegmatites (Ukraine, Namibia, Brazil, USA, Pakistan, and Afghanistan).

The pegmatites most renowned and abundant in Li-, Fe-, Mn and Zn phosphates are found in SE Germany, Namibia, USA, Czech Republic, the Iberic Peninsula, Rwanda, Brazil Mozambique. They may be attractive host rocks of gem-quality apatite and Fe-Mn phosphates as well as Al phosphates. The latter formed from alteration of primary pegmatite-related (Mn)apatite. They are of no use as a source of phosphate.

The major source of feldspar and quartz seldom lies in the parental granitic bodies but in the satellite pegmatites or aplites. Some of them are anatectic pegmatites which formed during the collisional stage of the orogen and commonly associated with migmatitic rocks or retrograde processes. The parent material of residual pegmatites lies within the granitic

suite of magmatic rocks and from the geodynamic point view they are syn-collisional or post-collisional. In places an aplitic margin developed at the contact between the true pegmatite and the metamorphic country rocks. These pegmatites are an important source of ceramic raw materials.

At Mangari, Kenya, a ruby mineralization is related to kyanite pegmatites (plumasite: coarse-grained rock consisting of anhedral corundum crystals in an oligoclase matrix). Typical corundum-bearing pegmatites also occur at Dac Lac in southern Vietnam.

Graphite occurs in alkaline pegmatites at Hackman Valley, Mt. Yukspor and Chibina Massif, Russia. It is associated with minerals including aegirine, apatite, albite, nepheline and natrolite. Graphite-bearing pegmatitic dikes occur side-by-side with wollastonite-bearing calcsilicates and gneiss-*charnockite* horizons in the supracrustal terrain of the Kerala *Khondalite Belt*.

White mica (muscovite) is found in booklets and large plates in many pegmatite and leucosomes, related to granitic intrusions or reflecting the retrograde path of regional metamorphism, respectively. Often mica cannot be won economically as a stand-alone commodity and is only be sold as a by-product of quartz, feldspar or more precious commodities such as beryl or even metals (e.g., bismuth). Quite different from that, phlogopite-bearing pegmatoids

mined at Ambatoabo, Madagascar, deserve particular treatment as their dynamo-metamorphic. The dynamo-metamorphic processes leading to the phlogopite mineralization are correlated with the waning stages of the Pan-African Orogeny around the turn Late Precambrian – Early Paleozoic. These phlogopite deposits are genetically related to the afore-mentioned Pan-African Th-U skarn and orthoclase deposits at Itrongay, Madagascar, which also contain phlogopite concentrations.

FINAL USE

Granitic pegmatites and aplites as well as those pegmatitic and aplitic mobilizates in metamorphic terrains play an important part in the field of non-metallic raw material supply, especially when it comes to gemstones and ornamental stones. They are of lesser significance as a source of metal or fossil fuels.

ACKNOWLEDGEMENTS

I express my gratitude to Milan Novák for taking over the review of this paper.

REFERENCES

- Dill, H.G. (2010). The "chessboard" classification scheme of mineral deposits: Mineralogy and geology from aluminum to zirconium. *Earth Science Reviews* **100**: 1-420.

PRELIMINARY RESULTS OF A NEWLY-DISCOVERED LAZULITE-SCORZALITE PEGMATITE-APLITE IN THE HAGENDORF-PLEYSTEIN PEGMATITE PROVINCE, SE GERMANY

Harald G. Dill^{1§}, Radek Škoda² & Berthold Weber³

¹ Federal Institute for Geosciences and Natural Resources, P.O. Box 510163, D-30631 Hannover, Germany, §dill@bgr.de

² Institute of Geological Sciences, Faculty of Science, Masaryk University, Kotlářská 2, 611 37 Brno, Czech Republic

³ Bürgermeister-Knorr Str. 8 D-92637 Weiden i.d.OPf., Germany

Key words: Pegmatite, lazulite-scorzalite, phosphate, Variscan, Hagendorf-Pleystein, SE Germany

INTRODUCTION

The Hagendorf-Pleystein pegmatite province Oberpfalz-SE/ Germany, ranks among the largest concentrations of pegmatitic and aplitic rocks in Europe with the largest pegmatite of this mining district totaling 4.4 million tons of pegmatitic ore and mined until recently at Hagendorf-South. The various pegmatite are famous for their Al-K-Fe-Mn-Li phosphates which were mined during the initial stages of mining at Hagendorf-South. Magnesium is absent from the phosphates minerals encountered at Hagendorf-South, Hagendorf-North and Pleystein which are the largest pegmatites of this area (Fig. 1).

GEOLOGICAL SETTING

The current mapping of the newly discovered aplitic- to pegmatitic mobilizates reveals a swarm of phosphate-bearing feldspar-quartz-mica mobilizates which are aligned in NNW-SSE direction. They are embedded into banded biotite gneisses. The study area is part of the northeastern Bavarian Basement whose paragneisses underwent structural deformation in the between 450 to 330 Ma (Weber & Vollbrecht 1989). The mobilizates are assumed to have formed in the aftermaths of this structural adjustment prior to the intrusion of the Flossenbürg Granite which was dated by the Rb/Sr whole rock method at 311.9 ± 2.7 Ma (Wendt *et al.* 1994).

METHODS

Examination of thin sections, X-ray diffraction analysis and X-ray fluorescence analysis were performed routinely. Electron microprobe analyses were carried out using a CAMECA SX100 equipped with five wavelength-dispersive spectrometers and a Princeton Gamma Tech energy-dispersive system. Trivalent iron within the analyses was calculated taking into consideration the XRD analyses of the minerals.

RESULTS AND DISCUSSION

A poorly to unzoned aplitic mobilizate containing Fe-Mn-Mg-Sc-U-REE phosphates, some Cu-Pb-Zn sulfides, and barite has been discovered near Trutzhofmühle at the western border of the Hagendorf Pegmatite Province, Germany (Dill *et al.* 2008). Apart from the common phosphates, phosphoferrite, Mn-vivianite, rockbridgeite, whitemoreite, ferrolaueite, Al rockbridgeite, mitridatite, strunzite, triplite, wolfeite, triploidite, an unnamed K-Ba-Sc-Zr phosphate, an unnamed Zr-Sc phosphate-silicate and kolbeckite were found. Aggregates of deep blue lazulite occur in contact with apatite near the edge of the aplitic dike. The Fe contents of lazulite range from 2.3 to 3.4 wt. % Fe. Another phosphate closely resembles lazulite with respect to its bluish tint, yet it does not contain any Fe, but a higher H₂O content. This mineral is called gordonite, $\text{MgAl}_2(\text{PO}_4)_2(\text{OH})_2 \cdot 8\text{H}_2\text{O}$ documented by XRD.

Based upon these findings of hitherto unknown Mg phosphate mineral assemblages the areas was revisited for the distribution Mg phosphate minerals, in particular. In one old mine and during a new discovery different Mg phosphates have been encountered.

Investigation of an abandoned feldspar mine near Ploessberg which operated a vaguely zoned pegmatitic dike led to the discovery of the Ti-Mg phosphate paulkerrite. It is a shear-zone-hosted pegmatite running through biotite gneisses with interbedded calcsilicates. The Fe-bearing phosphates are similar to those of Hagendorf since they show similar Li contents and are also associated with columbite-(Fe). Unlike Hagendorf, the Ploessberg pegmatite is much smaller. It is conformably interbedded with the metapelitic country rocks, whereas the Hagendorf pegmatite stock is intrusive and cuts through the gneissic country rocks.

Another series of aplitic to pegmatitic mobilizates which has not been touched by mining activities was mapped in the Hagendorf-Pleystein Pegmatite Province. Even with the unarmored eyes the blue tint of the phosphate mineral association may be detected in the field. It is a mineral of the lazulite-scorzalite s.s.s. (solid solution series) (Table 1). Wagnerite is another Mg phosphate but far less widespread than the minerals of the lazulite-scorzalite s.s.s. The major phosphate mineral in these mobilizates is Mn-bearing apatite, ubiquitous also in the Pleystein and Hagendorf pegmatites. Iron phosphates present in the newly discovered aplitic to pegmatitic mobilizates belong to the rockbridgeite s.s.s., santabarbaraite, whitmoreite and minerals of the strengite-variscite s.s.s. In some Fe phosphates the Zn contents may be as high as 0.9

wt. ZnO. Unlike Hagendorf or Pleystein, neither Zn phosphates nor Li phosphates have been identified so far in the siliceous mobilizates under study.

The Mg-Ti phosphate paulkerrite in the shear zone-hosted pegmatite at Ploessberg is assumed to have originated from hydrothermal processes operative along the contact between the dike-like phosphate pegmatite and its surrounding chloritized biotite gneisses.

Minerals of the lazulite-scorzalite s.s.s which formed in the newly discovered aplitic-pegmatitic mobilizates are part of the phosphate association which was emplaced during the Late Variscan pegmatitic stage. There are no signs of hydration of these Mg-Al minerals resulting in the precipitation of gordonite as at Trutzhofmühle.

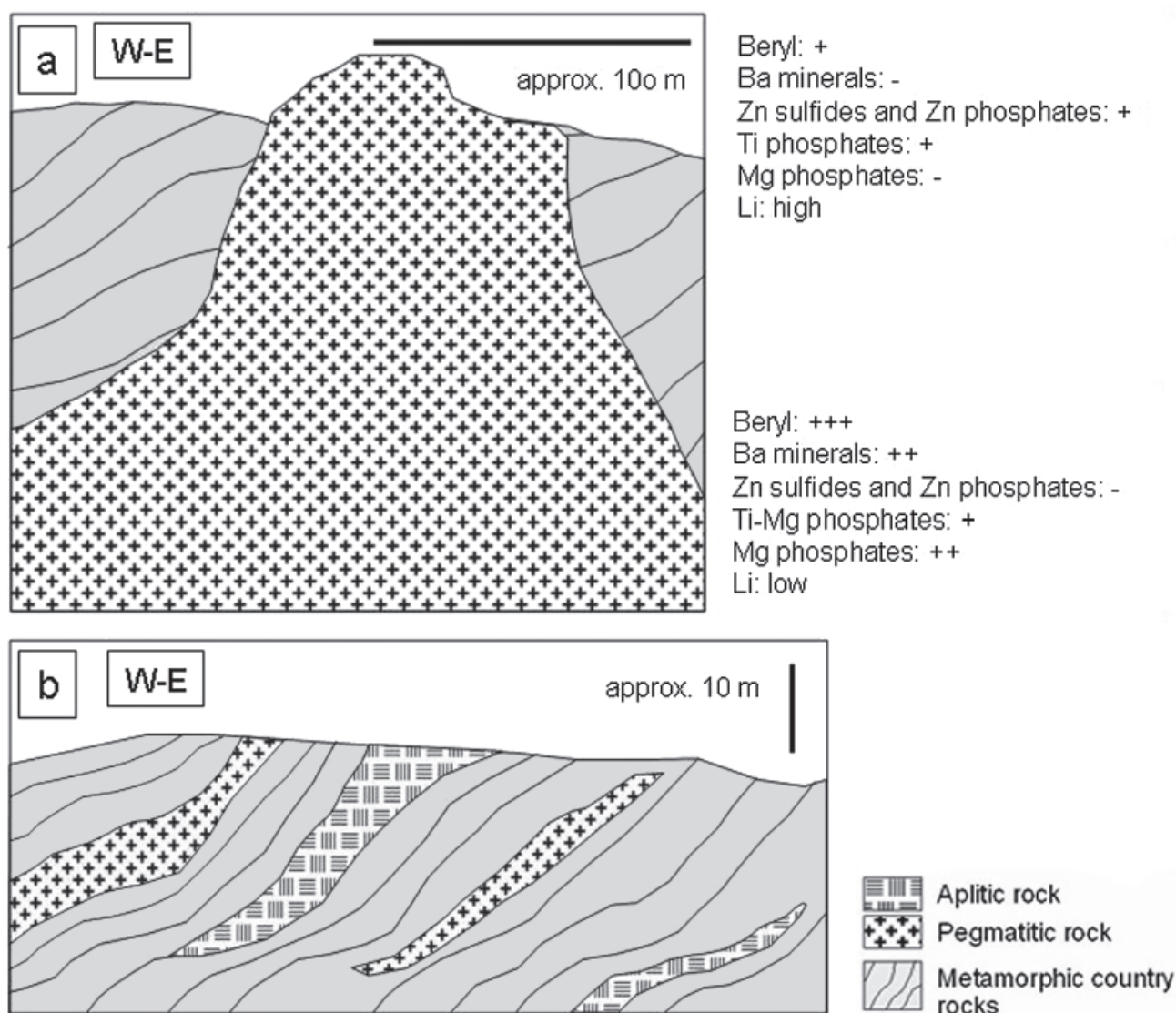


FIGURE 1. Structural type of pegmatitic and aplitic rocks in the NE-Bavarian Basement with marker minerals and chemical characteristics crucial for their distinction.

a) Intrusive (discordant) pegmatitic stocks. Hagendorf South, Hagendorf North, Pleystein.

b) Pegmatitic and aplitic mobilizates (concordant with little discordant pegmatitic veinlets). Trutzhofmuehle, Ploessberg.

+++ abundant ++ common + traces - absent

We interpret these findings of a Mg-Fe-Al phosphate mineralization as evidence of a deeper level of erosion cutting through the zone where the pegmatitic melt was reacting with the chloritized biotite gneisses.

Magnesium phosphates in poorly zoned pegmatitic and aplitic dikes are representative of the siliceous melt reacting with the metapelitic country rocks at an earlier stage and deeper level than the main well-zoned pegmatitic bodies at Hagendorf and Pleystein. The most recent discovery is held to be the deepest part of erosion, followed by the Trutzhofmühle level and the Ploessberg level. The shallowest part of the pegmatitic bodies is exposed in the Pleystein and Hagendorf pegmatites which are the most economic bodies of the pegmatite province and most well zoned.

The late discoveries of Mg phosphate-bearing aplite and pegmatites are due to the size and shape of these siliceous bodies which are interbedded sandwich-like into the metapelitic country rocks only of moderate thickness (less than 10 m) and poorly zoned into quartzose cores and a feldspar rim. Therefore they are of only minor importance as a source of K feldspar for the ceramic industry.

Magnesium phosphates which show up in the pegmatitic and hydrothermal stages of the formation of phosphate pegmatites reflect the interaction between the metapelitic country rocks and the pegmatites at different levels of erosion. They may be very attractive to mineral collectors, yet from the economic point of you they are a "negative ore guide" hallmarking the end of mining pegmatites for ceramic purposes. The quality of the lazulite-scorzalite s.s.s is only of showroom and not of gem quality.

These changes among Mg-bearing phosphates observed in the pegmatites and aplites in SE Germany are also paralleled by conspicuous trends of other minerals such as those bearing barium, zinc, lithium and beryllium (Fig. 1).

TABLE 1. Chemical composition of some selected phosphates (wt. %) from the newly –discovered lazulite-scorzalite pegmatite-aplite in the Hagendorf-Pleystein pegmatite province, SE Germany

Mineral	lazulite-scorzalite		santabarbaraite		strengite-variscite	
	s.s.s.				s.s.s.	
Sample	42	40	77	92	38	33
P ₂ O ₅	45.41	45.24	29.87	29.33	39.33	39.36
SiO ₂	0.27	0.07	0.08	0.17	0.01	0.07
Al ₂ O ₃	32.7	31.7	2.86	2.73	0.44	0.57
ZnO	0.00	0.00	0.00	0.04	0.14	0.03
CaO	0.08	0.04	0.02	0.26	0.01	0
MgO	8.12	8.27	0.64	0.69	0.04	0.04
Na ₂ O	0.08	0.03	0.00	0.08	0.14	0.22
H ₂ O (OH)	5.76	5.71	24.47	24.27	19.95	20.23
FeO	8.40	7.96	0.00	0.00	0.00	0.48
Fe ₂ O ₃	0.23	1.34	43.02	42.24	43.17	43.48
MnO	0.07	0.03	0.00	0.00	0.00	0.11
Mn ₂ O ₃	0.00	0.00	1.24	1.53	0.10	0.00
sum	101.12	100.39	102.20	101.34	103.33	104.59

ACKNOWLEDGEMENTS

We express our gratitude to an anonymous reviewer for taking over the review of this paper.

REFERENCES

- Dill, H.G., Melcher, F., Gerdes, A., & Weber, B. (2008). The origin and zoning of hypogene and supergene Fe-Mn-Mg-Sc-U-REE-Zn phosphate mineralization from the newly discovered Trutzhofmühle aplite (Hagendorf pegmatite province, Germany). *Can. Mineral.* **46**: 1131-1157.
- Weber, K. & Vollbrecht, A. (1989). The Crustal structure at the KTB Drill Site, Oberpfalz.- In.: Emmermann, R. & Wohlenberg, J. (eds.) *The continental deep drilling program (KTB)*. 5-36, Springer, Heidelberg.
- Wendt, I., Ackermann, H., Carl, C., Kreuzer, H., Müller, P. & Stettner, G. (1994) Rb/Sr-Gesamtgesteins- und K/Ar-Glimmerdatierungen der Granite von Flossenbürg und Bärnau. *Geol. Jb. E* **51**: 3-29.

THE WAUSAU SYENITE COMPLEX, MARATHON COUNTY, WISCONSIN

Alexander U. Falster^{1§}, Thomas W. Buchholz² & Wm. B. Simmons¹

¹ Department of Earth and Environmental Sciences, University of New Orleans, New Orleans, LA 70148. §afalster@uno.edu

² 1140 12th Street North, Wisconsin Rapids, Wisconsin 54494.

Key words: Wausau Syenite Complex, anorogenic, Proterozoic, pegmatite

INTRODUCTION

The anorogenic, NYF-type, Wausau syenite complex (WSC) is located in central Marathon Co., Wisconsin (Fig. 1) and is part of a NE-SW-trending belt of 1.770 to 1.030 Ga granitic plutons that extend from the Baltic shield to the SW United States (Anderson 1983a). The Proterozoic (ca. 1.5 Ga) complex consists of 4 intrusive centers (Fig. 1), from oldest and most alkalic to youngest and most silicic: Stettin complex (SC), Wausau pluton (WP), Rib Mountain pluton (RMP), and the Nine Mile pluton (NMP).

MAGMA ORIGIN AND TECTONIC CONDITIONS

Anderson (1983b) postulates that these plutons are of rapakivi affinity and crystallized between 790 to 640 °C under low total pressure of less than 2 kb. The intrusion of the magmas is likely the result

of thermal doming in the mantle which supplied the heat of fusion at lower crustal levels (Anderson 1983b). This thermal event was related to a failed rift (Anderson 1983b). According to VanSchmus and Bickford (1981), the time from the intrusion of the Stettin complex to the intrusion of the Nine Mile pluton spanned 0.02 Ga.

Geochemically, the WSC can be classified as within-plate granitoids (WPG), using the discrimination diagrams (Fig. 2) of Pearce *et al.* (1984), and as A₁ type (rift, plume and hotspot environments) granitoids (Fig. 3), according to Eby (1992). This interpretation is consistent with the anorogenic tectonic environment of the complex and suggests that the melts that formed the WSC are derived from lower crustal materials. The older rocks of the SC are enriched in Nb and Ga compared to the younger rocks of the NMP. Compared to the WSC, the WPG South Platte district in Colorado, is similar but falls in the A₂

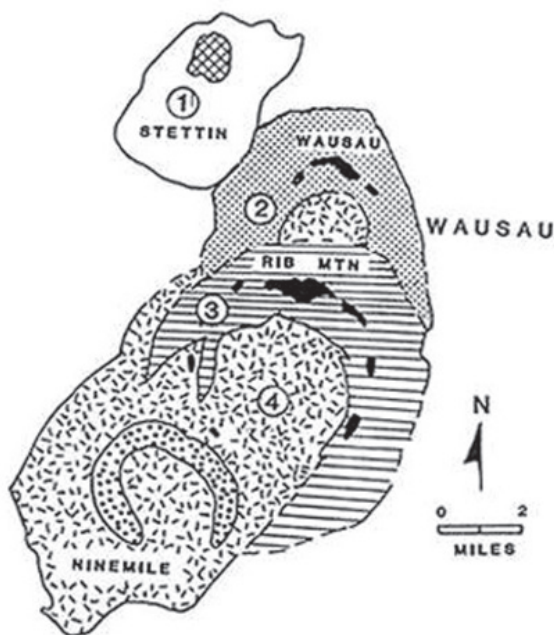


FIGURE 1. Schematic representation of the 4 intrusive centers of the WSC (Myers *et al.* 1984).

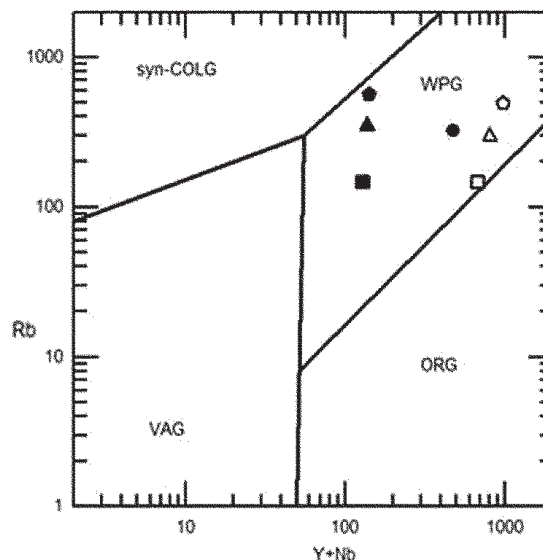


FIGURE 2. Tectonic discrimination plot of Rb vs. Y+Nb (average) applied to the rock suites of the WSC (Pearce *et al.* 1984). Symbols used: circle, overall average Wausau Syenite complex; Filled triangle, Nine Mile pluton average; Filled pentagon, Nine Mile rock average; filled square, Nine Mile wall zone average; open triangle, Stettin complex average; open pentagon, Stettin complex rock average; open square, Stettin complex wall zone average.

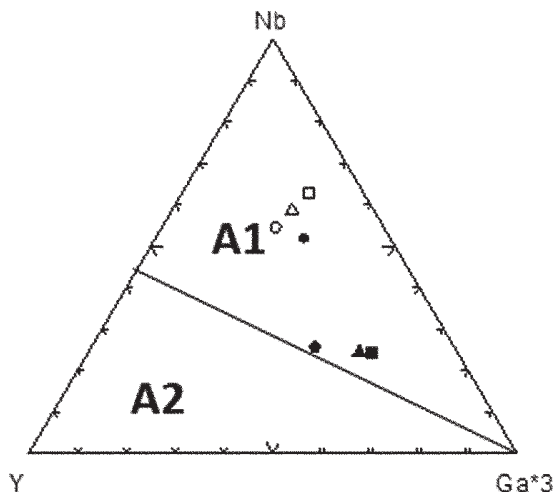


FIGURE 3. Ternary plot of Y vs. Nb vs. 3*Ga for A₁ and A₂ granitic rocks (Eby 1992).

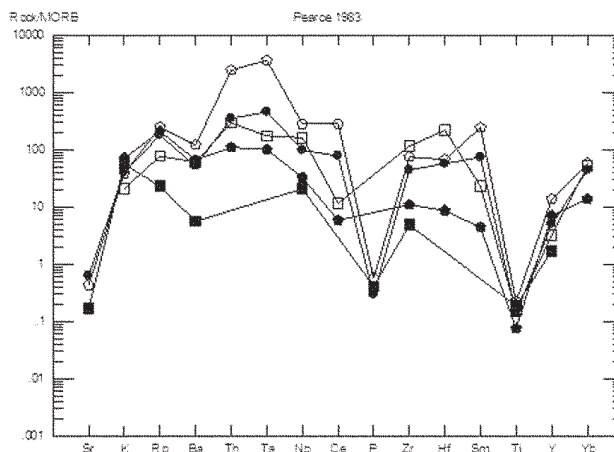


FIGURE 4. Spider diagram for rocks from the Wausau Syenite complex (after Pearce 1983).

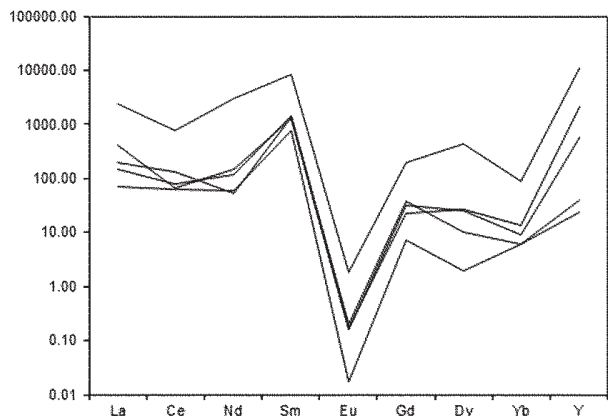


FIGURE 5. Chondrite-normalized REE plot of fluorite from the W & S portions of the Nine Mile pluton.

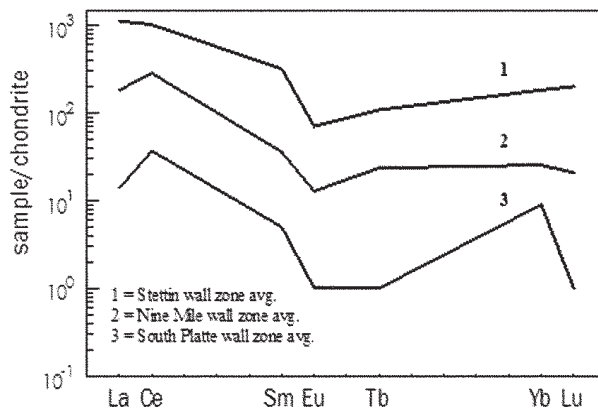


FIGURE 6. Chondrite-normalized plot of wall zone REE contents for the Stettin Complex, the Nine Mile pluton, and South Platte, Colorado.

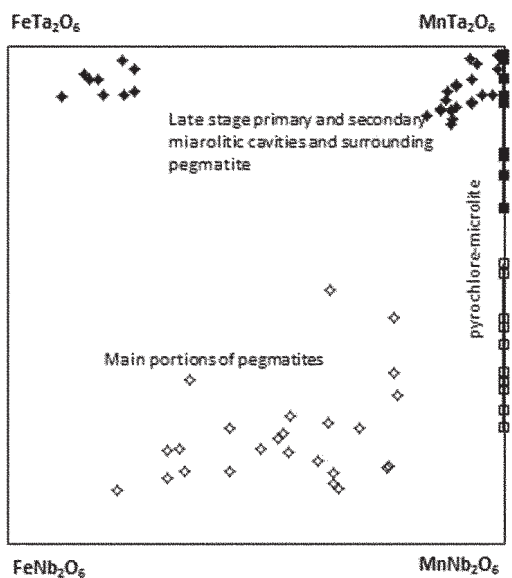


FIGURE 7. Columbite-tantalite quadrilateral for pegmatites in the Nine Mile Pluton.

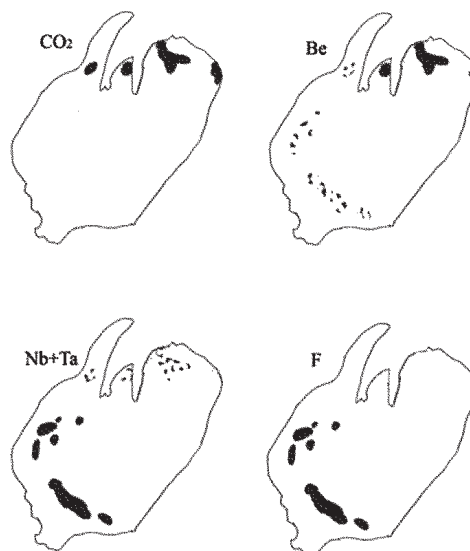


FIGURE 8. Key element distribution in the Nine Mile pluton.

type granitoids field (Simmons *et al.*, 1999). A distinct enrichment of the WSC in Rb, Th, Ta, Zr, Hf, Y and Yb as well as depletion in Sr, P and Ti is evident in a Spider Diagram According to Pearce (1983) (Fig. 4).

STETTIN COMPLEX

The Stettin complex is the oldest and most alkalic of the 4 intrusive centers. Rock types exposed include nepheline syenite, pyroxene and amphibole syenites as well as feldspar-dominant syenites. Pegmatites occur throughout the complex and often are well zoned. Mirolitic cavities are generally small. REE-bearing minerals are wide-spread throughout the pegmatites and pyrochlore species are common. Columbite group species are scarce and fluorite is common. Zircon is locally very abundant. Outcrops are less common than in the Nine Mile pluton.

NINE MILE PLUTON

The NMP (Fig. 1) is the best exposed of the 4 intrusive centers, a result of extensive mining of weathered rocks (grus) for road material and landscaping. Numerous pegmatite bodies exist throughout the complex (Falster *et al.* 2000). The pegmatites are of modest size, rarely reaching 100 m in maximum dimension. Pegmatites are well-zoned with distinctive wall zones, intermediate zones and core zones. Replacement units (usually albite) occur in some. The mineralogy of the pegmatites is rich in REE-bearing species such as monazite-group minerals, xenotime, bastnaesite-group species and numerous pyrochlore-group minerals. REE are also abundant in fluorite (Fig 5). The pegmatite wall zones of the WSC pegmatites contain substantial concentrations of REE, with those from the SC exceeding the ones from the NMP. It is interesting to note that wall

zone REE content is significantly lower in pegmatites from the South Platte district (Simmons *et al.* 2000) (Fig. 6). However, South Platte pegmatites exhibit an astonishing REE concentration in the inner zones and especially in the replacement units (Simmons *et al.* 1987). Be minerals occur sporadically, and B minerals are essentially absent, whereas F is widespread as REE-rich fluorite (Fig. 5) and other F-bearing minerals. In late-stage primary and secondary mirolitic cavities (left by dissolution of pre-existing quartz or fluorite), a highly-evolved mineral association is seen consisting of tantalite-(Mn), microlite, tantalian rutile, tantalian cassiterite, and tapiolite. In some non-mirolitic pegmatites, Ta-rich minerals (tantalite-(Mn), microlite, tantauxenite-(Y)) occur embedded in feldspar and quartz mainly along the inner intermediate zone and core margin. Typically, the Ta/Nb ratio steadily increases from the core of the crystals toward the rim, such that significant Ta-dominance is achieved (Fig. 7). Sometimes, Ta-rich microlite forms as a late overgrowth on and/or replacement of columbite-group minerals. Zircons found in this assemblage also reflect a similarly high enrichment trend expressed as very low Zr/Hf ratios. The abundance of fluorite suggests that F complexing is the controlling mechanism causing the late enrichment of Ta which produced a late-stage mineral association similar to that seen in highly evolved LCT-type pegmatites.

KEY ELEMENTAL DISTRIBUTION IN THE NINE MILE PLUTON

A comparison of key elemental abundances in the Nine Mile pluton shows a important relationships (Fig. 8): The northern portion which houses the large mirolitic cavity-bearing pegmatites is also the area where siderite is very abundant. Possibly, CO₂ plays an important role in the formation of these larger

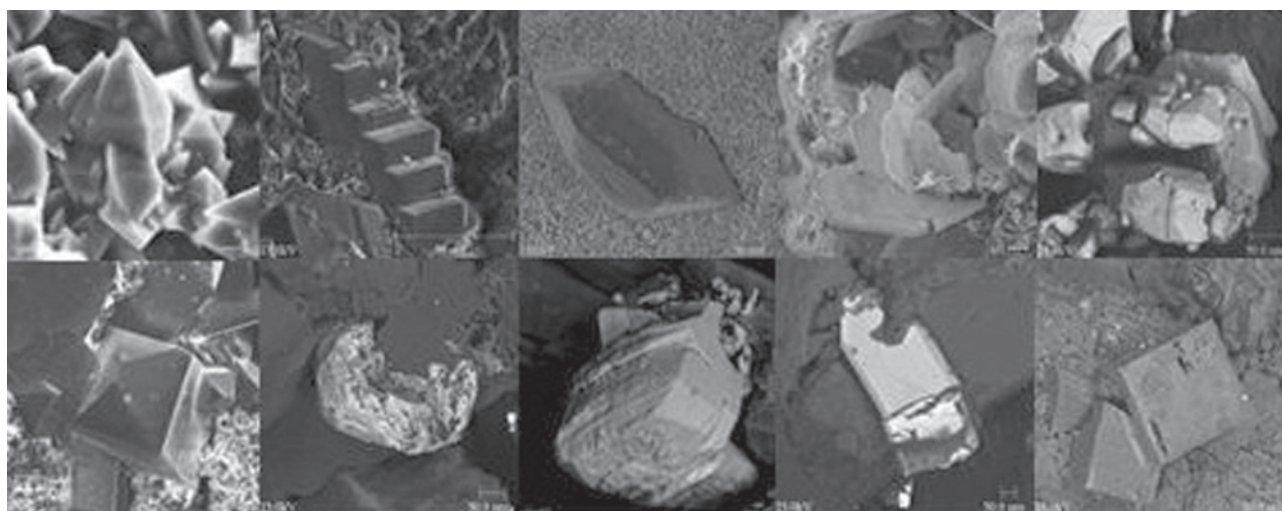


FIGURE 9. Scanning electron photomicrographs of selected mineral species from pegmatites in the Nine Mile pluton. Top row, left to right: anatase, bertrandite, phenakite, bastnaesite, monazite. Bottom row: xenotime, manganotantalite, ferrotapiolite, manganocolumbite and fluorite.

miarolitic cavities in the northern part. Be and Ti are also far more abundant in this part of the pluton. REE occur all over the pluton. Nb and Ta are widespread but favor the southern and western parts of the pluton. Interestingly, F favors the western and southern parts as well and is frequently a rock-forming mineral in this environment in pegmatites, granites and aplites. Many of the accessory minerals in the WSC occur in fine crystals (Fig. 9)

REFERENCES

- Anderson, J. L. (1983a). Proterozoic anorogenic granite plutonism of North America. Geological Society of America Memoir **161**.
- Anderson, J. L. (1983b). Mineral equilibria and crystallization conditions in the late Precambrian rapakivi massif, Wisconsin. *Am. Jour. of Science* **280**: 289-332.
- Eby, G. N. (1992). Chemical subdivision of the A-type granitoids: petrogenetic and tectonic implications. *Geology* **20**: 641-644.
- Falster, A. U., Wm. B. Simmons, K. L. Webber, & T. W. Buchholz (2000). Pegmatites and pegmatite minerals of the Wausau complex, Marathon Co., Wisconsin. *Memorie della Societa Italiana di Scienze Naturali e del Museo Civico di Storia Naturale di Milano* **XXX**: 13-28
- Myers, P. E., M. K. Sood, L. A. Berlin, & A. U. Falster (1984). Fieldtrip #3: The Wausau Syenite Complex, Central Wisconsin. 30th Annual Institute on Lake Superior Geology.
- Pearce, J. R., N. B. Harris, & A. G. Tindle (1984). Trace element discrimination diagrams for the tectonic interpretation of granitic rocks. *J. Petrol.* **25**: 956-983.
- Simmons, Wm. B., K. L. Webber, & A. U. Falster (2000). NYF pegmatites of the South Platte district, Colorado. *Can. Min.* **37**: 836-837.
- Simmons, Wm. B., M. T. Lee, & R. H. Brewster (1987). Geochemistry and evolution of the South Platte granite-pegmatite system, Jefferson Co., Colorado. *Geochim. Cosmochim. Acta* **51**: 455-471.
- VanSchmus, W. R. & M. E. Bickford (1981). Proterozoic chronology and evolution of the mid-continent region, North America: In *Precambrian plate tectonics*, Kroner, A., ed., New York Elsevier Scientific Publication Co.: 251-296.

ZONED FOITITE→SCHORL→DRAVITE→MAGNESIOFOITITE CRYSTALS FROM POCKETS IN ANATECTIC PEGMATITES OF THE MOLDANUBIAN ZONE, CZECH REPUBLIC

Petr Gadas^{1§}, Milan Novák¹, Jan Filip², Josef Staněk¹

¹ Department of Geological Sciences, Masaryk University, Kottlářská 2, 611 37 Brno, Czech Republic; §pgadas@centrum.cz

² Centre for Nanomaterial Research and Department of Experimental Physics, Palacký University, Tř. 17. listopadu 12, 771 46 Olomouc, Czech Republic

Key words: foitite, schorl, dravite, magnesiofoitite, compositional evolution, anatectic pegmatite, pocket.

INTRODUCTION

Compositional trends in tourmaline were widely studied in a variety of granitic pegmatites from barren to highly fractionated complex (Li) ones. During pegmatite evolution, they generally exhibit increase in Al and Li and decrease in Mg and Fe in the simplified sequence dravite/foitite→schorl→elbaite→rossmanite. In contrast, the examined anatectic pegmatites with primary andalusite and common pockets contain zoned tourmaline crystals showing foitite→schorl→dravite→magnesio foitite evolution. We present compositional data and evolution during crystallization of tourmalines from pockets of 14 pegmatites and 5 muscovite-rich veins.

INTERNAL STRUCTURE AND MINERALOGY OF ANATECTIC PEGMATITES AND TOURMALINE DESCRIPTION

Anatectic pegmatites with locally developed large pockets lined with attractive crystals of smoky quartz and tourmaline occur in several regions with migmatites in the Moldanubian Zone (Fig. 1). These pegmatites are similar to the HP massive Al, B-rich pegmatites of abyssal class with dumortierite, schorl-olenite and primary kyanite from the Kutná Hora Unit (Cempírek *et al.* 2006); however, common andalusite and cordierite in the anatectic pocket pegmatites suggest LP conditions at $P < 4$ kbar. The pegmatites form concordant and discordant dikes or irregular bodies with transitional to locally sharp contacts to the hosting migmatitized biotite-sillimanite gneisses or granulitic gneisses. Their internal structure evolves from common simply zoned thin dikes, from several cm to several dm thick, to rare more complicated large dikes, up to 2 m thick. Pegmatites are commonly built of an outermost, medium- to coarse-grained granitic unit ($Plg+Qtz+Kfs±Msc±Bt$), followed by a graphic unit ($Qtz+Kfs$) and sporadic pockets with crystals of smoky quartz, K-feldspar, albite, muscovite

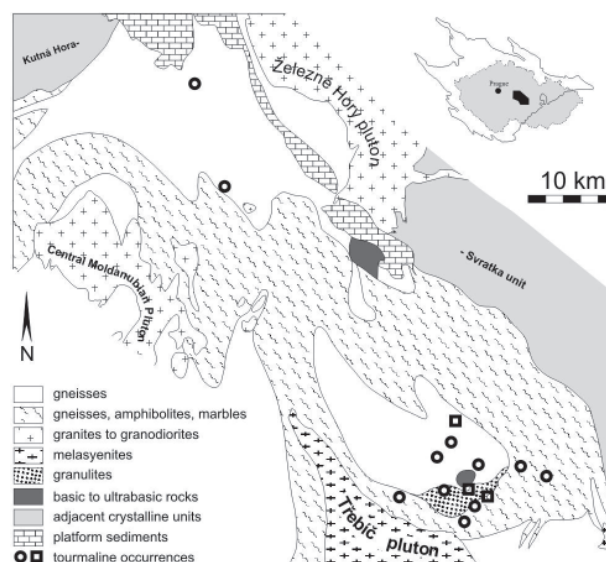


FIGURE 1. Occurrences of pegmatites and muscovite-rich veins on the simplified geological map of the northeasternmost part of the Moldanubian Zone. Circles – pegmatites, squares – muscovite-rich veins.

and tourmaline. Large dikes may contain blocky K-feldspar and rare albite-rich units and locally a quartz core. Pockets are randomly distributed close to the core of pegmatite bodies. In the area of anatectic pocket pegmatites, thin muscovite-rich veins different from pegmatite dikes in shape, size and internal structure, were sporadically found. They exhibit evident spatial relations to the pocket pegmatites, but they are built of porous masses of medium- to coarse-flaked muscovite as a dominant textural-paragenetic unit in veins with rare to minor crystals of albite, tourmaline and quartz. Similarities in the mineral assemblages indicate the muscovite-rich veins to be late satellites to anatectic pocket pegmatites.

The mineral assemblages of pegmatite bodies have major K-feldspar, albite, and quartz, minor muscovite and tourmaline, and minor to accessory

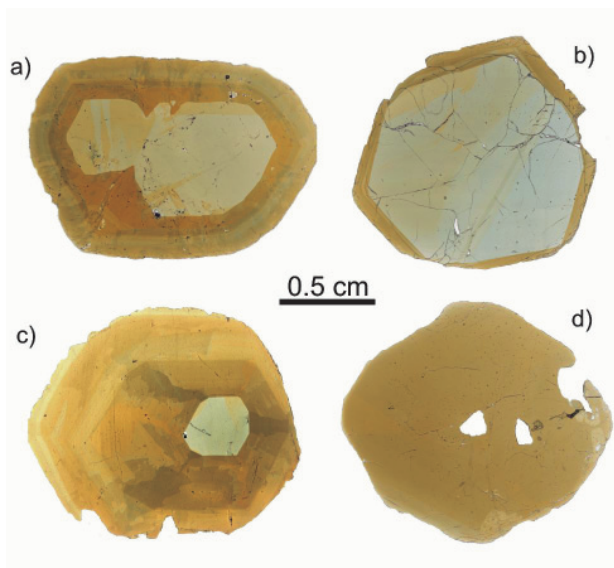


FIGURE 2. Thin sections of tourmalines from pegmatites (a, b, c) and from muscovite-rich veins (d).

biotite, andalusite, fluorapatite and altered cordierite. Rare accessory dumortierite, garnet, pyrite, ilmenite, rutile, anatase, brookite, monazite-(Ce), xenotime, Zn-rich hercynite and W-xiolite were also identified. The muscovite-rich veins exhibit a simpler assemblage: muscovite \geq albite, quartz and tourmaline; K-feldspar and most accessory minerals are commonly absent.

Black tourmaline is a common minor to accessory mineral present locally in several generations in the texturally more evolved anatectic? pegmatites. Prismatic crystals and their aggregates enclosed in blocky K-feldspar and massive quartz occur in large dikes; nevertheless, tourmaline from pockets is typical. It forms long prismatic to lens-shaped crystals and their parallel to subparallel intergrowths, up to 15 cm in size, typically with prismatic striations and strong vitreous lustre.

OPTICAL ZONING AND CHEMICAL COMPOSITION OF TOURMALINE

Crystals of tourmaline from pockets in the anatectic pegmatites typically exhibit striking zoning in optical microscope with variable pleochroism (Figs. 2a, b, c): core - O = greyish blue to khaki green, E = pale yellowish to colorless; intermediate zone - O = brown, E = pale brown to yellowish; rim are too narrow. Within the core, weak to moderate sectorial, fine-oscillatory and/or patchy zoning were observed. Crystals from muscovite-rich veins are rather homogeneous with O = brown, E = pale brown (Fig. 2d)

Electron microprobe study revealed that the optical zoning and compositional zoning in crystals from pockets are only partly correlated. Cores and

intermediate zones have very similar compositions, the main difference is higher concentration of Ti (up to 0.14 apfu; 1.06 wt.% TiO_2 , Fig. 3g) and slightly decreased $\text{Fe}_{\text{tot}}/(\text{Fe}_{\text{tot}} + \text{Mg})$ and X-site vacancy in the intermediate zone (Figs. 3a, b, e). Very narrow outer rims, only locally developed, are evidently Mg-enriched (Figs. 3c, f) but otherwise similar to the intermediate zone as well as with contents of Ti (Fig. 3g). Mössbauer spectroscopic study of two samples from pocket pegmatites yielded very low Fe^{3+} contents similar in core and intermediate zone. More homogeneous tourmaline from muscovite-rich veins (Fig. 2d) is evidently Mg-enriched (Fig. 3d, f), slightly Ca-enriched (Fig. 3e) and exhibits a narrower variation in $\text{Fe}_{\text{tot}}/(\text{Fe}_{\text{tot}} + \text{Mg})$, increasing X-site vacancy (Figs. 3d, e) and decreasing Ti (Fig. 3g) toward rims.

DISCUSSION

Tourmaline from anatectic pocket pegmatites exhibits rather primitive composition with low Li and F contents (see also Povondra 1981, Novák *et al.* 2004), high to low $\text{Fe}_{\text{tot}}/(\text{Fe}_{\text{tot}} + \text{Mg})$ and low to moderate Ti but high Al. Such primitive compositions are known mainly from Al-rich metapelites (Henry & Dutrow 1996), but only scarcely described in granitic pegmatites. In spite of a high variability in $\text{Fe}_{\text{tot}}/(\text{Fe}_{\text{tot}} + \text{Mg})$ in the crystal core and intermediate growth zone of tourmalines from pockets, the general trend exhibits an evident reverse evolution characterized by the decrease in $\text{Fe}_{\text{tot}}/(\text{Fe}_{\text{tot}} + \text{Mg})$ from core to rim of crystals in the pockets of pegmatites. Tourmaline from muscovite-rich veins is Mg-enriched in comparison with those from studied pegmatites and shows low variation in $\text{Fe}_{\text{tot}}/(\text{Fe}_{\text{tot}} + \text{Mg})$ with some overlaps with narrow late rims (Fig. 3c, d). General decrease in $\text{Fe}_{\text{tot}}/(\text{Fe}_{\text{tot}} + \text{Mg})$ from cores of crystals to narrow rims and to tourmaline from muscovite-rich veins is apparent and corroborate their genetic relations.

Presence of tourmaline in pockets and muscovite aggregates suggest that they crystallized likely from hydrothermal fluids at low-T relative to massive pegmatites. Reverse compositional evolution in $\text{Fe}_{\text{tot}}/(\text{Fe}_{\text{tot}} + \text{Mg})$ distinct from those typically found in granitic pegmatites may be related to the parental medium. Such tourmaline compositions also support, along with the mineral assemblage very similar to host migmatites, their origin during late (hydrothermal) stages of anatectic processes.

This work was supported by the research project GAČR P210/010/0743 to PG, MN and JF.

REFERENCES

- Cempírek, J. & Novák, M. (2006). Mineralogy of dumortierite-bearing abyssal pegmatites at Starkoč and Běstvína, Kutná Hora Crystalline

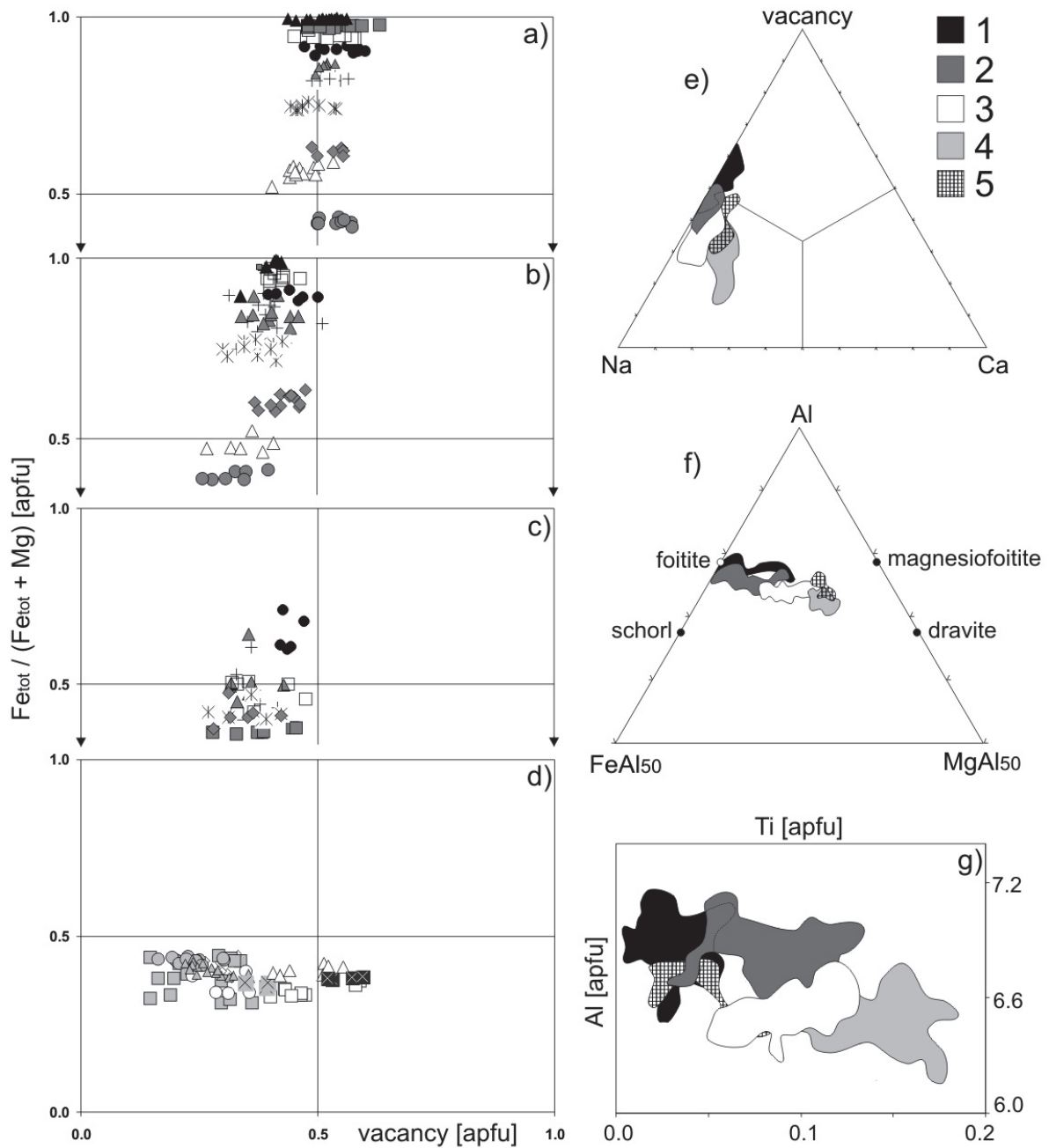


FIGURE 3. Left: Compositional evolution of tourmalines in $Fe_{tot}/(Fe_{tot}+Mg)$ plot. Individual pegmatite dikes (a - cores, b - intermediate zones, c - rims) are distinguished by different symbols as well as muscovite-rich veins (d) where grey-coloured symbols represents central parts and white-coloured symbols outer parts of tourmalines. Right: Triangular plots showing X-site composition (e), Fe-Al-Mg composition (f) and Ti/Al plot (g) of the individual tourmaline types: pegmatite dikes (1-cores, 2-intermediate zones, 3-rims) and muscovite-rich veins (4-central parts, 5-outer parts).

Complex. Journ. Czech Geol. Soc., 51: 259–270.

Henry, D.J. & Dutrow, B.L. (1996). Metamorphic tourmaline and its petrologic applications. In: Boron: Mineralogy, Petrology and Geochemistry (Grew, E.S., Anovitz, L.M., Eds). Rev. Mineral. 33: 503-557.

Novák, M., Povondra, P. & Selway, J.B. (2004). Schorl-

oxy-schorl to dravite-oxy-dravite tourmaline from granitic pegmatites; examples from the Moldanubicum, Czech Republic. Eur. J. Mineral. 16: 323-333.

Povondra, P. (1981). The crystal chemistry of tourmalines of the schorl-dravite series. Acta Univ. Carol., Geol. 1981: 223-264.

A MUSCOVITE PEGMATITE FIELD IN A LOWER PALEOZOIC OROGENIC ARC: THE VALLE FÉRTIL DISTRICT, SAN JUAN, ARGENTINA

Miguel Ángel Galliski¹, Brígida Castro de Machuca², Julio Oyarzábal³,
 Estela Meissl⁴, Alicia Conte-Grand⁴ and María Belén Roquet⁵

¹ IANIGLA, CCT Mendoza-CONICET, Avda. A. Ruiz Leal s/n, (5500) Mendoza, Argentina.

² CONICET-INGEO, Facultad de Ciencias Exactas, Físicas y Naturales, Universidad Nacional de San Juan, Argentina.

³ Gerencia de Geología y Minería, Loma Negra CIASA, Camargo Correa, Loma Negra, Buenos Aires.

⁴ INGEO, Facultad de Ciencias Exactas Físicas y Naturales, Universidad Nacional de San Juan.

⁵ Departamento de Geología, Universidad Nacional de San Luis, Chacabuco y Pedernera, (5700) San Luis, Argentina.

Key words: muscovite class, orogenic pegmatite district, allanite-monazite, Ordovician

INTRODUCTION

The muscovite class granitic pegmatites from the Sierras Pampeanas, Argentina, form several districts that flank both on the east and west a central rare-element pegmatite belt. These pegmatite fields were centers of considerable mining activity in the past, producing most of the mica of commercial grade. Nowadays, they continue producing the bulk of the mica and, in addition, a significant tonnage of ceramic-grade feldspar and quartz. However, these pegmatite districts have received comparatively little attention from the research point of view compared to the rare-element-enriched districts. Valle Fértil, in the province of San Juan, is the southwestern muscovite district, economically one of the most important of this kind, and we present in this communication a description of its main geological features.

GEOLOGICAL SETTING

The Valle Fértil pegmatite field, long. 67° 29' to 67° 43' W, lat. 30° 30' to 30° 47' S, is located in the Valle Fértil range, western Sierras Pampeanas (Fig. 1). The crystalline basement of this range consists of a sequence of wedge- or strip-shaped septa of metasedimentary quartzofeldspathic to pelitic migmatites, with rare calcareous lenses, interlayered with and intruded by metamafic and intermediate igneous rocks of tonalitic to granodioritic compositions (Otamendi *et al.* 2008, and references therein). The metasedimentary rocks are considered the upper crust levels of the sequence. Deeper levels are dominated by intermediate and metamafic rocks. Small lenses of granite also are present. The whole sequence underwent granulite-facies metamorphism during the Ordovician at peak conditions of 770–840 °C and 5.2–7.1 kbar (Otamendi *et al.* 2008), and 800–850 °C and pressures attaining 5 kbar in metagabbros (Delpino *et al.* 2008). The Valle Fértil range is considered to expose a cross section through a magmatic paleoarc of Famatinian age, developed approximately with a N-S orientation

during the Late Cambrian to Early Ordovician (Otamendi *et al.* 2009).

THE PEGMATITE FIELD

The granitic pegmatites of the Valle Fértil district are exposed along 40 km and distributed in three groups, Balilla, Aurora and Trinacria, from north to south. They were mined since the 1940s, mostly for muscovite and some for vermiculite. In the last twenty years, they have produced muscovite, K-feldspar, quartz and albite of ceramic grade. During a sampling survey, we located and described 46 bodies of pegmatite, from which approximately 50% are mined today. General geological aspects of the pegmatites were recorded by Herrera (1958) and Mirré (1971). Recently, Oyarzábal *et al.* (2010) described the geochemistry and structural state of the K-feldspar from four of them.

The pegmatites are usually tabular, with very variable thicknesses, between 2 to 50 m, with an average between 5 and 8 m. In the Balilla and Aurora groups, the pegmatites tend to be thicker and, in some cases, more globular than the thin tabular dikes that are more common in the Trinacria group. The lengths are also variable, between 10-12 m and 50-70 in most cases, with maximum lengths of 100, 150 or up to 200 m. Strikes and dips are not consistent, and pegmatites with NE-SW, N-S, N25-45°E or N20-30°W strikes and 5-10 to 45°E, 45°NW, 20°W dips or a subhorizontal attitude are frequent. Most of the pegmatites are hosted in metamafic rocks, some in diorites, and a few in pelitic gneisses. The thinner dykes show evidences of deformation, with fractures and megascopic folds. The pegmatites are invariably zoned, showing variable textural patterns. The internal structure is complex, and mainly symmetric and uniform across the district. We recognize border, wall, intermediate and core zones. The border zones are centimeters wide, fine-grained, with the assemblage Pl-Qtz-Kfs-Bt-Ms±Grt. They pass inward to decimetric wall-

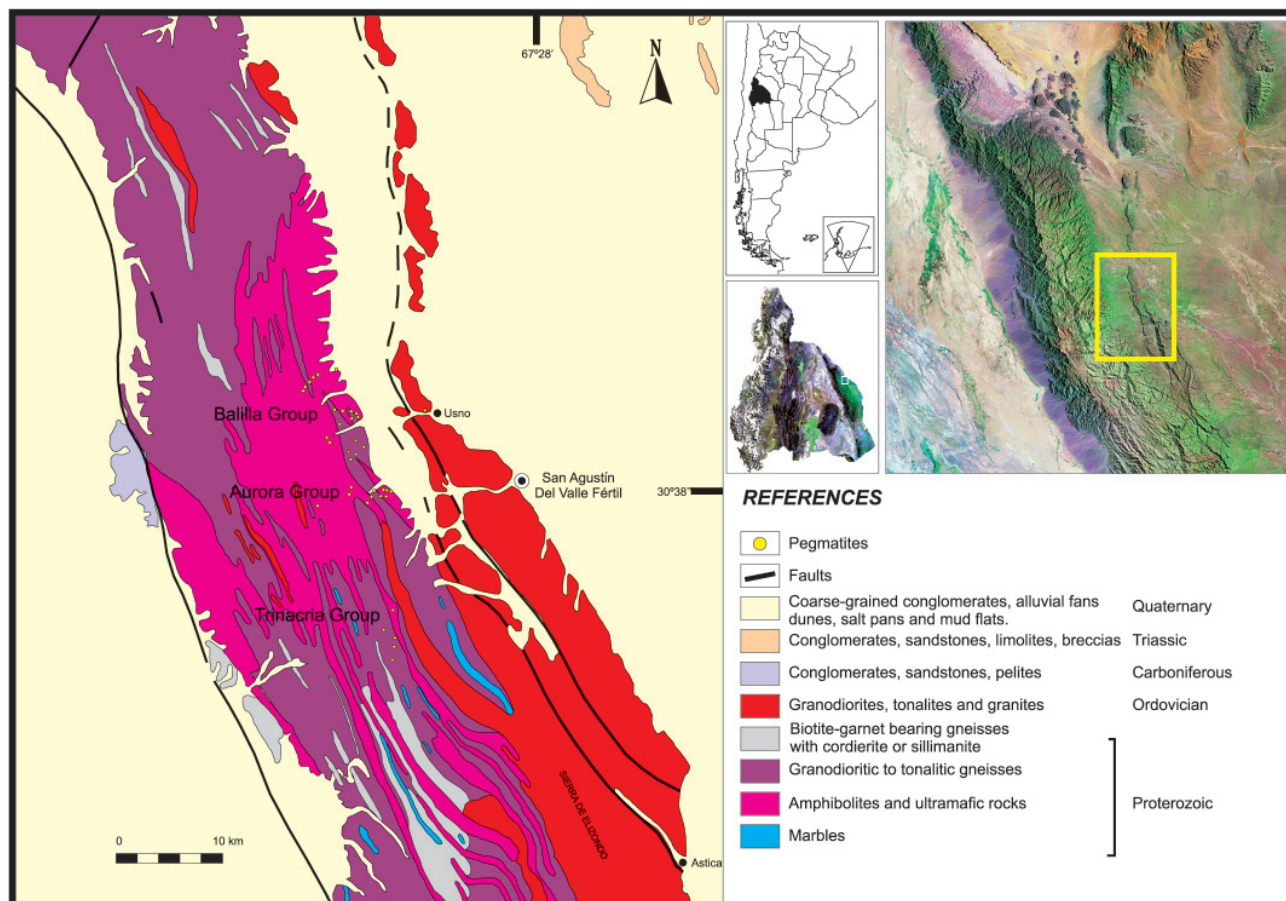


FIGURE 1. Geological map of the Valle Fértil pegmatite field with the distribution of the granite pegmatites from the different groups. Geology modified after Furque *et al.* (1998).

zones with the same composition and normally with two typical features: blades of biotite, in some cases in excess of one meter long, with incipient replacement of muscovite and, in the inner part, widespread graphic textures developed in Kfs + Qtz. This zone passes through an irregular but sharp limit to the intermediate zone, characterized by giant grain-size. The modal composition of this zone is dominated by K-feldspar and quartz, with albite that is generally interstitial. The K-feldspar occurs in subhedral to euhedral, meter-sized crystals of pink or pale brown color, blocky texture and moderate perthitic character. It shows a fully ordered structure typical of maximum microcline. The primitive values of K/Rb, K/Cs and Rb/Sr correlate well with the established ranges for muscovite-bearing or barren rare-element pegmatites of the Pampean pegmatitic province. The milky quartz is normally present in globular pods with a smoky border. Muscovite is frequent in centimetric sheets, and biotite occurs concentrated close to the wall zone or around xenoliths of mafic rocks. The core zone does not differ from the intermediate one, except that the micas disappear and quartz increases its modal proportion. The accessory minerals are scarce, in general. Garnet of almandine-dominant composition in cm-sized euhedral crystals is the most frequent minor phase. Occasionally, isolated

cm-sized crystals of allanite and some crystals of monazite associated with biotite are encountered. Epidote was found in one occurrence. Very seldom, crystals of beryl appear in some pegmatites, whereas in one pegmatite, we have found a small nodule of magnetite and in a few others, millimetric veinlets of chalcocite. Exceptionally, one pegmatite body of the Balilla group presents a different bulk-composition, with a greater incidence of sodic replacement, more beryl and scarce crystals of columbite-(Fe).

Most of the pegmatites studied have geological and mineralogical attributes that characterize them as members of the muscovite class. However, a few of them have accessory minerals indicative of incipient transition to pegmatites of muscovite-rare element (MSREL) class, MSREL-rare earth elements subclass of the Černý & Ercit (2005) classification.

The pegmatites are strongly deformed, and possibly they share the metamorphic ages of the Ordovician basement. Galindo *et al.* (1997) gave a Rb-Sr isochron of 455 ± 3 Ma (MSWD = 1.9) with a $^{87}\text{Sr}/^{86}\text{Sr}$ initial ratio of 0.7093 ± 0.0002 , whereas Casquet *et al.* (2003) dated garnet crystals with high contents of HREE by Sm-Nd, obtaining an age of 455 ± 3 Ma (MSWD = 1.4). More recently, Gallien *et al.* (2010) obtained a U-Pb zircon age of 478 ± 13 Ma

(MSWD = 0.21) from a pegmatite belonging to the Tinacria group.

Herrera (1958) tentatively ascribed the origin of the granitic pegmatites of the Valle Fértil district to the derivation of residual melts from the crystallization of small plutons of biotite granite outcropping in the west-central part of the field. Galliski (1994) discussed this and other possible interpretations, and considered as more viable an anatectic formation. Casquet *et al.* (2003) suggested that these pegmatites 1) owe their origin to partial melting of a crustal protolith, and 2) were emplaced after the peak of metamorphism.

ACKNOWLEDGEMENTS

The authors are very grateful to grants PIP 5907 and 857 of CONICET and PICT 21638 of FONCYT, which financed the research. They are also very grateful to the helpful review made by R. Martin.

REFERENCES

- Casquet, C., Galindo, C., Rapela, C., Pankhurst, R.J., Baldo, E., Saavedra, J. & Dahlquist, J. (2003). Granate con alto contenido en tierras raras pesadas (HREE) y elevada relación Sm/Nd en pegmatitas de la Sierra de Valle Fértil (Sierras Pampeanas, Argentina). *Bol. Soc. Esp. Min.* **26-A**: 133-134.
- Černý, P. & Ercit, T.S. (2005). The classification of granitic pegmatites revisited. *Can. Mineral.* **43**: 2005-2026.
- Delpino, S., Bjerg, E., Mogessie, A., Schneider, I., Gallien, F., Castro de Machuca, B., Previley, L., Meissl, E., Pontoriero, S. & Kostadinoff, J. (2008). Mineral deformation mechanisms in granulite facies, Sierra de Valle Fértil, San Juan Province: Development conditions constrained by the P-T metamorphic path. *Rev. Asoc. Geol. Argent.* **63**: 181-195.
- Furque, G., González, P. & Caballé, M. (1998). Hoja Geológica 3169-II, San José de Jáchal, provincias de San Juan y La Rioja. *Boletín 259, SEGEMAR*, Buenos Aires. Edición preliminar.
- Galindo, C., Pankhurst R.J., Casquet, C., Baldo, E., Rapela, C. W. & Saavedra, J. (1996). Constraints on the age and genesis of the Sierra de Valle Fértil pegmatites (western Sierras Pampeanas, Argentina). *13° Cong. Geol. Arg. y 3° Cong. Expl. Hidrocarburos, Actas V*: 333. Buenos Aires.
- Gallien, F., Mogessie, A., Bjerg, E., Delpino, S., Castro de Machuca, B., Thöni, M. & Klötzli, U. (2010). Timing and rate of granulite facies metamorphism and cooling from multimineral chronology on migmatitic gneisses, Sierras de La Huerta and Valle Fértil, NW Argentina. *Lithos* **114** (1-2): 229-252.
- Galliski, M. A. (1994). La Provincia Pegmatítica Pampeana II. Metalogénesis de sus Distritos Económicos. *Rev. Asoc. Geol. Argent.* **49**: 113-122.
- Herrera, A. O. (1958). Estructura interna de las pegmatitas micacíferas de Valle Fértil, San Juan. *Universidad de Buenos Aires, Contr. Cient.* **2**: 5-29.
- Mirré, J.C. (1971). Caracterización de una comarca de metamorfismo regional epizonal de alto grado: la Sierra de Valle Fértil, San Juan, Argentina. *Rev. Asoc. Geol. Argent.* **26** (1): 113-127.
- Otamendi J.E., Tibaldi A.M., Vujovich, C.I. & Viñao, G.A. (2008). Metamorphic evolution of migmatites from the deep Famatinian arc crust exposed in Sierras Valle Fértil-La Huerta, San Juan, Argentina. *J. South Am. Earth Sci.* **25**: 313-335.
- Otamendi, J.E., Vujovich, G.I., de la Rosa, J.D., Tibaldi, A.M., Castro, A., Martino, R.D. & Pinotti L.P. (2009). Geology and petrology of a deep crustal zone from the Famatinian paleo-arc, Sierras de Valle Fértil and La Huerta, San Juan, Argentina. *J. South Am. Earth Sci.* **27**: 258-279.
- Oyarzábal, J.C., Roquet, M.B., Galliski, M.A. & Perino, E. (2010). Caracterización geoquímica y estructural de feldespatos potásicos de algunas pegmatitas de los Grupos Balilla y Aurora, distrito pegmatítico Valle Fértil, San Juan, Argentina. *Rev. Asoc. Geol. Argent.* (in press).

ASSOCIATION OF SECONDARY Al-Li-Be-Ca-Sr PHOSPHATES IN THE SAN ELÍAS PEGMATITE, SAN LUIS, ARGENTINA

Miguel Ángel Galliski¹, Petr Černý²,
María Florencia Márquez-Zavalía¹, Ron Chapman²

- ¹ IANIGLA, CCT Mendoza-CONICET, Avda. A. Ruiz Leal s/n, -5500- Mendoza, Argentina. galliski@mendoza-conicet.gov.ar
² Dept of Geological Sciences, University of Manitoba, Winnipeg, MA, R3T 2N2, Canada

Key words: montebbrasite, augelite, hydroxylherderite, goyazite, crandallite, pegmatite

INTRODUCTION

Granitic pegmatites usually form, in the early stages of magmatic crystallization in a closed system, relatively isolated from the host rocks. However, in the late stages of formation during subsolidus hydrothermal reactions, exchange of components with country rocks can modify the pristine magmatic mineral assemblage. Particularly sensitive to these processes are the pegmatite phosphates. In this presentation we document a secondary assemblage where early magmatic phosphates were replaced by hydrothermal phases that coexist with secondary species formed by interaction with leached cations from the host rock.

THE PARENT PEGMATITE

The phosphate assemblage occurs in the San Elías pegmatite which is located in the Sierra de la Estanzuela, Chacabuco department, San Luis province, República Argentina, approximately at Latitude 31°51'S and Longitude 65°06'W. The pegmatite is emplaced in a quartz-mica schist of medium metamorphic grade, probably of Lower Paleozoic age, that is locally tourmalinized in contact with the hanging-wall part of the body.

San Elías is a rare-element-class pegmatite of the LCT petrogenetic family according to the classification of Černý & Ercit (2005). The internal structure and mineralogy of the pegmatite were summarized by Galliski *et al.* (1999). The pegmatite is a tabular body that is 140 m long, strikes N-S, and dips steeply to the east. It is only partially exposed because the eastern side is covered by Quaternary loess and consequently the outcropping width varies between 27 and 15 m. The pegmatite is zoned with border, wall, intermediate and core zones. The border and wall zones are fine- and medium-grained rocks respectively, that are principally composed of plagioclase (An₋₁₅), quartz and

muscovite, and are only visible in the western part of the pegmatite. The intermediate zone has a medium- to coarse-grained association of K-feldspar, quartz, and cleavelandite as main minerals. In the southern part of the pegmatite, there is a poorly defined subzone of cleavelandite and small crystals and nodules of amblygonite-montebbrasite, with blue, green, colorless and pink tourmaline as principal accessory minerals. Nb-Ta oxide minerals and yellow beryl are scarce in this zone. In the internal part, this subzone shows abundant gray, pink or purple, fine-grained, massive lepidolite. The core is irregular and is composed of quartz that includes a few large euhedral crystals of K-feldspar. In the core-margin assemblage there are abundant vugs in the cleavelandite, with late-stage growth of quartz, cookeite, hydroxylherderite and apatite. Mostly in the northern half of the pegmatite, there also are some relics of Mn-Fe-Li phosphates and "nodules" of a soft, white, kaolinized material which completely replaced an unknown phase. These are the focus of the present study.

PETROGRAPHY OF THE PHOSPHATES

In the west wall of the main quarry of the northern part of the San Elías pegmatite, the exposed units are mostly the intermediate zone and the quartz core zone. The intermediate zone is composed of K-feldspar in coarse crystals, quartz, platy albite and some mica. In some areas of this unit an irregular subzone is present, composed mainly of cleavelandite and montebbrasite with minor tourmaline. Especially interesting are some intergrowths of dendritic montebbrasite, hosted in creamy colored cleavelandite. In a closer view of the fresh material of this subunit, it is possible to see that the matrix of tan-colored cleavelandite contains abundant, skeletal, white crystals of montebbrasite and some small darker crystals of blue to green tourmaline.

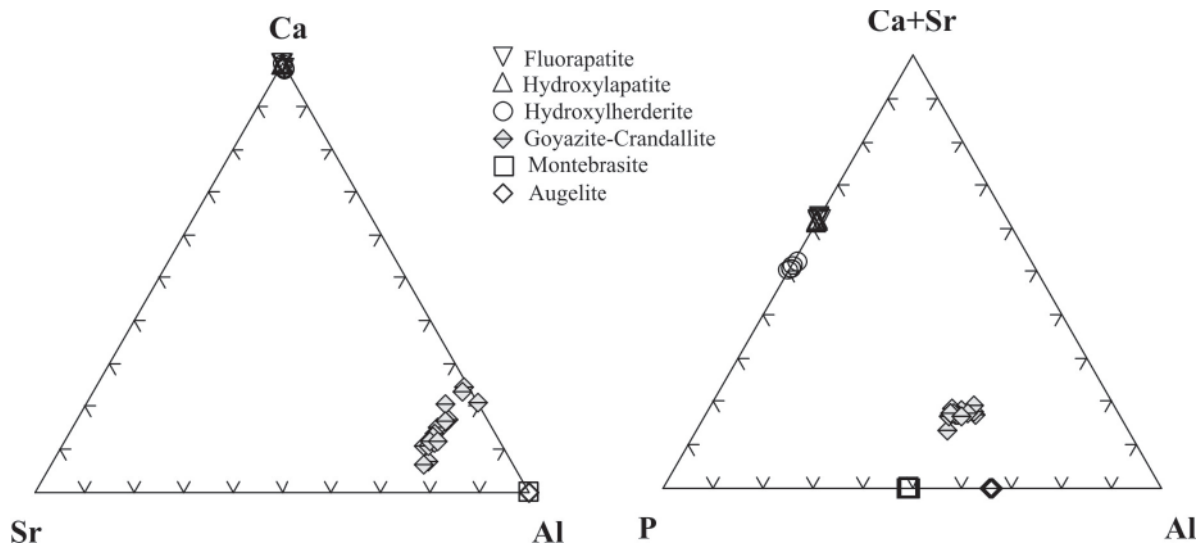


FIGURE 1. Triangular diagrams showing the compositions of the minerals of the hard ovoid nodule.

South of the dendritic montebrasite in the west wall of the quarry, we found several white "nodules" at the transition between the intermediate and quartz-core zones. One of them is a hard ovoid nodule formed by a fine-grained aggregate that is surrounded by a halo of altered and soft material. This halo compositionally corresponds to the other "nodules" that resemble subrectangular blocks, completely replaced by a white material of argillaceous appearance, dominantly kaolinite and quartz. Some thin veinlets of "limonite" suggest the presence of an approximately rectangular network of cleavage or parting in the primary phase(s). In other "nodules" that appear deformed, irregular veinlets of quartz crosscut the white aggregate, porcellaneous or soft depending on the degree of pervasive silicification.

The hard ovoid nodule, 15 by 10 cm in size, is white with a light gray to light blue tinge in some parts and very tenacious. It consists of a fine intergrowth of minerals, which decrease in grain size from 1 mm to 0.6 mm towards the center of the nodule. The association consists of euhedral tabular crystals of montebrasite (randomly distributed or in radial aggregates), euhedral but locally broken or corroded laths of augelite, anhedral fluorapatite, interstitial quartz (occasionally with hexagonal contours or as fine veinlets), and subhedral crystals of hydroxylherderite, hydroxylapatite, goyazite and crandallite.

The precursor of the ovoid nodule and the primary phase(s) of the subrectangular blocks were probably of magmatic origin: members of the amblygonite-montebrasite series that were replaced during the hydrothermal stage by the secondary phosphates. Electron-microprobe analyses of the phosphate minerals were carried out in the wavelength-dispersion mode on a Cameca Camebax

SX50 equipment, with a beam diameter of 3 μ m and an acceleration potential of 15 kV. A sample current of 20 nA measured on Faraday cup and a counting time of 20 s were used for Na, Mg, Al, Si, P, S, Cl, K, Ca, V, Mn, Fe, As, Sr, Y, Ba, La, Ce, Nd, Pb, Bi, Th and U. For F was used a counting time of 30 s. The textural relationships of all phases plotted in the ternary diagrams Ca-Sr-Al and Ca+Sr-Al (Fig. 1) show that the secondary montebrasite, fluorapatite, hydroxylherderite and augelite were followed by goyazite-crandallite with increased Ca and Sr influx and finally hydroxylapatite and quartz. After this reequilibration, facilitated by hydrogen metasomatism, the "nodules" evolved by extreme leaching and cation exchange to a mass of very fine-grained Li-muscovite (2M₁), adularia, kaolinite, fluorapatite, and some inclusions of microlite.

This secondary association of phosphates, somewhat variable at different localities, with brazilianite, lacroixite, gorceixite among others, has been described in several pegmatites worldwide: Palermo #1, White Picacho district, Buranga, Daheim (Mrose 1953, London & Burt 1982, Daltry & von Knorring 1998, Baldwin *et al.* 2000) and some albitized granites such as Beauvoir (Charoy *et al.* 2003). Strontium, Ca, and other cations that interact with the P-Al-bearing fluids produced by destabilized primary montebrasite are provided by fluids circulating in an open system, after the thermal reequilibration of the pegmatite with the host-rock that follows magmatic crystallization (Clark & Černý 1987, Charoy *et al.* 2003). The studied association of phosphates is not in equilibrium and consists of an assemblage produced by late hydrothermal pegmatitic fluids (montebrasite, hydroxylherderite, fluorapatite, augelite) overprinted by secondary Sr-rich fluids forming goyazite, crandallite, hydroxylapatite and quartz.

ACKNOWLEDGEMENTS

Grants from PIP 5907 and 857 of CONICET and PICT 21638 FONCYT financed the development of the project in Argentina. The EMP work at University of Manitoba was financed by an NSERC Research and Major Installation grants to PČ and Major Equipment plus Infrastructure Grants to Frank C. Hawthorne. The authors are very grateful to F. Hatert for the review of the manuscript and valuable suggestions.

REFERENCES

- Baldwin, J.R., Hill, P.G., von Knorring, O. & Oliver, G.J. H. (2000). Exotic aluminum phosphates, natromontebasite, brazilianite, goyazite, gorceixite and crandallite from rare-element pegmatites in Namibia. *Min. Mag.* **64** (6): 1147-1164.
- Černý, P. & Ercit, T.S. (2005): The classification of granitic pegmatites revisited. *Can. Mineral.* **43**: 2005-2026.
- Charoy B., Chaussidon, M., Le Carlier De Veslud, C. & Duthoud, J.L. (2003). Evidence of Sr mobility in and around the albite–lepidolite–topaz granite of Beauvoir (France): an in-situ ion and electron probe study of secondary Sr-rich phosphates. *Contrib. Mineral. Petrol.* **145**: 673-690.
- Clark, G.S. & Černý, P. (1987). Radiogenic ^{87}Sr , its mobility, and the interpretation of Rb-Sr fractionation trends in rare-element granitic pegmatites. *Geoch. et Cosmoch. Acta* **51**(4): 1011-1018.
- Daltry, V.D.C. & von Knorring, O. (1998). Type-mineralogy of Rwanda with particular reference to the Buranga pegmatite. *Geologica Belgica.* **1**: 9-15.
- Galliski, M.A., Černý, P., Márquez-Zavalía, M. F. & Chapman, R. (1999). Ferrotitanowodginite, $\text{Fe}^{2+}\text{TiTa}_2\text{O}_8$, a new mineral of the wodginite group from the San Elías pegmatite, San Luis, Argentina. *Am. Mineral.* **84**: 773-777.
- London, D. & Burt, D.M. (1982). Alteration of spodumene, montebasite and lithiophilite in pegmatites of the White Picacho district, Arizona. *Am. Mineral.* **67**: 97-113.
- Mrose, M.E. (1953). Palermoite and goyazite, two strontium minerals from the Palermo mine, North Groton, New Hampshire [abstract]. Proceedings of the Thirty-third Annual Meeting of the MSA, Boston, Massachusetts. *Am. Mineral.* **38**: 354.

THE DUMORTIERITE-BEARING ASSEMBLAGES OF VIORCO, SAN LUIS, ARGENTINA: ARE THEY PEGMATITIC DIKES OR HYDROTHERMAL VEINS?

Miguel Ángel Galliski^{1§}, María Florencia Márquez-Zavalía¹ & Raúl Lira²

¹ IANIGLA, CCT Mendoza-CONICET, Avda. A. Ruiz Leal s/n, -5500- Mendoza, Argentina.

[§]galliski@mendoza-conicet.gov.ar

² CICTERRA- CONICET, Museo de Mineralogía y Geología "Dr. A. Stelzner", F.C.E.F y N. Universidad Nacional de Córdoba. Av. V. Sarsfield 299, (5000) Córdoba, Argentina.

Key words: dumortierite-tourmaline-chrysoberyl-kyanite-veins, San Luis

INTRODUCTION

The descriptive mineralogy of dumortierite-bearing assemblages of Virorco was initially recorded by Gay & Galliski (1978). These rocks consist of zoned veins with dumortierite-tourmaline-kyanite-chrysoberyl, now regarded as an assemblage found in granitic pegmatites of the abyssal class (Černý & Ercit 2005). The mineralogy and geochemistry of these rocks were studied in more detail, including EPM and LA-ICPMS chemical analyses of minerals, and conventional chemical analyses of rocks, in order to clarify the origin and parameters of crystallization.

OCCURRENCE

The pegmatites are located in the eastern side of the Virorco River at latitude 33°05'44"S, longitude 66°07'24"W, and 1,284 m of altitude in the San Luis range. The geological setting consists of feldspathic quartzites, gneisses and migmatites intruded by lenses of norites and hornblende gabbros with minor ultramafics, belonging to a NNE-SSW trending discontinuous mafic-ultramafic belt. The host rocks of the mafic-ultramafic belt have undergone granulite-facies metamorphism, and belong to a complex which metamorphic grade transitionally passes to the east through several kilometers of strongly folded psamopelitic strata, to finish with greenschist facies in the upper levels of the sequence. All of these metamorphic lithologies were grouped in the Pringles Metamorphic Complex and dated at 530 Ma by U-Pb on zircon from pelitic gneisses (Sims *et al.* 1998); the age of the mafic rocks yielded 478±6 Ma (Sims *et al.* 1997).

The dumortierite-bearing veins are emplaced in norites and gabbros. They have thicknesses between 2 and 3 cm but exceptions of 1 or up to 10 cm do exist. The lengths vary from several decimeters to 2-3 m, and they strike approximately N-S with high angles of dip. The present work was concentrated in the 1 to 4 cm thick veins because they are the most representative dumortierite-bearing rocks, and the

most suitable for whole rock chemical analysis.

MINERALOGY AND PETROGRAPHY

Most of the veins show unidirectional growth texture of prismatic minerals, with approximately right angles between the crystal lengths and the contact in the thinner veins, and orientations oblique to the contacts in the thicker ones. The 2-3 cm thick veins are usually zoned, with dark border zones, 1 to 3 mm wide, rich in colored tourmaline. The intermediate zone is thicker and it normally concentrates light-colored minerals including quartz, feldspars, muscovite, plagioclase and/or kyanite. The core zone is commonly blue-tinged due to abundant dumortierite. Several veins show evidence of strain through deformed bundles of blue dumortierite, mortar textures developed in quartz, and flexures in the twin planes of plagioclase, the cleavage of muscovite, and in the prismatic crystals or twin plane of kyanite.

The mineralogy of the veins includes quartz, plagioclase, tourmaline-group minerals, dumortierite, muscovite, kyanite, beryl, chrysoberyl, garnet, fluorapatite, columbite-group minerals and a few more minor unidentified phases still under study, approximately in order of decreasing abundance. Staurolite and sillimanite were described by Gay and Galliski (1978), but they were not found *in situ* in the recent and new sampling sites. Quartz is abundant in anhedral grains with undulose extinction, commonly with mortar texture, and hence evidence that underwent strong deformation. Plagioclase is subhedral, deformed, with polysynthetic twinning and compositions that vary from $An_{15.7-27.3} Ab_{72.3-83.7} Or_{0.4-0.6}$. Tourmaline is a common phase, very abundant in the border zones and scarcer in the inner parts of the veins. It usually occurs as short prismatic, subidiomorphic crystals, sometimes totally or partially replaced by dumortierite. In thin section, tourmaline color varies from brownish green, to blue, light blue, and colorless according to compositional

changes. In general, border zone tourmaline is dravite that normally grades inward to schorl and later to olenite. Some colorless tourmaline has Mn-rich composition and possibly corresponds to elbaite. The textural relationships between tourmaline and dumortierite are complex but, in general, the later mineral replaced dark blue tourmaline. Dumortierite occurs in prismatic crystals, bundles and sprays included in quartz, normally in a beautiful blue color but sometimes also in apple green aggregates. It also replaces light blue crystals of kyanite. The chemical composition of blue dumortierite is typical of the species, but the yellowish green material is depleted $\approx 25\%$ in SiO_2 and 15% in Al_2O_3 , raising the possibility that it could actually be holtite. The EPM routine for the analyses performed to date does not include Ta, Sb and As, elements that are strongly enriched in the veins. Recent EDS shows the presence of the peaks corresponding to Nb, Ta, As and Sb. Kyanite is abundant in some veins. It forms long prismatic crystals with pointed terminations, and it occurs as aggregates of several crystals or as a replacement of muscovite. Kyanite and dumortierite are commonly associated. Muscovite occurs in scarce, tabular, dull pinkish crystals, some of which show flexures from deformation. Its composition is variable but normally Na-rich ($\text{K}_{1.181-1.611}\text{Na}_{0.411-0.294}$). Garnet is a frequent accessory phase in small quantities. It is commonly anhedral, it appears to be reabsorbed, and possesses a spessartine-rich composition ($\text{Sps}_{68.8-95.6}\text{Alm}_{2.5-26.5}\text{Grs}_{\text{tr}}\text{Uv}_{\text{tr}}$). Chrysoberyl occurs as sparse and generally anhedral to subhedral prismatic crystals, somewhat rounded, at times included in quartz or in dumortierite. Beryl can be associated in the same thin section with chrysoberyl. Fluorapatite is a common minor accessory.

GEOCHEMISTRY

The whole-rock chemical analyses of major elements show high SiO_2 contents (72.2-76.19 wt%) and very high contents of Al_2O_3 (16.73-18.7 wt%). The weight percents of MgO (0.13-1.28), FeO (0.70-2.66), MnO (0.06-0.36) and CaO (0.47-1.95) are invariably low. Alkalis are very depleted with Na_2O at 0.32 to 1.52 and K_2O between 0.04 and 0.87 wt. %. Phosphorus and boron are enriched with contents of 0.19-1.41 of P_2O_5 wt.% and of 0.27-1.48 wt.% of B_2O_3 .

Normalized trace element contents show depletion in Ba, Sr, Th, Ce, Zr, Hf and Y; Eu has a very strong anomaly. In contrast, most of the samples are enriched in Cs, Rb, Pb, U, Nb, Ta, Sn, Sb, As, B and Be. High concentrations of these trace elements (Fig. 1) are normally found in the highly evolved stages of pegmatites fractionation. Boron exceeds the 1% B_2O_3 maximum for natural granitic melts (Pichavant & Manning 1984).

The normalized REE contents are low, in the range of 0.1 to 30 times chondrite (Fig. 2). Most REE

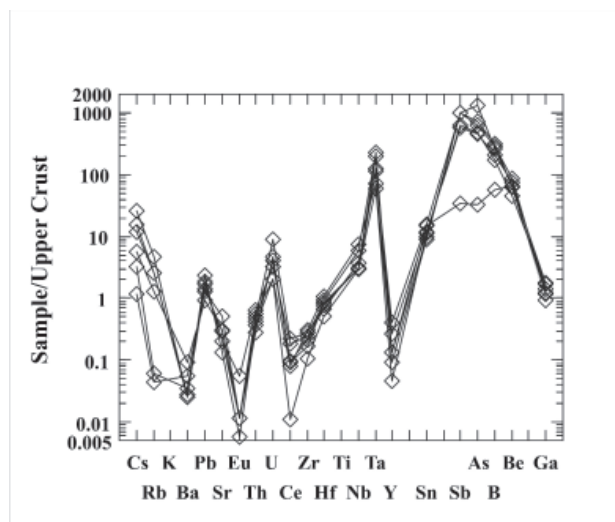


FIGURE 1. Spider diagram showing the plotting of the Virorco veins normalized to the values of the Upper Crust (Taylor & McLennan 1985).

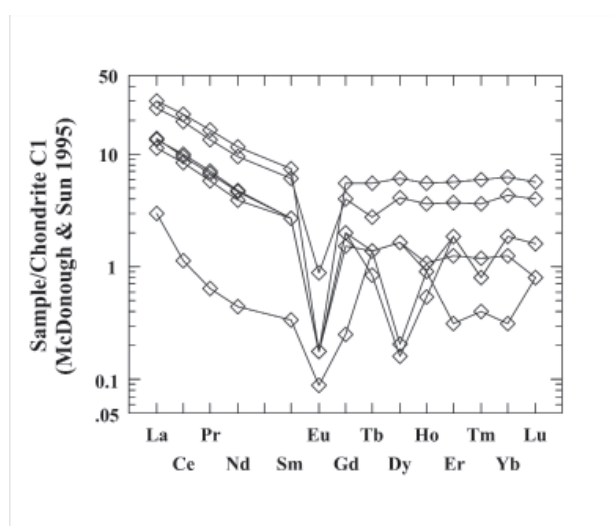


FIGURE 2. Chondrite normalized content of the Virorco dumortierite-bearing assemblages.

patterns display a strong Eu anomaly.

DISCUSSION

The origin of the dumortierite-bearing assemblages of Virorco represents a dilemma between two possibilities: are they pegmatite dykes or hydrothermal veins?

Considering the first possibility, the mineralogy and petrography of the veins are similar to the dumortierite-bearing pegmatite occurrences of the Starkoč and Bestvina in the Kutná Hora Crystalline Complex of the Bohemian Massif (Cempírek & Novák 2006). They were classified as belonging to the AB-BBe subclass of the Abyssal class of pegmatites of Černý & Ercit (2005). In the case of Virorco, the strong trace element concentration typical of the latest stages

of pegmatite crystallization, and the pronounced Eu anomaly indicative of considerable plagioclase fractionation, are sustainable arguments suggesting that these rocks owe their origin to the emplacement of highly fractionated pegmatite melts.

These light element-, volatile-, and Ta-enriched residual melts should possibly have been derived by tectonic extraction from a remnant of the last-stage fractionation of a rare-element pegmatite. This hypothesis could be possible because in the area, 2500 m to the north, there are at least two tourmaline-bearing pegmatites of more than 50 m long and several m thick.

Against this possibility and supporting the second, experimental runs were unsuccessful to melt quartz+tourmaline rocks of Cornwall, in the presence of a hydrous sodium borate melt, producing only ~5% melt at 750° C at 2 kb (London *per. com.*).

The studied assemblage has undergone, as in some other occurrences of abyssal class pegmatites, medium- to high-pressure metamorphism. In the case of the Virorco area, Delpino *et al.* (2007) indicated that mafic and adjacent basement mylonites were developed under upper amphibolite facies transitional to granulite facies metamorphic conditions at intermediate pressures (668–764°C, 6.3–6.9 kbar, $0.3 < X_{CO_2} < 0.7$) during a counterclockwise pattern of regional metamorphism. However, kyanite occurs in the veins replacing muscovite, which could be an indicator of slightly higher pressure conditions than the ones determined in the mylonites.

ACKNOWLEDGEMENTS

The authors are very grateful to C. A. Heinrich for the use of the EPM and LA- ICPMS facilities of the ETH Zurich, and to P. Černý of the University of Manitoba for the use of the EPM. Grants PIP 5907 and 857 of CONICET and PICT 21638 of FONCYT financed the research. The authors thank very much the helpful review of David London that improved the insights for interpreting genetic constraints of this interesting occurrence.

REFERENCES

- Cempírek, J. & Novák, M. (2006). Mineralogy of dumortierite-bearing abyssal pegmatites at Starkoè and Bstvina, Kutná Hora Crystalline Complex. *Journal Czech Geological Society* **51** (3-4):259-270.
- Černý, P. & Ercit, T.S. (2005). The classification of granitic pegmatites revisited. *The Canadian Mineralogist* **43**: 2005-2026.
- Delpino, S. H., Bjerg, E., Ferracutti, G. R. & Mogessie, A. (2007). Counterclockwise tectonometamorphic evolution of the Pringles Metamorphic Complex, Sierras Pampeanas of San Luis (Argentina). *Jour. South Amer. Earth Sci.* **23**: 147-175.
- Pichavant, M. & Manning D. A. C. (1984). Petrogenesis of tourmaline granites and topaz granites; the contribution of experimental data. *Phys. Earth and Planet. Int.* **35**: 31-50.
- Gay, H. D. & Galliski, M. A. (1978). Dumortierita, crisoberilo y minerales asociados de Virorco, San Luis. *Actas VII Cong. Geol. Argentino* **II**: 327-335.
- Sims, J. P., Skirrow, R. G., Stuart-Smith, P. G. & Lyons, P., (1997). Informe geológico y metalogénico de las Sierras de San Luis y Comechingones (Provincias de San Luis y Córdoba), 1:250000. *Anales XXVIII, Instituto de Geología y Recursos Minerales, SEGEMAR, Buenos Aires.*
- Sims, J. P., Ireland, T. R., Camacho, A. Lyons P., Pieters, R. G., Stuart-Smith, P. G. & Miró, R. (1998). U-Pb, Th-Pb and Ar-Ar geochronology from the Southern Sierras Pampeanas, Argentina: implications for the Paleozoic tectonic evolution of the western Gondwana margin. In: Pankhurst R. J. & Rapela C. A. (eds.) *The Proto-Andean Margin of Gondwana*. Geological Society, London. *Special Publications* **142**: 259-281.
- Taylor, S. R. & McLennan, S.M. (1985). *The Continental Crust: its Composition and Evolution*. Blackwell Scientific Publications, 312p.

THE CRYSTAL CHEMISTRY OF OLIVINE-TYPE PHOSPHATES

Frédéric Hatert^{1§}, Luisa Ottolini², François Fontan^{3,†}, Paul Keller⁴,
 Encarnación Roda-Robles⁵ & André Mathieu Fransolet¹

¹ Laboratory of Mineralogy B18, University of Liège, B-4000 Liège, Belgium. §email fhatert@ulg.ac.be

² C.N.R.-Istituto di Geoscienze e Georisorse (IGG), Unità di Pavia, Via Ferrata 1, I-27100 Pavia, Italy.

³ LMTG-UMR 5563, Observatoire Midi Pyrénées, 14 Avenue E. Belin, F-31400 Toulouse, France

⁴ Institut für Mineralogie und Kristallchemie, Universität Stuttgart, Pfaffenwaldring 55, D-70569 Stuttgart, Germany.

⁵ Dpt. Mineralogía y Petrología, UPV/EHU, Bilbao, Spain.

Key words: triphylite, lithiophilite, pegmatite phosphates, crystal chemistry, olivine structure.

INTRODUCTION

Iron-manganese phosphates are common accessory minerals occurring in granitic pegmatites, in metamorphic rocks, and in meteorites. In rare-elements pegmatites, primary phosphates of the triphylite-lithiophilite series $[\text{Li}(\text{Fe}^{2+}, \text{Mn}^{2+})(\text{PO}_4)]\text{-Li}(\text{Mn}^{2+}, \text{Fe}^{2+})(\text{PO}_4)$ form masses that can reach several meters in diameter, enclosed in silicates. During the oxidation processes affecting the pegmatites, these olivine-type phosphates progressively transform to ferrisicklerite-sicklerite $[\text{Li}_{1-x}(\text{Fe}^{3+}, \text{Mn}^{2+})(\text{PO}_4)\text{-Li}_{1-x}(\text{Mn}^{2+}, \text{Fe}^{3+})(\text{PO}_4)]$ and to heterosite-purpurite $[(\text{Fe}^{3+}, \text{Mn}^{3+})(\text{PO}_4)\text{-(Mn}^{3+}, \text{Fe}^{3+})(\text{PO}_4)]$, according to the substitution mechanism $\text{Li}^+ + \text{Fe}^{2+} \rightarrow \text{Fe}^{3+}$. This oxidation sequence was first observed by Quensel (1937), and then confirmed by Mason (1941).

The crystal structure of minerals of the triphylite-lithiophilite series (triphylite: $a = 4.690$, $b = 10.286$, $c = 5.987$ Å, $Pbnm$) has been investigated from synthetic samples and natural minerals (Finger & Rapp 1969, Losey *et al.* 2004), and is characterized by two chains of edge-sharing octahedra parallel to the c axis. The first chain is constituted by the $M(1)$ octahedra occupied by Li, while the second chain is formed by the $M(2)$ sites occupied by Fe and Mn. The chains are connected in the b direction by sharing edges of their octahedral sites, and the resulting planes are connected in the a direction by the PO_4 tetrahedra. Natrophilite, NaMnPO_4 , is another pegmatite phosphate with the olivine structure, in which the $M(1)$ site is occupied by Na while the $M(2)$ site contains the smaller divalent cations (Moore 1972).

Since the electrochemical investigation of $\text{LiFe}(\text{PO}_4)$ by Padhi *et al.* (1997), an increasing number of papers devoted to olivine-type phosphates were published. The exceptional performance of triphylite as cathode material for Li-ion batteries has initiated an increasing interest for these phosphates, which are now produced industrially and used in batteries for many applications such as electric cars, electric bicycles, or for the storage of green energy.

This paper presents new structural and chemical data on natural olivine-type phosphates, data that will help us to shed some light on the crystal chemistry of this complex group of minerals.

ANALYTICAL METHODS

Electron-microprobe analyses were performed with a Cameca SX-50 instrument located in Bochum, Germany (analyst H.-J. Bernhardt), which operated in the wavelength-dispersion mode with an accelerating voltage of 15 kV and a beam current of 15 nA. The standards used were graffonite from Kabira (for Fe, Mn, P), pyrope (Mg, Al, Si), ZnO (Zn), andradite (Ca), jadeite (Na), and a K-glass (K).

The Li_2O contents were determined with a Cameca IMS 4f ion microprobe (SIMS) installed at CNR-IGG, Pavia (Italy). We used a 12.5-kV accelerated $^{16}\text{O}^-$ primary-ion beam with a current intensity in the range 0.8–4 nA, corresponding to a beam diameter of 3–6 mm. The samples were polished, washed in an ultrasonic tank with ethanol, and Pt coated (400 Å thickness) before analysis. Secondary-ion signals of the following isotopes $^6\text{Li}^+$, $^{31}\text{P}^+$ and $^{57}\text{Fe}^+$ were detected at the electron multiplier. Acquisition times were 3 seconds for Li and P (each), and 6 seconds for Fe over 3 cycles. Analyses were done under *steady-state* sputtering conditions after 360-second sputtering using $\sim 75\text{--}125$ eV secondary ions. The choice of medium-to-high-energy (*energy filtering*) secondary ions as analytical ones is particularly useful to reduce matrix effects affecting light-element ionization and improve the reproducibility of analysis. We used as reference material for SIMS Li-analyses triphylite from the Buranga pegmatite, Rwanda; more details concerning the SIMS analytical procedure are given by Hatert *et al.* (2010).

The crystal structures of the samples were refined from data obtained by single-crystal X-ray diffraction techniques, with an Oxford Diffraction Gemini PX Ultra 4-circle diffractometer using the MoK_α radiation (50 kV, 40 mA).

TABLE 1. Chemical compositions of the olivine-type phosphates investigated in this study.

Sample	Mineral	Locality	Composition
PK-17	Triphylite	Hagendorf-Süd, Germany	$\text{Li}_{0.99}(\text{Fe}^{2+}_{0.73}\text{Fe}^{3+}_{0.05}\text{Mn}^{2+}_{0.19}\text{Mg}_{0.01})\text{PO}_4$
PK-20	Triphylite	Engelbrechts Claim, Brandberg, Namibia	$\text{Li}_{1.06}(\text{Fe}^{2+}_{0.65}\text{Mn}^{2+}_{0.34})\text{PO}_4$
K9-5-6 (colourless)	Lithiophilite	Koktokay #3 pegmatite, Altai, China	$\text{Li}_{0.93}(\text{Fe}^{2+}_{0.03}\text{Fe}^{3+}_{0.13}\text{Mn}^{2+}_{0.80})\text{PO}_4$
K9-5-6 (light yellow)	Lithiophilite-sicklerite	Koktokay #3 pegmatite, Altai, China	$\text{Li}_{0.96}(\text{Fe}^{2+}_{0.08}\text{Fe}^{3+}_{0.08}\text{Mn}^{2+}_{0.81})\text{PO}_4$
K9-5-6 (yellow)	Lithiophilite-sicklerite	Koktokay #3 pegmatite, Altai, China	$\text{Li}_{0.88}(\text{Fe}^{3+}_{0.16}\text{Mn}^{2+}_{0.80}\text{Mn}^{3+}_{0.01})\text{PO}_4$
K9-5-6 (orange)	Lithiophilite-sicklerite	Koktokay #3 pegmatite, Altai, China	$\text{Li}_{0.82}(\text{Fe}^{3+}_{0.16}\text{Mn}^{2+}_{0.75}\text{Mn}^{3+}_{0.06})\text{PO}_4$
K9-5-6 (deep orange)	Sicklerite	Koktokay #3 pegmatite, Altai, China	$\text{Li}_{0.69}(\text{Fe}^{3+}_{0.16}\text{Mn}^{2+}_{0.62}\text{Mn}^{3+}_{0.19})\text{PO}_4$
AB-2-2	Ferrisicklerite	Cañada pegmatite, Spain	$\text{Li}_{0.17}(\text{Fe}^{3+}_{0.75}\text{Mn}^{2+}_{0.08}\text{Mn}^{3+}_{0.10}\text{Mg}_{0.06})\text{PO}_4$
AB-X1-2-ME-3	Ferrisicklerite	Cañada pegmatite, Spain	$\text{Li}_{0.19}(\text{Fe}^{3+}_{0.57}\text{Mn}^{3+}_{0.19}\text{Mg}_{0.24})\text{PO}_4$
AB-X1-2-TB-5	Ferrisicklerite	Cañada pegmatite, Spain	$\text{Li}_{0.23}(\text{Fe}^{3+}_{0.67}\text{Mn}^{2+}_{0.14}\text{Mn}^{3+}_{0.10}\text{Mg}_{0.07})\text{PO}_4$
PK-1	Ferrisicklerite	McDonalds Claim, Brandberg, Namibia	$\text{Li}_{0.18}(\text{Fe}^{3+}_{0.67}\text{Mn}^{2+}_{0.13}\text{Mn}^{3+}_{0.12}\text{Mg}_{0.07})\text{PO}_4$
PK-18	Ferrisicklerite	Strathmore tin mine, Namibia	$\text{Li}_{0.18}(\text{Fe}^{3+}_{0.73}\text{Mn}^{2+}_{0.11}\text{Mn}^{3+}_{0.10}\text{Mg}_{0.06})\text{PO}_4$
PK-3	Heterosite	Ariakas, Usakos, Namibia	$(\text{Fe}^{3+}_{0.64}\text{Mn}^{2+}_{0.05}\text{Mn}^{3+}_{0.31}\text{Mg}_{0.01})\text{PO}_4$
PK-15	Heterosite	Sandamap, Usakos, Namibia	$\text{Li}_{0.02}(\text{Fe}^{3+}_{0.70}\text{Mn}^{3+}_{0.25}\text{Mg}_{0.03})\text{PO}_4$

CHEMICAL COMPOSITION

SIMS analyses of six natural triphylite samples show lithium contents from 9.51 to 9.88 wt. % Li_2O , while the analyses of four lithiophilites show higher Li_2O contents ranging from 10.23 to 11.15 wt. %. These compositions correspond to 0.99-1.04 Li atoms per formula unit (*a.p.f.u.*) in triphylites, and 1.07-1.15 Li *a.p.f.u.* in lithiophilites. The significant Li enrichment of lithiophilites indicates that Li can also occur in the *M*(2) site of the olivine structure. Eleven ferrisicklerite samples show Li_2O -contents from 1.65 to 2.84 wt. % (= 0.17 to 0.29 *a.p.f.u.*), and three heterosite samples contain 0.16 to 0.21 wt. % Li_2O (= 0.02 *a.p.f.u.*). The presence of significant amounts of Li in heterosites was unexpected, and the low Li content of ferrisicklerites indicates that trivalent manganese also occurs in this mineral. The formula of Li-poor ferrisicklerite corresponds to $\text{Li}_{0.17}(\text{Fe}^{3+}_{0.75}\text{Mn}^{3+}_{0.10}\text{Mn}^{2+}_{0.08}\text{Mg}_{0.06})(\text{PO}_4)$ (Table 1).

In order to shed some light on the chemical and structural modifications induced by the oxidation processes affecting lithiophilite, we investigated a natural sample from the Altai Mountains, China, in which a progressive transition from lithiophilite to sicklerite is observed. Under the polarizing microscope, lithiophilite is colorless, whereas sicklerite shows a deep orange color. Several grains also show intermediate

colors, suggesting a progressive transition from lithiophilite to sicklerite. This progressive transition is confirmed by the SIMS analyses, which indicate Li values from 0.96 to 0.69 Li *a.p.f.u.* (Table 1).

STRUCTURAL DATA

The crystal structures of 14 natural olivine-type phosphates were refined to an R_1 factor from 2.19 to 8.24 %, and the unit-cell parameters of these minerals are given in Table 2. The structures show an ordered cationic distribution, with Li located on the *M*(1) site, and with the divalent cations Fe, Mn, and Mg located on *M*(2). The refined site occupancy factors of Li on *M*(1) are in the ranges 0.93-0.95 for triphylites, 0.22-0.59 for ferrisicklerites, and 0-0.09 for heterosites. In the sample from the Altai (China), the occupancy factors on *M*(1) range from 0.99 Li *p.f.u.* (lithiophilite) to 0.75 Li *p.f.u.* (sicklerite). These values are in good agreement with the values measured by SIMS.

In the crystal structure of heterosite, Eventoff & Martin (1972) noticed that the *M*(1) site was empty, and that the complete oxidation of iron and manganese induced a Jahn-Teller distortion of the *M*(2) O_6 octahedron, characterized by two short bonds (1.912-1.914 Å) and four long bonds (2.030-2.163 Å). This observation is confirmed by our data, which show distortion coefficients (Bond length distortion,

TABLE 2. Crystal data for the olivine-type phosphates investigated in this study.

Sample	<i>a</i> (Å)	<i>b</i> (Å)	<i>c</i> (Å)	V (Å ³)	R ₁ (%)
PK-17	4.704(1)	10.365(1)	6.025(1)	293.7(1)	4.07
PK-20	4.711(1)	10.369(1)	6.038(7)	294.9(1)	3.56
K9-5-6 (colourless)	4.736(1)	10.432(2)	6.088(1)	300.8(1)	2.53
K9-5-6 (light yellow)	4.734(1)	10.423(2)	6.094(1)	300.7(1)	2.36
K9-5-6 (yellow)	4.740(1)	10.415(1)	6.080(1)	300.1(1)	2.94
K9-5-6 (orange)	4.767(1)	10.403(2)	6.072(1)	301.1(1)	2.67
K9-5-6 (deep orange)	4.765(1)	10.338(1)	6.060(1)	298.5(1)	2.19
AB-2-2	4.787(2)	9.954(3)	5.875(2)	280.0(2)	5.87
AB-X1-2-ME-3	4.776(3)	10.035(3)	5.883(3)	282.0(3)	8.24
AB-X1-2-TB-5	4.797(3)	9.978(5)	5.881(3)	281.5(3)	6.92
PK-1	4.795(1)	9.979(2)	5.890(1)	281.8(1)	4.01
PK-18	4.795(2)	9.959(6)	5.892(3)	281.3(3)	4.92
PK-3	4.776(3)	9.732(3)	5.826(3)	270.8(2)	6.32
PK-15	4.777(2)	9.776(3)	5.817(2)	271.7(2)	5.76

BLD) between 2.69 and 3.54 % for triphylites and ferrisicklerites, and between 4.46 and 5.01 % for heterosites.

Fransolet *et al.* (1984) investigated twenty natural and five synthetic olivine-type phosphates of the triphylite-lithiophilite series by X-ray powder diffraction, and established correlations between the unit-cell parameters and the chemical composition. We also attempted to correlate the unit-cell parameters of natural and synthetic Li-bearing olivine-type phosphates with the mean ionic radius of the cations occurring on the *M*(2) site. These correlations are excellent and generally follow Vegard's law, except for the *c* parameter which has been fitted with a second order polynomial curve. The correlations can be used to predict the unit-cell parameters of olivine-type phosphates, but also to estimate the Fe/(Fe+Mn) ratio within the triphylite-lithiophilite solid solution. Starting from the unit-cell parameters published by Fransolet *et al.* (1984) and by Losey *et al.* (2004) on natural minerals of the triphylite group, we estimated Fe/(Fe+Mn) ratios which fit fairly to those obtained by chemical analysis, except when the Mg content of the phosphates is higher than 0.016 atoms per formula unit (*a.p.f.u.*). Indeed, an increase of the Mg content induces a significant overestimation of the Fe/(Fe+Mn) ratio, which is characterized by an error reaching 35% for a Mg content of 0.23 *a.p.f.u.*

REFERENCES

- Eventoff, W. & Martin, R. (1972). The crystal structure of heterosite. *Am. Mineral.* **57**: 45-51.
- Finger, L.W. & Rapp, G.R. (1969). Refinement of the crystal structure of triphylite. *Carnegie Inst. Wash. Yearbook* **68**: 290-292.
- Fransolet, A.-M., Antenucci, D. & Speetjens, J.-M. (1984). An X-ray determinative method for the divalent cation ratio in the triphylite-lithiophilite series. *Mineral. Mag.* **48**: 373-381.
- Hatert, F., Ottolini, L. & Schmid-Beurmann, P. (2010). Experimental investigation of the alluaudite + triphylite assemblage, and development of the Na-in-triphylite geothermometer: applications to natural pegmatite phosphates. *Contrib. Mineral. Petrol.*, in press.
- Losey, A., Rakovan, J., Hughes, J.M., Francis, C.A. & Dyar, M.D. (2004). Structural variation in the lithiophilite-triphylite series and other olivine-group structures. *Can. Mineral.* **42**: 1105-1115.
- Mason, B. (1941). Minerals of the Varuträsk pegmatite. XXIII. Some iron-manganese phosphate minerals and their alteration products, with special reference to material from Varuträsk. *Geol. Fören. Stockholm Förh.* **63**: 117-175.
- Moore, P.B. (1972). Natrophilite, NaMnPO₄, has ordered cations. *Am. Mineral.* **57**: 1333-1344.
- Padhi, A.K., Nanjundaswamy, K.S. & Goodenough, J.B. (1997). Phospho-olivines as Positive-Electrode Materials for Rechargeable Lithium Batteries. *J. Electrochem. Soc.* **144**: 1188-1194.
- Quensel, P. (1937). Minerals of the Varuträsk Pegmatite. I. The lithium-manganese phosphates. *Geol. Fören. Stockholm Förh.* **59**(1), 77-96.

MAGMATIC LAYERING (UNIDIRECTIONAL SOLIDIFICATION TEXTURES AND Y-ENRICHED GARNET TRAIN TEXTURES) IN APLITE – PEGMATITES OF THE CADOMIAN BRNO BATHOLITH, CZECH REPUBLIC

Sven Hönig[§], Jaromír Leichmann & Milan Novák

Department of Geological Sciences, Masaryk University, Kotlářská 2, 611 37Brno, Czech Republic. [§] honig@mail.muni.cz

Key words: Unidirectional Solidification Texture (UST), A-type granite, magmatic layering, aplite-pegmatite, yttrium, garnet, Train texture

INTRODUCTION

A rarely occurring magmatic structure - unidirectional solidification textures (UST) - is known as a specific type of the magmatic layering. This non-genetic term describes the morphological features of layers with crystals oriented perpendicular to, or with high angle to, the strike/plan of a layer. Typical morphological features of UST are comb-like or crenulated shape of the crystals oriented perpendicularly to the layer. These crystals are present in layers and multilayered sequences, with textures indicative of mineral growth in one direction from a solid substrate.

The term UST was used for the first time by Shannon *et al.* (1982) for textures observed in subvolcanic granitic bodies at the Henderson Mine, Empire, Colorado; however, older russian texts also described identical textural features in the Transbaykal region. Similar textures were recently found in many strongly peraluminous, volatile-rich (B, F and H₂O) aplite-pegmatites as well (e.g., London 1992; Breiter *et al.* 2005).

Compared to these highly-fractionated, mica-bearing and peraluminous aplite-pegmatites, the UST were newly found in the felsic, A-type, metaluminous, garnet-bearing aplite-pegmatites of the Brno batholith, SE Czech Republic (Hönig *et al.* 2010), studied in this paper.

GEOLOGICAL SETTING

The Brno batholith is a Cadomian magmatic complex formed mainly by amphibole-biotite and biotite granitoids, pegmatites or other more evolved leucocratic granitic rocks are occurred very sporadically. Three distinct internal subunits were recognized in the Brno batholith, each separated by sharp tectonic boundaries: Central Metabasite Zone, Eastern Granitoid (*I*-type) Complex and Western Granitoid Complex, which show three distinctive granitic suites. Two of them are represented by evolved rocks of an active continental margin with S- and/or I-type granite affinities. The third suite (Hlína suite-studied in this paper), is built by felsic,

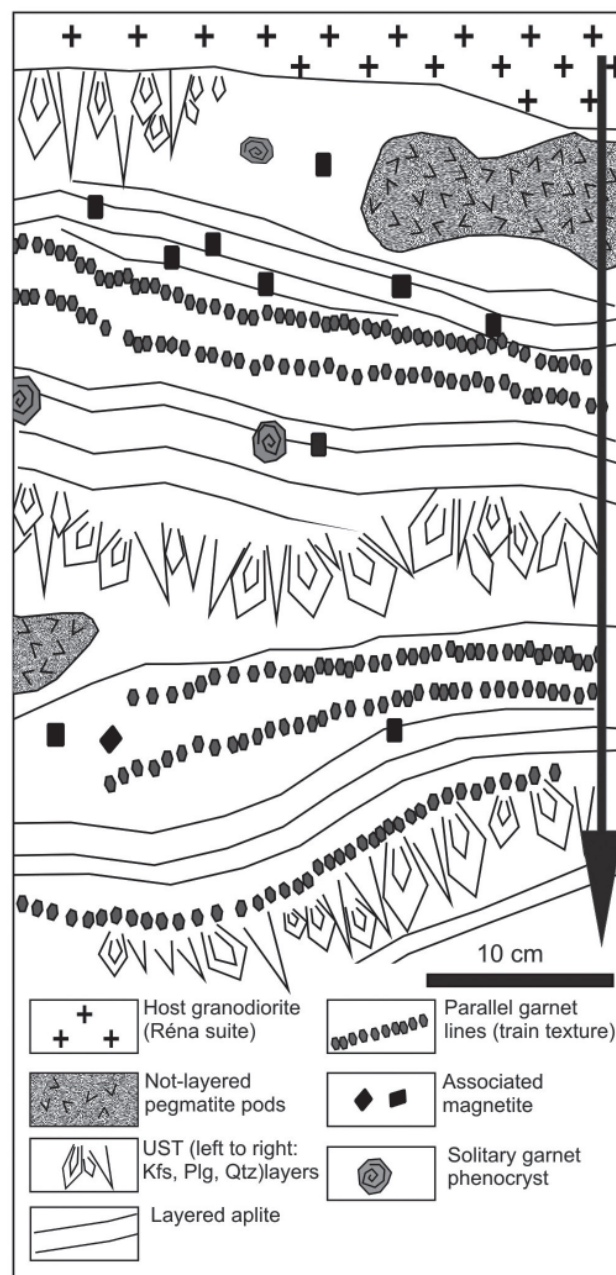


FIGURE 1: Idealized vertical section of the Hlína layered aplite-pegmatite. Arrow shows direction of crystallization. Individual layers and features are not to scale. Thickness of interlayered aplite typically vary from 0.1 to 0.5 m, UST unites are usually 0.2 – 10 cm thick.

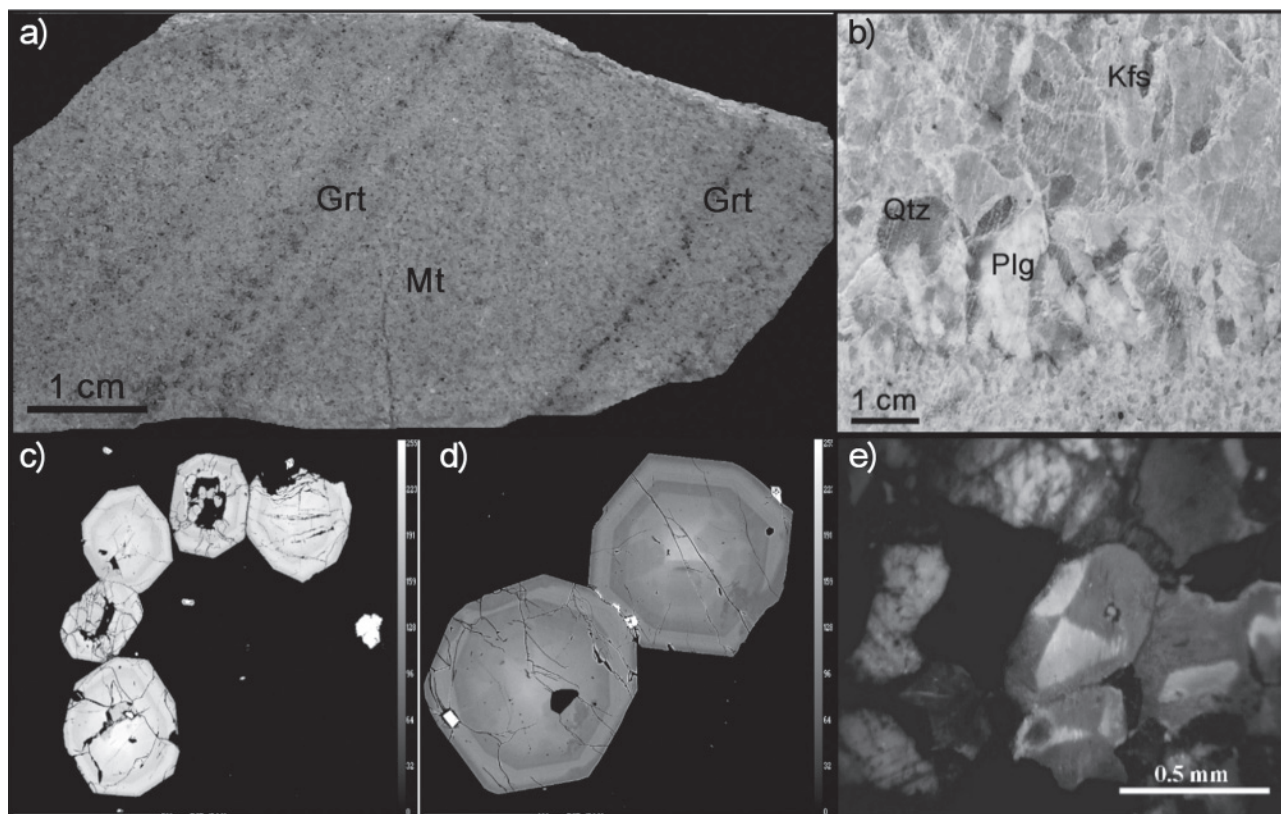


FIGURE 2: Upper row images – macrotextures of the layered Hlína suite; a – For the aplite unit parallel garnet stripes and associated magnetite are typical. b – UST unit characterized by comb-like shaped Kfs, Qtz and Plg. The tips of elongated crystals are grown into the fine-grained aplite unit with sharp boundary. Opposite sides of the UST have a transitional boundary. Lower row images – structures of garnets (c,d) and feldspars (e); c – BSE image of the train texture, garnets from the strip. d – garnets from the strip in BSE, with typical complex internal fabric (sector zones in the centre, oscillatory zones in the rims). e – CL image of the blue colored hourglass and sector zoning in K-feldspar.

layered, garnet-bearing, aplite–pegmatite intrusions, now classified as an A-type granite (Leichmann *et al.* 1999).

Dykes and lens-shaped bodies of the layered Hlína aplite–pegmatites and associated aplitic granites cut other S- and I-type granodiorites of the Western Granitoid Complex. The examined aplite–pegmatite bodies are ~2 to 50 m thick and up to 200 m long with a general NW–SE strike and either NE or SW 40–80° dip. Sharp contacts of the aplite–pegmatite dykes with host granodiorites are scarcely exposed and commonly strongly weathered.

TEXTURES AND STRUCTURES OF THE HLÍNA LAYERED SUITE

Studied dykes are characterized by alternating, generally fine-grained layered garnet-bearing aplite units with parallel comb-like, coarse-grained UST units (Fig. 1). Major minerals of UST include K-feldspar, plagioclase (An₁₅₋₁₀) and quartz; accessory minerals are extremely rare. The tips of elongated crystals are always growing into the fine-grained aplite unit with sharp boundaries. The bottom/opposite sides show typical transitional boundaries. Contacts of both aplite and UST units are typically sharp although gradual transitions were also observed. Thickness

of the individual zones varies from several cm to *ca.* 1–2 m for aplites and *ca.* 10 cm for UST zones. The layered character of aplitic rocks is pointed up by parallel stripes of Y-enriched garnet grains. These train textures are composed by numerous of small (< 0.5 mm) individual garnet grains always arranged into long lines (up to several meters long), where the individual garnet crystals are in direct contact (Figs. 2 a, c, d). Stripes are always parallel to the boundary plane of the aplite unit. Less abundant are similar associated stripes of magnetite.

Cathodoluminescence study of fine-grained aplite unit and coarse-grained UST exhibit several internal structures inside both K-feldspar and plagioclase. Zoned feldspars from aplite unit (Fig. 2e) are very common: K-feldspar, lacking perthites, are marked by a variable intensity of blue color with a well developed hourglass sector zoning in their middle parts as well as light blue sector zones dissolved on corroded rims. Subhedral grains of plagioclase (light green color) show multiple oscillatory zones. Feldspars represented in the coarse-grained UST unit have zoned texture too. The comb-like shaped crystals of K-feldspar show light-blue sector luminescence zoning with sharply jagged rims in their centre; no zoning was observed in their dark-blue outer parts.

A different modal composition as well as textural dissimilarity between alternated UST and aplite units is remarkable. The interlayered aplite units seems to have features of very rapid cooling such as hourglass zoning and abundant symplectite-granophyric textures between feldspars and quartz, unlike UST that shows effects of probably slightly slower crystallization as suggested by the CL observed oscillatory zoning of comb-like K-feldspar.

WHOLE-ROCK CHEMISTRY

All aplite-pegmatites of the Hlína suite have a felsic character documented by high contents of SiO₂ (74.6–75.7 wt. %), K₂O (4.61–4.94 wt. %), Na₂O (3.82–4.21 wt. %), moderate concentrations of CaO (0.94–1.11 wt. %), and low to very low concentrations of Fe₂O₃^T (0.62–0.93 wt. %), MgO (0.02–0.03 wt. %) and TiO₂ (d'' 0.03 wt. %). Slightly elevated concentrations of Rb (170–182 ppm) and MnO (0.12–0.32 wt. %) are positively correlated with Y and HREE concentrations. Low K/Rb (212–241) and high K/Ba ratios (1034–2303) with deep negative Eu anomalies indicate high degree of fractionation.

Depletion in LREE (*ca.* 10 times enrichment over chondritic abundances) relative to HREE (70–90 times enrichment relative to chondrite) is typical; noticeable are also the low contents of volatiles (B, F, P and H₂O).

The ASI of the Hlína suite is moderate (~ 1.01); affinity to calc-alkaline series (calc-alkali index = 15.1–16.2) is also typical. High content of Y (64–116 ppm), Nb (12–28 ppm) and Ga (18 ppm) classify these rocks into the fields of post-collisional, post-orogenic and anorogenic A-type granites (Eby 1992).

Garnet is the most common mineral besides feldspars and quartz. Small euhedral garnet grains from layered aplitic unit are slightly heterogeneous (Sps_{42–38} Alm_{32–28} And_{15–7} Grs_{21–15} Prp_{2–1}). This garnet is typically enriched in HREE + Y, with up to 1.10 wt. % Y₂O₃ (0.06 apfu), 0.53 wt. % Yb₂O₃ and 0.20 wt. % Er₂O₃. It is evident that distribution of REE in rock correlated well with REE contents in the garnet. Other accessories, mainly zircon or xenotime, are extremely rare and they do not contain elevated concentrations of Y and/or HREE. Garnet is dominant container of Y and HREE in the rock.

CONCLUSION

Based on above discussion, magma crystallization was probably interrupted several times (alternation of UST and interlayered aplite units); moreover, the process of non-equilibrium crystallization is characterized by the layered /striped structure of the magmatic Y-rich garnet (spessartine-almandine s.s.) also with evolved internal oscillatory and sector zoning. Mechanism of formation of garnet-rich and garnet-poor layers is considered an oscillatory

crystallization-related process active at the evolving chemical boundary front as suggested by Webber *et al.* (1999), next to the partly solidified surface of the UST unit.

All these features are strikingly different from other known UST-bearing intrusions worldwide, which are typically associated with strongly peraluminous, volatile-rich (B, F, P and H₂O) intrusions of distinct mineralogy.

Y and HREE reside mainly in the magmatic garnet which is dominant Y and HREE container of the rock. Low concentration of Phosphorus in the magma prevented primary xenotime from precipitating as well as very rare zircon could not accumulate substantial concentrations of Y and HREE because its sum of Y + HREE > Zr.

ACKNOWLEDGEMENTS

This work was supported by research projects GAČR IAA300130801 and MSM0021622412.

REFERENCES

- Breiter, K., Müller, A., Leichmann, J. & Gabašová, A. (2005). Textural and chemical evolution of a fractionated granitic system: the Podlesí stock, Czech Republic. *Lithos* **80**: 323–345.
- Eby, G.N. (1992). The A-type granitoids: a review of their occurrence and chemical characteristics and speculations on their petrogenesis. *Lithos* **26**: 115–134.
- Hönig, S., Leichmann, J. & Novák, M. (2010). Unidirectional solidification textures and garnet layering in Y-enriched garnet-bearing aplite-pegmatites in the Cadomian Brno Batholith, Czech Republic. *J. of Geosciences* **55**: 81–97.
- Leichmann, J., Novák, M. & Sulovský, P. (1999). Peraluminous whole-rock chemistry versus peralkaline mineralogy of highly fractionated, garnet-bearing granites from the Brno Batholith. *Ber. Deutsch. Miner. Ges.* **1**: 144.
- London, D. (1992). The application of experimental petrology to the genesis and crystallization of granitic pegmatites. *Can. Mineral.* **30**: 499–540.
- Shanon, J.R., Walker, B.M., Carten, R.B. & Geraghty, E.P. (1982). Unidirectional solidification textures and their significance in determining relative ages of intrusions at the Henderson Mine, Colorado. *Geology* **10**: 293–297.
- Webber, K.L., Simons, W.B., Falster, A.U. & Foord, E.E. (1999). Cooling rates and crystallization dynamics of shallow level pegmatite-aplite dikes, San Diego County, California. *Amer. Miner.* **84**: 708–717.

RECENT DEVELOPMENTS IN THE INVESTIGATION OF POLISH PEGMATITES

Janusz Janeczek[§] & Eligiusz Szełęg

Faculty of Earth Sciences, University of Silesia, Będzińska 60, 41-200 Sosnowiec, Poland. [§]janusz.janeczek@us.edu.pl

Key words: granitic pegmatite, Strzegom, Karkonosze Mtns., Sowie Mtns., Piława Górna, Poland

Poland seemed not to be particularly blessed with complex rare-element pegmatites. However, recent discoveries of LCT and NYF pegmatites may change this perception. Complex rare-element pegmatites

together with abundant common pegmatites crop out in the Sudety Mtns. and in their foreland, which together form the NE margin of the Bohemian Block in SW Poland (Fig. 1).

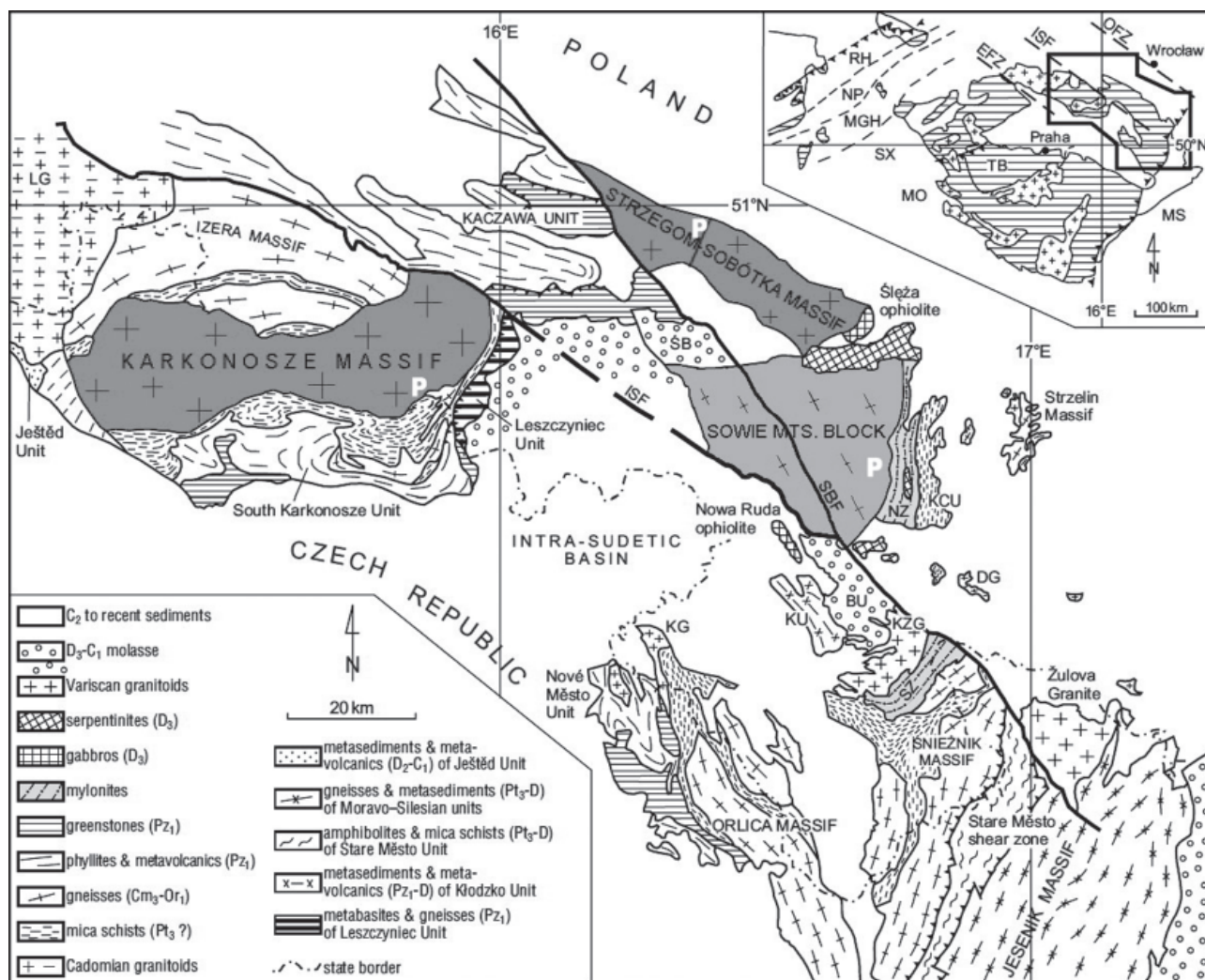


FIGURE 1. Geological map of the Sudety Mtns. (after Aleksandrowski *et al.* 1997 and Kryza *et al.* 2004); Symbols: BU: Bardo Unit, DG: Doboszwowice gneiss, ISF: Intra-Sudetic Fault, KCU: Kamieniec Unit, KG: Kudowa granite, KU: Kłodzko Metamorphic Unit (Complex), KZG: Kłodzko-Złoty Stok granitoids, NZ: Niemcza Zone, LG: Lusatian granitoids, SBF: Sudetic Boundary Fault, SSG: Strzegom-Sobótka granitoids. Inset map: EFZ: Elbe Fault Zone, ISF: Intra-Sudetic Fault, MGH: Mid-German High, MO: Moldanubian Zone, MS: Moravo-Silesian Zone, NP: Northern Phyllite Zone, OFZ: Odra Fault Zone, RH: Rhenohercynian Zone, SX: Saxothuringian Zone, TB: Teplá-Barrandian Zone, P: pegmatite occurrences mentioned in the text.

Among mineralogists and mineral collectors, the best known occurrences are miarolitic cavities in pegmatite segregations within two large Variscan (324–308 Ma) granite bodies: the Strzegom–Sobótka massif (hereafter referred to as SS) and the Karkonosze pluton (hereafter referred to as KP). They range in size from a few millimeters to a few meters. Miarolitic cavities in the classical locality of Strzegom (Striegau) have yielded many fine specimens of smoky quartz (many of gem quality), microcline, albite, fluorite, epidote, bavenite, milarite and zeolites (yellow stilbite and cherry-red chabasite). The list of minerals found in miarolitic cavities and in pegmatite dikes, veins, segregations and pods within granites of the SS massif is extensive and covers almost 100 species. Some of those minerals are rather unusual for granitic pegmatites, e.g., abundant stilpnomelane or manganiferous fayalite, together with products of their hydrothermal alteration, typical of banded iron-formations. The miarolitic pegmatites of the SS massif seem to belong to the MI REE subclass with a NYF signature. Their anatomy, mineralogy and origin are summarized in Janeczek (2007). Recently, a new type of miarolitic pegmatite was found, with the assemblage topaz – lepidolite – phenakite, and with Ta-bearing columbite-(Mn) as an accessory mineral in the amazonitic microcline zone. The chemical composition of that pegmatite seems to be intermediate between NYF and LCT (Szełęg & Szuszkiewicz 2010a).

Intracrystalline pegmatites within KP include miarolitic cavities, which are in many respects similar to the miarolitic pegmatites of the SS massif, beryl-bearing pegmatites, REE-pegmatites and peculiar nodular pegmatites (Kozłowski & Sachanbiński 2007, and literature therein). Granites of KP are highly enriched in actinides and REE, and this enrichment results in the occurrence of uranyl minerals and metamict REE-minerals, e.g., gadolinite, fergusonite, allanite, “cheralite-(Nd)”, among others. Pegmatite dikes occur also in the metamorphic cover of the KP. Currently, a corundum-bearing pegmatite of the Krucze Rocks (“Crows Rocks”) is under investigation. Irregular bodies of corundum pegmatite (up to 40 cm in diameter), bordered by a thick mica–corundum layer, occur within two quartz-rich pegmatite pods connected by a common pegmatite dike in gneiss (Fig. 2). The corundum pegmatite lacks quartz and consists of orthoclase, biotite, muscovite, albite, Fe-rich chlorite (chamosite) and blue corundum as major minerals. Schorl, rutile, ilmenite, anatase and ferberite are accessory minerals. A new mineral with a chemical composition of ScNbO_4 was found within anatase, Nb-bearing rutile and ilmenite (Szełęg *et al.* 2010b).

The largest pegmatite fields in Poland are associated with the Sowie Mtns. (Owl Mtns.) and their foreland (Fig. 1). Pegmatites occur there within gneisses, migmatites, serpentinites and amphibolites. They were extensively mined for feldspars in the XIX

century, including underground operations. Metallic beryllium was for the first time smelted from the Sowie Mtns. beryl (Sachanbiński 1973). The Sowie Mtns. host the type locality of sarcopside, which was described from one of the pegmatites by Martin Websky in 1868. Pegmatites of the Sowie Mtns. consist of abyssal class pegmatites genetically associated with migmatites, abundant common pegmatites, and rare-element pegmatites of the beryl type. The most abundant are common pegmatites, generally with abundant tourmaline of the schorl–dravite series. Recently, elbaite was found for the first time in Poland (Pieczka *et al.* 2004). Cordierite-bearing pegmatite occur within a small body of serpentinite as a result of hybridization of the pegmatite-forming melt (Kryza 1977). Some pegmatites are enriched in P, resulting in the occurrence of numerous rare phosphates including sarcopside, hureaulite, ferrisicklerite, graftonite, Carich beusite, staněkite, and alluaudite (Pieczka *et al.* 2003). The source of the Sowie Mtns. pegmatites is unknown with the exception of the undoubtedly authigenic abyssal class pegmatites.



FIGURE 2. Pegmatite dike hosting corundum-bearing pegmatite enclaves within gneiss of the Krucze Rocks in the metamorphic cover of the Karkonosze pluton. Large cavities are remnants of mining blue corundum (“sapphire”).

In 2007, a group of beryl-bearing pegmatite dikes was discovered in the newly opened amphibolite quarry in Piława Górna in the Sowie Mtns. foreland (Fig. 1). Those pegmatites are being progressively exposed owing to quarrying activities, therefore enabling observations of various cross-sections through the dikes (Fig. 3). Over 20 pegmatite dikes have been encountered so far within amphibolites and migmatitic gneisses. The pegmatites, up to 4 m across, are internally zoned, with the following sequence from the contact with host rocks: 1) a thin and discontinuous fine-grained border zone, 2) a coarse- to very coarse-grained wall zone featuring elongate and oriented biotite crystals several cm long, 3) graphic intergrowths of quartz and alkali feldspar in a gradual transition to a blocky microcline zone with numerous patches of muscovite-quartz, tourmaline-quartz and garnet-quartz intergrowths, and 4) a quartz core. The pegmatite-forming minerals are: microcline, albite, quartz, biotite and muscovite. Those pegmatites are enriched in beryl, tourmaline-group minerals, almandine-spessartine garnet, and a suite of primary Nb-Ta minerals: ishikawaite, euxenite-(Y), polycrase-(Y), columbite-(Fe), columbite-(Mn), tantalite-(Fe), tantalite-(Mn), fersmite and ixiolite. The secondary Nb-Ta minerals include pyrochlore, ytropyrochlore, microlite, plumbomicrolite, bismutomicrolite, betafite and ytrobetafite (Szełęg *et al.* 2010b, Pieczka *et al.* 2010a, b). On the basis of their mineral and chemical compositions, those pegmatites belong to the rare-element class with NYF signature (Černý & Ercit 2005).

In 2010, a Cs-bearing, lithium-dominated pegmatite with Li-rich tourmalines (elbaite, olenite, rossmanite and liddicoatite), lepidolite, pollucite, Cs-rich beryl, Nb-rich cassiterite, zircon, spessartine, columbite-(Mn) and tantalite-(Mn) was found in the quarry (Pieczka *et al.* 2010c). This is the first occurrence of an LCT pegmatite in Poland.



FIGURE 3. Beryl-bearing pegmatite within amphibolite in Piława Górna, the Sowie Mtns. foreland.

REFERENCES

- Aleksandrowski, P., Kryza, R., Mazur, S. & Zaba, J. (1997). Kinematic data on major Variscan strike-slip faults and shear zones in the Polish Sudetes, northeast Bohemian Massif. *Geol. Mag.* **133**: 727–739.
- Černý, P. & Ercit, T.S. (2005). The classification of granitic pegmatites revisited. *Can. Mineral.* **43**: 2005–2026.
- Janeczek, J. (2007). Intragranitic pegmatites of the Strzegom-Sobótka massif – an overview. In: *Granitoids in Poland, AM Monograph 1*: 193–201, Warsaw.
- Kozłowski, A. & Sachanbiński, M. (2007). Karkonosze intragranitic pegmatites and their minerals. In: *Granitoids in Poland, AM Monograph 1*: 155–178, Warsaw.
- Kryza R. (1977). Cordierite-bearing pegmatite within serpentinites near Lubachów (Sowie Mtns.). (In Polish, English summary). *Rocznik PTG* **47** (2): 247–263.
- Kryza, R., Mazur, S. & Oberc-Dziedzic, T. (2004). The Sudetic geological mosaic: Insights into the root of the Variscan orogen. *Przegląd Geologiczny.* **52** (8/2): 761–773.
- Pieczka, A., Gołębiowska, B. & Skowroński, A. (2003). Ferrisicklerite and other phosphate minerals from the Lutomia pegmatite (SW Poland, Lower Silesia, Góry Sowie Mtns). Book of abstracts. International Symposium on Light Elements in Rock-forming Minerals, Nové Město na Morav, Czech Republic, June 20 to 25: 63–64.
- Pieczka, A., Łobos, K. & Sachanbiński M. (2004). The first occurrence of elbaite in Poland. *Miner. Pol.* **35** (1): 3–14.
- Pieczka, A., Szełęg, E., Łodziński, M., Szuszkiewicz, A., Nejbort, K., Turniak, K. & Ilnicki, S. (2010a). Nb-Ta minerals in pegmatites of the DSS mine at Piława Górna, Góry Sowie block, southwestern Poland. *Mineralogia – Special Papers, Vol. 37*: 101.
- Pieczka, A., Szełęg, E., Łodziński, M., Szuszkiewicz, A., Nejbort, K., Turniak, K. & Ilnicki, S. (2010b). Mn-Fe fractionation in tourmalines from pegmatites of the DSS mine at Piława Górna, Góry Sowie block, southwestern Poland (preliminary data). *Mineralogia – Special Papers.* **37**: 100.
- Pieczka, A., Szełęg, E., Szuszkiewicz, A., Łodziński, M., Nejbort, K., Turniak, K., Ilnicki, S., Banach, M., Michałowski, P. & Różniak, R. (2010c). Lithium pegmatite from the DSS Piława Górna mine, Góry Sowie block, southwestern Poland. *Mineralogia – Special Papers.* **37**: 99.

- Sachanbiński M. 1973. Occurrence of the beryllium minerals in Lower Silesia. *Biul. Inst. Geol.* **264**: 249-257.
- Szełęg, E. & Szuszkiewicz, A. (2010a): Topaz, lepidolite and phenakite-bearing pegmatite from Zołkiewka quarry, Strzegom–Sobótka granite massif, Lower Silesia, SW Poland. *Mineralogia – Special Papers* **37**: 112.
- Szełęg, E., Gałuskina, I. & Prusik, K. (2010b). Sc–Nb oxide from corundum pegmatite of the Krucze Skały in Karpacz (Karkonosze massif, Lower Silesia, Poland) – a potentially new mineral of the ScNbO_4 – FeWO_4 series. 20th General Meeting of the IMA (IMA2010), Budapest, Hungary, August 21-27, CD of Abstracts **6**: 501.
- Szełęg, E., Szuszkiewicz, A., Pieczka, A., Nejbort, K., Turniak, K., Łodziński, M., Ilnicki, S., Banach, M., Michałowski, P. & Różniak, R. (2010c). Geology of the Julianna pegmatite vein system from the Piława Górna Quarry (Dolnośląskie Surowce Skalne S.A.), Sowie Mts. block, SW Poland. *Mineralogia – Special Papers* **37**: 111.

THE OCCURRENCE OF BETAFITE IN PEGMATITIC SHEETED URANIFEROUS GRANITES OF THE CENTRAL ZONE OF THE DAMARA OROGEN

Judith Kinnaird¹, Paul Nex^{1,2}, Guy Freemantle¹

¹ School of Geosciences, University of the Witwatersrand, 2050 Wits, South Africa. Judith.kinnaird@wits.ac.za

² Umbono Financial Services, Johannesburg

Key words: uraniferous sheeted granite, Betafite, Namibia.

INTRODUCTION

Although a relatively rare mineral, betafite, a Ti-rich pyrochlore with <30% uranium, is a widespread but minor accessory in some leucogranite sheets in Namibia. During ore processing, uranium is not released from betafite and is lost to the tailings. It is therefore important to understand the controls on formation of this mineral and to investigate its abundance in new uranium prospects. However, the fact that betafite retains actinides within its structure may have direct application to the titanite ceramic designed for disposal of partially reprocessed nuclear fuel elements so the study of betafite is of much more than local interest.

GEOLOGICAL SETTING OF SHEETED INTRUSIONS

The Neoproterozoic Pan-African Damara Orogen is a polydeformed and polymetamorphic orogenic belt with a north-south trending coastal belt and an intracontinental inland branch trending northeastwards across Namibia. This inland trending orogen has been divided into a number of zones distinguished by distinct variations in stratigraphy, structure, metamorphic grade and igneous activity (Barnes & Sawyer 1980; Clifford 1967; Miller 1983). The boundaries between the zones are marked by major linear structures, such as faults or lineaments with a major aeromagnetic expression (Miller 1987). The Central Zone of the Damara Orogen which is bounded to the north by the Omaruru Lineament and to the south by the Okahandja Lineament is characterised by a dome and basin structural style and by more than 300 intrusions with an outcrop area of at least 75,000 km². Of these, 96% are granitic with 4% minor calc-alkaline gabbroic to granodioritic rocks (Miller 1987). The Orogen is considered to represent the root zone of a volcanic arc associated with a subduction zone (Stanistreet *et al.* 1991). It exhibits high-temperature low-pressure metamorphism and an apparent metamorphic grade increase from east to west where granulite facies has been attained near the coast (Masberg *et al.* 1992; Nex *et al.* 2001). At a late-stage in the development of the Orogen sheeted granites were

emplaced in the high-grade terrane of the western Central Zone within 80 km of the Atlantic coast.

GRANITE PETROLOGY

Early workers noted that uranium mineralisation appeared to be confined to some of the late undeformed sheeted intrusions, which were called alaskites (Jacob 1974) a term used in 1900 for alkali feldspar-rich granites with little or no dark component. More recently, the term has become synonymous with alkali feldspar granites and whilst 'alaskite' is still a useful field term, the sheeted leucogranites range in composition from granodiorite, through monzo- and syenogranite to alkali feldspar granite (Nex and Kinnaird 1995, and Nex *et al.* 2001). These range in texture from granophyric, aplitic and fine-, medium-, or coarse-grained granitic to pegmatitic. Six types have been recognised (A-F), three of which are barren of U mineralisation and were pre-D₃ while post D₃ sheets are more prospective for uranium. Leucogranite sheets are common as cross-cutting irregular, anastomosing dykes and concordant bodies following the trend of the gneissosity in the Neoproterozoic Damara sediments. The sheets vary in size from a few centimetres in width to >100 m across and the larger sheets, some of which may be composite, tend to show mineralogical banding. Mineralogically, albite or oligoclase ranges in size from a few mm to several cm and in abundance from 20->80% in any one sheet while alkali feldspars constitute 3-47% and vary from massive microcline with occasional albite lamellae to a perthitic intergrowth of equal proportions of K and Na components. Accessory minerals are wide-ranging in composition although rarely more than 5% except close to country-rock contacts. Quartz varies from clear and glassy through milky and smoky to almost black when sheets are U-rich.

URANIUM MINERALISATION

Uranium mineralisation within the Central Zone was first noted in the early 1920's by the occurrence of davidite in the vicinity of Rössing Mountain. Further prospecting and exploration ultimately resulted in the discovery of the Rössing uranium deposit

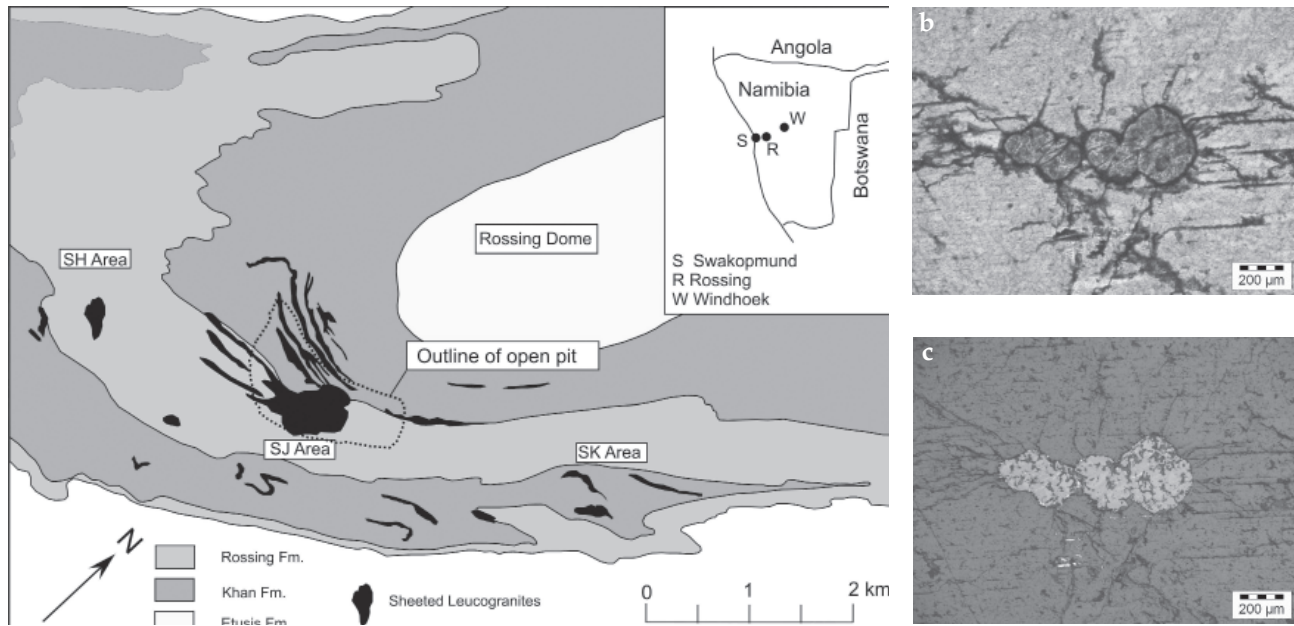


FIGURE 1: (a) Simplified geological map (after Smith, 1965) showing the locations of the SJ pit, and the SH and SK uranium anomalies. Inset shows the location of Rössing Mine within Namibia. (b) betafite in transmitted light showing iron-oxides in radial cracks and (c) in reflected light.

which has been commercially mined since 1978 (Fig. 1a). Uraninite accounts for 50% of the U-species, betafite, a Ti-rich pyrochlore hosts 5% while 45% is recovered from secondary minerals such as coffinite, betauranophane and U-phosphates. In the environs of the Rössing Mine, betafite although a relatively rare mineral, is the dominant U-species in some leucogranite sheets.

URANIUM SPECIATION

Uraninite forms small subhedral to euhedral crystals that are generally black and resinous ranging in size from a few microns to 500 µm although commonly 30-50 µm. It occurs typically within feldspar, or at crystal boundaries between feldspar, quartz, and biotite. Many uraninite crystals are altered in their core to thorite $[(\text{Th,U})\text{SiO}_4]$, jarosite and secondary uranium minerals and with rims of pyrite or magnetite or U-silicates that may also be Pb rich.

Betafite, the Nb+Ti-rich pyrochlore group mineral is defined by $2\text{Ti} \geq \text{Nb} + \text{Ta}$ for the B-site cation population (Hogarth, 1977) with a general formula of $(\text{Ca,Na,U,REE})_{16-x}(\text{Nb,Ti})_{16} \text{O}_{48}(\text{O,OH,F})_{8-y} \cdot z\text{H}_2\text{O}$, although rare worldwide, locally reaches significant proportions in the Rössing SH and SK areas (Fig. 1a). Betafite, is typically dark brown or yellowish brown (Fig. 1b), with a resinous lustre and conchoidal fracture. It occurs predominantly in the medium-grained microcline-perthite facies of the leucogranites although it has been noted in pegmatitic facies, often within smoky quartz or at the contact between quartz and feldspar grains and surrounded by a halo of radial cracks. It occurs as small octahedra to sub-rounded

isolated dodecahedral crystals or clusters of crystals up to 2 cm in size, although commonly of 1-3 mm diameter, characteristically surrounded by a 5-10 µm rim with 1-2 micron sized galena or pyrite and TiO_2 -bearing minerals or orange-coloured altered rims of iron oxides and clays.

CONTROLS ON BETAFITE FORMATION

There is no apparent difference in the composition or abundance of feldspar, or in the proportions of quartz and feldspar in betafite-bearing or betafite-absent granitic sheets or correlation between alkali feldspar triclinicity and U grade. In contrast, the country rocks may exert an effect on betafite formation. Betafite is frequently found where sheeted leucogranites cross-cut Ti- and Nb-bearing amphibole schist, and amphibolite of the Khan Formation, and cordierite gneisses of the Rössing Formation. However, this cannot be the only control, otherwise betafite would be more abundant in the SJ Main Pit where sheeted leucogranites cut the same lithologies.

Betafite-bearing granites appear to occur preferentially in the cores of antiforms where it is envisaged that the associated fluid did not escape, or where fluid movement was ponded by amphibolite dykes or where thick overlying marbles inhibited fluid loss. However, the major difference between betafite-bearing and uraninite-bearing sheets is in the trapped fluid abundance and composition (Herd 1996; Nex *et al.* 2002). Samples from the SJ-pit where betafite is rare and uraninite is the main primary phase have a total fluid content in excess of 10, and typically 20-40 micromoles per gram, whereas fluid content in

betafite-bearing S sample to the west was consistently low, typically 3-5 micromoles per gram. Absolute values of CO₂ show little difference between the pit and SH areas (typically 1-2 micromoles per gram). However, since the SH samples contain much lower amounts of water, the CO₂:H₂O ratio is much higher. This high CO₂ activity has clearly been important in influencing betafite crystallisation.

There is therefore no simple single factor that controls betafite crystallisation. Rather there appears to be a combination of host-rock chemistry, fluid chemistry and structural factors that combine to favour betafite crystallisation.

BETAFITE COMPOSITION

Brown betafite has close to full A-site occupancy with Ca and U and <14.5 wt% REE's, whereas altered yellow betafite has >1 atom pfu vacancy in the A site and 1-3.5 wt% REE. This A-site vacancy in yellow betafite is linked to loss of Ca, Na and REE, whereas the U has been retained. Previous authors (e.g., Chakhmouradian & Mitchell 1999; Ohnenstetter & Piantone 1992) have suggested that A-site cation deficiency is related to loss of U or Th in pyrochlore minerals. Our data shows that this is not the case for betafite, rather the cation-deficiency in the A-site is due to depletion of Ca and Na. Artificial materials of betafite composition are therefore potential repositories for the containment of radioactive waste. The titanite ceramic designed for disposal of partially reprocessed nuclear fuel elements consists of betafite of near ideal stoichiometry (CaUTi₂O₇) as a major phase (Ball *et al.* 1989). Our studies indicate that the long-term stability of the natural analogue of the ceramic may be partly governed by leaching of Ca and REE during alteration whereas U is effectively retained in the A-site of betafite. Since the Rössing betafites are c.500 million years old our results concur with Lumpkin and Ewing (1996) that a titanite ceramic of betafite composition is an effective repository for actinide waste disposal.

QEMSCAN STUDIES

Other primary granite-hosted anomalies in the south Central Zone which are currently under exploration and evaluation are Valencia, the Ida Dome, Goanikontes and Rossing South. The uranium deportment for all these prospects has been studied by detailed QEMSCAN analysis to investigate the uranium speciation to evaluate whether refractory betafite, brannerite or davidite may host significant uranium that would not be released during acid processing. Results show that beyond the Rössing area, betafite and other refractory oxides are absent or only present in trace proportions in the uranium-bearing mineral assemblage.

REFERENCES

- Ball, C.J., Buykx, W.J., Dickson, F.J., Hawkins, K., Levins, D.M., St. C. Smart, R., Smith, K.L., Stevens, G.T., Watson, K.G., Weedon, D., & White, T.J. (1989). Titanite ceramics for the stabilization of partially reprocessed nuclear fuel elements. *J. Amer. Cer. Soc.* **72**: 404-414.
- Barnes, S.J & Sawyer, E.W. (1980). An alternative model for the Damara mobile belt: ocean crust subduction and continental convergence. *Precamb. Res.* **13**: 297-336.
- Chakhmouradian, A.R., & Mitchell, R.H. (1999). Primary, agpaitic and deuteric stages in the evolution of accessory Sr, REE, Ba and Nb-mineralization in nepheline-syenite pegmatites at pegmatite Peak, Bearpaw Mts. Montana. *Min. Pet.* **67**: 85-110.
- Clifford, T. N. (1967). The Damaran episode in the Upper Proterozoic-Lower Palaeozoic structural history of southern Africa. *Geol. Soc. Am. Spec. Pap.* **92**.
- Herd, D.A. (1996). Geochemistry and mineralisation of alaskites in selected areas of the Rössing Uranium Mine, Namibia', MSc thesis, University of St. Andrews, St. Andrews, Scotland, UK.
- Hogarth, D.D. (1977). Classification and nomenclature of the pyrochlore group. *Am. Mineral.* **62**: 610-633.
- Jacob, R.E. (1974). The radioactive mineralisation in part of the central Damara Belt, South West Africa, and its possible origin. Pretoria, Atomic Energy Board: 17.
- Lumpkin, G.R., & Ewing, R.C. (1996). Geochemical alteration of pyrochlore group minerals: Betafite subgroup. *Am. Mineral.* **81**: 1237-1248.
- Miller, R.McG. (1983). Evolution of the Damara Orogen of southwest Africa/Namibia. *Geol. Soc. S. Afr. Spec. Pub.* **11**, 515. Johannesburg, Geol. Soc.S. Africa.
- Masberg, H.P, Hoffer, E, & Hoernes, S. (1992). Microfabrics indicating granulite-facies metamorphism in the low-pressure central Damara Orogen, Namibia. *Precamb. Res.* **55**: 243-257.
- Nex, P.A.M., & Kinnaird, J.A. (1995). Granites and their mineralisation in the Swakop River around Goanikontes, Namibia. *Comm. Geol. Svy. Namibia.* **10**: 51-56.
- Nex, P.A.M., Kinnaird, J.A., & Oliver, G.J.H. (2001). Petrology, geochemistry and uranium mineralisation of post-collisional magmatism around Goanikontes, southern Central Zone, Damaran Orogen, Namibia. *Jnl. Afr. Earth Sci.* **33**: 481-502.

- Nex, P. A. M., Herd, D., & Kinnaird, J. (2002). Fluid extraction from quartz in sheeted leucogranites as a monitor to styles of uranium mineralisation: an example from the Rossing area, Namibia. *Geochemistry: Exploration, Environment, Analysis* **2**(1): 83-96.
- Ohnenstetter, D., & Piantone, P. (1992). Pyrochlore-group minerals in the Beauvoir peraluminous leucogranite, Massif Central, France. *Canadian Mineralogist* **30**: 771-784.
- Smith, D.A.M. (1965). The geology of the area around the Khan and Swakop Rivers in southwest Africa. *Southwest Africa Series. Memoir 3*, Geological Survey of South Africa, Pretoria South Africa.
- Stanistreet, I. G., Kuçkla P. A. & Henry, G. (1991). Sedimentary basinal responses to a Late Precambrian Wilson Cycle: the Damara Orogen and Nama Foreland, Namibia', *Jnl. Afr. Earth Sci.* **11**: 141-156.

GEOCHEMICAL EVOLUTION AND PETROGENESIS OF RARE ELEMENT PEGMATITES IN THE SOLBELDER RIVER BASIN (SOUTH SIBERIA, RUSSIA)

Liudmila Kuznetsova

Vinogradov Institute of Geochemistry SB RAS, Irkutsk, Russia, lkuzn@igc.irk.ru

Key words: pegmatites, rare-elements, fluids, contamination, evolution

INTRODUCTION

Rare-element pegmatites in the Solbelder river basin represent much more variable mineral assemblages (Li and Li-Cs-Ta specialized), than those known in the other pegmatitic fields of the Sangilen region in South Siberia. In the Solbelder field, dyke swarms of spodumene-rich pegmatites (spodumene subtype) predominate. Some of them are considerably contaminated, while the others, less contaminated and more evolved, contain late stage quartz-clevelandite assemblage with lepidolite, elbaite, and pollucite in their upper parts. In the NW flank of the field pegmatite of lepidolite subtype with elbaite occurs separately in two dyke swarms. The petrological and geochemical features of pegmatites of different types and the role of fluids in their formation have been investigated.

GEOLOGICAL SETTING

The Solbelder field of rare-element pegmatites is located in the centre of the Sangilen mountain area (South Siberia, Russia). It includes several localities of Li- and Li-Cs-Ta-specialized pegmatites, hosted by the Cambrian limestones and metapelites displaying metamorphism of greenschist facies. The Sangilen Highland represents part of the Tuva-Mongolian terrain within Early Paleozoic (Caledonian) folded area in the southern termination of the Siberian Platform. It is characterized by a block-and-fold structure. The disjunctive dislocations, which resulted in formation of thrusts and shears, largely contribute to the emplacement of pegmatite-bearing granites and associated pegmatites. Most of rare-element pegmatite dykes occur near the linear fracture zones in the vicinity of Bystrinsko-Karginsky granite massif of the Early Paleozoic age. Small stocks and veins of leucocratic two-micaceous granites occupy the same position, but they have not any contacts with rare-element pegmatites.

Among rare-element pegmatites of this field the spodumene-rich variety predominates. These granitoids make up dense swarms of several bodies; the biggest of them are in Shuk-Byul, Kara-Adyr and Nadejda localities. Every swarm includes over 10

dykes, commonly subvertical and elongated, sized in length as $n \times 100$ m and from 1 up to 6 m thick. All dykes display typical intrusive features. The Kara-Adyr and Nadejda dyke swarms are hosted by limestone, whereas, the Shuk-Byul dyke swarm is located in metapelites.

Pegmatites with Ta, Li, Cs rare-metal specialization – lepidolite subtype with elbaite - occur in the NW periphery of the Solbelder field. One dyke swarm of such pegmatites is situated in the Ozerniy locality and the other one lies in the NW flank of the Shuk-Byul locality. In the last case, these pegmatites are intruded along the fracture zones crosscutting submeridian dykes of spodumene pegmatites. In both places pegmatites with lepidolite and elbaite are hosted by metapelites.

INTERNAL STRUCTURE, PETROLOGICAL AND MINERALOGICAL FEATURES

Spodumene-subtype pegmatites display weakly zoned internal structure. Fine-grained quartz-oligoclase mineral assemblage occurs in thin (3-10 cm) border zone. The central part of pegmatite bodies is almost completely occupied by fine- to medium-grained mineral assemblage of quartz, K-feldspar, plagioclase and spodumene with minor amounts of tourmaline and mica (Table 1).

This assemblage represents a rather wide evolutionary sequence of compositions (from quartz-spodumene-two-feldspars to almost biminerall quartz-spodumene), tending towards enrichment of rocks in spodumene instead of feldspars. In the Qz-Ab-Ort ternary plot their bulk normative composition vary from the vicinity of minimum haplogranitic melts at total pressures 2-3 kb towards the Qz apex (Fig.1). In the Qz-Fsp-Spd ternary plot their bulk normative composition closely approaches to petalite (Pet) apex. Such evolution trend may be due to superliquidus differentiation (delaminating) of the melts under the influence of reduced C-O-H fluids (Kuznetsova & Prokofiev 2009). Spodumene granitoids have oriented "directional" structure (defined by parallel growth of spodumene laths), if they crystallized in steady-state tectonic environments (Shuk-Byul), and massive,

TABLE 1. Mineral assemblages of rare-element pegmatites in the Solbelder river basin

Spodumene subtype				Lepidolite subtype	
Strongly contaminated		Slightly contaminated		Uncontaminated	
Less evolved	More evolved	Less evolved	More evolved	Less evolved	More evolved
Mineral assemblages (Qz and Kfs are always present)					
Sc+Sp	Olig+Sp	Olig+Sp	Ab+Sp+Lp	Ab+Tour	Ab+Lp+Tour
Associated mica and tourmalines composition					
-	Fe-Mn-lepidolite	Li-muscovite	Trilithionite	±Muscovite	Cs-rich trilithionite
Li-uvite	Liddicoatite, tsilaisite	Schorl-elbaite	Elbaite	Schorl-elbaite	Elbaite
Main accessories					
Cassiterite Pyrochlore Zircon Helvite	Cassiterite Pyrochlore-microlite Columbite-tantalite Zircon Helvite	Cassiterite Columbite-tantalite Zircon Garnet Beryl	Cassiterite Tantalite Zircon Garnet Beryl Pollucite	Cassiterite Columbite-tantalite Pyrochlore-microlite Zircon Garnet Beryl	Cassiterite Tantalite Microlite Zircon Garnet Beryl

Qz: quartz, Kfsp: K-feldspar, Ab: albite, Olig: oligoclase, Sp: spodumene, Sc: scapolite, Lp: lepidolite, Tour: tourmaline

tangled-columnar or fluidal structure if crystallization occurred in unstable tectonic environments (Kara-Adyr and some veins of Nadejda locality).

Mineralization in spodumene-subtype pegmatites becomes more complicated in some particular cases. For example, in the upper part of the Shuk-Byul locality the dykes of spodumene pegmatites have bulges, which contain core zones of late stage coarse-grained quartz-clevelandite assemblage with lepidolite, elbaite, and pollucite. In the Kara-Adyr and Nadejda localities, hosted by limestone, mineral composition of spodumene pegmatites show distinct signs of contamination: they include oligoclase instead of albite and some Ca-bearing accessory minerals (Table 1). One spodumene-bearing pegmatite dyke from Nadejda locality demonstrates a higher degree of contamination. In this dyke, scapolite crystallized instead of plagioclase; tourmaline and accessory minerals are represented by Ca-rich varieties not typical for granitic rare-element pegmatites (Table 1).

Lepidolite-subtype pegmatites exhibit a strong internal zoning in the distribution of two main mineral assemblages: (a) less evolved quartz-K-feldspar-albite variety with tourmaline (schorl) and minor muscovite occurs in the outer zone; (b) more evolved quartz-lepidolite-albite variety with elbaite is common in the inner zone. Normative compositions of lepidolite pegmatites display evolution trend towards the albite (Ab) apex of the Qz-Ab-Or ternary plot - quite distinct from the trend of spodumene pegmatites (Fig.1). Expansion of the liquidus field toward the Ab apex for Li-F-rich granites is supposedly caused by the influence of fluorine (Manning 1981).

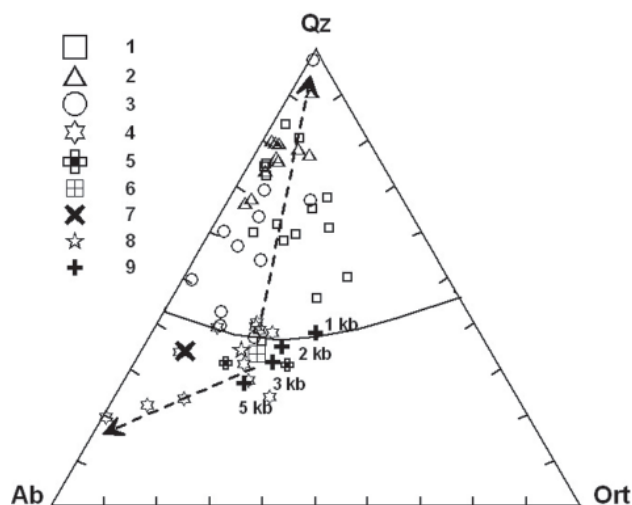


FIGURE 1. Position of the Solbelder rare-element pegmatites normative composition on the diagram Qz-Ort-Ab-H₂O. 1-3 samples of spodumene-subtype pegmatites from localities, 1: Kara-Adyr; 2: Nadejda (the vein with scapolite); 3: Shuk-Byul; 4-5 samples of lepidolite-subtype pegmatites from localities, 4: Shuk-Byul; 5: Ozerniy; 6: average bulk composition of the Tastyg dyke swarm of spodumene pegmatites - chemical data from Polkunov *et al.* 1961 (unpublished account); 7: average bulk composition of some world's known spodumene pegmatite veins, 8: composition of spodumene-rich granite of the Alakhinsky intrusion, South Siberia (7-8 from Beskin *et al.* 1999) 9: minimum granite melt compositions determined at various water activities (Tuttle & Bowen 1958). The shaped lines point the direction of the rock's evolution.

GEOCHEMISTRY

Average chemical composition of quartz-spodumene-two-feldspar mineral assemblages predominating in spodumene pegmatites of the Solbelder field corresponds to peraluminous leucogranite with ASI index - mole $A/CNK = 1.4-1.5$, $A/NKL = 1.1-1.2$, and $(Na_2O+K_2O+Li_2O) = 8.0-8.3$ (wt. %). These spodumene pegmatites demonstrate the low ratio of $Na/K = 0.7-1.5$ and are fairly poor in volatiles: $F = 0.02-0.12$; $B < 0.02$, $H_2O < 0.7$; $P_2O_5 < 0.02$ (wt. %). In the evolutionary sequence of their compositions Si, Li contents increase (SiO_2 to 76, Li_2O to 4.5 wt. %), while K, Na content almost totally decrease; Al content and ASI index - mole $A/NKL = Al_2O_3/(K_2O + Na_2O + Li_2O)$ remain constant. The iron total concentrations (as Fe_2O_3) vary from 1.3 to 1.5 wt. %. The CaO and CO_2 contents of some Solbelder's spodumene pegmatites are heightened up to 1-1.5 and 0.4-0.8 wt. %. In pegmatite with scapolite, they reach extreme levels (6-7 wt % CaO and 2.2-2.4 wt % CO_2), though average chemical composition of this rock in terms of Si, Al, Fe, and Mg contents, corresponds to leucogranite with unusually low contents of alkalis ($K_2O + Na_2O < 2$ wt %) and $A/CNK = 0.8$ (Kuznetsova & Sizykh 2004).

In spodumene pegmatites of the Solbelder field parallel increase in contents of Li and Ta, Nb, Sn was revealed. Their contents exhibit rather weak correlation with fluid components. Steady low values of whole-rock element ratios K/Rb (40-20), Nb/Ta (5.7-3.2), Zr/Hf (5.6-4.6) in all samples of spodumene pegmatites indicate rather high granite evolution.

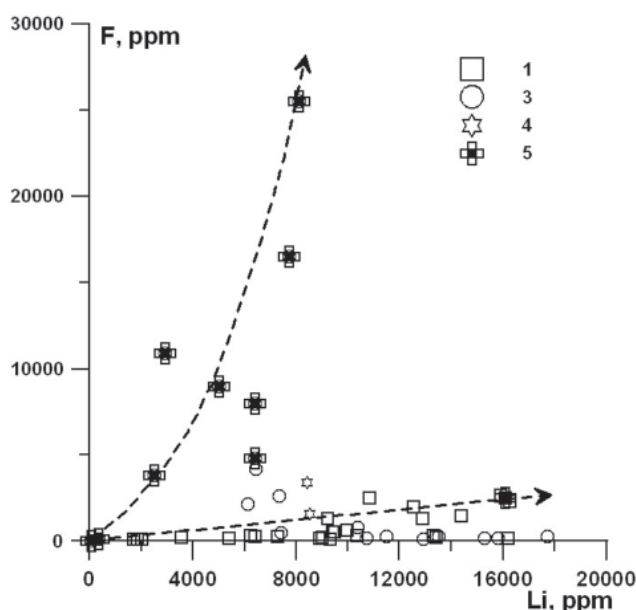


FIGURE 2. Li versus F in rare-element pegmatites of different types (symbols same as in Fig. 1)

Spodumene pegmatite with scapolite has high concentrations of Li, Rb, Cs, Be, Nb and Sn, i.e. the elements characteristic of rare-element pegmatite, as well as some elements not typical for this system (Sr, Zr, Hf, U, Th). These peculiarities may result from contamination of pegmatite melts which took place before their emplacement into the vein site, because at the surface we observed only inessential signs of their *in situ* contamination.

Average chemical composition of quartz-lepidolite-albite mineral assemblages in lepidolite-subtype pegmatites is peraluminous and subalkaline: $A/CNK = 1.4-1.5$, $A/NKL = 1.1-1.2$, $(Na_2O+K_2O+Li_2O) = 9-10$ (wt. %). Compared to spodumene pegmatites, in these rocks Na/K ratio is higher (2.5-3.5) and they are enriched in volatiles: F, B, and H_2O (up to 2.5; 0.5 and 1.8 wt. % respectively). They are characterized by high Li content (up to 1.7 wt. %) together with high contents of Ta, Be, Cs. In lepidolite pegmatites, a vivid correlation between Li and F contents was revealed in distinction to spodumene pegmatites (Fig. 2). Characteristic element ratios of these rocks - K/Rb (12-3), Nb/Ta (0.5) and Zr/Hf (4.7) indicate a higher degree of fractionation of granite than in spodumene varieties.

To reveal the conditions of Li-rich melts crystallization microtermometric study of primary fluid inclusions in minerals of spodumene pegmatites together with gas-chromatographic study of fluid compositions was conducted. It demonstrated that spodumene pegmatites crystallized at temperature 550-650 °C and pressure about 5 kb from the melts undersaturated in respect to H_2O , F, and B, but in the presence of highly dense fluid composed of CO_2 with admixed CH_4 and N_2 . It was expected that the degree of contamination depended on CO_2 activity in the melts and increased with fluid pressure (Kuznetsova & Prokofiev 2008). This regime contrasted to the environments of lepidolite pegmatites crystallization: lower P-T conditions and noticeably intense activity of H_2O , F, and B. Diversity of volatiles activity may have been responsible for the difference between the evolutionary trends and rare-elements specialization of the two pegmatites types studied.

ACKNOWLEDGMENTS

This work was supported by the Russian Foundation for Basic Research, project 09-05-01181-a; Interdisciplinary Integration Project SB RAS 29.

REFERENCES

- Beskin, S.M., Marin, Yu.B., Matias, V.V. & Gavrilova, S.P. (1999). Rare-metal granite (history of the problem, terminology, types, approach to the genesis). *Zap. VMO.* **128** (6): 28-39.

- Kuznetsova, L.G. & Sizykh, Yu.I. (2004). Problem of the origin of scapolite in rare-metal pegmatites of Sangilen. *Dokl. Earth Sci.* **395** (3): 406-410.
- Kuznetsova, L.G. & Prokofiev, V.Yu. (2008). The role of fluids in the formation of limestones-hosted Li-rich aplites and pegmatites. Proceedings of XIII Intern. Conf. on Thermobarogeochemistry and IVth APIFIS Symposium. (IGEM RAN, Moscow). 1: 102-105.
- Kuznetsova, L.G. & Prokofiev, V.Yu. (2009). Petrogenesis of anomalous Li-rich spodumene aplites of the Tastyg deposit (Sangilen area, Tuva Republic, Russia). *Dokl. Earth Sci.* **429** (8): 1262-1266.
- Manning, D. A. C. (1981). The effect of fluorine on liquidus phase relationships in the system Qz-Ab-Or with excess water at 1 kb. *Contrib. Mineral. Petrol.* **76**: 206-215.
- Tuttle, O.F. & Bowen, N.L. (1958). Origin of granite in the light of experimental studies in the system NaAlSi₃O₈-KAlSi₃O₈-SiO₂-H₂O. *Geol. Soc. Amer. Mem.* **74**: 153-16

UNUSUAL TEXTURAL RELATIONSHIPS BETWEEN SPODUMENE AND PETALITE AT SPODUMENE BEARING APLITE-PEGMATITE OF BARROSO-ALVAO FIELD (NORTHERN PORTUGAL)

Alexandre Lima^{1§} & Tania Martins²

¹ Centre of Geology of Porto University, Porto, Portugal §allima@fc.up.pt

² Department of Geological Sciences, University of Manitoba, Canada

Key words: spodumene, petalite, pegmatite, aplite, Barroso-Alvão, Portugal.

INTRODUCTION

Spodumene and petalite are common minerals in Barroso-Alvão pegmatite field. Pegmatites with spodumene were the first lithium-bearing bodies described in this area. The initial discovery report was followed by several studies focused on these spodumene aplite-pegmatite bodies (e.g., Charoy *et al.* 1992, 2001; Lima 2000). Later on, a suite of aplite-pegmatite bodies in which petalite is a dominant phase was identified (e.g., Lima *et al.* 2003; Martins 2009). Both spodumene and petalite that are present in this pegmatite field have a peculiar relationship and textures not found in the literature. In this work, we describe a particular case of these uncommon textures.

GEOLOGICAL SETTING

The Barroso-Alvão pegmatite field is located in the Iberian Peninsula, the most westerly portion of Europe. Of the several geotectonic zones that compose the Iberian Peninsula, the study area belongs to the Galicia-Trás-os-Montes Zone (Farias *et al.* 1987), and is close to the thrust that represents the southern boundary with another geotectonic zone, the Central Iberian Zone. The main hosts for the spodumene-bearing pegmatites of the Barroso-Alvão pegmatite field are meta-pelitic, mica-shists, and rarely carbonaceous or graphitic schists of upper Ordovician to lower Devonian age (Ribeiro *et al.* 2000). Spodumene-bearing pegmatites at Barroso-Alvão pegmatite field are unzoned and have the thickness between 10 and 30 m.

METHODOLOGY

The studied sample of a spodumene-bearing pegmatite was obtained from drill core at 60 meters depth. The drill core is from the Portuguese Geological Survey drill holes campaign in 1996. The sample was studied under the polarizing microscope and Raman apparatus at the Centre of Geology, Porto University. Backscattering imaging and quantitative data were obtained at the LNEG laboratory, in São Mamede de Infesta, Portugal using an electron microprobe JEOL JXA 8500-F.

RESULTS

In the studied spodumene-bearing aplite-pegmatites, spodumene is the dominant Li-bearing mineral. Petalite and eucryptite can also be observed, mostly as accessory phases. Spodumene occurs in three petrographic varieties: 1) Primary poikilitic crystals with irregular shape and containing sparse blebs of quartz (Charoy *et al.* 1992); 2) Matted aggregates of very fine-grained needles preferentially oriented surrounding earlier coarser-grained spodumene (Charoy *et al.* 1992); 3) Intimate intergrowth of spodumene and petalite in a banded sequence found in the studied sample (Fig. 1A, B).

Petalite occurs in three petrographic varieties: 1) secondary petalite surrounding spodumene, as described by Charoy *et al.* (2001); 2) Euhedral to subhedral crystals of primary petalite (Lima *et al.* 2003, Martins 2009) 3) Intimate intergrowths of petalite and spodumene in a banded sequence found in the studied sample (Fig. 1A, B).

Eucryptite is found in the fractures of spodumene or petalite crystals (primary or secondary), and as infill of angular vugs as described by Charoy *et al.* (2001) (Fig. 1A).

Cookeite crystals were observed, along fractures or in open vugs of spodumene and/or petalite, as fine-grained radial aggregates (Lima *et al.* 2010).

The electron microprobe analyses of the two minerals of studied sample are summarized on Table I.

DISCUSSION

When the system is quartz-saturated, and when the reactant and product phases are near end-member compositions as is the case on the studied pegmatite, according to London's (1984) petrogenetic grid, the existence of spodumene and petalite are a function of pressure and temperature. The existence of this peculiar micro-texture in Barroso-Alvão pegmatite field suggests a variation of the range of pressure (or temperature) during pegmatite emplacement and evolution. Based on London's (1984) petrogenetic grid we tried to explain the pressure and temperature

TABLE I. Average chemical composition of the EMPA analyses in petalite (pet) and spodumene (spd). (Li_2O^* is calculated from stoichiometry; n=number of analysis; O number of oxygens).

Pet	Wt %	n=7	20 O	Spd	Wt %	n=7	24 O
SiO_2	77.79	Si	7.990	SiO_2	64.60	Si	7.953
TiO_2	0.00	Ti	0.000	TiO_2	0.00	Ti	0.000
Al_2O_3	16.58	Al	2.007	Al_2O_3	27.75	Al	4.026
FeO	0.04	Fe	0.004	FeO	0.38	Fe	0.039
MnO	0.03	Mn	0.002	MnO	0.02	Mn	0.002
MgO	0.00	Mg	0.000	MgO	0.00	Mg	0.000
CaO	0.01	Ca	0.001	CaO	0.01	Ca	0.001
Na_2O	0.02	Na	0.004	Na_2O	0.10	Na	0.025
K_2O	0.02	K	0.002	K_2O	0.02	K	0.002
Li_2O^*	4.82	Li	1.990	Li_2O^*	8.03	Li	3.975
Total	99.30			Total	100.90		

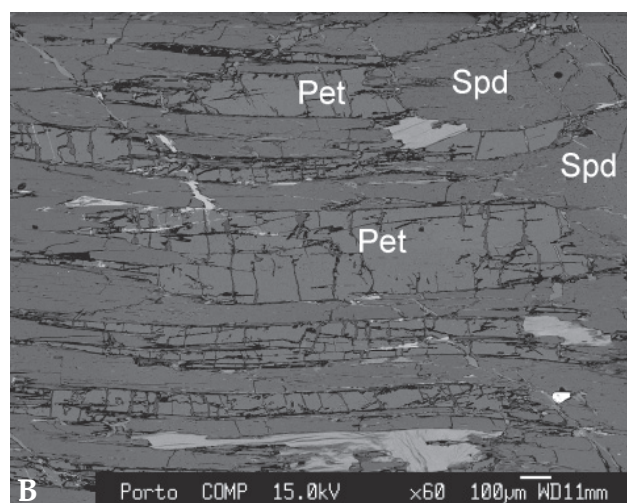
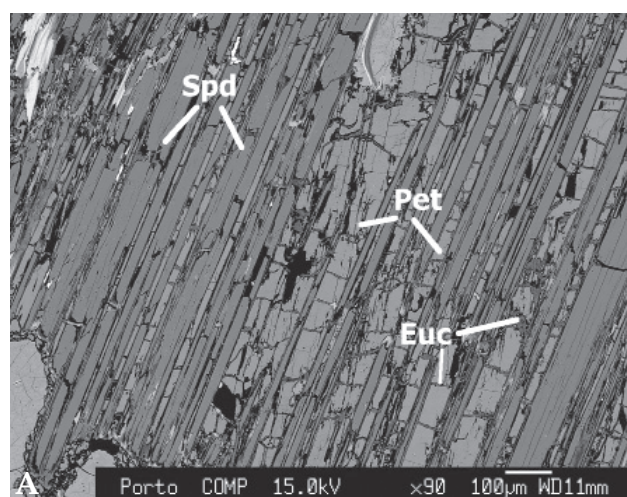


FIGURE 1. Relationships between spodumene and petalite in spodumene-bearing pegmatite of the Barroso-Alvão field. A) BSE imaging spodumene (Spd) and petalite (Pet). Eucryptite (Euc) is replacing Pet in the fractures. B) Petalite isolated micro-crystals in spodumene crystal.

conditions for the studied Li-rich pegmatite: the primary crystallisation of spodumene and petalite demonstrated principally by the intimate growth texture can be explained if existing P and T conditions coincide with the univariant curve for these two minerals, the only position in the diagram where spodumene and petalite coexist at equilibrium. Another hypothesis is having P and T conditions very close to the univariant curve and any variation of pressure, for example, would make the precipitation of the different minerals.

These findings seem to imply a variability of pressure and temperature greater than what should be expected for a system at equilibrium.

The most probable geological reason is that some of these aplite-pegmatites are affected by shear zones that contribute to variability on pressure.

ACKNOWLEDGEMENTS

We would like to acknowledge the use of the LNEG facilities in São Mamede de Infesta, Portugal.

REFERENCES

- Charoy, B., Lothe, F., Dusausoy, Y. & Noronha, F. (1992). The Crystal Chemistry of Spodumene in some Granitic Aplite-Pegmatite from Northern Portugal. *Can. Mineral.* **30**: 639-651.
- Charoy, B., Noronha, F. & Lima, A.M.C. (2001). Spodumene-Petalite-Eucryptite: mutual relationships and alteration style in pegmatite-aplite dykes from Northern Portugal. *Can. Mineral.* **39**: 729-746.
- Farias, P., Gallastey, G., Lodeiro, F.G., Marquinez, J., Parra, L.M.M., Catalán, J.R.M., Macia, G.P. & Fernandez, L.R.R. (1987). Appontaciones al Conocimiento de la Litoestratigrafia y Estructura de Galicia central. (Insights on the lithostratigraphy and structure of the Central Galicia) IX Reunión de Geología do Oeste Peninsular. Publicação do Museu e Laboratório Mineralógico e Geológico da Faculdade de Ciências, Universidade do Porto, Program Abstr 1: 411-431 (in Spanish)
- Lima, A. (2000). Structure, Mineralogy and Genesis of the spodumene-rich aplite-pegmatite bodies from Barroso-Alvão (Northern Portugal). PhD thesis. University of Porto, Portugal and INPL, Nancy, France, 270 p. (in Portuguese)
- Lima, A. M. C., Vieira, R. C., Martins, T. C., Noronha, F. & Charoy, B. (2003). A ocorrência de petalite como fase litinífera dominante em numerosos filões do campo applitopegmatítico do Barroso-Alvão (Norte de Portugal). VI Congresso Nacional de Geologia. Costa da Caparica. Almada, p. F52-F55. (in Portuguese)

- Lima, A. M. C., Vieira, R., Martins, T. & Noronha, F. (2010). Minerais de Lítio. Exemplos dos campos aplitopegmatíticos de Barroso-Alvão e Almendra-Barca d'Alva. In Neiva, J MC., Ribeiro, A., Mendes Victor, L., Noronha, F., M.M Ramalho, Eds. "Ciências Geológicas – Ensino e Investigação e sua História", Volume I, Geologia Clássica, Capítulo I - Cristalografia e Mineralogia 89-98.
- London, D. (1984). Experimental phase equilibria in the system $\text{LiAlSiO}_4\text{-SiO}_2\text{-H}_2\text{O}$: a petrogenetic grid for lithium-rich pegmatites. *Am. Mineral.* **69**: 995-1004.
- Martins, T. (2009). Multidisciplinary study of pegmatite and associated Li and Sn-Nb-Ta mineralisation from the Barroso-Alvão region. PhD thesis, University of Porto, Portugal, 196 p
- Ribeiro, M.A., Martins, H.C., Almeida, A. & Noronha, F. (2000). Carta Geológica de Portugal, escala 1:50 000, 6-C (Cabeceiras de Basto), Notícia Explicativa, Serviços Geológicos de Portugal, 48 p. (in Portuguese)

GRANITIC PEGMATITE CHRYSOBERYL IN A SHEAR ZONE OF THE ACHALA BATHOLITH, CÓRDOBA, ARGENTINA

Raúl Lira^{1§} & Jorge Sfragulla²

- ¹ CICTERRA-CONICET. Museo de Mineralogía "Dr. A. Stelzner", Facultad de Ciencias Exactas, Físicas y Naturales, Universidad Nacional de Córdoba. Vélez Sarsfield 299. 5000 Córdoba, Argentina. § rlira@com.uncor.edu
² Cátedra de Petrología Ígnea y Metamórfica, Facultad de Ciencias Exactas, Físicas y Naturales, Universidad Nacional de Córdoba. Vélez Sarsfield 1611. 5016 Córdoba, Argentina.

Key words: chrysoberyl, beryl, granite pegmatite, shear zone, Achala batholith.

INTRODUCTION

Chrysoberyl of granitic pegmatite affiliation was found in the Ethel Mary mine, at coordinates S 31° 42' 24.8" and W 64° 57' 25.1", in the western margin of the Sierra Grande, San Alberto Department, Córdoba province, Argentina (Fig. 1).

Up to date, the sole published finding of chrysoberyl in Argentina was reported by Gay & Galliski (1978) and Galliski *et al.* (2011), near Virorco, Sierra de San Luis. At this site, chrysoberyl occurs as a subordinate phase in the assemblage dumortierite-tourmaline-kyanite, in zoned veins or dikes of uncertain origin, emplaced in norite and hornblende gabbro.

This contribution describes the geological setting and mineralogical peculiarities of this finding of granitic pegmatite chrysoberyl in the country, in an attempt to constrain its formation environment.

PEGMATITE GEOLOGY

Arias (1983) described the Ethel Mary mine as a 120 m NNE-SSW extended and 50 m wide lens-shaped pegmatite, recognizing four major zones: a fine grained "contact" zone (Qtz-Kfs-Ms-Bt), followed by a "marginal" zone (external and internal), with the same mineralogy, distinguishing 7cm long bladed biotite crystals in the external zone and a few prismatic beryl crystals up to 20 cm long in the internal zone; the innermost zone was described as a quartz core. Surface mine workings were done for beryl extraction. Chrysoberyl was not identified at that time.

Chrysoberyl is hosted in a fracture-filling Qtz-Mc-Ab-Ms (\pm Bt \pm Brl) pegmatitic assemblage that crosscuts the zoned pegmatite described by Arias in 1983 (Sfragulla 2001). Both bodies are emplaced in a coarse grained, equigranular biotite-muscovite monzogranite facies of the extended Achala batholith of Devonian age (Rapela 1982; Lira & Kirschbaum 1990; Demange *et al.* 1996; Dorais *et al.* 1997; Rapela *et al.* 2008).

The older pegmatite body is tabular shaped, striking 25° and dipping 25°E; zonation consists in a 3 to 4 m thick massive quartz core in contact with an intermediate zone about 10 m thick composed of

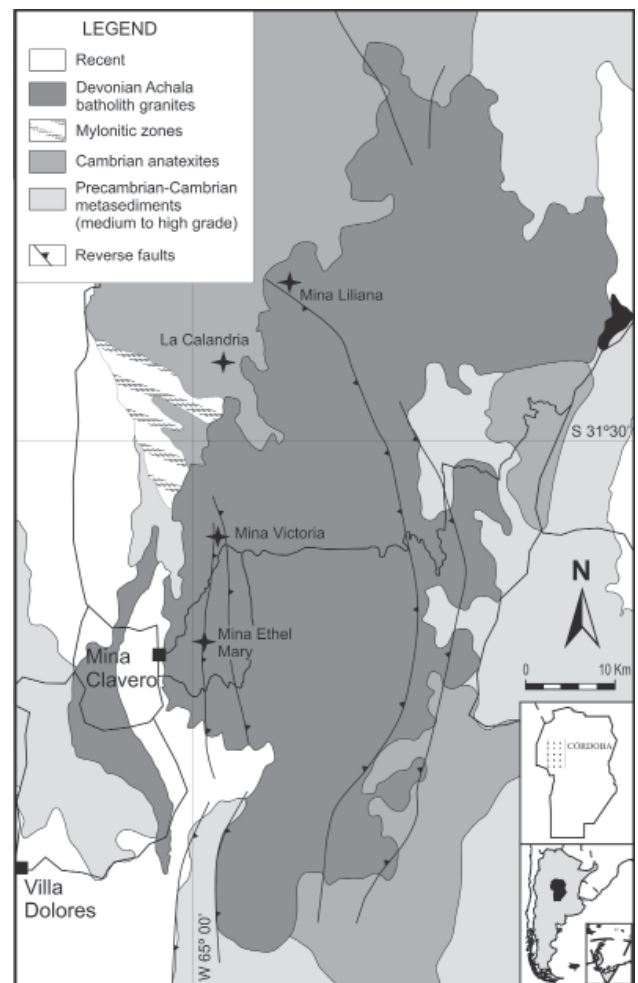


FIGURE 1. Location of the Ethel Mary beryl-chrysoberyl mine within the ca. 2500 km² Achala batholith. Three neighboring topaz bearing pegmatites of the Punilla district are drawn for reference (Liliana, La Calandria and Victoria). Regional geology summarized after Bonalumi *et al.* (1999).

50% volume plagioclase in anhedral crystals (0.5-2 cm), 30% blocky pink K-feldspar (5-20 cm, partially graphic), 10% greyish white anhedral quartz (0.5-1 cm), and 10% volume of micas (muscovite and biotite) occurring in small booklets (up to 1cm), being biotite partially oxidized. Only prismatic beryl is found as

an accessory phase (1 to 20 cm long). This pegmatite body is crosscut by granite dykes varying in width from 0.2 to 2 m thick.

The younger infilling pegmatite body is thin (0.5 to 1 m wide), and shows two main textural domains evidenced by a fine grained (0.5-1 cm) mica-rich zone ($Ms \pm Bt \pm Ab$) that resembles a replacing assemblage which irregularly passes into a distinct coarser grained zone (1-2 cm) composed of moderately

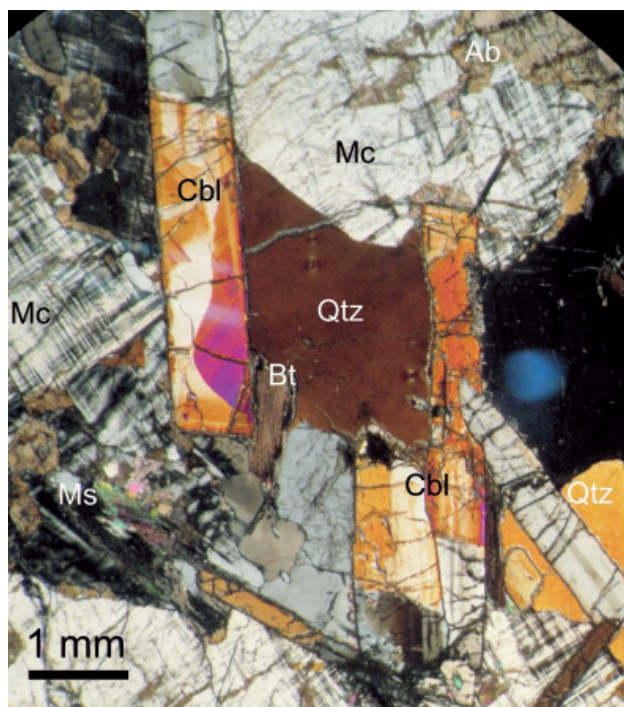


FIGURE 2A. Representative chrysoberyl (Cbl) - bearing assemblage. Most Cbl tabular crystals are twinned and show complex color zoning; some show a replacing alteration rim. Mc: perthitic microcline, Ab: albite (partially replacing Mc), Qtz: quartz, Bt: biotite, Ms: muscovite.

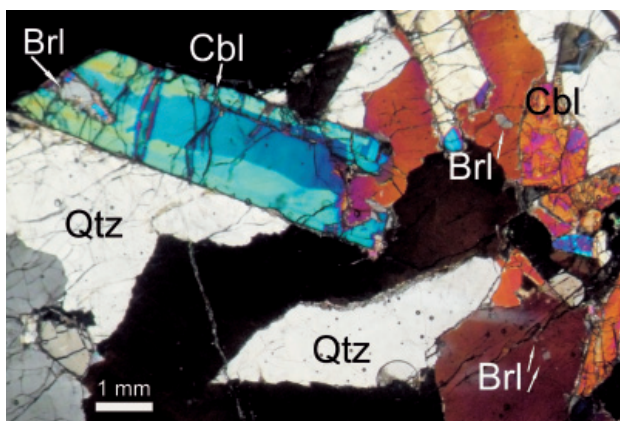


FIGURE 2B. Anhedrally relic beryl (Brl) included in chrysoberyl (Cbl), interpreted as remnants of its breakdown into the latter. Qtz: quartz.

albitized perthitic microcline, albite and quartz, where chrysoberyl is preferentially concentrated ($Mc - Ab - Qtz - Cbl \pm Brl$, Fig. 2A). Quartz is always the latest anhedral phase. In the mica-rich zone, both subhedral Ms and Bt are intergrown in equilibrium; muscovite in contact with microcline has developed myrmequitic texture.

Some sectors of the infill/replacement assemblage show textural evidence of ductile to brittle deformation as evidenced by bent and fractured feldspars and chrysoberyl crystals, and undulose extinction of quartz, partially with mosaic texture.

CHRYSOBERYL DESCRIPTION

Chrysoberyl is yellowish green. It occurs as tabular individual crystals parallel to (001) which commonly associate to each other in a "tree branch"-like habit. Few tabular crystals have grown as parallel aggregates. Individual crystal sizes are not longer than 1.5 cm and 0.5 to 2 mm thick. Both multiple contact {130} pseudo-hexagonal twins with re-entrant angles and the heart-shaped type are present.

Some crystals include subhedral biotite and muscovite booklets. Chrysoberyl is distributed in both the quartz-feldspar zone and the replacement mica-rich zone, though the largest ones are found included in quartz or feldspars. Relics of anhedral beryl grains included in chrysoberyl and adjacent patchy quartz provide textural evidence of beryl breakdown into chrysoberyl+quartz (Fig. 2B).

In thin section chrysoberyl is weakly pleochroic varying within light yellow to pale green hues. Optical, strong complex zoning is commonly evidenced by anomalous birefringence shown as blue and brown interference colours, usually like sharp wedged blades developed along the *c* axis (Fig. 2 A-B).

Practically all chrysoberyl crystals are rimmed by a thin aggregate of fine grained replacing muscovite, developed at the intergranular contact with enclosing feldspars; besides feldspars, in some cases muscovite weakly replaces chrysoberyl centripetally. This second generation of muscovite also locally replaces biotite.

In some sectors, chrysoberyl crystals are bent, fractured and strongly replaced by muscovite aggregates.

REGIONAL GEOLOGY AND FORMATION ENVIRONMENT

The Ethel Mary intragranitic pegmatites are located within the Punilla district according to the geographic distribution established by Galliski (1994 a, b; 1999). Pegmatites of this district are representative of the REE class, Beryl type, Beryl-Columbite-Phosphate subtype, despite phosphates and columbite-group species were not found in some of them. Mineralogical

indicators for the whole district suggest to classify them as of the Hybrid family between NYF and LCT (Galliski 1994 b), characterization that would also apply for the Ethel Mary pegmatites.

Despite that it was not found in the Ethel Mary mine, topaz is a common accessory mineral present in neighbouring pegmatites like La Calandria and Liliana (Gay & Lira 1984) and La Victoria (Gay & Sfragulla 1992; Fig. 1).

The lonely occurrence of chrysoberyl in the Ethel Mary mine, is interpreted as a by-product of the breakdown reaction of beryl, i.e., $\text{beryl} \rightarrow \text{chrysoberyl} + 3\text{quartz} + 2\text{BeO}$ (Černý *et al.* 1992) or $\text{beryl} + 2 \text{aluminosilicate} \rightarrow 3 \text{chrysoberyl} + 8\text{quartz}$ (Franz & Morteani 2002). Its location in a reverse fault zone and textural evidence that shearing was active during pegmatite infill/replacement stage, suggest that chrysoberyl formation was favored by its confinement to a regional shear-stress environment, like other worldwide known examples (*e.g.*, Černý *et al.* 1992; Černý 2002; Manimaran *et al.* 2007). The stable assemblage $\text{Cbl} + \text{Qtz}$ would be achieved at high T°C-low P conditions (Franz & Morteani 2002).

Strongly fractured and partially replaced chrysoberyl by muscovite aggregates suggest that a hydrothermal fluid was channelled through the fault zone during post-deformation stage.

ACKNOWLEDGEMENTS

Research work was granted by SeCyT-UNC Res. 214/10 (2010). We thank F. Colombo for providing some references and M. Galliski for a preliminary critical review. Meticulous review of F. Hatert is sincerely acknowledged.

REFERENCES

- Arias, S.C. (1983). Informe del relevamiento topográfico- geológico- económico de la mina "Ethel Mary", ubicada en pedanía Tránsito, departamento San Alberto, provincia de Córdoba. Dirección de Minería. Informe inédito. 7 pp.
- Bonalumi, A., Martino, R., Sfragulla, J.A., Baldo, E., Zarco, J., Carignano, C., Tauber, A., Kraemer, P., Escayola, M., Cabanillas, A., Juri, E. & Torres, B. (1999). Hoja Geológica 3166-IV. Villa Dolores. (Memoria y Mapa Geológico). Boletín 250. SEGEMAR. Buenos Aires.
- Černý, P. (2002). Mineralogy of beryllium in granitic pegmatites. *Rev. Min. Geoch.* **50**: 405-444. *Min. Soc. Amer.*
- Černý, P., Novák, M. & Chapman, R. (1992). Effect of sillimanite-grade metamorphism and shearing on Nb-Ta oxide minerals in granitic pegmatites: Maršíkov, Northern Moravia, Czechoslovakia. *Can. Min.* **30**: 699-718.
- Demange, M., Álvarez, J.O., López, L. & Zarco, J.J. (1996). The Achala Batholith (Córdoba, Argentina): a composite intrusion made of five independent magmatic suites. Magmatic evolution and deuterite alteration. *J. South Amer. Earth Sc.* **9** (1-2): 11-25.
- Dorais, M.J., Lira, R., Chen, Y. & Tingey, D. (1997). Origin of biotite-apatite-rich enclaves, Achala batholith, Argentina. *Contributions to Mineralogy and Petrology* **130**: 31-46.
- Franz, G. & Morteani, G. (2002). Be-minerals: synthesis, stability, and occurrence in metamorphic rocks. *Rev. Min. Geoch.* **50**: 551-589. *Min. Soc. Amer.*
- Galliski, M.A. (1994 a). La Provincia Pegmatítica Pampeana. I: Tipología y distribución de sus distritos económicos. *Rev. Asoc. Geol. Arg.* **49** (1-2): 99-112.
- Galliski, M.A. (1994 b). La Provincia Pegmatítica Pampeana. II: Metalogénesis de sus distritos económicos. *Rev. Asoc. Geol. Arg.* **49** (1-2): 113-122.
- Galliski, M.A. (1999). Distrito pegmatítico Punilla. In: Zappettini, E.O. (ed.), Recursos Minerales de la República Argentina. *Inst. de Geol. y Rec. Min., SEGEMAR, Anales* **35**: 547-550. Buenos Aires.
- Galliski, M.A., Márquez-Zavalía, M.F. & Lira, R. (2011). The dumortierite-bearing assemblages of Virorco, San Luis, Argentina: are they pegmatitic dikes or hydrothermal veins? PEG2011, abstract, this volume.
- Gay, H.D. & Galliski, M.A. (1978). Dumortierita, crisoberilo y minerales asociados de Virorco, San Luis. *Actas VII Cong. Geol. Argentino, II*: 327-335.
- Gay, H.D. & Lira, R. (1984). Presencia de topacio en la provincia de Córdoba. Yacencia, mineralogía y paragénesis en Tanti y Cañada del Puerto. *Revista de la AMPS* **15** (3-4): 62-66.
- Gay, H.D. & Sfragulla, J.A. (1992). Fosfatos de la pegmatita Victoria, Departamento San Alberto, Córdoba. Iª Reunión de Mineralogía y Metalogenia, *Actas*: 137-146. *Public. N° 2, Inst. Rec. Min., UNLP, La Plata.*
- Lira, R. & Kirschbaum, A.M. (1990). Geochemical evolution of granites from the Achala batholith of the Sierras Pampeanas, Argentina. In: Kay, S.M. & Rapela C.W. (eds.), *Plutonism from Antarctica to Alaska.. Geological Society of America, Special Paper* **241**: 67-76. Boulder, Colorado.
- Manimaran, G., Bagai, D. & Chacko, R. (2007). Chrysoberyl from Southern Tamil Nadu of

- South India, with implications for Gondwana studies. In: Rajendran, S., Aravindan, S. & Srinivasamoorthy, K.(eds.). *Mineral Exploration: Recent Strategies*. 63-76.
- Rapela, C.W. (1982). Aspectos geoquímicos y petrológicos del Batolito de Achala, Provincia de Córdoba. *Rev. Asoc. Geol. Arg.* **XXXVII** (3):313-330. Buenos Aires.
- Rapela, C.W., Baldo, E.G., Pankhurst, R.J. & Fanning, C.M. (2008). The Devonian Achala Batholith at the Sierras Pampeanas: F-rich, aluminous A-type granites. 6° South Amer. Symp. on Isot. Geol., 8pp. S. C. de Bariloche, Argentina..
- Sfragulla, J.A. (2001). Ficha mina yacimiento Ethel Mary. In: Rubio, M., Bonalumi, A., Pérez, D., Sfragulla, J.A., López, A., Guerreschi, A., Cuffini, S.L., Spahn, G., Vázquez, C. and Gozávez, M.: Informe final Proyecto BID 802/OC. AR. PICT N° 1004059. "Investigación petro mineralógica y geoquímica de cuarzo y feldespatos alcalinos en la Provincia de Córdoba, direccionada a su aplicabilidad en la industria de la fibra óptica y cerámicas especiales", FONCyT (inédito).

COMPETING MODELS FOR THE INTERNAL EVOLUTION OF GRANITIC PEGMATITES

David London

ConocoPhillips School of Geology & Geophysics: dlondon@ou.edu
University of Oklahoma, 100 East Boyd Street, room 710 SEC, Norman, OK USA 73019

Key words: pegmatite, granite, granitic liquid, fluxing components, gel, aqueous fluid

These models for the generation and internal evolution of granitic pegmatites were proposed by the early decades of the 20th century: (1) precipitation from an aqueous fluid phase; (2) crystallization of silicate liquid through an aqueous fluid interface; (3) crystallization from a hydrous silicate gel; (4) crystallization from a flux-rich silicate liquid, and (5) crystallization of a granitic melt from margins to center. Each of these models has its advocates today. What is different today, however, from the early 20th century is that there is now a large and relevant data base on which to assess each of these models.

(1) *Precipitation from an aqueous phase.* Hunt (1871) proposed this model as an extension of "granitization." Gresens (1969) revised the concept, and Roedder (1981) endorsed it, at least for the formation of rare-element pegmatites. The problems with the model are primarily associated with the low solute-carrying capacity of aqueous fluids at moderate (pegmatite-forming) P and T. In a single-phase H₂O-CO₂-NaCl fluid that would be typical of an evolving granitic magma, the solubility of silica is < 0.5 mg SiO₂/l of fluid (London 2009, from Fournier & Potter 1982). Alumina is less soluble by over orders of magnitude (Anderson & Burnham 1983). The fluid:rock volumetric ratios necessary to transport enough alumina to make a feldspathic pegmatite are of the order of 10⁶. The interactions of such fluids with host rocks along the path of a pegmatite-producing fracture are generally nonexistent.

(2) *Crystallization of silicate liquid through an aqueous fluid interface.* The concept was proposed by Brögger (1890), endorsed by Landes (1933), and it became the core concept of Jahns and Burnham (1969). Jahns and Burnham (1969) recognized the problem of solute transport in an aqueous fluid phase, which is why they stated that the process might work if given sufficient time. However, London (2008) has outlined numerous lines of evidence that fail to demonstrate evidence for an aqueous fluid phase during pegmatite consolidation. Moreover, the timeframes for crystallization are now in the range of days to

years, not the many thousands of years that would be necessary to effect the mass transport (same problem as (1) above). Jahns and Burnham (1969) suggested that thermal gradients across the pegmatite melt might provide the driving force to speed-up the mass transfer, but Jahns (1982) abandoned this mechanism, perhaps because he realized that the feldspar zonation that would result from transport through an aqueous fluid along thermal gradients would be just the opposite to that found in pegmatites. Aqueous fluid fractionates a number of the rare and incompatible elements (Rb, Cs, B, etc.) from melt, and early separation of aqueous vapor will deplete melt in such trace elements, leading to their depletion, not enrichment, as crystallization advances.

(3) *Crystallization from a hydrous silicate gel.* Merritt (1924) proposed this mechanism based on the similarity of zoned pegmatites to zoned agates, which have fortification bands that resemble layered aplites, and cores of coarse-grained quartz; the gel hypothesis has been reintroduced as the medium from which all granitic pegmatites solidify (Taylor 2006). Merritt (1924) and others (Oehler 1976) found that such silicate gels are unstable and decompose to crystals plus aqueous fluid at temperatures well below those of near-solidus melts. There is no plausible mechanism by which gels or sols that normally contain > 10 wt% H₂O (> 80 mol% H₂O) could evolve from an initially H₂O-undersaturated granitic melt; the wide miscibility gap between aqueous fluid and silicate melt at moderate P and T has been confirmed by analyses of quenched products and corroborated by chemographic methods (Burnham and Jahns, 1962). Gels are also more viscous than their liquid counterparts, which makes an already intractable problem of pegmatite dike extraction from granites (Rubin 1995) even more problematic. In addition, gels promote crystal growth by impeding solute diffusion, and thereby keeping the solvent phase of the gel at or below crystal saturation (as compared to liquids). Like most other pegmatite petrologists, Jahns (1953) recognized that the problem of making giant crystals amounted to finding a mechanism

that promoted more rapid diffusion than afforded by a simple granitic melt; relative to silicate liquids, gels of a corresponding composition diminish, not increase, the rates of diffusion needed to transport a large flux of insoluble material over large distances to growing crystal surfaces.

(4) *Crystallization from a flux-rich silicate liquid.* The vast majority of pegmatites are common granites in composition. They lack any evidence of formerly large quantities of the fluxing components that are conserved at least partially in minerals (B, P, and F); though probably hydrous as liquids, they also lackmiarolitic cavities, internal alteration by hydrothermal fluids, and any observable hydrothermal overprint on their host rocks. Even the most fractionated pegmatites are not far from the granite composition and low in total fluxing components (Stilling *et al.* 2006), and the more astute petrologists of pegmatites have observed that “the differences in composition between some complex and simple pegmatites are more mineralogical than chemical and more apparent than real” (Heinrich 1953). In addition to evidence from field studies, generally low flux contents in the bulk compositions of pegmatites are indicated by mineral-melt equilibria as calibrated through experimental methods (reviewed in London 2009), and by the widespread and characteristic occurrence of graphic granite, which owes its origins to crystallization from a granitic melt of high viscosity in the absence of an intervening aqueous fluid phase (Fenn 1986). Purported evidence for highly fluxed melt compositions as manifested by crystalline solid inclusions within minerals is mostly dubious. Such inclusions from pegmatites of Western Europe (Thomas *et al.* 1996) possess solidus temperatures in the range of ~550° to 650°C and liquidus temperatures from 750° to 950°C (Thomas 1994; Thomas *et al.* 1996; Thomas and Webster 2000). As such, these inclusions (many of which contain 6-8 wt% H₂O and several wt% each of the components B, P, and F; see the citations above) cannot represent flux-enriched melts derived from the extended liquidus fractionation in the granite system. As derivative melts, their solidus and liquidus must be lower, not higher, than their parental melts. One possibility is that these inclusions constitute mixtures of fluids that were immiscible at the conditions of entrapment, and this is one of the hypotheses put forward by Thomas and Webster (2000) and by Veksler *et al.* (2003). However, entrapment of immiscible fluids might account for the high liquidus temperatures of these inclusions, but not their high solidi, which should be close to the solidus of hydrous macusanite (i.e., if one of the phases trapped was a low-melting flux-rich melt). Alternatively, inclusions with final melting temperatures as high as 750° to 950°C could easily be explained as

cases of trapped melt plus accidentally trapped crystalline phases, leading to widely variable compositions (e.g., 100 to 7,000 ppmw Sn in a single quartz sample: Thomas and Webster 2000) or immiscible liquids resulting from complete laboratory melting (Thomas *et al.* 1996).

(5) *Crystallization of a granitic melt from margins to center.* A model based on constitutional zone refinement by crystallization from a granitic liquid that contains low but significant quantities of the fluxing components of H, B, P, or F at temperatures below the solidus and well below the liquidus of the pegmatite-forming melt can reconcile all of the disparities and inconsistencies cited above (London 2008, 2009). The bulk liquids have high viscosity (but not as high as gels of comparable composition), and the boundary layer of melt that evolves ahead of the crystallization front can sufficiently concentrate the fluxes so as to promote a high mass-transfer of normally slow-diffusing components over long distances at low temperatures and at rates that are amenable to crystallization in days to years. In this model, the fine-grained, graphic, and oriented textures of the outer pegmatite zones are dominated by the effects of liquidus undercooling, whereas the coarser-textured interior zones result from the eventual accumulation of fluxes through constitutional zone refining (London 2009). The sharp transition from granitic pegmatite to inner zones rich in rare-element minerals marks the transition from crystallization of bulk granitic melt through the flux-rich boundary layer liquid to the eventual crystallization of the flux-rich liquid itself. The additional fluxing components that are not conserved by these latest-stage zones are lost to host rocks, where they may induce a narrow but intense zone of metasomatic alteration. This model was implicit (though not fully elucidated) in the concepts of pegmatite crystallization that were summarized by Cameron *et al.* (1949), and endorsed by Jahns (1953). Those authors believed that pegmatites formed “...as successive layers upon the walls of the chamber enclosing a body of pegmatitic liquid, and hence are due primarily to fractional crystallization” (Cameron *et al.* 1949, p. 105), and that “... All known features of pegmatite zones seem reasonably explainable on the basis of crystallization from a melt of low viscosity, with or without end-stage deuteric or hydrothermal activity” (Jahns 1953).

REFERENCES

- Anderson, G.M. & Burnham, C.W. (1983). Feldspar solubility and the transport of aluminum under metamorphic conditions: *Am. J. Sci.* **283-A**: 283-297.
- Brögger, W.C. (1890). Die mineralien der syenitpegmatitgänge der Südnorwegischen augit und nephelinsyenite: *Zeit. Krist. Mineral.* **16**: 1-63 and 213.

- Burnham, C.W. & Jahns, R.H. (1962). A method for determining the solubility of water in silicate melts: *Am. J. Sci.* **260**: 721-745.
- Cameron, E.N., Jahns, R.H., McNair, A.H., & Page, L.R. (1949). Internal structure of granitic pegmatites: *Econ Geol. Mon.* **2**: 115 p.
- Fenn, P.M. (1986). On the origin of graphic granite: *Am. Mineral.* **71**: 325-330.
- Fournier, R.O. & Potter, R.W. II (1982). An equation correlating the solubility of quartz in water from 25° to 900°C at pressures up to 10,000 bars: *Geochim. Cosmochim. Acta* **46**: 1969-1973.
- Gresens, R.H. (1969). Tectonic-hydrothermal pegmatites. I. The model: *Contrib. Mineral. Petrol.* **15**: 345-355.
- Heinrich, E.W. (1953). Zoning in pegmatite districts: *Am. Mineral.*, **38**, 68-87.
- Hunt, T.S. (1871). Notes on granitic rocks: *Am. J. Sci.* **1**: 82-89, 182-191.
- Jahns, R.H. (1953). The genesis of pegmatites. I. Occurrence and origin of giant crystals: *Am. Mineral.* **38**: 563-598.
- Jahns, R.H. (1982). Internal evolution of pegmatite bodies. In: Černý, P. (Ed.) *Granitic Pegmatites in Science and Industry*: Mineral. Assoc. Can. *Sht. Crse. Hndbk.* **8**: 293-327.
- Jahns, R.H. & Burnham, C.W. (1969). Experimental studies of pegmatite genesis: I. A model for the derivation and crystallization of granitic pegmatites: *Econ. Geol.* **64**: 843-864.
- Landes, K.K. (1933). Origin and classification of pegmatites: *Am. Mineral.* **18**: 33-56.
- London, D. (2008). *Pegmatites*: Sp. Pub. 10, Can. Mineral., 368 p.
- London, D. (2009). The origin of primary textures in granitic pegmatites: *Can. Mineral.* **47**: 697-724.
- Merritt, C.A. (1924) The function of colloids in pegmatitic growths. *Trans. Roy. Soc. Can.* **17**: 61-68.
- Oehler, J.H. (1976). Hydrothermal crystallization of silica gel: *Geol. Soc. Am. Bull.* **87**: 1143-1152.
- Roedder, E. (1981). Natural occurrence and significance of fluids indicating high pressure and temperature: *Phys. Chem. Earth* **13**: 9-39.
- Rubin, A.M. (1995). Getting granite dikes out of the source region: *J. Geophys. Res.* **100B**: 5911-5929.
- Stilling, A., Černý, P., & Vanstone, P.J. (2006). The Tanco pegmatite at Bernic Lake, Manitoba. XVI. Zonal and bulk compositions and their petrogenetic significance: *Can. Mineral.* **44**: 599-623.
- Taylor, M.C. (2006). The gel model for the formation of gem-bearing pockets within granitic pegmatites, and implications for gem synthesis: (abstr) *Gems Gemol.* **42**: 110-111.
- Thomas, R. (1994). Fluid evolution in relation to the emplacement of the Variscan granites in the Erzgebirge region: a review of the melt and fluid inclusion evidence: In *Metallogeny of collisional orogens* (Seltmann, R., Kämpf, H., and Möller, P. eds.). *Czech Geol. Surv.* 70-81.
- Thomas, R., Reide, D., & Turnbull, R.B. (1996). Microthermometry of volatile-rich silicate melt inclusions in granitic rocks. *Zeit. Geol. Wiss.* **24**: 505-526.
- Thomas, R. & Webster, J.D. (2000). Strong tin enrichment in a pegmatite-forming melt: *Mineral. Dep.* **35**: 570-582.
- Veksler, I.V., Thomas, R., & Schmidt, C. (2002) Experimental evidence of three coexisting immiscible fluids in synthetic granitic pegmatite: *Am. Mineral.* **87**: 775-779.

PETALITE RARE-METAL PEGMATITES OF THE EAST SAYAN BELT, EASTERN SIBERIA, RUSSIA: GEOLOGICAL SETTING, MINERALOGY, GEOCHEMISTRY AND GENESIS

Vladimir Makagon

Institute of Geochemistry, SB RAS, Irkutsk, Russia, vmak@igc.irk.ru

Keywords: petalite pegmatites, minerals, geochemistry, genesis

INTRODUCTION

The East Sayan pegmatite belt has extension of about 500 km along the south-western Siberian craton margin. The Vishnyakovskoye, the Alexandrovskoye and another petalite pegmatite fields are situated in north-western part of this belt. Referred to most perspective for Ta mining in Russia Vishnyakovskoye rare-metal deposit (Komin *et al.* 2004) is settled down in the field of the same name. Li, Rb, Cs, Be, Sn and Nb are accompanying components in this deposit.

GEOLOGICAL SETTING

Pegmatite fields are located within the Elash graben which belongs to the Tagul-Tumanshet mobile zone (Bryntsev 1994). Graben is composed of the sedimentary and volcanic rocks of the Low Proterozoic Subluk series, which are metamorphosed in conditions of green shists and epidote-amphibolite facies of andalusite-sillimanite metamorphism type. The Elash-Tenishet granite massif of Sayan complex is located also in the Elash graben. These granites are considered to be fertile for rare-metal pegmatites of this region. Granitoids of this complex form two associations, early biotite-amphibole granodiorites, low-alkali granites and late intrusions of biotite, muscovite-biotite leucocratic granites, pegmatoid granites, pegmatite and aplite veins. Age of granites of the Elash-Tenishet massif is 2120-1960 Ma (Bryntsev 1994) and age of granites of the Sayan complex is determined by Levitsky *et al.* (2000), using the U-Pb zircon method, as 1858 Ma. Dykes and massif of rapakivi-granites with age, dated by thermoisochron Pb-Pb zircon method, as 1780 Ma (Bryntsev 1994), are located close to the pegmatite fields. They are united in the Elash complex. Zones of deep-seated faults are the main factor controlling pegmatite field position. Age of petalite pegmatites of Vishnyakovskoye field, determined by Rb-Sr method, is 1490 Ma, as well age of altered amphibolites in exocontact zones of these pegmatites is 1480 Ma (Makagon *et al.* 2000).

INTERNAL STRUCTURE

Pegmatites of the Alexandrovskoye field belong to phosphorus-tantalum-lithium geochemical

sequence of petalite rare-metal pegmatites. They form some vein series. Bodies of lepidolite-albite pegmatites are studied most completely. Single gently dipping veins lie in amphibolites. One of them has the biggest width and drop-like shape. Its length is near 200 m and width in swell is 20 m. This vein shows zonation. In endocontact quartz-muscovite rim is of different width reaching 2 m. In addition to quartz and muscovite it contains green tourmaline, columbite-tantalite and beryl. Near swell albite occurs as well. Zone of blocks of microcline, which is altered into albite in a swell, follows rim. Saccharoidal albite with clevelandite portions is in next zone. This pegmatite is replaced by quartz-lepidolite and quartz-albite-lepidolite aggregates with white beryl, rose tourmaline, tantalite, microlite, amblygonite-montebrazite, topaz. Here blocks of petalite are located, sometimes they are substituted by quartz-spodumene aggregate. Quartz core is situated in central part of vein. It contains in outer part large blocks of amblygonite-montebrazite, white and pinkish beryl, white, rose and blue tourmaline, small grains of cassiterite and tantalite. Described vein has apophyse, composed by lepidolite glimmerites and tourmalinites.

The Vishnyakovskoye field includes pegmatites of complex (Ta-Cs-Li) geochemical sequence. Gently dipping pegmatite veins form series in orthoamphibolites. Largest single bodies have extension up to 2 km and width near 12 m and are characterized by asymmetrical zoning. Small muscovite-quartz or albite-muscovite-quartz rim with cassiterite is observed in upper endocontact. It is followed by lower intermediate block zone, composed of potash feldspar blocks and cryptocrystalline quartz-albite ("porcelain") aggregate portions with rare unaltered petalite blocks and isolated quartz blocks. Parallel-columnar quartz-spodumene aggregates and coarse-crystalline eucryptite excretions are sometimes observed in this zone. This block zone is divided into two parts; the central zone of middle – and coarse-plate albite and clevelandite with muscovite-quartz nests and aggregates of tantalite-(Mn), wodginite and microlite is found between these two parts. The quartz core and large potash feldspar blocks sometimes occur in the central zone. Accumulations

of wodginite, tantalite-(Mn) and microlite are situated between large potash feldspar blocks. Sections of fine-scaly rosy and greenish muscovite with high Rb content and with abundant Ta mineralization are observed under quartz cores. Zone of fine-grained albite is occurred in lying wall of pegmatite veins. This schematic generalization of zoning is complicated by significant inhomogeneity of pegmatite body structure on strike and dip.

Petalite pegmatites of studied belt were formed in conditions lowered original pressure in comparison with their spodumene ones, it was about 2.5 kbar. Early magmatic, late magmatic, autometasomatic and hydrothermal stages are distinguished in pegmatite formation process.

MINERALOGY AND GEOCHEMISTRY

Composition peculiarities of minerals concentrating Li (aluminosilicates and phosphates of Li and micas), Rb and Cs (potash feldspars and micas), Be (beryl), Ta and Nb (Nb-Ta oxide minerals) point out very high degree of melt differentiation from which petalite pegmatites of the Vishnyakovskoye and Alexandrovskoye fields were formed. Increase of differentiation degree is obvious from low parts of gently dipping vein series to their upper horizons.

Pegmatites of the Alexandrovskoye field contain blocks of petalite, which is partly substituted by spodumene. All three Li aluminosilicates occur in the Vishnyakovskoye field pegmatites, where petalite is substituted by spodumene and quartz, afterwards eucryptite is formed, sometimes it is followed by calcite. Thus, petalite with 4.3-4.7% Li_2O is crystallized on early magmatic stage, spodumene with 7.3-7.7% Li_2O and eucryptite, which contains 10.66% Li_2O , are generating on late stage of crystallization from the residual melt. Also Li phosphates (lithiophilite and montebasite) are crystallized on this stage.

Primary potash feldspars have different structural state in petalite pegmatites. In Alexandrovskoye field there are only microclines with ordered Al-Si arrangement, pegmatites of Vishnyakovskoye field have both orthoclases and microclines. Orthoclases contain highest Li, Rb, Cs, Tl and Sr amount. High Sr concentration is caused by large quantity of its radiogenic isotope. Two stages of autometasomatic and hydrothermal alteration of orthoclases are distinguished. At the first stage potash feldspars are ordered up to high and intermediate microclines with Cs, Tl, Pb removal and Ba supply. Afterwards ordering to low microcline and intensive Na, Li, Rb, Cs, Tl, Pb extraction, as well K, Ba content increase occur. During second stage feldspar is albitized, Na amount increases and other studied elements are removed.

Micas of petalite pegmatites are related to series of muscovite-lepidolite. They are characterized by increase of Li content from early magmatic stage,

when muscovite was crystallizing, to late magmatic stage, when Li-bearing muscovite and lepidolite were formed. Sharp lowering of Li amount is marked in muscovites of autometasomatic stage. Rb and Cs contents are increased at both late magmatic and autometasomatic stages. Main concentrating Be mineral is beryl, phenakite is very rare. Li and Cs contents in beryl increase from early to late magmatic stage, then they become lower at autometasomatic stage. Tourmaline is widespread in pegmatites of Alexandrovskoye field, where it forms series of schorl-dravite in microcline pegmatite veins and schorl-elbaite and elbaite-olenite series in lepidolite-albite pegmatite bodies. The latest tourmaline in these pegmatites is dravite, which forms aggregates with muscovite and quartz in thin cracks cutting across crystals of tourmaline of elbaite-olenite series.

Petalite pegmatites of studied fields are distinguished from spodumene ones by different Nb-Ta mineralization, in which varieties enriched by Ta are predominant. So, the trend of fractionation of columbite group minerals is rather short, it includes columbite-(Mn) of early magmatic stage and tantalite-(Mn) of late magmatic and autometasomatic stages, which contains up to 87.2% Ta_2O_5 . Wodginite and microlite widespread in pegmatites of Vishnyakovskoye field are crystallized on two last stages. The latest Ta oxide in studied pegmatites is rynersonite, crystallized on autometasomatic and hydrothermal stages. Composition of wodginite changes in pegmatite formation process from early Ti containing variety to the mineral with maximum Sn amount and afterwards to wodginite, which contains up to 84% Ta_2O_5 . Abundant wodginite with such high Ta_2O_5 content and significant predominance of tantalite-(Mn) in oxides of columbite group led to formation of ores rich in Ta, Ta content in which reaches 0.877% with ratio of Ta/Nb more than 30.

Intense differentiation of zones on composition is typical for petalite pegmatite vein series and is characterized most obviously by ratio $\text{Na}_2\text{O}/\text{K}_2\text{O}$. It changes by several tens of times –from 0,14 in block potash feldspar zone up to near 10 in micrograined (“porcelain”) quartz-albite pegmatites of the Vishnyakovskoye field. Contents of SiO_2 and F show wide variations as well. Obvious Rb and Cs accumulation is observed from outer zones to inner potash feldspar zone. Li is mainly concentrated in block petalite and substituting spodumene, and eucryptite and lepidolite sections. Isolated melt, from which glimmerites and tourmalinites of main vein apophyse were formed in the Alexandrovskoye field, was rich in H_2O , F, B and P. Ta, Nb and Sn distribution is very irregular in pegmatites of both studied fields. Ta and Nb enrichment goes on from outer zones to central parts, like in micaceous aggregates of autometasomatic alteration, where ratio Ta/Nb increases in comparison with zones, crystallized from the melt. Petalite pegmatites of studied fields contain

very low concentrations of REE, total amount of which composes 1-2 ppm only.

GENESIS OF PETALITE PEGMATITES

It is necessary to point out the following circumstances, turning into genetic features of studied petalite pegmatites: (1) significant time gap between emplacement granites of Sayansk complex and rapakivi-granites of Elash complex on one hand and petalite pegmatites on the other hand; (2) absence of pegmatite field zoning relative to granite massifs; (3) control of pegmatite field location by deep-seated fault zones; (4) obvious increase of pegmatite body differentiation extent from deep horizons to apical part; (5) very irregular distribution of petrogenic and rare elements under high primary alkalinity of melts enriched by volatiles (especially H₂O and F) and P, as well as rare metals (Li, Rb, Cs, Ta, Nb, Be, Sn); (6) extreme pegmatite enrichment by granitophile rare elements.

Obtained data are not in accordance with hypothesis of pegmatite formation as a result of fractionation of granite magma, from which granite massifs of Sayansk and later Elash complexes were formed, they point out the absence of fertile granites for studied pegmatites. Available data can be explained most correctly assuming, that these pegmatites were formed from melt originated in long-lasting process of granite magma transformation in deep-seated chambers under the influence of mantle or low crust fluids enriched in granitophile elements. Such transformation of granite magmas into pegmatite melts occurred in accordance with metamagmatic model of pegmatite formation (Zagorsky 2007) in the Low Proterozoic in conditions of significant earth crust reorganization and was caused by a powerful impulse of energy and matter from the mantle as fluid flows penetrating along deep-seated fault zones. Pegmatite melts, enriched by rare metals and volatiles, intruded along these zones into location places. Their differentiation happened on the intrusion ways, what

is a reason of high geochemical heterogeneity of pegmatitic melts. Fractionation of these rich in fluids melts in crystallization chambers and autometasomatic alterations of pegmatites caused the highest rare metal concentration in some individual zones of veins.

ACKNOWLEDGEMENTS

This work was supported by RFBR (projects 10-05-00964, 11-05-01061) and by SB RAS (project IIP 29).

REFERENCES

- Bryntsev, V.V. (1994). Precambrian granitoids of North-Western Cissayan. Novosibirsk. Nauka. 184 p. (In Russian).
- Komin, M.F., Usova, T.Yu. & Zuyeva, T.I. (2004). Mineral raw material base of rare metals in Russia: conditions and development ways. *Razvedka i ochrana nedr.* **11**: 32-37. (In Russian).
- Levitsky, V.I., Melnikov, A.I., Reznicky, L.Z., Bibikova, T.I., Kirnozova, T.I., Kozakov I.K., Makarov, V.A. & Plotkina, Yu.V. (2002). Early Proterozoic postcollisional granitoids in southwestern Siberian craton. *Geologiya i geofizika.* **43**: 717-731. (In Russian).
- Makagon, V.M., Lepin, V.S. & Brandt, S.B. (2000). Rubidium-strontium date of rare-metal pegmatites of the Vishnyakovskoye deposit. *Geologiya i geofizika.* **41**: 1783-1789. (In Russian).
- Zagorsky, V.Ye. (2007). Deep fluid flow – melt interaction and problems of granite-pegmatite system petrogenesis. *Memorias Universidade do Porto.* **8**: 58-59.
- Zagorsky, V.Ye., Makagon, V.M. & Shmakin, B.M. (1999). The systematics of granitic pegmatites. *Can. Mineral.* **37**: 800-802.

THE REGIONAL DISTRIBUTION OF TRACE ELEMENTS IN QUARTZ OF SOUTH NORWEGIAN PEGMATITES AND ITS TECTONOMAGMATIC IMPLICATIONS

Axel Müller

Geological Survey of Norway, 7491 Trondheim, Norway, Axel.Muller@ngu.no

Key words: pegmatite, quartz, LA-ICP-MS, Evje, Iveland, Froland

In this study the Al, Ti, Li and Ge concentrations in pegmatitic quartz are analysed by laser ablation inductively coupled plasma mass spectrometry (LA-ICP-MS) on samples from the intermediate zone of about 200 NY(F)-type pegmatites from the Froland and Evje-Iveland pegmatite fields. The pegmatite fields are part of the Bamble and Evje-Iveland pegmatite districts in South Norway. These were formed during the Sveconorwegian orogeny (1.14-0.90 Ga) at the western margin of the Fennoscandian shield, when the Bamble Complex was thrust over the Telemark Block along the Porsgrunn-Kristiansand Fault Zone (PKFZ) at 1.09-1.08 Ga (Bingen *et al.* 2008). Both fields differ, however, in age and tectonometamorphic setting. The Froland pegmatites are situated above the PKFZ thrust zone in the Bamble Complex and intruded at 1.09-1.06 Ga. The field is 20 km long and 5 km wide and strikes NE-SW parallel to the PKFZ. The Evje-Iveland pegmatites were emplaced ~0.91 Ga and are located in the interior of the Telemark Block, in the foot wall of the thrust zone. The N-S-striking Evje-Iveland field is 30 km long and up to 10 km wide. The pegmatites of both fields are temporarily unrelated to adjacent granitic plutons, namely the Herefoss pluton SW of the Froland field and the Høvringsvatnet pluton NE of the Evje-Iveland field.

The regional distribution of the Ti, Al, Li and Ge contents of pegmatitic quartz are used to evaluate the differentiation pattern and crystallisation temperatures within both pegmatites fields. Quartz of the Froland pegmatites has relative homogeneous composition with 11.8 ± 6.7 ppm Li, 1.5 ± 0.8 ppm Ge, 44.7 ± 22.7 ppm Al, and 7.7 ± 3.3 ppm Ti. The relative low Ti corresponds to crystallisation temperatures of $511 \pm 46^\circ\text{C}$ according to Ti-in-quartz geothermometer by Wark & Watson (2006). The thermometer can be applied even in the absence of rutile if the TiO_2 activity of the system is known. In the case of the Froland and Evje-Iveland pegmatites the TiO_2 activities were determined by applying the TiO_2 saturation model for granitic melts by Hayden *et al.* (2005). The whole rock composition of medium- to coarse-grained border zones of some pegmatites were analysed to calculate the TiO_2 activities considering that

composition of the border zone is representative for the pegmatite bulk composition. The TiO_2 activities vary between 0.7 and 1. The calculated crystallisation temperatures are higher along the NW margin of the Froland pegmatite field, close to the PKFZ. The most differentiated pegmatites occur along the northern SE margin of the field, away from the PKFZ. The regional pattern of the quartz chemistry implies that the formation and emplacement of pegmatite melts occurred in conjunction with the Sveconorwegian overthrusting, which is consistent with the geological model presented by Henderson & Ihlen (2004) for their emplacement.

Quartz of the Evje-Iveland pegmatites has more variable composition with 7.3 ± 4.5 ppm Li, 3.0 ± 2.9 ppm Ge, 81.7 ± 58 ppm Al, and 21.4 ± 11.4 ppm Ti. The high average Ti indicates crystallisation temperatures of $591 \pm 70^\circ\text{C}$. Highest crystallisation temperatures were detected along the margin of the pegmatite field. The two areas of relative low crystallisation temperatures and highly differentiated quartz composition are developed in the central and south-central part of the field. The areas are characterised by gadolinite- and columbite-rich NY(F) pegmatites. In these pegmatites gadolinite and columbite crystals are up to 40 cm in size. The irregular regional distribution of temperatures and differentiation indexes in the Evje-Iveland field excludes the possibility of an underlying parent granite intrusion. Such an intrusion is expected to have caused a more regular zoning of the quartz chemistry. The lack of coeval granite intrusions in both pegmatite fields suggest that the source of the pegmatite melts is to be found at deeper crustal levels and remains enigmatic at the current stage of knowledge.

REFERENCES

- Bingen, B., Nordgulen, Ø. & Viola, G. (2008). A four phase model for the Sveconorwegian orogeny, SW Scandinavia. *Norwegian J. Geol.* **88**: 43-72.
- Breiter, K. & Müller, A. (2009). Evolution of rare-metal granitic magmas documented by quartz chemistry. *Eur. J. Miner.* **21**: 335-346.

- Hayden, L.A., Watson, E.B. & Wark, D.A. (2005). Rutile saturation and TiO₂ diffusion in hydrous siliceous melts. EOS (Transactions, American Geophysical Union), **86**, Fall meeting supplement, abs. MR13A-0076.
- Henderson, I. & Ihlen, P.M. (2004). Emplacement of polygeneration pegmatites in relation to Sveco-Norwegian contractional tectonics: examples from southern Norway. *Precamb. Res.* **133**: 207-222.
- Müller, A., Behr, H.-J., van den Kerkhof, A.M., Kronz, A. & Koch-Müller, M. (2009). The evolution of late-Hercynian granites and rhyolites documented by quartz – a review. *Earth Environ. Sc. Trans. Royal Soc. Edinburgh* **100**: 185-204.
- Wark, D.A. & Watson, E.B. (2006). TitaniQ: a titanium-in-quartz geothermometer. *Contrib. Mineral. Petrol.* **152**: 743-754.

GEOCHEMISTRY OF GRANITIC APLITE-PEGMATITE VEINS AND SILLS AND THEIR MINERALS FROM CABEÇO DOS POUPOS, SABUGAL, CENTRAL PORTUGAL

Ana M.R. Neiva^{1§}, Paulo B. Silva² & João M.F. Ramos²

¹ Department of Earth Sciences and Geosciences Center, University of Coimbra, 3000-272 Coimbra, Portugal, neiva@dct.uc.pt

² LNEG, 4466-956 S. Mamede de Infesta, Portugal

Key words: granites, aplite-pegmatites, zoned micas and columbite-tantalite

INTRODUCTION

Pegmatites are derived from granitic melts and experimental work supports this mechanism (London 2008), which has been successfully tested (e.g. Shearer *et al.* 1992; Neiva *et al.* 2008) although pegmatites contain fluxes such as B, F, P and Li in addition to H₂O. The mineralogy, geochemistry and petrology of granites from the Sabugal area and aplite-pegmatite veins and sills from Cabeço dos Poupos within this area are presented, using the data to identify the mechanisms responsible for the origin of these rare-element pegmatites. The zoning of micas and columbite-tantalite crystals from these aplite-pegmatite veins and sills are described.

GEOLOGY

In the Sabugal area, seven Variscan two-mica granites intruded the Cambrian schist-metagraywacke complex (Fig. 1). The emplacement of the granites was controlled by the last ductile deformation phase D3 of Namurian-Westphalian age. The ID-TIMS U-Pb zircon and monazite ages show that granite G1 is 309.2±1.8 Ma and syn- to late-D3, while most of the other granites are 300±3 Ma and late-D3, and G7 is 299±3 Ma and late- to post-D3. Many granitic aplite-pegmatite veins and sills trending mainly E-W and WNW-ESE, cut granites G2, G6 and G7. An area was selected to study these veins and sills cutting the granite G6 (Fig. 1), which produced a metasomatic

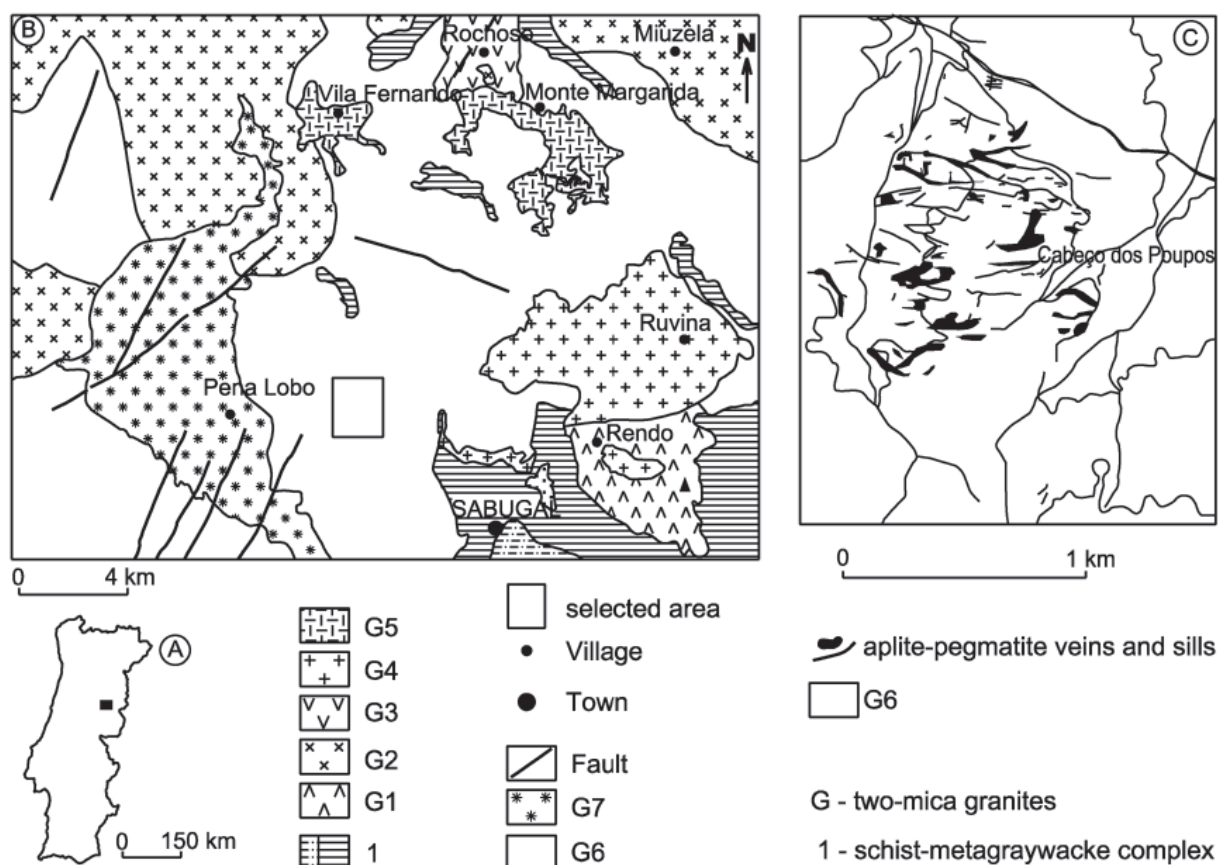


FIGURE 1. (a) Location of the Sabugal area on the map of Portugal. (b) Simplified geological map of the Sabugal area, mainly to show the granites and location of the Cabeço dos Poupos area. (c) Geological map of the Cabeço dos Poupos area.

zone enriched in zinnwaldite and up to 15 cm thick in the host granite. Pegmatites are of beryl-columbite-phosphate subtype. Most aplite-pegmatite veins and sills have an aplite layer at the footwall followed upward by a pegmatite layer and an aplite-pegmatite layer at the hanging wall. Some veins and sills contain up to 5-6 layers. The veins are 10 cm - 15 m thick and up to 700 m long, whereas the sills are up to 2.5 m thick and 200 m long.

PETROGRAPHY

All granites have phenocrysts of K-feldspar and some also contain phenocrysts of plagioclase. The granites contain quartz, micropertthitic orthoclase and microcline, plagioclase, biotite, muscovite, zircon, apatite, monazite and ilmenite. Most of them also contain tourmaline. Sillimanite occurs in G1 and andalusite in G2.

The aplite-pegmatite veins and sills contain quartz, micropertthitic orthoclase and microcline, albite, muscovite, lithian muscovite, tourmaline, beryl, zircon, columbite-tantalite, cassiterite, apatite and triplite. Rare zinnwaldite and very rare lepidolite also occur close to the contact with the host granite G6, whereas rare polyolithionite occurs in an aplitic intermediate layer.

WHOLE-ROCK GEOCHEMISTRY

All granitic rocks are peraluminous with A/CNK ranging between 1.11 and 1.50. Granites G2, G3 and G7 define a series, whereas granites G5 and G6 define another series (Fig. 2). Some granitic aplite-pegmatite veins and sills have similar CaO, MgO, Sn, Rb, Sr and Li contents to those of granite G7 and others also have similar MgO, Rb and Li contents to those of G3 (Figs. 2a, b, c). There are gaps between the veins and sills and granites G1 and G4 (Fig. 2a, b, c) and G1 is one of the richest granites in total FeO, Sr and Ba contents. Variation diagrams for granites G5 and G6 and aplite-pegmatite veins and sills define fractionation trends (Figs. 2d, e, f) and veins and sills have lower total FeO, MgO, CaO, Sr, Zr, Y and Ba contents and higher SiO₂, F, Sn, Rb and Li contents than these two granites. The chondrite normalized REE pattern of a pegmatite is subparallel to those of granites G5 and G6. All the REE contents of the pegmatite are lower than those of the granites. Whole-rock $\delta^{18}\text{O}$ values plotted versus total FeO values show a gap between aplite-pegmatite veins and sills and granites G1 and G4. Most veins and sills have lower $\delta^{18}\text{O}$ values than the granite G7, but similar or higher than those of the granite G6 and up to 0.46‰. These rare-element pegmatites belong to the REL-Li subclass, beryl type and beryl-columbite-phosphate subtype (Černý & Ercit 2005).

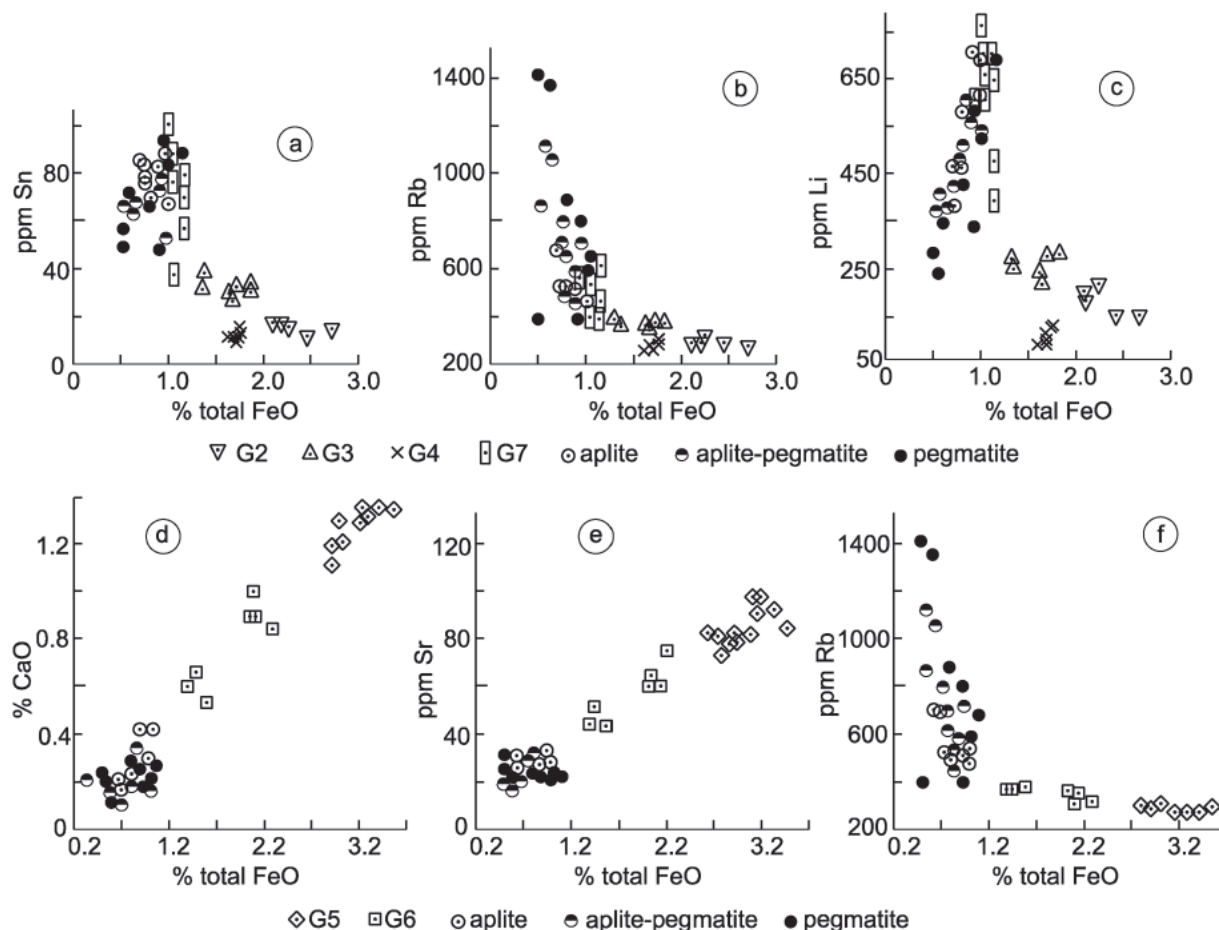


FIGURE 2. Selected variation diagrams of granites from the Sabugal area and granitic aplite-pegmatite veins and sills from Cabeço dos Poupos, suggesting that these veins and sills are related to the series G5-G6.

GEOCHEMISTRY OF MINERALS

Ba content of K-feldspar from aplite-pegmatite veins and sills is similar to lower than that of K-feldspar from all granites of the area. Albite (An_0 - An_5) from these veins and sills has lower Ca content than phenocryst and matrix plagioclase from all granites, except G7. In general, K-feldspar has higher P_2O_5 content than coexisting plagioclase. P_2O_5 contents of feldspars may depend on phosphorus content in the crystallizing melt. P_2O_5 contents of K-feldspar and albite from aplite-pegmatite veins and sills reach higher values than in feldspars from all granites. D[P]Kf/Pl ranges between 1.0 and 2.4, showing no significant fractionation of phosphorus between coexisting feldspars. The distribution of P between Kf-Pl pairs is only in equilibrium in granites G5 and G6.

In aplite and pegmatite, subhedral lithian muscovite surrounds relics and penetrates along cleavages of primary muscovite and contacts are sharp, showing an apparent oscillatory zoning. The former has higher Fe^{2+} , Li, F, Rb contents and lower Al^{VI} , $Al^{IV}+Al^{VI}$ and OH contents than the latter. Subhedral and radial lithian muscovite from aplites are apparently oscillatory zoned, showing sharp contacts between lighter and darker zones. The lighter zones are richer in Fe^{2+} , Li, F and poorer in Al^{VI} , $Al^{IV}+Al^{VI}$ and OH than the darker zones. Primary muscovite and lithian muscovite from aplite-pegmatites have higher Fe^{2+} , Li, Rb, F contents and lower Mg content than primary muscovite from granites G5 and G6 and define a trend in the Li-Mg diagram. In aplite-pegmatite, very rare lepidolite partially surrounds lithian muscovite and has higher Si, Fe^{2+} , Mn, Li, K, Rb, F contents and lower Al^{IV} , Al^{VI} , Na contents than lithian muscovite. Zinnwaldite from aplite-pegmatite penetrates along cleavages and partially surrounds lithian muscovite. Locally zinnwaldite and lithian muscovite from aplite-pegmatite are intergrown and show different orientations. All the contacts are sharp. Zinnwaldite has higher Fe^{2+} , Mn, Li, F contents and lower Al^{VI} , $Al^{IV}+Al^{VI}$ and OH contents than associated lithian muscovite. Rare polyolithionite partially surrounds lithian muscovite from aplite and the contact is sharp. The border has higher Si, Li, Rb and F contents and lower Al^{VI} , $Al^{IV}+Al^{VI}$, OH contents than the core.

Columbite-tantalite occurs associated with albite, K-feldspar, quartz, muscovite and beryl. Columbite-(Fe) is more abundant than columbite-(Mn). Tantalite-(Fe) is rare. Individual crystals of columbite-(Fe) or consisting of columbite-(Fe) and columbite-(Mn) are oscillatory zoned, involving several elements, and

locally present a partial thin rim of tantalite-(Fe). The contacts are sharp. Cassiterite crystals are rare, unzoned, consist of nearly pure SnO_2 and contain similar small Fe, Nb and Ta contents. Fluorapatite is the most abundant phosphate. The triplite shows a significant range in $F/(F+OH)$.

MAGMA RELATIONS

Variation diagrams of major and trace elements (Fig. 2) suggest that the aplite-pegmatite veins and sills from Cabeço dos Poupos are related to the series defined by granites G5 and G6, which is supported by the facts that the REE pattern of a pegmatite is subparallel to those of these two granites, $\delta^{18}O$ values of veins and sills are close to those of G6 and primary muscovites from the two granites and aplite-pegmatites and lithian muscovite from the latter define a trend in the Li-Mg diagram. Least squares analysis of major elements shows that the aplite-pegmatite veins and sills are derived from the granite G5 magma by fractional crystallization of quartz, K-feldspar, plagioclase, biotite and ilmenite. The calculated Sr and Ba contents decrease and Rb content increases versus the decrease in the weight fraction of melt remaining during fractional crystallization. However, the calculated Sr and Ba contents are up to 2 and 6 times higher, respectively, than the determined contents, while the calculated Rb content ranges from 0.7 to 1.0 times lower to similar to the determined content, indicating that LIL elements are controlled by magmatic fluxes and fluids. Cassiterite and columbite-tantalite minerals are also probably controlled by these fluxes and fluids.

REFERENCES

- London, D. (2008). Pegmatites. *Can. Mineral. Sp. Publ.* **10**: 347 pp.
- Neiva, A.M.R., Gomes, M.E.P., Ramos, J.M.F. & Silva, P.B. (2008). Geochemistry of granitic aplite-pegmatite sills and their minerals from Arcozelo da Serra area (Gouveia, central Portugal). *Eur. J. Mineral.* **20**: 465-485.
- Černý, P. & Ercit, T.S. (2005). The classification of granitic pegmatites revisited. *Can. Mineral.* **43**: 2005-2006.
- Shearer, C.K., Papike, J.J. & Jolliff, B.L. (1992). Petrogenetic links among granites and pegmatites in the Harney Peak rare-element granite-pegmatite system, Black Hills, South Dakota. *Can. Mineral.* **30**: 785-810.

REGIONAL ZONATION OF PEGMATITES AND SYNCHRONOUS MINERALIZATION IN THE CENTRAL ZONE OF THE DAMARA OROGEN, NAMIBIA

Paul Nex^{1,2}, Judith Kinnaird² & Luisa Broccardo²

¹ Umbono Financial Services, Johannesburg, South Africa. pnex@umbono.co.za

² School of Geosciences, University of the Witwatersrand, Johannesburg, South Africa

Key words: Pegmatites, Regional Zonation, Mineralization, Uranium, Gold, Tin,

INTRODUCTION

The Central Zone of the Damara Orogen is the northeast trending (inland) branch of the Pan-African orogenic assembly of Gondwana within Namibia. It formed as a result of continental collision between the Congo and Kalahari cratons. The inland branch of the Damara Orogen has been divided into a number of zones based on metamorphism, the nature of the intrusive rocks and structural style generally delimited by major structural and geophysical lineaments (Miller 1983), (Fig. 1). The Central Zone of the Damara Orogen is characterized by high-temperature, low-pressure metamorphism, abundant voluminous granitoid intrusions and a dome and basin structural style with a dominant structural trend parallel to the orogen. Within this zone there are well-known mineral deposits including, the Rubicon and Helicon zoned lithium pegmatites, tourmaline producing pegmatites in the Usakos area,

uranium-bearing pegmatitic sheeted leucogranites at Rossing, tin pegmatites at Uis, and shear-hosted gold mineralization at Navachab. These deposits exhibit similar structural controls on their genesis and all are broadly synchronous considering the age-data currently available.

MINERALIZATION ZONED LCT PEGMATITES

The Rubicon and Helicon pegmatites are zoned LCT pegmatites which were exploited for lithium from 1951-1994. Rubicon is the largest zoned pegmatite in the Usakos-Karibib area and together with Helicon was studied in detail by Roering (1963) Further mineralogical work on micas (Roda *et al.* 2007) microlite and tapiolite (Baldwin *et al.* 2005) and phosphate minerals (Baldwin *et al.* 2000) has been undertaken. The Rubicon pegmatite has been dated by U-Pb on columbite-tantalite at ~500 Ma (Oberthur pers comm.)

DAMARAN TOURMALINE PEGMATITES

According to Schneider and Seeger (1993) tourmaline is the most valuable of semi-precious stones found in Namibia. The tourmaline-producing pegmatites of Damaran age include the Usakos pegmatite, Becker's Pegmatite and Neu Schwaben, found in the Usakos-karibib area These have not been directly dated however they cross-cut D3 structures and are likely to have been emplaced at ~ 500 Ma. Tourmaline compositions of various pegmatites, possibly including those of Mesozoic age, have been investigated from the Erongo-Karibib-Usakos area by Keller *et al.* (1999).

URANIUM PSLG'S

The uranium-bearing sheeted leucogranites comprise 5 major discrete deposits which have been exploited (Rossing) or are currently being explored and evaluated (Goanikontes, Valencia, Ida Dome and Rossing South). They all exhibit the same lithostratigraphic and structural controls (Kinnaird & Nex 2007) and have been dated at between 509 and 506 Ma (Briqueu *et al.* 1980; Longridge *et al.* 2009).

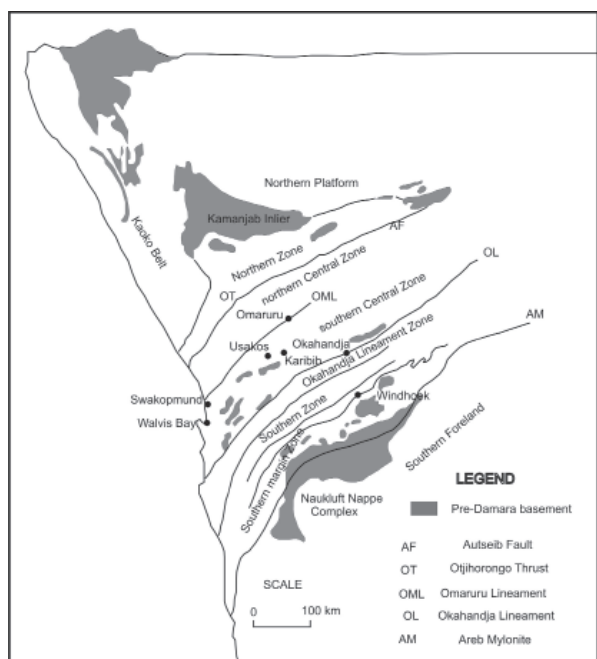


FIGURE1. Map of tectono-stratigraphic zones of the Damara Orogen (Miller 1983).

SN PEGMATITES

The tin pegmatites of Damaran age are confined to the northern Central Zone and occur in three sub-parallel NNE-trending belts, named from east to west Uis, Karlowa and Strathmore. Within each belt the pegmatites are emplaced en-echelon with an east-west strike and dipping to the north (Diehl 1993a,b). The Uis belt generally exhibits simple unzoned tin pegmatites while within the Strathmore swarm, and to a minor extent in the Karlowa swarm, zoned lithium-rich tin-niobium-tantalum pegmatites occur and exhibit the same structural control and country-rock relationships as the tin pegmatites (Diehl 1993a).

NAVACHAB GOLD MINERALIZATION

Gold mineralization is hosted at Navachab by sets of quartz veins developed in a NNE-trending ductile-brittle shear zone on the NW margin of a D3 dome structure (Kisters 2005). The quartz veins crosscut all lithologies and fold-related structures while the origin of the deposit is controversial, either as a skarn- or orogenic-gold deposit (Dziggel *et al.* 2009). These authors also noted that pegmatites both cross-cut and are cut by gold-bearing quartz veins indicating that pegmatite intrusion and gold mineralization were contemporaneous. There is no consensus on the age of the mineralization and estimates range from 550-494 Ma (Dziggel *et al.* 2009) although recent work by Longridge *et al.* (2009) has dated late-tectonic intrusions at 536-520 Ma which are probably the earliest possible dates for the mineralization.

REGIONAL ZONATION

The regional zonation exhibited by these deposits is immediately apparent from an inspection of a regional deposit and occurrences map (Fig. 2). Uranium mineralization is confined to the southwest of the orogen, gold mineralization occurs in the northeast, and tin mineralization occurs in three sub-parallel NNE trending structures in the northern part of the Central Zone. Curiously, LCT pegmatites are not as well-constrained as the other pegmatitic rocks and occur in two areas. In the northeast of the Central Zone, Rubicon and Helicon pegmatites occur southeast of Usakos together with various tourmaline pegmatites. In addition, there is a further cluster of LCT pegmatites in the Strathmore and Petalite pegmatite swarms in the northern Central Zone west and along strike from the tin pegmatites.

It would appear to be unlikely that the regional zonation exhibited by these pegmatites and other mineral deposits is related to a single extensive granite extending over an area of some 150 by 175 km. It is much more likely that the zonation is a result of contemporaneous processes, controlled by the prevailing stress-field, with variations in partial

melting, assimilation and transport parameters superimposed on the earlier crustal metamorphic architecture. The host rock metamorphic grade is a function of M1 metamorphism which took place at between 540 and 520 Ma (Nex *et al.* 2001, Jung & Mezger 2003 Longridge *et al.* 2009) and has no bearing on the petrological characteristics of the pegmatites apart from constraining post peak metamorphism partial melting of the crust. The simultaneous emplacement of these pegmatites, associated with the transition from ductile to brittle deformation, has implications for pegmatite classification schemes. There has been a suggestion that the uraniferous pegmatitic leucogranites are associated with post-collisional A-type magmatism, which although not geochemically based in the sense of Whalen *et al.* (1987) or Eby (1992) is suggested by the association of Nb-rich pyrochlore (betafite), and accessory fluorite and spatially minor amazonite. They could be considered incipient NYF pegmatites. This to some extent reinforces the proposal by Martin and de Vito (2005) that the depth zone classification is invalid however it additionally suggests that the LCT-compressional and NYF-extensional association is not applicable in the case of the Damara Orogen.

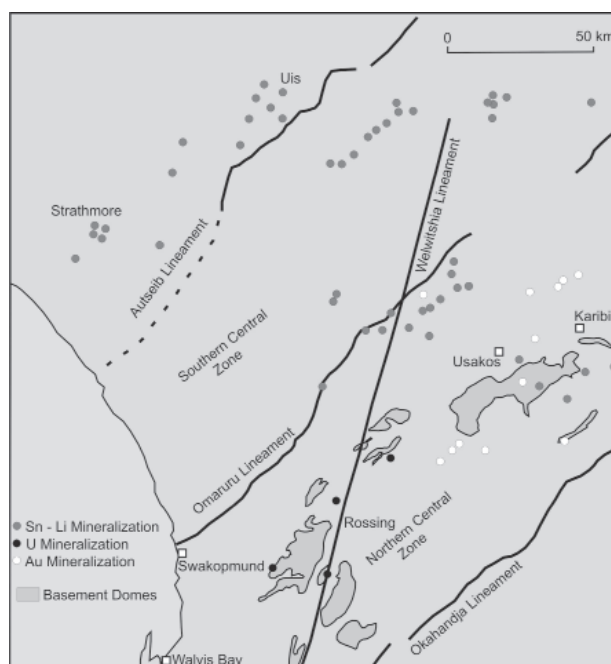


FIGURE 2. Map showing the location of uranium, gold and tin-lithium pegmatite occurrences in the Central Zone of the Damara Orogen.

REFERENCES

- Baldwin, J.R., Hill, P.G., von Knorring, O. & Oliver, G.J.H. (2000) Exotic aluminium phosphates, natromontbrasite, brazilianite, goyazite, gorceixite and crandallite from rare-element pegmatites in Namibia. *Min. Mag.* **64**: 1147-1164.

- Baldwin, J.R., Hill, P.G., Finch, A.A., von Knorring, O. & Oliver, G.J.H. (2005). Microlite-manganotantalite exsolution lamellae: evidence from rare-metal pegmatite, Karibib, Namibia. *Min. Mag.* **69**: 917-935.
- Briqueu, L., Lancelot, J.R., Valois, J-P. & Walgenwitz, F. (1980). Géochronologie U-Pb et genèse d'un type de mineralization uranifère: les alaskites de Goanikontès (Namibie) et leur encaissant. *Bull. Centre Rech. Explor. Prod. Elf. Aquitaine* **4**: 759-811.
- Diehl, B.J.M. (1993a). Tin. In: *Mineral Resources of Namibia*
- Diehl, B.J.M. (1993b). Rare metal pegmatites of the Cape Cross-Uis pegmatite belt, Namibia: geology, mineralization, rubidium-strontium characteristics and petrogenesis. *Jnl. Afr. Earth Sci.* **17**: 167-181.
- Dziggel, A., Wulff, K., Kolb, J. & Meyer, F.M. (2009). Processes of high-T fluid-rock interaction during gold mineralization in carbonate-bearing metasediments: the Navachab gold deposit, Namibia. *Min. Dep.* **44**: 665-687.
- Eby, G.N. (1992). Chemical subdivision of the A-type granitoids: Petrogenetic and tectonic implications. *Geology* **20**: 641-644.
- Jung, S. & Mezger, K. (2003). Petrology of basement-dominated terranes: I. Regional metamorphic T-t path from U-Pb monazite and Sm-Nd garnet geochronology (Central Damara orogen, Namibia). *Chem. Geol.* **198**: 223-247.
- Keller, P., Robles, E.R., Perez, A.P. & Fontan, F. (1999). Chemistry, paragenesis and significance of tourmaline of the Southern Tin Belt, central Namibia. *Chem. Geol.* **158**: 203-225.
- Kinnaird, J.A. & Nex, P.A.M (2007). A review of geological controls on uranium mineralization in sheeted leucogranites with the Damara Orogen, Namibia. *App. Earth Sci. (Trans. IMM, B)* **116**: 68-85.
- Kisters, A.F.M. (2005). Controls of gold-quartz vein formation during regional folding in amphibolite-facies, marble-dominated metasediments of the Navachab Gold Mine in the pan-African Damara Belt, Namibia. *South African Jnl Geol.* **108**: 365-380.
- Longridge, L., Gibson, R.L., Kinnaird, J.A. & Armstrong, R.A. (2009). Crustal thickening and high-grade metamorphism in the Central Zone of the Damara Orogen, Namibia: New results from SHRIMP dating. *Out of Africa Conference, University of the Witwatersrand, Johannesburg, South Africa.*
- Martin, R.F. & De Vito, C. (2005). The patterns of enrichment in felsic pegmatites ultimately depend on tectonic setting. *Can. Min.* **43**: 2027-2048.
- Miller, R. McG. (1983). The Pan-African Damara Orogen of South West Africa / Namibia. In: Miller, R. McG. (Ed.) 1983 *Evolution of the Damara Orogen of South West Africa / Namibia*. *Geol. Soc. South Afr. Spec. Pub.* **11**: 431-515.
- Nex, P.A.M., Oliver, G.J.H. & Kinnaird, J.A. (2001). Spinel-bearing assemblages and P-T-t evolution of the Central Zone of the Damaraa Orogen, Namibia. *Jnl. Afr. Earth Sci.* **32**: 471-489.
- Roda, E., Keller, P., Pesquera, A. & Fontan, F. (2007). Micas of the muscovite-lepidolite series from Karibib pegmatites, Namibia. *Min. Mag.* **71**: 41-62.
- Roering, C. (1963). Pegmatite investigations in the Karibib District, South West Africa. Ph.D thesis (unpublished), University of the Witwatersrand, pp130.
- Schneider, G.I.C. & Seeger, K.G. (1993). Semi-precious stones. In: *Mineral Resources of Namibia*.
- Whalen, J.B., Currie, K.L. & Chappell, B.W. (1987). A-type granites: geochemical characteristics, discrimination and petrogenesis. *Cont. Min. & Pet.* **95**: 407-419.

COMPOSITIONAL VARIATIONS IN PRIMARY AND SECONDARY TOURMALINE FROM THE QUINTOS PEGMATITE, BORBOREMA PEGMATITE PROVINCE, BRAZIL; REDISTRIBUTION OF Cu, Mn, Fe AND Zn IN SECONDARY TOURMALINE

Milan Novák¹, Petr Gadas¹, Radek Škoda¹,
Hartmut Beurlen², Odúlio J.M. Moura³

¹ Department of Geological Sciences, Masaryk University, Kotlářská 2, 611 37 Brno, Czech Republic; mnovak@sci.muni.cz

² Universidade Federal de Pernambuco, Rua Acad. Hélio Ramos, 54740-530, Recife, State of Pernambuco, Brazil

³ H&R Exportação e Importação de Minérios, Governador Valadares, Minas Gerais, Brazil

Key words: tourmaline, copper, zinc, manganese, secondary crystallization, Borborema, Brazil

INTRODUCTION

“Paraíba tourmalines” typically contain elevated concentrations of Cu, Zn and Mn and chiefly “electric” blue varieties of elbaite were studied in numerous gemmological and mineralogical papers (e.g., Peretti *et al.* 2010 and references therein). Also compositional trends within the individual pegmatite dikes and zoned single crystals, and concentrations of minor elements, were examined in detail (e.g., Beurlen *et al.* 2009, Peretti *et al.* 2010). However, distributions of Cu, Zn and Mn during primary *versus* secondary tourmaline crystallization have not been studied. Multicolored zoned crystals of elbaite altered to muscovite from the Quintos Mine, Borborema pegmatite province, State of Rio Grande do Norte were examined in detail using electron microprobe and evidently two distinct stages of tourmaline crystallization were recognized. We present compositional variations of primary and secondary tourmaline and relations to hydrothermal alteration producing muscovite, borocookeite and clay minerals.

LOCALITY AND SAMPLES

The zoned Quintos pegmatite dike, up to 150 m long and up to 20 m thick, is enclosed in quartzites of the Equador Formation. Its internal structure consists of a texturally heterogeneous border zone, wall zone, outer and inner intermediate zones, and discontinuous quartz core (Soares *et al.* 2008). Intermediate zones underwent locally strong albitization and lepidolitization. Typical minor to accessory minerals include muscovite, lepidolite, spessartine, apatite, gahnite, zircon, beryl, spodumene and Nb,Ta-oxide minerals. Comb-like crystals of zoned multicolored tourmaline, up to 25 cm long, from albite-rich portions of the inner intermediate unit are typically oriented toward a quartz core. Commonly, pink to red core is followed by a narrow zone of “electric” blue elbaite and narrow green or black Fe-rich elbaite rim.

TEXTURAL RELATIONS OF PRIMARY/ SECONDARY TOURMALINE AND OTHER REPLACEMENT PRODUCTS

Two zoned comb-like crystals of multicolored tourmaline enclosed in coarse-grained white albite were examined. The core of primary pink tourmaline I, locally replaced by pinkish muscovite, is overgrown by a narrow zone of “electric” blue elbaite sharply limited from the core and from the outermost thin rim of black Fe-rich elbaite (Fig. 1a). Thickness of the individual outer zones is several times higher on basal planes relative to prismatic ones (Fig. 1a). Thin sections and BSE images of tourmaline crystals cut parallel or perpendicular to c-axes manifest complex evolution and a variety of textures (Fig. 1). Core of the tourmaline I crystals is partly replaced by flakes of muscovite I, up to 5 mm in diameter, which are commonly oriented parallel to c-axis of tourmaline I. Its rare irregular or elongated relics occur in highly altered portions of the core (Fig. 1b). The coarse muscovite I is commonly replaced by fine-grained aggregates of muscovite II (Fig. 1b). Formation of muscovite in the expense of tourmaline I is associated with the formation of tourmaline II as irregular veinlets and heterogeneous masses, up to 1 mm in size, developed typically close to muscovite (Fig. 1b).

The relics of tourmaline I associated with secondary muscovite contain irregular aggregates and veining of tourmaline II (Fig. 1b). They texturally differ in the cuts parallel or perpendicular to c-axes. On the cuts parallel to c-axes, newly-formed terminations of tourmaline II, up to 100 µm in long, are developed. They are always growing parallel to c-axis (Fig. 1b), but in an opposite direction than black terminations of large crystals. In the cuts perpendicular to c-axes, complicated zoning is common varying from patchy to simple oscillatory.

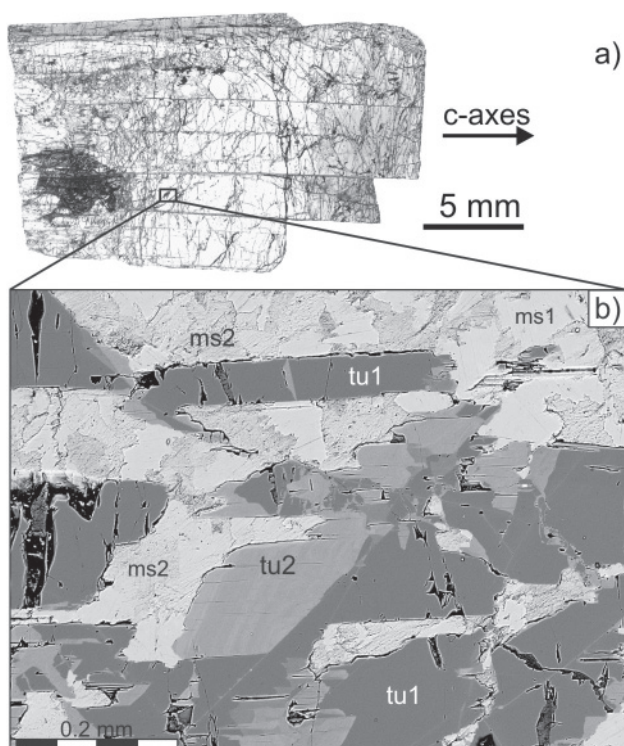


FIGURE 1. Thin section and BSE image of tourmaline crystal cut parallel to c-axes. tu1 and tu2 -tourmaline 1 and 2, ms1 and ms2 - muscovite 1 and 2. Dark area in core – clay minerals.

CHEMICAL COMPOSITION

Tourmaline is highly variable in chemical composition (Fig. 2). Primary tourmaline I is formed by large core characterized by moderate to high vacancy in the X site (0.30-0.51 pfu), low Ca \leq 0.05 apfu, moderate F = 0.33-0.51 apfu and low ΣR^{2+} = 0.15-0.47 apfu (Fe>Mn~Cu>Mg>Zn) increasing from the core outwards. The intermediate zone shows increasing in Fe, Ti, Cu and Mg with $\Sigma R^{2+} \leq$ 0.70 apfu (Fe>Cu>Mn>Mg>Zn) and high F = 0.46-0.72 apfu. Dark rim is Fe,Ti,Mg-enriched showing $\Sigma R^{2+} \leq$ 0.96 apfu (Fe>>Mg~Mn>Cu>Zn) and moderate F = 0.38-0.57 apfu (Fig. 2).

Secondary tourmaline II is highly heterogeneous and differs from tourmaline I generally by higher contents of Mn and Zn, and lower contents of Fe (Fig. 2). We found three distinct compositional types: (i) Mn>Cu>Zn, $\Sigma R^{2+} \leq$ 0.88 apfu; (ii) Cu>Mn>Zn, $\Sigma R^{2+} \leq$ 0.82 apfu, and (iii) Mn \geq Zn>Cu, $\Sigma R^{2+} \leq$ 1.03 apfu, the latter usually enriched in Ca \leq 0.25 apfu and Mg \leq 0.21 apfu (Fig. 2). The compositional types differ in textures; (i) commonly form thin veinlets and irregular aggregates in relics of tourmaline I (Fig. 1b), (ii) and (iii) occur chiefly in late prismatic ongrowths parallel to c-axis (Fig. 1b). Texturally distinct muscovite I and muscovite II have very similar composition; the only differences are elevated Ba and lower F contents in some muscovite II analyses.

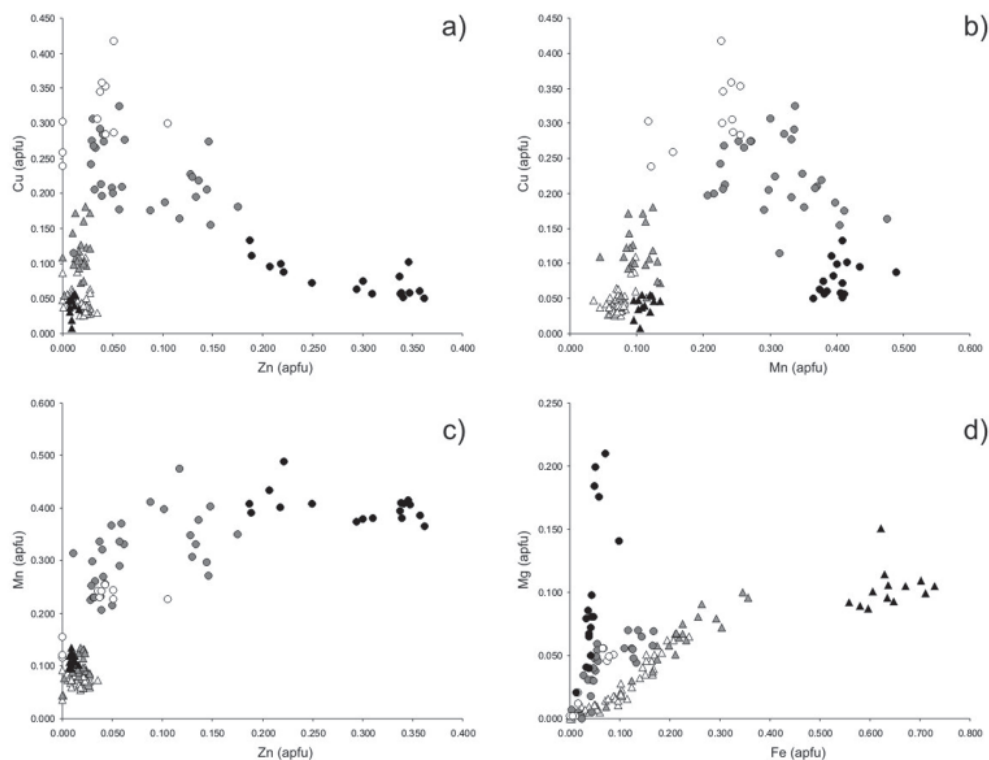


FIGURE 2. Chemical composition of tourmaline I and II, plots a) Cu-Zn, b) Cu-Mn, c) Mn-Zn, d) Mg-Fe. Triangles - tourmaline I (white - core, gray - intermediate zone, black - rim) circles - tourmaline II (white - Mn>Cu>Zn, gray - Cu>Mn>Zn, black - Mn \geq Zn>Cu).

DISCUSSION

Primary compositional trend in tourmaline from elbaite in core to Fe-enriched fluor-elbaite in rim was observed in many multicolored "watermelon" tourmalines as well as quite sharp boundaries between the individual zones. However, low to moderate concentrations of Cu ($\text{CuO} = 0.22\text{-}0.93$ wt.%; $\text{Cu} \leq 0.11$ apfu in core, and $\text{CuO} \leq 1.50$ wt.%, $\text{Cu} \leq 0.17$ apfu in intermediate zone; Figs. 2a,b) are unusual relative to ordinary complex pegmatites worldwide but similar to other samples from the Borborema region (Peretti *et al.* 2010). Slightly elevated contents of Mg and Ti in rims relative to the core (Fig. 2d) indicate opening of the system to host rocks during crystallization.

The replacement of tourmaline I core by muscovite (and borocookeite) and formation of tourmaline II is associated with evident redistribution of most elements. Part of B and Li was released from the system, whereas Al and Si seem quite constant and input of K and H_2O is apparent. Behavior of Mn, Cu, Fe, Mg and Zn are complicated. Their elevated concentrations in tourmaline II relatively to tourmaline I, except for Fe, manifest their evident enrichment, but whether these elements were at least in part released from the system is uneasy to estimate. Nevertheless, their mobility related to alteration of elbaite cores with low to moderate Cu contents may yield mobile Cu for formation of "electric" blue tourmaline in late pockets. The composition of

three types of secondary tourmaline II seems to be controlled by crystal-structural constraints such as the Jahn-Teller effect - evident avoidance of Cu and Zn (Fig. 2a). High Mg in (iii) $\text{Mn} \geq \text{Zn} > \text{Cu}$ secondary tourmaline (Fig. 2d) may suggest opening of the system to host rocks, but crystal-structural constraints also may have played a role.

This work was supported by the research project GAČR P210/10/0743 to MN, PG and RŠ.

REFERENCES

- Beurlen, H., Moura, O.J.M., Soares, D.R., Da Silva, M.R.R., Rhede, D. (2009). "Paraiba tourmaline" in pegmatites of the the Borborema pegmatite province, NE Brazil: geological and geochemical control. *Estudos Geológicos* **19**: 67-71
- Peretti, A., Bieri, W.P., Reusser, E., Hametner, K., Günther, D. (2010). Chemical variations in multicolored "Paraiba"-type tourmaline from Brazil and Mosambique: Implications for origin and authenticity determination. *Contributions to Gemology*: 1-84.
- Soares, D.R., Beurlen, H., Barreto, S.B., Da Silva, M.R.R., Ferreira, A.C.M. (2008). Compositional variation of tourmaline-group minerals in the Borborema pegmatite province, northeastern Brazil. *Can. Mineral.* **46**: 1097-1116.

RHEOLOGY OF FLUID-SATURATED GRANITIC AND PEGMATITE-FORMING MELTS

Igor S. Peretyazhko

Institute of Geochemistry, SB RAS, Irkutsk, Russia, pgmigor@igc.irk.ru

Key words: granitic melt, pegmatite-forming melt, density, viscosity, ascent velocities of a bubble.

INTRODUCTION

The occurrence of miaroles in granites and granitic pegmatites suggests that the parental melts of these rocks contained a free fluid phase (segregations or bubbles). The ascent velocity of a spherical bubble in a viscous liquid is described by the Navier–Stokes equation:

$$V = gD^2(\rho_m - \rho_f) / 12\mu_m, \quad [1]$$

where ρ_m and ρ_f are the density (kg/cm^3) of the melt and fluid, respectively; g is the acceleration due to gravity; D is the diameter of the bubble (m), and μ_m is the viscosity of the melt ($\text{Pa}\cdot\text{s}$). It is possible to evaluate the probable ranges of some of these parameters (Peretyazhko, 2010).

DENSITY OF MAGMATIC FLUIDS AND GRANITIC OR PEGMATITE-FORMING MELTS

Most evaluations of the density of magmatic fluids are obtained by studying primary fluid inclusions in minerals. The density is calculated from the thermometric and cryometric characteristics of the liquid phase of the inclusions in terms of the H_2O – NaCl system or any other system whose P – V – T – X characteristics are known. The density of magmatic fluids with relatively low concentrations of dissolved components (predominantly Na, K, Ca, and Mg chlorides) varies from 0.2 to 0.8 g/cm^3 . Carbon dioxide and aqueous salt solutions with CO_2 have a higher density, which can reach 1 g/cm^3 . The concentration of H_3BO_3 in fluids during the crystallization of minerals in miaroles granitic pegmatites is known to be 12–27 wt% (Peretyazhko *et al.*, 2000). The density of H_3BO_3 – H_2O solutions with up to 30 wt% H_3BO_3 varies from 0.6 to 1 g/cm^3 within broad P – T ranges (Peretyazhko *et al.*, 2004). Much more rarely, minerals in granites and pegmatites contain inclusions with daughter crystals, which either dissolve or do not dissolve as temperature is increased, and which

account for more than a half of the inclusion volume. With regard to data on the volumetric proportions of crystalline, liquid, and gaseous phases in fluid inclusions, the density of magmatic fluids with high concentrations of salt and other soluble components reaches 1.2–1.3 g/cm^3 and can occasionally be as high as 1.5–1.7 g/cm^3 .

The density of silicate melts can be calculated from the change in the partial molar volumes V_i (cm^3/mol) of molten oxides depending on temperature and pressure (*e.g.*, Lange, 1994). The density of a melt (g/cm^3) can be calculated as:

$$\rho_m = \sum X_i M_i / \sum X_i [V_i T_{ref} + dV_i / dT (T - T_{ref}) + dV_i / dP (P - 1 \text{ bar})] [2]$$

where X_i and M_i are the mole fraction and molecular mass of oxide i , T is the temperature ($^\circ\text{C}$) at which the density value was calculated, T_{ref} is the temperature ($^\circ\text{C}$) at which the V_i were determined, and P is the pressure (bar). Inasmuch as the values of dV_i / dP ($^\circ\text{C}/\text{mol}\cdot\text{bar}^{-1}$) of most major oxides are of the order of $n \cdot 10^{-4}$ (Lange 1994), pressure only insignificantly affects the density of silicate liquids of various compositions. The $V_{i,750^\circ\text{C}}$ values of numerous oxides reported in Knoche *et al.* (1995) are recommended to calculate the density of silicate melts under pressures of a few kilobars.

TABLE 1: Density (g/cm^3) of melts corresponding to pegmatitic complexes at various temperatures

$T, ^\circ\text{C}$	1	2	3	4	5
650	2.317	2.321	2.337	2.353	2.349
750	2.304	2.312	2.326	2.344	2.334
850	2.291	2.302	2.315	2.336	2.320

Complexes: (1) quartz–tourmaline (multicolored)–albite–lepidolite, (2) two feldspars, (3) graphic with blocks of K-rich feldspar, (4) oligoclase-bearing pegmatite, (5) albite–“rubellite”–lepidolite with pollucite.

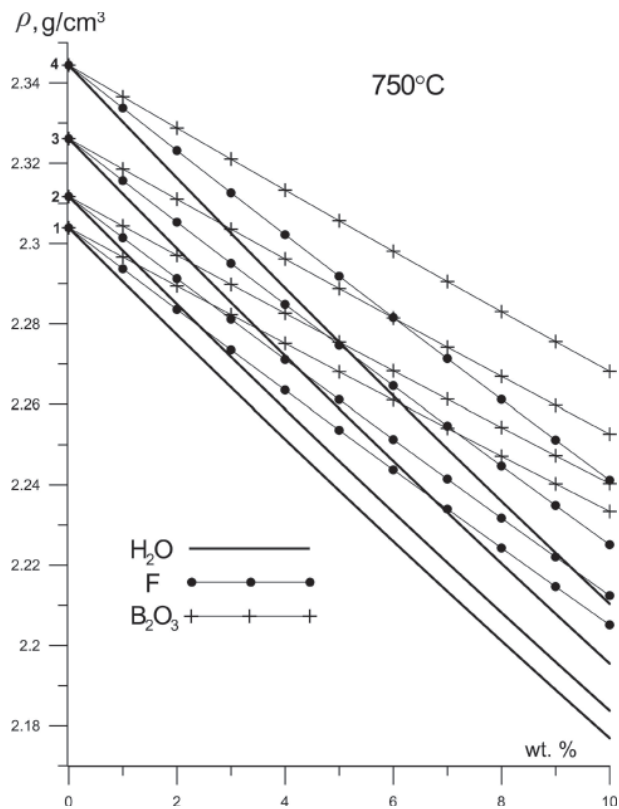


FIGURE 1: Density of granitic (pegmatite-forming) melts at 750°C whose initial composition corresponds to complexes (numbers 1-4, see in the table) with the addition H₂O, F, and B₂O₃ (figure from Peretyazhko, 2010).

The calculations were carried out for the compositions of the mineralogically most contrasting pegmatite complexes in the Malkhan field (Transbaikalia): potassic feldspar, two-feldspar, oligoclase, and rare-metal with albite, lepidolite, tourmaline, and pollucite. A temperature increase from 650 to 850°C decreases the density of the melts that compositionally approximate these complexes by about 0.02 g/cm³, and variations in the melt composition at a constant temperature result in changes in the density of 0.01-0.04 g/cm³ (Table 1).

It should be mentioned that the density of rare-metal melts with minimal SiO₂ (55-60 wt%) and high concentrations of Li, B, F, Rb, and Cs differ insignificantly from the density of "normal" granitic or pegmatite-forming melts. For a temperature of 750°C, the density of the melts is calculated as a function of their H₂O, B₂O₃, or F concentrations by proportionally adding up to 10 wt% of each of these components to the original compositions. The density of melts rich in H₂O, B₂O₃, and F decreases relative to the original values by 0.04-0.10 g/cm³ (Fig. 1). Both H₂O and F affect the density of the melts more significantly than B₂O₃. Thus, the density of granitic (pegmatite-forming) melts of various composition, containing volatile components varies insignificantly: from ~2.20 to 2.35 g/cm³.

VISCOSITY OF GRANITIC (PEGMATITE-FORMING) MELTS

An analysis of experimental data leads to the conclusion that total pressure only insignificantly affects the viscosity of silicate melts. According to their effect on the viscosity of granitic (pegmatite-forming) melt, H₂O and other minor components can be arranged in the following sequence (at constant *P-T* parameters): H>Li>F>Na>K>B>Cs>P>Be (Dingwell *et al.*, 1996). The addition of equal mass-fractions of oxides of adjacent elements in this succession changes the viscosity by 10-100 Pa·s. According to the evaluations of Holtz *et al.* (2001), the viscosity of granitic melts at 5-8 kbar and 1-7 wt% H₂O dissolved in them varies from 10^{4.5} to 10^{5.4} Pa·s. Giordano *et al.* (2004) studied the viscosity of haplogranitic and peraluminous melt (A/CNK ≥ 1) at 2 kbar with the addition of H₂O and F. The addition of ~2 mol.% (H₂O + F₂O₁) decreases the viscosity of granitic melts by four orders of magnitude, and a further increase in the total concentration of these components by more than 5 mol.% results in an insignificant further decrease. The simultaneous occurrence of F and H₂O in a melt does not appreciably affect the viscosity of this melt more than H₂O alone in equimolar amounts. Chlorine and CO₂ also modify the viscosity of granitic melts. The viscosity of a Cl-bearing H₂O-saturated granitic melt is slightly greater than in the Cl-free case. The presence of CO₂ affects melt viscosity only through a decrease in the partial pressure of H₂O and the corresponding decrease in its solubility in the melts.

Some other factors can also significantly modify the viscosity of silicate melts. For example, at pressures above 6 kbar and temperatures of 700-1100°C, a haplogranitic melt can contain >11 wt% dissolved H₂O (Holtz *et al.*, 2001), and this should result in a viscosity decrease to 10⁴-10² Pa·s. Within a single *P-T* range, the viscosity of a H₂O- and F-bearing granitic melt decreases by one order of magnitude with increasing alkalinity and the transition from a peraluminous to a peralkaline variety. According to Thomas and Webster (2000), the viscosity of a melt trapped in inclusions in minerals in a granitic pegmatite containing 17.3 wt% H₂O + F at 600°C is 4.7 Pa·s, which is equivalent to that of castor oil at 20°C.

ASCENT VELOCITY OF BUBBLES IN A MELT

According to Eq.[1], this velocity is directly proportional to the difference between the densities ($\Delta\rho$) of the melt and fluid in the bubbles. The density of a pegmatite-forming melt at temperatures of 650-850°C and pressures of 1-2 kbar is close to 2.3 g/cm³, and the density of magmatic fluids generally lies within the range of 0.5-0.8 g/cm³. Deviations from the average value $\Delta\rho = 1.5-1.8$ g/cm³ of more than ± 0.2 g/cm³ occur mostly because of changes in the density of the

fluids, because the density of a granitic or pegmatite-forming melt varies insignificantly within its P - T - X field of stability.

I calculated the ascent velocity of bubbles from 10 μm to 1 cm in diameter in a granitic melt at $\Delta\rho = 1.7 \text{ g/cm}^3$ and 650, 750, 850°C. The viscosity of the melt was obtained, depending on the temperature and concentration of dissolved H_2O , up to ~10 wt% (30 mol.%), by the equation of Giordano *et al.* (2004). At H_2O concentrations of ~1 wt% and a viscosity of 10^{10} to $10^{7.7}$ Pa·s, bubbles (10-100 μm) travel a vertical distance of 10^{-7} - 10^{-5} m per year, whereas bubbles 1-10 mm in diameter buoyantly ascend 0.001-0.1 m. A decrease in the viscosity to $10^{5.3}$ - $10^{4.6}$ Pa·s results in the ascent of bubbles of the same size over a vertical distance roughly 100 times greater. The greatest distances are covered by bubbles in the melts richest in H_2O and less viscous (at a given temperature). For instance, in one year, bubbles 10-100 μm in diameter should ascend through melts with 30 mol.% dissolved H_2O over a distance of 0.02-1.6 cm (650°C, $\eta=10^{4.44}$ Pa·s), 0.11-10.9 cm (750°C, $\eta=10^{3.61}$ Pa·s), and 0.55-54.8 cm (850°C, $\eta=10^{2.29}$ Pa·s). Bubbles of the same diameter in granitic melts of viscosity 10^5 - 10^6 Pa·s remain practically at the sites of their nucleation for hundreds to thousands of years. The velocity of buoyant ascent of bubbles in a melt can increase to a few meters per year only if the diameter of the bubbles increases to 1-10 mm. The evaluations quoted above pertain exclusively to homogeneous superliquidus melts and cannot be applied to melts containing a significant fraction of crystalline phases. Suspended in the melts, these phases will notably hamper the buoyant ascent of bubbles.

The ascent velocity of fluid bubbles in a magma chamber can increase by several orders of magnitude if these bubbles are involved in convection flows of the melt. It is known that stable flows develop in a volume of liquid (for example, melt) heated from below, if the Rayleigh criterion is met :

$$\text{Ra} = \beta g \Delta T l^3 / \nu a > \sim 1700, \quad [3]$$

where β is the volumetric thermal expansion coefficient ($^\circ\text{C}^{-1}$), g is the acceleration due to gravity, ΔT is the temperature difference ($^\circ\text{C}$) between the lower and upper boundaries of the layer, l is the thickness of the layer (m), a is the thermal conductivity coefficient (m^2/s), $\nu = \eta/\rho$ is the kinematic viscosity coefficient (η is the viscosity Pa·s of the melt, and ρ is its density in kg/m^3). A turbulent character of flow in the volume of a horizontal layer of melt is established at $\text{Ra} > 10^6$. Using Eq. [3], one can calculate the critical thickness of the melt layer:

$$l_{cr} = (10^6 \nu a / \beta g \Delta T)^{1/3} \quad [4]$$

The horizontal component of the flow U in a layer of thickness l at a temperature difference of ΔT is determined by the expression $U = 0.24a(\text{Ra} - 1708)^{1/2}/l$ (Dobretsov *et al.* 2001). With regard for the uncertainty in the values of l and ΔT , it is possible to merely

approximately estimate the size of the l_{cr} and the order of magnitude of the velocity of horizontal flow. For example, in a granitic melt having a viscosity of $10^{4.5}$ - $10^{5.5}$ Pa·s and a density of 2200–2300 kg/m^3 at $\beta = 5 \cdot 10^{-5} \text{ }^\circ\text{C}^{-1}$ and $a = 10^{-6} \text{ m}^2/\text{s}$, $\Delta T = 50^\circ\text{C}$, the l_{cr} should be 10-32 m thick. The maximum velocity of horizontal flow of melt in this layer should vary from 2.1 to 0.5 m/day, and the analogous velocity in a layer 50 m thick should vary from 5.2 to 1.9 m/day. The vertical components of the velocity of convective flows can also be significant. Experimental results and calculations suggest that the velocity of convection in flows of melt significantly decrease in the course of its crystallization.

Hence, the vertical distances over which bubbles can travel in large magma chambers with granitic melt before the onset of its crystallization are controlled, first of all, by the velocity of convective flow. The gravitational component should significantly contribute to these movements only during the long-term residence of the melt (over thousands of years) under P - T parameters above the liquidus or at a low crystallinity of the melt. It follows from rough evaluations of the thickness of the critical layer l_{cr} that active convective flow of melts are unlikely to occur in pegmatite chambers less than 10 m thick, even above the liquidus temperature. The development of large bodies (>20-30 m thick) of pegmatite or their parts can be accompanied by the convective flow of melt with bubbles before the onset of crystallization of the melt or in its early stages.

ACKNOWLEDGEMENTS

The study was supported by RFBR grant 11-05-00841.

REFERENCES

- Dingwell, D.B., Hess, K.U. & Knoche, R. (1996). Granite and granitic pegmatite melts: volumes and viscosities. *Trans. R. Soc. Edinb.: Earth Sci.* **87**: 65-72.
- Dobretsov, N.L., Kidryashkin, A.G. & Kidryashkin, A.A. (2001). *Deep Geodynamics*. (SO RAN, Fil. TGEOU). Novosibirsk. 409 p [in Russian].
- Giordano, D., Romano, C., Dingwell, D.B., Poe, B. & Behrens, H. (2004). The combined effects of water and fluorine on the viscosity of silicic magmas. *Geochim. Cosmochim. Acta* **68**: 5159-5168.
- Holtz, F., Johannes, W., Tamic, N. & Behrens, H. (2001). Maximum and minimum water contents of granitic melts generated in the crust: a reevaluation and implications. *Lithos* **56**: 1-14.
- Knoche, R., Dingwell, D.B. & Webb, S.L. (1995). Melt densities for leucogranites and granitic pegmatites: partial molar volumes for SiO_2 , Al_2O_3 , Na_2O , K_2O , Li_2O , Rb_2O , Cs_2O , MgO , CaO , SrO , BaO , B_2O_3 , P_2O_5 , F_2O , TiO_2 , Nb_2O_5 , Ta_2O_5 , and WO_3 .

- Geochim. Cosmochim. Acta **59**: 4645-4652.
- Lange, R.A. (1994). The effects of H₂O, CO₂ and F on the density and viscosity of silicate melts. *Rev. Mineralogy*. **30**: 331-369.
- Peretyazhko, I.S. (2010). Genesis of mineralized cavities (miaroles) in granitic pegmatites and granites. *Petrology* **18**: 183-208.
- Peretyazhko, I.S., Prokof'ev, V.Yu., Zagorsky, V.Ye. & Smirnov, S.Z. (2000). Role of boric acids in the formation of pegmatite and hydrothermal minerals: petrologic consequences of sassolite (H₃BO₃) discovery in fluid inclusions. *Petrology* **8**: 214-237.
- Peretyazhko, I.S., Zagorsky, V.Ye., Smirnov, S.Z. & Mikhailov, M.Y. (2004). Conditions of pocket formation in the Oktyabrskaya tourmaline-rich gem pegmatite (the Malkhan field, central Transbaikalia, Russia). *Chem. Geol.* **210**: 91-111.
- Thomas, R. & Webster, J.D. (2000). Strong tin enrichment in a pegmatite-forming melt. *Mineral. Deposita* **35**: 570-582.

OCCURRENCE OF COMPLEX PEGMATITES IN THE SOUTH OF TOCANTINS STATE, BRAZIL

Hudson Queiroz[§], Rúbia R. Viana, Gislaine A. Battilani, Luana Laiame de Oliveira, Gilliard Medeiros Borges & Denis L. Guerra

Federal University of Mato Grosso - UFMT [§] hudsonq@gmail.com

Key words: Tourmaline, granitic pegmatite, Tocantins State, Brazil

INTRODUCTION

Brazil is famous internationally in the mineral sector, not only in metal minerals, but also as one of the leading producers of non-metal minerals, especially colored gems. Minas Gerais state is the largest producer, given the great variety, quality and quantity of gem minerals from pegmatite rocks of Eastern Brazilian Pegmatite Province. In addition to Minas Gerais, part of the Bahia, Espírito Santo and Rio de Janeiro states also belong to this province that makes it the largest pegmatitic province of Brazil.

In the Tocantins State, northern Brazil, there are several poorly studied pegmatite bodies. In the south of this state, near the border of Goiás State, NE-SW striking granitic pegmatite bodies occur. Five pegmatite bodies, Marimbondo, Marimbondinho, Índio, Zé do Fole and Marta Rocha, from the southern region containing colored tourmaline mineralization and their host rocks have been studied in this work.

GEOLOGIC SETTING

The pegmatites studied in this work, are intruded into the Central sector of Tocantins Structural Province (TSP) (Almeida & Hasui 1984) and are hosted in metasedimentary rocks of the Serra da Mesa Group.

The TSP is the result of the collage of different cratonic fragments from Amazon and São Francisco cratons, due to their collision during the Paleoproterozoic. This province has been affected and partly reworked in the Brasiliano orogenic cycle (Almeida *et al.* 1981). Almeida & Hasui (1984) subdivided the TSP into three sectors: North, South and Central. The Central sector is represented by the Goiás Massif, the Brasília Belt and the Goiás Magmatic Arc.

The Goiás Massif consists of different lithologies that comprise the oldest basement in the Central sector region of TSP. This structural high is situated between the Paraguay-Araguaia and Brasília belts, forming a narrow and elongated shape (Fuck *et al.* 1993). The Goiás Massif covers different geological-tectonic

domains (Pimentel *et al.* 2000) from the Proterozoic to the Brasiliano orogeny.

The Brasília Belt is a Neoproterozoic mobile belt located in the eastern portion of the TSP, extending over 1000 km, in approximately a NS direction, along the western edge of the São Francisco Craton. The northern and southern segments are separated in the central portion by a system of dextral ductile shear zones, responsible for an abrupt change in structural directions (Costa & Angeiras 1971; Araújo Filho 1999).

The Goiás Magmatic Arc is located in the western portion of the Brasília Belt. According to Dardenne (2000), the arc is represented by a narrow belt of volcanic and meta-sedimentary rocks, with structural direction NNW-SSE ranging from NNE-SSW, separated by orthogneisses of dioritic to granitic composition, often mylonitized.

The pegmatite bodies are hosted in the rocks of the Goiás Massif.

HOST ROCKS

The host rocks of these pegmatite bodies are represented by metamorphic sequences, ranging from slightly to highly altered. The alteration and dense vegetation cover make the exact identification of these rocks difficult.

The host rocks of the studied pegmatites are represented by quartzites and schists of the Serra da Mesa Group.

The lithotypes, described as Serra da Mesa, are better preserved in the higher altitudes. The abrupt contact between pegmatite and host is best observed only in Zé do Fole pegmatite, which displays only moderate alteration.

The quartzite is gray, to greenish due to the presence of mafic minerals. On the slope of the Serra Dourada coarse-grained, reddish quartzite with small plates of muscovite occurs. The unaltered schist, is gray and thin bands of biotite interspersed with

quartz, produces the schistosity of the rock. Altered schist is red and very friable.

In general, the host rocks next to the veins show foliation ranging between 13 and 30° NE with dips ranging from 50° to 65° SE. The contact between the pegmatite bodies and host rocks seems to be high angle. In the Zé do Fole pegmatite the contact dip is around 70° SE.

PEGMATITE BODIES

Except for the Marta Rocha pegmatite, which displays a roughly circular form, the pegmatites have elongated shapes. The outcrops vary from a few tens of meters in the Marta Rocha and Indian pegmatites, to hundred of meters in the Zé do Fole, Marimbondinho and Marimbondo pegmatites. The latter, the largest of them, are about 200 m in N-S direction and 150 m in E-W.

The pegmatite bodies are zoned, with a narrow border zone (maximum at 20 cm) and a wall zone, composed of an intergrowth of quartz and potassic feldspar. The intermediate and core zones are composed of very large blocks of crystals aggregates of K-feldspar, quartz, schorl and muscovite. Some replacement bodies of metasomatic minerals, like cleavelandite, tourmalines, some clay-minerals and lithium-micas (muscovite and lepidolite) also occur.

The mineralogy of pegmatites studied consists primarily of quartz, feldspar, mica (muscovite, biotite and lepidolite) and tourmaline, with clay minerals, beryl, spodumene and garnet.

The quartz occurs as fine crystals intergrown with microcline, large as anhedral blocks and also as euhedral crystals over 50cm in length. In some bodies smoky quartz crystals up to 5 cm in length are found, associated with lepidolite, tourmaline and albite.

Feldspar group minerals are represented by microcline and albite showing some differences in the distribution and arrangement in the pegmatites. Typical massive microcline makes up the wall zone. Few crystals show preserved faces and most are altered to clay minerals. Albite is typically massive and occurs in the inner and replacement zones. In the Marimbondo, Marta Rocha and the Zé do Fole pegmatites, cleavelandite, is associated with replacement bodies.

The mica group is represented by muscovite, lepidolite and minor amounts of biotite (found only in pegmatites Marimbondinho and Marimbondo). The muscovite occurs as aggregated plates (Fig. 1b) up to 20cm and it has mafic inclusions of Fe and Ti oxides. In inner zones, muscovite plates are yellowish green in color when combined with tourmaline, lepidolite, and albite. Sometimes, muscovite crystals show a

chemical zoning with purple or lilac edges and yellow cores. The occurrence of lepidolite is restricted to inner zones and its color varies in shades of purple, in most cases aggregates of plates are millimeter size (Fig. 1c). Biotite is restricted to Marimbondinho and Marimbondo pegmatites and appears as small crystals in the wall zone.

Tourmaline group varieties consist dominantly of schorl, with some pink (Fig. 1a), green and watermelon tourmalines. Based on chemical analyses and cation distribution, it was possible to identify two subgroups of colored tourmaline: first between elbaite rossmanite and second between liddicoatite and rossmanite. Liddicoatite and rossmanite were identified in Indio, Zé do Fole and Marta Rocha Pegmatites. Schorl is normally black, but rare crystals with dark green portions also occur. This mineral shows euhedral crystals, varying from a few millimeters to more than 50cm in length. Most crystals are fractured, usually filled by quartz veinlets. Schorl is present mainly in the border and intermediate zone, it is also found associated with large blocks of quartz, muscovite and lepidolite, from the intermediate zone.

Elbaite, liddicoatite and rossmanite are found associated with large crystals of quartz and feldspars (mainly albite) and also aggregates of lepidolite. The watermelon variety is found in Indio and Marta Rocha pegmatites and the crystals are often opaque, with green edges and black cores. These varieties were found in contact with aggregates of muscovite or as inclusion in these aggregates. The crystals are prismatic with well-formed faces, normally fractured and the crystals rarely exceed 5 cm. All samples of these specimens were collected in the tailings area.

Clay group minerals, primarily kaolinite group species, are found in all pegmatites as alteration product, mainly of feldspars.

Beryl was identified only in Marimbondo pegmatite and is associated with feldspar. The crystals are anhedral with opaque blue-green color. The samples are between 1 and 7 cm in length.

Spodumene crystals are associated with albite/cleavelandite, quartz, colored tourmaline and lepidolite (Fig. 1d). The crystals are white to beige in color, and sometimes appear superficially colored in shades of green or purple, probably due to alteration of lepidolite or tourmaline. The habit of the crystals is tabular, striated and rarely exceed 12 cm in length. This mineral was found only in Zé do Fole Pegmatite.

The garnet group is represented by the variety spessartite, which was found only in Marta Rocha pegmatite. The crystals are millimeter size, and are moderately altered, and can be included in tourmaline (schorl) or associated with microcline, albite and quartz.

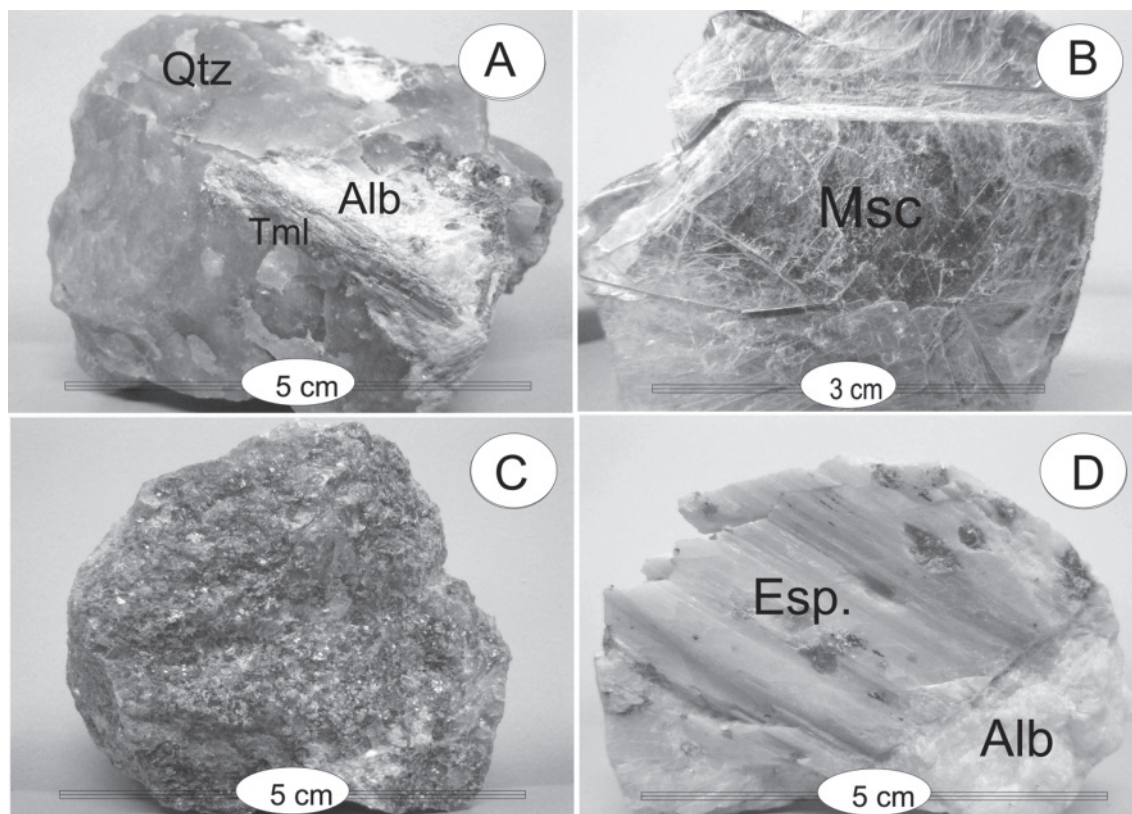


FIGURE 1. Mineral samples from Tocantins Pegmatites. (A) Pink tourmaline, gray quartz and white albite. (B) yellowish muscovite plates. (C) massive lepidolite. (D) spodumene.

REFERENCES

- Almeida, F.F.M & Hasui, Y. (1984). O Pré-Cambriano do Brasil. São Paulo, Ed Edgard Blucher.
- Almeida, F.F.M., Hasui, Y., Neves, B.B.B., Fuck, R.A. (1981). Brazilian Structural Provinces: an introduction. *Earth Sci. Rev.* **17**: 1-29.
- Araújo Filho, J.O. (1999). A Sintaxe dos Pirineus: um exemplo de dois cinturões Brasileiros no centro oeste do Brasil. In: SBG, Simpósio de Geologia do Centro-Oeste; 7, Simpósio de Geologia de Minas Gerais, 10, Boletim de Resumos, 79.
- Costa, L.A.M & Angeiras, A.G. (1971). Geosynclinal evolution of the epi-Baykalian platform of Central Brazil. *Geol.Runds.* **60**(3): 1024-1050.
- Dardenne, M.A. (2000). The Brasília Fold Belt. In: Cordani, U.G., Milani, E.J., Tomas Filho, A., Campos, D.A. *Tectonic Evolution of South America.* 231-263.
- Fuck, R.A., Jardim de Sá, E.F., Pimentel, M.M., Dardenne, M.A. & Pedrosa Soares, A.C. (1993). As faixas de dobramento marginais do Cráton do São Francisco. In: O Cráton do São Francisco. Salvador, Sociedade Brasileira de Geologia. 161-185.
- Pimentel, M.M., Fuck, R.A. & Gioia, S.M.C.L. (2000). The neoproterozoic Goiás Magmatic Arc, central Brazil: A review and new Sm-Nd isotopic data. *Revista Brasileira de Geociências* **30** (2): 35-39.

CATION PARTITIONING BETWEEN MINERALS OF THE TRIPHYLITE ± GRAFTONITE ± SARCOPSIDE ASSOCIATION IN GRANITIC PEGMATITES

Encarnación Roda-Robles^{1§}, Miguel Galliski², James Nizamoff³, William
Simmons³, Paul Keller⁴, Alexander Falster³, Frédéric Hatert⁵

¹ Dpt. Mineralogía y Petrología, UPV/EHU, Bilbao, Spain §encar.roda@ehu.es

² IANIGLA-CCT Mendoza, CONICET, Mendoza, Argentina

³ Dpt. Earth & Env. Sci, Univ. New Orleans, New Orleans, LA, USA

⁴ Institut für Mineralogie und Kristallchemie, Universität Stuttgart, Germany

⁵ Lab. Cristallografie, Université Liège, Belgium

Key words: graffonite, triphylite, sarcopside, textures, cation partitioning

INTRODUCTION

Phosphates of the graffonite-beusite ($\text{Fe}^{2+}, \text{Mn}^{2+}, \text{Ca}$)₃(PO_4)₂, and the triphylite-lithiophilite $\text{Li}(\text{Fe}^{2+}, \text{Mn}^{2+})\text{PO}_4$ solid-solution series, as well as sarcopside ($\text{Fe}^{2+}, \text{Mn}^{2+}, \text{Mg}$)₃(PO_4)₂, are primary phases that frequently occur together in intimate intergrowths in some granitic pegmatites. These and other phosphates generally appear in the intermediate zones and/or core margin of the pegmatites, mainly in nodules that vary widely in size range, from a few millimeters up to ~2m in diameter. Most commonly, silicates are absent or scarce inside these nodules, with quartz, muscovite and plagioclase the most commonly observed. Nevertheless, it is not unusual to observe some Fe-Mn-Mg-rich silicates, such as tourmaline, biotite and/or garnet, in close contact with these phosphates.

Despite studies on this phosphate association, which are relatively numerous, genetic relationships between these minerals are not fully understood. Consequently, phosphate assemblages from 11 pegmatites - Cañada, Pereña, La Fregeneda (Spain); Nossa Senhora de la Assunção (Portugal); Cema, Santa Ana, La Empleada (Argentina); Boavista (Brasil); Palermo#1 (USA); and Tsaobismund, Abbabis (Namibia) - have been tested for cation partitioning of Fe-Mn-Mg by electron microprobe techniques, in order to determine some evidence for their genetic relationships, and for a discussion of pegmatite evolution in general. In this study we present the

petrographic results and the preliminary data on partitioning of Fe-Mn-Mg between these phases.

SELECTED MATERIALS

The different localities where the studied phosphates occur and their main petrographic features are listed in Table 1. The Fe/(Fe+Mn) ratio of triphylite-lithiophilite (or its topotactic replacement product, ferrisicklerite-sicklerite) is given as well. A broad range for this ratio is presented by the studied samples, from Mn-rich members (Fe/(Fe+Mn) = 0.25 in La Empleada), to Fe-rich terms (Fe/(Fe+Mn) = 0.89 in Palermo #1). The Fe/(Fe+Mn) ratio in phosphates indicates the degree of fractionation of the initial pegmatitic melt as well as the evolutionary stage of pegmatite formation (e.g., Fransolet *et al.* 1986, Keller *et al.* 1994). This way, the phosphates with the lowest Fe/(Fe+Mn) ratios would have crystallized from the most evolved pegmatitic melt fractions. However, in some cases this ratio seems to be anomalously lower than expected, which is interpreted as a result of an impoverishment in Fe of the pegmatitic melt due to the previous crystallization of other Fe-rich phases, such as schörl or almandine (Roda-Robles *et al.* 2009). This could be the case in some of the studied samples, such as Cema, Santa Ana and La Empleada pegmatites. Anyway, the important differences in this ratio between the different samples, allow us to check if cation partitioning is influenced by changes in the Fe-Mn proportions.

TABLE 1. List of selected samples with coexisting members of the triphylite-lithiophilite and graffonite-beusite series and sarcopside, and main features of the hosting pegmatites.

PEGMATITE	Country Rock	Main minerals	Phosphate association	Phosphate textures	trph(fsck) Fe/(Fe+Mn)
Cañada (border) (Salamanca, Spain)	leucogranite & gabbro	Qtz, Pl, Kfs, Ms, tur, phos±Bt±Grt	fsck, grft , mgtr, jhsm, Mn-apt, xnt, allu, stnk	granoblastic texture an- to subhedral habit	0.74-0.78
Cañada(core margin) (Salamanca, Spain)	leucogranite & gabbro	Qtz, Pl, Kfs, Ms tur, phos	trph, srcp, fsck, grft , wolf, mtbr	srcp lamellae inside granoblastic trph granoblastic grft	0.80-0.83
Pereña (Salamanca, Spain)	leucogranite	Qtz, Pl, Kfs, Ms, brl, Bt, py, phos	fsck, het, srcp, grft , allu, stnk	srcp lamellae inside granoblastic fsck/het granoblastic grft	0.84-0.88
La Fregeneda (Salamanca, Spain)	micaschists	Qtz, Pl, Kfs, Ms	fsck, het, srcp, grft , allu, wyll-rsm, Mm-apt	srcp lamellae inside granobl. Fsck and grft	0.77-0.78
N ^ª S ^a de Assunçao (Aguiar, Portugal)	two-mica granite	Qtz, Pl, Kfs, Ms, Bt, brl, phos	trpl, trph, srcp , isok, apt	srcp lamellae inside granoblastic trph	0.50-0.53
Cema (San Luis, Argentina)	schists	Qtz, Pl, Kfs, Ms, tur, Grt, brl, phos, spd	sck, beus , var, qng, apt, joos	granoblastic sck and beus	0.46-0.48
Santa Ana (San Luis, Argentina)	micaschists	Qtz, Pl, Kfs, Ms, tur, Grt, brl, phos, crd	ltph, sck, beus , qng, apt,	ltph/sck lamellae inside beus	0.35-0.40
La Empleada (San Luis, Argentina)	micaschists	Qtz, Pl, Kfs, Ms, tur, Grt, brl, phos, crd	ltph, sck, srcp, beus , qng, var	srcp lamellae inside ltph/sck	0.25-0.28
Tsaobismund (Karibib, Namibia)	Kfs-bearing quartzites	Qtz, Pl, Kfs, Ms, tur, brl, col, phos	trph, fsck , het, trpl, srcp , apt, allu, beus	srcp and beus irregular grains or srcp lamellae inside trph/fsck	0.63-0.64
Abbabis I (Karibib, Namibia)	micaschists	Qtz, Pl, Ms, brl, col, phos	fsck, het, srcp , arroj, Fe-wyll	srcp lamellae inside granoblastic trph	0.84
Palermo#1 (New Hampshire, USA)	schists	Qtz, Pl, Kfs, Ms, brl, phos±tur	grft, trph, fsck ,	trph/fsck lamellae inside grft. granoblastic grft and trph/fsck	0.74-0.82
Palermo#1 (New Hampshire, USA)	schists	Qtz, Pl, Kfs, Ms, brl, phos±tur	grft, trph, fsck, srcp ,	trph/fsck lamellae inside grft. srcp lamellae inside trph	0.89
Boavista (Galiléia, Brasil)	schists	Qtz, Pl, Kfs, Ms, brl, spd, phos	trph, srcp	srcp lamellae inside granoblastic trph	0.79-0.80

Symbols of rock-forming minerals taken from Kretz (1983)

Members of the triphylite-lithiophilite series (or ferrisicklerite-sicklerite) are present in all the studied pegmatites. However, members of the graffonite-beusite series and sarcopside are only present in some of them (Table 1). By this way, three different associations have been distinguished: 1) trph/fsck + grft + srcp, where the three phases are present; 2) trph/fsck + grft, where sarcopside has not been identified; and 3) trph/fsck + srcp, where members of the graffonite-beusite series are absent. Textures in every association may be different. In associations 1 and 2 the most common is that triphylite-lithiophilite and graffonite-beusite members appear together in discrete grains of granoblastic texture (Cañada

border, Cañada core margin, Pereña, La Fregeneda, Cema, Tsaobismund, and Palermo#1), whereas an intergrowth of graffonite containing coarse lamellae of triphylite-lithiophilite, or its topotactic replacement products ferrisicklerite-sicklerite, is less frequently observed (Palermo#1, Santa Ana and La Empleada). In this case most lamellae are platy and form a single set that share a quite uniform optical orientation, enclosed in monocrystalline graffonite, giving rise to a laminated parallel intergrowth. In associations 1 and 3, the triphylite hosts lamellae of sarcopside. These lamellae usually show two preferential crystallographic orientations, and are restricted just to the triphylite, usually inside it (Cañada core margin,

Pereña, La Fregeneda, Nossa Senhora de la Assunção, La Empleada, Tsaobismund, Abbabis, Palermo#1 and Boavista) and, more rarely, as a rim between triphylite and graffonite (Cañada core margin and Palermo#1). Sarcopside lamellae are usually lenticular, expanding inward and pinching out at the boundary of triphylite with graffonite in association 1.

ANALYTICAL METHODS

Representative phosphates were collected from the 11 pegmatites listed in Table 1. Mineral

identification was carried out by a combination of petrographic, powder XRD, and EPM techniques. Close to 850 chemical analyses were performed at the LMTG (Laboratoire des Mécanismes et Transferts en Géologie, Toulouse, France), with a Camebax SX 50 electron microprobe. The analytical conditions were an operating voltage of 15 kV and a beam current of 20 nA. Standards used for the phosphates were: CaF₂ for F, albite for Na, orthoclase for K, corundum for Al, andradite for Fe, Ca and Si, graffonite for Mn and P, titanite for Ti, olivine for Mg, and ZnS for Zn.

TABLE 2. Representative K_D and Fe/(Fe+Mn) ratios from the studied phosphates. Associations: 1 = trph/fsck + grft + srcp; 2 = trph + grft; 3 = trph + srcp.

ASSOC LOCALITY	1 Cañada Core m.	1 Pereña	1 Fregen.	1 Emplea.	1 Tsaob.	1 Pal.#1	2 Cañada border	2 Cema	2 S. Ana	2 Pal.#1	3 Cañada Core m.	3 NSAss.	3 Abbabis	3 Boavista
Fe/(Fe+Mn)	0.83	0.79	0.77	0.25	0.64	0.89	0.77	0.46	0.37	0.79	0.80	0.52	0.84	0.79
K _D _{Fe grft/trph}	0.79	0.75	0.76	-	-	0.88	0.90	0.80	0.80	0.83	-	-	-	-
K _D _{Mn grft/trph}	2.33	1.95	1.85	-	-	2.51	2.44	1.27	1.32	1.91	-	-	-	-
K _D _{Mg grft/trph}	0.24	0.18	0.17	-	-	0.29	0.25	0.28	0.30	0.31	-	-	-	-
K _D _{Fe grft/srcp}	0.78	0.78	0.78	-	-	0.85	-	-	-	-	-	-	-	-
K _D _{Mn grft/srcp}	2.10	1.70	1.69	-	-	2.30	-	-	-	-	-	-	-	-
K _D _{Mg grft/srcp}	0.39	0.25	0.27	-	-	0.50	-	-	-	-	-	-	-	-
K _D _{Fe srcp/trph}	1.01	0.96	0.98	1.43	1.04	1.03	-	-	-	-	1.01	1.02	1.13	1.04
K _D _{Mn srcp/trph}	1.11	1.15	1.09	0.91	0.98	1.09	-	-	-	-	1.06	0.98	1.19	1.08
K _D _{Mg srcp/trph}	0.61	0.75	0.65	0.49	0.54	0.58	-	-	-	-	0.57	0.54	0.56	0.53

FE-MN-MG PARTITIONING AND DISCUSSION

Correlated pairs of data have been used to calculate empirical partition coefficients on molar basis (K_D). For associations 2 and 3 the analyses used in these calculations were made on common interfaces between two phosphates (trph(fsck)/grft and trh(fsck)/srcp respectively). In association 1, this was done in the same way for these pairs of phosphates. However, sarcopside and graffonite do not exhibit common interfaces. In that case, to calculate the K_D we used pairs of data from the same sample. No chemical zoning has been observed in any of the studied samples, permitting us to use these data in such a way.

The evaluated mole fractions are $X_{Fe} = Fe/(Fe+Mn+Mg)$, $X_{Mn} = Mn/(Fe+Mn+Mg)$ and $X_{Mg} = Mg/(Fe+Mn+Mg)$. The partition coefficients are defined as follows: $K_{D_{M_{A/B}}} = X_A/X_B$, where M = Fe, Mn or Mg; A = graffonite or sarcopside, and B = triphylite or sarcopside (Table 2). Plots of the mole fractions (Fig. 1) let us draw some conclusions in relation to the distribution of Fe, Mn and Mg among

coexisting phases. In all the cases, the crystal structure of graffonite shows a strong preference for Mn. This preference seems to decrease as the Fe/(Fe+Mn) decreases. This way, in the samples from Santa Ana and Cema, where the phosphates correspond to the Mn-rich terms, the K_D_{Mn grft/trph} are in the range 1.27-1.32, whereas for the rest of the occurrences, which are Fe-richer, K_D_{Mn grft/trph} values are significantly higher, ranging from 1.75 to 2.57. Fe is preferentially partitioned into triphylite-lithiophilite and sarcopside over graffonite, with K_D_{Fe grft/trph} in the range 0.75-0.88 and K_D_{Fe grft/srcp} in the range 0.77-0.93. For the pairs trph-srcp there is not a clear tendency for the distribution of Fe and Mn as, in general, K_D are quite close to unity. However, mainly in the association 1, where the three phases coexist, there is a tendency to increase the K_D_{Mn srcp/trph} with increasing Fe/(Fe+Mn) (R² = 0.640), whereas the K_D_{Fe srcp/trph} tends to decrease (R² = 0.857). Finally, Mg is clearly partitioned preferentially into triphylite, with graffonite the Mg-poorest of the three phases, with K_D_{Mg grft/trph} in the range 0.17-0.35, K_D_{Mg grft/srcp} in the range 0.25-0.53 and K_D_{Mg srcp/trph} in the range 0.17-0.77.

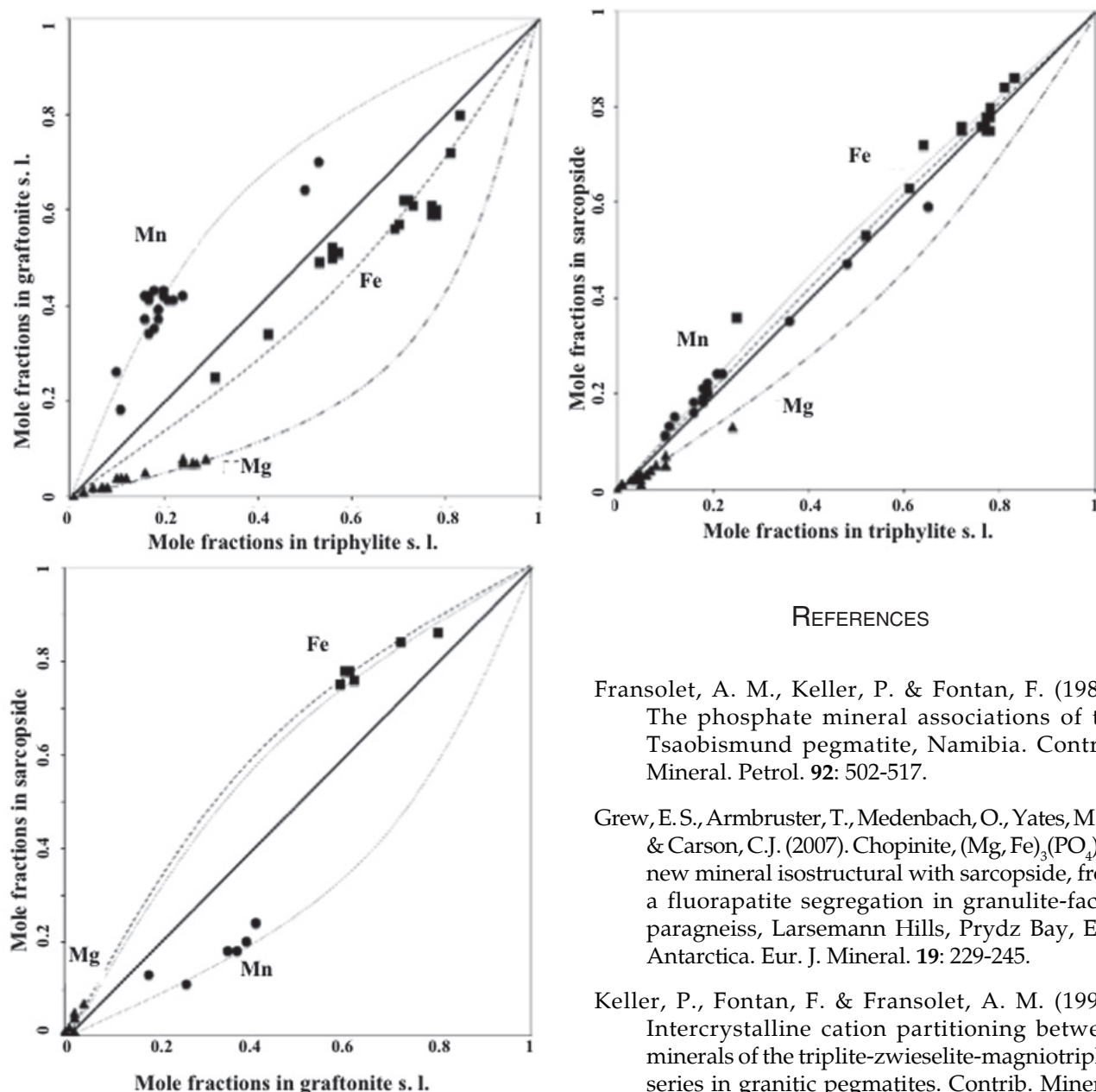


FIGURE 1. Partitioning of Fe, Mn and Mg between coexisting sarcopside and members of the triphylite and graffonite series. Legend: squares = Fe^{2+} ; circles = Mn^{2+} ; and triangles = Mg

The strong preference of minerals of the graffonite-beusite series for Mn was already reported in the literature (Smeds *et al.* 1998), and is certainly due to the presence of the large 7-coordinated M(1) site in the graffonite structure, which is able to contain significant amounts of Ca (Wise *et al.* 1990). On the other hand, the preference of the sarcopside structure for Mg, compared to graffonite, explains the recent discovery of chopinite, $\text{Mg}_3(\text{PO}_4)_2$, in granulite-facies rocks from East Antarctica (Grew *et al.* 2007).

ACKNOWLEDGMENTS

This study has been carried out with the support of the UPV/EHU (project n° 08/02)

REFERENCES

- Fransolet, A. M., Keller, P. & Fontan, F. (1986). The phosphate mineral associations of the Tsaobismund pegmatite, Namibia. *Contrib. Mineral. Petrol.* **92**: 502-517.
- Grew, E.S., Armbruster, T., Medenbach, O., Yates, M.G. & Carson, C.J. (2007). Chopinite, $(\text{Mg}, \text{Fe})_3(\text{PO}_4)_2$, a new mineral isostructural with sarcopside, from a fluorapatite segregation in granulite-facies paragneiss, Larsemann Hills, Prydz Bay, East Antarctica. *Eur. J. Mineral.* **19**: 229-245.
- Keller, P., Fontan, F. & Fransolet, A. M. (1994). Intercrystalline cation partitioning between minerals of the triphylite-zwieselite-magniotriphylite series in granitic pegmatites. *Contrib. Mineral. Petrol.* **118**: 239-248.
- Kretz, R. (1983). Symbols for rock-forming minerals. *American Mineralogist* **68**: 277-279.
- Roda-Robles, E., Galliski, M., Roquet, M. B., Hatert, F. & de Parseval, P. (2009). Phosphate mineral associations in the Cema pegmatite (San Luis province, Argentina): paragenesis, chemistry and significance in the pegmatite evolution. *Estudios Geológicos* **19** (2): 300-304.
- Smeds, S.-A., Uher, P., Černý, P., Wise, M.A., Gustafsson, L. & Penner, P. (1998). Graffonite-beusite in Sweden: primary phases, products of exsolution, and distribution in zoned populations of granitic pegmatites. *Can. Mineral.* **36**: 377-394.
- Wise, M.A., Hawthorne, F.C. & Černý, P. (1990). Crystal structure of a Ca-rich beusite from the Yellowknife pegmatite field, Northwest Territories. *Can. Mineral.* **28**: 141-146.

CHEMICAL VARIATION IN TOURMALINE FROM THE BERRY-HAVEY PEGMATITE (MAINE, USA), AND IMPLICATIONS FOR PEGMATITIC EVOLUTION

Encarnación Roda-Robles^{1§}, William Simmons², James Nizamoff², Alfonso Pesquera¹, Pedro P. Gil-Crespo¹, José Torres-Ruiz³

¹ Dpt. Mineralogía y Petrología, UPV/EHU, Bilbao, Spain §encar.roda@ehu.es

² Dpt. Earth & Env. Sci, Univ. New Orleans, New Orleans, LA, USA

³ Dpt. Mineralogía y Petrología, Universidad de Granada, Spain

Key words: tourmaline, pegmatites, mineral chemistry, Maine, USA

INTRODUCTION

The Berry-Havey pegmatite (Androscoggin County, Maine, USA), is a highly evolved rare-element pegmatite enriched in Li, F, B, Be and P. It belongs to the Oxford pegmatite field, located in the western portion of the state of Maine, in proximity to the Sebago granitic batholith. In this field pegmatites concentrate along the northwest, northeast and eastern margins of the granite. Different degrees of evolution are attained by pegmatites in this region, with an internal zonation that varies from poor to well developed, sometimes with the occurrence of pockets, where gem tourmaline may be present. The Berry-Havey pegmatite belongs to this group of highly evolved pegmatites.

This study deals mainly with the textural characteristics and compositional variation of tourmaline in the different zones of the Berry-Havey pegmatite, and its implications for the evolution of this body.

GEOLOGY OF THE PEGMATITIC BODY

With the present exposure of the Berry-Havey pegmatite it is not easy to determine the shape of the pegmatite, or its internal structure. A straight contact is observed in the southern limit of the open pit, whereas in the western zone the pegmatite exhibits some dyke-like branches that cross-cut the schists of the country rock. In the rest of the quarry it is not possible to observe the contact. In the southern part of the open pit the pegmatite is conformable to the country rock, with a dip close to 40° SSE, whereas in the northern part the body seems to be more horizontal. Regarding the internal structure, five different zones have been distinguished: wall zone, first intermediate zone, second intermediate zone, core margin and core zone. Tourmaline is present in all of them, with important textural and compositional differences among the different zones. The main features of these zones appear in Table 1.

TEXTURAL CHARACTERISTICS OF TOURMALINE

The main textural features of tourmalines from the different zones of the pegmatite are reported in Table 1. In the wall zone tourmaline is scarce, occurring as very fine-grained prismatic black crystals, together with quartz, feldspars, muscovite, garnet and biotite. The first intermediate zone is characterized by the abundance of graphic intergrowths of quartz and K-feldspar, with schorl occurring as a minor constituent. On the contrary, in the second intermediate zone the quartz-K-feldspar graphic intergrowths are not so common, whereas schorl may be very abundant, appearing as black prismatic crystals up to 6 × 40 cm. In the core margin, tourmaline is quite abundant and many crystals exhibit a tapered black prism growing perpendicular to the pegmatite contacts that increases in width in the direction of the core of the pegmatite. The thick ends of most crystals are crowned by black ± green tourmaline + albite (clevelandite) ± quartz. The tourmaline crystals, which show a sharp boundary between the black and the greenish zones, are commonly broken, giving rise to a pull-apart structure. Finally, the core represents the innermost zone of the pegmatite, which is the most complex zone, not only because of its mineralogy, but also because of its textures. It is not a continuous unit, but several pods of different sizes, generally with diameters < 3 m that appear aligned over the tourmalines of the core margin, and usually embedded in meter-scale masses of blocky K-feldspar and quartz. The other main minerals of this zone are micas from the muscovite-lepidolite series and tourmaline. The core also contains rounded pods of Fe-Mn phosphate, montebasite, beryl, and greenish, fine-to-medium-grained tourmaline crystals associated with medium-to-coarse book crystals of muscovite. Lepidolite occurs as fine-grained, irregular to rounded purple masses close to the muscovite + green tourmaline-containing areas.

TABLE 1. Main characteristics of the Havey pegmatitic units and the associated tourmaline.

ZONE	Mineralogy	General Textures	Tourmaline Texture	compositional Variation
WALL	Qtz, Kfs, Pl, Bt, Ms ± Grt ± BLACK TOURMALINE	Homogeneous, very fine to medium grained facies Locally greenish Kfs	Very fine grained, black prismatic crystals. Very scarce	Dravite-Schorl
INTERMEDIATE-I	Qtz, Kfs ± Grt ± Bt ± BLACK TOURMALINE	Qtz-Kfs graphic intergrowths (> 90% volume)	Fine to medium subhedral crystals	Schorl-Foitite
INTERMEDIATE-II	Qtz, Kfs, BLACK TOURMALINE	Blocky Kfs and Qtz	Coarse prismatic black crystals	Schorl-Foitite
CORE MARGIN	Ab, Qtz, BLACK ± GREEN TOURMALINE	Matrix of tabular crystals of Clv, where coarse tourmaline crystals occur	Coarse black tourmaline prisms (< 70 cm length) crowned by an intergrowth of black±green Tur and AbSharp contact between black and green tourmaline	From Schorl -Foitite to Elbaite
CORE	Lpd, Ms, Qtz, Kfs, Amb, Ab, Brl, Fe-Mn PhoGREEN, PINK & MULTICOLORED TOURMALINE	Irregular pods of fine grained Lpd, coarse book Ms, Amb, Fe-Mn-Pho ±Cst±Col-Tan Coarse morganite (Brl) sub- to euhedral crystals are common Pockets with elbaite in a Cookite matrix	In the pods, subhedral, fine to medium zoned crystals (watermelon, or longitudinal zoning). Also fine individual pink or green crystals (together with lepidolite and muscovite respectively). In the pockets, some green, teal or watermelon gem quality crystals	Pods:Elbaite- Rossmanite Pockets (gem): Elbaite - Rossmanite

In "Mineralogy", the following abbreviations have been used: Qtz=quartz; Kfs=feldspar; Pl=plagioclase; Ms=muscovite; Bt=biotite; Grt=garnet; Tur=tourmaline; Ab=albite; Clv=clevelandite; Amb=amblygonite; Cst=cassiterite; Col-Tan=columbite-tantalite; Lpd=lepidolite; Pho=phosphates; Brl=beryl; Cook=cookeite. *Grain size: very fine = <6 mm; fine = 6 mm to 2.5 cm; medium = 2.5 cm to 10 cm; coarse = >10 cm.

Small pinkish tourmaline crystals have been observed inside the lepidolite masses. Prismatic crystals of watermelon tourmaline have also been observed in this zone, but most are replaced by clay minerals. Moreover, radial prisms of multicoloured tourmaline embedded in feldspars and quartz are also abundant. Finally, pockets are common in the core and may contain multicoloured gem-quality tourmaline, smoky quartz, hydroxylherderite, cassiterite, cookeite, lepidolite, and beryl, among others.

TOURMALINE CHEMISTRY AND DISCUSSION

Tourmaline structural formulae have been normalized on a 15 T+Z+Y basis (Table 2). Tourmaline compositions have been recast into end-member

components according to the scheme of Pesquera *et al.* (2008). Overall, all the tourmalines from the Berry-Havey pegmatite are alkali tourmalines (Fig. 1a, Table 2), although important contents of vacancies are present in many cases (foitite component up to 52% and rossmanite component up to 45%). It is also noteworthy that some of the tourmalines from the core margin and core zone are F-rich. Tourmalines from the wall zone may be classified as schorl-rich dravites (Figs. 1a, b, Table 2). In the intermediate zones schorl and foitite are the two dominant tourmaline components, whereas in the core margin elbaite content increases and most greenish and bluish crystals are elbaite. In the core zone all the tourmalines are elbaite with high rossmanite content. In addition, some gemmy elbaite crystals from the pockets show a significant olenite component.

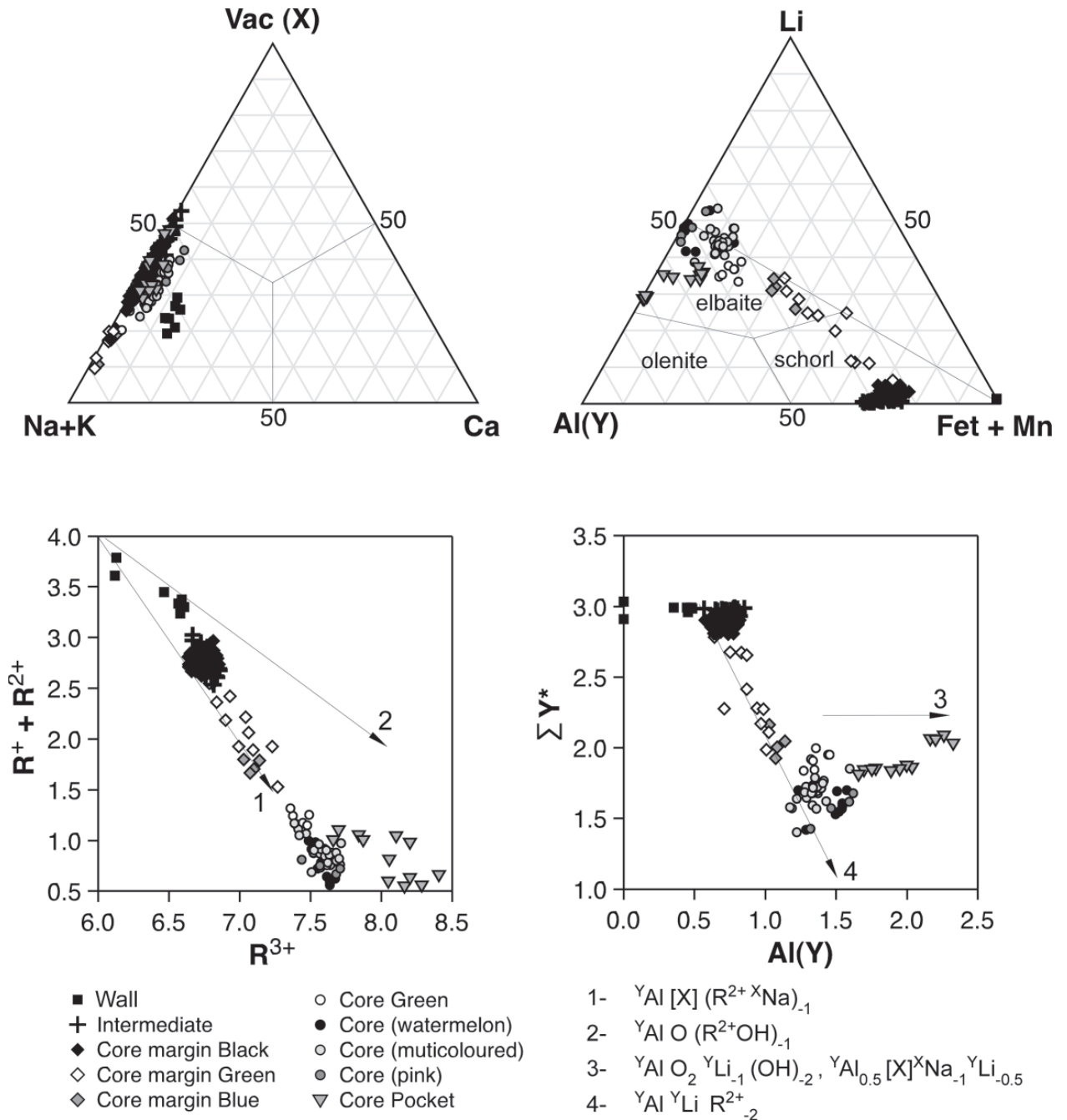


FIGURE 1. Chemical composition of tourmalines from the Berry-Havey pegmatite. (SY*=SY-Li)

The compositional variation of the Berry-Havey tourmalines accounts for fractionation processes via different mechanisms (Fig. 1 c, d). At the beginning of the crystallization the compositional changes observed in tourmaline may be explained by the exchange operators FeMg_{-1} and $\text{Al}[X]^X(\text{R}^{2+}\text{Na})_{-1}$. Starting with a dravite-rich composition, these exchange operations proceeded until the end of the crystallization of the intermediate zones. Later, during most of the crystallization of the core margin the Li and Al may have been incorporated according to the substitution schorl-elbaite (${}^Y\text{Al}{}^Y\text{Li}{}^Y\text{R}^{2+}_{-2}$), but at the

end, the exchange vector $[X]^Y\text{Al}_{0.5}{}^X\text{Na}_{-1}{}^Y\text{Li}_{-0.5}$ seems to have a strong influence for the crystallization of the pinkish crystals. During the crystallization of the gem tourmaline from the pockets, the enrichment of Al in tourmaline may be explained by the exchange vector ${}^Y\text{AlO}_2{}^Y\text{Li}_{-1}\text{OH}_{-2}$. The decrease in F and Li contents observed in some of the tourmalines from the pockets, in comparison with the elbaite from the core zone, could be related to the crystallization of late lepidolite, which would have depleted the Li and F contents.

Regarding the trace elements, no significant differences have been observed between the

TABLE 2. Structural formulae and components of tourmalines from the Havey pegmatite. WZ=Wall Zone, IZ= Intermediate Zones, CM= Core Margin, CZ= Core Zone, CZP= Core Zone Pockets, B= Black, G=green, Blu= Blue, P= Pink, WT= Watermelon, MC= Multicolored.

Sample n°	1	2	3	4	5	6	7	8	9	10	11	12	
Zone	WZ	IZ	IZ	CM	CM	CM	CZ	CZ	CZ	CZ	CZP	CZP	
Color	B	B	B	B	G	Blu	G	MC	P	WT	G	G	
Si	6.01	5.99	6.06	5.95	5.85	6.08	6.05	6.01	5.92	5.96	5.95	6.02	
Ti	0.09	0.01	0.01	0.01	0.00	0.01	0.02	0.00	0.00	0.01	0.01	0.00	
Al(T)	0.00	0.01	0.00	0.05	0.15	0.00	0.00	0.00	0.08	0.04	0.05	0.00	
Al(Z)	6.00	6.00	6.00	6.00	6.00	6.00	6.00	6.00	6.00	6.00	6.00	6.00	
Al(Y)	0.48	0.75	0.78	0.72	0.86	1.07	1.32	1.35	1.68	1.58	1.73	2.03	
Fe2+	1.03	1.82	1.72	2.10	1.08	0.71	0.29	0.23	0.00	0.00	0.09	0.00	
Fe3+(*)	0.00	0.00	0.00	0.00	0.36	0.00	0.00	0.04	0.00	0.02	0.00	0.00	
Mn	0.01	0.04	0.02	0.06	0.05	0.17	0.18	0.15	0.02	0.02	0.06	0.02	
Mg	1.37	0.34	0.40	0.00	0.00	0.00	0.00	0.00	0.00	0.00	0.00	0.00	
Li	0.01	0.03	0.02	0.08	0.72	0.92	1.10	1.20	1.38	1.41	1.13	0.92	
Zn	0.00	0.00	0.00	0.06	0.07	0.03	0.00	0.03	0.00	0.00	0.03	0.00	
Ca	0.13	0.02	0.02	0.01	0.00	0.02	0.02	0.06	0.07	0.01	0.04	0.00	
Na	0.63	0.60	0.51	0.59	0.80	0.79	0.71	0.68	0.50	0.59	0.57	0.59	
K	0.01	0.01	0.02	0.00	0.00	0.00	0.01	0.00	0.00	0.02	0.00	0.01	
(X)	0.23	0.37	0.46	0.40	0.20	0.19	0.26	0.26	0.42	0.38	0.38	0.39	
F	0.00	0.27	0.24	0.23	0.82	0.48	0.58	0.52	0.36	0.12	0.76	0.35	
Cl	0.00	0.00	0.00	0.00	0.00	0.00	0.00	0.01	0.00	0.02	0.00	0.00	
Schorl	23.6	38.8	33.4	45.9	23.7	19.3	6.8	5.2	0.0	0.0	0.6	0.0	
Dravite	27.0	6.7	7.1	0.0	0.0	0.0	0.0	0.0	0.0	0.0	0.0	0.0	
Olenite	12.4	12.6	10.7	8.9	0.0	0.0	0.3	0.0	0.0	0.0	9.0	24.1	
Elbaite	0.4	1.4	0.9	3.4	43.1	53.9	60.2	56.9	50.0	60.4	47.3	35.8	
Liddicoatite	0.0	0.0	0.0	0.9	0.0	0.0	2.0	2.3	6.0	7.2	0.6	4.0	0.2
Rossmannite	0.1	0.4	0.4	1.4	7.7	7.7	10.3	18.3	20.7	41.7	37.7	33.8	38.9
Foitite	10.0	30.8	36.5	37.1	11.5	7.9	4.9	3.9	0.0	0.0	2.8	0.0	
Mg-foitite	13.3	5.8	8.4	0.0	0.0	0.0	0.0	0.0	0.0	0.0	0.0	0.0	
Others	13.2	3.4	2.6	2.5	14.0	6.6	7.2	7.2	1.1	1.3	2.6	0.9	

tourmalines from the different zones except for some elements, and especially in the gem tourmalines from the pockets. Mn, Nb and Sn show a slight increase from the wall zone towards the core, with a final decrease in the pockets. The highest contents in Sc, Sr, and LREE are observed in the tourmaline from the wall zone, whereas the highest contents in W, Tl and HREE belong to the gemmy tourmaline from the pockets.

The textural and chemical variations observed in tourmaline from the pegmatite, from the wall zone to the core, suggest an inward crystal fractionation model. The development of the quartz-K-feldspar and quartz-tourmaline graphic intergrowths could indicate undercooling of the pegmatite melt. The development of quartz-tourmaline crowns around elongated tourmaline crystals frequently showing

pull-apart structures could be related to a sudden change in P conditions. Finally, the pockets located along the core zone of the pegmatite suggest elevated fluid activity during the last stages of crystallization of this pegmatite.

ACKNOWLEDGMENTS

This study has been carried out with the support of the UPV/EHU (project n° 08/02) and the Spanish CICYT (project n° CGL 2009-12677).

REFERENCES

Pesquera, A., Torres, F., Gil-Crespo, P. & Torres-Ruiz, J. (2008). *Min. Mag.* **72** (5): 1021-1034.

THE NYF PEGMATITES OF THE POTRERILLOS GRANITE, SAN LUIS RANGE, ARGENTINA

María Belén Roquet¹, Federico Bernard²,
Raúl Lira³ & Miguel Ángel Galliski⁴

- ¹ Departamento de Geología, Universidad Nacional de San Luis, Chacabuco y Pedernera, (5700) San Luis, Argentina.
² YPF, 9 de Septiembre esquina Roca s/n, Las Heras, Santa Cruz.
³ CONICET-CICTERRA, Museo de Mineralogía y Geología "Dr. A. Stelzner", F.C.E.F y N. Universidad Nacional de Córdoba. Av. V. Sársfield 299, (5000) Córdoba, Argentina.
⁴ IANIGLA, CCT Mendoza-CONICET, Avda. A. Ruiz Leal s/n, (5500) Mendoza, Argentina.

Key words: allanite-monzite - NYF pegmatites - intragranitic - Carboniferous

INTRODUCTION

The intragranitic pegmatites of Potrerillos have been less studied than the comparatively more widespread LCT pegmatites typically hosted in metamorphic rocks of the San Luis range. They were considered as possible examples of NYF or Hybrid pegmatites by Galliski (1994 a,b). This interpretation was supported by preliminary trace element geochemistry of K-feldspar and muscovite, which evidenced some primitive patterns typical of barren or poorly evolved granitic pegmatites (Galliski *et al.* 1997). In this communication, we address their geological setting, mineralogy and geochemistry, based on recent detailed studies carried out by Bernard (2009) and Roquet (2010), whose data classify the studied Potrerillos units as rare-element pegmatites of the *REL-REE* subclass and allanite-monzite type.

THE PEGMATITES

The pegmatites are located in the surroundings of the Potrerillos village, in the Libertador General San Martín department, San Luis province, Argentina. As a subgroup, they belong to the Conlara pegmatitic field, which is hosted in a granite suite of the post-orogenic Devonian to Carboniferous Las Chacras-Potreriillos batholith. The geological setting, petrology and geochemistry of the batholith was addressed by several researchers, particularly by Brogioni (1993, 1997), and more recently by Siegesmund *et al.* (2004) and López de Lucchi *et al.* (2007).

The subgroup is composed of six medium-sized bodies called: Rancul, La Elsa, Casa de Piedra, San Osmar, Potrerillos 2 and Catriel. Pegmatite body shapes are usually rounded or elliptical, less commonly irregular, with discrete sizes averaging from 10 to 50 m in diameter. The pegmatites show a vertical development, that possibly look like the turnip-shaped bodies described by other authors or are similar to thick lenses. They were mined for K-feldspar and quartz and minor beryl as a by-product, and all of them have open quarries with good exposures.

The mineralogy and fabric of the pegmatites are simple (Table 1). The zonation is ill-defined with

TABLE 1: Mineralogy of the Potrerillos Pegmatites

	Rancul	La Elsa	Piedra	Osmar	Potr2	Catriel
Quartz	▲	▲	▲	▲	▲	▲
K-feldspar	▲	▲	▲	▲	▲	▲
Albite	▲	▲	▲	▲	▲	▲
Biotite	■		■	■	■	■
Muscovite	■	■	■	■	■	■
Tourmaline	■	■	■	■	■	■
Beryl	●	●				●
Allanite				●	●	*
Fluorite		●				
Fluorapatite	●		●	●	●	
Monazite		*				*
Ilmenite	●					
Ilmenorutile	●				●	●
Rutile	●			●		●
Pyrochlore	*					
Scheelite			*			
Hematite	●	●		●	●	
Pyrite	●	●				●
Bismuthinite			*			
Molibdenite			*			
Bismuthite	*					
Clinovisbanite	*					
Goethite	●		●	●		
Mn-oxides	●					
Opal			*			

Minerals: ▲ major, ■ accessory, ● subordinate, * rare

a border-wall zone where the granite transitionally grades to a coarse-grained intermediate zone composed of K-feldspar and quartz, with minor albite, normally interstitial, or forming spherical aggregates in some bodies.

The core zone is irregular and discontinuous, poorly defined, normally made of milky to pink or gray quartz with inclusions of large, isolated crystals of K-feldspar and primary anhedral pods of fluorite

as in the La Elsa pegmatite. Biotite is a common accessory mineral occurring as 5 to 10 cm wide black booklets, irregularly concentrated in the intermediate zone. Muscovite is more widespread, associated with K-feldspar or quartz. Black tourmaline, in radiating crystals or in broken prisms, is a common minor accessory mineral in all the studied pegmatites. Beryl in blue, sometimes gemmy crystals or more commonly in yellowish green prisms up to 5-7 cm long is abundant and is associated with albite, tourmaline or included in quartz. Fluorapatite is also abundant, in anhedral gray to green crystals or in thin prisms. Prismatic allanite-(Ce) up to 2 cm long occurs included in quartz but is not found in all the pegmatites; scarce monazite-(Ce) occurs in small, cm-sized crystals, though it is more common in microscopic sizes. Ilmenorutile is a quite common accessory and contains inclusions of U-bearing pyrochlore. Hematite is a common oxide in masses of 5 to 10 cm. A couple of pegmatites contain aggregates of rutile crystals sized 0.5 to 3 cm, often with profuse hematite exsolution. Scheelite is very rare and only occurs in one pegmatite. Pyrite in 2 to 10 cm anhedral masses, variably replaced by goethite, is present in most pegmatites normally included in core quartz. Bismuthinite is occasionally present but it is more commonly altered to bismuthite or, more rarely, to clinobisvanite. Goethite, Mn-oxides and opal occur in some of the pegmatites. Muscovite of the San Osmar pegmatite was dated in 359 ± 12 Ma by Galliski and Linares (1999).

THE PARENTAL GRANITE

The Potrerillos pluton is the southernmost intrusive of the Las Chacras-Potreriillos (LCPC) batholith. It is composed of three predominant facies that according to Siegesmund *et al.* (2004) are a biotite porphyritic granite (BPG), a biotite-bearing equigranular red granite (BRG) and a muscovite-bearing equigranular red granite (MRG). The BPG has been dated by the same authors yielding a U-Pb zircon age of 382 ± 5 Ma and cooling ages in biotite of 362 ± 8 and 352 ± 7 Ma.

Studied pegmatites are hosted by two main lithologic units, one of them being a coarse-grained porphyritic monzogranite equivalent to the BRG and the other a coarse grained equigranular monzogranite equivalent to the MRG.

The porphyritic monzogranite is composed by $Qtz + Mc + Pl + Bt \pm Ttn \pm Zrn \pm Mnz \pm Aln \pm Ap \pm Rt \pm Mag$. It is of metaluminous chemistry, enriched in Fe_2O_3 , CaO, MgO and TiO_2 relative to the equigranular facies. It shows enrichment in some trace elements like Sr (360-430 ppm), Zr (204-286), Ba (453-922), Y (31-49) and depletion in Rb (150-178), Nb (14-20) and Th (19.7-26.7), with a La/Lu_N ratio that ranges from 19.35 to 27.88 and Eu/Eu^* that varies from 0.42 to 0.54.

The equigranular monzogranite is a pink rock composed by $Qtz + Mc \pm Pl \pm Ms \pm Bt \pm Zrn \pm Ap \pm$

$Mag \pm Hem$. Secondary albite and muscovite are common. This granite is calc-alkaline, mildly peraluminous with a high-K, high silica chemical signature and shows depletion in Fe_2O_3 , CaO, MgO, TiO_2 , Sr, Ba, Zr and enrichment in Rb, Y, Nb and Th compared to the porphyritic monzogranite. It is also characterized by a moderate Eu anomaly ($Eu/Eu^* = 0.23$).

The post-Famatinian orogenic emplacement of the LCPC batholith, the petrographic signature, the metaluminous to slightly peraluminous chemistry and the REE normalized pattern, very similar to typical NYF granites though more depleted in HREE (Fig. 1), are attributes that suggest that both, the Potrerillos

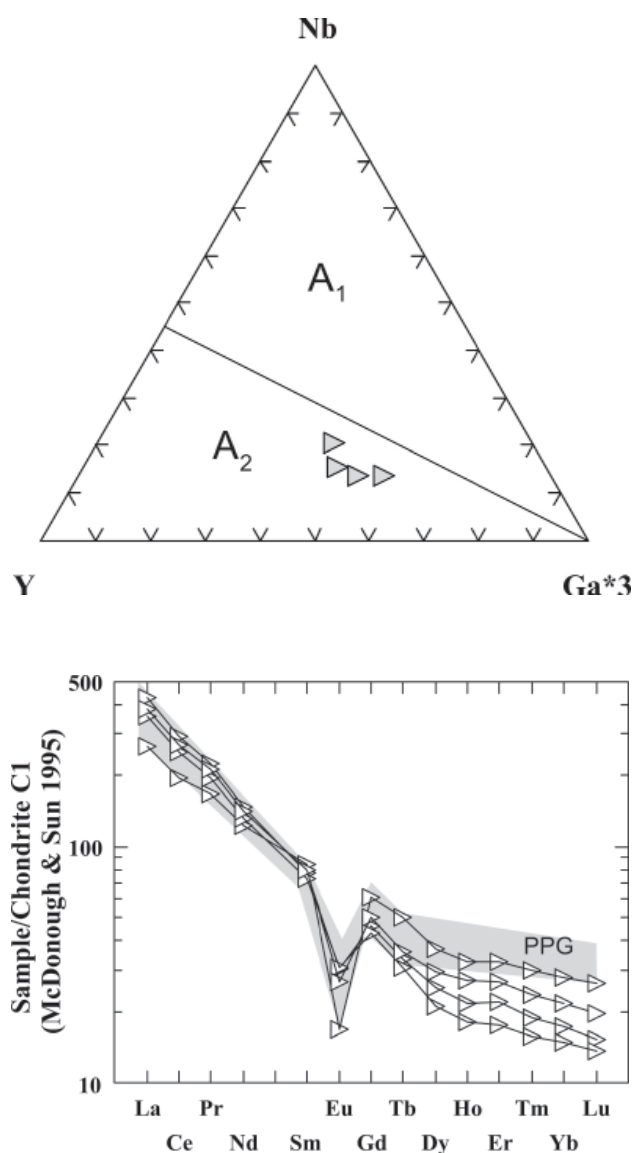


FIGURE 1: Plot of the Potrerillos granite in the Eby (1992) A-type granites discrimination triangle, and chondrite normalized REE profiles of the Potrerillos granite compared with the typical pattern of the Pikes Peak granite taken from Smith *et al.* (1999).

pegmatites and their parental granites, belong to an aluminous suite of A-type granites possibly originated by partial melting of a depleted garnet-bearing lower crust, previously metasomatized by a mantle fluid component. The mineralogy of the pegmatites ascribes them to the allanite-monazite type, *REL-REE* subclass of the Černý and Ercit (2005) classification scheme.

ACKNOWLEDGEMENTS

Grants PIP 5907 and 857 of CONICET, PICT 21638 of FONCYT and Project 349001 of CyT financed the research. The authors are very grateful to the careful review of Wm. Simmons, K. Webber. A. Falster.

REFERENCES

- Bernard, F. (2009). Pegmatitas intragraníticas del plutón Potrerillos, Sierras de San Luis: geología, mineralogía y génesis. Graduate thesis, Facultad de Ciencias Exactas, Físicas y Naturales, Universidad Nacional de Córdoba, 103 p.
- Brogioni, N. (1993). El batolito de Las Chacras-Piedras Coloradas, provincia de San Luis, geocronología Rb-Sr y ambiente tectónico. XII Congreso Geológico Argentino y II Congreso de Exploración de Hidrocarburos, Actas IV: 54-60.
- Brogioni, N. (1997). Mineralogía y petrografía del batolito de Las Chacras-Piedras Coloradas, San Luis. *Rev. Asoc. Geol. Argentina* **52**(4): 515-538.
- Černý, P. & Ercit, T.S. (2005). The classification of granitic pegmatites revisited. *Can. Mineral.* **43**: 2005-2026.
- Eby, G. N. (1992). Chemical subdivision of the A-type granitoids: Petrogenetic and tectonic implications. *Geology* **20**: 641-644.
- Galliski, M. A. (1994a). La Provincia Pegmatítica Pampeana: I Tipología y Distribución de sus Distritos Económicos. *Rev. Asoc. Geol. Argentina* **49**: 99-112.
- Galliski, M. A. (1994b). La Provincia Pegmatítica Pampeana: II Metalogénesis de sus Distritos Económicos. *Rev. Asoc. Geol. Argentina* **49**: 113-122.
- Galliski, M. A. & Linares, E. (1999). New K-Ar muscovite ages from granitic pegmatites of the Pampean Pegmatite Province. In II South American Symposium on Isotope Geology, Actas, 63-67. SEGEMAR, Anales 34. Buenos Aires, Argentina.
- Galliski, M. A., Perino, E., Gásquez, J., Márquez Zavalía, M. F. & Olsina, R. (1997). Geoquímica de feldespatos potásicos y muscovitas como guía de exploración de pegmatitas graníticas de las sierras Pampeanas. *Rev. Asoc. Geol. Argentina* **52**: 24-32.
- López de Luchi, M. G., Siegesmund, S., Wemmer, K., Steenken, A. & Naumann, R. (2007). Geochemical constraints on the petrogenesis of the Paleozoic granites of the Sierra de San Luis, Sierras Pampeanas, Argentina. *J. South American Earth Sciences* **24**: 138-166.
- Roquet, M. B. (2010). Mineralogía, geoquímica, tipología y relación con los granitoides de las pegmatitas del grupo Villa Praga-Las Lagunas, distrito Conlara, Sierra de San Luis. Ph D thesis, Universidad Nacional de Córdoba, 409 p.
- Siegesmund, S., Steenken, A., López de Luchi, M. G., Wemmer, K., Hoffmann, A. & Mosch, F. (2004). The Las Chacras-Potrerillos batholith (Pampean Ranges, Argentina): structural evidences, emplacement and timing of the intrusion. *Int. J. Earth Sciences* **93**: 23-43.
- Smith, D.R., Noblett, J., Wobus, R.A., Unruh, D., Douglass, J., Beane, R., Davis, C., Goldman, S., Kay, G., Gustavson, B., Saltoun, B. & Stewart, J. (1999). Petrology and geochemistry of late-stage intrusions of the A-type, mid-Proterozoic Pikes Peak batholith (Central Colorado, USA): implications for petrogenetic models. *Precambrian Research* **98**: 271-305.

TECHNOLOGICAL CHARACTERIZATION OF MUSCOVITE FROM THE PEGMATITES DISTRICTS OF CRISTAIS - RUSSAS (DPCR) AND SOLONÓPOLE - QUIXERAMOBIM (DPSQ) – CEARÁ, NORTHEAST BRAZIL

Gabriela Meireles Rosa¹, Martha Noélia Lima², Débora Macedo do Nascimento¹, Tereza Falcão de Oliveira Neri¹, Francisco Diones Oliveira Silva¹, Andressa de Araujo Carneiro¹, José de Araújo Nogueira Neto¹ & José Cleyton Vasconcelos³

¹ Federal University of Ceará (UFC), Geology Department, Campus of Pici – Pici. Zip code: 60.455-760 Fortaleza, CE – Brazil. gabrielameirelesrosa@hotmail.com

² University of Aveiro (UA), Department of Geociencias, Campus of Santiago – Aveiro. Zip code: 3810-193 Aveiro, Portugal.

³ Master Teacher In Memorium

Key words: Pegmatite, Muscovite, Technological Characterization

INTRODUCTION

The pegmatites that carry muscovites are important both in terms of geological and economical point of view. They represent sources of minerals that are used by industrial technology. Pegmatite districts Cristais - Russas (DPCR) and Solonópole - Quixeramobim (DPSQ) are inserted in the central region of the state of Ceará - Brazil, representing two major producers of muscovite, which have large scale applications in the electric and electronic industries. This work presents the characterization of two parameters useful as background information and quantification of industrial processes using muscovites of the DPCR and DPSQ: dielectric constant (K) and colorimetric indices.

GEOLOGICAL FRAMEWORK

The Sub-Pegmatite Province of Ceará (SPCE) is inserted in the Province of Borborema (PB), which exhibits great diversity in lithostratigraphic and tectonic-metamorphic characteristics. Among the several Precambrian terrains of Ceará, we can find the pegmatites in the Domains Orós-Jaguaribe (DOJ) and Ceará Central (DCC), both cut by major shear zones. The subdivision of Pegmatite Province of Ceará, proposed by Souza (1985) differentiates two main districts: District of Cristais-Russas (DPCR) and District Solonópole-Quixeramobim (DPSQ), which are the targets of this research (Fig. 1).

The Senador Pompeu and Orós shear zones limit the great two pegmatite districts and seem to have influenced the regional structure, not only the rocks from the basement (“paleoproterozoic terranes”) but also the plutonic rocks (Marques Jr. et al, 1988; Marques Jr, 1992, Marques Jr & Nogueira Neto, 1992). The factors that control the positioning and the mineralization of the pegmatites in the region are: tectonics, lithology, size, and internal arrangement of

the bodies (Marques Jr, 1992). These occur as veins filling discontinuities (faults, fractures, and foliation) or as more expressive bodies whose thickness and length reach tens of meters.

Regarding lithological control, the complex heterogeneous pegmatites are generally restricted to the intrusions in the gneisses, while the simple homogeneous pegmatites occur both in gneisses as in granites. The homogeneous pegmatites show a simple mineralogy consisting of feldspars, quartz, and muscovite, but may be mineralized in beryl and tourmaline. Some more simple heterogeneous terms show a slightly zoning with predominance of aplitic textures in the rims and coarse texture in the cores of the bodies, often with tourmaline, beryl, apatite, and amblygonite (Marques Jr et al, 1988; Marques Jr, 1992 and Marques Jr & Nogueira Neto, 1992).

The pegmatites of these regions intruded in a biotite-muscovite granite, along a normal fault. They are tabular shaped, heterogeneous complex with sometimes incomplete zoning, being characterized by “body replacement” with albite, muscovite, and lepidolite. In the rims of the body predominate aplitic texture (zone I). The zone II is marked by the presence of graphic texture of quartz-feldspar and by the association potassium feldspar + quartz + mica. The zone III presents small “concentrations” of the remains of potassic feldspar in contact with albite and tourmaline are found in these areas. The association tourmaline + albite is close to the quartz core (zone IV).

TECHNOLOGICAL CHARACTERIZATION

The dielectric constant measures the ability of the material to store charge, being an intrinsic property of each material, which allows to predict the behavior of the material and the electrical properties (insulators, conductors, etc.).



FIGURE 1. Geological map of the state of Ceará with your major shear zones and location of studied area highlighting the pegmatite districts from Cristais-Russas (DPCR) and Solonópole-Quixeramobim (DPSQ), Ceará-Brazil.

In the specific case of muscovites this constant is of extreme importance, since they correspond to the raw material used in industrial processes for the manufacture of electrical and electronic components, given their high dielectric constant (Lima 2006; Gomes 2006). (Fig. 2).

The color corresponds to a physical property of materials, which depends on the light radiation that can be absorbed, filtered, reflected, refracted or interfere with each other, and also represents relevance in technological products.

DIELECTRIC CONSTANT AND COLORIMETRIC INDICES

The dielectric constants (K) for employment in industrial electronics must have minimum values of approximately 4 (K~4). In this context, the muscovites DPCR exhibited K values ranging 2.65 to 5.51. It is noteworthy that the most significant values of K are present in pegmatites in the region of crystals within the DPCR. DPSQ on the values of K in turn, were positioned between 3.09 and 5.03. So far the data on dielectric constants found in DPCR, as those obtained in DPSQ, record for the most likely values to use as feedstock for industrial processes for the manufacture of components and instruments insulators.

The colorimetric readings of muscovites DPCR exhibited the values of E^* (Full Color) ranged from 60.68 to 77.36 on average. In its turn the parameters registered in the E^* DPSQ showed values between 45.92 and 76.63. The set of colorimetric analysis of muscovite in both districts (DPCR and DPSQ) shows that those specimens known by miners as "Ruby" intense purple color, like dark gray coloring, have color values that vary total E^* between approximately 44.9 and 60.1. Micas said "champagne" have values



FIGURE 2. Muscovites extracted from pegmatites of the region, widely applied in electric and electronic industries.

of E^* between 61 and 65 approximately. For E^* e'' 65 and below 70 muscovites demonstrate the colors light green, on the other hand, those with values above 70 are located as silver-gray.

REFERENCES

- Gomes, I. P. (2006). Mapeamento Geológico e Potencial Metalogenético de uma Área Localizada no Município de Banabuiú, NE do Estado do Ceará (Área I). Universidade Federal do Ceará – UFC, Fortaleza – CE. Relatório de Graduação, 69p.
- Lima, M. N. (2006). Mapeamento Geológico e Potencial Metalogenético de uma Porção Localizada no Município de Banabuiú, Nordeste do Estado do Ceará (Área II). Universidade Federal do Ceará – UFC, Fortaleza - CE. Relatório de Graduação, 92p.
- Marques JR., F., Nogueira Neto, J. A. & Néri, T. F. O. (1988). Contribuição à Geologia do Campo Pegmatítico de Berilândia, Ceará. IN : Anais do XXXV Congresso Brasileiro de Geologia, Belém 1: 329–337.
- Marques JR., F. (1992). Geologia do Campo Pegmatítico de Berilândia-CE. Instituto de Geociências. Universidade de São Paulo. São Paulo. Dissertação de Mestrado. 152p.
- Marques JR., F. & Nogueira Neto, J. A. (1992). Considerações Petrogenéticas do Campo Pegmatítico de Berilândia (CE). In: 37º Congresso Brasileiro de Geologia, São Paulo. Anais do 37º Congresso Brasileiro de Geologia. São Paulo: Sociedade Brasileira de Geologia 2: 53-54.
- Souza, J. V. de (1985). Geologia dos Pegmatitos de Metais Raros da Região W e NW de Solonópole – CE. Tese de Professor Titular. Departamento de Geologia - UFC. Fortaleza - CE. 109p.

K-FELDSPAR MINERALS DEFINED FROM THEIR TWIN-STRUCTURES: APPLICATION TO A PRELIMINARY CLASSIFICATION OF PEGMATITES

Luis Sánchez-Muñoz^{1§}, Javier García-Guinea², Victor Ye. Zagorsky³, Odulio J.M. de Moura⁴ & Peter J. Modreski⁵

¹ Institute for Ceramics and Glasses (CSIC), Campus de Cantoblanco, Kelsen 5, 28049 Madrid, Spain. § lsm@icv.csic.es

² Museo Nacional de Ciencias Naturales (CSIC), C/ Jose Gutierrez Abascal 2, 28006 Madrid, Spain

³ Vinogradov Institute of Geochemistry, Siberian Branch of Russian Academy of Sciences, Irkutsk, Russia

⁴ Joaquim Neves Ferreira, 238, Barrio Vila Bretas, CEP 35030-391 Governador Valdares, MG, Brazil

⁵ U.S. Geological Survey, Federal Center Denver, CO 80225-0046, USA

Key words: K-feldspars, twin-structures, classification of pegmatites

INTRODUCTION

The more common minerals in the earth crust, i.e., quartz and feldspars, teach us in a very different way about what a crystal is and how it behaves. While most quartz specimens are in general terms apparently very similar, feldspars exhibit astounding diversity particularly from the microstructural point of view. However, it is generally thought that this problematical mineral group is not able to supply any valuable information to geologists, except as a chemical compound to be used in rock classifications. The consequence of such a pessimistic view is that petrologists, when investigating tectonic setting or petrogenetic processes in igneous rocks, have always preferred geochemical data to other structural information like Si/Al order in feldspars. Actually, the only application of the K-feldspars (with the conventional definitions) in igneous petrology is the obvious distinction between volcanic (sanidine) and plutonic rocks (orthoclase or microcline). This work is an attempt to differentiate K-feldspars by means of the twin-structure (-ts) concept (Sánchez-Muñoz *et al.* 2009a, b), hence being useful in understanding granite pegmatites and their tectonic setting from a new perspective.

THE PROBLEM OF FELDSPARS

The conventional definition of a mineral accepted by most geologists is directly related to the view that most solid-state physicists have about the *crystalline state*, a scientific field that supposedly started (from their particular historical point of view) in the early twentieth century with the first experiment of X-ray diffraction by a crystal. The local geometrical order from short-range forces, as well as homogeneity and constant chemical composition are the fundamental features that define mineral species, and equilibrium thermodynamics is expected to make

correct predictions about the existence or not of a certain "phase". Twins are seen as non-equilibrium and undesirable defects, away from the relevant information that supposedly mainly concerns the cell lattice to build up perfect polyhedral solids. Thus, the crystalline state is reduced to a *simple system* where the crystal size is totally irrelevant.

In feldspars, and specifically in K-feldspars, homogeneity is not the appropriate characteristic used to describe their mineral structures. When extended pristine volumes of this particular *crystalline medium* are studied in detail using large specimens (i.e. from pegmatites), long-distant regularities as twin-structures formed during the subsolidus stage can be seen as the essential feature to develop their genuine natural identity. These crystalline patterns are interpreted as the result of not only short-range atomic diffusion but also long-range elastic-strain correlations, where not only a deterministic but also stochastic phenomenon must be invoked (Sánchez-Muñoz *et al.* 2009a, b). In this view, the crystalline medium should be considered as a *complex system* (Sánchez-Muñoz *et al.* 2006a, b), and the elastic strain distribution as well as the crystal size effects are needed to understand their behaviour when building such a kind of patterns (Sánchez-Muñoz *et al.* 2008).

K-FELDSPAR TWIN-STRUCTURES

Sanidine, orthoclase and microcline are the three *mineral species* recognized by IMA for K-feldspars, and thus our nomenclature system is based on those terms. However, in our proposal, homogeneity to obtain certain averaged or bulk values on pulverized samples is not the final objective, but to study extended mineral patterns on large crystalline volumes.

The term *sanidine-ts* is proposed for the primary mineral directly formed from melt with absence of any microstructural signature from subsolidus Si/

TABLE 1. Preliminary classification of pegmatites using twin-structure characteristics in perthitic K-feldspars

FEATURES	SUB-VOLCANIC ROCKS	OROGENIC EVENTS		PLUTONIC ROCKS		NON-OROGENIC EVENTS	
		Syn-orogenic ("peraluminous") suites	Late-orogenic suites	Late-orogenic suites	Post- or an-orogenic suites		
Typical features in the twin-structure see reference (1)	Absent	Tweed partially recrystallized into A/P twins from interfaces	Coarse poly synthetic and chessboard twinning, with very residual tweed	Large A/P twins with serrated boundaries mainly along P twins	From crypto- to micro-crosshatched texture partially recrystallized into A/P twins with many different configurations and orientations		
K-feldspars as defined in this work from their twin-structure (-ts)	Sanidine-ts	Orthoclase-ts > Microcline-ts	Microcline-ts (residual orthoclase-ts)	Microcline-ts	Orthoclase-ts (minor microcline-ts)		Microcline-ts (minor orthoclase-ts)
Schemes of local Si/Al order	HS to LS	HM > from IM to LM end member	Close to LM end-member (also LM in OR)	Close to LM end-member	Close to LM end-member		Close to LM end-member
SAN → OR	Absent	Si/Al ordering can be inhibited chemically by some elements like P (6) (11)			Tweed, crypto- to micro-crosshatched		
OR → MIC	Absent	Rational ± A and ± P twins with many crossovers (chessboards)			Absent		Rational and irrational ± A and ± P twins
MIC → MIC	Absent	Absent and ± A and ± P twins can be preserved	By fine twins, mainly ± A twin from ± P twins, ("energy storage")	To form twins as single-crystal volumes ("energy release")	Absent		Either by fine or coarse twins, in several different episodes
Perthites and Na-feldspars	Corrugated nano-films	Bimodal sizes, with films and veins/patches	Films, veins and sizes in between the two types	Mainly very large veins	Veins to patches		Irregular veins
Color or varieties	Moonstone	Transparent, white, yellow, pink					Yellow, red, black, green-blue (amazonite)
Luminescence (TL, CL, PL)	UV, blue and a low TL effects	UV, blue with a very strong TL effect	UV and blue in pristine areas, only red when interaction with water-rich fluids				Strong UV and blue in low iron samples, red in iron-rich samples, IR en REE-rich samples
Geochemistry (2)	-	LCT suite (B-Be-P-Ta-Li-enriched pegmatites)					NYF suite (REE-Nb-Y-F-Ti-U-enriched pegm.)
Classification (3)	-	AB, MS and REL classes					MS and MI class MS class -REE subclass
Examples of pegmatites and K-feldspars from other rocks (references)	Rabb Park, NM, USA (4)	-La Isla pegm., Belvis de Monroy, Spain (5) -South Mt Batholith, Nova Scotia, Canada (6) -Fermin pegm., Linópolis, MG, Brazil (7)	-Golconda III, Gov. Valadares, MG, Brazil (5) -Helio pegm, Itambé, Bahia, Brazil (5) -Specimen from Wyangala, Australia (8)	-Wray pegmatite, Spruce Pine, NC, USA -Pau Alto, Jequitinhonha River, MG, Brazil -Specimen 292, from Norway in ref (8)	-Voinovka charnockite from Novo-Ukraine Massif (9) -Zarzalejo porphyry (Madrid, Spain)		- Madagascar pegms. -Karelia-Kola Peninsula region, Russia (9,10)

(1) Sánchez-Muñoz *et al.* (2009a,b); (2) Martin & De Vito (2005); (3) Černý & Ercit (2005); (4) O'Brient (1986); (5) Sánchez-Muñoz *et al.* (2006a and b); (6) Kontak *et al.* 1996; (7) Sánchez-Muñoz *et al.* (2008); (8) Fitz Gerald & McLaren (1982); (9) Marfuntin (1966); (10) Shimakin *et al.* (1999); (11) Breiter *et al.* (1997). *Abbreviations:* Schemes of local Si/Al order: HM high microcline, IM intermediate microcline, LM low microcline (see Bamberger *et al.* 1989). Luminescence techniques: TL thermoluminescence, CL cathodoluminescence and PL photoluminescence. Pegmatite classification: AB abyssal class; MS muscovite class; REL rare-element class; MI miarolitic class, REE rare-earth element subclass (see Černý and Ercit 2005).

Al ordering, thus with a high local disorder, showing schemes of Si/Al order ranging from those of the high to low sanidine (HS to HS) as defined by Ribbe (1984) if considering a monoclinic topology.

The name *orthoclase-ts* is proposed for patterns in triclinic K-feldspars directly produced after sanidine by the homogeneous nucleation of many coexisting and woven discrete solid-state recrystallization events following mainly four orientation variants (\pm Albite, \pm Pericline) separated by more or less diffuse or sharp limits. The resulting grid microstructure can be resolved in transmission electron microscopy as “tweed” contrasts, or seen at the optical scale as crypto-to-micro crosshatched patterns. As a result of the many intersections between the different variants, volumes with mixed orientations and wavy patterns in obliquity (deviations from the orthogonality) occur throughout the crystalline medium. The local schemes of Si/Al order are also highly heterogeneous and range from the high to low microcline end-member (HM to LM). In this definition, local order is not the criteria used for defining the mineral species but its critical behaviour to give the typical tartan patterns at different size scales. Thus occasionally the cell angles α and γ can be very close (or even equal) to 90° but the “m” plane and the “two-fold” axis of the monoclinic symmetry are absent at the atomic scale.

The word *microcline-ts* is proposed to designate patterns produced by the solid-state recrystallization of orthoclase, in the form of avalanche-like events (as discrete pulses or in self-organized sets) that become regular and relatively homogeneous regions with sharp boundaries, either as rational or irrational (diagonal and anti-diagonal) twins, locally always close to the LM Si/Al order. Irregular microcline as defined by Bambauer *et al.* (1989) is a transitional product from the conversion of orthoclase into microcline (Sánchez-Muñoz *et al.* 2009b). The many recrystallization events can be crossed to form many “crossovers” as in the chessboard microstructure, or not, as in the parquet microstructure. Microcline patterns are very often recrystallized into newer ones, either with finer twins (storage of tectonic energy) or evolving to form single-crystal like regions (release of internal energy), with serrated boundaries (Fitz Gerald & McLaren, 1982) as a typical intermediate configuration.

K-FELDSPAR BASED CLASSIFICATION OF PEGMATITES

The usefulness of these definitions is tested in trying to systematically classify granitic pegmatites (Table 1) by considering mainly tectonic setting (Martin & De Vito, 2005). Other characteristics have also been included such as color, luminescence and typical perthitic textures. The types of pegmatite were distinguished by the predominance of a particular K-feldspar-ts in their inner parts (intermediate zone

or core): i) sub-volcanic pegmatites with preserved sanidine-ts; ii) syn-orogenic pegmatites with “tweed” orthoclase-ts typically having a high content in P_2O_5 ; iii) syn-orogenic pegmatites with microcline-ts formed by fine twins; iv) late-orogenic pegmatites with a microcline-ts formed mainly by a single orientation variant; v) post- and anorogenic pegmatites formed by several orthoclase-ts partially or totally replaced by microcline-ts. Some examples of each type of pegmatite from the author work as well as from selected references can be found in Table 1.

REFERENCES

- Bambauer, H.U., Krause, C., & Kroll, H. (1989). TEM-investigation of the sanidine/ microcline transition metamorphic zones: the K-feldspar varieties. *Eur. J. Mineral.* **1**: 47-58.
- Breiter, K., Fryda, J., Seltmann, R. & Thomas, R. (1997). Mineralogical evidence for two magmatic stages in the evolution of an extremely fractionated P-rich rare-metal granite: the Podlesí stock, Krusne Hory, Czech Republic. *J. Petrol.* **38**: 1723-1739.
- Černý, P. & Ercit, T.S. (2005). The classification of granitic pegmatites revisited. *Can. Mineral.* **43**: 2005-2026.
- Fitz Gerald, J.D. & McLaren, A.C. (1982). The microstructures of microcline from some granitic rocks and pegmatites. *Contrib. Mineral. Petrol.* **80**: 219-229.
- Kontak, D.J., Martin, R.F. & Richard, L. (1996). Patterns of phosphorus enrichment in alkali feldspars, South Mountain Batholith, Canada. *Eur. J. Mineral.* **8**: 805-824
- Marfunin, A.S. (1966). The feldspars. Phase relations, optical properties, and geological distribution. Israel Program for Scientific Translations, Jerusalem, 317pp.
- Martin, R.F. & De Vito (2005). The patterns of enrichment in felsic pegmatites ultimately depend on tectonic setting. *Can. Mineral* **43**: 2027-2048.
- O'Brient, J.D. (1986). Preservation of primary magmatic features in subvolcanic pegmatites, aplites and granite from Rabb Park, New Mexico. *Am. Mineral.* **71**: 608-624
- Ribbe, P.H. (1984). Average structures of alkali and plagioclase feldspars: systematic and applications. En: *Feldspars and Feldspathoids. Structures, Properties, and Occurrences*, Ed. W.L. Brown, Proc. NATO, Series C, 137, Reidel Publishing Comp. Dordrecht, 1-54.
- Sánchez-Muñoz, L., García Guinea, J. & Sanz, J. (2006a). Static and dynamic regimes in the structural evolution of perthitic microclines. *Bol. Soc. Esp. Ceram.V.* **45**: 289-299.

- Sánchez-Muñoz, L., Rouer, O., Sanz, J. & García Guinea, J. (2006b). Mechanism of construction-destruction of macrostructural patterns in perthitic microclines as complex systems. *Bol. Soc. Esp. Ceram.* V. **45**: 321-329.
- Sánchez-Muñoz, L., García-Guinea, J., Beny, J.M., Rouer, O., Correcher, V., Sanz, J. & De Moura, O.J.M. (2008). Mineral self-organization during the orthoclase-microcline transformation in a granite pegmatite. *Eur. J. Mineral.* **20**: 439-446.
- Sánchez-Muñoz, L., Crespo, E., García-Guinea, J., de Moura, O.J.M. & Zagorsky, V. Ye. (2009a). What is a twin-structure? An answer from microcline minerals from pegmatites. *Estudios Geológicos* **19**: 240-245.
- Sánchez-Muñoz, L., García-Guinea, J., Crespo, E. & Rubio, J. (2009b). Twinning in K-feldspars from the interplay between the ionic and electronic lattices. *Estudios Geológicos* **19**: 234-239.
- Shmakin, B.M., Makagon, V.M., Zagorsky, V.Ye. & Peretyazhko, I.S. (1999). On the extreme concentration of some minor elements in pegmatites. *Can.Mineral.* **37**:843-844.

K-FELDSPAR TWIN-STRUCTURES FROM OROGENIC AND ANOROGENIC GRANITIC PEGMATITES IN CENTRAL NORTH AMERICA

Luis Sánchez-Muñoz^{1§}, Peter J. Modreski² & B. Ronald Frost³

¹ Institute for Ceramics and Glasses, CSIC, Kelsen 5, Campus de Cantoblanco, 28049 Madrid, Spain. § lsm@icv.csic.es

² U.S. Geological Survey, Federal Center Denver, CO 80225-0046, USA

³ Dpt. Geology and Geophysics, University of Wyoming, Laramie, WY 82071, USA

Keywords: K-feldspars, twin-structures, orogenic-anorogenic pegmatites

INTRODUCTION

Nowadays, systematic classifications, petrogenetic and geotectonic analyses of igneous rocks use minerals as being simple and homogeneous solid phases, including K-feldspar, although most would accept that “no two feldspars are alike”. Geochemical data are considered as the most valuable source of information, whereas structural-microstructural mineral features are seen as complementary facts. The suggestion of Marmo (1971) to distinguish orthoclase granites and microcline granites (the former being mainly post-kinematic granites, such as Rapakivi and Alpine granites, and the latter mainly syn- or late-kinematic granites) has not been accepted in general terms. In this work, that hypothesis is explored by studying the perthitic K-feldspars of twenty-four Proterozoic pegmatites from central North America. Samples with well preserved features that were formed in the subsolidus stage were studied by optical microscopy, X-ray powder diffraction and X-ray fluorescence. The K-feldspar minerals and their microstructures were analyzed by means of the twin-structure (-ts) concept (Sánchez-Muñoz et al. 2009; Sánchez-Muñoz et al. 2011).

SELECTED PEGMATITES FROM CENTRAL NORTH AMERICA

LCT-, NYF- and hybrid pegmatites (Table I) were distinguished from their mineral paragenesis (Černý & Ercit 2005; Martin & De Vito 2005). In most cases it was possible to correlate the LCT and NYF pegmatites with the Roult & Berthoud suites of Tweto (1987), or the 1.7 Ga orogenic plutonism, and the 1.4

Ga and 1.1 Ga anorogenic plutonism of Anderson & Cullers (1999). One rock (Clora May pegmatite) shows a hybrid character; Hanson et al. (1992) provided information on other pegmatites of this district.

The more distinctive characteristics of the LCT suite are: i) presence of B-Be-P-Ta-Li-rich minerals, ii) lens shaped or elongate dikes hosted in metamorphic rocks (mainly high-grade sillimanite gneisses); iii) a peraluminous character is noted from the crystallization of muscovite, garnet and cordierite as primary minerals, with biotite being a major mineral only in one pegmatite of the abyssal class (i.e., Roscoe Beryl pegm.); iv) their external zone consist of a porphyritic texture with perthite (in some cases in a graphic texture) as phenocrysts in a finer-grained matrix composed of quartz, albite and muscovite; v) the degree of zonation can show a great variability, from a simple increase in grain size to the center (i.e., in the Douglas Mt. pegm.), to a well-developed internal structure, as in the Black Hill pegmatites.

On the other hand, the main features of the NYF pegmatites are: i) presence of REE-Ti-F-Nb-U-rich minerals; ii) an elliptical-circular shape in plan view, hosted in their parental granites with gradational contact; iii) biotite is a major primary mineral, whereas muscovite appears sometimes in secondary replacement units; iv) their external zone is almost always composed of a graphic intergrowth; v) a very well-developed concentric and sharp internal zonation occurs in most cases, either as bizonal (small external zone with a large composite internal zone formed by K-feldspar and quartz) or polyzonal bodies (a perthite-bearing intermediate zone and a quartz core), as in the McGuire and Elkhorn I-II pegmatites, respectively.

TABLE 1. Classification of granite pegmatite studied in this work

A.- LCT pegmatites

Area	Locality (district)	Pegmatite name (CODE)	Coordinates	Mineralogy: major and main accessories	General description (class system)
Denver Mountain Parks CO	Clear Creek Prov., Jefferson Co, CO	Roscoe Beryl (RC)	39° 44' 10.02" N 105° 21' 33.34" W	Qtz-P-Ab-Bt>Ms-Mgt-Grt <i>Brl-Gad-Mnz</i>	Swarm in migmatites and gneisses, i.e., the MMmg (AB class) locally zoned
	Golden, Jefferson Co,	Douglas Mt (DG)	39° 45' 49.06" N 105° 23' 15.63" W	Qtz-P-Ab-Ms-Grt <i>Srl</i> in the MMmg (MS class)	Discordant poorly zoned in gneisses- amphibolites
	Upper Bear Creek Clear Creek Co, CO	Evans Ranch (ER)	39° 37' 51.3" N 105° 27' 31.3" W	Qtz-P-Ab-Ms-Grt <i>Elb-Lpd-Mic</i>	Discordant and asymmetrically zoned in gneiss (REL class)
Crystal Mountain class)	Larimer Co, CO	Hyatt (HT)	40° 27' 37" N 105° 21' 23.23" W	Qtz-P-Ab-Ms-Grt <i>Brl-Ap-Trp-Lph-U-Bi</i>	Discordant lenticular body in ISF sillimanite gneisses (MS)
		TheTourmaline prospect (TP)	40° 34' 20.40" N 105° 25' 32.50" W	Qtz-P-Ab-Ms-Grt <i>Be-Srl</i>	Simple, zoned and concordant in ISF sillimanite gneisses (MS class)
		Big Boulder (BB)	40° 31' 16.60" N 105° 24' 32.20" W	Qtz-P-Ab-Ms-Spd-Grt <i>Srl-Brl-Tri-Trp-Lph-U</i>	Complex well zoned body in andalusite schist (REL class)
Twin Mountain Batholith	Micanite, close to Guffey, frontier between Fremont Co, and Park Co, CO	Climax mica (CM)	38° 41' 44" N 105° 28' 54.17" W	Qtz-P-Ab-Ms>Bt-Grt <i>Crd-Ap-Srl-Tri</i>	Irregular star shaped, weak albitization, hosted in sillimanite gneiss (MS class)
		Rose Dawn (RD)	38° 41' 51.09" N 105° 28' 59.62" W	Qtz-P-Ab-Ms-Grt <i>Srl-Brl-Ap-Tri-Clb-Tnt</i>	Strongly albitized, Ms filling fractures, in sillimanite gneiss (MSREL class)
	Eight Mile Park, Fremont Co, CO	Mica Lode (ML)	38° 28' 41.98 N 105° 18' 07.39" W	Qtz-P-Ab-Ms-Grt <i>Srl-Brl-Tri-Ap-Clb-Tnt-Bi</i>	Lens like sill, well zoned in gneisses from the ISF (MSREL class)
	Texas Creek, Fremont Co, CO	Devils Hole (DH)	38° 28' 16.33" N 105° 35' 10.75" W	Qtz-P-Ab-Ms-Grt-Brl-Mgt <i>Ghn-Srl-Ap-Clb-Tnt-Cu-Bi</i>	Lens shaped, well zoned in sillimanite gneisses from the ISF (MSREL class)
		Chief Lithium (CL)	38° 29' 18.03" N 105° 35' 10.75" W	Qtz-P-Ab-Ms-Grt <i>Elb-Lpd-Tz-Clb-Tnt-Bi</i>	Irregular shape zoned with a F-Li rich-unit, in ISF gneiss (MSREL class)
Harney Peak Granite Co, CO	Custer, Custer Co, Black Hills, SD	Tin Mountain (TM)	43° 44' 48.01" N 103° 43' 18.21" W	Qtz-P-Ab-Ms-Spd <i>Ap-Brl-AM-Cst-Pol-Clb-Tnt</i>	200x20x30 L-shaped, zoned, discordant in sillimanite schist REL class)
		Tip Top (TT)	43° 42' 56.58" N 103° 40' 11.70" W	Qtz-P-Ab-Ms-Amb-Mbr-Brl <i>Srl-Trp-Lph-Ap-Spd</i>	190 x 90 lenticular zoned, more than 80 minerals mostly phosphates (REL class)
	Keystone, Black Hills, Pennington	Hugo (HP)	43° 52' 57.16" N 103° 25' 26.89" W	Qtz-P-Ab-Ms-Brl-Spd <i>Amb-Mbr-Srl-Ap-Lpd-Clb-Tnt</i>	One of the largest bodies in BH, irregular shape, well zoned
		Etta (ET)	43° 52' 51.33" N 103° 25' 00.46" W	Qtz-Spd-P-Ab-Ms <i>Srl-Ap-Bt-Clb-Tnt-Cst</i>	Inverted teardrop shape 76 x 69 m, in staurolite schist (REL class)

Abbreviations: Aes aeschynite; Aln allanite; Ab albite; Amb amblygonite; Ap apatite; Bsn bastnäsite; Brl beryl; Bt biotite; Bi bismuth minerals; Clb columbite; Crd cordierite; Cst cassiterite; Cu copper minerals; Elb elbaite; Eux euxenite group; Fer fergusonite; Fl fluorite; Gad gadolinite; Ghn gahnite; Grt garnet; Lph lithiophilite; Mbr montebrasite; Mgt magnetite; Mnz monazite; Ms muscovite; Lpd lepidolite; Mic microlite; NbR niobian rutile; P perthite; Pcl pyrochlore; Pol pollucite; Qtz quartz; Sk samarskite; Spd spodumene; Srl schorl; Syn synchysite; Tnt tantalite; Toz topaz; Trp triphylite; Tri triplite; U uranium minerals. ISF Idaho Spring Formation; MMmg Mount Morrison migmatites and gneisses also called Early Proterozoic metasedimentary and meta-igneous rocks. AB abyssal class; MS muscovite class; REL rare-element class; MI miarolitic class, from Černý & Ercit (2005).

B.- NYF pegmatites

Area	Locality (district)	Pegmatite name (CODE)	Coordinates	Mineralogy: major and main accessories	General description (class system)
Sherman Granite	Tie Siding, Albany Co, WY	Elkhorns I - II (EH1 and EH2)	41° 1' 56.31" N 105° 26' 02.46" W	Qtz-P-Bt <i>Gte-Pcl</i>	Two polyzonal bodies, circular shape, hosted in granite ("MS" class?)
Pikes Peak Batholith	South Platte, Jefferson Co, CO	White Cloud (WC)	39° 23' 44.79" N 105° 10' 35.12" W	Qtz-P-Ab-Bt-FI <i>Sk-Fer-Aes-Gad-Syn-Aln</i>	Polyzonal, elliptical shape, in granite (REL-REE subclass)
		Oregon (OG)	24' 50.38" N 39° 105° 16' 43.11" W	Qtz-P-Ab-Bt Fta	Polyzonal, elliptical shape, in granite (REL-REE subclass)
		No name (NN)	39° 25' 39.42" N 105° 16' 26.10" W	Qtz-P-Ab <i>Bt</i>	Polyzonal, elliptical shape, in granite ("MS" class?)
	Park Co, CO	McGuire mine (MG)	39° 19' 56.43" N 105° 24' 45.55" W	Qtz-P-A-Bt-Toz <i>Aln-Bsn-Fl-NbR</i>	Bizonal circular shape, in Rapakivi granite (REL-REE subclass)
	Crystal Peak, Park and Teller Cos., CO	Ray Berry (RB) sample 11924	-----	Qtz-P-Ab-Bt <i>Fte-Zr-Clb-Tnt-Goe</i>	Amazonite pegmatite, well zoned and small size (MI class)

C.- Hybrid pegmatite

Trout Creek Pass	Buena Vista, Chaffee Co, CO	Clora May (CIM)	38° 50' 48.85" N 105° 58' 53.99" W	Qtz-P-Ab-Bt-Grt <i>Mgt-Eux-Aes-Gad-Aln</i>	Bizonal formed by a composite Qtz-P core, oval shape in schist (REL-REE subclass)
------------------	-----------------------------	-----------------	---------------------------------------	--	---

TABLE 2: Major, minor (% wt) and trace (ppm) element chemical analyses

	SiO ₂	Al ₂ O ₃	Fe ₂ O ₃	CaO	Na ₂ O	K ₂ O	P ₂ O ₅	Total	Cs	Rb	Sr	Ba	Ni	Cr	Pb
RC	64.31	19.94	0.07	0.15	3.42	11.47	0.02	99.38	55	624	7	127	22	11	74
DG	64.37	19.89	0.04	0.13	3.50	11.33	0.02	99.28	40	413	9	388	13	12	116
ER	64.51	19.92	0.03	0.09	3.20	11.64	0.04	99.43	56	1116	11	80	47	11	50
TP	63.30	20.44	0.04	0.27	3.14	11.61	0.49	99.29	88	392	49	235	13	7	93
HY	63.12	20.66	0.05	0.17	2.51	12.64	0.35	99.50	476	1073	203	930	32	17	65
BB	63.53	20.53	0.06	0.07	2.13	12.94	0.25	99.51	234	1133	40	140	34	19	64
CM	64.26	19.91	0.04	0.12	3.16	11.95	0.17	99.61	81	421	50	388	13	18	106
RD	64.04	20.11	0.04	0.08	3.69	11.03	0.32	99.31	54	902	11	128	28	9	85
ML	63.93	20.16	0.04	0.11	2.72	12.38	0.12	99.46	130	499	35	162	15	17	85
DH	64.49	19.74	0.04	0.09	3.82	10.90	0.11	99.19	77	645	7	172	20	19	17
CL	64.35	19.93	0.03	0.08	3.27	11.79	0.08	99.53	230	664	9	191	20	19	22
TM	63.19	20.63	0.01	0.23	1.92	12.83	0.56	99.35	716	7294	64	10	202	14	91
TT	63.56	20.49	0.02	0.09	2.36	12.44	0.32	99.28	358	2368	37	210	68	11	26
HG	63.55	20.34	0.02	0.10	2.83	12.23	0.33	99.40	111	1041	17	186	30	30	40
ET	64.33	19.97	0.02	0.09	1.87	13.14	0.19	99.61	398	1409	97	142	41	12	107
EH1	64.27	19.90	0.12	0.18	3.42	11.76	0.01	99.64	78	300	12	272	11	11	41
EH2	64.67	19.74	0.05	0.19	3.56	11.17	0.01	99.39	76	331	9	232	10	9	38
WC	64.66	19.61	0.03	0.08	3.69	11.12	0.01	99.20	72	957	11	268	29	7	88
MG	64.57	19.88	0.04	0.10	3.79	10.74	0.03	99.15	29	628	32	299	20	10	54
OG	64.96	19.84	0.06	0.13	4.28	10.25	0.02	99.54	70	364	12	305	11	13	70
NN	64.27	19.83	0.11	0.12	3.05	11.99	0.02	99.39	26	272	39	1026	10	16	35
CIM	64.34	19.87	0.03	0.07	2.43	12.77	0.02	99.53	259	2290	11	102	65	9	64

TABLE 3: K-feldspar twin structures in (001) sections by optical microscopy

Pegm	K-Feld.-ts	Basic descriptions of the twin-structures
RC	MI (OR?)	Diffuse very fine twinning replaced by polysynthetic $\pm A$ twins from Na-veins
DG	MI (OR?)	Diffuse very fine twinning partially replaced by large $\pm A/\pm P$ needle twins, and also by smaller polysynthetic $\pm A$ twins from Na-veins
ER	MI	Sharp very fine twinning formed by needle twins and set of polysynthetic twins (locally as parquets) only partially transformed by the later twin generations from Na-veins
TP	MI	Large $+A/+P$ single-twin regions strongly transformed into polysynthetic $\pm A$ twins developed from NaF veins, later finer $+A/+P$ twins on the polysynthetic twins
HY	MI	Large $+A/+P$ twins replaced by polysynthetic $\pm A$ twins from veins, late finer $+A/+P$ twins
BB	MI	Very large $+A/+P$ needle twins transformed into polysynthetic $\pm A$ twins developed from NaF veins and later replaced by finer $+A/+P$ twins
CM	MI	$+A/+P$ twinning formed by needles and sets of twins locally transformed into polysynthetic $\pm A$ twins developed from Na-veins
RD	MI	Large needle and polysynthetic $\pm P$ twins transformed into polysynthetic $\pm A$ twins from Na-veins
ML	MI	$+A/+P$ twinning formed by needles, strongly transformed by sets of polysynthetic $\pm A/\pm P$ twins forming some chessboards
DH	MI	$+A/+P > -A/-P$ needle twins partially transformed by sets of polysynthetic $\pm A/\pm P$ twins, with later very fine twins giving blurred interfaces
CL	MI	$\pm P$ needle twins partially transformed into polysynthetic $\pm A$ twins, with a strong later replacement of the polysynthetic twins by very fine $\pm A/\pm P$ twins
TM	MI	Very large $\pm A < \pm P$ twins replaced by $\pm A$ polysynthetic twins, later fine $\pm A/\pm P$ twins from veins
TT	MI	Large $\pm P$ twins being replaced by $\pm A$ polysynthetic twins from P interfaces and also by smaller polysynthetic $\pm A > \pm P$ twins from Na-veins
HG	MI1-MI2 (OR)	(1) Small $\pm A-A^*/\pm P-P^*$ needle and polysynthetic twins, and square OR-ts; (2) Large needle and polysynthetic $\pm A/\pm P$ twins with chessboards. Replacement by smaller polysynthetic $\pm A/\pm P$ twins
ET	MI (OR)	Polysynthetic $\pm A/\pm P$ twins in different sizes (residual OR-ts), replaced by finer $\pm A/\pm P$ twins
EH1	MI-OR	OR-ts with a tweed-like contrast preserved away from veins, large $\pm A/\pm P$ uneven twins and ill-defined polysynthetic $\pm A/\pm P$ twins from Na-veins
EH2	MI-OR	OR-ts with a tweed-like contrast and some $\pm A^*/\pm P^*$ twins preserved away from Na-veins, large $\pm A/\pm P$ uneven twins, and ill-defined polysynthetic $\pm A/\pm P$ twins from Na-veins
MG	MI-OR	Large mainly $\pm P^*$ needle twins, discrete thin $\pm A-A^*/\pm P-P^*$ twins from Na-veins (residual OR-ts)
WC	OR (MI)	OR-ts without resolved microstructure, and discrete $\pm A > A^*/\pm P > P^*$ twins from Na-veins
OG	OR (MI)	OR-ts without resolved microstructure, and discrete $\pm A > A^*/\pm P > P^*$ twins from Na-veins
NN	OR (MI)	OR-ts without resolved microstructure, and discrete $\pm A/\pm P$ twins from Na-veins
RB	MI	Large $\pm A/\pm P$ needle twins transformed into finer polysynthetic $\pm A$ twins from Na-veins
CIM	MI	Single variant with homogeneous optical extinction, partially replaced by very fine $\pm A/\pm P$ twins

Notes: MI microcline, OR orthoclase, $\pm A$ left- and right-handed Albite twins, $\pm P$ left- and right-handed Pericline twins; later twins from MI-ts \rightarrow MI-ts are often developed from the interface between the Na-feldspar veins and the K-feldspar matrix of the perthitic texture; the symbol "*" is used for "irrational" twins; the pegmatite codes are as in Table 1. "Replaced by" and "transformed into" are used as synonymous words for a solid-state process of K-feldspar "recrystallization" in the subsolidus stage in which a certain orientation variant is converted into another one with a different relative orientation.

GEOCHEMISTRY AND TWIN STRUCTURES OF K-FELDSPAR SAMPLES

The chemical composition of the samples is given in Table 2. Samples from the LCT pegmatites are characterized by a higher content in Cs and Rb. The more typical feature of the NYF suite is the extremely low content of P_2O_5 , when compared with the other rocks. The Na_2O content of K-feldspar in the samples of the NYF suite is higher than those of the LCT suite because of a higher temperature of crystallization and also a stronger postmagmatic albitization. The hybrid character CIM pegmatite is shown by the high content in Cs and Rb.

The basic features of the K-feldspar-ts are in Table 3. The LCT suite is principally formed by microcline-ts, consisting of discrete needle twins from the orthoclase-ts \rightarrow microcline-ts recrystallization, being typical in many Colorado pegmatites as in the Big Boulder pegmatite, and polysynthetic-chessboard twinning from microcline-ts \rightarrow microcline-ts conversion, as seen in the South Dakota pegmatites. Conversely, the NYF suite contain orthoclase-ts in a significant proportion (being the main mineral in the samples studied from non miarolitic pegmatites of the Pikes Peak granite, although it is only partially preserved in the Sherman granite pegmatites), and the microcline-ts is characterized by "irrational" twinning.

CONCLUSIONS

The pessimistic view that K-feldspar shows an erratic heterogeneity as worthless and random pseudomorphs and, consequently, a limited usefulness in understanding petrological problems has been supported in part by studies on igneous and metamorphic rocks (small grain-size) that experienced strong interactions with fluids at lower temperatures. However, when pristine features formed during the subsolidus stage are identified, as in the gigantic crystals of K-feldspars from the inner zones of gran-

ite pegmatites, Marmo's approach could be useful if the -ts concept is applied. Hence, K-feldspar can aid to recognize tectonic setting, and well-identified geological environments must help suggesting right terms for K-feldspar minerals.

REFERENCES

- Anderson, J.L. & Cullers, R.L. (1999). Paleo- and Mesoproterozoic granite plutonism of Colorado and Wyoming. *Rocky Mountain Geology* **34**: 149-164.
- Černý, P. & Ercit, T.S. (2005). The classification of granitic pegmatites revisited. *Can. Mineral.* **43**: 2005-2026.
- Hanson, S.L., Simmons, W.B., Webber, K.L. & Falster, A.U. (1992). Rare-earth-element mineralogy of granitic pegmatites in the Trout Creek Pass district, Chaffee County, Colorado. *Can. Mineral.* **30**: 673-686
- Martin, R.F. & De Vito, C. (2005). The patterns of enrichment in felsic pegmatites ultimately depend on tectonic setting. *Can. Mineral* **43**: 2027-2048.
- Marmo, V. (1971). *Granite petrology and the granite problem*. Elsevier, 244p.
- Sánchez-Muñoz, L., Crespo, E., García-Guinea, J., de Moura, O.J.M. & Zagorsky, V.Ye. (2009). What is a twin-structure? An answer from microcline minerals from pegmatites. *Estudios Geológicos* **19**(2): 240-245.
- Sánchez-Muñoz, L., García-Guinea, J., Zagorsky, V.Ye., De Moura, O.J.M. & Modreski, P. (2011). K-feldspar minerals defined from their twin-structures: Application to a preliminary classification of pegmatites (this issue).
- Tweto, O. (1987). Rocks units of the Precambrian basement in Colorado. U.S. Geol. Survey Prof. Paper 1321-A, 1-54.

Rb-Sr GEOCHRONOLOGY FOR THE “LA AURORA” ANDALUSITE-BEARING PEGMATITE FROM MAZÁN RANGE, NW ARGENTINA

Fernando Sardi^{1§} & José Manuel Fuenlabrada Pérez²

¹ INSUGEO-CONICET. Miguel Lillo 205 (4000)- San Miguel de Tucumán, Argentina. § fgsardi@csnat.unt.edu.ar

² CAI de Geocronología y Geoquímica Isotópica, Facultad de Geología, Universidad Complutense de Madrid, 28040 Madrid, Spain

Key words: Rb-Sr geochronology, errorchron, pegmatite, Mazán range, Argentina.

INTRODUCTION

The pegmatite's rock-forming minerals such as K-feldspars, micas, and plagioclase commonly contain variable amounts of potassium. The geochemical characteristics such as ionic size and charge allow the trace radiogenic element Rb to substitute for the major element potassium into these minerals. For this reason, the Rb/Sr method can be properly used for geochronology studies on pegmatites. However, the highly probable post-consolidation disturbance of the system by the mobility of the radiogenic element (⁸⁷Sr) may cause some problems in the dating and interpretation of the initial ⁸⁷Sr/⁸⁶Sr ratio, particularly for Early Proterozoic and older pegmatites (Černý, 1991).

The goal of this work is to determine the absolute age of the crystallization of the “La Aurora” pegmatite using the Rb/Sr method and to realize some pegmatogenesis considerations based on the initial ⁸⁷Sr/⁸⁶Sr ratio. This work represents the first isotopic study in pegmatites from the Mazán pegmatitic field, La Rioja province, northwestern Argentina.

GEOLOGY AND MAZÁN GRANITE

Geographically, the Mazán range is located in the north-east sector of the La Rioja province (Argentina) and it is considered a north-east extension of the very big Velasco range (Fig. 1).

Geologically, the Mazán range forms part of the Sierras Pampeanas province. The Sierras Pampeanas geological province is located in the north-western sector of Argentina. It contains abundant crystalline rocks, mainly metamorphic rocks and granitoids of different genesis and evolution (Rapela *et al.*, 2001). The granitoids were generated mainly during the Paleozoic and some of them are fertile and formed pegmatites, mainly of the rare-element class, constituting the Pampeana Pegmatitic Province (Galliski, 2009).

The oldest rocks in the Mazán range are low grade metamorphic rocks, essentially phyllites and

metapsammities, located in the southern and south-western portions of the range. These rocks constitute the La Cébila Formation (González Bonorino, 1951). In this formation, located in the neighboring Ambato range, Verdecchia *et al.* (2007) have recently discovered lower Ordovician marine fossils.

The dominant rock in the Mazán range is the homonymous granite. The Mazán granite is porphyritic with idiomorphic megacrysts of perthitic microcline immersed in an equigranular groundmass composed of feldspars, quartz, biotite, muscovite and cordierite. Schalamuk *et al.* (1989) also recognized andalusite, garnet and apatite. Tourmaline appears occasionally. On the other hand, it is common to observe rounded and elongated enclaves of metapelites and metapsammities in the Mazán granite, some of them displaying relict sedimentary structures.

Geochemically, the Mazán granite is highly peraluminous with ASI (molar ratio Al₂O₃/(CaO+Na₂O+K₂O) between 1.47 and 1.67 (Sardi *et al.*, 2009a). Likewise, Schalamuk *et al.* (1989) and Toselli *et al.* (1991) obtained ASI values > 1. The highly peraluminous composition of the Mazán granite may be attributed to assimilation of clastic metasedimentary packages of the very Al-rich La Cebila Formation. The Mazán granite has been dated at 484.2 ± 3.1 Ma using U-Pb SHRIMP (Pankhurst *et al.*, 2000).

“LA AURORA” PEGMATITE

The “La Aurora” pegmatite occurs in its parental Mazán granite. The pegmatite is zoned and ellipsoidal in shape with dimensions of 45 by 15 meters (Fig. 1; Sardi *et al.*, 2009b). The coordinates are 28° 42' 50" S – 66° 34' 15" W. “La Aurora” is a barren pegmatite, as no rare-element bearing minerals have been found. The mineralogy of the pegmatite is very simple with an andalusite-corundum assemblage (Sardi *et al.*, 2009b). The “La Aurora” pegmatite, as are the other bodies from the Mazán pegmatitic field, is considered transitional between muscovite class and rare-element class.

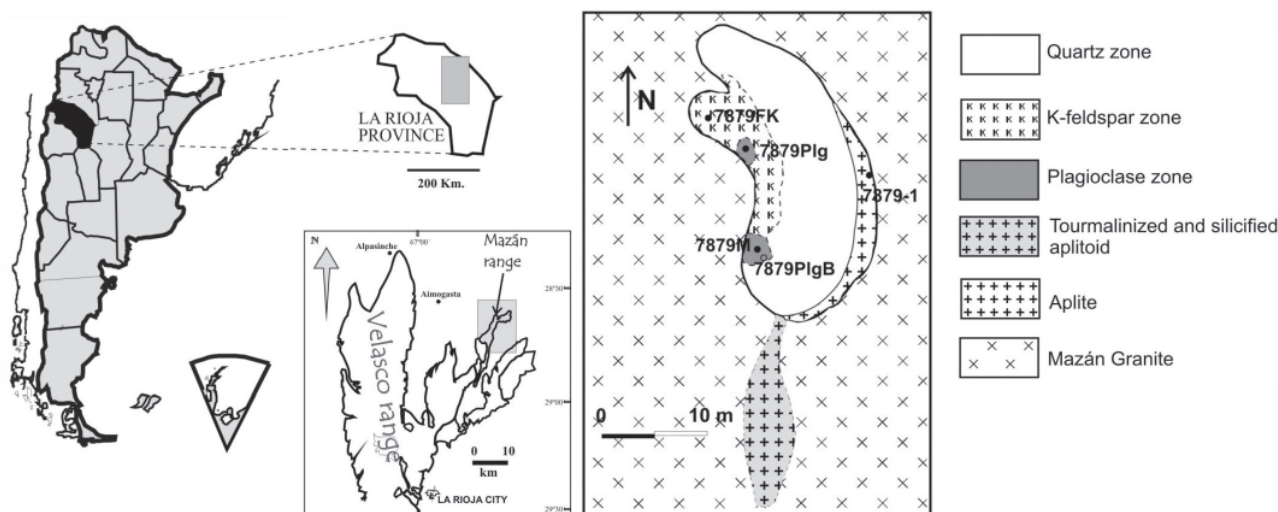


FIGURE 1. Schematic geological map of the "La Aurora" pegmatite (after Sardi *et al.* 2009b) showing sampling points.

The Rb-Sr geochronology of the "La Aurora" pegmatite was determined from *aplite* from the border of the pegmatite and *K-feldspar*, *plagioclase* and *muscovite* from the intermediate zone. Sample purity was checked under the binocular microscope before the grinding and submission of samples to the laboratory.

RESULTS AND CONCLUSIONS

Isotopic analysis of five samples from the "La Aurora" pegmatite (*aplite*, *K-feldspar*, *muscovite* and two *plagioclases*) was performed at the Centro de Geocronología y Geoquímica Isotópica (Universidad Complutense de Madrid). For Sr isotopic mineral analysis by isotope dilution-thermal ionization mass spectrometry (ID-TIMS), the samples were first dissolved in ultra-pure reagents in order to perform isotopic separation by exchange chromatography (Strelow 1960), and subsequently analysed using a Sector 54 VG Micromass multicollector spectrometer. The measured $^{87}\text{Sr}/^{86}\text{Sr}$ isotopic ratios (Table 1) were corrected for possible isobaric interferences from ^{87}Rb ; and normalized to $^{88}\text{Sr}/^{86}\text{Sr}=0.1194$ in order to correct mass fractionation. The NBS 987 international isotopic standard was analysed during sample measurement, and gave an average value of $^{87}\text{Sr}/^{86}\text{Sr}=0.710262$ for 7 replicas, with an internal precision of ± 0.00007 (2σ). These values were used to correct the measured ratios for possible sample drift. The error estimated for the $^{87}\text{Rb}/^{86}\text{Sr}$ ratio is 1% and 0.01% for the $^{87}\text{Sr}/^{86}\text{Sr}$ ratio. Plotting of the isotopic data (Fig. 2) and age calculations were performed using the Isoplot/Ex 3.00 program (Ludwig, 2003).

The results are shown in Table 1. The ratio of Rb/Sr is always > 1 , and is much higher in the *muscovite* sample. Due to the very high MSWD value obtained, the linear array shown in the $^{87}\text{Sr}/^{86}\text{Sr}$ vs

$^{87}\text{Rb}/^{86}\text{Sr}$ orthogonal diagram in Figure 2 would not be considered an isochron but an 'errorchron'.

The 'errorchron' defines an age of 461.8 ± 9.0 Ma, with a $^{87}\text{Sr}/^{86}\text{Sr}$ initial ratio = 0.704. This date represents the crystallization age of the "La Aurora" pegmatite and falls into the Ordovician period. In general, the age obtained can be considered in agreement with the crystallization age of the parental Mazán granite, but with a gap of around 22 Ma between the granitic-magmatic episode and pegmatitic crystallization. This is a very long time compared to the experimental and observational measurement made by Webber *et al.* (1999) for pegmatite body crystallization. A probable explanation for the 22 Ma gap could be the frequent ^{87}Sr loss from the Rb-Sr system during the post-consolidation stage, which would give an unrealistically younger age (e.g., Černý 1991).

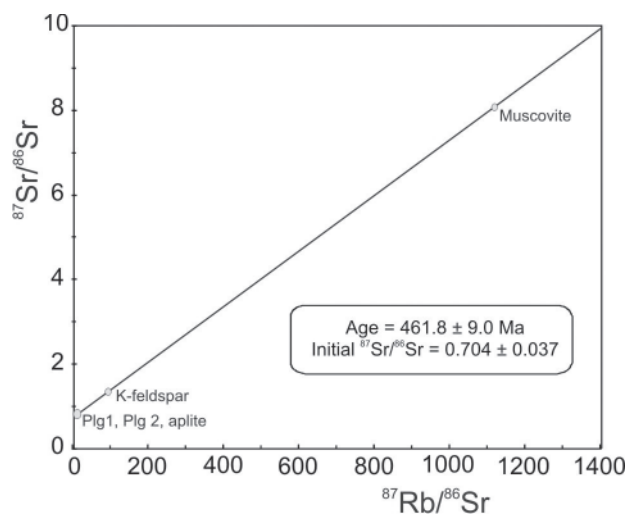


FIGURE 2. $^{87}\text{Sr}/^{86}\text{Sr}$ vs $^{87}\text{Rb}/^{86}\text{Sr}$ diagram ('errorchron') for the "La Aurora" pegmatite from Mazán range.

TABLE 1. Analytical isotope data for aplite and cogenetic minerals of the "La Aurora" zoned pegmatite.

Sample	Description	Rb (ppm)	Sr (ppm)	Rb/Sr	⁸⁷ Rb/ ⁸⁶ Sr	⁸⁷ Sr/ ⁸⁶ Sr	2s (2-sigma)	⁸⁷ Sr/ ⁸⁶ Sr init
7879-1	Aplite	82.2	31.3	2.63	7.641	0.765460	5	0.715385
7879FK	K-feldspar	931.3	28.5	32.68	100.309	1.331040	8	0.673679
7879M	Muscovite	2883	12.8	225.23	1123.082	8.102516	57	0.742535
7879Plg	Plagioclase	39.3	8.212	4.79	13.969	0.798192	9	0.706649
7879PlgB	Plagioclase	31.24	14.90	2.10	6.096	0.760521	6	0.720569

The ⁸⁷Sr/⁸⁶Sr initial ratio of 0.704 suggests an upper mantle contribution. However this value seems too low for the "La Aurora" pegmatite considering that the parental Mazán granite is peraluminous, is cordierite bearing, has an S-type granite affinity, contains metasedimentary enclaves, and is probably crustal in origin. In agreement, Toselli *et al.* (1991) infer that magmatism in the Mazán range is crustal in origin, with magma generation in the middle crust with a minimum pressure of ~ 5-6 Kb and shallow level emplacement at a pressure of ~ 1.5Kb.

REFERENCES

- Černý, P. (1991). Rare-element granitic pegmatites. Part I: Anatomy and internal evolution pegmatite deposits. *Geosc. Canada*. II: 29-47.
- Galliski, M. (2009). The Pampean Pegmatite Province, Argentina: a review. *Estudios Geol.* 19 (2):30-34.
- González Bonorino, F. (1951). Una nueva formación Precámbrica en el noroeste Argentino. *Comunic. Cient. Museo La Plata*. N° 5: 4-6.
- Ludwig, 2003 K.R. Ludwig, User's Manual for Isoplot 3.00. A Geochronological Toolkit for Microsoft Excel, Spec. Public. vol. 4a, Berkeley Geochronology Center, Berkeley, California.
- Pankhurst, R. J., Rapela, C. & Fanning, C. (2000). Age and origin of coeval TTG, I- and S- type granites in the Famatinian belt of NW Argentina. *Trans. of the Royal Society of Edinburgh: Earth Sciences*. 91:151-168.
- Rapela, C. W., Casquet, C., Baldo, E., Dahlquist, J., Pankhurst, R., Galindo, C. & Saavedra, J. (2001). Las Orogénesis del Paleozoico Inferior en el margen proto-andino de América del Sur, Sierras Pampeanas, Argentina. *Journal Iberian Geology*, 27:23-41.
- Sardi, F., Murata, M., Lozano Fernández, R., Báez, M., Fogliata, A. & Lazo, M. (2009a). Geological and geochemical setting of the Mazán Granite containing andalusite-pegmatites, Argentina. *Estudios Geol.* 19 (2): 326-331.
- Sardi, F., Bengochea, L. & Maz, G. (2009b). The mineral assemblage andalusite-corundum from "La Aurora" pegmatite from Mazán Pegmatitic Field, Northwestern Argentina. *Estudios Geol.* 19 (2): 332-336.
- Schalamuk, I., Toselli, A., Saavedra, J., Echeveste, H. & Fernández, R. (1989). Geología y mineralización del sector este de la sierra de Mazán, La Rioja, Argentina. *Asoc. de Miner. y Petrol.* 20 (1-4): 1-12.
- Strelow, F.W.E., 1960. An Ion exchange selectivity scale of cations based on equilibrium distributions coefficients. *Anal. Chem.* 32: 1185-1188.
- Toselli, G., Saavedra, J., Córdoba, G. & Medina, M. (1991). Petrología y geoquímica de los granitos de la zona Carrizal-Mazán, La Rioja y Catamarca. *Rev. Asoc. Geol. Arg.* XLVI (1-2): 36-50.
- Verdecchia, S., Baldo, E., Benedetto, J. & Borghi, P. (2007). The first shelly fauna from metamorphic rocks of the Sierras Pampeanas (La Cébila Formation, Sierra de Ambato, Argentina): age and paleogeographic implications. *Ameghiniana*, 44:493-498.
- Webber, K., Simmons, W., Falster, A. & Foord, E. (1999). Cooling rates and crystallization dynamics of shallow level pegmatite-aplite dikes, San Diego County, California. *Am. Mineral.* 84: 708-717.

MAGMATIC DIFFERENTIATION IN THE HUACO GRANITE AND ITS ASSOCIATED Be-PEGMATITES FROM THE VELASCO DISTRICT, ARGENTINA

Fernando Sardi^{1§}, Mamoru Murata² & Pablo Grosse³

¹ INSGUEO-CONICET. Miguel Lillo 205, (4000) San Miguel de Tucumán, Argentina. § fgsardi@csnat.unt.edu.ar

² Naruto University of Education, Department of Geosciences. 7772-8502, Tokushima, Japan.

³ CONICET and Fundación Miguel Lillo. Miguel Lillo 251, (4000) San Miguel de Tucumán, Argentina.

Keywords: geochemistry, fractional crystallization, granite, Be-pegmatite, Velasco, Argentina.

INTRODUCTION

The Velasco Pegmatitic District is located in the central-eastern area of the Sierra de Velasco in La Rioja province (NW Argentina). The pegmatites are classified as rare-element class, beryl type, beryl-columbite-phosphate subtype, belonging to the Mixed LCT-NYF petrogenetic family. The pegmatites have been exploited for beryl, especially during the first half of the last XXth century. More recently, the pegmatites have been exploited only sporadically for heliodor and aquamarine, the gem-quality varieties of beryl.

GEOLOGICAL SETTING

The Sierra de Velasco is the biggest range of the Sierras Pampeanas geological-structural province of NW Argentina. The Sierras Pampeanas province is located in center and northwestern region of Argentina and they are characterized by widespread outcrops of the crystalline basement consisting of low-to-high grade metamorphic rocks and several Paleozoic igneous intrusives, usually of granitic composition. The Sierras Pampeanas contain ~95% of the productive pegmatites of Argentina (Galliski 1994).

The Sierra de Velasco is formed essentially of granitoids, but meta-sedimentary rocks (metapelites and metapsamites) form small outcrops on its eastern. The granitoids have different ages and evolutions (Toselli *et al.* 2005). Two main magmatic episodes can be recognized, a pre-tectonic Ordovician episode, and a post-tectonic Carboniferous episode. The undeformed, post-orogenic Carboniferous granites intruded the previous rocks of the Sierra de Velasco. The Carboniferous Huaco granite, which has been dated at 350-358 Ma (U-Pb on monazite) by Grosse *et al.* (2009), contains most of the Be-rich pegmatites that comprise the Velasco pegmatitic district.

In general, the Huaco granite is characterized by a porphyritic texture of idiomorphic perthitic microcline megacrysts immersed in a coarse- to medium-grained groundmass. The lithologic composition is syeno- to

monzogranitic. The main accessory minerals are biotite and muscovite, and minor phases are apatite, zircon, monazite and scarce opaque minerals.

HUACO GRANITE PHASES

Four facies of the Huaco granite are distinguished on the basis of their textural and mineralogical features: (i) border of Huaco granite, BHG; (ii) main (~ regional) porphyritic granite, RPG; (iii) granite adjacent to the pegmatites, APG; and (iv) marginal aplite of the Be-pegmatites, MA. These facies were recognized by Sardi *et al.* (2010), except for the first phase which is added here. The table 1 shows some petrographic and geochemical features.

BHG is a thin (< 100 m) border phase that grades into the main Huaco granite, RPG. The texture of BHG is slightly porphyritic, with scarce microcline megacrysts (5-20%) immersed in a medium to fine grained equigranular groundmass. It has a monzogranitic composition and the modal composition is quartz (34-40%), twinned and zoned plagioclase (23-34%), twinned and perthitic microcline (19-33%), biotite (5%) and muscovite (2-4%). Apatite, zircon and opaque minerals are usually included in biotite.

RPG constitutes the bulk of the Huaco granite. It has a syenogranitic to monzogranitic composition, porphyritic texture with abundant microcline megacrysts (~32%) immersed in a medium to coarse grained equigranular groundmass. The mineralogy is quartz (~22%), plagioclase (~17%), microcline (~48%), biotite (~8%), muscovite (~4%), apatite (~1%) and zircon. The biotite/muscovite ratio is typically ~2.

APG surrounds the Be-pegmatites to distances not more than 6 m from their contacts. APG is distinguished by a decrease in the grain size of the groundmass and in the abundance of megacrysts (~29%). Relative to the RPG, the quartz content increases, microcline content decreases, and the biotite/muscovite ratio decreases to 1.4 in APG.

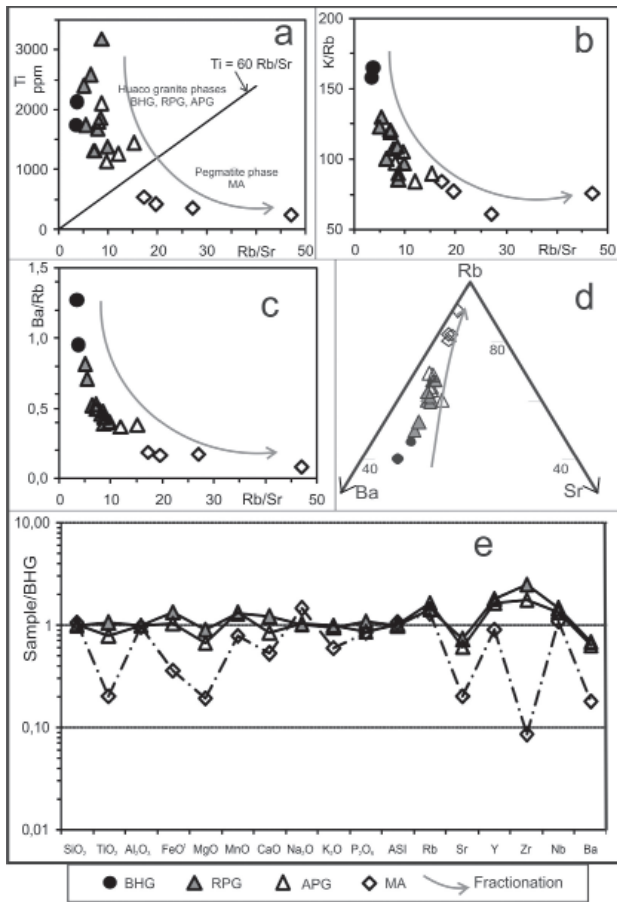


FIGURE 1. Geochemical diagrams. a) Ti-Rb/Sr orthogonal diagram; b) K/Rb-Rb/Sr orthogonal diagram; c) Ba/Rb-Rb/Sr orthogonal diagram; d) Ba-Rb-Sr triangular diagram; e) multi-elemental diagram normalized to the BHG phase.

MA constitutes the outer margins of the pegmatites. It commonly consists of aplites or more rarely of muscovite-rich equigranular leucogranites with topaz. The thickness of the MA is variable, but not greater than 2 m. It has a monzogranitic to granodioritic composition. The rock contains quartz (~37%), K-feldspar and plagioclase in similar amounts (~24%); muscovite (~10%) is the main accessory mineral, whereas biotite (~2%) is scarce and sometimes absent, being the biotite/muscovite ratio ~0.3. Topaz can be identified under the microscope. The MA is considered as the earliest crystallization phases of the pegmatites.

GEOCHEMISTRY

Twenty-one samples of the Huaco granite and the marginal aplites of the Be-pegmatites were analyzed by XRF for major and some trace elements (Rb, Ba, Sr). The analyses were carried out at the Geosciences Department of Naruto University (Japan), Huelva University (Spain) and at ACTILAB (Canada). The data include analyses previously published by Grosse *et al.* (2009) and Sardi *et al.* (2010), as well as new unpublished analyses.

The silica content of all phases is high, especially in the MA phase. The K_2O/Na_2O ratio is >1 in the BHG, RPG and APG phases whereas it is ≤ 1 in the MA. The concentration of ferromagnesian elements is low in the three Huaco granite phases (BHG, RPG and APG), between 2.2 and 5.4 %, but is notably lower in the MA (0.6-1.1 %). Sardi *et al.* (2010) suggested that this decrease from the granite to the pegmatites was caused by fractional crystallization of biotite. All phases have very low CaO contents (less than 1.2 %) and are peraluminous, with ASI (molar $Al_2O_3/[CaO+Na_2O+K_2O]$) > 1 .

The Rb, Sr and Ba contents in the analyzed rocks are variable. The lowest Rb contents are found in the BHG, increasing towards the RPG and the APG. Rb contents then decrease in the MA possibly because of declining K_2O concentrations evidenced by the change in the modal composition. On the other hand, Sr and Ba decrease continuously in the sequence BHG-RPG-APG-MA.

The elements alone or their ratios can serve as indicators of fractionation processes (e.g., Černý *et al.* 1985, Černý 1991). Figures 1a, 1b and 1c use such ratios (Rb/Sr, K/Rb and Ba/Rb). In these figures, a continuous fractionation trend can be observed for the BHG-RPG-APG, especially in figures 1b and 1c. Figure 1a shows a clear separation between the granitic phases (BHG, RPG and APG) and the MA. Similar considerations about the fractionation trend can be drawn from the triangular figure 1d.

Figure 1e is a multi-element diagram normalized to the BHG phase. The RPG and APG have quite parallel designs with values similar to the BHG, although showing slight Zr, Rb and Y peaks and Sr and Ba lows. The MA shows a small Na_2O peak and several strong lows, notably TiO_2 , FeO^t , MgO, Sr, Zr and Ba.

CONCLUSIONS

The Huaco granite shows four distinct phases (BHG, RPG, APG, MA) from the border of the intrusion towards the margins of the included Be-pegmatites. These phases originated from the same magma source, but show textural, mineralogical and geochemical differences that indicate a continuous sequence of fractional crystallization of the granite (BHG→RPG→APG), followed by the crystallization of the MA as the first pegmatitic phase. Large-ion lithophile elements such as Rb, Ba and Sr can be used as monitors of the magmatic differentiation in the Velasco district. The Rb/Sr and Ba/Rb ratios are good examples of them in order to show such evolution. The Ti concentrations clearly separate the Huaco granite phases (BHG, RPG and APG) from the pegmatite phase (MA). The equation $Ti = 60 Rb/Sr$ is a useful empirical expression for separating between granite and pegmatite crystallization.

TABLE 1. Petrographic and geochemical features of the phases of the Huaco granite, Sierra de Velasco, Argentina.

	BHG		RPG		APG		MA	
Texture Composition	Slightly porphyritic Monzogranite		Porphyritic Syenogranite to monzogranite		Porphyritic Monzogranite to syenogranite		Equigranular Granodiorite to monzogranite	
Mc	~ 26 %		~ 48 %		~ 36 %		~ 25 %	
Qz	~ 37 %		~ 22 %		~ 37 %		~ 37 %	
Pl	~ 29 %		~ 17 %		~ 15 %		~ 24 %	
Ms	~ 3 %		~ 4 %		~ 5 %		~ 10 %	
Bt	~ 5 %		~ 8 %		~ 6 %		~ 2 %	
	<i>n</i> ¹ = 2		<i>n</i> = 8		<i>n</i> = 7		<i>n</i> = 4	
<i>wt. %</i>	<i>x</i> ²	<i>range</i>	<i>x</i>	<i>range</i>	<i>x</i>	<i>range</i>	<i>x</i>	<i>range</i>
SiO ₂	71.82	71.64-71.99	71.37	68.06-73.94	72.11	70.06-74-34	75.77	72.93-81.16
TiO ₂	0.32	0.29-0.35	0.34	0.22-0.53	0.25	0.19-0.35	0.07	0.04-0.09
Al ₂ O ₃	14.17	14.15-14.19	13.95	12.81-14.85	14.07	13.20-14.63	13.56	10.34-15.01
Fe ₂ O ₃ ^t	2.22	1.92-2.53	2.95	2.28-4.31	2.30	1.84-3.25	0.74	0.55-0.87
MnO	0.05	0.04-0.06	0.06	0.04-0.09	0.07	0.05-0.09	0.04	0.03-0.05
MgO	0.41	0.38-0.44	0.37	0.24-0.60	0.16	0.28-0.41	0.08	0.04-0.10
CaO	0.87	0.86-0.88	1.04	0.75-1.51	0.73	0.27-0.97	0.46	0.17-0.60
Na ₂ O	3.05	3.04-3.05	3.08	2.79-3.43	3.12	2.20-3.52	4.40	2.63-5.35
K ₂ O	5.55	5.51-5.59	5.24	4.69-5.65	5.51	4.60-7.07	3.29	2.76-4.39
P ₂ O ₅	0.27	0.25-0.30	0.29	0.15-0.40	0.24	0.12-0.37	0.23	0.14-0.26
ppm								
Rb	286	282-290	405	343-480	470	393-658	367	327-434
Ba	318	268-368	216	181-301	201	166-254	57.9	28.0-82.7
Sr	77.5	73.6-81.3	56.3	46.0-73.0	47.2	37.1-55.6	15.6	7.0-25.0

¹n: number of samples; ²x: average value.

REFERENCES

- Černý, P. (1991). Rare-element granitic pegmatites. *Geoscience Canada* **18** (2): 49-81.
- Černý, P., Meintzer, R. & Anderson, A. (1985). Extreme fractionation in rare-element granitic pegmatites: selected examples of data and mechanisms. *Canadian Mineral.* **23**: 381-421.
- Galliski, M. (1994). La Provincia Pegmatítica Pampeana. *Asoc. Geol. Argentina, Revista* **49** (1-2): 99-122.
- Grosse, P., Söllner, F., Báez, M., Toselli, A., Rossi, J. & De La Rosa, D. (2009). Lower Carboniferous post-orogenic granites in central-eastern Sierra de Velasco, Sierras Pampeanas, Argentina: U-Pb monazite geochronology, geochemistry and Sr-Nd isotopes. *Inter. Journal of Earth Sci.* **98**:1001-1025.
- Sardi, F., Murata, M. & Grosse, P. (2010). Petrographical and geochemical features of the granite-pegmatite transition in the Velasco Pegmatitic District, NW Argentina. *N. Jahrbuch für Geol. und Paläont.* **258** (1): 61-71.
- Toselli, A., Rossi, J., Miller, H., Báez, M., Grosse, P., López, J. & Bellos, L. (2005). Las rocas graníticas y metamórficas de la Sierra de Velasco. *Serie Correl. Geol.* **19**: 211-220.

MINERALOGY OF THE LITHIUM BEARING PEGMATITES FROM THE CONSELHEIRO PENA PEGMATITE DISTRICT (MINAS GERAIS, BRAZIL)

Ricardo Scholz¹, Mário Luiz de Sá Carneiro Chaves², Klaus Krambrock³

¹ Departamento de Geología, Escola de Minas, UFOP – r_scholz_br@yahoo.com

² Departamento de Geología, Instituto de Geociências, UFMG

³ Departamento de Física, Instituto de Ciências Exatas, UFMG

Keywords: lithium bearing pegmatite, montebrasite, triphylite.

INTRODUCTION

The Eastern Brazilian Pegmatite Province (EBPP) encompasses a large region of about 150,000 km², from Bahia to Rio de Janeiro states, but more than 90% of its whole area is located in eastern Minas Gerais State. In this context, the Conselheiro Pena pegmatite district is located in the northeast portion of the Minas Gerais state, ca. 360 km from Belo Horizonte. The Conselheiro Pena pegmatite district is inserted in the domains of Araçuaí fold belt (Almeida 1977), that is a mobile belt developed in the eastern margin of the São Francisco craton during the Brazilian orogenic cycle (630-490 Ma). Geologic units in this belt show structural direction north-south in Minas Gerais state, changing to east-west direction in southern Bahia state.

In the studied region mainly occur granitoid rocks of several suites, such as Urucum and Palmital of Eocambrian to Paleozoic age, and Galiléia of Neoproterozoic age, as well as gneiss, schist, quartzite, and calcisilicate rock of Neoproterozoic age, such as the Tumiritinga and São Tomé formations. Structurally, the region seems to be a synclinorium megastructure that has basically north-south direction, where metasediments are found in syncline parts of this structure, while in adjacent anticline parts granitoid rocks occur. Ages of the pegmatite bodies are about 580 Ma (Nalini 1997), and are related to granite G2 supersuite (Pedrosa-Soares *et al.* 2001; 2009) intrusive in the metasediment units. They consist mostly of S-type peraluminous granites and minor metaluminous granites, generated during the syn-collisional stage of Araçuaí orogen.

PEGMATITES OF THE CONSELHEIRO PENA DISTRICT

Most pegmatites of this region are residual bodies from G2 S-type two-mica granites of the Urucum suite, crystallized around 582 Ma (Nalini 1997). Granites and pegmatites were mainly emplaced along high-angle-dip strike-slip shear zones (Nalini 1997). The most important pegmatites are generally external bodies hosted by amphibolite facies rocks,

like sillimanite-staurolite-garnet-mica schist of the São Tomé Formation. Netto *et al.* (1998) reported mining activities in 205 pegmatites of the Conselheiro Pena district, many of them large (15 to 50 m thick) to very large (> 50 m thick) bodies.

Pegmatite bodies are tabular- or lens-shaped, and a few are irregular-shaped balloons. They generally display complex zoning and diversified mineralogy. The Conselheiro Pena district is characterized by remarkable phosphate assemblages, such as those of the Sapucaia pegmatite (Cassedanne 1983). Triphylite is the main primary phosphate that formed dozens of metasomatic and secondary phosphates, such as eosphorite, huréaulite, reddingite, variscite, vivianite and frondelite (Chaves & Scholz 2008). Spodumene and montebrasite also occur as primary lithium minerals.

In the past, this district was very important for the production of gem-quality tourmaline, morganite, aquamarine and kunzite, besides industrial minerals, such as microcline, albite and mica, and beryl ore. Nowadays, these pegmatites are mined for industrial feldspar, besides collection of rare minerals. Figure 1 shows the geological map of the region, including the locations of the pegmatites and the type of primary lithium mineralization.

MINERALOGY

The pegmatites were divided in four groups, according to the presence or absence of primary lithium minerals or their secondary mineral paragenesis. This classification is related to the type of primary lithium minerals. The pegmatite groups are described below:

I – Pegmatites very poor or without primary Li-minerals. In this group of pegmatites, the primary lithium mineral or its paragenesis of secondary minerals was not described. Some of them are rich in gem quality minerals, such as the green and red elbaïtes from the Sapó pegmatite and Jonas Lima pegmatite. The pegmatite bodies classified in this group are hosted in rocks of different stratigraphic

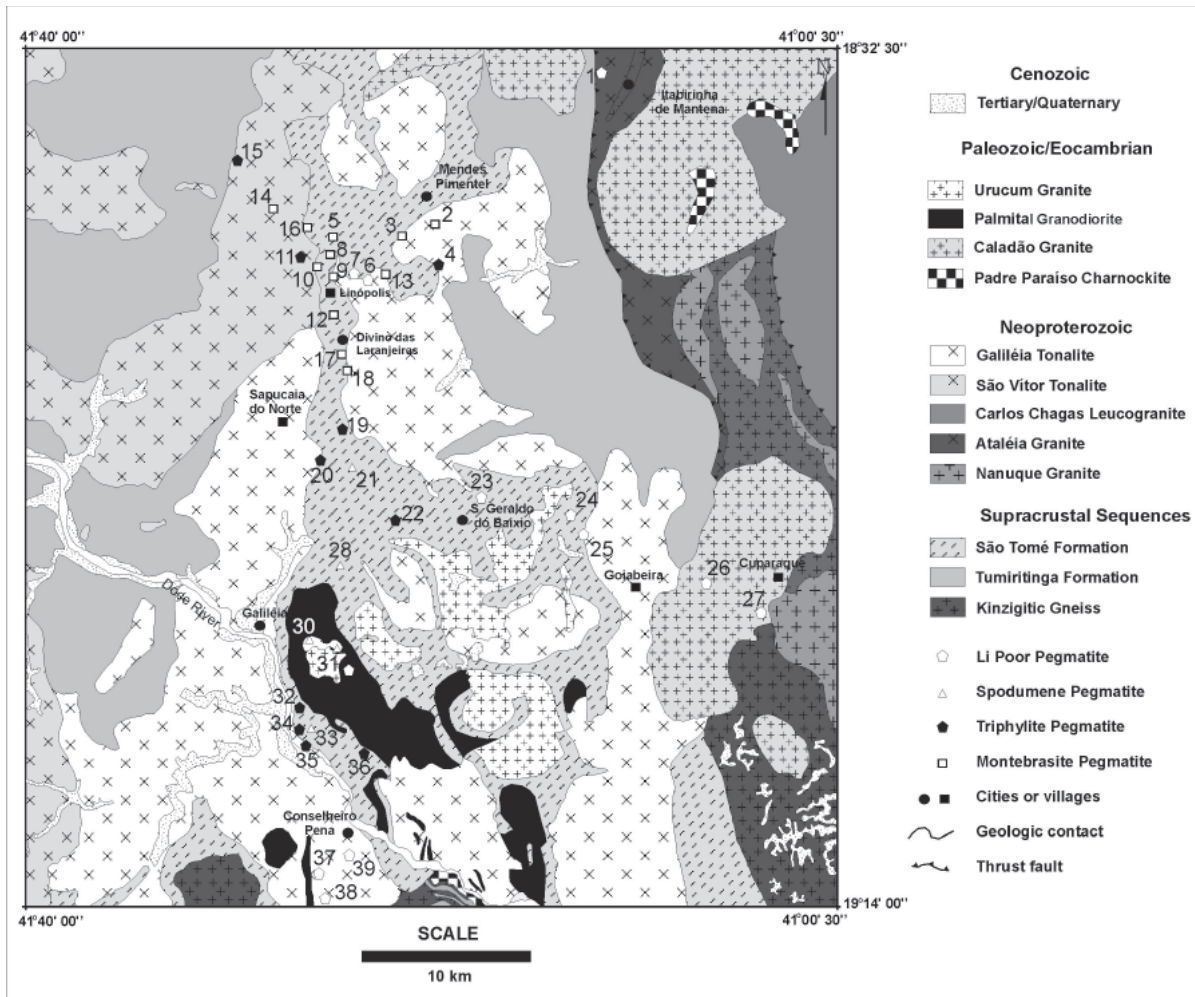


FIGURE 1: Geology and main pegmatite bodies of the Conselheiro Pena pegmatite district (Netto *et al.* 1998). Pegmatite mines or “garimpos”: 1. Geraldinho; 2. Boa Esperança; 3. Indaiá; 4. Gentil; 5. Piano; 6. Cristalão; 7. Confusão; 8. Roberto; 9. Osvaldo Perin; 10. Pomarolli I; 11. Pomarolli II; 12. Evaldo; 13. Jove Lauriano; 14. João Firmino; 15. Pomarolli II; 16. Córrego Frio; 17. Boa Vista I; 18. Boa Vista II; 19. Boca Rica; 20. Sapucaia; 21. Berilo Branco; 22. Sapucaia Proberil; 23. Viúva; 24. Sapo; 25. Formiga; 26. Km 04; 27. Aldeia; 28. Unnamed; 29. Rogério I; 30. Urucum; 31. Orozimbo Coelho or Navegadora; 32. Espessartine or Rogério II; 33. Córrego Boa Vista; 34. Marcelo; 35. Bode; 36. Cigana; 37. Bernardino; 38. Tatiaia; 39. Jonas Lima. Lithium mineralogy: in green, triphylite pegmatites; in red, montebrasite pegmatites; in yellow, spodumene pegmatites and; in blue, pegmatites very poor or without primary Li-minerals.

units, including the schists of the São Tomé Formation and granitoids of the Caladão, Galiléia and São Vítor suites. They show well development of internal zones and the substitution bodies to late crystallization bodies are larger than 1.0 m³. The accessory minerals that occur in such pockets are helvine, spessartine (Orozimbo/Navegadora mine), elbaite (Jonas and Sapo mines), and cassiterite and columbite (Sapo mine). The phosphate mineralogy is rare, mainly composed by fluorapatite from Aldeia and Sapo pegmatites, and monazite from Geraldinho pegmatite (Chaves *et al.* 2005). Hydroxylherderite is rare, identified only in Sapo pegmatite.

II – Pegmatites with spodumene. The spodumene-rich pegmatites are hosted mainly in rocks of the São Tomé formation and in the Urucum granitic suite. Such pegmatites are poor in gem quality minerals, except the Urucum pegmatite, an important source

for beryl (morganite) and spodumene (kunzite). In some pegmatites are also found other primary lithium minerals or their secondary paragenesis, as the Córrego Boa Vista pegmatite. In minor amount triphylite also can occur as a primary lithium mineral; a secondary phosphate paragenesis can be found, including an association of huréaulite, lithiophilite, reddingite, phosphosiderite and vivianite. In this group, substitution bodies to late crystallization bodies are rare, usually smaller than 0.01 m³, covered by muscovite, quartz and albite. In some bodies the spodumene was partially replaced by cookeite, as in Córrego Boa Vista pegmatite.

III – Pegmatites with triphylite. The triphylite-rich pegmatites are hosted mainly in rocks of the São Tomé Formation. Pegmatites related to this group are poor in gem quality minerals, with rare occurrences of elbaite in Pomarolli I and II pegmatites. In all of

the studied pegmatites, secondary phosphates occur replacing partially or completely the triphylite-lithiophilite assemblage. The mineralogy comprises several iron and manganese phosphates, resulting in a complex mineralogical paragenesis, that include: sicklerite-ferrisickerite, heterosite-purpurite, frondelite-rockbrigeite, huréaulite, reddingite, barbosalite, gormanite, phosphosiderite-strengite, variscite, cyrilovite, and vivianite.

IV – Pegmatites with montebrasite. The montebrasite-rich pegmatites are hosted mainly in rocks of the São Tomé Formation. Pegmatites classified in this group are poor in gem quality minerals, with rare occurrences of elbaite in João Firmino and Evaldo pegmatites. In this group of pegmatites, small amounts of triphylite and their secondary minerals also can be found as in Telfrio pegmatite.

Primary montebrasite occurs associated with fluorapatite, hydroxylherderite, brazilianite, beryllonite, eosphorite, siderite, zanazziite, and crandalite. Other two types of secondary montebrasites also can be found in substitution bodies, and show lower fluorine content (Scholz *et al.* 2008). The primary montebrasite shows fluorine content ranging 3.52% to 5.57%; relevant cationic substitutions were not found. In this group of pegmatites, substitution bodies to late crystallization bodies are common, usually smaller than 0.1 m³, covered by secondary montebrasite, muscovite, quartz, albite and others secondary phosphates.

CONCLUDING REMARKS

Pegmatites of Conselheiro Pena district were classified in four groups depending on the presence or absence of primary lithium minerals: (i) pegmatites very poor or without primary Li-minerals; (ii) pegmatites with spodumene; (iii) pegmatites with triphylite and; (iv) pegmatites with montebrasite.

Such pegmatites are mainly related to the Urucum suite, that compose G2 granitic supersuite. These pegmatites are distributed in north-south trend around the Urucum pluton, located in central portion of the district. The most important bodies are Urucum, Navegadora, Cigana and Rogério II. Most of the pegmatites that occur surrounding the Urucum granite were classified as type II and III. The absence of montebrasite pegmatites (type IV) is characteristic.

Main occurrences of montebrasite-rich pegmatites are located in the north portion of this

region, near the locality of Linópolis. The most important mines are Córrego Frio, Telfrio and João Firmino pegmatites. The grade of differentiation of the pegmatites of Conselheiro Pena district and the complex paragenesis of secondary minerals seems to be an important aspect for the potential discovery of new species.

REFERENCES

- Almeida, F.F.M. (1977). O Craton do São Francisco. *Revista Brasileira Geociências* 7: 349-364.
- Cassedanne, J.P. (1983). Famous mineral localities: the Córrego Frio mine and vicinity, Minas Gerais, Brazil. *Mineral. Rec.* 14: 227-237.
- Chaves M. L. S. C., Scholz R., Atencio D. 2005. Assembléias e paragéneses minerais singulares nos pegmatitos da região de Galiléia (Minas Gerais). *Geociência* 24: 143-161.
- Chaves, M.L.S.C. and Scholz, R. (2008). Pegmatito Gentil (Mendes Pimentel, MG) e suas paragéneses mineralógicas de fosfatos raros. *Rev. Escola de Minas* 61: 125-134.
- Nalini Jr., H.A. (1997). Caractérisation des suites magmatiques néoprotérozoïques de la region de Conselheiro Pena et Galiléia (Minas Gerais, Brésil). Saint Etienne, These de Docteur, Ecole Nationale Superieure des Mines de Saint Etienne, 237 pp.
- Netto, C., Araujo, M.C., Pinto, C.P. and Drumond, J.B.V. (1998). Projeto Leste – Província Pegmatítica Oriental. Belo Horizonte, CPRM, 223 pp.
- Pedrosa-Soares, A.C., Noce, C.M., Wiedmann, C.M. & Pinto, C.P. (2001). The Araçuaí-West Congo orogen in Brazil: an overview of a confined orogen formed during Gondwanaland assembly. *Prec. Research* 110: 307-323.
- Pedrosa-Soares, A.C., Chaves, M.L.S.C. & Scholz, R. (2009). Eastern Brazilian pegmatite province. In: *Internat. Symp. on Granitic Pegmatites (PEG 2009)*, 4th, Recife, Field Trip Guide, 28 pp.
- Scholz, R., Karfunkel, J., Bermanec, V., da Costa, G.M., Horn, A.H., Cruz Souza, L.A. & Bilal, E. (2008). Amblygonite-montebrasite from Divino das Laranjeiras Mendes Pimentel pegmatitic swarm, Minas Gerais, Brasil. II. Mineralogy. *Romanian Journal of Mineral Deposits* 83: 135-139.

CONCURRENT TREATMENT OF METAMICT AND CRYSTALLINE FERGUSONITE BY U, Th AND Pb-RICH FLUIDS: AN EMPA AND TEM STUDY

Radek Škoda^{1§}, Renata Čopjaková¹ & Mariana Klementová²

¹ Institute of Geological Sciences, Faculty of Science, Masaryk University, Kotlářská.2, 61137 Brno, Czech Republic.

² Institute of Inorganic Chemistry ASCR, 250 68 Rež 1001, Czech Republic. §rskoda@sci.muni.cz

Key words: fergusonite, metamict state, experimental alteration, EMPA, TEM, FIB

INTRODUCTION

Complex Y, REE-Nb-Ta-Ti oxides, a typical accessory of more evolved granites and pegmatites commonly contain large amount of U and Th. Due to the accumulation of radiation induced damage over a long period of time, they usually occur in the metamict state. Metamictization, the transition from a crystalline to an amorphous state is accompanied by major changes in chemical and physical properties. Amorphization generally decreases the chemical durability of mineral; the dissolution rate of amorphous zircon is approximately two orders of magnitude greater than that of crystalline zircon. In fact, the diffusion coefficient in radiation-damaged zircon was determined to be 4–5 orders of magnitude greater than that of undamaged zircon (Cherniak & Watson 2001). Amorphous minerals are commonly highly hydrated. The process of metamictization can be generalized in three steps: 1) initial state - the isolated amorphous domains are surrounded by slightly disordered crystalline material. 2) The amorphous domains start to form percolation clusters at the first percolation point, 3) at the second percolation point, the crystalline domains cease to be interconnected (Geisler *et al.* 2003). Altered metamict Y-REE-Nb-Ta-Ti minerals commonly show enrichment of Si, Al, & Ca (e.g. Ruschel *et al.* 2010, Ercit, 2005), and they are usually replaced by pyrochlore group minerals (e.g. Ercit 2005). These alteration products also occur in the metamict state and they are assigned to the pyrochlore group minerals only on the basis of chemical composition, whereas due to the variable A-site vacancy, a number of different mineral compositions can be assigned to the pyrochlore group. The chemical composition of newly-formed pyrochlores differs significantly from primary ones, mainly by the presence of high amounts of Si and increasing vacancy (Lumpkin & Ewing 1995). Fergusonite group minerals used in experiments are tetragonal or monoclinic with general formula ABO_4 , where the A-site is occupied by Y, REE, U, Th, & Ca, and the B-site is occupied by Nb, Ta, Ti and W. High U and Th content usually assure its metamict state.

The aim of this work is a comparison of alteration processes of crystalline and metamict fergusonite and a detailed study of alteration products.

EXPERIMENTAL METHODS

A large grain of metamict fergusonite-(Y) from the NYF pegmatite Landsverk 1, Evje, Norway was crushed and sieved to the fraction 64-512 μm . The metamict state of natural fergusonite was confirmed by X-ray powder diffraction. After heating in air at 650°C for 12 hours, the fergusonite structure appeared on the powder X-ray diffraction pattern. The crystalline fergusonite-(Y) (crystals 10-200 μm in size) was prepared by flux growth technique in the Pt-crucible. Synthetic fergusonite-(Y) corresponds to the beta-modification of YNbO_4 .

The amount of 0.1 g (64-512 μm fraction) of crushed natural and synthetic fergusonite-(Y) was loaded into pressure vessels with a PFTE liner. Five ml of 1M solution containing $\text{Pb}(\text{NO}_3)_2$, $\text{Th}(\text{NO}_3)_4$ and $(\text{UO}_2)(\text{NO}_3)_2$ with a molar ratio U:Th:Pb 1:1:1 was added. The pressure vessels were then held at temperature of 200°C for 60 days.

After the run, the treated grains were mounted in epoxy resin, polished and carbon coated. Chemical composition of untreated and treated grains was determined by electron microprobe Cameca SX100. The operating parameters were: accelerating voltage 15 kV, the beam current 20nA, and spot size 1 μm . The mineral formulas were calculated on the basis of $\text{Nb}+\text{Ti}+\text{Ta}=1$. Although uranium was added to the solution as U^{6+} , for oxygen calculation uranium was assumed to be U^{4+} .

For the HRTEM observation, the thin foils from interesting areas were prepared by Focused Ion Beam (FIB) technique using FEI Quanta 3D Dualbeam electron microscope. The thin foils were consequently studied on the FEI Tecnai G2 F20 X-Twin transmission electron microscope (equipment located at GFZ Potsdam).

RESULTS

Besides a different degree of hydration, the chemical composition of natural fergusonite is almost homogeneous. The sum of oxides varies between 92.36-96.32 wt. % and the average content of major oxides in weight percents is as follows: Nb₂O₅ 43.56, Y₂O₃ 27.71, REE₂O₃ 12.50, UO₂ 3.61, CaO 1.43, SiO₂ 1.21, ThO₂ 1.20, Ta₂O₅ 1.18 and TiO₂ 0.82. Mineral formulas of studied fergusonites could be expressed as: (Y_{0.71} REE_{0.20} Ca_{0.07} U_{0.04} Th_{0.01})_{Σ1.00} (Nb_{0.95} Ti_{0.03} Ta_{0.02} Si_{0.05})_{Σ1.05} O_{4.13}.

During experimental treatment, the metamict fergusonite was locally replaced by patchy to collomorph-like domains up to tens of micrometers in size (bright in BSE, see Fig. 1a). These zones occur in the majority of fergusonite grains and propagate from the rim inwards, but a lot of metamict grains have some parts of edges unattached (Fig. 1a). Newly-formed areas have a sharp boundary with the neighboring host fergusonite and are depleted in Y and REE, but strongly enriched in either Th or U and Pb. Detailed study revealed that these phases form separate domains or occur in a mixture. The chemical compositions of fergusonite and newly-formed phases close to the contact zone do not differ from

compositions in their central parts. The interfacial area between the newly-formed phases and parent fergusonite contain numerous nanopores.

The U-rich phase has the following chemical composition: Nb₂O₅ 48.18, UO₂ 28.92, ThO₂ 6.69, PbO 6.35, Ta₂O₅ 1.21, TiO₂ 0.90, SiO₂ 0.57 and Y₂O₃ 0.28, which yields the empirical formula (U_{0.28} Th_{0.07} Pb_{0.04} Y_{0.01})_{Σ0.39} (Nb_{0.95} Ti_{0.03} Ta_{0.02} Si_{0.02})_{Σ1.02} O_{3.20}.

The chemical composition of the Th-rich phase is Nb₂O₅ 33.38, UO₂ 4.09, ThO₂ 48.23, PbO 1.12, Ta₂O₅ 1.03, TiO₂ 0.87 and Y₂O₃ 1.90, REE₂O₃ 1.11 and SiO₂ 0.54 yielding the formula (Th_{0.68} U_{0.06} Y_{0.06} REE_{0.02} Pb_{0.0})_{Σ0.83} (Nb_{0.94} Ti_{0.04} Ta_{0.02} Si_{0.02})_{Σ1.02} O_{4.04}.

The FIB sample preparation (Fig. 1b) in combination with TEM allows us to study the newly-formed phases in detail as well as the transition zone between unchanged fergusonite and newly-formed phases. The U-rich phase is nanocrystalline, which is well documented by High Angle Angular Dark Field (HAADF) images. It forms prismatic or platy crystals up to 400 nm, clearly visible in Figure 2a. In contrast, the Th-rich phase appears to be amorphous (Fig. 2b); crystals of similar composition a few nanometers

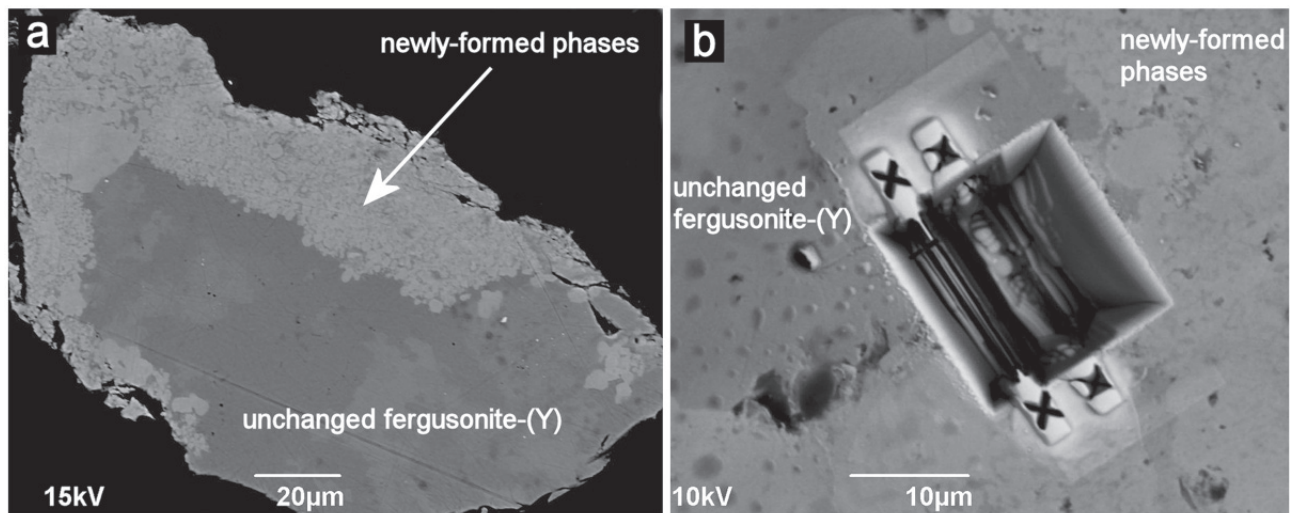


FIGURE 1: a) BSE image of the fergusonite-(Y) replaced by newly-formed U- and Th-rich phases, b) view (combination of BSE+SE image) of the area where the thin foils prepared by FIB were taken.

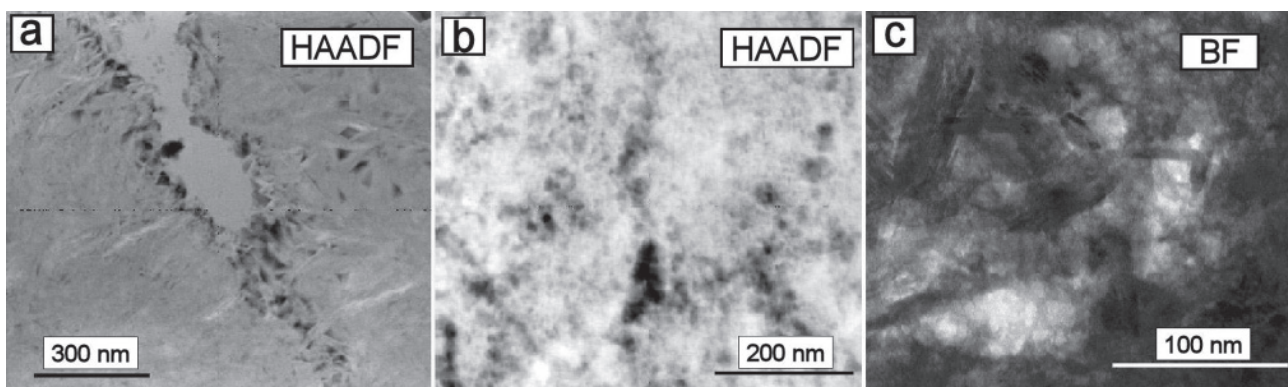


FIGURE 2: a) HAADF image of the crystalline U-rich phase in sub-micron scale, b) HAADF image of the amorphous and porous Th-rich phase, c) Bright Field image of the U-rich phase nanocrystals enclosed in the amorphous Th-rich phase.

in size were rarely observed. More frequently, the amorphous Th-rich phase encloses the U-rich crystals (Fig. 2c). Unfortunately, the larger thickness of the thin foils did not allow determination in detail of the structural parameters of the U-rich phase. Nevertheless, the following d values were obtained 3.15-3.17 Å, 2.47 Å, 1.80 Å and 1.47 Å.

The crystalline fergusonite does not show any apparent features of alteration. Its chemical composition remains unchanged and replacement textures or dissolution etch pits were not observed.

DISCUSSION

Uranium, thorium and lead from the solution interacted with metamict and hydrated Y, REE-Nb-Ta oxide, and replaced it by precipitation of crystalline (U-rich) and amorphous (Th-rich) phases, whereas Y, REE, and Ca were leached out. Dramatic alteration of metamict fergusonite and resistant crystalline fergusonite obviously confirms the strong negative influence of the metamict state on the mineral stability during low-temperature alteration processes, as described by several authors.

The absence of lateral changes in chemical composition close to the contact zone argues against mass transport by diffusion. On the other hand, the presence of abundant nanopores, chiefly close to the interface (Fig. 2a), suggests that dissolution and consequent precipitation could take place. Despite substantial compositional changes among the U-Th-Y, REE cations, the Ta/(Ta+Nb) ratio of newly-formed phases is nearly identical to the parent fergusonite, which suggests similar (im)mobility of Nb and Ta at the described conditions.

Obtained d values and chemical composition do not lead to unambiguous identification of the U-rich phase.

Although the chemical conditions of experimental alteration are different from that usually occurring in nature, the replacement textures on the micrometer scale are very similar. With regards to the long geological time, the natural newly-formed "pyrochlores", owing to their common U and Th content, are also metamict and their original

structure is not known. Our experiments show that newly-formed phases could be either amorphous or crystalline. According to the discrimination diagram for metamict Y, REE-Nb-Ta-Ti oxides published by Ercit (2005), both newly-formed phases fall in the pyrochlore field, but the Th-rich phase can not be a member of the pyrochlore group due its primary amorphous nature.

Different behavior of U and Th during the precipitation of newly-formed phases could indicate different oxidation state of uranium (U^{6+}) than thorium (Th^{4+}). Structural identification of the U-rich phase as well as the oxidation state of U requires further study.

ACKNOWLEDGEMENT

The authors wish to thank Anja Schreiber for FIB sample preparation and Richard Wirth for the TEM study.

This work was supported by project of Grant agency of Czech Republic nr. KJB 301630801

REFERENCES

- Cherniak, D., J., Watson, E., B. (2001). Pb diffusion in zircon. *Chem. Geol.* **172**: 5-24
- Ercit, T., S. (2005). Identification and alteration trends of granitic-pegmatite hosted (Y,REE,U,Th)-(Nb,Ta,Ti) oxide minerals: a statistical approach. *Can. Mineral.* **43**: 1291-1303.
- Geisler, T., Pidgeon, R., T., Kurtz, R., van Bronswijk, W., Schleicher H. (2003). Experimental hydrothermal alteration of partially metamict zircon. *Amer. Mineral.* **88**: 1496-1518.
- Lumpkin, G., R., Ewing, R., C. (1995). Geochemical alteration of pyrochlore group minerals: Pyrochlore subgroup. *Amer. Mineral.* **80**: 732-743.
- Ruschel K., Nasdala, L., Rhede, D., Wirth, R., Lengauer, Ch., Libowitzky, E. (2010). Chemical alteration patterns in metamict fergusonite. *Eur. J. Mineral.* **22**: 425-433.

TOWARDS EXPLORATION TOOLS FOR HIGH PURITY QUARTZ AND RARE METALS IN THE SOUTH NORWEGIAN BAMBLE-EVJE PEGMATITE BELT

Benjamin R. Snook^{1,2§}, Axel Müller², Ben J. Williamson¹ & Frances Wall¹

¹ Camborne School of Mines - University of Exeter, Penryn, Cornwall TR10 9EZ, U.K. § bs225@exeter.ac.uk

² Geological Survey of Norway, N-7491 Trondheim, Norway

Key words: Pegmatites; REE; high purity quartz; Bamble-Evje pegmatite; mineral chemistry.

INTRODUCTION

High purity naturally occurring quartz, defined as containing less than 50 ppm trace elements (Harben 2002), is of increasing demand due to emerging applications in the production of high-tech components such as solar cells and computer chips. However, high purity quartz deposits (including hydrothermal veins, pegmatites and granitic rocks) are extremely rare and volumetrically small. Unless significant new deposits are found, increasing demand for high purity quartz will raise its price, elevating the strategic nature of this limited commodity. Rare Earth Elements (REEs) have a multitude of uses such as rare-earth magnets (wind turbines), nuclear batteries (hybrid cars), super conductors, and optoelectronics (lasers, LCD screens). REEs are mainly sourced from the minerals bastnaesite, monazite and apatite, and to a lesser extent allanite, REE-bearing titanite and fluorite, with China currently contributing 97% of the global REE production. However, the Chinese government has recently implemented export restrictions for REEs, initiating a wave of global exploration. Ensuring security of supply requires the identification of deposits in a broader range of countries, particularly in Europe, and possibly of a different kind to those currently in production. A prerequisite for developing exploration tools for such deposits is to gain a better understanding of the nature of high purity quartz mineralisation.

Preliminary data will be presented for PhD studies being carried out on pegmatites and surrounding country rocks from the Evje-Iveland field of the Bamble-Evje pegmatite cluster, southern Norway. The area was targeted due to its well constrained geological setting and previously identified potential for high purity quartz (Larsen *et al.* 2000). The aims of the study are to determine the mode of occurrence and mineral chemistry of the pegmatites in order to better understand their formation history (i.e. their source, magmatic evolution and any hydrothermal

overprint) and to explain the nature and existence of REE mineralisation and high purity quartz.

PROJECT SYNOPSIS

The N-S-striking Evje-Iveland field is 30 km long and up to 10 km wide. It consists of around 350 major pegmatite occurrences, emplaced within migmatitic amphibolites and metagabbros, at the western margin of the Fennoscandian shield. The pegmatites were formed during the Sveconorwegian orogeny (1.14-0.90 Ga), when the Bamble Complex was thrust over the Telemark Block along the Porsgrunn-Kristiansand Fault (Bingen *et al.* 2008). They lie in the interior of the Telemark Block in the foot wall of the thrust zone (Fig. 1). The pegmatites, which were emplaced at 910.5 ± 1.6 Ma (Scherer *et al.* 2001), are spatially related to the Høvringsvatnet granite intrusion which lies to the NE and has an emplacement age of 945 ± 53 Ma (Rb-Sr whole-rock isochron, Pedersen (1981)).

Around 260 of the pegmatites have been mined for high purity K-feldspar for use in the ceramics industry and as dental porcelain. The granitic pegmatites are classified as rare-element pegmatites of the NYF (Niobium-Yttrium-Fluorine) family (Černý & Ercit 2005) consisting of K-feldspar, plagioclase, quartz, biotite and muscovite and with variable contents of a range of rare metal and REE minerals. The pegmatites are zoned, consisting of a granitic border zone ('chilled margin'), a megacrystic intermediate zone and core zone with crystal sizes of up to several meters. The 7 pegmatites under investigation (localities in Fig. 1) are beryl-gadolinite, gadolinite-fergusonite and allanite-monazite types. Some show late-pegmatitic (metasomatic) partial replacement, with an assemblage of cleavelandite, amazonite, topaz, garnet, beryl and tourmaline, and/or the presence of hydrothermal breccias and replacements containing high purity quartz, adularia, chlorite, calcite, fluorite and pyrite. Larsen (2002) suggested that the Evje-Iveland pegmatites share a common source and represent relatively primitive

melts. The relatively poorly fractionated nature of the melts was thought to have resulted in the formation of the high purity quartz as the melts would have been relatively low in incompatible elements (potential quartz impurities). This argument is at odds with the traditional view that cooler more evolved melts produce purer quartz (Larsen *et al.* 2000).

THE PROJECT AIMS TO ASSESS:

- ◆ The origin of the Evje-Iveland pegmatites; whether they represent late-stage melts from the Høvringsvatnet granite or partial melts of country rock gneisses, metagabbros (Fig. 2) or an unknown source.

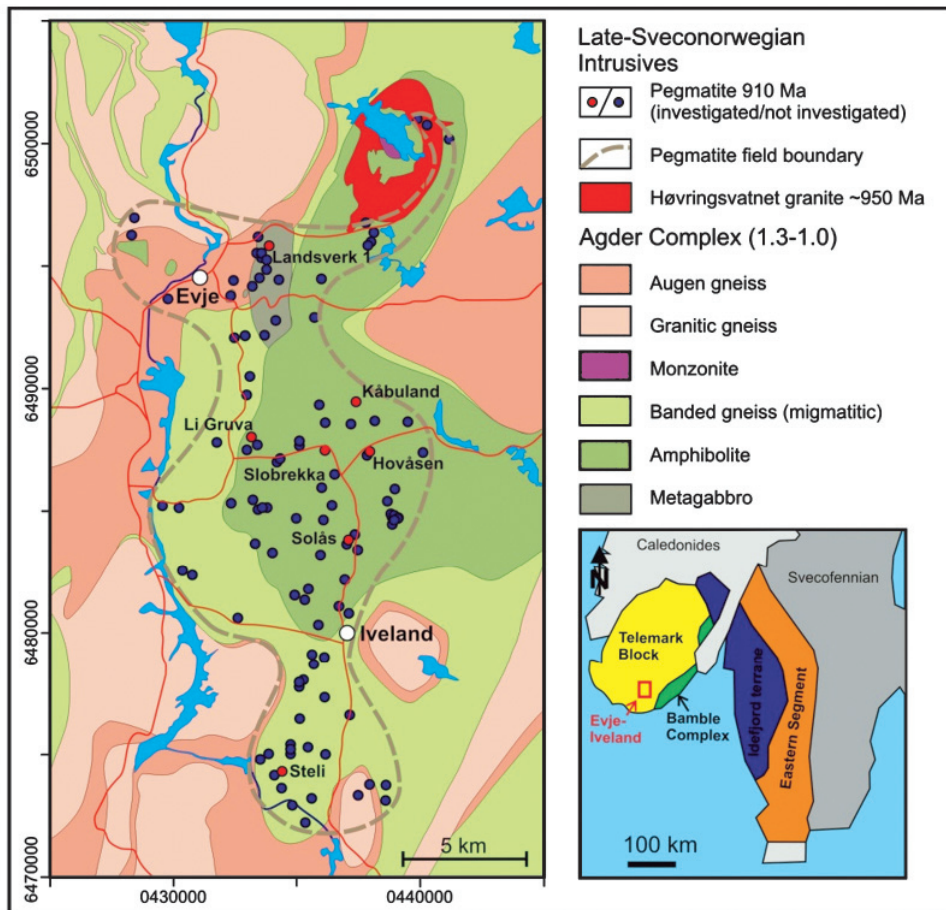


FIGURE 1. Geological map of the area under investigation.

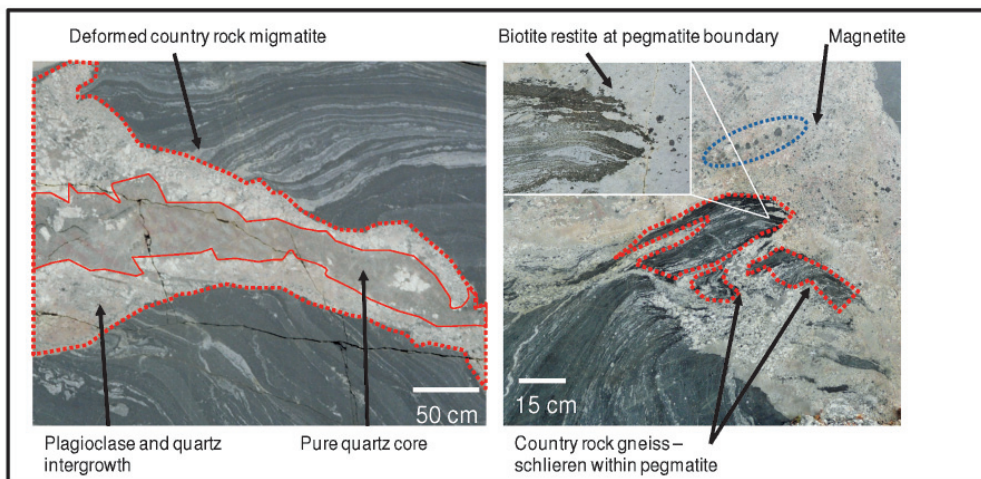


FIGURE 2. Images of a road cut in the town of Iveland showing evidence for partial melting of country rock migmatites to form pegmatitic melts.

- ◆ Whether the purity of pegmatite quartz is controlled by its (preferentially low) temperature of crystallisation or the degree of fractional crystallisation, variably linked to the extent of undercooling, the alkalinity of the pegmatite melts and the presence of fluxing agents.
- ◆ Whether rare metals and REEs are enriched in certain pegmatites due to differences in source composition, degrees of partial melting of the source and/or levels of fractionation.
- ◆ If in some pegmatites high purity quartz was generated by secondary processes (possibly at the magmatic-hydrothermal transition) such as hydrothermal alteration or secondary recrystallisation.

METHODOLOGIES

The study commenced with a mapping program to constrain the dimensions of the pegmatite bodies, their structural relations and internal mineralogical zonations. Quartz samples were collected from massive central and outer cores, roof and floor regions (relative to pegmatite body) and quartz/plagioclase intergrowth boundary zones to locate the highest purity quartz and to determine intra-pegmatite chemical variations. Samples were also collected of 'chilled margin' rocks (providing the closest approximation to the pegmatite melt composition on emplacement), country rocks (both proximal and distal to contacts). Feldspar and mica samples for five pegmatites (excluding Landsverk 1 and Kåbuland) were available from previous reconnaissance studies.

REFERENCES

- Bingen, B., Nordgulen, Ø. & Viola, G. (2008). A four phase model for the Sveconorwegian orogeny, SW Scandinavia. *Norwegian Journal of Geology* **88**: 43-72.
- Černý, P. & Ercit, T.S. (2005). The classification of granitic pegmatites. *Can. Mineral.* **43**: 2005-2026.
- Harben, P.W. (2002). *The industrial mineral handybook – a guide to markets, specifications and prices.* 4th edition, Industrial Mineral Information, Worcester Park, United Kingdom, 412 p.
- Larsen, R.B., Polvè, M. & Juve, G. (2000). Granite pegmatite quartz from Evje-Iveland: trace element chemistry and implications for the formation of high-purity quartz. *NGU-Bulletin* **436**: 57-65.
- Larsen, R.B. (2002). The distribution of rare-earth elements in K-feldspar as an indicator of the petrogenetic processes in granitic pegmatites: examples from two pegmatite fields in Southern Norway. *Can. Mineral.* **40**, pp. 137 -151.
- Müller, A., Ihlen, P.M. & Kronz, A. (2008). Quartz chemistry in polygeneration Sveconorwegian pegmatites, Froland, Norway. *Europ. J. Mineral.* **20**: 447-463.
- Pedersen, S. (1981) Rb/Sr age determinations on the late Proterozoic granitoids from the Evje area, south Norway. *Bulletin of the Geological Society of Denmark* **29**:129-143.
- Scherer, E., Münker, C., Mezger & K. (2001). Calibration of the lutetium-hafnium clock. *Science* **293**: 683-687.

MINERAL CHEMISTRY OF ELBAITE FROM THE SERRA BRANCA PEGMATITE, NEAR PEDRA LAVRADA, STATE OF PARAÍBA, NE-BRAZIL

Dwight Rodrigues Soares¹; Hartmut Beurlen²; Ana Cláudia Mousinho Ferreira¹ & Ranjana Yadav²

1 Instituto Federal de Educação, Ciência e Tecnologia da Paraíba (IFPB) – Campina Grande, Paraíba, Brazil

2 Universidade Federal de Pernambuco (UFPE) – Recife, Pernambuco, Brazil

Keywords: Serra Branca pegmatite, elbaite, Borborema Pegmatite Province, mineral chemistry

INTRODUCTION

The Serra Branca is one of over 700 Ta-Be-Li-gem bearing pegmatites of the Borborema Pegmatite Province (BPP). The BPP covers parts of the states of Paraíba and Rio Grande do Norte, in northeastern Brazil, and is known worldwide since World War II due to its production of Ta-ore and beryl, and later by the production of raw mineral products for the ceramics industry and subordinate gemstones like aquamarine, morganite, heliodor, gahnite, euclase, elbaite and spessartine. Nowadays, the most famous production of the BPP is the unique copper-bearing elbaite known under the fashion name “Paraíba Tourmaline”. The mineral chemistry of this peculiar gem was already studied by many authors (Soares *et al.* 2008 and references therein).

This study presents the chemical characteristics of further light blue gem quality elbaite free of copper, from the Serra Branca pegmatite, near Pedra Lavrada in the State of Paraíba, Brazil.

GEOLOGICAL SETTING

The Borborema Pegmatite Province (BPP) extends over an area of approximately 75 x 150 Km in the eastern-southeastern part of the Seridó Foldbelt in the Rio Grande do Norte Tectonic Domain, between 5°45' and 7°15' S and 35°45' and 37° W, in the states of Paraíba (PB) and Rio Grande do Norte (RN), in northeastern Brazil (Fig. 1).

The Seridó Foldbelt is composed of a Paleoproterozoic gneissic-granitic-migmatitic basement and a Neoproterozoic supracrustal meta-volcano-sedimentary sequence (the Seridó Group), which comprises, from base to top, gneisses and marbles (Jucurutu Formation), quartzites and meta-conglomerates (Equador Formation) and garnet-cordierite and/or sillimanite-biotite schists (Seridó Formation).

Several Neoproterozoic granite types are found intruding the Seridó Group. The youngest one is the

most probable source of the pegmatites of the BPP and consists of several small pegmatitic granite intrusions with peraluminous, S-type characteristics, with age determinations between 480 and 530 Ma (Beurlen *et al.* 2008).

The formation of Be-Li-Ta or gem-bearing (mineralized) rare-element granitic pegmatites is usually considered to be related to pegmatitic granites of a late- to post orogenic (Baumgartner *et al.* 2006 and references therein) phase.

THE SERRA BRANCA PEGMATITE

The Serra Branca granitic pegmatite occurs 10 km south of the township of Pedra Lavrada in the State of Paraíba and was mined sporadically for rare element mineral concentrates, mainly Ta-Nb and Sn oxides and some Li-minerals. In addition it is known by a great variety of phosphate minerals. The pegmatite strikes along 250 m N80°E with subvertical dip intruded in garnet-biotite-schists of the Neoproterozoic Seridó Formation, with a maximum thickness of 50 m. The internal zoning includes a border zone followed by a wall zone (K-feldspar quartz, muscovite and black tourmaline), an external intermediate zone (blocky K-feldspar, quartz, albite, muscovite and black tourmaline), an internal intermediate zone (albite, quartz, phosphates, - including the new species serrabrancaite, and elbaite) followed by a central quartz core with local blue quartz patches due to microscopic inclusions of blue tourmaline. Gem minerals include colored tourmaline and some phosphate minerals, mostly found in the internal intermediate zone, quartz-core or pockets.

CHEMICAL COMPOSITION OF ELBAITE

Electron microprobe analyses EMPA of 20 fragments of light blue gem-quality tourmaline allow to classify them as fluorelbaite according to Hawthorne & Henry (1999) with ^WF > 0.5 apfu (range between 0.41 and 0.83 apfu). The average

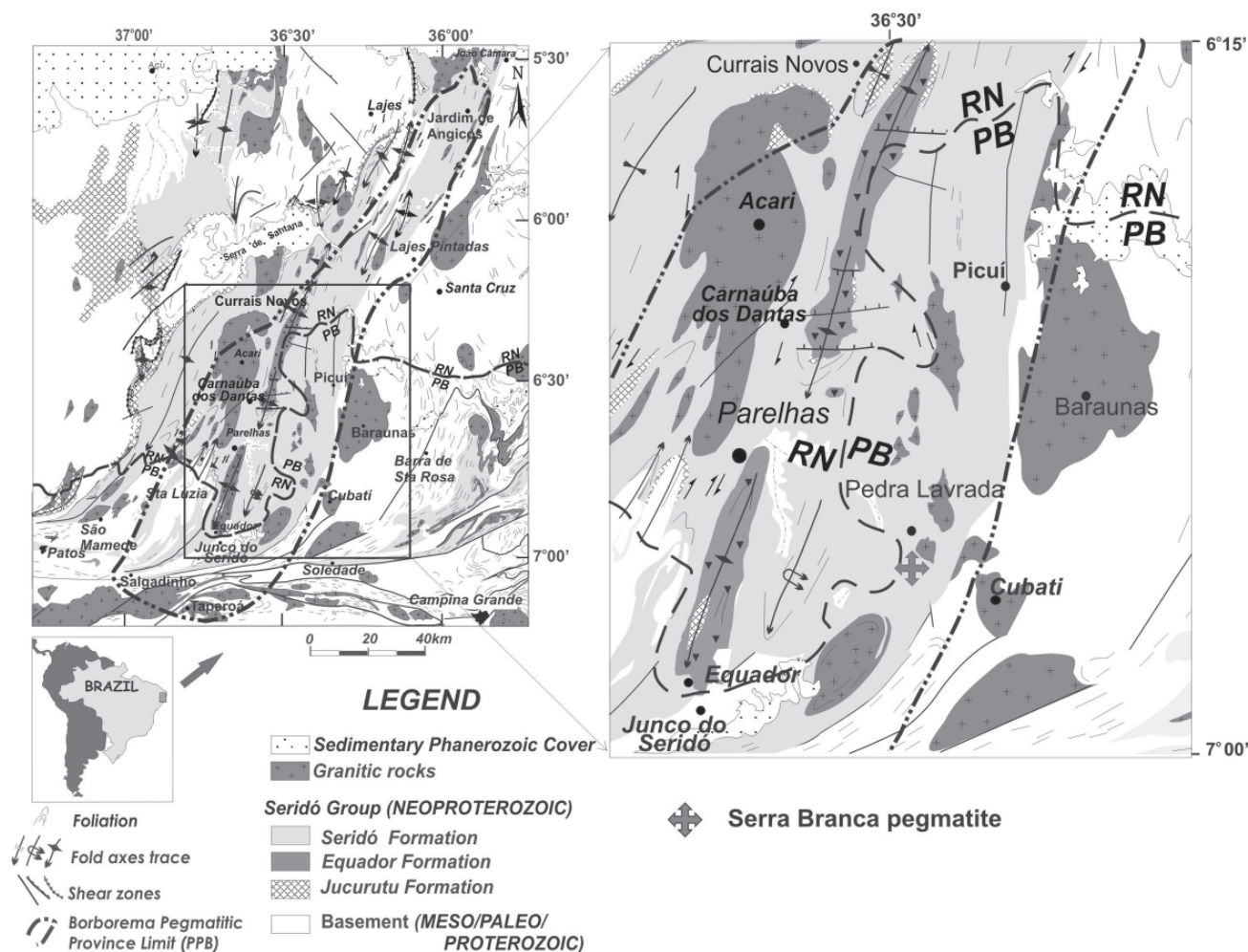
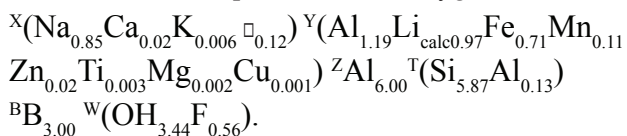


FIGURE 1: Simplified Geologic Map with the location of the Serra Branca Pegmatite.

stoichiometric composition for 31 oxygens is:



The compositional variation in the X-site, with dominance of Na+K, over vacancy and Ca, is shown in Figure 2.

The blue gemological Serra Branca elbaite is characterized by low ^TSi deficiency, low X-site vacancy (between 0.09 and 0.17 pfu), negligible Cu contents (0.000 to 0.007 apfu), high ^YFe (0.58 to 0.77 apfu) and high ^YFe/^Y(Fe+Mg) and ^XNa/(Na+Ca) values (0.97 to 0.98). There is observed a good (near 1/1) negative correlation between ^XNa and ^Xvacancy and between ^Y(Li+Al) and ^Y(Mg+Fe) as also reported in other elbaite in the BPP (Soares *et al.* 2008).

CONCLUSIONS

These data in association with the paragenetic variety of phosphates and the absence of minerals

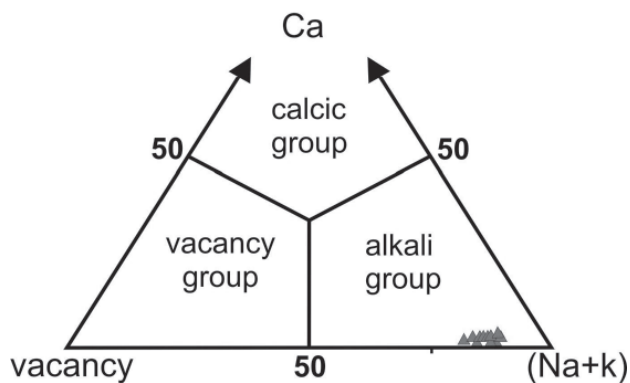


FIGURE 2: Compositional variation of the blue gem quality tourmaline from the Serra Branca pegmatite

characteristic for highly fractionated pegmatites, indicate a moderate degree of evolution (fractionation) of the Serra Branca pegmatite relative to Li-rich pegmatites with abundant spodumene and/or lepidolite common in the BPP.

REFERENCES

- Beurlen, H., Da Silva, M.R.R., Thomas, R., Soares, D.R. & Olivier, P. (2008). Nb-Ta-(Ti-Sn) oxide mineral chemistry as tracer of rare-element granitic pegmatite fractionation in the Borborema Province, Northeastern Brazil. *Mineral. Deposita* **43**: 207-228.
- Baumgartner, R., Romer, R.L., Moritz, R., Sallet, R. & Chiaradia, M. (2006). Columbite-tantalite-bearing granitic pegmatites from the Seridó belt, Northeastern Brazil: genetic constraints from U-Pb dating and Pb isotopes. *Can. Mineral.* **44**:69-86.
- Hawthorne, F.C. & Henry, D.J. (1999). Classification of the minerals of the tourmaline group. *Eur. J. Mineral.* **11**: 201-215.
- Soares, D. R., Beurlen H., Barreto S. B., Da Silva M.R.R. & Ferreira A.C.M. (2008). Compositional variation of tourmaline group minerals in the Borborema Pegmatite Province, Northeastern Brazil. *Can. Mineral.* **46**: 1097-1116.

SECONDARY Ta-Nb OXIDE MINERALS OF THE ARCHAEOAN WODGINA PEGMATITE DISTRICT, WESTERN AUSTRALIA, AND THEIR SIGNIFICANCE

Marcus T. Sweetapple^{1§} and Gregory R. Lumpkin²

¹ CSIRO Earth Science and Resource Engineering, P.O. Box 1130, Bentley, Western Australia, 6102. [§]email: Marcus.Sweetapple@csiro.au

² Institute of Materials Engineering, Australian Nuclear Science and Technology Organization, PMB 1, Menai, New South Wales 2234, Australia

Key words: pyrochlore, microlite, fersmite, tantalum mineralization, Wodgina, Australia.

INTRODUCTION

We describe here the secondary tantalum minerals, principally belonging to the pyrochlore group, occurring within the Wodgina pegmatite district. These secondary Ta mineral species are interpreted to have late magmatic to subsolidus parageneses. Although these secondary species are of less economic significance than primary minerals such as wodginite and columbite-tantalite, they are also of interest as indicators of late stage pegmatite petrogenetic processes, as well as having potential implications for long term actinide storage.

The Wodgina pegmatite district has been a globally important source of tantalum since 1905. Prior to the suspension of mining operations by Talison Minerals Pty. Ltd. in 2008, the district was providing more than 30% of world tantalum production (TIC 2008). Mining is currently suspended on account of market conditions.

GEOLOGICAL SETTING

The Wodgina pegmatite district is located near the north-western coast of Western Australia (Fig. 1), lying in the centre of the Archaean Pilbara Craton. The pegmatite district is comprised of three distinct pegmatite groups (Fig. 1), which may be classified according to the schema of Černý & Ercit (2005):

- i) **Wodgina pegmatite group**, comprised of layered albite-type pegmatites hosted in metakomatiite and metabasalt; the most important body is the Wodgina mainlobe pegmatite, which forms a dyke approximately 1 km long and up to 40 metres thick. Modern open pit mining of this pegmatite took place over the years 1987-1994.
- ii) **Mt. Cassiterite pegmatite group**, consisting of a substantial complex of interlinked sills and dykes of the albite-spodumene pegmatite type, hosted in a psammopelitic sequence. Internally, these pegmatites are weakly layered to homogenous.

At surface, this pegmatite group covers an area of approximately 1.2 x 0.8 km, with a depth extent of at least 350 metres. Open pit mining of this pegmatite was carried out from 1995-2008.

- iii) **Beryl pegmatite group** (beryl-columbite subtype), consisting of pegmatites no more than 140 m long x 15 m wide, with simple zonation, containing beryl and columbite-(Mn) mineralization, intruded semi-concordant with the foliation of a sheared mafic schist unit.

Changes in distribution of pegmatite type appear to be directly controlled by host rock type, and have different structural controls. Both major pegmatite groups display geochemical and mineralogical characteristics typical of highly fractionated rare metal pegmatites. Columbite-tantalite from the pegmatites has been age dated at 2830 Ma, related to the emplacement of a 2830-2890 Ma 'younger' granite suite across the Archaean Pilbara Craton (Kinny 2000; summary of Sweetapple & Collins 2002). Further details of the pegmatite groups and their host rocks may be found in Sweetapple *et al.* (2001, 2008), and Sweetapple and Collins (2002).

PRIMARY TANTALUM-NIOBIUM (-TIN) MINERALIZATION

The three pegmatite groups have distinctly different tantalum-niobium mineral assemblages. These are summarized in Table-1. These minerals have a largely quasi-homogeneous distribution in the Mt. Cassiterite pegmatite group, whereas Ta-Nb-Sn mineral assemblages vary significantly between different petrogenetic units in the Wodgina mainlobe pegmatite. In the latter pegmatite, the most important variations are the concentration of niobium-rich minerals in central granitic-aplitic textured (GAP) units, whereas tantalum-rich primary minerals reflecting a high degree of fractionation are concentrated in albite-rich units, especially paragenetically late sugary albite units containing wodginite.

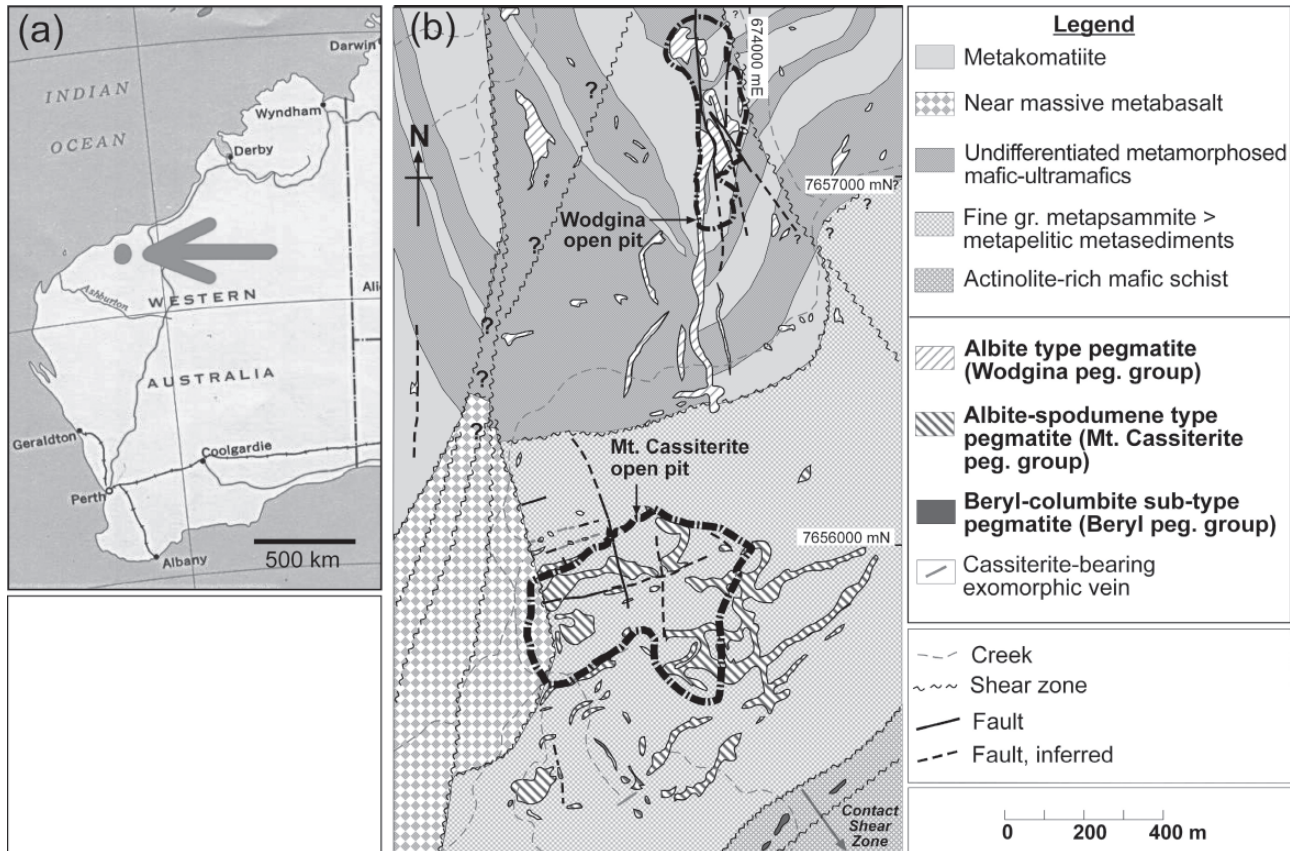


FIGURE 1: (a) Location map of Western Australia, and (b) geology and pegmatite group distribution in the Wodgina district.

PYROCHLORE SUPERGROUP MINERALS

Pyrochlore supergroup minerals are less abundant than columbite-tantalite and wodginite in all of the pegmatite groups. They occur both as direct replacements of primary columbite-tantalite and wodginite, as well as grain aggregates or more rarely, discrete grains. A number of the pyrochlore supergroup species of the two main pegmatite

groups reflect the Ta and Nb contents of the primary Ta-Nb minerals. Microlite is the only species present in the Mt. Cassiterite pegmatite group, whereas pyrochlore is also present, subordinate to microlite, in the Wodgina mainlobe pegmatite, as an alteration product of columbite (Fig. 2).

Conversely, in the Beryl pegmatite group, zero valence dominant (zvd) microlite occurs as inclusions within columbite-(Mn), rather than forming an

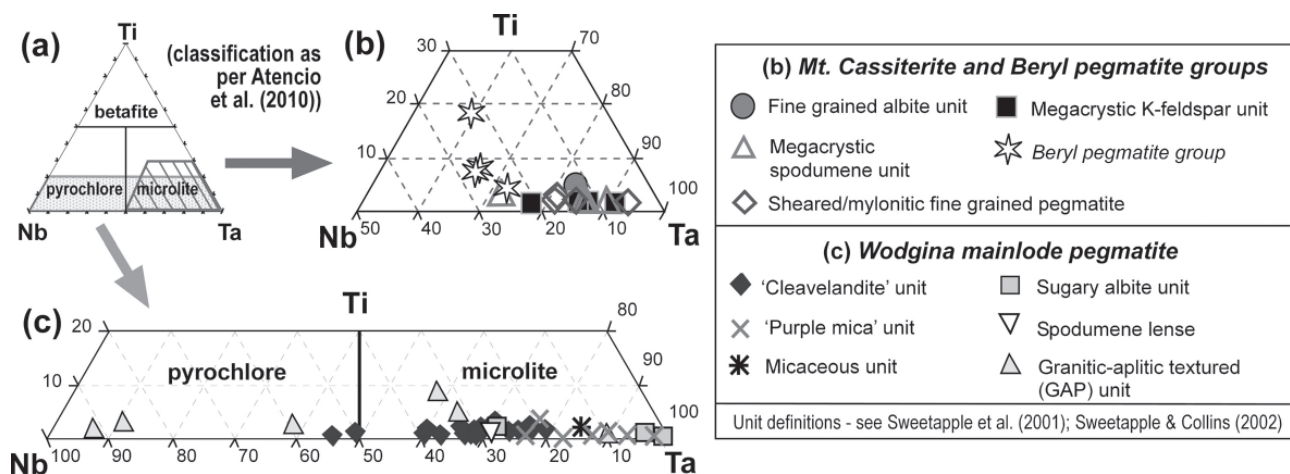


FIGURE 2: Classification of pyrochlore group minerals by B-site cation occupancy. (a) Distribution of data by host pegmatite group within fields of dominant cation occupancy; for (b) Mt. Cassiterite and Beryl pegmatite groups and (c) Wodgina mainlobe pegmatite.

TABLE 1: Summary of Ta-Nb-Sn mineralogy for the pegmatite groups of the Wodgina District. Minor species are in brackets. Minerals are listed in decreasing order of abundance.

Pegmatite Group	Primary mineralogy	Secondary mineralogy
Wodgina	Tantalite-(Mn), Columbite-(Mn) (Wodginite, Cassiterite)	Fluorcalciomicrolite, Calciomicrolite (zvd Microlite, Fluorcalciopyrochlore, Calciopyrochlore, Fersmite, Titanite, Rutile, Euxenite/ Aeschynite?)
Mt. Cassiterite	Wodginite, Cassiterite, Tantalite-(Mn), Columbite-(Mn) (Ferrowodginite)	Fluorcalciomicrolite, zvd Microlite
Beryl	Columbite-(Mn) (zvd Microlite inclusions in Columbite-(Mn))	?

zvd = zero valence dominant (nomenclature of Atencio *et al.* 2010)

alteration product *per se*. This is interpreted to be a consequence of a significantly different paragenesis within a fluid-rich shear zone, where the formation of columbite-(Mn) or microlite depended on the local availability and ion exchange of species such as Mn^{2+} and Ca^{2+} (cf. Lumpkin & Ewing 1992). A similar reversible mechanism may also be used to explain the appearance of secondary columbite-(Mn) overgrowths on microlite as a by-product of alteration of primary tantalite-(Mn) at Mt. Cassiterite.

Broadly, pyrochlore supergroup minerals may be texturally divided into three morphological types when observed in SEM imaging:

- ♦ a uniform 'solid' type, mostly as crusts on primary Ta-Nb mineral grains;
- ♦ a type with visible porosity, which mostly appears where primary Ta-Nb mineral grains have been completely replaced;
- ♦ crystallites with cubic or hexagonal outlines, typically ranging in 1-10 μm diameter, occurring as either discrete crystals or crystal aggregates.

There appears to be some degree of overlap between these different types, e.g. the apparently uniform 'solid' microlite is shown by TEM to contain micropores of < 100 nm diameter. The variation in textural types may be considerable over a distance of only a few centimetres, suggesting that interactions between primary Ta-Nb minerals with late calcian fluids was highly heterogeneous, dependant on microscale fluid pathways. There is little difference in compositions between the different textural types, although some crystallites may contain higher U and Pb contents, particularly in the Wodgina main lode pegmatite. Significantly, the crystallite form of microlite has been identified in samples from the two main pegmatites as discrete particles in the size range of 50-500 nm, from both SEM and TEM studies. Pyrochlore supergroup minerals almost invariably lack primary growth zoning.

Chlorite geothermometry on chlorite overgrowths on microlite in the Wodgina main lode pegmatite indicates a lower temperature boundary of 200-300 °C.

Together with paragenetic criteria, this is suggestive of pyrochlore supergroup mineral crystallization continuing from magmatic to subsolidus conditions.

The B-site chemistry of pyrochlore supergroup minerals is chiefly controlled by the local mineralogical and geochemical assemblages where these species are found, including primary Ta-Nb mineral compositions, rather than specific pegmatite unit types. Pyrochlore supergroup minerals display compositional evolution toward A and Y-site vacancies with increasingly later parageneses (cf. Lumpkin & Ewing 1992). Microlite from Mt. Cassiterite displays more consistent trends toward defected compositions than the Wodgina main lode pegmatite, consistent with the greater degree of elevation and weathering of the former pegmatite group.

Pyrochlore group minerals are major hosts of U and Th in the two main pegmatite groups. Beside very rare accessory minerals such as zircon, the main primary source of U and Th is uraninite inclusions within primary columbite-tantalite. Therefore, there is good evidence to link the derivation of U-enriched crystallite microlite with elevated A and Y-site vacancies, to the alteration of primary Ta-Nb minerals. Given the absence of any other known primary sources of U and Th, either within or outside of the pegmatites, it seems reasonable to presume very limited mobility of radionuclides in unweathered pegmatite over the last 2.8 Ga.

OTHER SECONDARY TA-NB MINERALS

Other Ta-Nb minerals are volumetrically minor compared to pyrochlore group minerals. Fersmite ($CaNb_2O_6$) occurs with pyrochlore as an alteration product of columbite in GAP units of the Wodgina main lode pegmatite, together with a very fine (< 5 μm diameter) euxenite/aeschynite-like phase, Nb-bearing titanite, and traces of REE minerals. Traces of thorite found in the Mt. Cassiterite pegmatite post-dates microlite replacement of wodginite, and displays complex intergrowths with apatite, cassiterite and pyrite.

REFERENCES

- Atencio, D., Andrade, M.B., Christy, A.G., Gieré, R. & Kartashov, P.M. (2010). The pyrochlore supergroup of minerals: nomenclature. *Can. Mineral.* **48**: 673-698.
- Černý, P. & Ercit, T.S. (2005). The classification of granitic pegmatites revisited. *Can. Mineral.* **43**: 2005-2026.
- Kinny, P. (2000). U-Pb dating of rare-metal (Sn-Ta-Li) mineralized pegmatites in Western Australia by SIMS analysis of tin and tantalum bearing minerals. *New Frontiers in Isotope Geoscience Conference*: 113-116. Univ. Melbourne, Lorne, Victoria.
- Lumpkin, G.R. & Ewing, R.C. (1992). Geochemical alteration of pyrochlore group minerals: Microlite subgroup. *Am. Mineral.* **77**: 179-188.
- Sweetapple, M.T. & Collins, P.L.F. (2002). Genetic Framework for the Classification and Distribution of Archean Rare Metal Pegmatites in the North Pilbara Craton, Western Australia. *Econ. Geol.* **97**: 873-895.
- Sweetapple, M.T., Collins, P.L.F. & Lumpkin, G.R. (2008). A genetic model for regional zonation and evolution of mineralized pegmatites from the Archaean Wodgina pegmatite district, Pilbara Craton, W.A. *Aust. Earth Sci. Conv., Geol. Soc. Aust. Abs.* **89**: 236.
- Sweetapple, M.T., Cornelius, H. & Collins, P.L.F. (2001). Tantalum Mineralization of the Wodgina pegmatite district: The Wodgina and Mt. Cassiterite pegmatite orebodies. *Excursion guide for Pilbara Metallogeny, Geol. Surv. W.A., Record 2001/11*: 41-58.
- T.I.C. (2008). News of member companies. *Ta-Nb Int. Study Centre Newsletter*, 136: 8 pp.

MINERALS FROM THE CROSS LAKE PEGMATITE, MANITOBA, CANADA

Kimberly T. Tait¹§, Frank C. Hawthorne² & Petr Černý²

¹ Royal Ontario Museum, Department of Natural History-Mineralogy, 100 Queens Park, Toronto, Ontario M5S 2C6 §ktait@rom.on.ca

² Department of Geological Sciences, University of Manitoba, Winnipeg, MB R3T 2N2

Key words: Cross Lake pegmatite, Mn-rich apatite, manitobaite, bobfergusonite, alluaudite-group minerals

INTRODUCTION

The Cross Lake pegmatite field is located in central Manitoba, approximately 100 km south of Thompson, Manitoba, Canada. The Cross Lake pegmatite field extends from the Minago River in the west, to the eastern edge of Cross Island (Fig. 1). The pegmatites are en echelon and comprise narrow linear east to northeast-trending zones that are parallel to the axial trend of the Cross Lake greenstone belt (Anderson 1984).

Anderson (1984) has subdivided the pegmatite field into four series, the Northern, Southern, Nelson and Minago series. One mineralogically unique pegmatite, designated "Pegmatite #22" by Anderson (1984), is on the southeastern shoreline of a small unnamed island in Cross Lake, Manitoba, about 5 km north-northwest of the Cross Lake settlement, longitude 54° 41' N, latitude 97° 49' W. Pegmatite #22 occurs in the Northern Series, which consists of muscovite-bearing pegmatites that intrude the metasedimentary rocks north of Cross Island (Anderson 1984) and has very unique paragenesis. Most pegmatites of the Northern series belong to

the beryl-columbite type of the rare-element class of pegmatites. The overall geochemical signature of this series is rather unusual among the pegmatites of the Superior Province in Canada. The series is poor in rare alkali metals, particularly Li and Rb, relative to Cs and shows enrichment in Mn and F, with pegmatite #22 being the most fractionated member of the series (Anderson 1984). Pegmatite #22 intrudes metagreywacke of the Cross Lake group, which grades into a metaconglomerate south of the dyke. The main part of the pegmatite is 40 m long and up to 6.7 m wide in outcrop. Two main zones were mapped by the Manitoba Geological Survey (pers comm. Paul Lenton 1983 field season), the interior and wall zones (shown in purple, Fig. 2), and the core zone (light green), which includes phosphate nodules (mapped as "triphylite masses", which have since been determined to be apatite) and massive brown microcline.

Approximately forty-five samples were collected in 2000 (by FCH and KTT, with assistance from the Manitoba Geological Survey) for a systematic mineralogical investigation of the pegmatite. In general, there are two distinct occurrences of

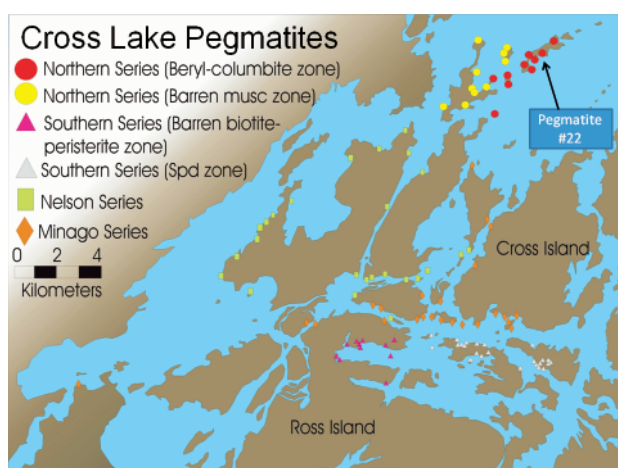


FIGURE 1: Cross Lake pegmatite field, with the pegmatites subdivided into four separate series (modified from Anderson 1984).

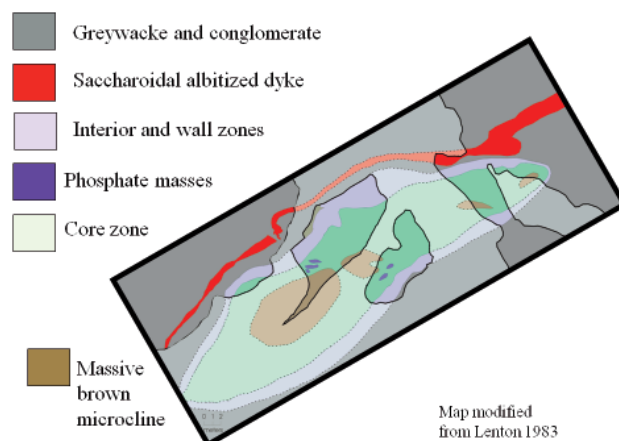


FIGURE 2: Pegmatite #22 in plan view (modified by mapping done by the Manitoba Geological Survey, Lenton 1983 field season) outcrop area is outlined by solid lines, inferred boundaries by dashed lines

phosphate minerals in pegmatite #22 that were investigated: (1) Phosphate nodules in the interior and wall zones of the pegmatite, and (2) phosphate masses in the core zone. All primary phosphates present have very high values of Mn/(Mn + Fe²⁺) and in some cases, these minerals have the highest Mn-values known for their species. The pegmatite has a surprisingly simple mineralogy, with three main phosphate minerals of interest: Mn-rich apatite, bobfergusonite and a recently described new mineral, manitobaite.

MN-RICH APATITE

Apatite is a common accessory mineral in granitic pegmatites and occurs at all stages of pegmatite formation. The earliest formed apatites are fluoride- or hydroxyl-bearing apatites and usually contain significant amounts (up to 4 wt%) of MnO (Moore 1973). High (OH + Cl)/F is a particularly diagnostic indicator of late-stage (presumably fluid-derived) pegmatite units (Papike *et al.* 1984). As the most evolved melts are expected to be relatively depleted in Ca and REE but enriched in incompatible elements such as Mn, As and Bi, one would expect higher concentrations of these elements in the apatite structure (Černý *et al.* 2001). Chlorine-enriched apatite is typical of late, secondary stages of pegmatite evolution or of some low-temperature hydrothermal assemblages (Černý *et al.* 2001).

Switch *et al.* (1985) suggested that the upper compositional limit for Mn-bearing apatite is one atom of Mn per unit cell, corresponding to 6.9 wt% for Mn-bearing fluorapatite. Hughes *et al.* (1991) reported 7.87 wt% MnO in apatite, giving 1.17 Mn atoms/unit cell and suggest that the apatite structure could possess more than the proposed one atom/unit cell. Apatite minerals from Cross Lake have far higher MnO content than any apatite minerals reported in the literature to date.

Apatite-group minerals are the primary phosphates in the core zone, forming blue-black masses up to 15 cm across; these were misidentified as triphylite in the original mapping by the Manitoba Geological Survey (Fig. 1). Figure 3 is a representative BSE image of apatite-group minerals in the core zone. Based on F vs. Cl content, CaO vs. MnO and the textural relations of the mineral, there are three stages of apatite-group minerals formation in these samples, designated (1)-(3), (1) being the youngest. Fluorapatite (1) and (2) have a relatively low MnO content (for this pegmatite). Chlorapatite (3) is a late-stage apatite-group mineral with high MnO, much greater than that of the primary fluorapatite. Apatite-group minerals also occur as anhedral grains in complex fine-grained "masses" that form at grain boundaries between phosphates and silicates. These "masses" likely crystallized from trapped fluids, forming fine-grained assemblages similar to the adjacent coarse-grained

phosphates. Minor phosphates (such as triploidite, bobfergusonite and manitobaite) and (Nb,Ta,Sn)-bearing-oxide minerals also occur in these "masses." Apatite-group minerals are common in the interior-wall zone, second in abundance to manitobaite, and typically occurring in fractures and veins that crosscut manitobaite. Minor goyazite occurs with apatite in the fractures and veins of manitobaite.

BOBFERGUSONITE

Bobfergusonite, Na₂Mn²⁺₅Fe³⁺Al(PO₄)₆ was first described from pegmatite #22 (Ercit *et al.* 1986) and has only been described from one other locality, the Nancy pegmatite, San Luis Range, Argentina (Tait *et al.* 2004). Bobfergusonite occurs as a constituent of the nodules in the intermediate zone of the pegmatite associated with other primary phosphate minerals, but large isolated crystals of bobfergusonite with no associated phosphates are also present. Bobfergusonite is closely related to the alluaudite-group and wyllieite-group minerals.

MANITOBAITE

Manitobaite, ideally (Na₁₆□)Mn²⁺₂₅Al₈(PO₄)₃₀ is a member of the alluaudite-super group minerals, and has only recently been formally described (Ercit *et al.* 2010), although has been known to occur at this locality for many years. It forms large (up to 2 cm across) crystals or cleavage masses intergrown with other phosphate minerals in phosphate nodules in the intermediate and core zones. It is the most common phosphate mineral in this pegmatite and has not been described from any other locality thus far.

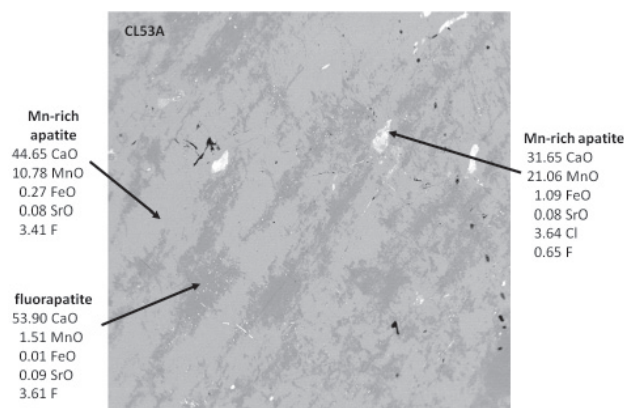


FIGURE 3: BSE image of apatite in the core zone of pegmatite #22, sample CL53A. Note only selected wt% values are listed.

ALLUAUDITE-SUPERGROUP MINERALS

Alluaudite-, wyllieite-, bobfergusonite- and manitobaite-group minerals are topologically very similar but are distinguished by different cation-ordering schemes over the octahedrally coordinated cation sites. The four subgroups differ primarily in their Al content and the pattern of cation order over the trimer of edge-sharing octahedra. The minerals of the alluaudite group (*sensu stricto*) contain negligible Al ($\text{Al}_2\text{O}_3 < 0.10$ wt %), the minerals of the wyllieite group contain moderate Al ($\text{Al}_2\text{O}_3 \approx 3$ wt %), and bobfergusonite contains far more Al than wyllieite ($\text{Al}_2\text{O}_3 \approx 7.5$ wt %) (Huminicki & Hawthorne 2002). Manitoabaite has the most Al_2O_3 (~15 wt % Al_2O_3) of the alluaudite-group minerals. Pegmatite #22 is unique in having three of the four groups in one assemblage, which gives us a unique opportunity to analyze three members of this complicated group from one locality, and understand their relations.

SUMMARY OF THE PEGMATITE #22'S
MINERALOGY

Apatite-group minerals are the main phosphates in the core zone, forming blue-black masses up to 15 cm. Blocky K-feldspar, quartz and book muscovite up to tens of cm to several metres across surround the phosphate masses. Apatite-group minerals also occur as anhedral grains in complex fine-grained "masses" that occur at grain boundaries between phosphates and silicates, with manitoabaite, bobfergusonite triploidite, eosphorite, dickinsonite, gahnite (Nb,Ta,Sn)-bearing oxide minerals and minor secondary alluaudite.

Manitoabaite is the most common phosphate mineral in the interior-wall zone of pegmatite #22. Apatite-group minerals are common minerals in the interior-wall zone, second in abundance to manitoabaite, typically occurring in fractures and veins in manitoabaite with goyazite. Eosphorite is a common accessory phosphate in the interior-wall zone, commonly associated with apatite, whereas dickinsonite, which is associated with eosphorite, is rare. Triploidite, goyazite, perloffite (Nb,Ta,Sn)-bearing oxides and gahnite are minor phases in fractures and veins crosscutting manitoabaite. Saccharoidal to medium-grained albite and quartz are the main silicates in the interior-wall zone, with books of muscovite, greenish columnar beryl and scattered spessartine and schorl.

REFERENCES

- Anderson, A.J. (1984). The Geochemistry, Mineralogy and Petrology of the Cross Lake Pegmatite Field, Central Manitoba. M.Sc. thesis, Univ. Manitoba, Winnipeg, Manitoba.
- Černý, P., Fryer, B.J., & Chapman, R. (2001). Apatite from granitic pegmatite exocontact in Moldanubian serpentinites. *Jour. of the Czech Geol. Soc.* **46**: 1-2, 15-20.
- Ercit, T.S., Anderson A.J., Černý P. & Hawthorne F.C. (1986). Bobfergusonite: A new primary phosphate mineral from Cross Lake, Manitoba, Can. Mineral. **24**: 599-604.
- Ercit, T.S., Tait, K.T., Hawthorne, F.C., Ball, N., Cooper, M.A., Abdu, Y., Galliski, M.A. & Anderson, A.J. (2010). The crystal structure and crystal chemistry of manitoabaite, ideally $(\text{Na}_{16}\square)\text{Mn}^{2+}_{25}\text{Al}_8(\text{PO}_4)_{30}$, from Cross Lake, Manitoba. *Can. Mineral.* (accepted).
- Hughes, J.M., Cameron, M., & Crowley, K.D. (1991). Ordering of divalent cations in the apatite structure: Crystal structure refinements of natural Mn- and Sr-bearing apatite. *Am. Min.* **76**, 1857-1862.
- Huminicki, D. & Hawthorne, F.C. (2002). The crystal chemistry of the phosphate minerals. *In* Phosphates: Geochemical, Geobiological, and Materials Importance (M.L. Kohn, J. Rakovan & J.M. Hughes, eds.). *Reviews in Mineralogy* **48**, 123-253.
- Moore, P. B. (1973). Pegmatite phosphates: Descriptive mineralogy and crystal chemistry. *Min. Rec.* **4**(3): 103-130.
- Papike J.J., Jensen, M., Shearer, C.K., Simon, S.B., Walker, R.J. & Laul, J.C. (1984). Apatite as a recorder of pegmatite petrogenesis. *Geological Society of America Abstracts with Programs* **16** (6): 617.
- Suitch P.R., LaCout, J.L., Hewat, A & Young, R.A. (1985). The structural location and role of Mn^{2+} Partially substituted for Ca^{2+} in fluorapatite. *Acta Cryst.* **B41**: 173-179.
- Tait, K.T., Hawthorne F.C., Černý P., Galliski M.A. (2004). Bobfergusonite from the Nancy pegmatite, San Luis Range, Argentina: crystal-structure refinement and chemical composition, *Can. Mineral.* **42**: 705-716.

PARAGENETIC CONTROL AND COMPOSITIONAL EVOLUTION OF THE COLUMBITE-TANTALITE OXIDES FROM THE FREGENEDA-ALMENDRA LITHIUM-RICH PEGMATITES (PORTUGAL & SPAIN)

Romeu Vieira^{1§}, Encarnación Roda-Robles², Alexandre Lima³, Alfonso Pesquera², Petr Gadas⁴ & Milan Novák⁴

¹ Centro de Geologia da Universidade do Porto, Rua do Campo Alegre, 687, 4169-007 Porto, Portugal §romeu.vieira@fc.up.pt

² Dpto. Mineralogía y Petrología, Universidad del País Vasco/EHU, Apdo. 644, 48080, Bilbao, Spain

³ Dpto. Geología, Ambiente e Ordenamento do Território, FCUP, Rua do Campo Alegre, 687, 4169-007 Porto, Portugal

⁴ Dept. of Geological Sciences, Masaryk University, Kotlářská 2, 602 00 Brno, Czech Republic

Key words: columbite-tantalite; lithium-pegmatites; Fregeneda-Almendra.

INTRODUCTION

The Fregeneda-Almendra (FA) pegmatite field (Spain-Portugal) is characterized by occurrence of numerous pegmatites of different types. Most of these pegmatites are barren, but lithium-rich bodies are also abundant in the northern part of the field. Minerals of the columbite-tantalite group (CT) and cassiterite are very common as accessory phases in the FA aplite-pegmatite veins, particularly in the most evolved veins enriched in Li and F. These two oxides are always associated in lithium-rich pegmatites assemblages from the FA, with predominance of cassiterite over CT phases (Roda *et al.* 1999; Vieira 2010).

In this preliminary study, we evaluate the control of cassiterite and Li- and F-rich assemblages on the compositional evolution of the columbite-tantalite group of minerals.

GEOLOGICAL SETTING & PEGMATITES DESCRIPTION

The FA area is located in the Central-Iberian-Zone, in the western part of a narrow metamorphic belt, with an E-W trend. This belt is bordered by the syn-tectonic Variscan Méda-Penedono-Lumbrales leucogranitic complex (Carnicero 1981) to the south, and by the late-tectonic Saucelle granite to the NE. They are both two-mica peraluminous granites. These granites and most of the pegmatites intruded pre-Ordovician metasediments of the Schist-Metagreywacke Complex.

Most of the pegmatites from the FA field correspond to the less evolved ones, grouped onto two main categories: (i) barren pegmatites with quartz, K-feldspar > albite, muscovite, tourmaline ± andalusite ± garnet (types 1, 2, 3 & 4). They are intragranitic (types 1 and 3) or conformable to the

hosting-rocks and occurring near the contact with the granite (types 2 and 4); and (ii) intermediate discordant pegmatites (types 5 and 6), characterized by the occurrence of Fe-Mn phosphates, montebrasite, and both micas and feldspars with higher Rb and Cs contents.

A third category of pegmatites (Table 1) represents ~10% of the aplite-pegmatite veins from the FA. They are mainly rich in Li-minerals (types 7, 8, 9 and 10) and/or cassiterite (type 11). They are discordant, the Li-rich dykes showing similar strikes, close to N10E, and similar dipping, close to the vertical. They intruded late-tectonic Variscan fractures. The main Li-bearing mineral assemblages are petalite (type 7), spodumene (type 8), *lepidolite* + spodumene (type 9), and *lepidolite* (type 10) (Roda *et al.* 1999; Vieira 2010).

COLUMBITE-TANTALITE OCCURRENCE AND TEXTURAL RELATIONSHIPS

In the lithium-rich pegmatites from the FA two textural types of CT were recognized (Table 2, Fig. 1). The CT exhibits typical zonation patterns, mainly progressive and oscillatory, normal or reversed. Patchy zonation, with embayment corrosion textures, is a common feature shown by the CT crystals from the Li-rich pegmatites (Fig. 1).

Columbite-tantalite, along with cassiterite, is particularly abundant in the petalite-pegmatites (type 7). They appear in assemblages containing mainly quartz, petalite, albite, microcline, muscovite, montebrasite, apatite and Fe-Mn phosphates (e.g., alluaudite). In the spodumene-pegmatites (type 8), CT and cassiterite are less common. Both phases are associated with quartz, spodumene, albite, microcline, muscovite, montebrasite and Fe-Mn phosphates.

TABLE 1. Main characteristics of the lithium-rich pegmatites recognized in the Fregeneda-Almendra area.

Type	Mineralogy		Morphology and structure	Examples	Enrichment
	Main	Other			
(7)	Qtz, Pet, Ab, Kfs	Ms, Cst, CT, \pm Mbs, Fe-Mn Pho, \pm Ecr	Discordant vein without internal zonation; thickness 5-30 m	Bajoca, Pombal and Hinojosa del Duero	Li, Sn, P
(8)	Qtz, Spd, Ab, Kfs	Ms, Mbs, Pet, Cst, CT, Fe-Mn Pho, \pm Ecr	Discordant vein without internal zonation; thickness 4-15 m	Alberto and Valdecoso	Li, P, (Sn)
(9)	Qtz, Ab, Kfs, Li-ms, Ms, Spd	Mbs, Cst, CT, Ap, \pm Ecr, Fe-Mn Pho	Discordant vein; internal zoning common; < 15 m thick.	Feli	Li, Sn, P, F, (Rb, Cs)
(10)	Qtz, Ab, Li-ms, Kfs	Ms, Cst, CT, Mbs	Discordant vein; internal zoning common; < 3 m thick.	C�rmen, Riba d'Alva and Ramalha	Li, Sn, P, F, (Rb, Cs)

Qtz – quartz; Kfs – K-feldspar; Ms – muscovite; Ab – albite; Pho – phosphates; Mbs – montebrasite; Pet – petalite; Spd – spodumene; Cst – cassiterite; CT – Nb-Ta oxides; Ap – apatite; Ecr – eucryptite.

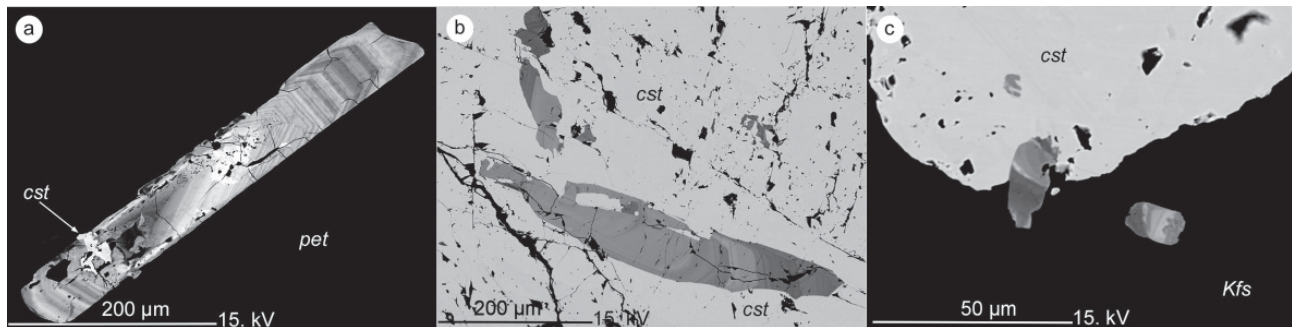


FIGURE 1. BSE images of columbite-tantalite grains (a) disseminated (CT I) columbite-(Fe) crystal exhibiting oscillatory zonation on the extremities, embayment and patchy zonation in the central zone; (b) columbite-(Fe) inclusion (CT II) on cassiterite exhibiting reversed oscillatory zonation; and (c) columbite-(Fe) partially included or nearby cassiterite grain (CT II) (cst – cassiterite; pet – petalite; Kfs – K-feldspar).

In the *lepidolite*-bearing pegmatites (types 9 and 10), CT and cassiterite appear in assemblages containing essentially Li-muscovite, quartz, albite and montebrasite.

CHEMISTRY AND DISCUSSION

The CT composition from the FA lithium-rich pegmatites corresponds mainly to columbite-(Fe) (type 7 and 8) and columbite-(Mn) (type 9 and 10) (Fig. 2).

Tantalite-(Fe) compositions are associated to dissolution of earlier ferrocolumbite crystals and recrystallization of a late Ta-enrichment zone, marked by embayment and patchy zonation (Fig. 1a).

Variations on $X_{Ta}/(X_{Ta} + X_{Nb})$ ratio, both on columbite-(Fe) and columbite-(Mn), only occur at crystal level. Differences on the ratio $X_{Mn}/(X_{Mn} + X_{Fe})$ are observed between the different types of pegmatites, especially among types 7 and 8 (Li-aluminosilicate-rich veins) and the *lepidolite*-bearing pegmatites (types 9 and 10).

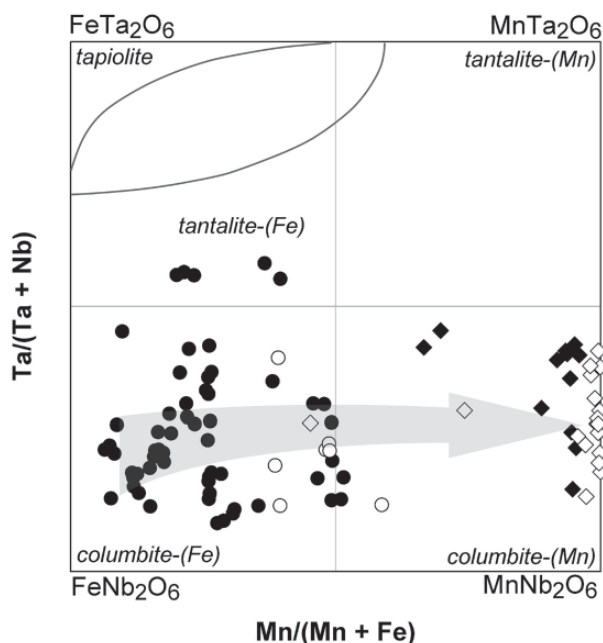
The marked evolution trend on the X_{Ta} versus X_{Mn} diagram, as well geological and mineralogical data, indicate a cogenetic relation among type 7 & 8 \rightarrow 9 \rightarrow 10. This evolution was mainly controlled by (i) abundance of Fe, Mn, Nb and Ta in the pegmatite-forming melts; (ii) partition of elements such as Nb and Ta among coexistent mineral assemblage; and (iii) the solubility of the Nb-Ta oxides on Li, F and Al-rich pegmatite forming melts (e.g., Keppler 1993; Mulja *et al.* 1996.).

In the Li-rich FA pegmatites we observe an enrichment in Mn in the CT from the F-rich pegmatites (types 9 and 10), similar to other examples reported in the literature (e.g., Bailey 1977;  ern y *et al.* 1986). Also in the phosphates the Fe/(Fe+Mn) ratio tends to decrease as the evolution degree of the pegmatites increases (Roda *et al.* 2010). In this way, there is a clear correlation between F and Mn and the trend from columbite-(Fe) (types 7 and 8) to columbite-(Mn) (types 9 and 10) could be driven via fluorine-complexes carrying Mn.

As described by  ern y *et al.* (1985) for complex F and Li-rich pegmatites, it should be expected the

TABLE 2. Cassiterite and columbite-tantalite petrographic characteristics (CT – columbite-tantalite).

Type	Shape	Size	Texture
Cassiterite	Euhedral to subhedral	Fine to medium	Chromatic zonation; «elbow» tin twin; inclusions of columbite-tantalite minerals Columbite-Tantalite
Columbite-Tantalite	CT I Euhedral to subhedral	Fine to medium	Disseminated across aplitic and pegmatitic facies
	CT II Euhedral to subhedral	Very fine to fine	Total or partially included in cassiterite or nearby cassiterite grains



Legend:

- petalite-rich (type 7)
- spodumene-rich (type 8)
- ◆ lepidolite + spodumene-rich (type 9)
- ◇ lepidolite-rich (type 10)

FIGURE 2. Ta/(Ta + Nb) versus Mn/(Mn + Fe) diagram for the columbite-(Fe), columbite-(Mn) and tantalite-(Fe) from the Fregeneda-Almendra Li-rich pegmatite types. Shaded arrow marks the evolution trend between F-poor and F-rich pegmatites.

projection for the tantalite-(Mn) field after a Mn-enrichment, but this evolution is not observed in the CT from the FA. Hence, we can assume that volumetrically essential cassiterite controlled the Ta partition into CT in all the evolution sequence.

REFERENCES

- Bailey, J. C. (1977). Fluorine in granitic rocks and melts: a review. *Chem. Geol.* **19**: 1–42.
- Carnicero, M. A. (1981). Granitoides del Centro Oeste de la Provincia de Salamanca. Clasificación y correlación. *Cuad. Lab. Xeol. Laxe* **2**: 45–49.
- Černý, P., Goad, B. E., Hawthorne, F. C. & Chapman, R. (1986). Fractionation trends of the Nb- and Ta-bearing oxide minerals in the Greer Lake pegmatitic granite and its pegmatite aureole, southeastern Manitoba. *Am. Mineral.* **71**: 501–517.
- Černý, P., Meintzer, R. E., & Anderson, A. J. (1985). Extreme fractionation in rare-element granitic pegmatites: selected examples of data and mechanisms. *Can. Mineral.* **23**: 381–421.
- Keppler, H. (1993). Influence of fluorine on the enrichment of high field strength trace elements in granitic rocks. *Contrib. Mineral. Petrol.* **114**: 479–488.
- Mulja, T., Williams-Jones, A. E., Martin, R. F. & Wood, S. A. (1996). Compositional variation and structural state of columbite-tantalite in rare-element granitic pegmatites of the Preissac-Lacorne batholith, Quebec, Canada. *Am. Mineral.* **81**: 146–157.
- Roda, E., Pesquera, A., Velasco, F. & Fontan, F. (1999). The granitic pegmatites of the Fregeneda area (Salamanca, Spain): characteristics and petrogenesis. *Mineral. Mag.* **63** (4): 535–558.
- Roda, E., Vieira, R., Pesquera, A. & Lima, A. (2010). Chemical variations and significance of the phosphates from the Fregeneda-Almendra pegmatite field, Central Iberian Zone (Spain and Portugal). *Mineral. Petrol.*, **100** (1-2): 23–34.
- Vieira, R. (2010) Aplitopegmatitos com elementos raros da região entre Almendra (V. N. de Foz-Côa) e Barca D'Alva (Figueira de Castelo Rodrigo). Campo aplitopegmatítico da Fregeneda-Almendra. Ph.D thesis, Univ. of Porto, Portugal. 275 p.

U-Pb LA-ICPMS COLUMBITE-TANTALITE AGES FROM THE PAMPEAN PEGMATITE PROVINCE: PRELIMINARY RESULTS

Albrecht von Quadt^{1§} & Miguel A. Galliski²

¹ Institute of Geochemistry and Petrology, Department of Earth Sciences, ETH Zurich. Clausiusstrasse 25, CH-8092 Zurich,

§vonquadt@erdw.ethz.ch

² IANIGLA, CCT Mendoza-CONICET, Avda. A. Ruiz Leal s/n, (5500) Mendoza, Argentina.

Key words: U-Pb ages - columbite – LA-ICPMS – granitic pegmatites.

INTRODUCTION

The granitic pegmatites have the same cooling path like their host rocks after magmatic crystallization. During this process, subsolidus hydrothermal re-equilibration tends to disturb some isotopic systems. Consequently, the K-Ar method applied on muscovite or K-feldspar at its best only gives the cooling age of the pegmatites. These ages for the pegmatites of the Pampean pegmatite province were broadly grouped in three major periods based on K-Ar dates by Rinaldi & Linares (1973) and Galliski & Linares (1999). However, since more precise methods are needed for bracketing these ages of pegmatite intrusion, we address this research to date primary phases of rare-element granitic pegmatites, specifically columbite-group minerals (CGM), which isotopic system usually remain undisturbed after their magmatic crystallization.

Romer & Wright (1992) showed that CGM are a suitable material for U-Pb dating. Thermionen mass spectrometer analyses (TIMS; Romer & Smeds 1994, Romer & Lehmann 1995, Romer *et al.* 1996) or Laser Ablation Inductively Coupled Plasma Mass Spectrometry (LA-ICP-MS; Smith *et al.* 2004) analyses were shown as appropriate methods to determine the crystallization age of CGM. Combined U-Pb dating with major, trace and REE element analysis, additionally give a fingerprint for tracing the provenance of some CGM ores (Melcher *et al.* 2008). This approach was shown to be a useful tool for certificate the origin of CGM (coltan) produced in conflictive areas of Africa or elsewhere.

EXPERIMENTAL METHODS

We have selected CGM samples from the Pampean pegmatite province (Argentina). This study includes the pegmatite field of El Quemado, Conlara, El Totoral, La Estanzuela and Altautina (Galliski & Černý, 2006). The trace and REE element data were analyzed with a LA-ICP-MS system (Excimer laser-193 nm, Elan 6100) using NIST 610 as an external standard.

The U-Th-Pb analyses on CGM were investigated on a LA-ICP-MS system using GJ-1 and NIST 610 as external standard material.

GEOLOGICAL SETTING

The granitic pegmatites of the economic fields from the Pampean pegmatite province extend along a discontinuous belt that exceeds 800 km in N-S and 300 km in W-E directions, mostly in the Sierras Pampeanas of Central and Northwestern Argentina (Fig. 1). They can be subdivided in orogenic and post-orogenic pegmatite fields. The orogenic pegmatite fields evolved mainly in the Lower Paleozoic during the Pampean and Famatinian orogenic cycles. They can be differentiated muscovite, muscovite rare-element or rare-element pegmatitic fields following the classification of Černý & Ercit (2005). The rare-element pegmatite fields form a belt extended in a polyphasic High-T Low-P Abukuma metamorphic belt. They contain most of the tantalum, lithium and beryllium worth of the province and their pegmatites provide good samples of CGM for geochemical purposes (Galliski & Černý 2006) and dating.

RESULTS

Preliminary U-Pb ages show for the pegmatite field of El Quemado, Conlara and Altautina magmatic ages around 480 Ma. For example, the concordia diagram for columbite-(Mn) from La Totoral pegmatite, a rare-element pegmatite of the Conlara district, gives an interception at 476 Ma (Fig. 2) which is significantly older than the K-Ar value of 413 ± 7 obtained by Galliski & Linares (1999). There are some evidences for younger events at 440 Ma at El Quemado and Conlara and El Totoral pegmatitic districts, and a 350 Ma event in the pegmatite field of La Estanzuela.

In the El Totoral pegmatite field, the tantalite-(Mn) sampled at the San Luis II pegmatite, gives a concordia diagram (Fig. 3) that intercepts at 450 ± 10 Ma. This value is different from the K-Ar age of 317 ± 11

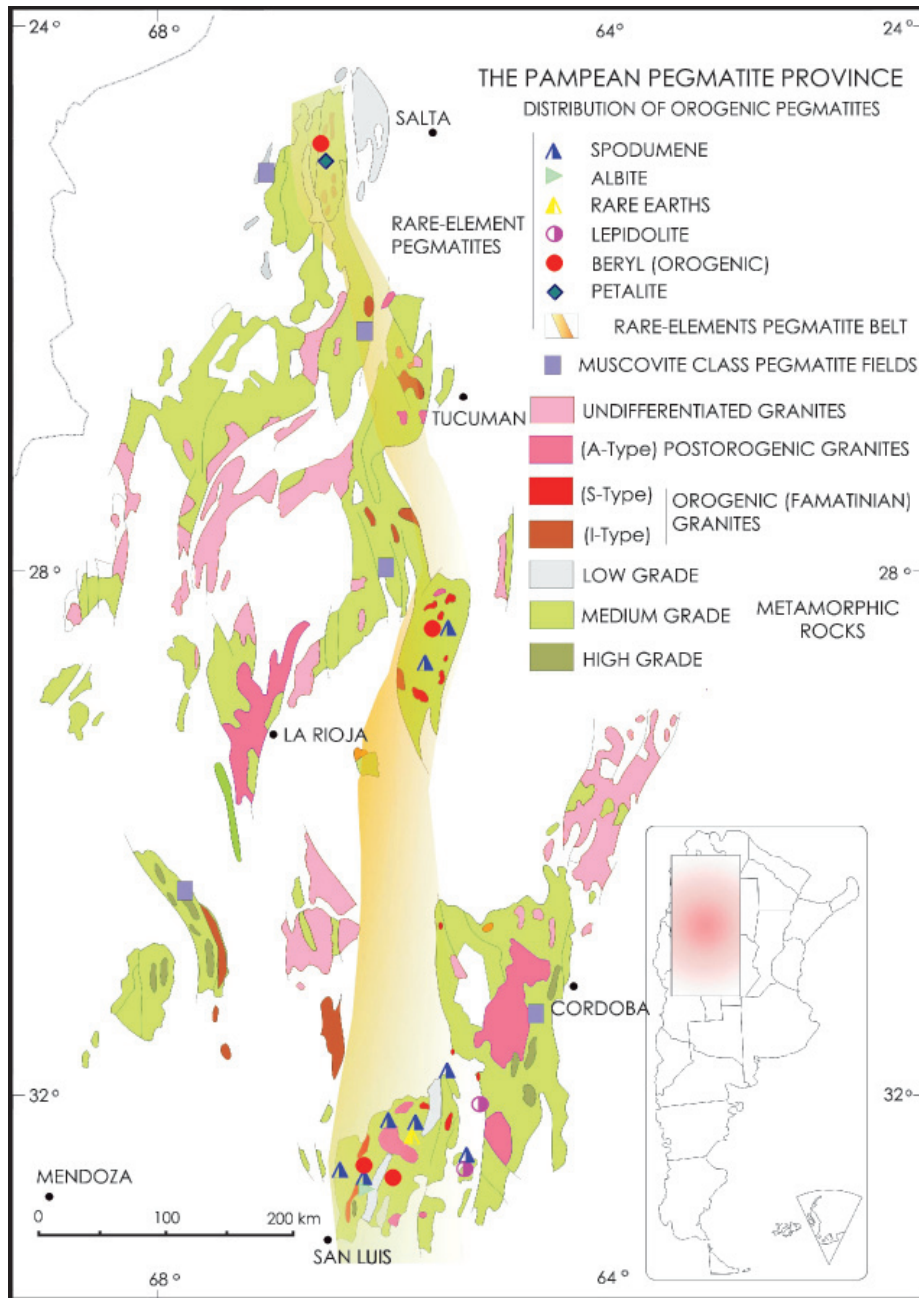


FIGURE 1. Schematic map with the location of the rare-element pegmatite belt mostly of Famatinian age of the Pampean pegmatite province with some of the different types of pegmatites that contain (modified from Galliski & Černý 2006). The rare-element pegmatite belt does not include the post-orogenic pegmatite fields, nor the rare-element orogenic pegmatites of the Córdoba ranges, presumably of the Pampean orogenic cycle, mostly belonging to the Comenchingones and Altautina pegmatitic fields.

Ma obtained on muscovite from the paired San Luis I albite-spodumene subtype pegmatite by Galliski & Linares (1999). The new age is in good agreement with the 460 ± 15 Ma value obtained by U-Pb on uraninite from the Santa Ana beryl-type pegmatite outcropping in the same district (Linares 1959). The new date is also in excellent agreement with the age of the considered parental granite called Paso del Rey and located 300 m to the west of the San Luis II pegmatite. The Paso del Rey leucogranite gives a Rb-Sr errorchron of 454 ± 21 Ma (Llambías *et al.* 1991), and some controversial U-Pb

values on zircon (Cf. Steenken *et al.* 2008). According to one interpretation of the last authors, the age of 456 ± 30 Ma (MSWD 0.26) would be in excellent agreement with the columbite age.

The preliminary U-Pb determination on CGM demonstrates that the previous K-Ar ages gave too young ages. The U-Th-Pb determination of "geological ages" with the LA-ICPMS technique is sometimes limited by the high content of common lead within the CGM.

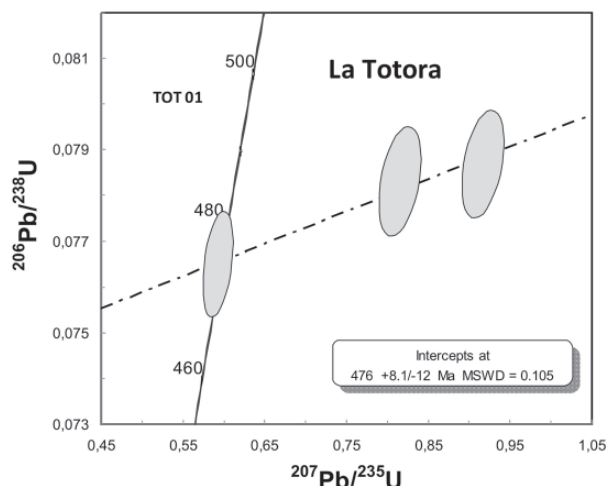


FIGURE 2. Concordia diagram of the columbite-(Mn) from the La Tatora pegmatite.

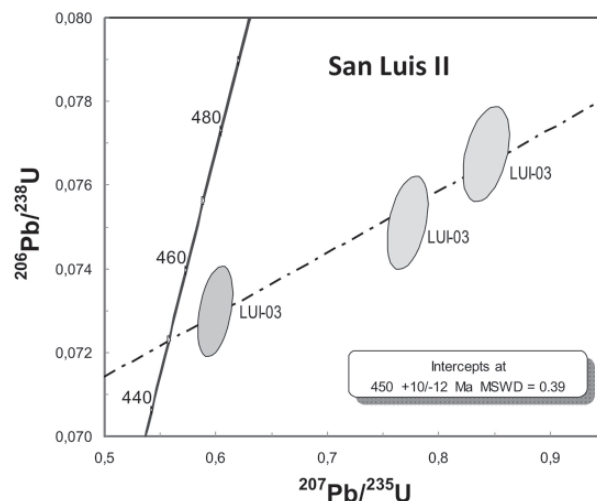


FIGURE 3. Concordia diagram of the tantalite-(Mn) from the San Luis II pegmatite.

ACKNOWLEDGEMENTS

Grants from PIP 5907 and 857 of CONICET and PICT 21638 FONCYT financed the development of the project in Argentina. The review and suggestions of Milan Novák are very appreciated.

REFERENCES

- Černý, P. & Ercit, T.S. (2005). The classification of granitic pegmatites revisited. *Can. Mineral.* **43**: 2005-2026.
- Galliski, M. A. & Černý, P. (2006). Geochemistry and Structural State of Columbite-Group minerals from granitic pegmatites of the Pampean Ranges. *Can. Mineral.* **44**: 645-666.
- Galliski, M. A., & Linares, E. (1999). New K-Ar muscovite ages from granitic pegmatites of the Pampean Pegmatite Province. *Actas II Segundo Simposio Sudamericano de Geología Isotópica, Anales XXXIV SEGEMAR*: 63-67.
- Linares, E. (1959). Los métodos geocronológicos y algunas edades de minerales de la Argentina obtenidas por medio de la relación plomo-uranio. *Rev. Asoc. Geol. Arg.* **14**: 181-217.
- Llambías, E., Cingolani, C., Varela, R., Prozzi, C., Ortiz Suárez, A., Caminos, R., Toselli, A. & Saavedra, J. (1991). Leucogranodioritas sincinemáticas ordovícicas en la Sierra de San Luis, República Argentina. In proceedings of the 6th Congreso Geológico Chileno. Viña del Mar, Chile 187-191.
- Melcher, F., Sitnikova, M. A., Graupner, T., Martin, N., Oberthür, T., Henjes-Kunst, F., Gäbler, E., Gerdes, A., Brätz, H., Davis, D. W. & Dewaele, S. (2008). Fingerprinting of conflict minerals: columbite-tantalite ("coltan") ores. *SGA News* **23**: 7-14.
- Rinaldi, C. A. & Linares, E. (1973). Edades K-Ar de pegmatitas de la provincia de San Luis. *Actas 5to. Cong. Geol. Arg.* **1**: 411-418, Buenos Aires.
- Romer, R.L. & Lehmann, B. (1995). U-Pb columbite age of Neoproterozoic Ta-Nb mineralization in Burundi. *Econ. Geol.* **90**: 2303-2309.
- Romer, R.L. & Smeds, S.A. (1994). Implications of U-Pb ages of columbite-tantalites from granitic pegmatites for the Paleoproterozoic accretion of 1.90-1.85 Ga magmatic arcs to the Baltic Shield. *Precambrian Research* **67**: 141-158.
- Romer, R. L. & Wright J. E. (1992). U-Pb dating of columbites: A geochronologic tool to date magmatism and ore deposits. *Geoch. et Cosmoch. Acta* **56**: 2137-2142.
- Romer, R.L., Smeds, S.-A. & Černý, P. (1996). Crystal-chemical and genetic controls of U-Pb systematics of columbite-tantalite. *Mineral. & Petrol.* **57**: 243-260.
- Smith, S. R., Foster, G. L., Romer, R. L., Tindle, A. G., Kelley, S. P., Noble, S. R., Horstwood M. & Breaks F. W. (2004). U-Pb columbite-tantalite chronology of rare-element pegmatites using TIMS and Laser Ablation-Multi Collector-ICP-MS. *Contrib. Mineral. Petrol.* **147**: 549-564.
- Steenken, A., Siegesmund, S., Wemmer, K. & López de Luchi, M.G. (2008). Time constraints on the Famatinian and Achaian structural evolution of the basement of the Sierra de San Luis (Eastern Sierras Pampeanas, Argentina). *Jour. South American Earth Sciences.* **25**: 336-358.

MIAROLITIC PEGMATITES AND GRANITES FROM THE SEARCHLIGHT DISTRICT, COLORADO RIVER EXTENSIONAL CORRIDOR, NEVADA, USA

Karen Webber[§], William Simmons & Alexander Falster

University of New Orleans, MP² Research Group, Department of Earth & Environmental Science, New Orleans, LA 70148 USA

[§] email kwebber@uno.edu

Key words: miarolitic, pegmatites, Newberry Mountains, Searchlight district

INTRODUCTION

Shallowly emplaced mid-Miocene granites exposed near Searchlight in the Newberry Mountains, Clark Co., Nevada, are located in the Northern Colorado River Extensional Corridor (NCREC) in the Basin and Range Province of the western United States (Fig.1). Newberry granites host numerous miarolitic pegmatites and were the focus of this study. Miarolitic cavities range from microscopic to meter size with thin rims of pegmatitic material surrounding the larger cavities. Miaroles host an assemblage of well-crystallized mineral species including smoky quartz, microcline, albite, biotite, zircon, titanite, thorite, manganocolumbite, ilmenite-pyrophanite, magnetite, monazite-Ce, bastnaesite-Ce, polycrase-Y, spessartine and fluorite.

GEOLOGIC SETTING

The NCREC is a 50 to 100 km-wide region of moderately to highly extended crust through which the Colorado River flows. In Miocene time, the southward and northward advancing magmatic and extensional fronts converged toward the NCREC. Thus, this region was one of the last parts of the Basin and Range to experience widespread volcanism, plutonism, and large-magnitude extension (Faulds *et al.* 2001). The Newberry Mountains consist largely of Miocene (15-18 Ma) granitic plutons and multiple dike swarms that intruded Proterozoic (~ 2 Ga) basement rocks of the Mojave terrane (Bachl *et al.* 2001). In addition to Proterozoic crystalline rocks, the Miocene plutons are underlain in places by Mesozoic granitoids such as the Cretaceous Ireteba pluton (D'Andrea Kapp *et al.* 2002) emplaced in response to Jurassic to early Tertiary subduction of the Farallon plate beneath North America. Miocene uplift accompanied by rotation on high angle normal faults has exposed complete sections of some of the Miocene plutons including the 10 km thick Searchlight Pluton and the Aztec Wash Pluton (Bachl *et al.* 2001; Falkner *et al.* 1995). The Searchlight pluton extends from the Eldorado Mountains south to the northern part of the Newberry Mountains. Bachl *et al.* (2001) subdivide the Searchlight Pluton into three zones: an upper fine-grained granite believed to represent a downward crystallizing solidification front, a middle granite zone locally in contact with a large mafic pod, and a lower heterogeneous granite zone characterized by numerous mafic enclaves. Miarolitic cavities are locally found in the upper part of the middle granite zone of the Searchlight Pluton.

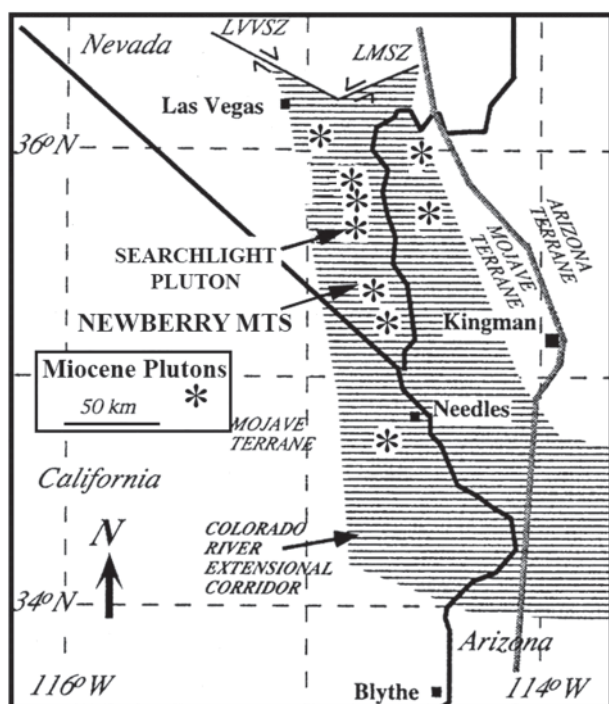


FIGURE 1 Location map for the Newberry Mountains in the NCREC. Modified from Bachl *et al.* (2001).

MINERALOGY AND GEOCHEMISTRY

For this study, samples were collected from miarolitic cavities and the wall zones of larger cavities as well as associated granites and aplite dikes. At first glance, the mineral assemblage found in the miarolitic cavities (smoky quartz, microcline, albite, biotite, zircon, titanite, thorite, manganocolumbite, ilmenite-

pyrophanite, magnetite, monazite-(Ce), bastnaesite-(Ce), polycrase-(Y), spessartine and fluorite) suggests enrichment in Mn, Ti, Zr, Nb>Ta, LREE>HREE, Th and F, consistent with emplacement of NYF pegmatites in the NCREC extensional tectonic setting. However, there are inconsistencies with a strictly NYF anorogenic source. Geochemically, the Searchlight district (SLD) suite can be classified as high-K calc-alkaline; dominantly metaluminous but ranging from peralkaline to peraluminous; and magnesian based on Fe^* ($FeO^T/(FeO^T + MgO)$ after Frost *et al.* 2001). There is a distinctive Mn-enrichment in several mineral phases. Garnet, crystallized primarily in the lining of miarolitic cavities, is spessartine rich with core and rim compositions averaging $Alm_{13}Sps_{87}$ and $Alm_{17}Sps_{83}$ respectively. The miarolitic cavities carry a primary assemblage of Ti-,Nb-,Ta-oxide minerals. Compositions of columbite group minerals correspond to near end member manganocolumbite. Ilmenite is also Mn enriched, with compositions close to pyrophanite. Additional accessory phases in the miarolitic cavities include zircon with intergrowths of thorite, polycrase-(Y) and titanite.

Biotite is the dominant ferromagnesium mineral found in both granites and miarolitic cavities and is strikingly different in composition compared to biotites we have looked at from a number of both anorogenic and orogenic localities including the ~1 Ga anorogenic South Platte (SP) district associated with the Pikes Peak Batholith, Colorado, the ~1.48 – 1.52 Ga anorogenic Wausau Syenite Complex (WSC), the ~1.7 Ga post orogenic Trout Creek Pass (TCP) district associated with the Boulder Creek Orogeny, Colorado and numerous pegmatites in the Oxford Pegmatite field in SW Maine (ME) associated with the ~300 Ma Appalachian Orogeny. Compared to all the localities mentioned above, SLD biotites are much more Mg-rich and in fact are close to phlogopite in composition (Fig.2). Many of the SLD biotites are also enriched in Mn (Fig. 3) and F (Fig. 4) and show a progressive enrichment in both Mn and F from granites to pegmatites to miarolitic cavities.

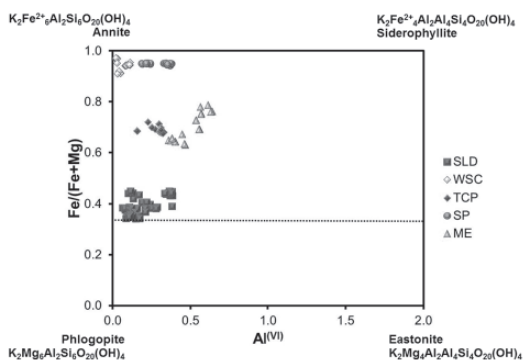


FIGURE 2. Composition of SLD biotites on the biotite quadrilateral compared to orogenic suites from Maine (ME) and Trout Creek Pass (TCP) and anorogenic suites from South Platte (SP) and the Wausau Complex (WSC).

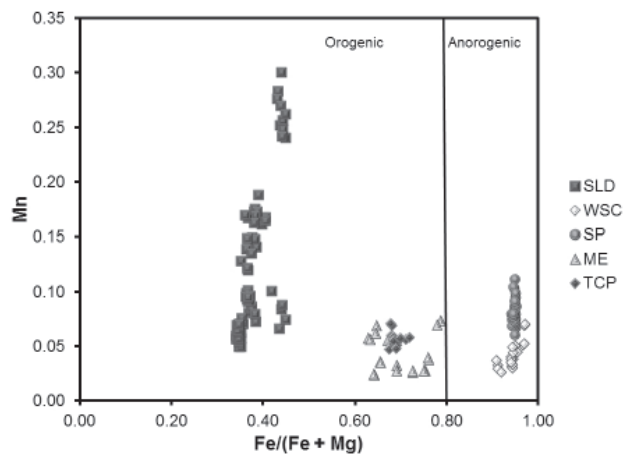


FIGURE 3. $Fe/(Fe+Mg)$ ratio vs. Mn diagram for biotite compositions from the SLD. Analyzed samples from orogenic and anorogenic suites shown for comparison (symbols as in Fig. 2).

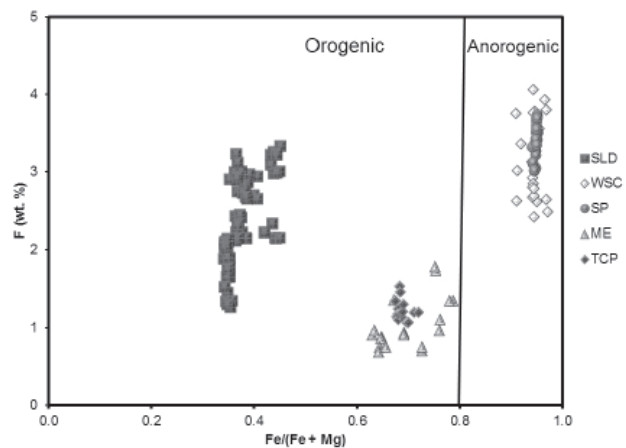


FIGURE 4. $Fe/(Fe+Mg)$ ratio vs. F (wt.%) diagram for biotite compositions from the SLD. Analyzed samples from orogenic and anorogenic suites shown for comparison (symbols as in Fig. 2).

Following the tectonic discrimination diagram of Abdel-Rahman (1994) SLD biotites fall in the I-type calc-alkaline field in the $FeO-MgO-Al_2O_3$ ternary (Fig. 5). On Nb vs. Y and Rb vs. Y+Nb (Fig. 6) trace element tectonic discrimination diagrams, SLD samples straddle the boundary between the WPG (anorogenic) and VAG (orogenic) fields. They can be classified as A-1 type granites using the discrimination diagram of Eby (1992; Fig. 7) and straddle the general fields between fractionated granites and A-type granites on the $10,000 * Ga/Al$ vs. $Zr+Nb+Ce+Y$ diagram of Whalen *et al.* (1987; Fig. 8).

The mineralogy and geochemistry of SLD granites and pegmatites is not entirely consistent with either a WPG (NYF pegmatites) anorogenic signature or a VAG (LCT pegmatites) orogenic signature. Additionally the high Mn and Mg in SLD mineral phases suggest a mafic source and there is evidence for mingling between mafic and felsic magmas in other

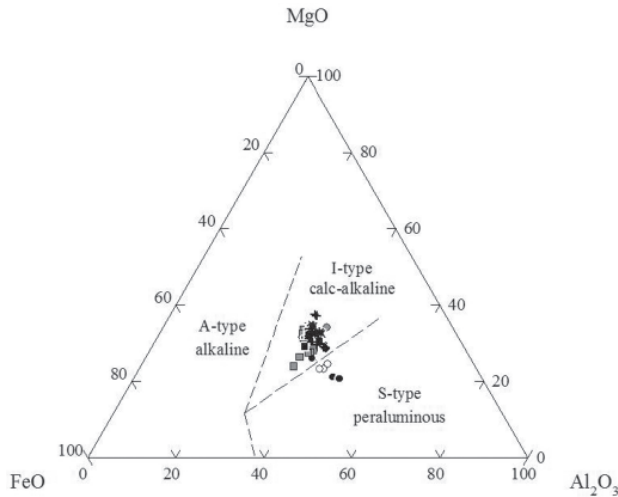


FIGURE 5 FeO-MgO-Al₂O₃ discrimination diagram for SLD biotite compositions (diagram after Abdel-Rahman, 1994). Includes biotite analyzed from granites, aplites and wall zones from larger miarolitic pockets from three different localities (Searchlight, Bat Ears, South Ridge) within the SLD.

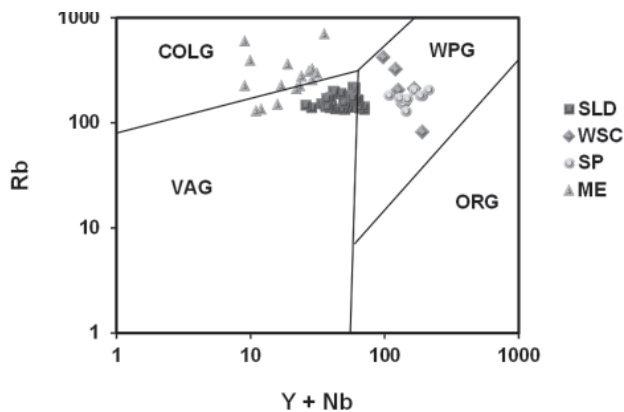


FIGURE 6. Rb vs. Y + Nb trace element tectonic discrimination diagram for SLD as well as comparison anorogenic and orogenic suites (symbols as in Fig. 2). Diagram after Pearce *et al.* 1984.

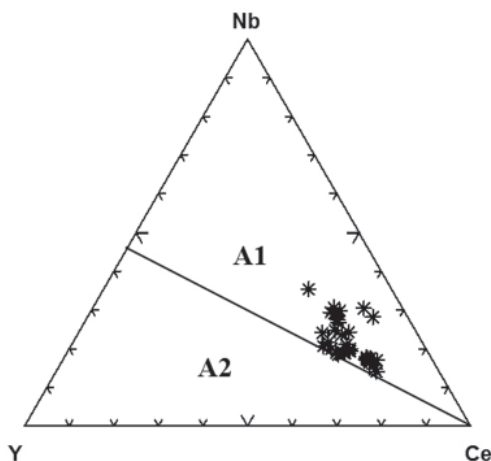


FIGURE 7 Nb-Y-Ce tectonic discrimination diagram. SLD samples fall in the A1 - rift related granites field of Eby (1992).

plutons in the NCREC (Bachl *et al.* 2001). Magmatism associated with the Basin and Range Orogeny likely reprocessed lithosphere that had previously been strongly affected by arc and collisional processes, first when the majority of the crust and probably the lithospheric mantle was formed and reworked in the Proterozoic forming the Mojave Terrane, and then again during Mesozoic arc magmatism. Thus, determination of tectonic setting for igneous rocks using discrimination diagrams can be misleading unless all the potential magmatic source reservoirs are identified. Otherwise, the petrochemistry may record dominant earlier events, rather than existing tectonic settings.

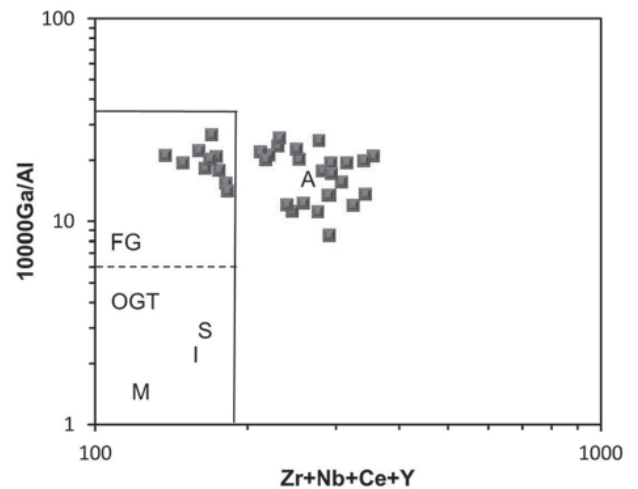


FIGURE 8. 10000*Ga/Al vs. Zr+Nb+Ce+Y discrimination diagram of Whalen *et al.* (1987). SLD samples are in both the fractionated granite (FG) field and anorogenic (A) field.

REFERENCES

- Abdel-Rahman, A.F.M. (1994). Nature of biotites from alkaline, calc-alkaline and peraluminous magmas. *Jour. Petrol.* **35**: 525-541.
- Bachl, C.A., Miller, C.F., Miller, J.S. and Faulds, J.E. (2001). Construction of a pluton: Evidence from an exposed cross section of the Searchlight Pluton, Eldorado Mountains, Nevada. *Geol. Soc. Am. Bull.* **113**: 1213-1228.
- D'Andrea Kapp, J., Miller, C.F. and Miller, J.S. (2002). Ireteba Pluton, Eldorado Mountains, Nevada: Late, deep-source, peraluminous magmatism in the cordilleran interior. *Jour. Geol.* **110**: 649-669.
- Eby, G.N. (1992). Chemical subdivision of the A-type granitoids: Petrogenetic and tectonic implications. *Geology* **20**: 641-644.
- Falkner, C.M., Miller, C.F., Wooden, J.L. and Heizler, M.T. (1995). Petrogenesis and tectonic significance of the calc-alkaline, bimodal Aztec Wash pluton, Eldorado Mountains, Colorado River extensional corridor. *Jour. Geophy. Res.* **100**: 10453-10476.

- Faulds, J.E., Feuerbach, D.L., Miller, C.F. & Smith, E.I. (2001). Cenozoic evolution of the northern Colorado River extensional corridor, southern Nevada and northwest Arizona. *Utah Geol. Assoc. Publ.* **30**: 239-272.
- Frost, B.R., Barnes, C.G., Collins, W.J., Arculus, R.J., Ellis, D.J. & Frost, C.D. (2001). A geochemical classification for granitic rocks. *Jour Petrol.* **42**: 2033-2048.
- Pearce, J.A., Harris, N.B.W. & Tindle, A.G. (1984). Trace element discrimination diagrams for the tectonic interpretation of granitic rocks. *Jour. Petrol.* **25**: 956-983.
- Whalen, J.B., Currie, K.L. & Chappell, B.W. (1987). A-type granites: geochemical characteristics, discrimination and petrogenesis. *Contrib. Mineral. Petrol.* **95**: 407-419.

THE ZAVITAYA LITHIUM-RICH GRANITE-PEGMATITE SYSTEM, EASTERN TRANSBAIKALIA, RUSSIA: GEOLOGY, GEOCHEMISTRY AND PETROGENETIC ASPECTS

Victor Zagorsky

Vinogradov Institute of Geochemistry, SB RAS, Irkutsk, Russia victzag@igc.irk.ru

Key words: granite, pegmatite, metasomatic rock, spodumene, lithium, petrogenesis

INTRODUCTION

In Eastern Transbaikalia, Russia, the Mesozoic province of rare-metal and miarolitic pegmatites is developed within the Mongol-Okhotsk folded belt. The majority of pegmatite fields of the province are predominantly found within the marginal parts of the Aginsky terrane, which is found between the two branches of the Mongol-Okhotsk suture, produced by the collision of the Siberian platform and the Mongol-Chinese continent in Jurassic times. Of specific interest is the Zavitaya granite-pegmatite system, including a large lithium deposit of spodumene pegmatites located 15 km west of confluence of the Onon and Ingoda rivers. This system combines (para) genetically related Mesozoic granites, pegmatites and metasomatic rocks (Zagorsky & Kuznetsova 1990).

GEOLOGICAL SETTING AND TYPES OF GRANITES AND PEGMATITES

The contours of the Zavitaya granite-pegmatite system approximately coincide with the boundaries of the pegmatite field of the same name, elongate in a sublatitudinal direction (20 x 7 km) along the Ingoda-Shilka branch of the Mongol-Okhotsk suture, which field is adjacent to the south. This is where the Ingoda-Shilka trough was formed in Upper Triassic times. It is filled with volcanogenic and terrigenous sediments (conglomerates, sandstones, siltstones, coaly siltstones, with felsic volcanic interludes), which were metamorphosed to the greenschist facies and were transformed into schists. They are cut by dykes of lamprophyre and microgranite porphyry. All these rocks host abundant granites and pegmatites, being the substratum for pre-pegmatite and syn-pegmatite metasomatic assemblages.

GRANITES

Considering the structure-textural features, mineral and chemical compositions, three main types of granites are distinguished. Taken together, they are referred to as the *Kukulbey* magmatic complex (J_3-K_1):

- 1) inequigranular porphyritic biotite granites (adamellites) (Gr1);
- 2) fine-grained two-mica granites-leucogranites (Gr2);
- 3) fine- to medium-grained (in places pegmatitic variety) muscovite-bearing subalkaline leucogranites (Gr3).

Gr1 occur as linearly elongate bodies (up to 5 x 1.5 km) on the western and the eastern terminations of the pegmatite field. Their relationships with Gr2 and Gr3 are not established. The average mineral composition of Gr1 (%): quartz 24.9, plagioclase 49.7, K-feldspar 13.6, and biotite 11.8. The accessory minerals are apatite, rarely garnet, zircon, tourmaline and monazite.

Gr2 and Gr3 occur both as separate comparatively small bodies (200–500 m across, rarely larger), and within stock-like granite-pegmatite bodies of very complicated internal anatomy (see below). Gr3 is more typical of granite-pegmatites than Gr2. Zones of quenching on the contacts of Gr2 and Gr3 are absent. The average mineral composition of Gr2 (%): quartz 31.6, plagioclase 38.9, K-feldspar 17.8, biotite 4.0, muscovite 7.7. Of accessory minerals, apatite is mostly common. Gr3 is distinguished from Gr2 by higher content of muscovite, absence of biotite, presence of garnet, and significant variations of K-feldspar content.

PEGMATITES

Four types of pegmatites are recognized in the Zavitaya field:

- 1) granite-pegmatites (Peg1);
- 2) inequigranular to blocky quartz-two-feldspar pegmatites (Peg2);
- 3) porphyry-like quartz-albite pegmatites (Peg3);
- 4) banded quartz-spodumene-albite aplite-pegmatites (Peg4).

Peg1 form isometric bodies some hundred meters across, or merged bodies of intricate shape.

They are basically composed of Gr3 containing numerous K-feldspar and quartz blocky enclosures, portions of coarse-grained quartz–two-feldspar and quartz–K-feldspar pegmatite varieties, as well as quartz–muscovite aggregate. The boundaries between granite matrix and pegmatitic parts proper within Peg1 bodies are irregular and generally indistinct. The quantitative proportions of “granite” and “pegmatite” in different parts of Peg1 bodies are not constant.

Peg2 compose apophyses of some granite–pegmatite bodies and single veins up to 200 m long and 25 m thick in swells. As regards composition and structure, they are close to the pegmatite constituent proper in the Peg1 bodies.

Peg3 are composed of fine- or medium-grained quartz–albite aggregate with particles of white K-feldspar 3–7 cm or larger. Albite is tabular, rarely bladed. Quartz is found as glomeroblasts about 3–5 cm across. Besides, scaly or platy muscovite is regularly dispersed throughout the rock.

Peg4 produces series of numerous closely juxtaposed veins extending for 2.5 km, and up to 1.2 km wide as a whole. The largest bodies of pegmatite reach several hundred meters long and 15–20 m thick. Having the most complicated composition

and internal structure, *Peg4* are composed by several structure–mineral varieties of rocks:

- a) fine-grained quartz–albite (“white aplites”);
- b) fine-grained spodumene–quartz–albite (“grey aplites”, in places “felsites”);
- c) medium-grained quartz–albite granite-like rocks (in places with rare spodumene);
- d) coarse-grained to giant-crystal-bearing spodumene–K-feldspar–quartz–albite, commonly with muscovite, in places containing the sites of bimineralic quartz–spodumene aggregates (pegmatites proper);
- e) coarse-grained quartz–muscovite (“greisen”).

A specific feature of *Peg4* is banding (Fig. 1), which is created by the irregular alternation of the above-listed varieties parallel to the contacts of vein bodies, even where they show a knee-like bend. Varieties *a*, *b* and *d* are predominant in *Peg4*. The thickness of the bands varies from 2–3 cm to 2.5 meters and more. In places, the bands branch, are wedge-shaped and reappear. The contacts of the spodumene-bearing rocks with spodumene-free ones may be either sharp or gradational. The spodumene



FIGURE 1. Typical banded structure of spodumene-rich pegmatites

and K-feldspar crystals, with rare exceptions, are oriented perpendicular to the contacts of bands. In a cross-section of a body, there may be up to a few dozen alternations of rocks. In swollen parts of veins, the banding is often distorted by pairing or crossing of bands. In the cases of veins dipping to a depth of 70-100 m, the proportion of aplite-like rocks increases relative to the pegmatites proper. Accessory garnet, tourmaline and beryl occur in all types of pegmatites, whereas Peg3 and Peg4 contain cassiterite and columbite-tantalite as well.

METASOMATIC ROCKS

The granite-pegmatite system includes metasomatic assemblages formed in two stages: (1) post-metamorphic pre-pegmatitic, and 2) syn-pegmatitic.

Metasomatic rocks of stage 1 represent the fracture-veinlet formations making up linear zones, occurring beyond the area of Peg4 branching veins. Their external parts are dominated by micaceous metasomatic assemblages with albite and tourmaline, whereas the axial parts are composed by tourmaline-bearing assemblages. In cases of a very high degree of metasomatic transformations, lenses of biotite-dominant glimmerites and anchimonomineralic tourmaline-dominant rocks with a carbonaceous substance are developed. Metasomatic rocks of this stage are generally cut by pegmatites.

Metasomatic rocks of stage 2 are linked with Peg4 bodies, in general, but they can infrequently occur around Peg3 as well. They represent exocontact rims some centimeters wide, rarely 2-3 m or more. The external parts of the metasomatic rims are composed of Li-rich biotite predominantly, which is replaced by association of Li-rich phengite and Li-rich muscovite, with quartz, tourmaline and apatite close to the contacts with pegmatites. Metasomatic rocks of stage 2 are developed at the expense of both the host metamorphic rocks and pre-pegmatite metasomatic assemblages.

WHOLE-ROCK GEOCHEMISTRY

The data acquired for granites, pegmatites and metasomatic assemblages allow the evolution of granite-pegmatite system as a whole to be deduced. In the series Gr1 → Gr2 → Gr3, while the Si contents increase and the femic components decrease in abundance, the alkalinity of the rocks increases. It is noteworthy that in Gr3, the dispersion of K and Na increases drastically, with $K_2O/(K_2O + Na_2O)$ varying from 0.25 to 0.59. On the diagram Qtz – Ab – Or – H₂O, the normative composition of granites in this series deviate from the line of cotectic minimum toward Qtz–Ab. The tendencies reported above, even if non-essential, are also preserved in the series from Peg1 to Peg4, but spodumene-rich Peg4 are enriched in

iron (1.20–1.50 wt.% Fe₂O_{3tot}) substantially, compared to other pegmatites and Gr3. Furthermore, on the background of an increase in the role of Na relative to K, and then Li relative to Na in the Peg1–Peg4 sequence, pegmatites show a much more profound intravein differentiation than in Gr3 as regards the alkalis: K and Na in Peg1 and Peg2, Na and Li in Peg4. No volatile component accumulates in pegmatites relative to granites. Furthermore, concerning B and F, a slight tendency to decrease their abundances in pegmatites is established.

Pegmatites of all recognized types are rich in granitophile rare elements relative to granites. Only Li contents in Peg1 and some Peg2 are lower than in Gr3. In the series from Peg1 to Peg4, the rocks are sequentially enriched in Li, Rb, Cs, Sn, Be, Ta and Nb parallel to a reduction in K/Rb, from 60-85 to 25-30. It is noteworthy that Peg4 is enriched in Li in an “explosive” manner. At the site of some bodies composed of a bimineralic quartz–spodumene aggregate, the Li₂O contents reach 3.9%, which is two-fold higher than in albite “aplitites” of the same bodies, as well as in pegmatites of the other types. The various types of pegmatites are practically indistinguishable or only slightly different in Ta/Nb (0.3–0.6) and Zr/Hf (commonly 15–25), commonly used as indicators of differentiation in magmatic systems. In Peg4, aplitic zones show three-fold lower values of Zr/Hf (15–18) than the pegmatite zones proper.

The formation of pre-pegmatitic metasomatic rocks was accompanied by enrichment of rocks in alkalis, B, F, Sn, W, Be, but their concentrations did not attain high values. In the case of the formation of the biotite-dominant glimmerite, an input of Fe and Mg (basification) is established as well. The process of formation of the syn-pegmatitic metasomatic assemblages was caused by a depletion of rocks in femic components and their significant enrichment in K, F, B, rare alkalis (especially Li) and, to a lesser degree, Sn and Be.

PETROGENETIC ASPECTS

The primary magmatic nature of granites and pegmatites of the Zavitaya field is verified by a set of geological and P–T geochemical data, in particular the presence of melt inclusions in quartz and spodumene of Peg4. At the same time, many available geological and geochemical data agree poorly with the classical model of lithium pegmatite formation due to the process of fractional crystallization of a magmatic system. They involve: (a) a large total volume of spodumene-rich pegmatites, comparable or even superior to that of “parent” leucogranites; (b) an absence of zonation in the distribution of Peg4 relative to the granites and pegmatites of other types; (c) a very sharp (“explosive”) mode of Peg4 enrichment in lithium at a low content of volatile components; (d) higher Eu/Eu* values (including positive anomalies)

in Peg4 as compared to leucogranites; (e) a significant time-gap between Rb–Sr ages of Gr2 (167.4 ± 3.5 Ma) and Peg4 (136.3 ± 3.5 Ma) (Zagorsky & Dril' 2009).

The data available are most consistent with the *metamagmatic model* of granite–pegmatite systems. According to this model, pegmatite-forming melts are interpreted as being more evolved and “mature”, rather than residual, in comparison to the parental granitic magma; they are supra-eutectic metamagmatic products, which appear as a result of fluid–melt interaction in zones of the most intense drainage of deep fluids within magma chambers (Zagorsky 2007). In terms of the model granites, pegmatites and metasomatic rocks seem to be closely interrelated constituents of the united fluid–magma system formed in the process of transformation of a granitic magma into pegmatitic one, which was accompanied by the input of lithium to the magmatic chamber and metasomatic conversion of the roof rocks. The lithium specialization of the granite–pegmatite system begins to be important with the pre-pegmatitic stage of metasomatism.

The Zavitaya granite–pegmatite system is polychronous. The time of its formation coincides with the stage in the geodynamic regime of change in the region at the Jurassic–Cretaceous boundary;

the age of the early granitic members of the system corresponds to the time of termination of collision, whereas the formation of Peg4 is related to the onset of a rifting stage.

ACKNOWLEDGEMENTS

The study was supported by RFBR (project 10-05-00964), SB RAS (IIP-29).

REFERENCES

- Zagorsky V. Ye. (2007). Deep fluid flow–melt interaction and problems of granite-pegmatite system petrogenesis. *Memorias Universidade do Porto*. **8**: 58-59.
- Zagorsky V. Ye. & Dril' S.I. (2009). Rb–Sr age of two-mica granites and spodumene pegmatites of the Zavitaya granite–pegmatite system. In: *Isotope systems and time of geological processes (Proceedings of the IV Russian conference on isotope geochronology)*. St. Petersburg. **1**: 192-195 (in Russian).
- Zagorsky V. Ye. & Kuznetsova L.G. (1990). *Geochemistry of spodumene pegmatites and alkaline-rare metal metasomatites*. Nauka Press. Novosibirsk, Russia. 141 pp. (in Russian).

“In view of the advanced geochemical evolution attained by the parental leucogranites, and the factors affecting the pegmatite melts themselves, it is understandable that some of the LCT rare element pegmatites represent the most fractionated terrestrial igneous rocks”.

Černý et al. (Econ. Geol. 100th Ann. Vol. p. 356, 2005)



AGENCIA
NACIONAL DE PROMOCIÓN
CIENTÍFICA Y TECNOLÓGICA

